UNIVERSITY OF SALAMANCA

FACULTY OF CHEMICAL SCIENCES

ORGANIC CHEMISTRY DEPARTMENT



ANTINEOPLASTIC PRODRUGS ACTIVATED BY CELLULAR HYPOXIA

PhD Thesis

Asmaa Habib

Supervisors

Joaquín Rodríguez Morán

Ángel Luis Fuentes de Arriba

© ASMAA HABIB, **2024**

UNIVERSIDAD DE SALAMANCA

FACULTAD DE CIENCIAS QUÍMICAS

DEPARTAMENTO DE QUÍMICA ORGÁNICA

PROFÁRMACOS ANTINEOPLÁSICOS ACTIVADOS POR HIPOXIA CELULAR

TESIS DOCTORAL

Asmaa Habib

Directores

Joaquín Rodríguez Morán

Ángel Luis Fuentes de Arriba

© ASMAA HABIB, **2024**

UNIVERSITY OF SALAMANCA

FACULTY OF CHEMICAL SCIENCES

ORGANIC CHEMISTRY DEPARTMENT



VNiVERSiDAD D SALAMANCA

CAMPUS DE EXCELENCIA INTERNACIONAL

ANTINEOPLASTIC PRODRUGS ACTIVATED BY CELLULAR HYPOXIA

PhD Thesis

Thesis presented by Ms. Asmaa Habib for the degree of Doctor by the University of Salamanca.

VNiVERSiDAD D SALAMANCA
CAMPUS OF INTERNATIONAL EXCELLENCE

DEPARTAMENTO DE QUÍMICA ORGÁNICA
FACULTAD DE CIENCIAS QUÍMICAS
UNIVERSIDAD DE SALAMANCA

Prof. Ricardo Escarcena Romero, Director of the Department of Organic Chemistry at the University of Salamanca

CERTIFIES:

That the present thesis entitled 'Antineoplastic prodrugs activated by cellular hypoxia' has been carried out by Asmaa Habib in the Department of Organic Chemistry at the University of Salamanca to opt for the title of Doctor by the University of Salamanca, and has been developed under the supervision of D. Joaquín Rodríguez Morán, Full Professor of the Department of Organic Chemistry at the University of Salamanca and Dr. Ángel L. Fuentes de Arriba, Associate Professor of the Department of Organic Chemistry at the University of Salamanca.

And for the appropriate purposes, I sign the present document

[redacted]

:

Ricardo Escarcena Romero

VNiVERSiDAD D SALAMANCA
CAMPUS OF INTERNATIONAL EXCELLENCE

DEPARTAMENTO DE QUÍMICA ORGÁNICA
FACULTAD DE CIENCIAS QUÍMICAS
UNIVERSIDAD DE SALAMANCA

D. Joaquín Rodríguez Morán, Full Professor of the Department of Organic Chemistry at the University of Salamanca and Dr. Ángel L. Fuentes de Arriba, Associate Professor of the Department of Organic Chemistry at the University of Salamanca

CERTIFY:

That the present document entitled 'Antineoplastic prodrugs activated by cellular hypoxia' has been carried out by Asmaa Habib in order to qualify for the title of Doctor by the University of Salamanca, and has been developed under his joint direction in the Department of Organic Chemistry at the University of Salamanca and authorise its presentation to be qualified as a Doctoral Thesis.

And for the record, they sign the following document

[redacted] [redacted]

Prof. Joaquín Rodríguez Morán Dr. Ángel L. Fuentes de Arriba

SCIENTIFIC CONTRIBUTIONS DERIVED FROM THE DOCTORAL THESIS

The scientific articles published in scientific journals and contributions presented at congresses and symposia, which include part of the results obtained in this Doctoral Thesis report, are listed below:

Publications in scientific journals.

1. José J. Garrido-González, Estela Sánchez-Santos, Asmaa Habib, Ángel V. Cuevas Ferreras, Francisca Sanz, Joaquín R. Morán, Angel L. Fuentes de Arriba, Transesterification of Non-Activated Esters Promoted by Small Molecules Mimicking the Active Site of Hydrolases, *Angew. Chem. Int. Ed.* **2022**, *61*, (35), e202206072. **https://doi.org/10.1002/anie.202206072**

   Impact factor: 16.6 (JCR, 2022).
   Ranking: Q1 (13/178).

2. Sánchez-Santos, E.; Garrido-González, J.J.; Rodríguez-Sahagún, L.F.; Habib.A.et al; Alcázar, V.**2022**. Tryptophan association in water driven by charge-transfer interactions with electron-deficient aromatic haptens. *Org. Biomol. Chem. 20* (40), 7972-7980**.** **https://doi.org/10.1039/D2OB01650H.**

   Impact factor: 3.2 (JCR, 2022).
   Ranking: Q2 (14/52).

3. Habib, A.; Garrido-González, J. J.; Sánchez-Santos, E.; Boya del Teso, I.; Sanz, F.; Alcázar, V.; Fuentes de Arriba, Á. L.; Morán, J. R. 5-chloro-8-nitro-1-naphthoyl (NNap): A Selective Protective Group for Amines and Amino Acids. *Org. Lett.* **2023**, *25* (22), 4103–4107. **https://doi.org/10.1021/acs.orglett.3c01334.**

   Impact factor: 5.5 (JCR, 2023).
   Ranking: Q1 (4/58).

4. Habib, A-; Sánchez-Santos, E.; Boya del Teso, I.; Sanz, R.; Simón, L.; Morán, J. R. Fuentes de Arriba, Á. L. An unusual rearrangement of a 1,8-naphthalene derivative. *J . Org. Chem.* **2024.** [Manuscript in preparation]

Contributions presented at conferences and symposia.

1. Title : "Antineoplastic Drugs Activated Under Hypoxia Conditions"

- Type of contribution: Poster.

- Authors: Asmaa Habib,* José J. Garrido-González, Estela Sánchez Santos, Ángel L. Fuentes de Arriba, Joaquín R. Morán.

- Conference name: RSEQ Symposium. 27/10/2021 – 30/09/2021.

- Organising Entity: Royal Spanish Society of Chemistry.

- Place of celebration: Online format, Spain.

2. Title : "Antineoplastic prodrugs activated by cellular hypoxia"

- Type of contribution: Oral communication.

- Authors: Asmaa Habib*

- Conference name: III Jornadas de Jóvenes Investigadores en Ciencia y Tecnología Químicas. 15/07/2021 – 16/07/2021.

- Organising Entity: Faculty of Chemical Sciences, USAL.

- Place of celebration: Salamanca, Castilla y León, Spain.

3. Title : "Targeting cancer cells by using new pro-drugs activated under hypoxic medium"

- Type of contribution: Poster.

- Authors: Asmaa Habib,* J. J. Garrido-González, E. Sánchez Santos, I. Boya del Teso, I. de Dios Pérez, Á. L. Fuentes de Arriba, J. R. Morán.

- Conference name: III Jornadas de Jóvenes Investigadores en Ciencia y Tecnología Químicas. 15/07/2021 – 16/07/2021.

- Conference name: XXXVIII Biennial RSEQ Meeting.

- Organising Entity: Spanish Royal Society of Chemistry. 27/06/2022- 30/06/2022.

- Place of celebration: Granada, Spain.

4. Title : "Synthesis of new theranostic pro drugs against cancer"

- Type of contribution: Oral communication.

- Authors: Asmaa Habib*

- Conference name: IV Jornadas de Jóvenes Investigadores en Ciencia y Tecnología Químicas. July, 2022.

- Organising Entity: Faculty of Chemical Sciences, USAL.

- Place of celebration: Salamanca, Castilla y León, Spain.

5. Title : "Synthesis of antineoplastic pro-drugs activated under hypoxia conditions"

- Type of contribution: Oral communication.

- Authors: Asmaa Habib*

- Conference name: 8th EuChemS Chemistry Congress. 28/08/2022- 01/09/2022.

- Organising Entity: Portuguese Chemical Society and Portuguese Electrochemical Society.

- Place of celebration: Lisbon, Portugal.

6. Title : "8-Nitro-1-Naphthoic Acid as a Novel Amine Protecting Group and Molecular Trigger of Drugs"

- Type of contribution: Poster

- Authors: Asmaa Habib*, J. J. Garrido Gonzalez, E. Sánchez-Santos, I. Boya Del Teso, Á. L. Fuentes de Arriba, J. Rodríguez. Morán

- Conference name: XXXIX REUNIÓN BIENAL. 25/06/2023- 29/06/2023.

- Organising Entity: Spanish Royal Society of Chemistry.

- Place of celebration: Zaragoza, Spain.

7. Title : "Nitro-1-Naphthoic Acid: as a Selective Protecting Group for Amines and Drugs Activator".

- Type of contribution: Poster

- Authors: Asmaa Habib*, Ángel L. Fuentes de Arriba, Joaquín R. Morán.

- Conference name: V Jornadas de Jóvenes Investigadores en Ciencia y Tecnología Químicas

- Organising Entity: Faculty of Chemical Sciences, USAL

- Place of celebration: Salamanca, Castilla y León, Spain.

8. Title : “Solubility Enhancement of Antineoplastic Prodrugs and their Activation Under Hypoxia Conditions”.

- Type of contribution: Poster

- Authors: Asmaa Habib *, Ángel L. Fuentes de Arriba, Joaquín R. Morán.

- Conference name: V Jornadas de Jóvenes Investigadores en Ciencia y Tecnología Químicas

- Organising Entity: Faculty of Chemical Sciences, USAL

- Place of celebration: Salamanca, Castilla y León, Spain.

9. Attendance at the 3-hour conference on research-based learning, held at the School of Industrial Engineering of the Polytechnic University of Madrid, on 20 October 2022.

10. Attendance at the IX Jornadas de Investigadoras de Castilla y León: the Adventure of Science and Technology, held in Salamanca, from 9 to 10 February 2023, with a duration of 16 hours.

For my parents, my sister and brothers, for all the people who love me

For all cancer patients around the world

Cancer the scourge that we fight always…

Acknowledgements

With a great pleasure, I would like to express my sincere appreciation and gratitude to all the people who have accompanied me during this important phase of my life and helped me to make it possible, moments of joy, setbacks and many challenges have marked this stage.

First and foremost, I would like to extend my heartful appreciation and gratitude to my thesis supervisors, Prof. Joaquín Rodríguez Morán "Quino", Full Professor of the Department of Organic Chemistry at the University of Salamanca and Dr. Ángel Luis Fuentes de Arriba, Contratado Doctor Professor of Organic Chemistry at the University of Salamanca for giving me the support to accomplish this work, for their guidance, advices and dedication through the entire process of investigating and writing this thesis over these years. I am very grateful for the knowledge they shared, their expertise and mentorship which have been invaluable to me. Thank you for trusting on me and giving me the opportunity to be integrated in your research group and laboratory to achieve this work.

To Dr. José Javier Garrido González, postdoctoral researcher from USAL, currently Marie Curie fellow at University of Padova (Italy) for his support, selfless help and his constant desire to create a family atmosphere among the group members.

To Dr. Maria Victoria Alcázar Montero, professor in the department of Industrial Chemical and Environmental Engineering (Universidad Politécnica de Madrid) , for her valuable scientific contributions, constant willingness and her collaborative spirit have been influential in the successful completion of this work.

To Dr. Eva Martín del Valle and Dr. Inmaculada De Dios Pérez (Chemical and Textile Engineering Department, USAL) for their valuable collaboration, wide experience and for their affective contribution in performing the biological assays and analysing our moieties by providing cells and experimental protocols.

To Dr. Luis Simón Rubio for his valuable scientific contributions in molecular modelling and his constant willingness to fend off obstacles.

To Dr. Anna Lithgow Bertelloni (NMR Service, NUCLEUS, University of Salamanca) for the NMR spectra done in the Bruker Avance NEO 400 MHz, for her permanent availability, responsibility and her competence in analysing the samples and broadening our knowledge in resonance.

To all the staff of Mass Spectrometry Service, especially to Dr. César Raposo Funcia and Dr. Juan Francisco Boyero Benito, for their inexhaustible patience, their expertise in analysing and processing a large number of samples and obtaining good results. I can only say thank you very much.

To Dr. Francisca Sanz González and Dr. José Manuel Compaña Prieto from X-ray Diffraction Service for their important contribution, and dynamism in treating so many crystals and finding their morphological structures.

To the staff of the Analytical Chemistry department, especially Dr. Diego García Gómez for his generous contribution in analysing and measuring the fluorescence of our samples.

To my laboratory colleagues: Dr. Ghibom Bhak, Estela Sánchez Santos and Irene Boya del Teso, I am sincerely grateful for the good atmosphere I have been able to enjoy over the years in the laboratory, which has made the work considerably easier, for their friendship and dedication in this work. Thank you from the bottom of my heart for everything.

To all the members of Moran group, as well as to those who were passing through, thank you for the pleasant moments shared inside and outside the faculty.

To María José Pérez Martín and Javier Vicente Díaz, for being available for equipping the laboratory with everything necessary, for keeping the department in order and their endless kindness and availability. Special mention also to the cleaning team, who allow us to work comfortably and keep everything in perfect conditions. Especially Toñi, for all her love, her constant interest and her great conversations.

To Elena Hernández García and Alba María Morales López for their valuable contribution in this work, seriousness and punctuality, also I would like to say a big thank you to all the wonderful people I have met who have given me moments of joy and beautiful memories: Ruth Pecker, Camille, Betul Kamis, Lucia Lacasta, Nerea Cobo, Aida Sanchez, Ligzajaya Rodríguez.

To Vicen and Sonia, thank you for making our stay in the faculty cafeteria a moment of disconnection and enjoyment.

To the entities which provided us with financial support: MICINN (PID2019-108994RB-I00, PID2020-118732RAI00 and CNS2022-135656), Junta de Castilla y León (European Regional Development Fund-SA069P17), the University of Salamanca (Own Research Programs-

KCEP/463AC01 and 18K155/463AC01) and Fundación Memoria de D. Samuel Solórzano Barruso (FS/8-2019).

To the Algerian government and the Ministry of Higher Education and Scientific Research for financing the predoctoral fellowship and of course the Algerian Embassy in Madrid for the invaluable commitment, thank you is not enough to express my gratitude message for giving me this precious opportunity, I really appreciate your dedication and support.

To my Algerian colleagues and friends whose unfailing friendship and attentiveness have been a constant source of comfort and motivation, I am grateful to have met you.

To my beloved parents, today my life has a purpose and a goal, all thanks to your unceasing efforts and your confidence in me, for your blessings and constant support. Actually, the word 'thank you' is not enough to express my love and gratitude to you.

Thank you, mum, for everything you have given me, your valuable advices, your supportive words, and for being by my side in my difficult and happiest times. May God heal and protect you for us.

Thank you, dad, for your confidence, your material and moral support, your love, thank you for the values and principles you instilled in me, which has become a source of inspiration and strength, without you I would not be here. May God protect you for us.

To my dearest sister Fatima Zahra, my role model and idol, for her support, advices and her wisdom in dealing with things, thank you and your husband Walid for your endless patience, understanding and encouragement.

To my dearest brothers, Adel, Yasser and Mohamed Abdelhai, your love, support, and words of encouragement have always been my source of strength, and for that, I am deeply thankful. May God bless and protect you.

To my little nephews, Joud and Abelbar "Banino" for being part of my life, thank you for making me smile when I see you little angels. May God bless you.

"There are no incurable diseases, only the lack of will. There are no worthless herbs, only the lack of knowledge."

Avicenna

"Without the curiosity of the mind, where would we be? That is the beauty and nobility of science: a never-ending desire to push back the frontiers of knowledge, to track down the secrets of matter and life without any preconceived idea of the possible consequences."

Marie Curie

INDEX

Summary 1
Resumen 5
Abbreviations and Acronyms 9
1. General Objectives 13
2. Introduction 13
2.1. Cancer: definition, history, epidemiology and characteristics 14
2.1.1. What is cancer? 14
2.1.2. Cancer history 14
2.1.3. Epidemiology and statistics 16
2.1.4. Cancer progression 17
2.1.5. Causes and genetic process 18
2.1.6. Tumor cells *versus* healthy cells 20
2.1.7. Energetic metabolism 21
2.1.8. Morphological differences 22
2.1.9. Tumor microenvironment 23
2.1.10. What is hypoxia? 24
2.1.11. Angiogenesis 25
2.1.12. Glutathione 26
2.1.13. Glutathione in cancer microhabitat 26
2.1.14. Tumour microenvironment features: Promising Prospects in Cancer Therapy 27
2.2. Chemotherapy 28
2.2.1. What are antineoplastic drugs? 29
2.2.2. Conventional chemotherapy 30
2.2.3. Targeted chemotherapy 34
2.2.4. Theranostic therapy: An opportunity to make chemotherapy selective 37
2.2.5. Prodrug strategy 38
2.3. Protective groups: New Moieties for Chemoselectivity, Regioselectivity and Stereoselectivity 44
2.3.1. Protecting groups 44
2.3.2. Characteristics 44
2.3.3. Protecting group´s chemoselectivity 45
2.4. Antineoplastic prodrugs hydro-solubility 46
2.4.1. Prodrugs solubility enhancement via polar functionality addition 46

2.5. An unusual rearrangement of a 1,8-naphtalene derivative.....50
3. References……..51

CHAPTER 1: PRODRUGS FUNCTIONALIZED WITH SULFUR-SULFUR BONDS……57

1. Objectives 57
2. Introduction 58
   2.1. Optimisation.....61
   2.2. Histone Deacetylases.....62
      2.2.1. Histone Deacetylases inhibitors.....63
   2.3. Background 65
      2.3.1. Pregnenolone and Farnesol 65
   2.4. Biological trials: MTT assay 67
      2.4.1. Cell Viability: MTT Assay technique.....68
3. Methodology.....70
   3.1. Synthesis of disulfide bonded compounds 70
   3.2. Study of functional groups able to react with acid chlorides **4** and **6** 71
   3.3. Synthesis of Tacedinaline.....78
   3.4. Functionalization of Tacedinaline with acid chloride **4** 82
   3.5. Prodrug synthesis 83
   3.6. Cell assays 84
4. Conclusions 86
5. Experimental Section.....87
   5.1. Materials and instrumentation.....87
   5.2. Cell lines and culture conditions 88
   5.3. Cell viability determination.....88
   5.4. Synthetic details and characterization 89
6. References 96

CHAPTER 2: PRODRUGS FUNCTIONALIZED WITH NITRO GROUPS 99

1. Objectives 99
2. Introduction 100
   2.1. Nitroaromatics.....101
      2.1.1. Nitroaromatics attached to mustard gas.....101
   2.2. Our strategy 102

2.3. Fluorescence contribution in anti- cancer drugs (ACDs) pharmacokinetics.....103
2.3.1. 1-Naphtoic acid.....103
2.4. The proposed challenge.....104
2.5. Bioreducible Mustards: New Scope for Exploitation.....105
2.5.1. Nitrogen Mustards Hybrids.....106
2.5.2. *N*,*N*-bis(2-chloroethyl)amine.....107
2.6. Nitroaromatics attached to antimetabolites(pyrimidine analogues) 5-Fluorouridine.....107
2.6.1. 5-Fluorouridine (5-FUrd).....107
3. Methodology.....109
3.1. Synthesis of nitro-based prodrugs (Nitrogen mustard/bis(2-chloroethyl)amine).....109
3.2. Synthesis of nitro-based prodrugs (5-Fluorouridine).....111
3.2.1. 5-Fluorouridine prodrug **1**.....111
3.2.2. 5-Fluorouridine prodrug **2**.....112
3.3. Synthesis of the auxiliary group.....113
3.4. Synthesis of other auxiliary groups.....120
3.5. Fluorescence properties.....122
3.6. Biological trials: MTT assay.....124
4. Conclusions.....127
5. Experimental Section.....128
5.1. Materials and instrumentation.....128
5.2. Synthetic details and characterization.....128
5.3. NMR spectra.....141
6. References.....153

CHAPTER 3: 5-CHLORO-8-NITRO-1-NAPHTHOYL (NNAP): A SELECTIVE PROTECTIVE GROUP FOR AMINES AND AMINO ACIDS.....157
1. Objectives.....157
2. Introduction.....158
2.1. Protecting groups.....158
2.2. Amino groups protection.....159
2.2.1. Protection varieties.....160
2.3. Background.....162
3. Methodology.....164
3.1. Amine's protection using the protective group NNap.....164

3.2. The NNap protective group formation 166
3.3. Amide crystallographic study 167
3.4. Deprotection study of NNap 167
3.5. Isolation of intermediate amines produced in the deprotection process 170
3.6. Deprotection using Hantzsch Ester 171
3.7. NNap a multi-applicable protective group 172
3.7.1. Peptides synthesis using NNap 172
3.7.2. Orthogonal protection of L-lysine using NNap 172
3.7.3. NNap application to indanolamines 174
4. Conclusions 175
5. Experimental Section 176
5.1. Materials and instrumentation 176
5.2. Synthetic details and characterization 178
5.3. General Procedure (**A**) for amine (**5-11**) protection using NNapCl 179
5.4. Procedure for deprotection 184
5.5. Capture of the intermediate amine 186
5.6. Synthesis of H-Leu-Leu-O*t*Bu 188
5.7. Orthogonal protection of lysine 191
5.8. Reaction with 1-amino-2-indanol (**11**) 193
5.9. NMR spectra 196
5.10. Crystallographic data 222
5.10.1. Potassium carboxylate (K•**3**) 222
5.11.2. Amide **17** 225
5.12. Modelling studies 226
6. References 230

CHAPTER 4: SYNTHESIS OF WATER-SOLUBLE PRODRUGS 233
1. Objectives 233
2. Introduction 234
2.1. What is solubility? 234
2.2. Hydro-solubility improvement in prodrugs 235
2.3. Background: Examples of solubilizing anticancer prodrugs from poorly-soluble drugs 236
2.4. Carboxylic acid functional group 237
2.4.1. Pharmaceutical applications 237

2.4.2. *First strategy*: Click reaction 238
2.4.3. *Second strategy*: Thioglycolic acid integration 244
2.5. What is Farnesol? 245
2.5.1. Anticancer chemotherapeutic properties of Farnesol 246
2.6. What is pregnenolone? 247
2.6.1. Anticancer chemotherapeutic properties of Pregnenolone 248
3. Methodology 250
3.1. Synthesis of 5-azide-8-nitro-1-naphtoic acid 250
3.2. Optimisation: Synthesis of Tacedinaline 251
3.3. Coupling of Tacedinaline with the protective group 256
3.4. Synthesis based on click reaction 259
3.5. Bioreductive medium mimicry 261
3.6. Synthesis of prodrugs soluble in water using a thioglycolic acid fragment 262
3.6.1. Fischer Esterification 263
3.6.2. Acid activation using $C_2O_2Cl_2$ 263
3.6.3. Antineoplastic agents' attachment 264
3.6.4. The hydrolysis of the prodrug's esters 268
3.6.5. Hydrolysis general procedure 269
3.7. Biological trials 269
3.7.1. Cell lines and culture conditions 269
3.7.2. Cell viability determination 270
3.7.3. Results 273
3.7.4. Cell counting 278
3.7.5. Mass spectrometry results 281
4. Conclusions 285
5. Experimental Section 287
5.1. Synthetic details and characterization 287
5.2. NMR Spectra 304
6. References 317

CHAPTER 5: AN UNUSUAL REARRANGEMENT OF A 1,8-NAPHTHALENE DERIVATIVE 323

1. Objectives 323
2. Introduction 324
3. Methodology 325

3.1. Compound **4** synthesis 325
4. Conclusions 336
5. Experimental Section.....336
5.1. Materials and instrumentation.....336
5.2. Synthesis and characterization 337
5.3. Crystallographic Data.....342
5.4. Computational Studies 345
5.5. NMR spectra 346
6. References 362

Publications ……367

Summary

Cancer is a broad term that encompasses a group of diseases, characterized by the uncontrolled growth and spread of abnormal cells from their original location to adjacent tissues or other organs, this mechanism is often known as metastatic stage. Because cancer is ranked as third in incidence worldwide and second in mortality, its early detection is vital for survival, with a range of treatment options, from surgery for the earliest stages to the more complex alternatives for the advanced stages.

In spite of the marked rate of progress in struggling against cancer over decades, the ongoing investigations are always focused on reducing side-effects by improving anti-cancer substances selectivity and therefore optimizing patient´s quality of life.

Among the major challenges in cancer treatment are the poor bioavailability and the lack of discrimination of antineoplastic agents towards healthy and tumor cells.

These issues arising from the use of conventional chemotherapy, led to heighten interest in targeted therapy which is based essentially on modifying the conventional chemotherapy substances by growing the understanding of tumor microenvironment features.

For these reasons, strategies of anticancer drugs delivery and targeting have been developed in order to enhance their biodistribution, therapeutic kinetics, and targeted selectivity.

The thesis objectives have been designed to optimize the current therapies efficiency, and diminish side effects by synthetising antineoplastic prodrugs taking advantage of the distinction between tumor and healthy tissues, in which the anticancer prodrugs were designed specifically to be cleaved in particular under the hypoxic medium which is a special feature of cancer cell clusters. Three strategies were employed to achieve the aims.

The **first strategy** focused on synthesizing compounds with disulfide bonds with the aim of attaching them to several antineoplastic drugs by exploiting two essential factors in the tumour microenvironment, hypoxia and high level of glutathione, so that, the resulting prodrugs functionalized with sulfur-sulfur bonds will be cleaved under the expected conditions by liberating the cytotoxic agent selectively.

Subsequently, the use of the *tert*-butyl group as an adjacent fragment to the disulfide has been a good option to be able to obtain the prodrug, then Tacedinaline has been synthesized and coupled resulting by that a cytotoxic compound derivatized with a disulfide bond that is stable in water at cellular pH.

The synthesized antitumor prodrug has been tested on cancer (colorectal carcinoma **HCT-116**) and healthy cells (fibroblasts **HS-5**). However, its behaviour was unexpected in which according to MTT assay results a lack of selectivity has been observed, in addition the effectiveness of the pure Tacedinaline was higher than the cytotoxic prodrug itself.

In light of this, a **second strategy** has been implemented, involving the synthesis of prodrugs functionalized with nitro groups. Initially, nitroaromatics derivatives have been designed and synthesized to be linked with another range of antineoplastic drugs such as bis(2 chloroethyl)amine and 5-fluorouridine, subsequently the two prodrugs have been realised successfully . In fact, bis(2 chloroethyl)amine prodrug was able to be used as a theranostic agent thanks to its fluorescence emitted by the cleavage of a fluorescent lactam when exposed to tumour hypoxia. 5-fluorouridine attached to a nitro aromatic trigger is a promising prodrug, and we have studied its ability to liberate the cytotoxic moiety under an analogous hypoxic medium using zinc as a reductant.
In vitro toxicity assessment was realised for bis(2 chloroethyl)amine prodrug. Surprisingly an insolubility issue appeared, which has affected the correct validation of the cytotoxic effect of the prodrug on cells.

In parallel we these studies we envisioned that the molecular trigger could be used as an orthogonal protecting group for amines, amino acids and aminoalcohols. Thus, extensive investigations were performed to explore the properties of the trigger 5-chloro-8-nitro-1-naphthoyl (NNapCl) as a protecting group. This group characterizes by an easy protection under Schotten-Baumann conditions and easy deprotection under reducing conditions. As a result, the study culminated by an effective protective group with a great potential to be included as alternative protecting group in the amine protection groups arsenal.

In order to resolve the prodrugs insolubility obstacle a **third strategy** was proposed which involves modifying the trigger 5-chloro-8-nitro-1-naphthoyl (NNapCl) by integrating a polar functional group through aromatic nucleophilic substitution or using click chemistry. Then, four antineoplastic drugs were suggested to be linked to the innovative molecular configuration of water-soluble molecular trigger. These drugs were: Pregnenolone, Farnesol, Bis(2 chloroethyl)amine (nitrogen mustard) and Tacedinaline. However, similar to many anticancer drugs, the latters are hydrophobic, consequently their attachment to the modified protective group was a successful step to produce the four prodrugs with hydro- solubility enhancement.

Actually, two different approaches were carried out to improve the solubility, first, the triggering moiety was modified by click chemistry and attached to Tacedinaline, nevertheless, the complexity of its purification pushed us to perform the second approach which was the integration of thioglycolic acid. Once the antitumor prodrugs have been obtained *in vitro* toxicity assessment (MTT assays) was applied on two cell lines: healthy fibroblasts **HS-5** and colorectal carcinoma **HCT-116** to validate the prodrugs cytotoxicity selectively towards cancer cells by their detachment only under the hypoxic medium. Curiously, the MTT assay results have shown a variance in reducing the cellular viability of cancer and healthy cells and a complete solubility of the four prodrugs within the cellular medium. Pregnenolone prodrug has attracted our attention since it was the more effective in reducing the cell viability, in this case additional analysis steps were carried out for further confirmation in which MTT assays have been repeated using different concentrations from the pregnenolone prodrug, also counting cells test and HPLC-MS have been achieved for an in-depth investigation of pregnenolone prodrug. Overall, the results were promising in which the HPLC-MS results have shown the release of the drug inside the cells.

To conclude this thesis, during the coupling of bis(2-chloroethyl)amine) to a 1,8-nitronaphthalene derivative (5-((2-methoxy-2-oxoethyl)thio)-8-nitro-1-naphthoic acid), a novel compound was obtained, probably due to an unusual rearrangement caused by the steric hindrance between the nitro and the carboxylic acid group in *peri* positions. To assign the structure of this compound, a full study has been realised using ^{1}H NMR, ^{13}C NMR, bidimensional NMR, IR, HRMS. Also, we have obtained the X-ray diffraction analysis of a product derivative and modelling studies have been performed to study the mechanism of this unusual rearrangement.

Resumen

Cáncer es un término amplio que engloba un grupo de enfermedades, caracterizadas por el descontrolado crecimiento y propagación de células anormales desde su localización original a tejidos adyacentes u otros órganos; este mecanismo suele conocerse como fase metastásica. Dado que el cáncer ocupa el tercer lugar en incidencia a nivel mundial y el segundo en mortalidad, su detección precoz es vital para la supervivencia, existiendo diversas opciones de tratamiento, desde la cirugía para los estadios más tempranos hasta las alternativas más complejas para los estadios avanzados.

A pesar de los notables avances registrados en la lucha contra el cáncer durante décadas, las investigaciones en curso se centran siempre en reducir los efectos secundarios mejorando la selectividad de las sustancias anticancerígenas y, por tanto, optimizando la calidad de vida de los pacientes.

Entre los principales retos en el tratamiento del cáncer se encuentran la escasa biodisponibilidad y la falta de discriminación de los agentes antineoplásicos entre células sanas y tumorales.

Estos problemas derivados del uso de la quimioterapia convencional suscitaron un mayor interés por la terapia dirigida, que se basa esencialmente en la modificación de las sustancias quimioterapéuticas convencionales mediante un mayor conocimiento de las características del microentorno tumoral.

Por estas razones, se han desarrollado estrategias de administración y focalización de fármacos anticancerígenos con el fin de mejorar su biodistribución, cinética terapéutica y selectividad dirigida.

Los objetivos de la tesis se han diseñado para optimizar la eficacia de las terapias actuales y disminuir los efectos secundarios mediante la síntesis de profármacos antineoplásicos aprovechando la distinción entre el tumor y los tejidos sanos, en los que los profármacos anticancerosos se diseñaron específicamente para ser escindidos en particular en el medio hipóxico, que es una característica especial de los grupos de células cancerosas. Se emplearon tres estrategias para alcanzar los objetivos.

La **primera estrategia** se centró en sintetizar compuestos con enlaces disulfuro con el objetivo de unirlos a varios fármacos antineoplásicos aprovechando dos factores esenciales en el microambiente tumoral, la hipoxia y el alto nivel de glutatión, de forma que los profármacos

resultantes funcionalizados con enlaces disulfuro se escindan en las condiciones esperadas liberando el agente citotóxico de forma selectiva.
Posteriormente, el uso del grupo *terc*-butilo como fragmento adyacente al disulfuro se ha considerado como una buena opción para poder obtener el profármaco. Por tanto, se ha sintetizado y acoplado Tacedinalina resultando así un compuesto citotóxico derivatizado con un enlace disulfuro que es estable en agua a pH celular.
El profármaco antitumoral sintetizado se ha ensayado en células cancerosas (carcinoma colorrectal **HCT-116**) y sanas (fibroblastos **HS-5**). Sin embargo, los resultados no han sido los esperados, puesto que en el ensayo MTT se ha observado una falta de selectividad, además la eficacia de la Tacedinalina pura fue superior a la del propio profármaco citotóxico.

En vista de ello, se ha puesto en marcha una **segunda estrategia**, consistente en la síntesis de profármacos funcionalizados con grupos nitro. Inicialmente, se han diseñado y sintetizado derivados nitroaromáticos para unirlos a otra serie de fármacos antineoplásicos, como la bis(2-cloroetil)amina y la 5-fluorouridina, y posteriormente se han sintetizado con éxito los dos profármacos. De hecho, el profármaco bis(2-cloroetil)amina pudo utilizarse como agente teranóstico gracias a su fluorescencia emitida por la escisión de una lactama fluorescente cuando se expone a la hipoxia tumoral. La 5-fluorouridina unida a un activador nitro aromático parece un profármaco prometedor, y hemos estudiado su capacidad para liberar el fármaco citotóxico en un medio hipóxico análogo utilizando zinc como reductor.
Se realizó una evaluación de la toxicidad *in vitro* del profármaco bis(2-cloroetil)amina. Sorprendentemente apareció un problema de insolubilidad, que ha afectado a la correcta validación del efecto citotóxico del profármaco sobre las células.

Paralelamente a estos estudios, nos planteamos la posibilidad de utilizar el activador molecular como grupo protector ortogonal para aminas, aminoácidos y aminoalcoholes. Así pues, se llevaron a cabo extensas investigaciones para explorar las propiedades del activador 5-cloro-8-nitro-1-naftoílo (NNapCl) como grupo protector. Este grupo se caracteriza por una fácil protección en condiciones Schotten-Baumann y una fácil desprotección en condiciones reductoras. Como resultado, el estudio culminó con un grupo protector eficaz con un gran potencial para ser incluido como grupo protector alternativo en el arsenal de grupos protectores de aminas.

Para resolver el obstáculo de la insolubilidad de los profármacos, se propuso una **tercera estrategia** que consiste en modificar el activador 5-cloro-8-nitro-1-naftoílo (NNapCl) integrando un grupo funcional polar mediante sustitución nucleofílica aromática o utilizando química *click*. A continuación, se propusieron cuatro fármacos antineoplásicos para unir al activador molecular hidrosoluble. Estos fármacos fueron: Pregnenolona, Farnesol, Bis(2 cloroetil)amina (mostaza nitrogenada) y Tacedinalina. Puesto que, al igual que muchos fármacos anticancerígenos, estos últimos son hidrófobos, su unión al grupo protector modificado fue un paso exitoso para producir los cuatro profármacos con hidrosolubilidad mejorada.

Se llevaron a cabo dos aproximaciones diferentes para mejorar la solubilidad. En primer lugar, el fragmento soluble en agua se unió al activador molecular mediante química *click* y a continuación se unió a Tacedinalina. Sin embargo, la complejidad de su purificación nos empujó a realizar la segunda aproximación que fue la integración de ácido tioglicólico. Una vez obtenidos los profármacos antitumorales se evaluó la citotoxicidad *in vitro* (ensayos MTT) en dos líneas celulares: fibroblastos sanos **HS-5** y carcinoma colorrectal **HCT-116** en medio hipóxico y normoxia. Curiosamente, los resultados del ensayo MTT han mostrado una variación en la reducción de la viabilidad celular de las células cancerosas y sanas y una solubilidad completa de los cuatro profármacos en el medio celular. El profármaco de pregnenolona ha atraído nuestra atención, ya que fue el más eficaz en la reducción de la viabilidad celular, en este caso se llevaron a cabo pasos adicionales de análisis para una mayor confirmación en la que los ensayos de MTT se han repetido utilizando diferentes concentraciones de la pregnenolona profármaco. Además, se hicieron experimentos de recuento celular tras el tratamiento con el profármaco de pregnenolona. En general, los resultados fueron prometedores, ya que los resultados de HPLC-MS mostraron la liberación del fármaco en el interior de las células.

Para concluir esta tesis, durante el acoplamiento de bis(2-cloroetil)amina) a un derivado de ácido 1,8-nitronaftalenocarboxílico (ácido 5-((2-metoxi-2-oxoetil)tio)-8-nitro-1-naftóico), se obtuvo un compuesto novedoso, probablemente debido a un reordenamiento inusual causado por el impedimento estérico entre el grupo nitro y el ácido carboxílico en posiciones *peri*. Para asignar la estructura de este compuesto, se ha realizado un estudio completo utilizando ^{1}H RMN, ^{13}C RMN, RMN bidimensional, IR, HRMS. También se ha obtenido el análisis de difracción de rayos X de un derivado del producto y se han realizado estudios de modelización para estudiar el mecanismo de este inusual reordenamiento.

Abbreviations and Acronyms

Throughout this manuscript, abbreviations and acronyms recommended by the American Chemical Society in the Organic Chemistry Area (updated in the Journal of Organic Chemistry on April 2018; https://pubs.acs.org/paragonplus/submission/joceah/joceah_authguide.pdf) have been employed.

Symbol/abbreviation	**Significance**
[ ]	Concentration
Å	Ångström
Ac	Acetyl group
Ac_2O	Acetic anhydride
ACDs	Anticancer drugs
AcOH	Acetic acid
ATP	Adenosine Triphosphate
Boc	*tert*-butyloxycarbonyl
Bu	Butyl group
Cbz	Benzyl chloroformate
^{13}C NMR	^{13}C Nuclear Magnetic Resonance
CD_3OD	Deuterated methanol
$CDCl_3$	Deuterated chloroform
COSY	Correlation SpectroscopY
CuAAC	Copper-catalysed azide–alkyne cycloaddition
Cys	Cysteine
δ	Chemical shift
d	Doublet
DCM	Dichloromethane
dd	Doublet of doublets
DIPEA	N, N -Diisopropylethylamine
DMEM	Dulbecco´s Modified Eagle´s Medium
DMEM+	DMEM supplemented with 10% FBS and 1% P-S
DMF	Dimethylformamide
DMSO	Dimethylsulfoxide

DMSO-d_6	Deuterated Dimethylsulfoxide
DNA	Deoxyribonucleic acid
dt	Doublet of triplets
DTT	Dithiothreitol
ECM	Extra cellular matrix
EDTA	Ethylenediamine tetraacetic acid
Eq	Equivalent
ESI	Electrospray Ionization
Et	Ethyl group
EtOAc	Ethyl acetate
FBS	Fetal bovine serum
Fmoc	Fluorenylmethyloxycarbonyl
5-FUrd	5-Fluorouridine
G6PD	Glucose-6-phosphate dehydrogenase
GCO	Global Cancer Observatory
GLUT-1	Glucose transporter 1
Gly	Glycine
GSH	Glutathione(γ-glutamylcysteinyl glycine)
GSSG	Glutathione disulfide
h	Hours
HAPs	Hypoxia activated prodrugs.
HDACi	Histone Deacetylase Inhibitors
HIF-1α	Hypoxia-inducible factor 1 subunit alpha.
HIF-1β	Hypoxia-inducible factor 1 subunit beta
HMBC	Hetero Nuclear Multiple Bond Correlation
^{1} HNMR	^{1}H Nuclear Magnetic Resonance
HPLC	High Performance Liquid Chromatography
HRMS	High Resolution Mass Spectrometry
HSQC	Heteronuclear Single Quantum Correlation
IARC	International Agency for research on Cancer
IC_{50}	Concentration inhibitory 50
IR	Infrared spectroscopy
Mp	Melting point

MDR	Multi drug resistance
MeOD	Deuterated methanol
NAD^+	Nicotinamide adenine dinucleotide
NADH	Nicotinamide adenine dinucleotide hydrogen.
NCEs	Novel chemical entities
NMs	Nitrogen Mustards
NNap	5-Chloro-8-nitro-1-naphthoyl
NSAIDs	Non-steroidal anti-inflammatory drugs
PBS	Phosphate-buffered saline
PG	Protective group.
ppm	Parts per million
PPP	Pentose phosphate pathway
Pyr	Pyridine
RIPA	Radio Immuno Precipitation Assay
RNA	Ribonucleic acid
ROS	Reactive oxygen species
r.t.	Room temperature
S_N2	Bimolecular Nucleophilic Substitution
TEA	Triethylamine
TGA	Thioglycolic acid
THF	Tetrahydrofurane
TKI	Tyrosine kinase
TLC	Thin Layer Chromatography
TME	Tumor microenvironment
TOPO	Trioctylphosphine oxide
VEGF	Vascular endothelial growth factor.
q	quartet
quant	Quantitative
ROESY	Rotating frame Overhauser Effect SpectroscopY
UV	Ultraviolet
Zn	Zinc

1. General Objectives

The general objective of this Thesis is the design and synthesis of molecules which can be attached to antineoplastic drugs in order to create the selectivity for cancer cells, or in the strict sense a prodrug that is capable of selectively attacking cancer cells without affecting healthy ones, knowing that these drugs are made basically to treat cancer but are unable to distinguish healthy cells.

The strategy is essentially based on the association of an antineoplastic drug well selected thanks to its lethal effect and a new molecule which is considered as protector and trigger for the drug. The activation to release the drug is due to the exploitation of the cancerous cells medium in which these molecules play the role of a protective group. They are functionalised with a disulfide bond or a nitro group, which can be reduced under the cellular microenvironment especially in the presence of the intrinsic factors such as hypoxia and the high concertation of glutathione for an *in situ* releasing of the drug.

This targeted liberation will trigger a direct mode of action aimed at cancer cells only, without leaking to healthy tissues.

In this way, many of the side effects of current cancer treatments could be avoided. Prodrugs are able to attack this disease in a more effective and direct way, contrary to conventional chemotherapy.

2. Introduction

Cancer has become a real public health problem, all the diagnoses and statistics carried out by oncologists and experts from World Health Organisation have shown that cancer is the principal cause of the mortality with around 10 million of deaths in 2020. The incidence of cases worldwide is expected to double by 2030.[1]

Fighting cancer is therefore more important than ever, especially as the burden of cancer increases. Today's research focuses on understanding the molecular and genetic bases involved in the mechanisms of oncogenesis, the search for diagnostic, prognostic and therapeutic targets, and the development of an appropriate therapeutic arsenal. So, what is cancer?

2.1. Cancer: definition, history, epidemiology and characteristics

2.1.1. What is cancer?

According to the World Health Organization cancer is an immense group of diseases that can develop in almost any organ or tissue in the body, when abnormal cells become uncontrollable and invade the adjacent parts of the body and spread to other organs. The latter process is called metastasis which is considered as the leader to death in the most infected cases.

The term cancer actually encompasses a group of closely related diseases that have in common unregulated cell division.[2] Tumor, neoplasm or malignancy are also common names for cancer.[1]

The original tissue gives a distinctive characteristic of cancer, about 85% arise in cells which are classified as carcinomas, it derivates from mesodermic cells as sarcomas (e.g., bone, muscle), it can originate also from the glandular tissue and these are called adenocarcinomas (e.g., breast).[3]

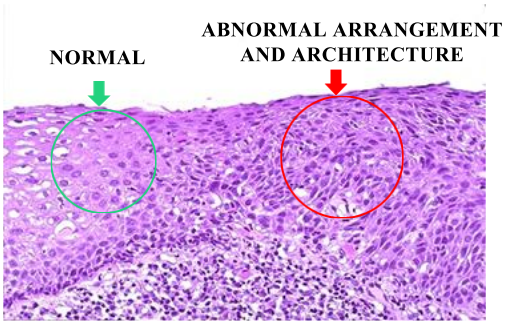


Figure 1. *Dysplasia microscopic observation of histologic section from a biopsy of the uterine cervix.*[4]

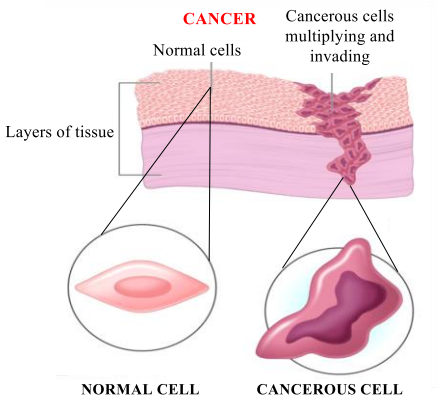


Figure 2. *Morphological dissimilarity between normal and cancer cells.*[5]

2.1.2. Cancer history

Cancer has a long history as an afflicting scourge for humanity, that can be observable in some neolithic fossilized human bones, actually, the latter have been interpreted as nasty excrescences.[2]

Dating back to the primitive times, the oldest cancer cells refer to dinosaur bones and mummies. In fact, **the Egyptians** were the leaders of describing the cancer process, in which

they have mentioned on their papyrus pages details with the same symptoms of nowadays in breast and cervical cancer.

The Greek historians and physicians Herodote and Hippocrates wrote as early as the 5th century BC about cancer, explained all cancer's stages, giving the name "*karkinos"* which refer to cancer disease but originally to "crab" due to the similarity of the tumors invasive and mortal effect.

The Roman physician Celsius, influenced by Greek and Egyptian medicine, described the degrees in the evolution of the disease and explained that cancer treatment depends on the degree of advancement of the disease.

The Italian physician Galien in the 150's believed in the humoral theory. He said that tumour was caused by an excess of "fluid "as black bile, which solidified in certain parts of the body. His proposal of treatment was based on administering purges to dissolve the solidified bile, if the lesion did not regress, he would then perform an excision. He introduced the term "oncos" to describe a nodule or lamp with a malignant appearance.

The Muslim doctor Avicenna was the first to describe the tumor process and progression. It was at the end of the first millennium, in the 1000s, he observed that tumor grows and invades slowly until spreading and destroying the surrounding tissues, eventually creating an absence of sensation in the affected area which later became known as metastasis.

The British surgeon John Ardern in 1390 was able to describe the rectal cancer, however he reported later that he was unable to cure at least a single case, autopsies were also authorized at this time permitting the discovery of human anatomy.

By the 17th century, cancer has taken another definition as a contagious disease. But in the 18th century, Gallian's theory explaining the lymph node territories of ganglia was taken up again.[6]

In 1853, the identification of cancer was fixed officially as a group of transformations explained by the successive proliferation of healthy cells and from here the struggle was established.

Two years after, Roentgen discovered X-rays, and in 1898 Pierre and Marie Curie detected radium radiation for the first time (Figure 3). This combination was essential in cancer diagnostic and treatment.

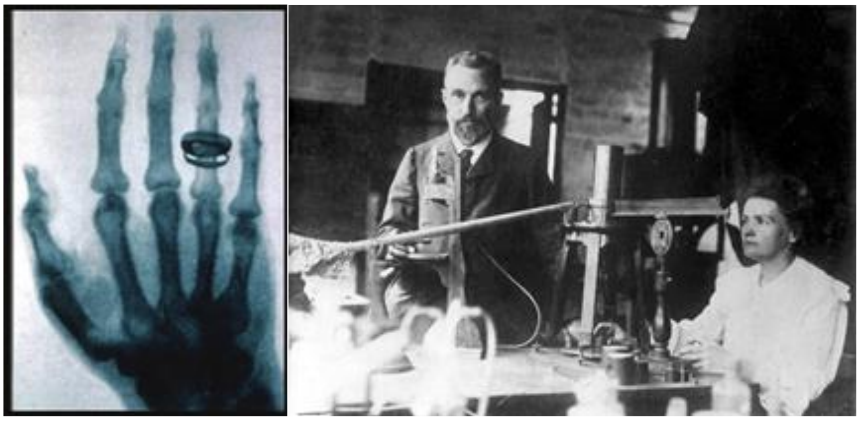


Figure 3. *Wilhelm Roentgen's first X-rays produced in 1895 (Left), Marrie and Pierre Curie radium discovery in 1898 (Right) which has contributed essentially in cancer dignostic.*[7,8]

2.1.3. Epidemiology and statistics

Cancer remains one of the major causes of morbidity and mortality worldwide along with cardiovascular diseases (Figure 4). Actually the diversity of the disease across the world, the influence of available health facilities, and other socio-economic factors affect the appropriate management of this malady.[7] Its burden has put the majority of the countries around the world in a significant disorder due to the types of cancer, death's number and the investigation for therapeutic solutions. According to reported data more than 19.3 million people were newly diagnosed as cancer case leading to the death of 10 million in 2020. It also forecasts an increase of up to 30.2 million new cases and a mortality of more than 16 million by 2040.[7]

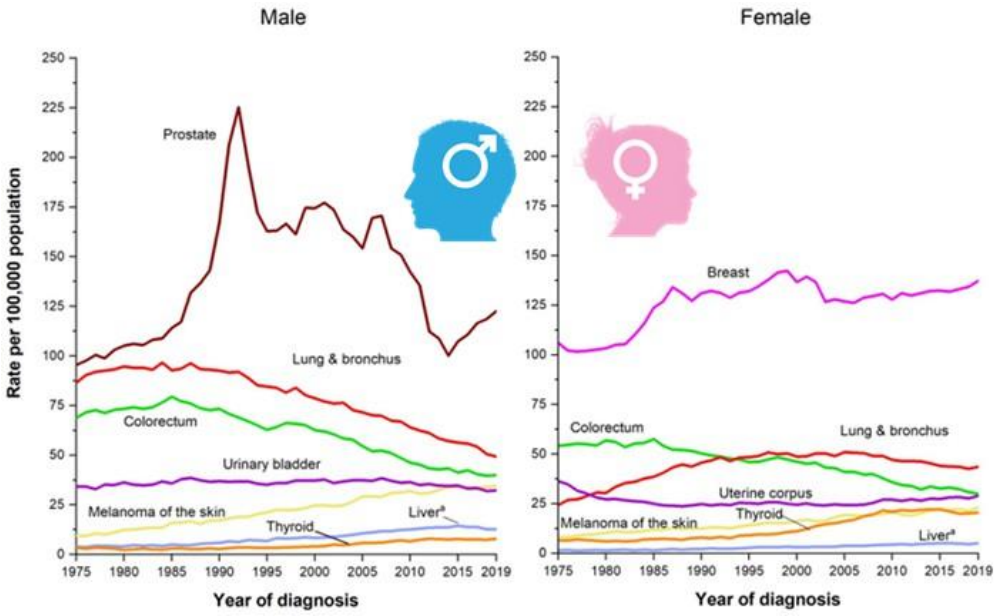


Figure 4. *Cancer incidence and mortality rates by type and gender*.[8]

The prevalence of cancer has taken a trend of analysing and reporting the percentages of incidences and deaths rates by several institutions, agencies and sites. The global estimations are saved by IARC's Global Cancer Observatory (GCO) (gco.iarc.fr), incorporated in visualized graphics in which the data are organised according to the region, the gender and other characteristics.[7] Figure 5 represents the prevalence and mortality of different kind of cancers.

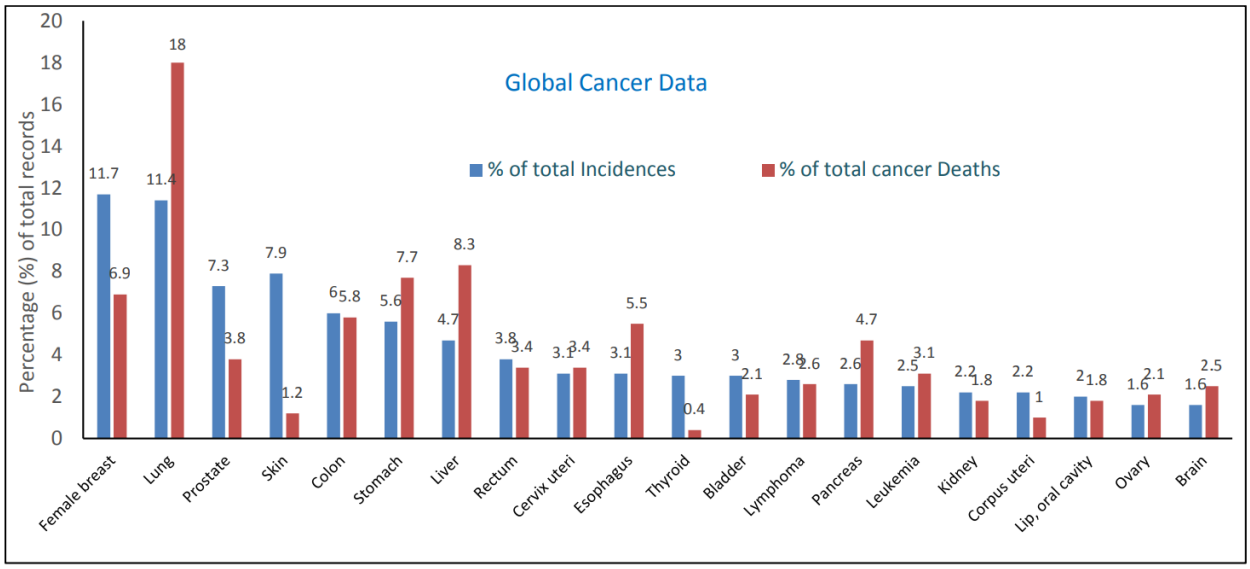


Figure 5. *Graphic representation of proportional relation between incidence and death caused by several cancer.*[7]

2.1.4. Cancer progression

Clinically, the evolution of human cancer has been well identified.[9] Hence, decades of oncology research has produced the understanding of tumorigenesis steps from the progressive growth until the metastasis stage.[10] In fact, before the formation of a full malignancy, intraepithelial neoplasm (pre-cancer) could be recognized in any organ, the latter is the consequence either of a genetic damaging (DNA alteration /mutations) or environmental features such as a viral infection, intense UV exposure or chemical products.[9] Consequently, spreading of cancer cells from their original tissue or agglomeration generates metastasis which is also known as stage IV (4) cancer, so that the cells propagates through the lymphatic system and/or the bloodstream to other parts of the body[11] (Figure 6).

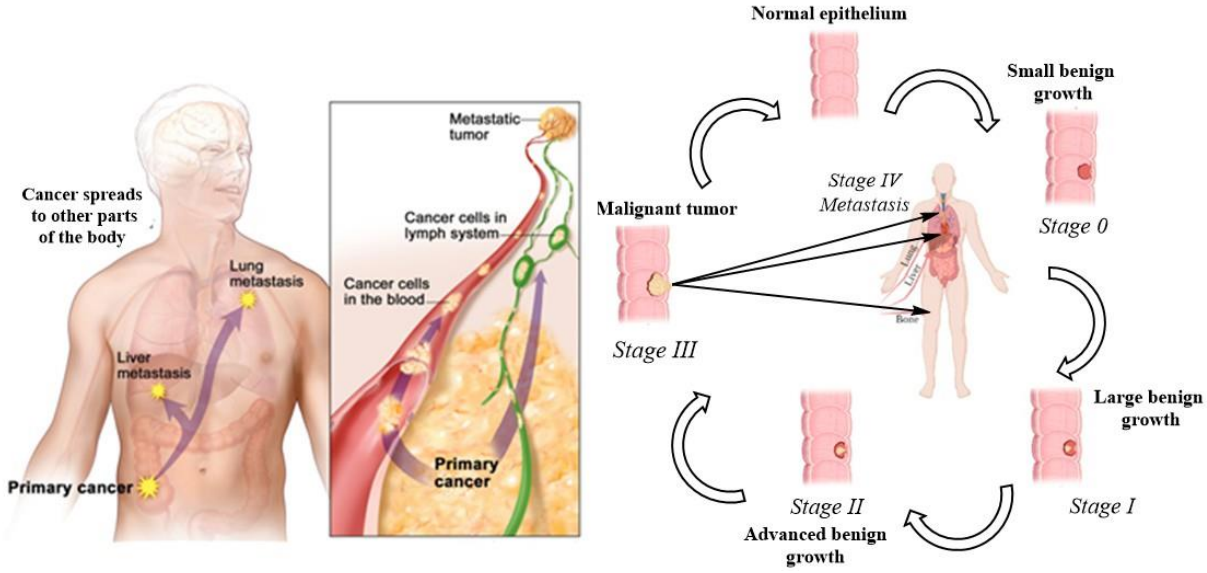


Figure 6. *Malignancy progression from pre-malignant stage until metastasis*[11,12] *(adapted).*

2.1.5. Causes and genetic process

Usually, the balance between cell birth and death is regulated by a system called apoptosis which is a genetic control system responsible for the programmed cellular death, along with other genetic mechanisms that occur in releasing signals of control for growth and cellular inhibition, the failures of these mechanisms can be the leading cause of cancer problems.

Tumors are generated from genetic damages so that it can be the consequences of a consumption or exposure to chemicals (e.g. medicines, detergents) intense exhibition to radiation, hormonal disorder and viruses, etc., the latter are responsible for the majority of cancer cases[13] (Figure 7).

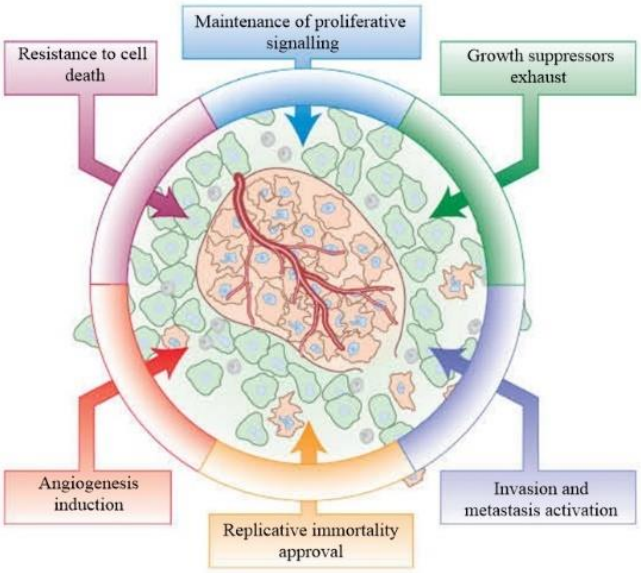


Figure 7. *Synopsis of modifications in cells leading to cancer: tumour appear when one from the six fundamental cellular properties arise.*[13]

DNA (Deoxyribonucleic Acid) is the hereditary material which codes genetic information in almost all prokaryotic and eukaryotic cells responsible of the control and production of proteins, indeed the intact passage of genetic information ensures its integrity and stability to assure high-performance gene expression. However, our genes are subject to a variety of attacks which are the result of environmental and endogenous effects which leads in the most cases of mutations (Figure 8).

In fact, normal functionality of DNA is guaranteed by defensive strategies against mutations which is by definition a DNA damage. These protecting mechanisms contribute to the reparation and correction of malformed ordered stratification of nucleic bases at the DNA level which is important during the pre-cell division period when detecting an error during replication, before passing the wrong genetic message to the daughter cell.

Cancer is a disease that involves alterations to gene structure and gene expression at the cellular level. When considering the process of carcinogenesis, it must be aware that cells are equipped with defensive mechanisms against mutations, such as the detection and repair of DNA damage. This detection of damaged DNA is particularly crucial in the period preceding cell division, as existing errors will be passed on to the daughter cells. Otherwise, the structure and gene expression may be affected by mutagenic alterations, which will subsequently cause cancer [3] as it is mentioned in figure 8.

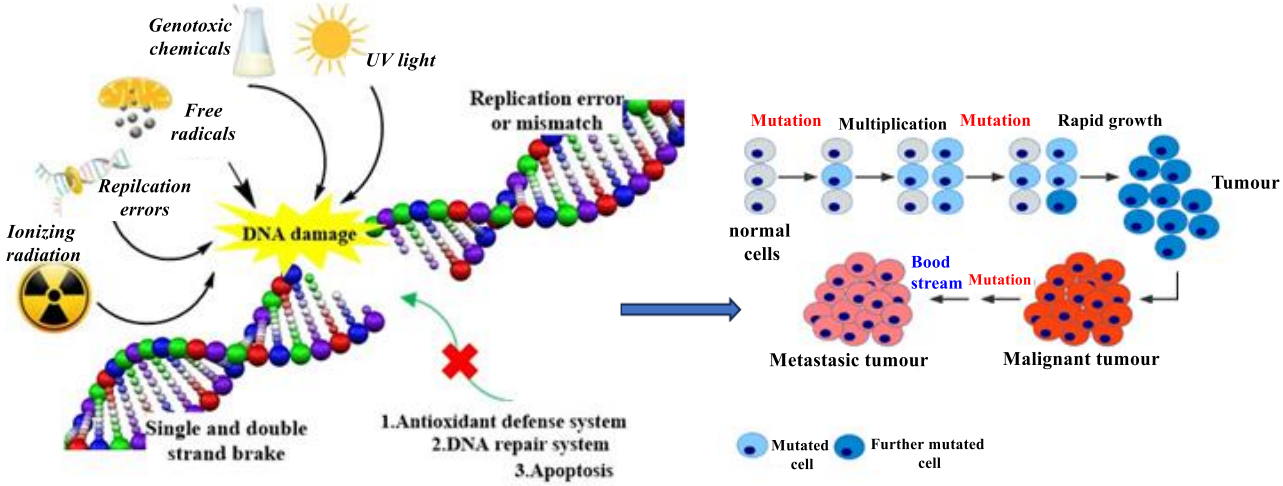


Figure 8. *The contribution of environmental causes and the failure of reparative genetic systems which induces cell mutations, then the formation of tumors (source: own elaboration).*

2.1.6. Tumor cells *versus* healthy cells

The production of new cells in the human body is a constant phenomenon which ensures the continuity of the living being existence, through the frequent birth of normal cells that obeys well-defined life cycle: growth, division, and death.

Numerous genetic amendments caused by oncogenesis are responsible of principal cells characteristics alterations, leading the latter to elude obvious signals from the growth system regulator resulting finally in the entire carcinogenic phenotype.[13]

Cellular regulatory activities at the molecular level can create the discrimination that enables differentiation between cancer cells and healthy cells, in which tumour cells vary from the normal not only in rampant and anarchic extension but also in their protein composition and energy utilization.[13]

Table 1. *The difference in functional mechanism between cancer cells and healthy cells.*[14]

Molecular activities	Normal cells	Cancerous cells
Growth	Controlled, when there is enough it stops.	Uncontrolled.
Communication	Sensitive to signals from other cells.	Inert towards other cells signals.
Cell repair/death	Reparation or replacement of aged and damaged cells.	Cells are neither repaired or replaced.
Stickiness/spread	Well arranged in a stratified cellular tissue.	Anarchic with the ability to migrate from one tissue to another or within the body.
Appearance	Uniform and regular shape.	Irregular with varied sizes, and darker center.
Maturation	Achieve the full growth.	Do not reach cellular maturity.
Evasion of immune system	Can be targeted and eliminated.	Elusive, with uninterrupted growth.
Function	Carry out designated tasks.	Failure in performing the appropriate labour.
Blood supply	Blood vessels develop to fuel normal growth and facilitate repairs.	The blood vessels develop independently, constantly "feeding" the tumour.

2.1.7. Energetic metabolism

Cells in their normal differentiation state obtain energy from the oxidative phosphorylation, ensured by the mitochondria in which they metabolize glucose to carbon dioxide and ATP, using the pyruvate oxidation through the tricarboxylic acid cycle.

By contrast to healthy cells, tumour cells are able to produce lactate even by aerobic glycolysis which mean in the presence of oxygen , this phenomenon is known as Warburg effect.[13]

In fact, Warburg noted that even in the presence of oxygen, cancer cells have a propensity to engage in glycolysis rather than mitochondrial oxidative phosphorylation, which results in aerobic glycolysis (the "Warburg effect"). Compared to oxidative phosphorylation, this kind of metabolism is less effective in producing energy. However, it is vital for cancer cells.[15,16,17]

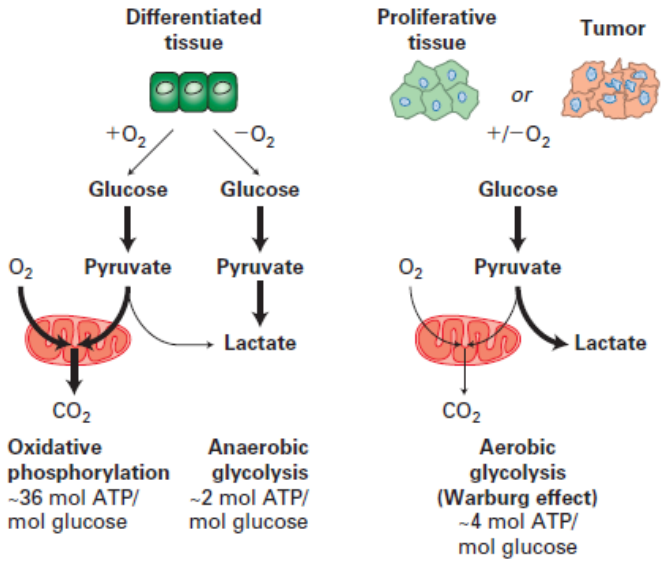


Figure 9. *Energy pathway production for normal and cancer cells (Warburg effect).*[13]

2.1.8. Morphological differences

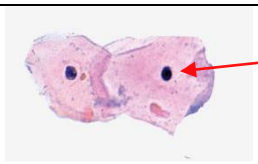
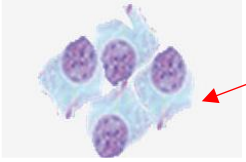
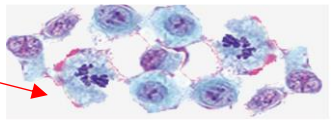
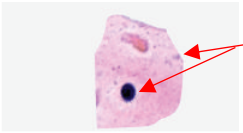
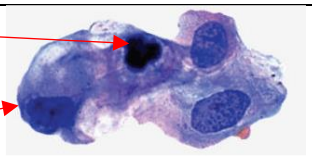
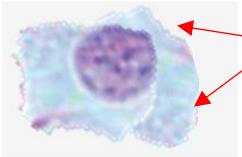
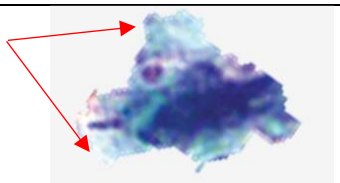
Several morphological attributes are considered as hallmarks which the histopathologists use to distinguish between cancerous and normal cells, since cancer is a state of immense cellular changes, the latter frequently affects size, appearance, nucleus dimension and cells arrangement. Their detection is usually made by biopsy and microscopic observation as diagnosis ways. The description of their most common features description is shown below:

-Dimension and cells appearance: usually the normal cells are elongated, round or spheric however the cancer cells can be shorter or larger than normal, this abnormality affects even their functionality.

-Cell's Nucleus: cancer cells nucleus is decentralized, sizeable and darker than normal cells nucleus.

-Cell tissue arrangement: the cells of a cancerous tissue are less attached to each other because of their deformation, rapid and uncontrolled progression, and their invasive effect in which their detachment from the tissue create a circulatory effect in the body *via* the blood or lymphatic system known as metastasis.[18]

Table 2. *Morphologic dissimilarity between normal an tumors cell (microscopic biopsy images).*[18]

Normal cells	Dissimilarities	Tumor cells
	Centered cell nucleus with regular shape	Abnormal nucleus huge and dark 
	Cells integrated in the same cluster organized distribution	Desorganized arrangement 
	Normal appearance	Various nucleus dimension Abnormal cell shape 
	Clearly defined surroundigs	Featers and morphology decay 

2.1.9. Tumor microenvironment

Tumour microenvironment (TME) is the biosphere that borders the malignancy within the organism, the latter includes several components and specific systems which distinguishes from the normal cellular microenvironment.

It performs a crucial part in the dynamic complex of tumour cells by processing vascular system, connective tissue and extracellular matrix (ECM), these tissue features ensure the improvement, nourishment and oxygenation for cancer cells progression.

Because the cellular reproduction is the hallmark of tumours, it is obvious that the occupied zone will be large, consequently cancerous cells are exhibited to compressive strain and stretching due to tissue barriers deformation for both types healthy/tumour. In this case the supply of nutrients and oxygen will be reduced as a result of the abnormal blood vascularisation which will subsequently create a molecular induction to resolve this insufficiency, this induction leads to the apparition of two principal phenomena known as angiogenesis and hypoxia.[19]

2.1.10. What is hypoxia?

Tumour hypoxia is one of the hallmarks of cancerous microenvironment [20], it is by definition a condition in which the supply of oxygen to tissues is insufficient to ensure the usual biological functions.[21]

Actually, the reduced pressure of oxygen which is usually less than 1% is due to poor perfusion of tumour tissues. Among its most prominent causes are the limited and inefficient vasculature of tumour tissues, and high interstitial pressures, as a result, there is a great variability in the concentration of oxygen, as well as other nutrients, causing the presence of hypoxic regions in the vast majority of human solid tumors.[22]

In fact, hypoxia also contributes to tumour progression by activating genes that are related to tumour growth[22], since a cellular response occurs to prevent cell apoptosis. This response consists of the activation of hypoxia transcriptional factor HIF-1α, which is dimerized with HIF-1β to achieve a multiple cellular response that involves: (i) the activation of oncogenes, (ii) an increase in the production of VEGF (vascular endothelial growth factor), (iii) an increase in glucose transport (GLUT-1), (iv) an increase in the activity of carbonic anhydrase (CA9) and (v) the induction of several apoptotic genes.[23, 24.]

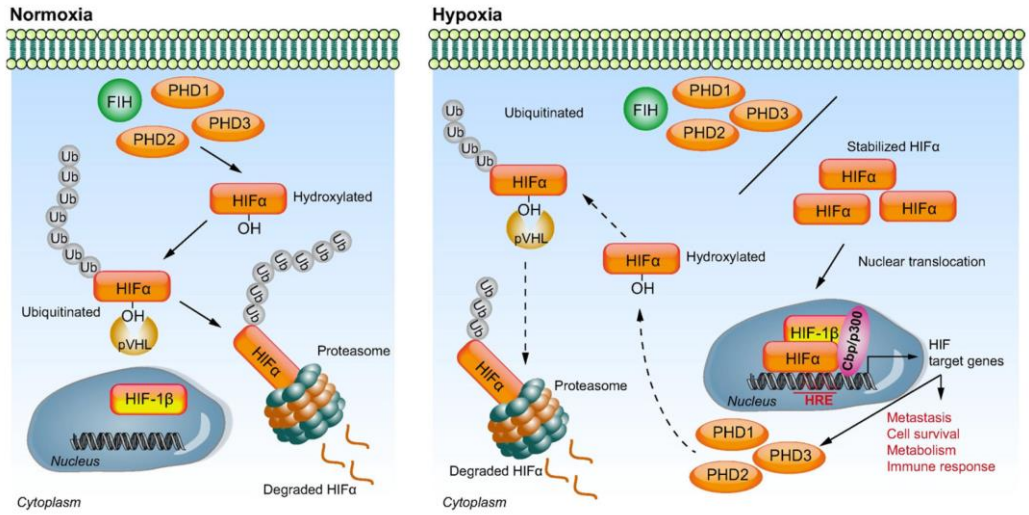


Figure 10. *Transcriptional system HIF under normoxic and hypoxic conditions.*[25]

Hypoxia can also be classified into two types:

-Transient or perfusion hypoxia: is due to the temporary closure of blood vessels. This leads to cellular hypoxia in shorter periods of time.

-Chronic hypoxia or hypoxia: due to diffusion. The cells are located away from the nearest blood capillary for long periods of time.[22]

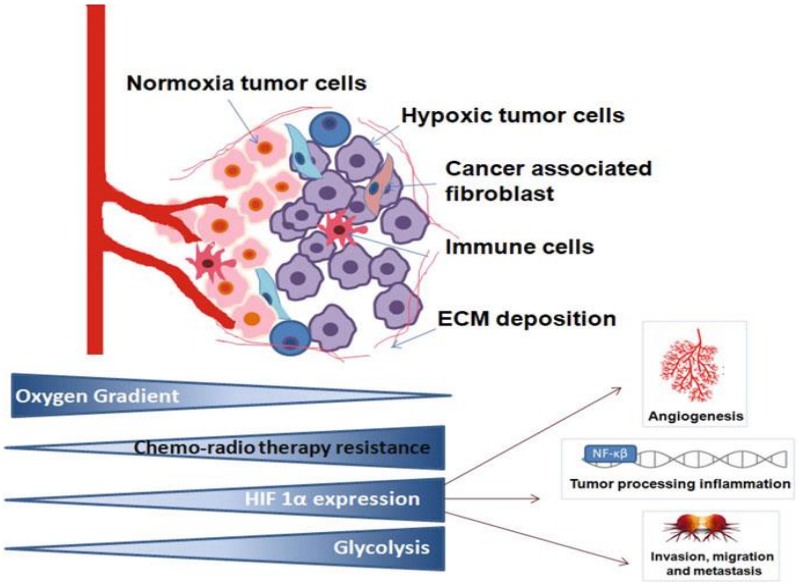


Figure 11. *Hypoxia manifestations with the different sections of tumor environment.*[26]

2.1.11. Angiogenesis

The angiogenesis is a specific phenomenon of solid tumours, in which a blood vessels network is created in order to cover oxygenation and nutrient deficiency in tumour cells (Figure 12) caused by the hypoxic state. The angiogenesis has a pivotal role in providing the welfare of tumour cell and protecting it from necrosis.[27]

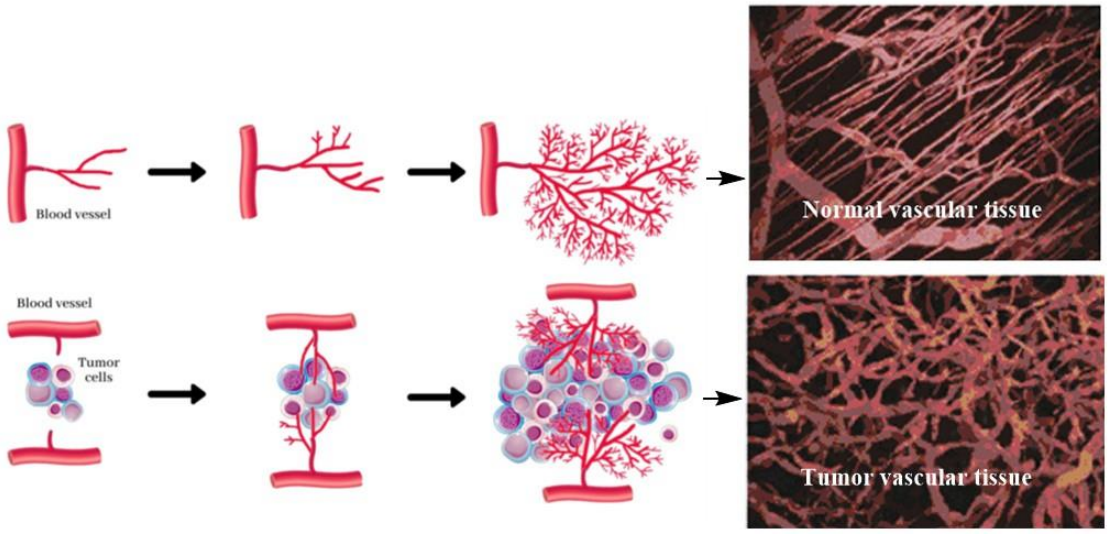


Figure 12. *Disorganized vessels arrangement in tumor cells versus ordered vascularity in normal cells (adapted).*[27, 28]

Indeed the hypoxic state and acidic conditions became a key factor that can influence the redox activity in tumor microenvironment (TME), including the increased concentration of glutathione.[29] In this environment, the concentration of glutathione, a type of antioxidant, is also characteristic, which is significantly higher than in normal cells.[23]

2.1.12. Glutathione

Glutathione (GSH) is a water-soluble tripeptide made up of three amino acids: glutamic acid, cysteine and glycine, it is also defined as an antioxidant that is involved in cellular homeostasis and plays a very important role in defending against oxidative damage.[30]

At millimolar concentration it is present in living organisms tissues as a thiol, and can integrate into a wide range of physiological functions such as cells proliferation, apoptosis, and immune system.[29]

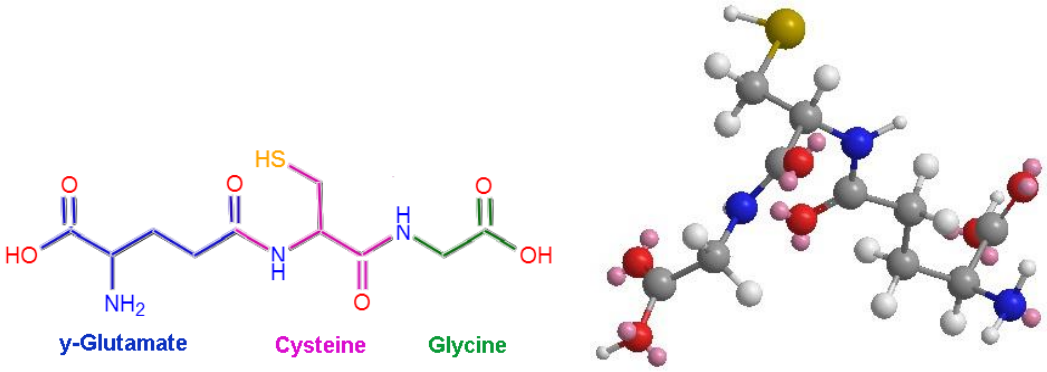


Figure 13. *Glutathione´s chemical structure 2D (Left) and 3D (Right).*

2.1.13. Glutathione in cancer microhabitat

Glutathione is one of the leading contributors of tumour cells progression, since the disruption in GSH homeostasis may cause molecular changes that involves in tumour proliferation[29]. This disturbance is expressed by an augmentation in GSH levels as it exerts a type of control signalling responsible for cell differentiation, detoxification, and endocellular redox maintenance.[31]

Generally, in oxidation reactions, electrons are transferred from a molecule to an oxidizing agent, which can produce free radicals. These free radicals are molecules that possess an unpaired electron in their outermost shell, making them highly reactive.

Antioxidants, such as glutathione, prevent the production of free radicals that are capable of initiating chain reactions that damage cells. They prevent this by removing some of the intermediates and inhibiting oxidation reactions by oxidizing themselves.

Studies indicate that free radicals and oxidative stress can induce cancer, at the same time, cancer cells generate more free radicals than healthy cells. This is why the concentration of glutathione in cancer cells is higher.[32]

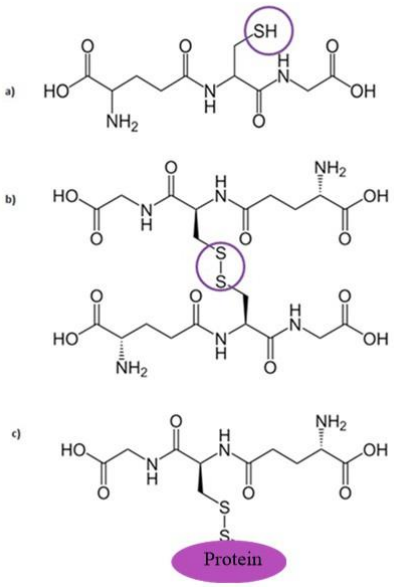


Figure 14. *Chemical structure of the different forms of glutathione: a) Reduced glutathione (GSH), its active group is the SH group of the cysteine residue. b) Oxidized glutathione, consisting of two GSH molecules linked by a disulfide bond (GSSG). (c) Protein-bound glutathione.*[30]

2.1.14. Tumour microenvironment features: Promising Prospects in Cancer Therapy

Despite the complexity of the tumour microenvironment, it is considered as double-edged sword since it is the terrain in which the disease manifestations take place and an attractive outlook of inspiring anti-cancer therapies. Actually, the examination of the TME throughout tumour progression process divulges several promising prognostic biological markers.[33]

To varying degrees, the TME contributes to the acquirement of tumor hallmarks, which include maintaining proliferative signalling, evading immune damaging, resisting apoptosis, inducing angiogenesis, metastasis activation and triggering tumor-promoting inflammation. Because of this dependency on the TME, there is a chance to target specific TME components or its signalling pathways for therapeutic intervention.[34]

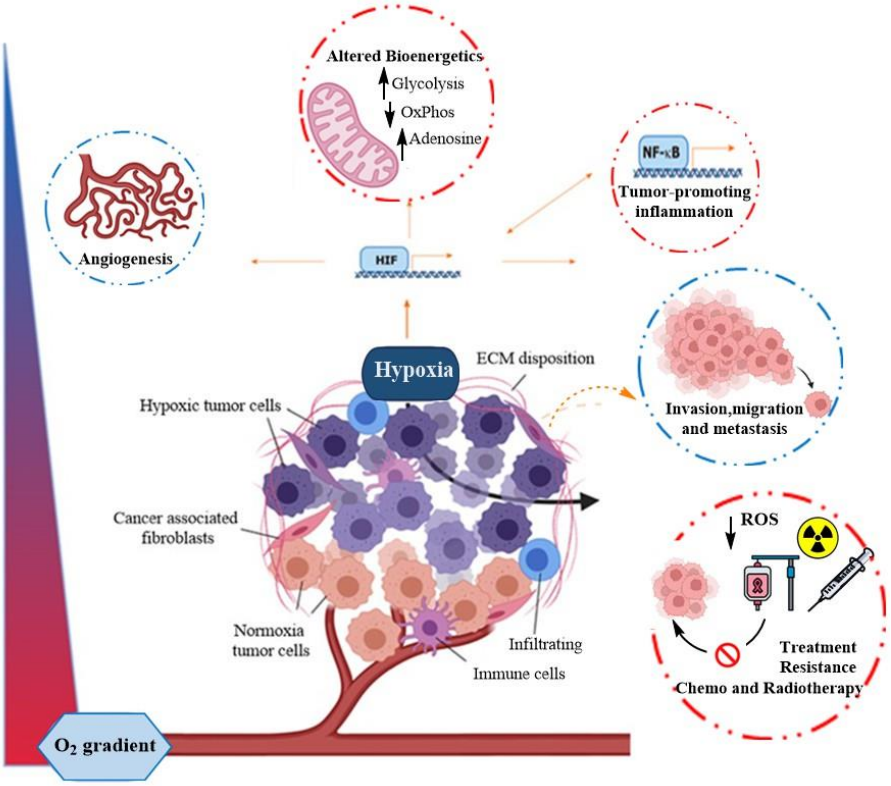


Figure 15. *Cancerous tumor microenvironment hallmarkers that can be exploited in therapy strategies (Adapted).*[35]

2.2. Chemotherapy

Chemotherapy is a major cancer treatment worldwide.[33] Aside from side effects, chemotherapy drugs are still the best choice for curing cancer until now; the latter depends on tumour juncture and patients tolerance so that it can be taken alone or as a therapeutic arsenal in conjunction with surgery and radiotherapy.[34]

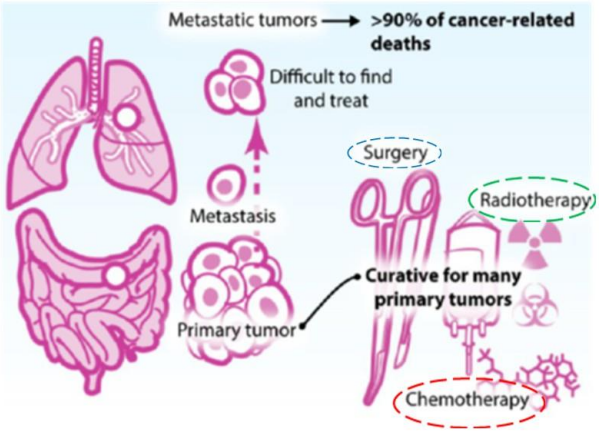


Figure 16. *Current curative strategies for primitive tumours: combination of chemotherapy with surgery and radiotherapy.*[36]

In fact, cancer drugs boost may require a therapeutic synergy that target and trigger the coexistence in TME[33], usually molecules known as antineoplastic drugs are the basic unit on which chemotherapy is based, so what are antineoplastic drugs?

2.2.1. What are antineoplastic drugs?

Antineoplastic drugs are a subset of drugs that aim to interfere cell growth thanks to its specific design and highly reactive moieties which relies on the inhibition of deoxyribonucleic acid (DNA) synthesis through several mechanisms.[37] Literally, the different types and the growing number of antineoplastic is proportionally related with the increasing cases diagnosed with cancer.[38]

The origins of antineoplastic remedy dates back by chance to World War I, at this time, the Germans used mustard gas as a poison gas.[2] Later, it was discovered that it could be used as an antineoplastic drug.

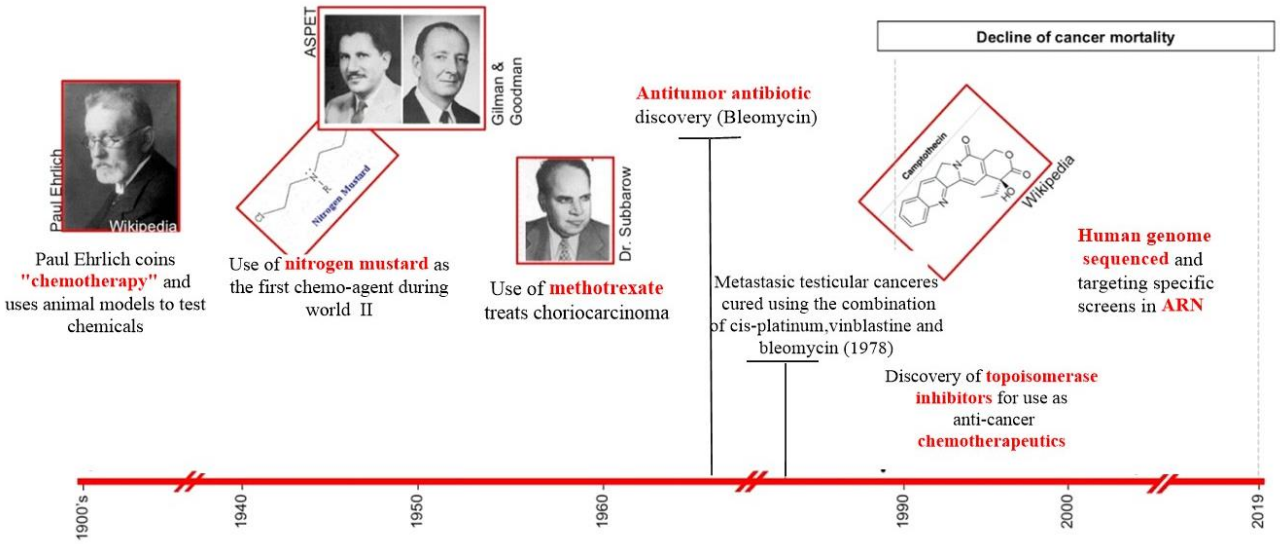


Figure 17. *Chemotherapy evolution and antineoplastic drugs advances.*[39]

Divergent generations of antineoplastic can be subdivided into two sections: conventional and targeted therapy.

2.2.2. Conventional chemotherapy

After the discovery of nitrogen mustard (figure 18) as an alkylating agent in 1942, a new stage in the development of cancer treatment began.[40]

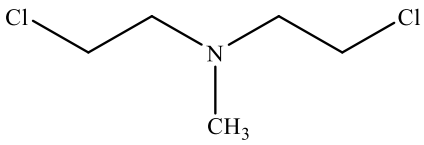


Figure 18. *Chemical structure of nitrogen mustard (Mechlorethamine).*

Decades after the first discovery of the lethal effect of nitrogen mustard, a cascade of trials to develop it from the raw molecule to a lower electrophilic agent was carried out. These are considered as steps of improvement in order to generate a group of safer analogues and generics clinically applicable. Some of these compounds are for instance: chlorambucil, mechlorethamine, melphalan, cyclophosphamide and estramustine.[40]

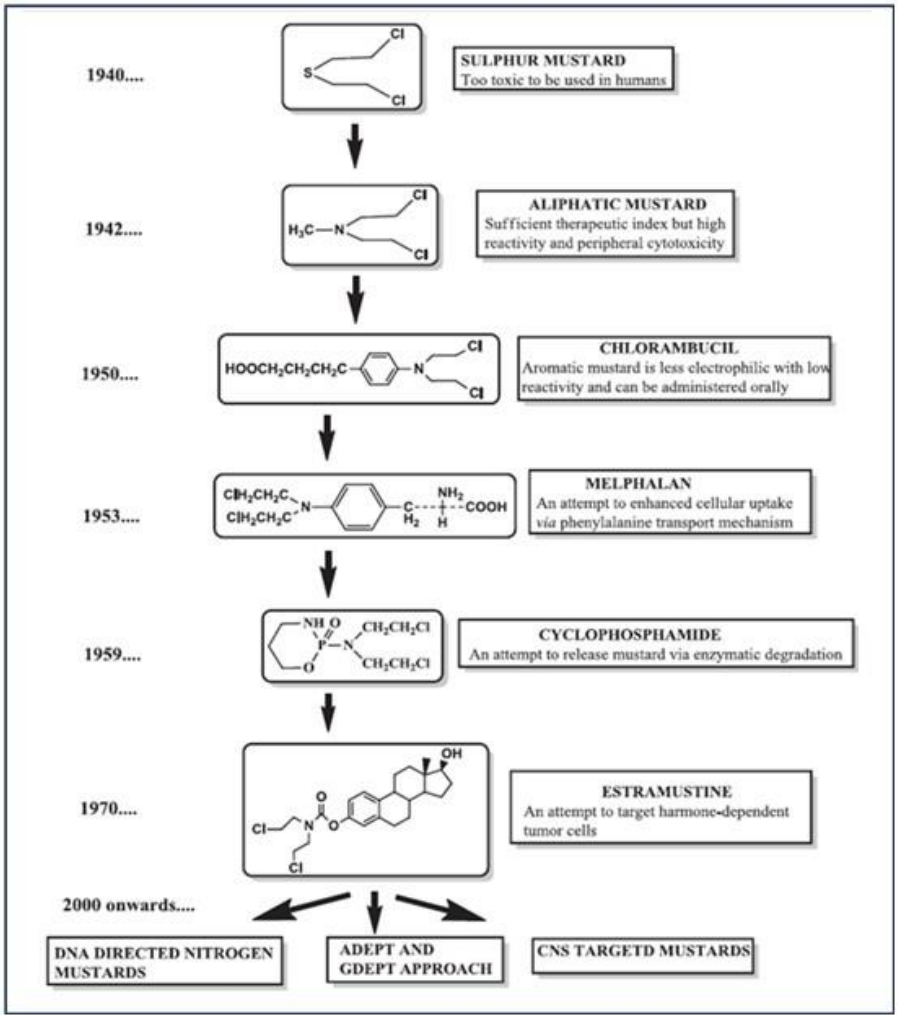


Figure 19. *Mustard nitrogen antineoplastic generations over time.*[40]

Conventional chemotherapy can be divided into three categories, the ranking is based usually on the mode of action: alkylating agents, antimetabolites and antitubulin agents.[38]

2.2.2.1. Alkylating agents

Alkylating agents are substances of organic origin, considered as the earliest antineoplastic family coincided with the discovery of the mustard gas as therapeutic agent throughout the first world war.[38]

In fact the DNA structure discovery in 1950 was a major step forward that has enabled chemists to understand the necessary structures for the creation of therapeutic agents by targeting special sites and exploiting the chemical and biological features of DNA and to strengthen the hypothesis of therapeutical effects of mustard gas.[2]

These organic molecules interact with DNA´s nucleophilic groups, by making covalent bonds to the nucleobases (such as guanine) from the double helix or proteins, this incorporation is based essentially on the integration of an alkyl group within DNA strands exploiting its electrophilicity.[38]

Consequently this chemobiological activity prevents DNA replication and transcription which leads eventually to cellular death.[40]

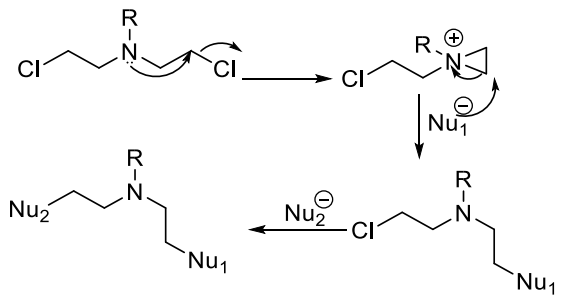


Figure 20. *Mechanism of DNA alkylation by nitrogen mustard.*

At the molecular scale, the non-bonding electron pair of nitrogen mustard nitrogen generates an aziridinium ion, which is a highly reactive intermediate with the DNA of tumour cells and healthy cells as well, causing adverse effects.

N-mustard alkylates DNA in a two-step process. First, bis(2-chloroethyl) amine undergoes intramolecular S_N2 cyclization at neutral or alkaline pH by a one-step reaction, with the

formation of a highly reactive and unstable aziridinium cation. In the second step, the aziridinium cation reacts with the N7 nitrogen of the nitrogenous base guanine, present in DNA, which acts as a nucleophile.

In the last decade, due to their high reactivity and cytotoxicity, numerous modifications have been made to the structure of nitrogen mustards to improve their efficacy and selectivity by tumour cells.[40]

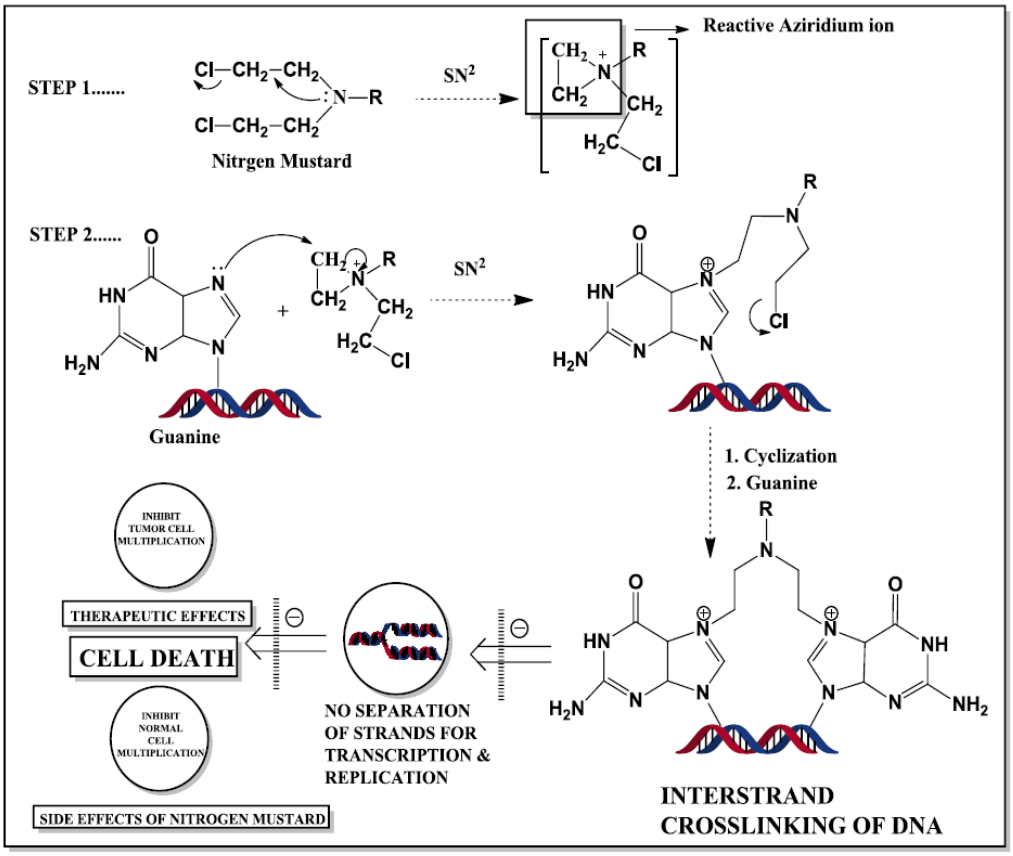


Figure 21. *Cytotoxicity through DNA alkylation (with the nucleotide base Guanine) caused by nitrogen mustard gas.*[40]

2.2.2.2. Antimetabolites agents

Antimetabolites are another class of antineoplastic drugs in which their mode of action is based on mimicking the substrates included in the biochemical activities inside the cells, more precisely the nitrogen bases of the DNA.

In fact, antimetabolites agents have a specific strategy of targeting which consists on blocking the natural functionality at DNA level thanks to its analogue structure with purine, pyrimidine,

hence these antimetabolites agents act as antagonists with the original components, so that the normal synthesis of DNA/RNA is achieved by attaching false substrates. Due to their chemical analogy inside the cell, these compounds indirectly replace the natural substrates, then deform the process, inhibit or block proliferation which can lead finally to cellular death.[2,38,41]

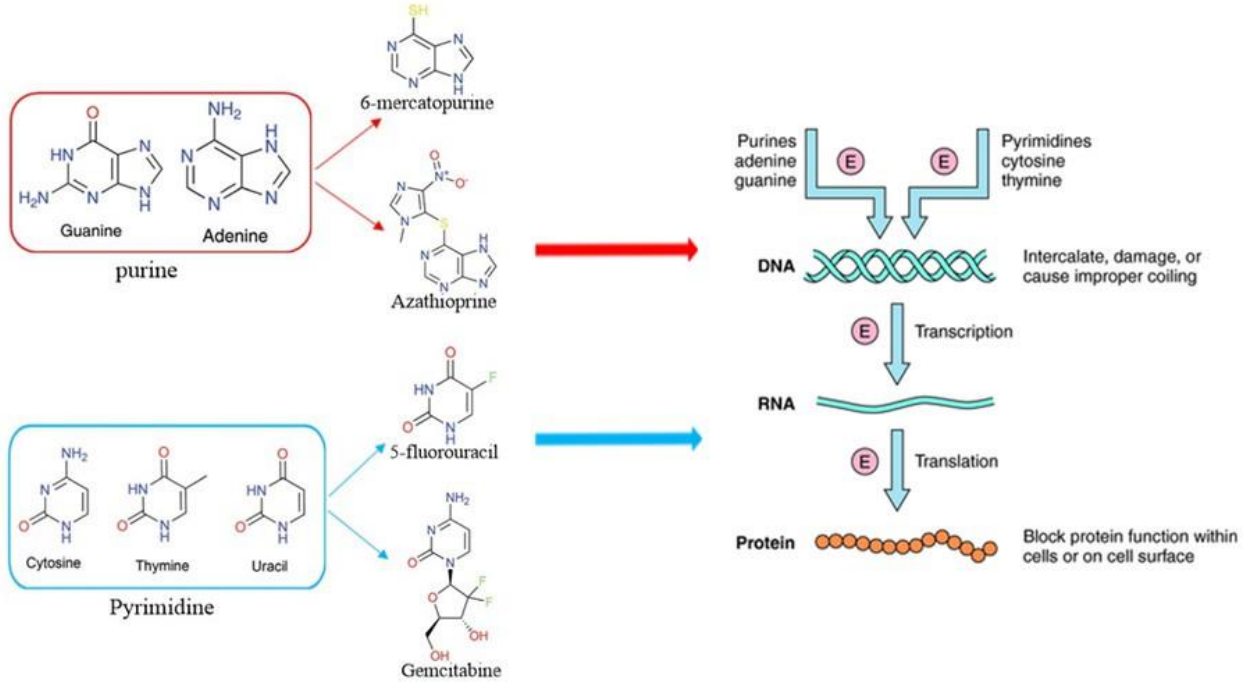


Figure 22. *Pyrimidine, purine and their analogues acting on DNA and RNA process (modified).*[38]

2.2.2.3. Antitubulin agents

Antitubulin drugs represent a huge category of antineoplastic drugs highly effective towards solid and hematologic malignancies, by attacking the microtubules (tubulin polymers) which are responsible for miotic spindles control.[43] As microtubules are one of nucleus division managers, antitubulin molecules work on blocking this process causing automatically cellular death. Antitubulin group includes principal classes as taxanes and Vinka alkaloids.[38, 42]

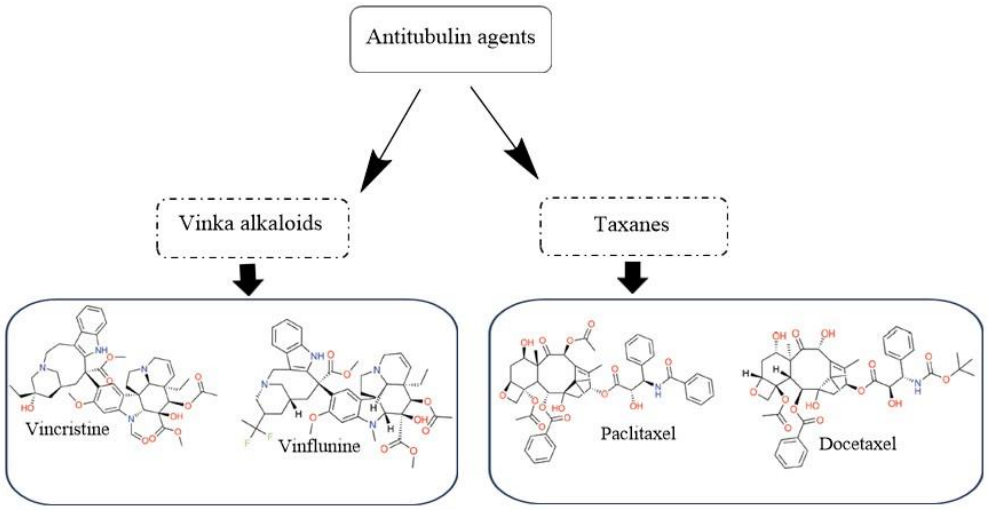


Figure 23. *Vinka alkaloids and taxanes structures (source: own elaboration).*

2.2.3. Targeted chemotherapy

Targeted chemotherapy, frequently referred as targeted therapy is a kind of drug therapy of cancer, it is used in particular to identify and attack tumor cells. Unlike conventional chemotherapy, targeted therapy aims to minimize damages to healthy cells by focusing on specific molecules pathways implicated in cancer cells growth and survival.[44, 45]

Consequently, a range small molecules specified for targeted therapy have emerged as a new generation that has refreshed the range of conventional chemotherapy, since the lack of discrimination between tumour and healthy cells is its limiting factor.[38,40]

Indeed, this new generation of small molecules carries a group of enhanced characteristics, those allow them to be integrated in the strategies of targeted therapy to be selective and cytotoxic only towards tumour tissues, a lot of examples can be mentioned:

-Hormone blocking anti-cancer drugs

-Topoisomerase inhibitors

-Matrix Metalloproteinase Inhibitors

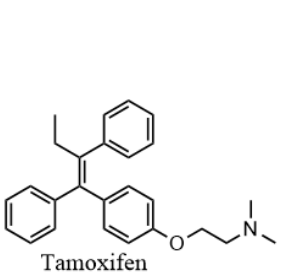
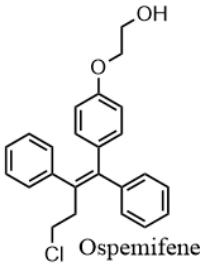
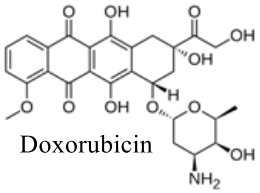
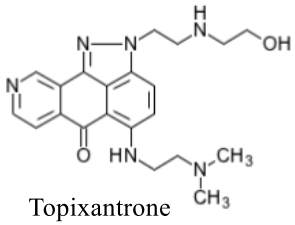
-Histone Deacetylase Inhibitors

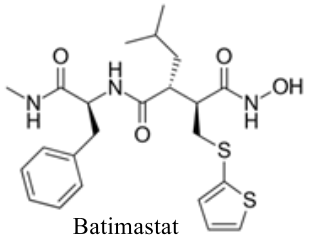
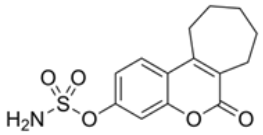
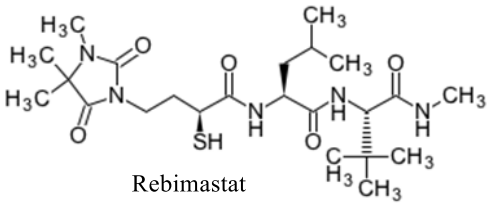
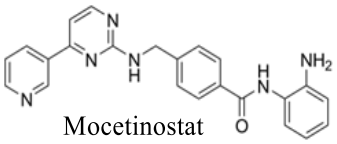
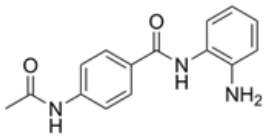
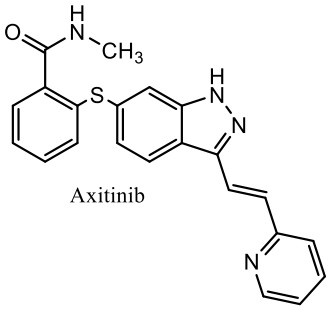
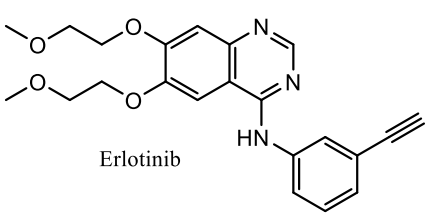
-Enzyme Inhibitor Tyrosine Kinases

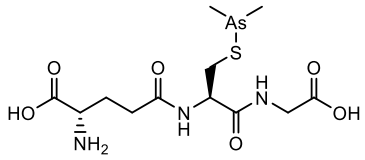
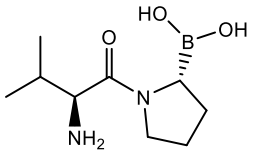
-Miscellaneous Antineoplastic Agents

The table below summarizes the classes, the modes of action and some chemical structures of the therapeutic substances.

Table 3. *Antineoplastic drugs, their mode of action and the chemical structures of the molecules integrated in cancer therapy.*[2]

Antineoplastic agent	Mode of action	Examples of therapeutic molecules
Hormone blocking anti-cancer drugs	Decrease the sexual hormones levels by exercising an antagonistic effect with estrogens and androgens on their specific receptors. (Anti-estrogens, anti-androgens, etc.)	 Tamoxifen  Ospemifene
Topoisomerase inhibitors	Topoisomerase blocking is the main action which lead to cell death by inhibiting its crucial role in DNA replication and transcription.	 Doxorubicin  Topixantrone

Matrix Metalloproteinase Inhibitors	Matrix Metalloproteinase hindrance and blocking by impeding cancerous cells proliferation since the Matrix Metalloproteinase are enzymes considered to be an intercellular communication bridge that maintains biological functionalities.	 Batimastat  Irosustat  Rebimastat
Histone Deacetylase Inhibitors (HDAC)	Diminish the deacetylation will cause genomic transcription to decline then the inhibition of proliferation which lead to cellular death.	 Mocetinostat  Tacedinaline
Enzyme Inhibitor Tyrosine Kinases (TKI)	Respond with the cytoplasmic catalysts or intracellular membranes to ensure their diffusion, then the disruption of the energetic process (ATP), since the tyrosine kinase is implicated.	 Axitinib  Erlotinib

Miscellaneous Antineoplastic Agents	Prevent progression and neoplastic spread by suppressing the cellular rapid dividing.	 Darinaparsin  Talabostat

2.2.4. Theranostic therapy: An opportunity to make chemotherapy selective

Attention has always been directed to chemotherapy as supplementary treatment in parallel with surgery and radiotherapy to eliminate any form of malignancies. However, as a result of its drawbacks caused by the lack of discrimination, and its undesirable attack on the active proliferation of normal cells which provokes a high level of cytotoxicity and the apparition of a lot of side effects such as hair loss, vomiting and weight loss, etc.[46], it became necessary to understand the intracellular regulation by focusing on the network signalling and exploitation responsible of cells survival.[47]

In order to solve the non-selectivity problem of conventional chemotherapy, several trials have been carried out and a wide range of molecules have been synthesised to avoid the side effects that can affect patients' quality of life. This is why visions have been directed towards a new perspective of treating tumors which are theranostic agents, so what are theranostic molecules?

2.2.4.1. Theranostic agents

Theranostic agents are a combination of therapy and diagnostics in a single unit aiming to control the disease progression and treatment response,[48] by dropping this concept on cancer therapy, theranostics have a double purpose strategy which consists on affording the cancer therapy customization by allowing the diagnosis, the staging and the treatment of cancer.[49]

As opposed to the anarchic assault of chemotherapy, theranostic molecules present a system of drug delivery performed by the usage of conjugates cleavable linkers which are regarded as a camouflage system allowing the reconversion and the release of the active ingredient under the intracellular physiological conditions of cancer cells (Figure 24).[49]

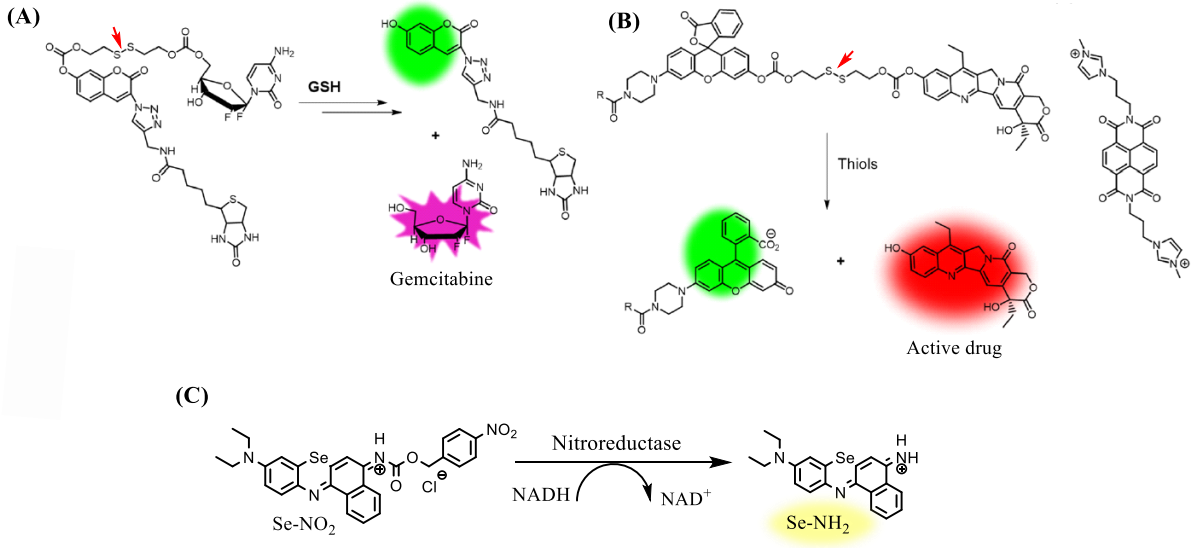


Figure 24. *Theranostics cleavage under GSH (A and B) and Nitroreductase medium (C) to release the cytotoxic and fluorophore agents.*[48]

In fact, this mechanism is known as drug delivery system which may be based on several new treatment tools against cancer, prodrugs can be seen as an example.

2.2.5. Prodrug strategy

2.2.5.1. What are prodrugs?

Prodrugs are molecules that belong to drug delivery systems, they are also regarded as drug moiety derivatives, these molecules are designed to be bioconverted within the body liberating the active parent drug under specific circumstances. Prodrugs are synthetised essentially to get over the complications of the inappropriate site specificity, insolubility, and the stability.

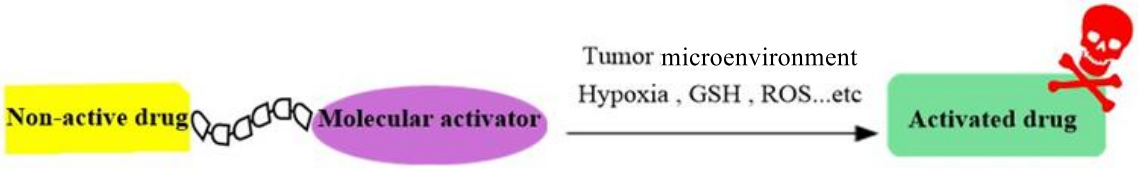


Figure 25. *The design overview of tumour-activated prodrug (Source: own elaboration).*

Thanks to their targeted delivery capabilities, they have created a new revolution in the personalisation of chemotherapy to improve its therapeutic efficacy, in which they are designed to inactivate the biodistribution of antineoplastic drugs in order to diminish the conventional

chemotherapy drawbacks and cytotoxicity by cleaving the prodrug and releasing the cytotoxic agent in the appropriate site.[50, 51]

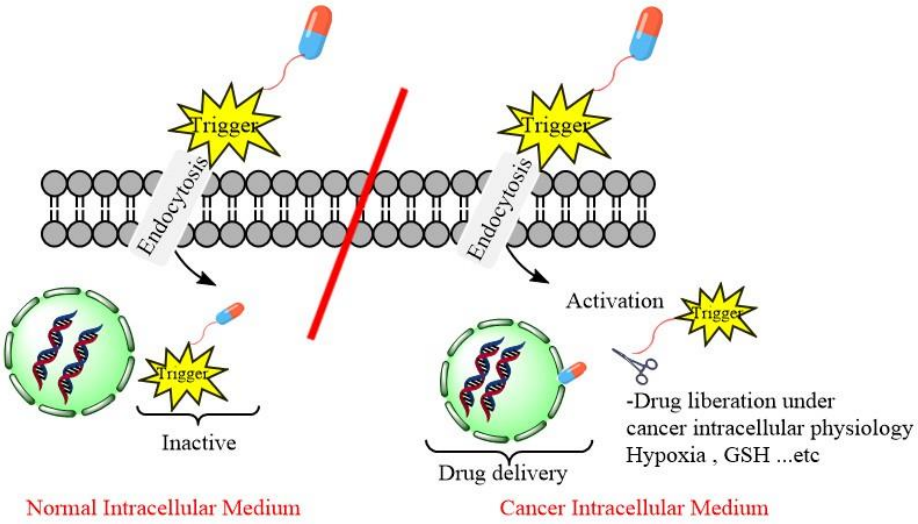


Figure 26. *The difference between the behaviour of the drug delivery process at the intracellular level for normal and cancerous cells.*[52]*(own elaboration).*

Based on the definitions provided and countless other examples, in this thesis we will talk specifically about prodrugs activated under hypoxia conditions, since hypoxia is still an attractive opportunity in the field of targeted therapy.

2.2.5.2. Hypoxia: double-edged sword in cancer therapy used on prodrugs triggering

Mentioned previously hypoxia is one of the crucial biomarkers at malignancies level with dual effects in which despite its negative contribution represented by the multi drug resistance (MDR), it did not prevent from being pivoted to the positive side known as hypoxia-activated prodrugs (HAPs).[51] In fact, tumour hypoxic microenvironment is the site where it exerts an excessive expression of nitro- reductase enzymes. This paved the way to develop nitro-linked triggers able to be attached to chemotherapeutic drugs to form a prodrug prone to release the drug upon reduction of the nitro group under hypoxia conditions.[49]

In fact, only a small proportion of tumour cells are in a hypoxia environment, which may seem ineffective when proposing a treatment. However, due to transient hypoxia, a high percentage of the tumour-forming cells at some point pass through this state, allowing the prodrug to activate, and eliminate a part of the cell population, cycle after cycle, until the tumour is completely eradicated. Prodrugs are able to function in this environment of transient hypoxia, killing tumour cells.

On the other hand, it is important to highlight the importance of combining these compounds with other treatments such as radiotherapy for greater effectiveness in the treatment.[22]

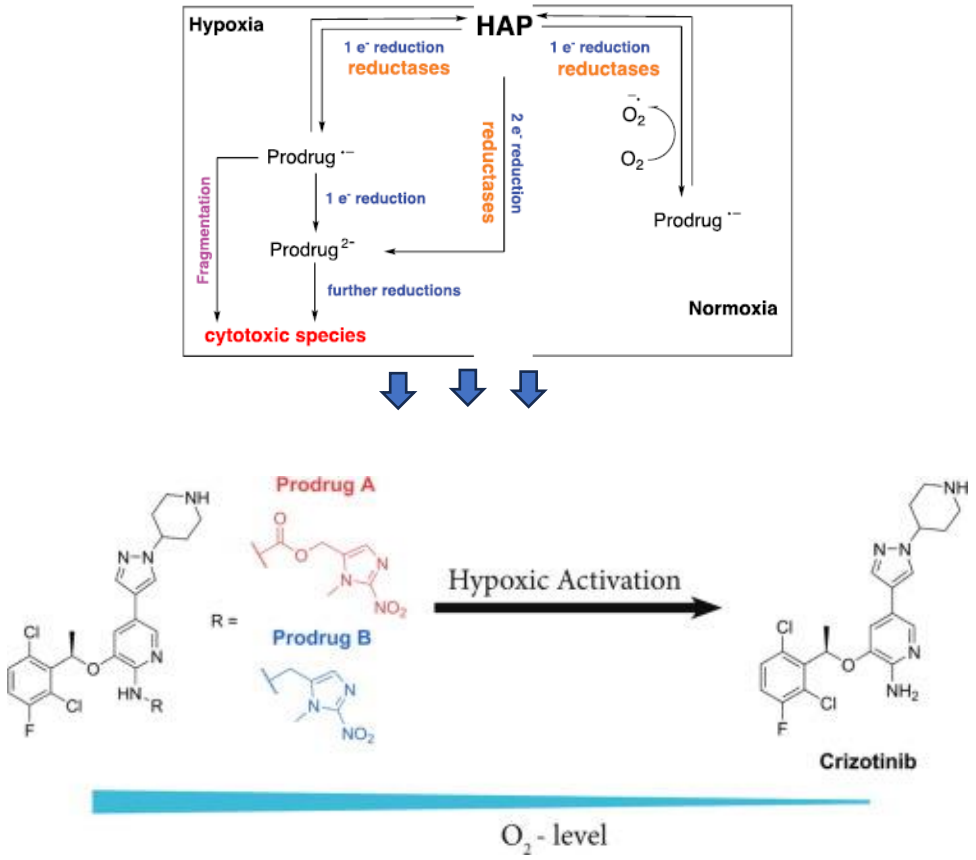


Figure 27. *Example of tyrosine kinase inhibitors prodrugs (A,B-Crizotinib) activation by hypoxia bioreductive medium and the illustrative process scheme (modified).*[22,53]

2.2.5.3. Background

Currently, there are multiple hypoxia-activated nitroaromatic compounds. Their great interest is due to the unique electronic properties of nitroaromatic compounds, which can accept up to six electrons from various reductase enzymes and undergo the successive formation of species, such as hydroxylamine and amines.

Nitrogen-based prodrugs can be classified into two broad groups:

(a) *Prodrugs activated by electronic redistribution*

The change in electron density can be harnessed for the activation of a cluster, for example, by greatly increasing the cellular toxicity of nitrogen mustards as DNA crosslinking agents.[54,55]

An example of this is the dinitroaziridine CB1954 (Figure 28). This compound was shown to have good bioactivity in rat tumours in *vivo*, due to its activation mainly by NQO1 reductase. In other mammals the enzyme is much less active, which limited the development of this compound. However, it was used as a comparison molecule and model.

Thus, variations of the prodrug CB1954 were designed and tested, leading to CP-506, which was shown to inhibit the growth of a wide range of hypoxic xenographed tumours. This compound is for the time being in a phase II clinical trial.[56]

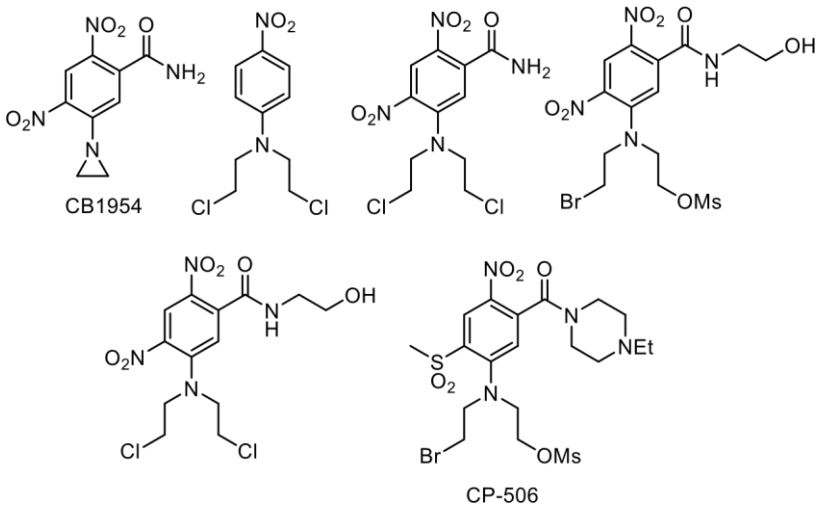


Figure 28. *Development of the prodrug CB1954 to CP-506.*[56]

b) Fragmentation-activated prodrugs

Most prodrugs fall into this group. They consist of two parts: the activator and the effector. The activator should undergo rapid reduction. In the presence of cellular oxygen, it must be able to reoxidize efficiently, so that the activation of the prodrug is limited only to cells in hypoxia. The effector is the part that, once released, is cytotoxic and therefore eliminates tumour cells. It must be able to perform its function at a wide variety of pH and proliferative states.[22]

There are several examples of prodrugs described in the literature, such as the one shown in the following image. The reduction of its nitro group leads to the fragmentation of the molecule to simultaneously release the kinase inhibitor semaxanib along with nitrogen mustard (Figure

29). The prodrug was evaluated in aerobic and hypoxic cultures of MDA-MB-468 breast cancer cells, but no increase in selectivity was recorded.[22, 57]

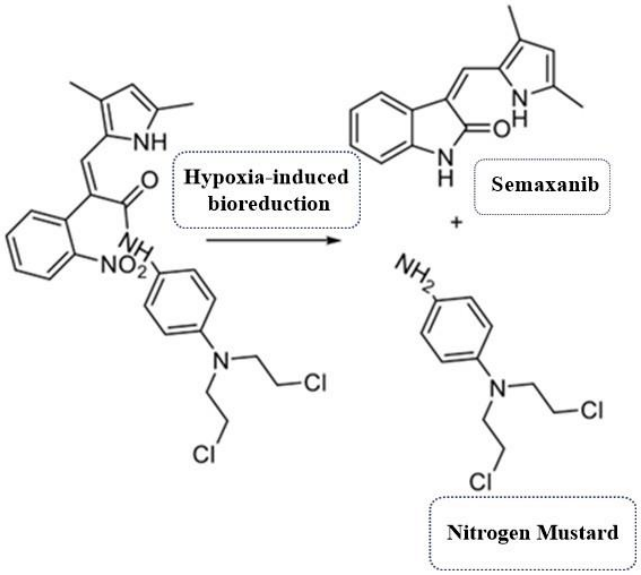


Figure 29. *Reduction of the prodrug example to release semaxanib and a nitrogen mustard*.[57]

Another example of theranostic agents activated under the hypoxic reducing medium is prodrug of figure 30 based on nitrobenzyl group attached to a sub-unit SN38 and a cancer targeting destabilizer responsible of biotinylation (biotin moiety/ topoisomerase 1 inhibitor). As a result of the bioreduction induced by tumour hypoxic area, the prodrug 28 from figure 30 detaches the antineoplastic agent due to the reduction of the nitro group to aniline derivative; at the same time the fluorescence of sub-unit SN38 turns on. This compound has been tested on HeLa cell-inoculated xenograft mice, showing a simultaneous triggering and activation of the nitrobenzene moiety, in which was exclusively gathered in the solid lump *in vivo* thanks to the fluorescence effect which has enabled the monitoring of tumour regression and shrinking.[49]

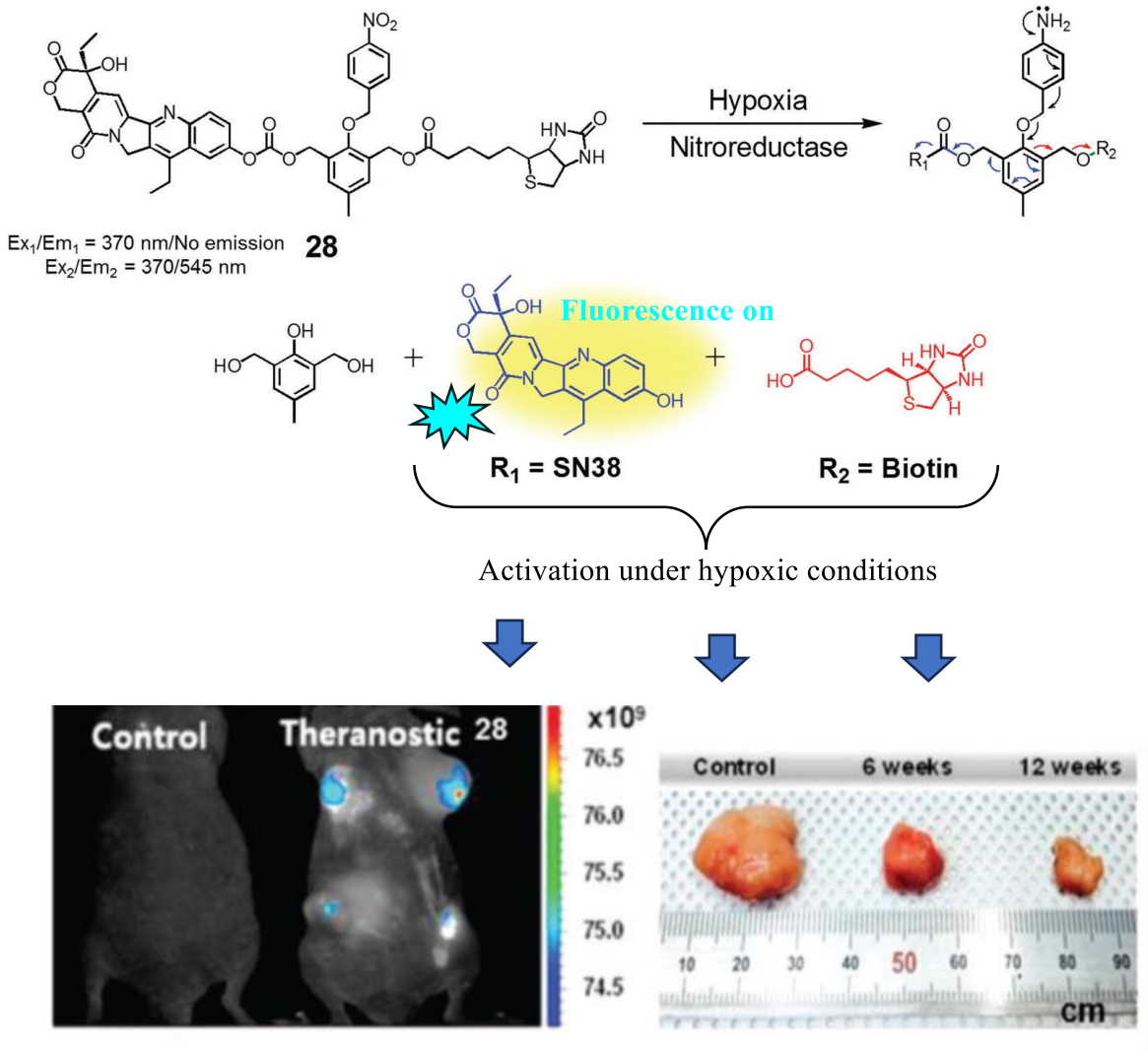


Figure 30. *Cleavage reaction of the prodrug **28** under the hypoxic reducing medium and its therapeutic effect induced by the theranostic agent shown by bioimaging and detected by fluorescence.*[49] *(adapted).*

As a matter of fact, advances in targeted therapy based on cytotoxic agents' delivery by the exploitation of cancer microenvironments biomarkers is not limited only on taking advantage from the hypoxic reducing medium but also by utilizing other features such as glutathione high concentrations within the malignancy area. Consequently, another range of prodrugs has been synthetized represented by the attachment of an anti-cancer agent with a disulfide bond exploiting the intracellular redox medium to reduce a disulfide bond to a thiol and then promote the drug liberation and activation.

That is what we will discuss in the first chapter from this thesis, while nitro-based theranostic drugs will be studied in the second chapter.

2.3. Protective groups: New Moieties for Chemoselectivity, Regioselectivity and Stereoselectivity

Usually, commercial molecules have complicated structures with many different functional groups. To carry out their synthesis many times is necessary to protect some of these functional groups as they can be sensitive to the reaction conditions employed to build the molecule. Thus, protecting groups need to fulfil a series of requirements.[58] Then, what are protecting groups ?

2.3.1. Protecting groups

Or protective groups (PG) are molecular structures integrated upon a functional group by chemical modification in poly- functional molecule in the aim of blocking the undesirable reactivity under a given conditions to achieve a certain selectivity such as chemoselectivity.[59,60]

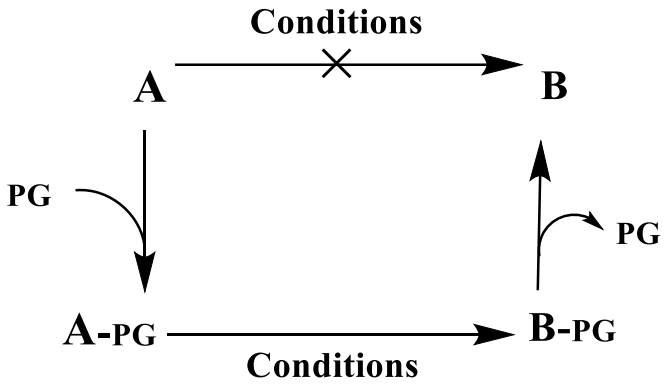


Figure 31. *Explanatory diagram for the protecting group operating mechanism.*[60]

2.3.2. Characteristics

Protective groups are usually used in the temporally masking avoiding the interfering with other reagents or sites, that is why a good protecting group requires a group of characteristics as it is shown in the figure 32 below.

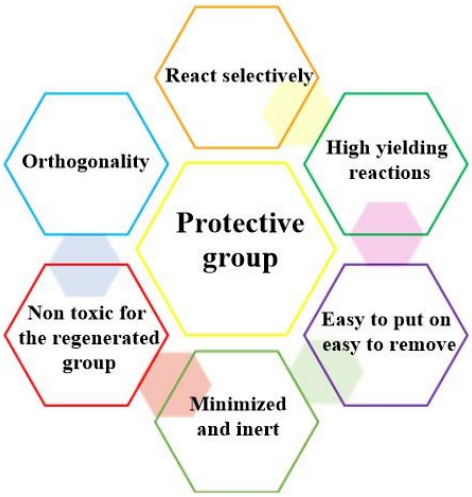


Figure 32. *Protective group characteristics.*[59, 61] *(modified).*

2.3.3. Protecting group´s chemoselectivity

Beside the great importance that protective groups occupy in organic synthesis, their mode of action has been considered as an opportunity to use them as triggering moieties in the pharmaceutical, biological or even medicinal fields by creating a chemobiological combination specialized in targeted therapy which can be used in cancer therapy for instance.

Due to chemotherapy non-specificity, recent advances in tumor microenvironment comprehension have strengthen the inspiration to investigate new molecular entities to improve the antineoplastic agents biodistribution.[62]

For these reasons, a robust protective group has been developed during our investigation (Chapter 3), which is specialized to protect the amines and the amino acids: 5-Chloro-8-nitro-1-naphtoyl (NNap) (Figure 33).

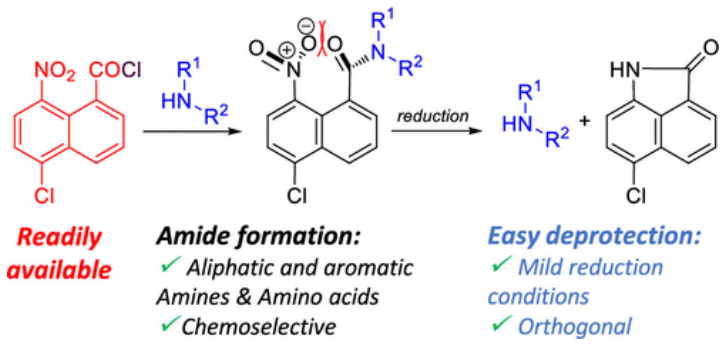


Figure 33. *NNapCl protecting group synthesis.*

NNap "5-Chloro-8-nitro-1-naphtoyl" allows aliphatic and aromatic amines as well as amino acid protection through amide formation. It offers a chemo-selective protection versus alcohols, for example. Also, NNap is compatible with acidic and basic media. Its deprotection is easy to perform and efficient using mild reaction conditions *via* Zn reduction. This makes NNap orthogonal with many other common protecting groups such as Boc, Cbz, Fmoc, etc.

Originally, NNap has been envisioned as a molecular trigger to be anchored to a chemotherapeutic drug (Chapter 2). However, as cancer cells are characterized for living in a reducing medium and NNap protecting group is released under reducing conditions, we envisioned that NNap could be used to liberate the drug only under the hypoxic influence of tumor cells. As a result, we realized that it could also be used as a protecting group tool in organic synthesis. More details will be discussed in the third chapter from this thesis.

2.4. Antineoplastic prodrugs hydro-solubility

The creation of novel chemical entities (NCEs) and their aqueous solubility is a critical step in the drug discovery process.[63] In order to optimize the physicochemical and pharmacological properties of drugs, prodrugs have been created as molecular modification for solubility enhancement, pharmacokinetic properties improvement and toxicity lessening.[64]

However, in spite of the fact that the prodrugs have no unexpected issues, their lack of solubility has become one of the undesirable features, the thing that can affect their bioconversion over chemical or enzymatic cleavage allowing the parent drug to be delivered with effective quantities.[64,65,66,67]

2.4.1. Prodrugs solubility enhancement via polar functionality addition

A prodrug could be considered as a parent drug derivative that enhances the molecule's physicochemical or biological characteristics to solve an inherent issue with the therapeutic use of the parent drug. In this context, low topical delivery due to the drug's poor solubility will be solved with the molecular fusion of a parent drug (known for its cytotoxic properties) with a promoiety that contains polar functional group and which will enhance the solubility.[72,73,74]

For these reasons formulation and conception strategies have been discussed in chapter 4 to overcome prodrugs low solubility of our antineoplastic moieties by introducing carboxylate functional group following two strategies: click chemistry with an azide and an alkyne and aromatic nucleophilic substitution with aromatic compound and sodium thioglycolate.

First strategy: *prodrugs solubility Enhancement via click chemistry*

Click chemistry has been introduced as one of the most pertinent chemical reactions in the twenty first century, in fact, Carolyn R. Bertozzi, Morten Meldal, and K. Barry Sharpless were awarded with the Nobel prize in Chemistry 2022 for "the development of click chemistry and bioorthogonal chemistry".[68,69] Also, Huisgen's 1,3-dipolar cycloaddition of alkynes and azides has been the most widely utilized synthetic and coupling tool among all the click reactions.

Actually, click chemistry is a notion that refers essentially to a group of chemical synthesis characterized by their simplicity, efficiency and selectivity in assembling molecular building blocks, hence it has been considered as an attractive chemical tool in producing high yields, easy to perform with minimum byproducts, and could be used in wide scope.

Copper(I)-catalysed azide-alkyne cycloaddition (CuAAC) is one of the most well-known click reactions, which effectively forms 1,2,3-triazoles, the latter can be carried out under milder condition which make it helpful in many fields such as material sciences and pharmaceutical products.[70] (Figure 34).

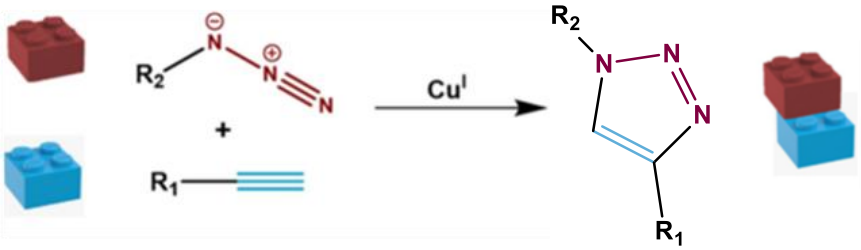


Figure 34. *The core of click chemistry is the Cu(I)-catalyzed cycloaddition of azide and alkynes (CuAAC) to afford 1,4- disubstituted-1H-1,2,3-triazoles (modified).*[68]

In Chapter 4, the solubility of Tacedinaline attached to *NNap* will be improved *via* click chemistry. Due to Tacedinaline toxicity, we expected that its attachment to a water soluble *NNap* (functionalized with two carboxylates by click chemistry) would reduce its toxicity while helping it to be soluble in aqueous environment. The presence of the nitro group in NNap should allow its reduction to the amino group under the hypoxic medium of the cancer cell with concomitant release of Tacedinaline (Figure 35). Also, the possibility to follow up the release of the triggering moiety by its fluorescence emission, could allow to use this prodrug as a theranostic compound.

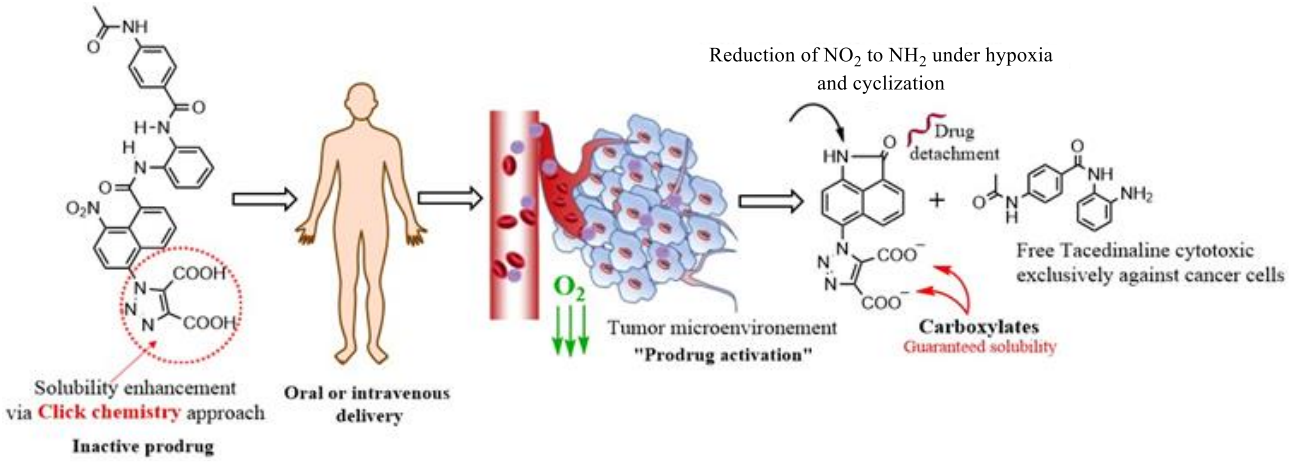


Figure 35. *Prodrug activation pathway with solubility properties enhanced via click chemistry conception (source: own elaboration).*

Second strategy: *aromatic nucleophilic substitution with aromatic compound and thioglycolate.*

One of the most promising strategies for prodrugs solubilization is the integration of an ionizable promoiety in a low soluble anticancer parent drug.[75]

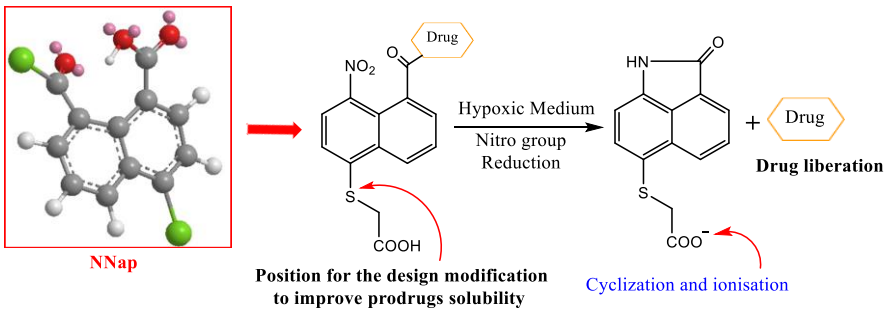


Figure 36. *Prodrug synthesis using 5-Chloro-8-nitro-naphthoyl (NNap) , and its behaviour under hypoxic condition with solubility enhancement (source: own elaboration).*

In order to apply the strategy, we decided to include a carboxylate from thioglycolate acid in *NNap* to increase its solubility in aqueous medium. The carboxylic group was chosen to perform the desired function thanks to its ionisation effect in the physiological medium *via* nucleophilic aromatic substitution between Cl-NNap and thioglycolate (Figure 36).

Then four anticancer agents have been selected: Bis(2-chloroethyl)amine, Tacedinaline, Farnesol and Pregnenolone to be linked to the modified NNap (Figure 37).

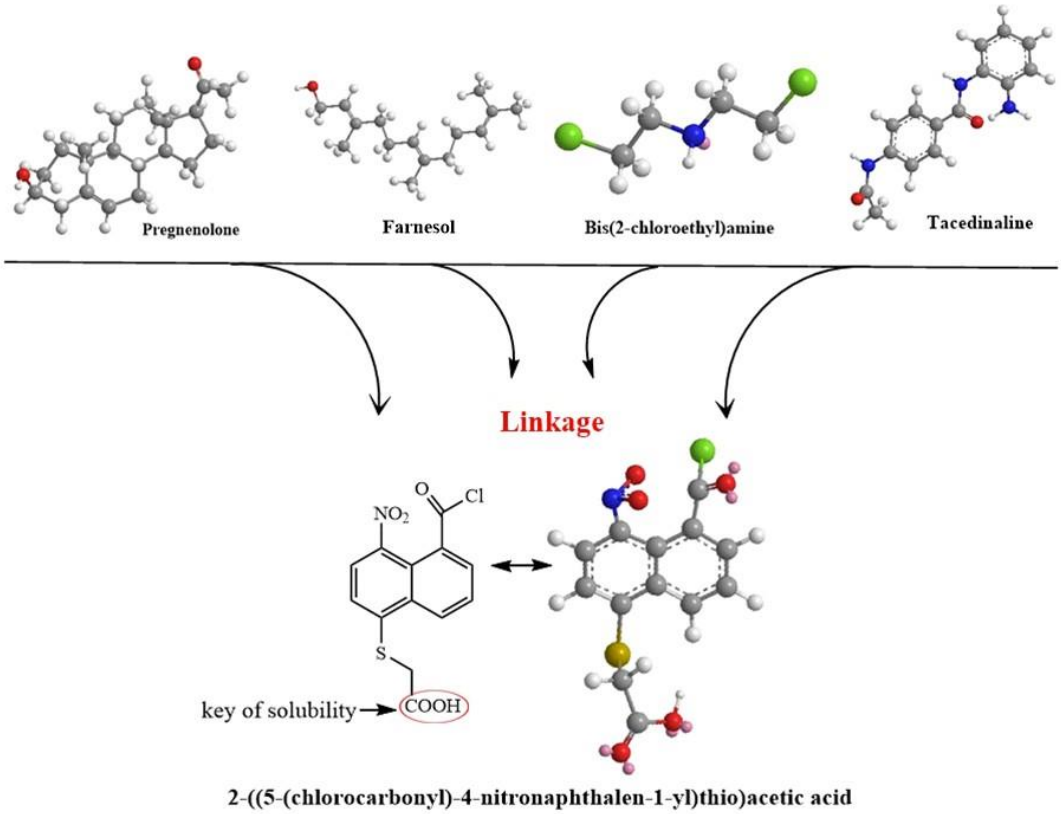


Figure 37. *Antitumor parent drugs linkage with the modified NNap over solubility enhancement (source: own elaboration).*

The corresponding linkage has afforded successfully four antineoplastic prodrugs as it has been expected, these have shown total performance in terms of solubility. Thanks to MTT assays that were realised in order to validate the reliability of the molecular conception. Fortunately, positive results have been obtained, more details are mentioned in chapter **4**.

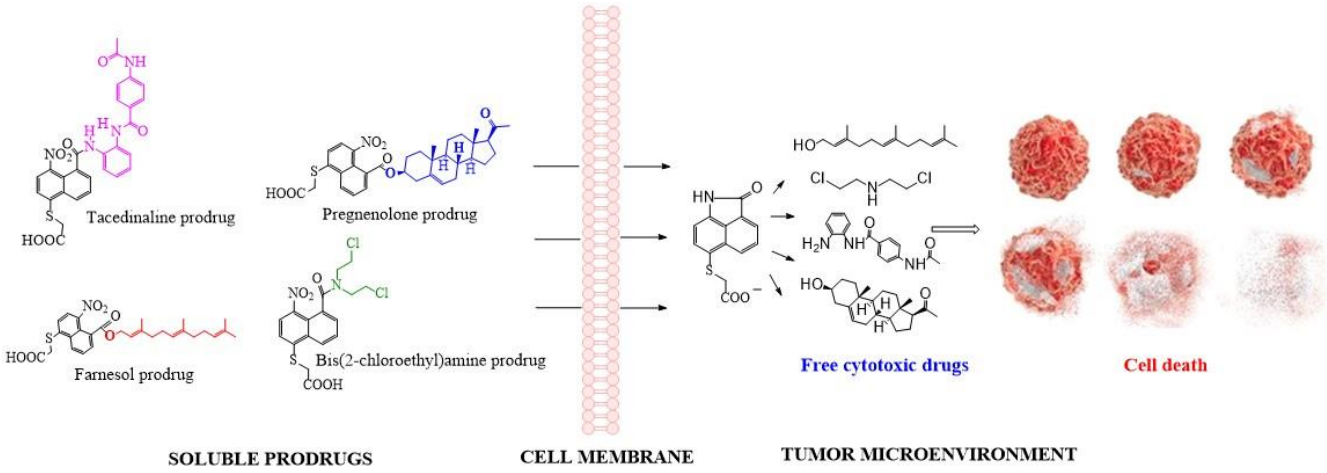


Figure 38. *Direct passage of prodrugs through the membrane thanks to solubility improvement and their cytotoxic effect towards cancer cells (source: own elaboration).*

2.5. An unusual rearrangement of a 1,8-naphtalene derivative

During the preparation of the acid chloride of NNap and its coupling with bis(2-chloroethyl)amine under Schotten-Baumann conditions we observed the formation of an unexpected compound with an aldehyde functional group and the rupture of the naphthalene ring. However, the molecular formula was the same of the starting material. Thus, an unusual and unexpected rearrangement was taking place. The 1,8-naphthalene rearrangement refers to a chemical transformation where the positions of substituents on the naphthalene ring change. In this context the rearrangement of a 1,8-nitronaphthalene carboxylate through the fragmentation of a naphthalene ring under mild reaction conditions was obtained. This led us to investigate and explain this unusual rearrangement which will be detailed in chapter 5.

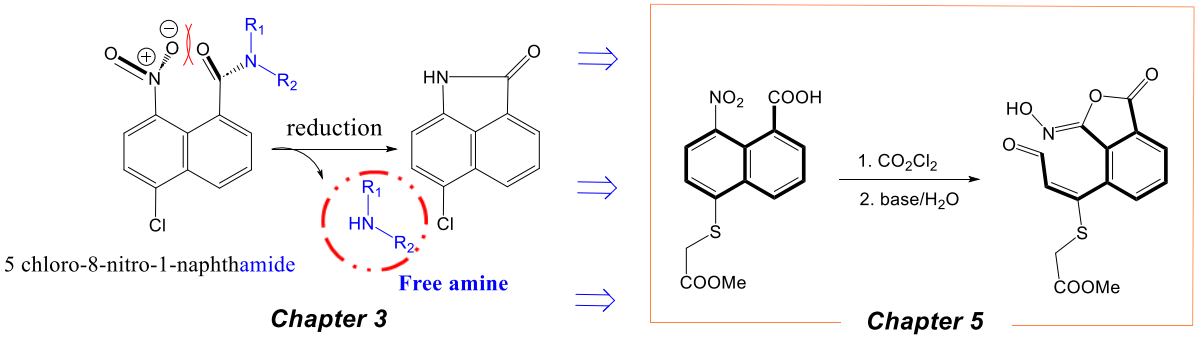


Figure 39. *Previous reactivity and unexpected rearrangement obtained.*[75]

6. References

(1) *Cancer*. https://www.who.int/es/news-room/fact-sheets/detail/cancer (accessed 2023-11-21).

(2) Lednicer, D. *Antineoplastic Drugs: Organic Syntheses*; John Wiley & Sons, **2015**.

(3) Pecorino, L. *Molecular Biology of Cancer: Mechanisms, Targets, and Therapeutics*, Third edition.; Oxford University Press: Oxford, 2012.

(4) *Female Genital Pathology*. https://webpath.med.utah.edu/FEMHTML/FEM141.html (accessed 2024-08-01).

(5) *What Is Cancer? Symptoms, Signs, Types & Causes*. Cleveland Clinic. https://my.clevelandclinic.org/health/diseases/12194-cancer (accessed 2024-08-01).

(6) Cancero_ch_1.Pdf. http://gwenr.free.fr/cancero/cancero_ch_1.pdf (accessed 2023-11-22).

(7) Chhikara, B. S.; Parang, K. Global Cancer Statistics 2022: The Trends Projection Analysis. **2023**.

(8) Siegel, R. L.; Miller, K. D.; Wagle, N. S.; Jemal, A. Cancer Statistics, 2023. *CA A Cancer J Clinicians* **2023**, *73* (1), 17–48. https://doi.org/10.3322/caac.21763.

(9) Yokota, J. Tumor Progression and Metastasis. *Carcinogenesis* **2000**, *21* (3), 497–503. https://doi.org/10.1093/carcin/21.3.497.

(10) Klein, C. A. Cancer Progression and the Invisible Phase of Metastatic Colonization. *Nat. Rev. Cancer* **2020**, *20* (11), 681–694. https://doi.org/10.1038/s41568-020-00300-6.

(11) *Metastatic Cancer: When Cancer Spreads - NCI*. https://www.cancer.gov/types/metastatic-cancer (accessed 2024-08-01).

(12) Hossain, M. S.; Karuniawati, H.; Jairoun, A. A.; Urbi, Z.; Ooi, D. J.; John, A.; Lim, Y. C.; Kibria, K. M. K.; Mohiuddin, A. K. M.; Ming, L. C.; Goh, K. W.; Hadi, M. A. Colorectal Cancer: A Review of Carcinogenesis, Global Epidemiology, Current Challenges, Risk Factors, Preventive and Treatment Strategies. *Cancers* **2022**, *14* (7), 1732. https://doi.org/10.3390/cancers14071732.

(13) Lodish, H; Berk, A ; Kaiser, C. A.; Krieger, M.; Bretscher, A.; Ploegh, H.; Amon, A.; Martin, K. C. *Molecular Cell Biology*, Eighth edition.; W. H. Freeman and Company: New York, **2016**.

(14) *Cancer Cells vs. Normal Cells: How Are They Different?* Very well Health. https://www.verywellhealth.com/cancer-cells-vs-normal-cells-2248794 (accessed 2023-11-30).

(15) Hanahan, D.; Weinberg, R. A. Hallmarks of Cancer: The Next Generation. *Cell* **2011**, *144* (5), 646–674. https://doi.org/10.1016/j.cell.2011.02.013.

(16) Liberti, M. V.; Locasale, J. W. The Warburg Effect: How Does It Benefit Cancer Cells? *Trends in Biochemical Sciences* **2016**, *41* (3), 211–218. https://doi.org/10.1016/j.tibs.2015.12.001.

(17) Burns, J. S.; Manda, G. Metabolic Pathways of the Warburg Effect in Health and Disease: Perspectives of Choice, Chain or Chance. *Int. J. Mol. Sci.* **2017**, *18* (12), 2755. https://doi.org/10.3390/ijms18122755.

(18) Kumar, R.; Srivastava, R.; Srivastava, S. Detection and Classification of Cancer from Microscopic Biopsy Images Using Clinically Significant and Biologically Interpretable Features. *J. Med. Eng.* **2015**, *2015*, 1–14. https://doi.org/10.1155/2015/457906.

(19) Simsek, H.; Klotzsch, E. The Solid Tumor Microenvironment—Breaking the Barrier for T Cells: How the Solid Tumor Microenvironment Influences T Cells. *BioEssays* **2022**, *44* (6), 2100285. https://doi.org/10.1002/bies.202100285.

(20) Choi, S. H.; Chung, A. R.; Kang, W.; Park, J. Y.; Lee, M. S.; Hwang, S. W.; Kim, D. Y.; Kim, S. U.; Ahn, S. H.; Kim, S.; Han, K.-H. Silencing of Hypoxia-Inducible Factor-1β Induces Anti-Tumor Effects in Hepatoma Cell Lines under Tumor Hypoxia. *PLoS One* **2014**, *9* (7), e103304. https://doi.org/10.1371/journal.pone.0103304.

(21) Nguyen, A. T.; Kim, H.-K. Recent Developments in PET and SPECT Radiotracers as Radiopharmaceuticals for Hypoxia Tumors. *Pharmaceutics* **2023**, *15* (7), 1840. https://doi.org/10.3390/pharmaceutics15071840.

(22) Anduran, E.; Dubois, L. J.; Lambin, P.; Winum J.-Y. Hypoxia-activated prodrug derivatives of anti-cancer drugs: a patent review 2006 – 2021. *Expert Opin. Ther. Pat. Vol* **2022**, *32* (1), 1-12. https://doi.org/10.1080/13543776.2021.1954617.

(23) Fraga, A. Hipoxia tumoral. Papel del factor inducible por hipoxia. *Actas Urol. Esp.* **2009**, *33* (9), 941-951. https://scielo.isciii.es/scielo.php?script=sci_abstract&pid=S0210-48062009000900003.

(24) Acker, T.; Plate, K. H. Role of Hypoxia in Tumor Angiogenesis?Molecular and Cellular Angiogenic Crosstalk. *Cell and Tissue Research* **2003**, *314* (1), 145–155. https://doi.org/10.1007/s00441-003-0763-8.

(25) Huynh, K. N.; Rao, S.; Roth, B.; Bryan, T.; Fernando, D. M.; Dayyani, F.; Imagawa, D.; Abi-Jaoudeh, N. Targeting Hypoxia-Inducible Factor-1α for the Management of Hepatocellular Carcinoma. *Cancers* **2023**, *15* (10), 2738. https://doi.org/10.3390/cancers15102738.

(26) Mukherjee, S.; Kanwar, J. R. *Hypoxia in Cancer: Significance and Impact on Cancer Therapy*; Springer: Bhopal, Madhya Pradesh, India, **2023**.

(27) Madu, C. O.; Wang, S.; Madu, C. O.; Lu, Y. Angiogenesis in Breast Cancer Progression, Diagnosis, and Treatment. *J. Cancer* **2020**, *11* (15), 4474–4494. https://doi.org/10.7150/jca.44313.

(28) Gray. J. W; Howley. P. M; Israel. M. A; Thompson. C. B, Mendelsohn. J. *The Molecular Basis of Cancer*, 4 th. edition; Saunders: Philadelphia, **2014**.

(29) Kennedy, L.; Sandhu, J. K.; Harper, M.-E.; Cuperlovic-Culf, M. Role of Glutathione in Cancer: From Mechanisms to Therapies. *Biomolecules* **2020**, *10* (10), 1429. https://doi.org/10.3390/biom10101429.

(30) Vulcano, L. A. D.; Soraci, A. L.; Tapia, M. O. Homeostasis del glutatión. *Acta Bioquím. Clín. Latinoam.* **2013**, 47 (3), 529-539. https:// https://www.redalyc.org/pdf/535/53529349007.pdf

(31) Traverso, N.; Ricciarelli, R.; Nitti, M.; Marengo, B.; Furfaro, A. L.; Pronzato, M. A.; Marinari, U. M.; Domenicotti, C. Role of Glutathione in Cancer Progression and Chemoresistance. *Oxidative Medicine and Cellular Longevity* **2013**, *2013*, 972913. https://doi.org/10.1155/2013/972913.

(32) Bansal,A; Simon,M celeste; Glutathione metabolism in cancer progression and treatment resistance. *Cell. Biol.* **2018**, 2;217(7):2291-2298. https://doi.org/10.1083/jcb.201804161. (33) Roma-Rodrigues, C.; Mendes, R.; Baptista, P. V.; Fernandes, A. R. Targeting Tumor Microenvironment for Cancer Therapy. *Int. J. Mol. Sci.* **2019**, *20* (4), 840. https://doi.org/10.3390/ijms20040840.

(34) Kharouf, N.; Flanagan, T. W.; Hassan, S.-Y.; Shalaby, H.; Khabaz, M.; Hassan, S.-L.; Megahed, M.; Haikel, Y.; Santourlidis, S.; Hassan, M. Tumor Microenvironment as a Therapeutic Target in Melanoma Treatment. *Cancers* **2023**, *15* (12), 3147. https://doi.org/10.3390/cancers15123147.

(35) King, R.; Hayes, C.; Donohoe, C. L.; Dunne, M. R.; Davern, M.; Donlon, N. E. Hypoxia and Its Impact on the Tumour Microenvironment of Gastroesophageal Cancers. *World J. Gastrointest. Oncol.* **2021**, *13* (5), 312–331. https://doi.org/10.4251/wjgo.v13.i5.312.

(36) Björnmalm, M.; Thurecht, K. J.; Michael, M.; Scott, A. M.; Caruso, F. Bridging Bio–Nano Science and Cancer Nanomedicine. *ACS Nano* **2017**, *11* (10), 9594–9613. https://doi.org/10.1021/acsnano.7b04855.

(37) Kümmerer, K.; Haiß, A.; Schuster, A.; Hein, A.; Ebert, I. Antineoplastic Compounds in the Environment—Substances of Special Concern. *Environ. Sci. Pollut. Res.* **2016**, *23* (15), 14791–14804. https://doi.org/10.1007/s11356-014-3902-8.

(38) Guichard, N.; Guillarme, D.; Bonnabry, P.; Fleury-Souverain, S. Antineoplastic Drugs and Their Analysis: A State of the Art Review. *Analyst* **2017**, *142* (13), 2273–2321. https://doi.org/10.1039/C7AN00367F.

(39) *Evolution of chemotherapy: A look back in time*. OncoBites. https://oncobites.blog/2019/04/26/evolution-of-chemotherapy-a-look-back-in-time/ (accessed 2024-08-01).

(40) Singh, R. K.; Kumar, S.; Prasad, D. N.; Bhardwaj, T. R. Therapeutic Journery of Nitrogen Mustard as Alkylating Anticancer Agents: Historic to Future Perspectives. *Eur. J. Med. Chem.* **2018**, *151*, 401–433. https://doi.org/10.1016/j.ejmech.2018.04.001.

(41) Chen, Y.; Jia, Y.; Song, W.; Zhang, L. Therapeutic Potential of Nitrogen Mustard Based Hybrid Molecules. *Front. Pharmacol.* **2018**, *9*, 1453. https://doi.org/10.3389/FPHAR.2018.01453/BIBTEX.

(42) Krause W. Resistance to anti-tubulin agents: from vinca alkaloids to epothilones. *Cancer Drug Resist.* **2019**, *2*, 82-106. http://dx.doi.org/10.20517/cdr.2019.06

(43) Barreca, M.; Stathis, A.; Barraja, P.; Bertoni, F. An Overview on Anti-Tubulin Agents for the Treatment of Lymphoma Patients. *Pharmacol. Ther.* **2020**, *211*, 107552. https://doi.org/10.1016/j.pharmthera.2020.107552.

(44) *Targeted Therapy for Cancer: What is It & How Does it Work?*. City of Hope. https://www.cancercenter.com/treatment-options/precision-medicine/targeted-therapy (accessed 2024-10-02).

(45) *Targeted Drug Therapy*. https://www.cancer.org/cancer/managing-cancer/treatment-types/targeted-therapy.html (accessed 2024-10-02).

(46) Min, H.-Y.; Lee, H.-Y. Molecular Targeted Therapy for Anticancer Treatment. *Exp. Mol. Med.* **2022**, *54* (10), 1670–1694. https://doi.org/10.1038/s12276-022-00864-3.

(47) Chabner, B. A.; Roberts, T. G. Chemotherapy and the War on Cancer. *Nat. Rev. Cancer* **2005**, *5* (1), 65–72. https://doi.org/10.1038/nrc1529.

(48) Pratihar, S.; Bhagavath, K. K.; Govindaraju, T. Small Molecules and Conjugates as Theranostic Agents. *RSC Chem. Biol.* **2023**, *4* (11), 826–849. https://doi.org/10.1039/D3CB00073G.

(49) Lee, M. H.; Sharma, A.; Chang, M. J.; Lee, J.; Son, S.; Sessler, J. L.; Kang, C.; Kim, J. S. Fluorogenic Reaction-Based Prodrug Conjugates as Targeted Cancer Theranostics. *Chem. Soc. Rev.* **2018**, *47* (1), 28–52. https://doi.org/10.1039/C7CS00557A.

(50) Dahan, A.; Zimmermann, E. M.; Ben-Shabat, S. Modern Prodrug Design for Targeted Oral Drug Delivery. *Molecules* **2014**, *19* (10), 16489–16505. https://doi.org/10.3390/molecules191016489.

(51) Delahousse, J.; Skarbek, C.; Paci, A. Prodrugs as Drug Delivery System in Oncology. *Cancer Chemother Pharmacol* **2019**, *84* (5), 937–958. https://doi.org/10.1007/s00280-019-03906-2.

(52) Lee, M. H.; Sharma, A.; Chang, M. J.; Lee, J.; Son, S.; Sessler, J. L.; Kang, C.; Kim, J. S. Fluorogenic Reaction-Based Prodrug Conjugates as Targeted Cancer Theranostics. *Chem. Soc. Rev.* **2018**, *47* (1), 28–52. https://doi.org/10.1039/C7CS00557A.

(53) Bielec, B.; Schueffl, H.; Terenzi, A.; Berger, W.; Heffeter, P.; Keppler, B. K.; Kowol, C. R. Development and Biological Investigations of Hypoxia-Sensitive Prodrugs of the Tyrosine Kinase Inhibitor Crizotinib. *Bioorg. Chem.* **2020**, *99*, 103778. https://doi.org/10.1016/j.bioorg.2020.103778.

(54) PubChem. *N,N-Bis(2-hydroxyethyl)benzamide*. https://pubchem.ncbi.nlm.nih.gov/compound/94109 (accessed 2023-12-25).

(55) *N,N-Bis(2-hydroxyethyl)benzamide | C11H15NO3 - PubChem https://pubchem.ncbi.nlm.nih.gov/compound/N_N-Bis_2hydroxyethyl_benzamide#section=GC-MS* (accessed 2023-12-25).

(56) Denny, W. A. Nitroaromatic Hypoxia-Activated Prodrugs for Cancer Therapy. *Pharmaceuticals (Basel)* **2022**, *15* (2), 187. https://doi.org/10.3390/ph15020187.

(57) Sansom, G. N.; Kirk, N. S.; Guise, C. P.; Anderson, R. F.; Smaill, J. B.; Patterson, A. V.; Kelso, M. J. Prototyping Kinase Inhibitor-Cytotoxin Anticancer Mutual Prodrugs Activated by Tumour Hypoxia: A Chemical Proof of Concept Study. *Bioorg. Med. Chem. Lett.* **2019**, *29* (10), 1215–1219. https://doi.org/10.1016/j.bmcl.2019.03.015.

(58) Fernandes, R. A. *Protecting-Group-Free Organic Synthesis*, John Wiley&Sons Ltd.; Indian Institute of Technology Bombay Mumbai, India, **2018**.

(59) *What is a protecting group in chemistry? [FAQ!]*. https://scienceoxygen.com/what-is-a-protecting-group-in-chemistry/ (accessed 2024-01-23).

(60) *Protecting Groups*. Chemistry LibreTexts. https://chem.libretexts.org/Courses/University_of_California_Davis/Chem_231A%3A_Methods_of_Organic_Synthesis/Text/Protecting_Groups (accessed 2024-01-23).

(61) *Greene's Protective Groups in Organic Synthesis*, 1st ed.; Wuts, P. G. M., Ed.; Wiley; Hoboken, **2014**. https://doi.org/10.1002/9781118905074.

(62) Chau, Y.; Tan, F. E.; Langer, R. Synthesis and Characterization of Dextran−Peptide−Methotrexate Conjugates for Tumor Targeting via Mediation by Matrix Metalloproteinase II and Matrix Metalloproteinase IX. *Bioconjugate Chem.* **2004**, *15* (4), 931–941. https://doi.org/10.1021/bc0499174.

(63) Jain, N. K.; Gupta, U. Application of Dendrimer-Drug Complexation in the Enhancement of Drug Solubility and Bioavailability. *Expert.Opin. Drug Metab. Toxicol* **2008**, *4* (8), 1035–1052. https://doi.org/10.1517/17425255.4.8.1035.

(64) Jornada, D. H.; Fernandes, G. F. D. S.; Chiba, D. E.; De Melo, T. R. F.; Dos Santos, J. L.; Chung, M. C. The Prodrug Approach: A Successful Tool for Improving Drug Solubility. *Molecules* **2016**, *21* (1), 42; https://doi.org/10.3390/molecules21010042.

(65) Rautio, J.; Kumpulainen, H.; Heimbach, T.; Oliyai, R.; Oh, D.; Järvinen, T.; Savolainen, J. Prodrugs: Design and Clinical Applications. *Nat. Rev. Drug Discov.* **2008**, *7* (3), 255–270. https://doi.org/10.1038/nrd2468.

(66) Huttunen K., Raunio H., Rautio J. Prodrugs: Design and clinical applications. *Pharmacol. Rev.* **2011**, *63*, 750–771. https://doi: 10.1124/pr.110.003459.

(67) Stella, V. J.; Nti-Addae, K. W. Prodrug Strategies to Overcome Poor Water Solubility. *Adv. Drug Deliv. Rev.* **2007**, *59* (7), 677–694. https://doi.org/10.1016/j.addr.2007.05.013.

(68) Lopez-Ruiz, A.; Ortega-Muñoz, M.; Santoyo-Gonzalez, F.; Megia-Fernandez, A. Click to Learn, Learn to Click: Undergraduate Synthetic Organic Chemistry Experiments. *Chem.Pap.* **2023**, *77* (9), 5227–5236. https://doi.org/10.1007/s11696-023-02858-5.

(69) Kolb, H. C.; Finn, M. G.; Sharpless, K. B. Click Chemistry: Diverse Chemical Function from a Few Good Reactions. *Angew. Chem. Int. Ed. Engl.* **2001**, *40* (11), 2004–2021. https://doi.org/10.1002/1521-3773(20010601)40:11<2004:AID-ANIE2004>3.0.CO;2-5.

(70) Worrell, B. T.; Malik, J. A.; Fokin, V. V. Direct Evidence of a Dinuclear Copper Intermediate in Cu(I)-Catalyzed Azide-Alkyne Cycloadditions. *Science* **2013**, *340* (6131), 457–460. https://doi.org/10.1126/science.1229506.

(71) Ma, N.; Wang, Y.; Zhao, B.-X.; Ye, W.-C.; Jiang, S. The Application of Click Chemistry in the Synthesis of Agents with Anticancer Activity. *DDDT* **2015**, *9*, 1585–1599. https://doi.org/10.2147/DDDT.S56038.

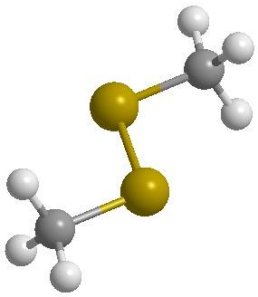
(72) Sloan, K. B.; Wasdo, S.; Ezike-Mkparu, U.; Murray, T.; Nickels, D.; Singh, S.; Shanks, T.; Tovar, J.; Ulmer, K.; Waranis, R. Topical Delivery of 5-Fluorouracil and 6-Mercaptopurine by Their Alkylcarbonyloxymethyl Prodrugs from Water: Vehicle Effects on Design of Prodrugs. *Pharm.Res.* **2003**, *20* (4), 639–645. https://doi.org/10.1023/A:1023207118209.

(73) Sloan, K. B. Functional group considerations in the development of prodrug approaches to solving topical delivery problems. In: Sloan, K. B., editor. Prodrugs: topical and ocular drug delivery. New York: Marcel Dekker; **1992**. pp. 17–116.

(74) Sloan, K. B.; Wasdo, S. Designing for Topical Delivery: Prodrugs Can Make the Difference. *Med. Res. Rev.* **2003**, *23* (6), 763–793. https://doi.org/10.1002/med.10048.

(75) Rautio, J.; Meanwell, N. A.; Di, L.; Hageman, M. J. The Expanding Role of Prodrugs in Contemporary Drug Design and Development. *Nat. Rev. Drug Discov.* **2018**, *17* (8), 559–587. https://doi.org/10.1038/nrd.2018.46.

CHAPTER 1: PRODRUGS FUNCTIONALIZED WITH SULFUR-SULFUR BONDS



In chapter 1 prodrugs functionalized with sulfur-sulfur bonds will be discussed.

Applying the starting theory and based on what is mentioned previously, compounds with disulfide bonds will be synthetised in order to attach several antineoplastic drugs, the solubility will also be taken into account to ensure its transition within the bloodstream.

Several linkers will be considered, structural studies will be afforded in order to develop a better design.

In this chapter, we will take advantage of the physiological structure and features of cancer tissue microenvironment, among them the hypoxia conditions and the large amount of glutathione, which can be used as a reductant of prodrugs to release the cytotoxic substance selectively.

1. Objectives

The main objective of this chapter is the design and synthesis of anti-cancer prodrugs based on linking an anti-cancer agent with a disulfide bond taking into consideration the following points:

- **Objective 1:** Looking for a functional group that is able to solubilize cytotoxic drugs in water by conserving their stability until they reach the target.
- **Objective 2:** It must be able to be reduced only under the hypoxic conditions to release the anti-tumor drug.
- **Objective 3:** Finding a cytotoxic drug that fits well to this functional group, remaining stable in the transport to its destination and ensure the triggering *in situ*.
- **Objective 4:** Once the prodrug is synthetized, it will be necessary to check the hypothesis validity by realising cytological tests *in vitro* as a kind of confirmation.

2. Introduction

Attractive opportunities have been adopted to be the alternative therapy for cancer, since the appearance of side effects caused by the routinely administration of the chemotherapeutic agents has become a real problem, as it affects the quality of patient's life. Hence it became necessary to find strategies by creating prodrugs based on the good understanding of cancer tissue physiopathology, in order to ensure the selectivity, the therapeutic efficiency and reduce the toxicity.

In fact, several hallmarkers in tumor microenvironment are considered promising for the targeted anti-cancer agents manufacturing, such as the endogenous thiols, more precisely glutathione (GSH, Figure 1).[1] Glutathione is well known as a non-protein thiol which play a crucial role in vital cell functions and maintenance.

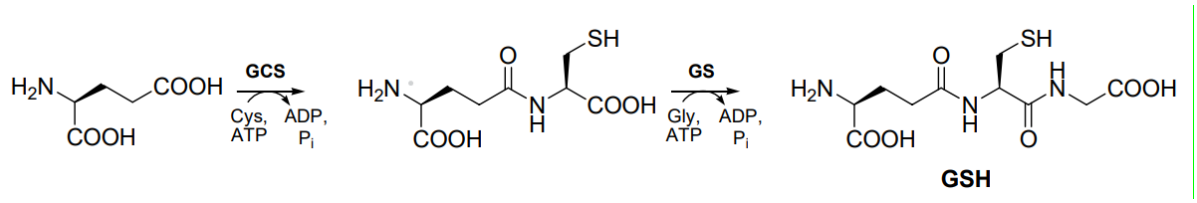


Figure 1. *GSH biosynthesis*.[1]

The redox state ensures a certain balance in the cell by maintaining cellular homeostasis and functionality, the latter may be affected with a non-equilibrium in the redox systems induced by cancer.

The redox system malfunctioning in cancer leads certainly to an overexpression of ROS (reactive oxygen species) and the reductive species such as the high concentration of glutathione (GSH). In the normal states GSH exists in millimolar concentration in intracellular medium and millimolar scale in the fluids as the blood.[1,2]

Usually, tumor cells are characterized by high levels of antioxidants, particularly GSH with a high concentration of ~10 mM, this value is ten times higher than in normal cells where it maintains an intracellular redox equilibrium and develop a potent antioxidant defense.[2,3]

As known, prodrugs are compounds with no pharmacological activity that can be metabolized into active drugs through chemical or enzymatic reactions. In the last 10 years, these compounds have contributed enormously to the discovery of new drugs to cure diseases.

Studying the structure of these prodrugs, it has been found that the combination of several functional groups to obtain multicomponent compounds is an interesting strategy that generates good results. This is due to the ability to deliver these multicomponent prodrugs in a targeted manner to cancer cells. The advantages obtained with this strategy are: (i) improved pharmacokinetics, (ii) reduced toxicity, (iii) new cytotoxic chemotherapies obtained, and (iv) easy monitoring of the location and efficacy of anticancer agents.

Among this type of compounds, those that involve functional groups capable of cleaving in their structure, such as disulfide bonds, stand out (Figure 2). In this way, the disulfide bonds should be able to deactivate the cytotoxic activity of the drug when it is conjugated with these bonds and being able to activate them when they reach the cancer cells, by breaking the disulfide bond.

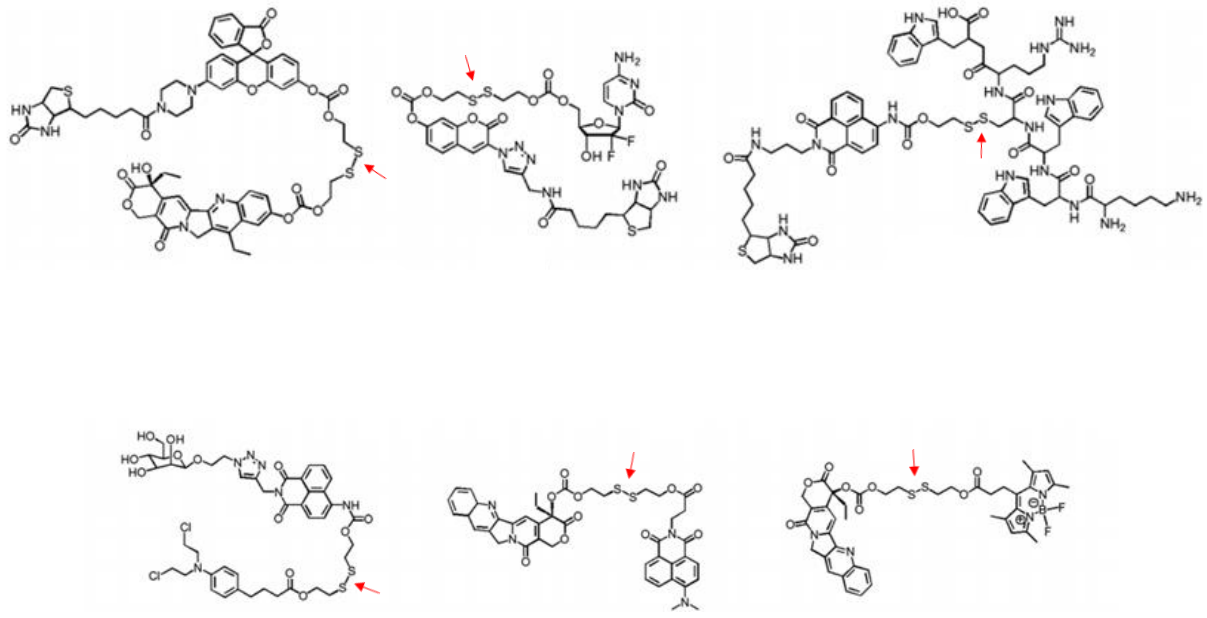


Figure 2. *Examples of disulfide-bonded prodrugs used as theranostic agents.*[4]

This can be achieved thanks to the reducing environment that exists in cancer cells, and the high concentration of glutathione that is present.

Our proposal for the prodrug design and development is shown in Figure 3, in which an acyl disulfide is bonded to the drug. Hence, under the hypoxic medium, the disulfide is reduced to thiol and the drug is released (Figure 3).

In addition, carbonyl sulfide (O=C=S) is generated in this process, which is also toxic and can contribute to damage cancer cells.[4,5]

The strategies that we have designed to release the drug are summarized in Figure 3:

- ✓ ***The proposed strategy**: Disulfide bonds.*

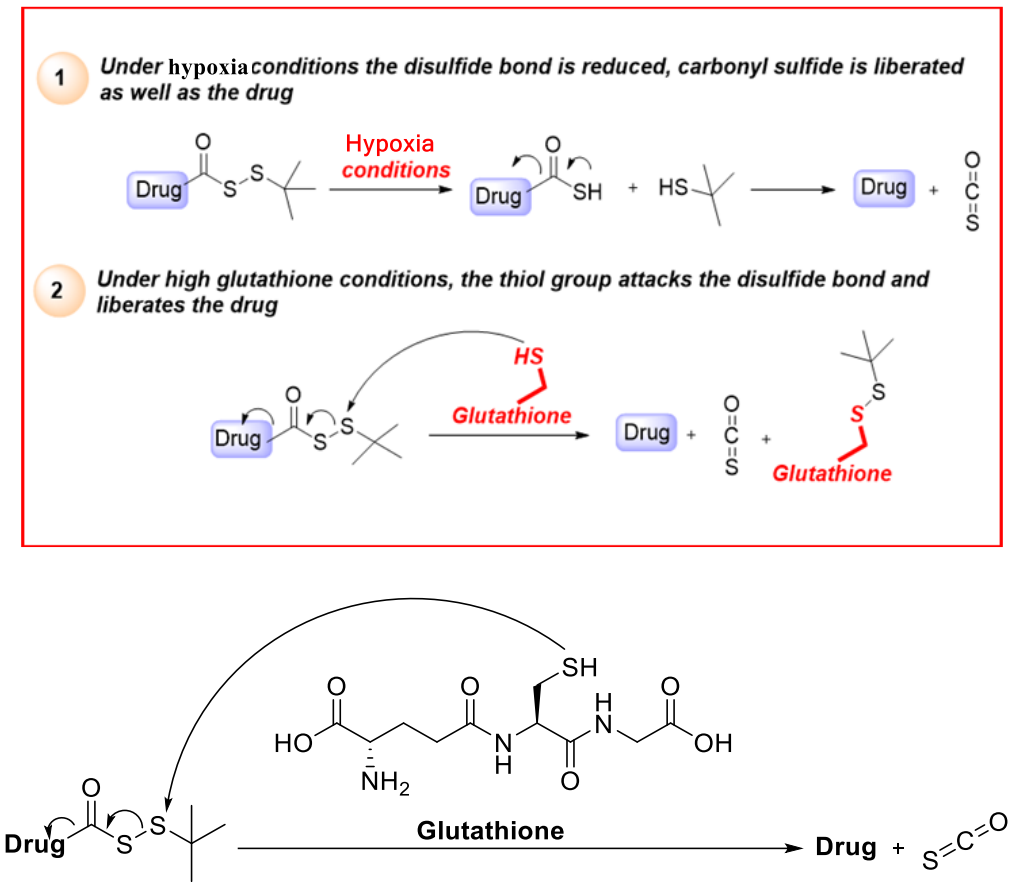


Figure 3. *Above: disulfide reduction mechanism. Below: Mechanism of action of glutathione on the prodrug.*

Disulfide bonds are of great biological importance as they help stabilize the tertiary and quaternary structure of proteins. They are arguably the most important redox covalent bonds that, in proteins, are made up of two cysteine residues (Figure 4).

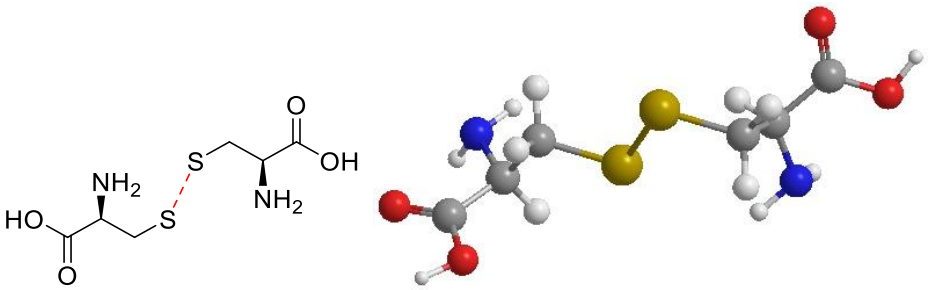


Figure 4. *2D and 3D representation of two cysteines forming a disulfide bond.*

2.1. Optimisation

An important point is the optimization of the disulfide bond cleavage so that this type of prodrug is selective and potent. It is necessary that: (i) the disulfide bond is stabilized in the bloodstream in order to prevent early release of the drug and (ii) there is a high rate of disulfide bond cleavage in cancer cells to ensure further drug release.

Disulfide bonded prodrugs synthesis is complicated because the formation of the desired disulfide bond is not always achieved. Therefore, it is mandatory to introduce protecting groups in order to stabilize it and allow its solubility in water, then being able to transport itself through blood vessels and reach its destination.[6]

In this work, different protective groups have been studied to form disulfide bonds (Figure 5):

- A thiol group attached to a *tert*-butyl group to study whether the steric hindrance is enough to prevent water molecules from attacking the disulfide bond and breaking it prematurely.
- A thiol group with three phenyl rings to test whether increased steric hindrance improves coupling and stability in aqueous solution.



tert-butylthiol tritylthiol

Figure 5. *Structure of the chosen protective groups.*

Once the structure of the disulfide has been designed, it is necessary to look for a drug that can be coupled to it. After successful laboratory tests with different model compounds, such as aniline and phenol, we looked for a drug that has one of these functional groups in its structure that fit well. After a literature search, it was found that some cytotoxic drugs, such as Tacedinaline, which is a histone deacetylase inhibitor, met these requirements.

2.2. Histone Deacetylases

Histone deacetylases, together with histone acetyltransferases, determine the acetylation status of histones. This affects the regulation of gene expression so that histone deacetylase inhibitors have been found to stop the growth, differentiation and/or apoptosis of many tumour cells. Thus, these inhibitors have emerged as an interesting treatment for cancer.[7]

Histone deacetylases (HDAC) are enzymes involved in the regulation of gene expression through the remodeling of chromatin, the structure that carries genetic information located in the nucleus of cells.

Chromatin remodeling, resulting from modification of the structure of nucleosomes (the fundamental units of chromatin) (Figure 6), plays an important role in the epigenetic regulation of gene expression.

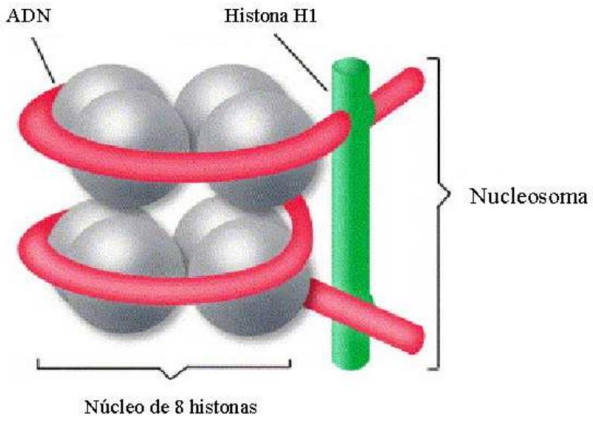


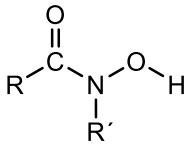
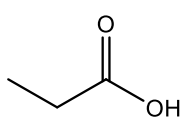
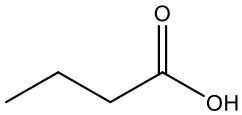
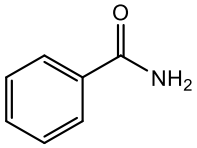
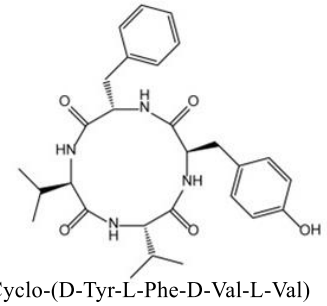
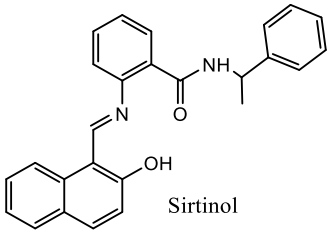
Figure 6. *Representation of the nucleosome.*[8]

Among the modification reactions of amino-terminal tails are: acetylation, methylation, phosphorylation, poly-ADP ribosylation, ubiquitinylation, sumoylation, carbonylation, and glycosylation. Specifically, HDACs catalyze the elimination of acetyl groups, resulting in chromatin condensation and transcriptional repression, thus deactivating the expression of one or more genes [9, 10, 11, 12, 13].

2.2.1. Histone Deacetylases inhibitors

Histone deacetylase inhibitors (HDACi) are a group of compounds that comprise diverse structures and can act as targeted anticancer agents (Table 1).

Table 1. *HDACi classification into 5 classes of compounds.*

HDACi	Structure
I. Hydroxamates	
II. Short-chain fatty acids (aliphatic)	 Propionic acid  Butyric acid
III. Benzamides	
IV. Cyclic tetrapeptides	 Cyclo-(D-Tyr-L-Phe-D-Val-L-Val)
V. Sirtuin inhibitors	 Sirtinol

HDACi act by promoting histone acetylation, which leads to chromatin conducting and activation of a number of genes implicated in cell survival regulation, proliferation, differentiation, and apoptosis.[14,15]

HDACi development may lead to design anti-cancer drugs that are safer and more effective than 'non-targeted' drugs. These kinds of compounds have the potential of inducing the death of cancer cells from a large number of neoplasms, even though their mechanisms of action need to be more studied. Several pathways are known by which they cause cancer cell growth arrest and death: (i) intrinsic or extrinsic apoptotic cell death, (ii) autophagy, and (iii) mitotic cell death. They also inhibit cell migration and tumour angiogenesis and alter the immune response.[11]

2.2.1.1. Tacedinaline

Tacedinaline, known as CI-994 or 4-acetamide-*N*-(2-aminophenyl)benzamide, is a histone deacetylase (HDACi) inhibitor that belongs to the benzamide group (Figure 7). It has a molecular weight of 269.30 g/mol, it is an inhibitor of histone deacetylase class I and has anticancer properties, thanks to its lethal effect against cancer cells. Its use in tumor therapy is possible since it can be combined with other antitumor treatments thereby improving the chemotherapeutic agent. Molecular studies have shown its mechanism of action represented by the histone deacetylation inhibition and cell cycle destabilization.[16]

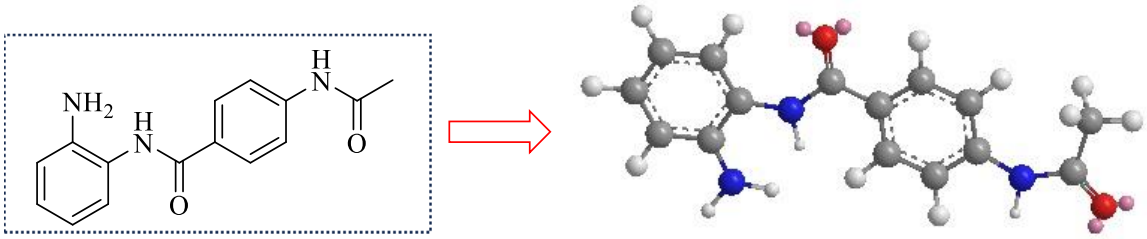


Figure 7. *Tacedinaline 2D and 3D representation.*

Tacedinaline is an anti-cancer agent that blocks angiogenesis, stops cell proliferation by inhibiting DNA repairs, that leads to the apoptosis in the tumour or cells (Figure 8).

The choice of this drug is due to its structure, which has an aniline. According to the studies which will be shown in the following pages, aromatic amines are well coupled to the carrier compound of the synthesized disulfide bond. In addition, the synthesis of this drug is apparently not very complicated. Due to the high price of Tacedinaline, it was decided to synthesize a prodrug containing this cytotoxic compound .[15]

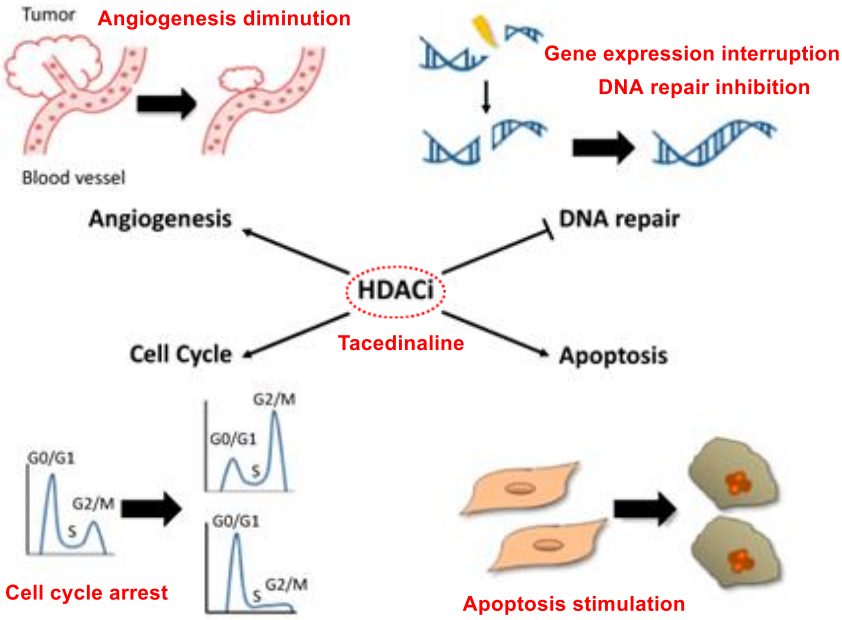


Figure 8. *HDACi effects on cellular processes by the decrease of histone acetylation (modified).*[17]

2.3. Background

2.3.1. Pregnenolone and Farnesol

The research group in collaboration with Prof. Eva Martín del Valle's group (Chemical Engineering Department, USAL) has also studied the development of antineoplastic agents that attack cancer cells by inhibiting the pentose phosphate pathway (Pregnenolone), as well as the production of phospholipids (Farnesol). In this sense, pregnenolone and farnesol are two compounds used as antitumor agents (Figure 9).[18]

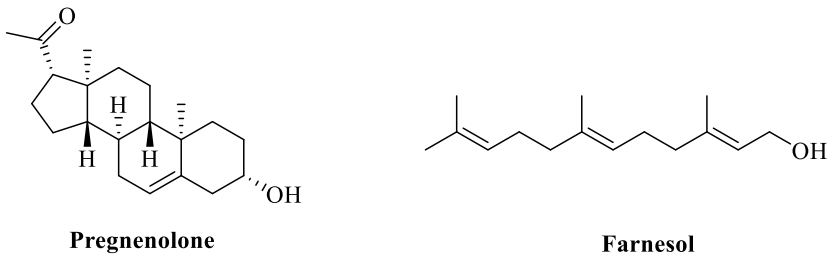


Figure 9. *Structure of Pregnenolone and Farnesol.*

One of the problems with farnesol is that it is a very hydrophobic compound. For this reason, an attempt was made to derivatize these compounds with polar groups containing a disulfide bond, to increase its solubility in water and to ensure its integration through the blood, by

releasing the drug into the reducing environment of the cancer cell. Sodium 2-mercaptoacetate and 2-mercaptoethan-1-aminium chloride were used as polar thiols to construct the disulfide bond by reaction with chlorocarbonylsulfonyl chloride (Figure 10).

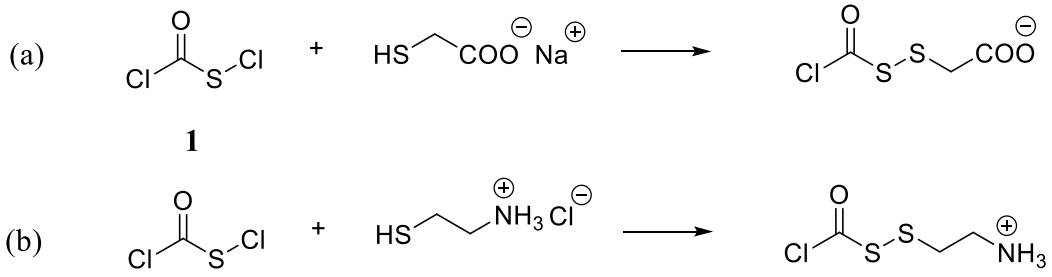


Figure 10. *Synthesis of two disulfides with (a) carboxylate group and (b) ammonium.*

These disulfides were then reacted with toluidine (**2**) as a model compound to form the corresponding amides (Figure 11).

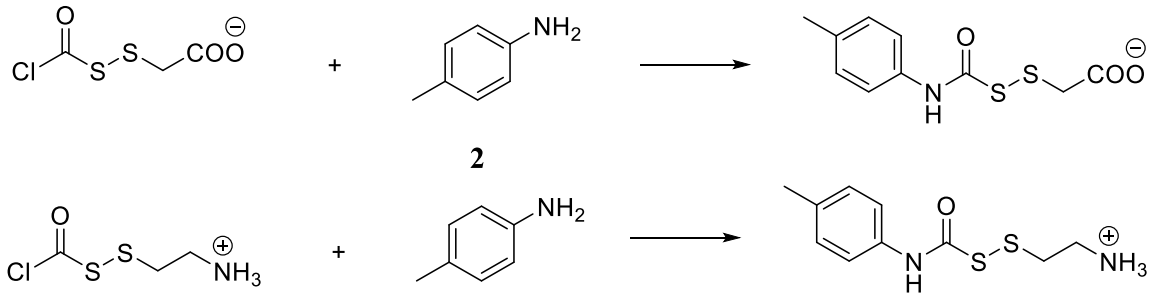


Figure 11. *Reactions of polar disulfides with toluidine.*

Although the goal of solubilization in aqueous solution was achieved, the synthesized compounds were not sufficiently stable in aqueous solution, even when buffering the medium at pH close to 7.

One of the sulfurs from the disulfide bond is thought to be attacked by the OH^- ions from the aqueous solution as shown in Figure 12, as does the SH of glutathione (Figure 3).

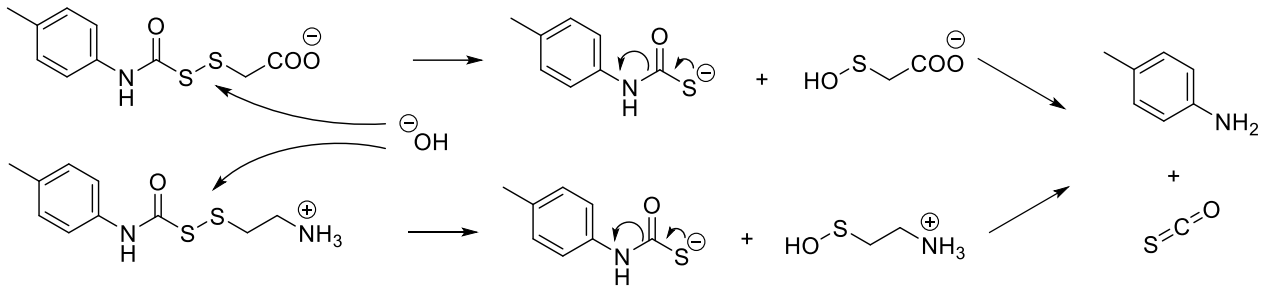


Figure 12. *Hydrolysis of disulfides. Toluidine and carbonyl sulfide (S=C=O) are released.*

As it was necessary for the prodrug to be stable in water at cellular pH so that the drug is not released before reaching the cancer cell, it was decided to continue the research by studying other functional groups that would increase the stability of the prodrug in aqueous solution.

Once the prodrugs are synthesized, their activity against cancer cells will be tested using MTT assay.

2.4. Biological trials: MTT assay

The MTT assay is a widely used method for assessing cellular metabolic activity, often employed to study cell toxicity, viability, and metabolic activity. Nevertheless , it is crucial to apply and interpret this assay correctly to avoid misleading conclusions.[19, 20]

The MTT assay entails the conversion of the water-soluble yellow dye MTT [3-(4,5-dimethylthiazol-2-yl)-2,5-diphenyltetrazolium bromide] to an insoluble purple formazan by the action of mitochondrial reductase.[21] So, this reaction only happens in the cells which are alive. Nearly all mammalian cell ranges reduce the tetrazolium salt sufficiently to carry out MTT assays, in order to obtain a significant 570-nm absorbance reading by the conversion of substrate to chromogenic product by live cells.[21,22]

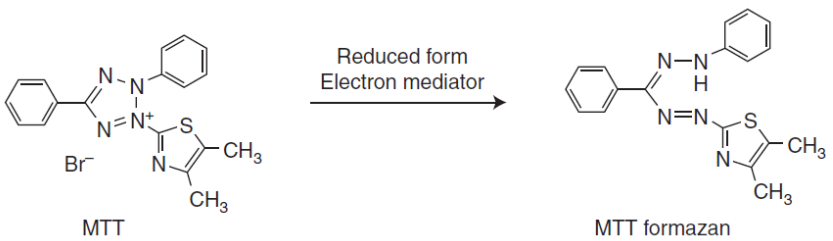


Figure 13. *Reduction of MTT-to-MTT formazan.*[19]

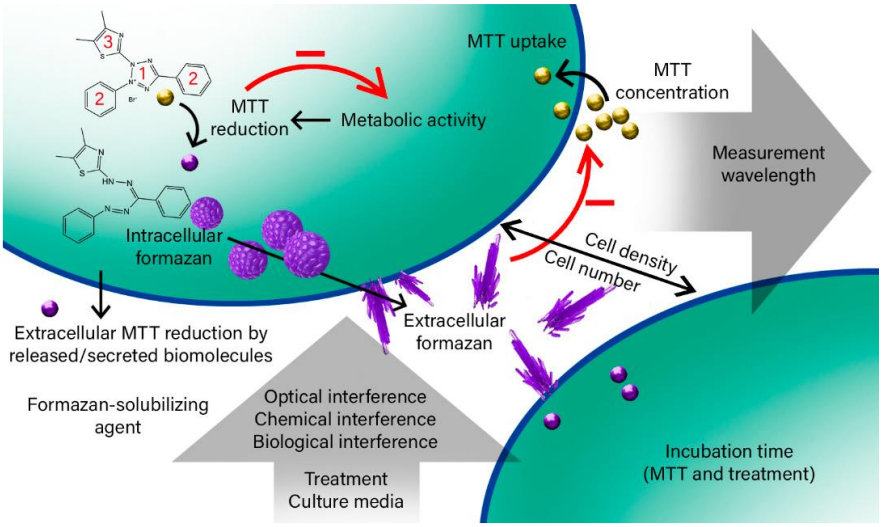


Figure 14. *Cellular factors influencing the final absorbance measurements obtained from MTT assay.*[19]

2.4.1. Cell Viability: MTT Assay technique

Since the MTT assay is realized in multi well plates, it is considered as a good option to implement several experiments (several cytotoxic syntheses) for a big range of samples in a short time, given its importance. The method has been extended and improved by several authors (Denizot and Lang, 1986; Gerlier and Thomasset, 1986; Carmichael *et al.*, 1987; McHale and McHale, 1988; Edmondson *et al.*, 1988; Plumb *et al.*, 1989; Niks and Otto, 1990; Heo *et al.*, 1990; Rubinstein *et al.*, 1990; Merlin *et al.*, 1992; Cedillo-Rivera et al., 1992; Hussain *et al.*, 1993; Thom *et al.*, 1993; Marshall *et al.*, 1995; Sieuwerts *et al.*, 1995; Chiba *et al.*, 1998).[23] In order to perform a successful MTT assay a well-defined material and protocol must be followed. In compliance with "*Animal Cell Culture: Principles and Practice"*[24]*(S. Mani and G. Swar.,2023)* the MTT assay should be carried out as follow :

Materials

(a) MTT solution (5 mg/ml MTT in PBS, pH 7.4, #M2128 Sigma Aldrich).
(b) PBS.
(c) Isopropanol or DMSO.
(d) DMEM.
(e) 96 well plates.

Protocol

(a) Prepare the MTT solution by dissolving 5 mg of MTT powder in 1 ml PBS solution (should be protected from light at 4 ºC and well solubilized).

(b) Add 10^4 cells and 100 µL of culture medium (e.g.DMEM) to each well of the 96-well plate. Remember to consider three replicates for each concentration. Then incubate the cells in 5% CO_2 and 37 °C for ~12 h to allow the cells to adhere to the plate bottom.

(c) Once the cells adhere, treat the cells with various concentrations of the desired compound, followed by incubation. Here, the incubation period is your required treatment time (e.g.24, 48 and 72 h).

(d) After the treatment period is over, discard the media and then pour 100 µL of culture medium into each of the wells followed by the addition of 10 µL of MTT solution per well. Then keep the plates for incubation in 5% CO_2 and 37 °C for 3–4 h.

(e) Discard the supernatant, followed by the addition of 100 µL of the suitable detergent, isopropanol or DMSO for dissolving the formazan crystals formed by the MTT. Preferably, slowly shake the plates for 10–15 mins to obtain a uniformly dissolved solution.

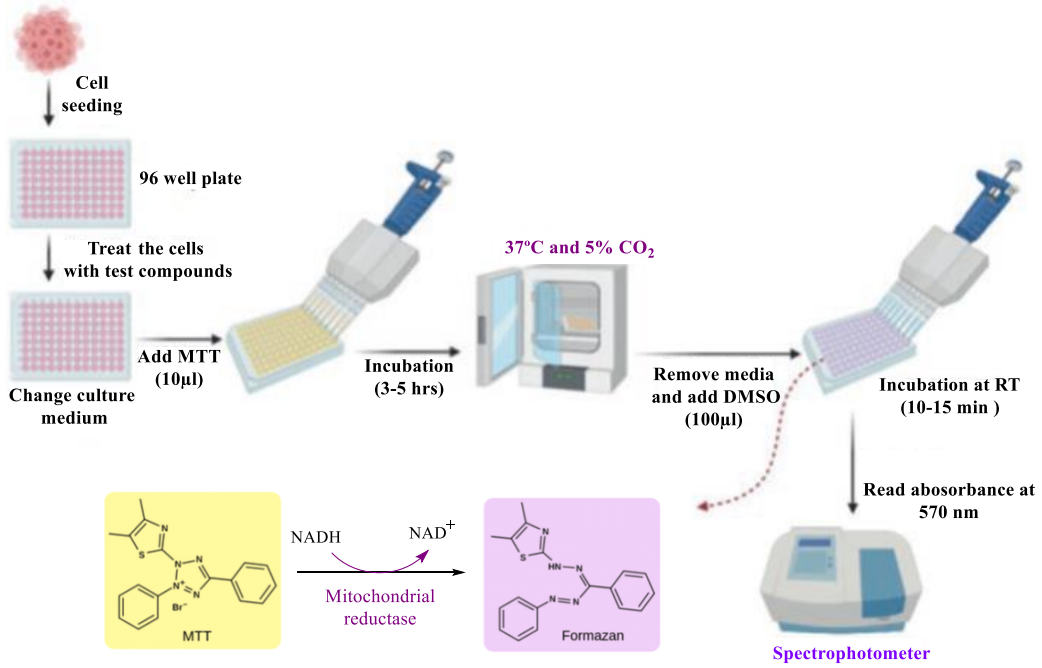


Figure 15.*The MTT assay procedure representation.*[24]

(f) Now, read the plates at wavelength 570 nm using a spectrophotometer.

(g) Compute the percentage of viable cells as follows:

$$\textbf{Viable cells (\%)} = \frac{\text{Total number of viable cells per mL of aliquot}}{\text{Total number of cells per mL of aliquot}} \times 100$$

(h) The data are reported in the form of a cell survival diagram (figure 16).

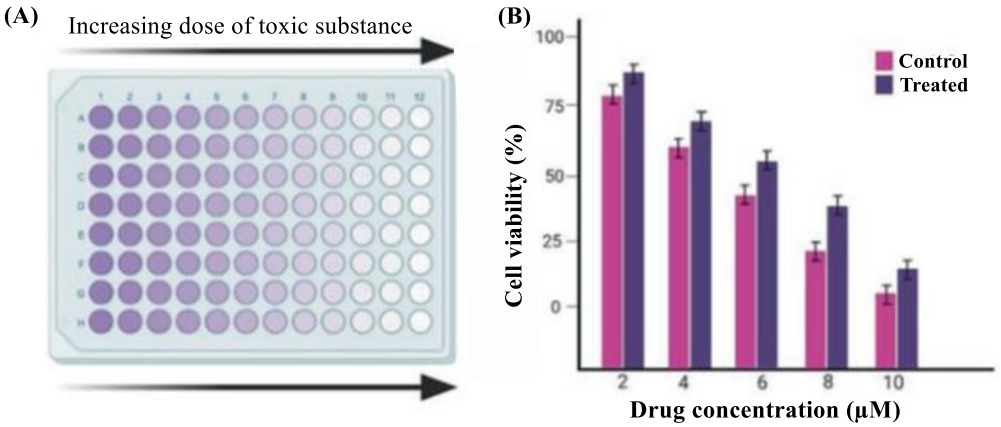


Figure 16. *The MTT assay results representation: (**A**) Sample of the 96 well-plates after MTT assay plate where the purple colour indicates MTT formazan. (**B**) Cell survival data are presented in the form of a bar graph.*[24]

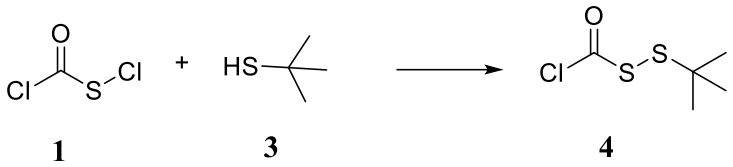
3. Methodology

As outlined above, we started by designing and developing other types of structures to be able to synthesize a prodrug that was enough stable in water. However, it should also be noted that this compound should not be too stable in water either, because it is necessary for the disulfide bond to be reduced or broken upon reaching its destination in order to release the drug.

3.1. Synthesis of disulfide bonded compounds

As a first hypothesis, the possibility was raised that, by increasing the steric hindrance around the S that undergoes nucleophilic attack by OH^-, it would be possible to increase the stability of the compound with the disulfide bond in aqueous solution. Thus, several structures containing a bulky group in the disulfide were designed and compounds **4** and **6** were synthesized (Figures 17 and 18).

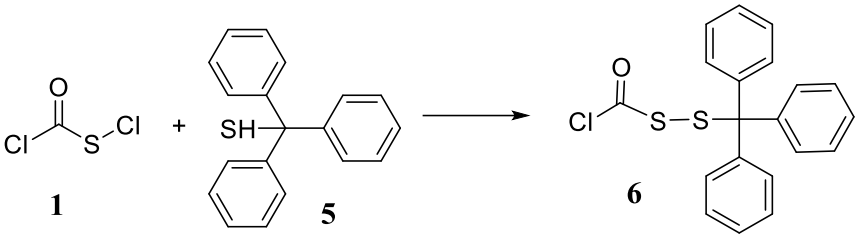
I. *S,S-tert*-butyl carbonchloride(dithioperoxoate)



1 **3** **4**

Figure 17. *Synthesis of compound **4**.*

II. *S,S*-trityl carbonchloride(dithioperoxoate)

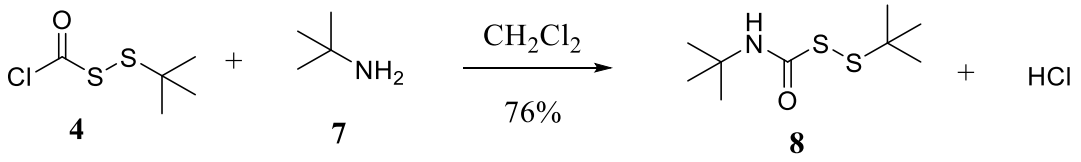


1 **5** **6**

Figure 18. *Synthesis of compound **6**.*

Reaction of compound **4** with *tert*-butylamine was performed to check the viability of compound **4** (Figure 19).

III. *S,S-tert*-butyl *tert*-butylcarbamate(dithioperoxoate)



4 **7** **8**

Figure 19. *Synthesis of compound **8**.*

3.2. Study of functional groups able to react with acid chlorides 4 and 6

Then, several experiments were carried out aimed at finding what kind of drugs could be functionalized with acid chlorides **4** and **6** containing the disulfide bond. Aliphatic and aromatic amines and aliphatic and aromatic alcohols were used as model compounds. In addition, in most cases, reactions were carried out at a concentration of 0.2 M in $CDCl_3$ to perform the analysis directly and quickly by ^1H NMR.

This would allow the coupling between the drug and the functional group containing the disulfide bond directly in the NMR tube, which has the advantage of being able to work with small amounts of drug (normally a few milligrams are needed to synthesize the product and perform the cell assays), while minimizing compound losses.

Due to the high price of the type of drugs to be functionalized, the possibility of carrying out the reaction directly in the NMR tube and being able to use the prodrug directly after washing with water and evaporating the solvent is highly attractive.

The study begins by performing a ^{1}H NMR spectrum of the molecule that simulates the drug. This makes it possible to assess whether the subsequent reaction with the disulfide takes place spontaneously. 2,4,6-collidine is then added to check if it is necessary to use an auxiliary base to form the compound since HCl is released when the reaction occurs, which may need to be neutralized to avoid amine protonation and deactivation.

Finally, it is checked if the compound is stable over time and aqueous conditions by removing the auxiliary base with an aqueous solution of HCl 2M.

The first reaction was made with benzyl alcohol (Figure 20).

I. *O*-benzyl *S*,*S*-*tert*-butyl carbon(dithioperoxoate)

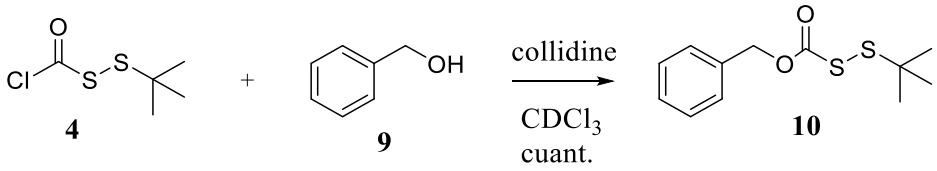


Figure 20. *Synthesis of compound **10**.*

The ^{1}H NMR spectra (in the aromatic region) for the synthesis of compound **10** (shown in Figure 21) correspond, in ascending order, to:

1. Benzyl alcohol.
2. Benzyl alcohol with the addition of disulfide **4**.
3. The above mixture after the addition of 1 equivalent of 2,4,6-collidine.
4. The reaction mixture 24 hours later.
5. The above solution after adding a few drops of HCl 2M.

It is observed that an auxiliary base (2,4,6-collidine) is necessary for the synthesis of compound **10**. This compound is stable for 24 hours, even after removing excess 2,4,6-collidine with 2M

HCl. This indicates that benzyl alcohol would be a good functional group in the drug structure to be functionalized with acid chloride **4**.

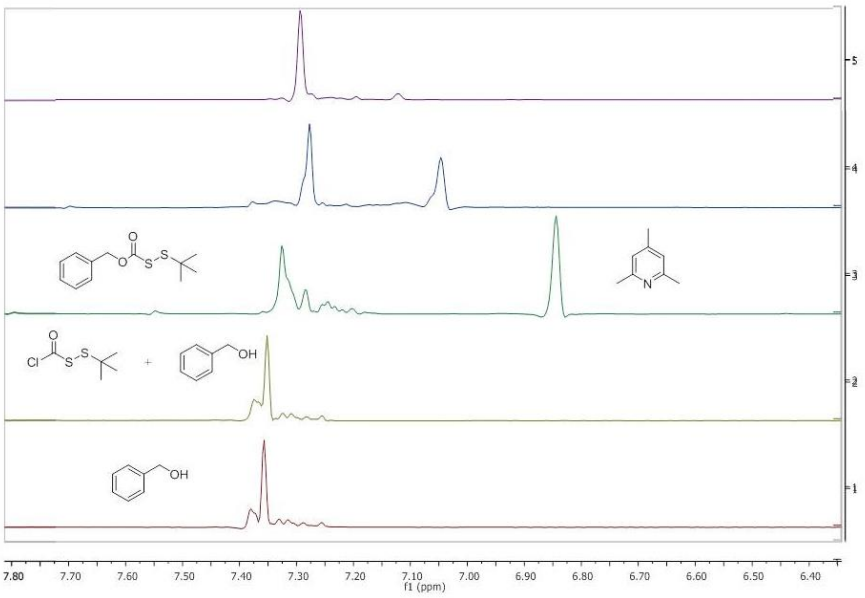


Figure 21. *^{1}H NMR spectra (6.40-7.80 ppm) in deuterochloroform at 20 ºC showing the evolution of reactions for the synthesis of compound **10**.*

Then, benzylamine was tested to be coupled with compound **4** (Figure 22).

II. *S,S-tert*-butylbenzylcarbame(dithioperoxoate)

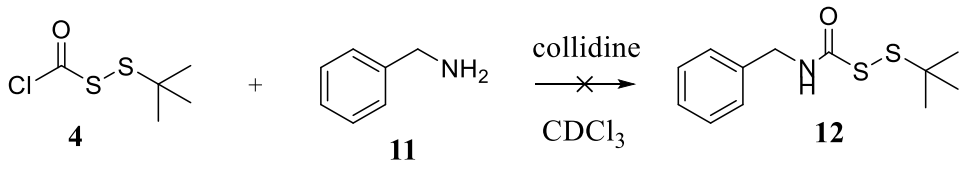


Figure 22. *Synthesis of compound **12**.*

The ^{1}H NMR spectra (in the aromatic region) for the synthesis of compound **12** (shown in Figure 23) correspond, in ascending order, to:

1. Benzylamine.
2. Benzylamine with the addition of disulfide **4**.
3. The above mixture after the addition of 1 equivalent of 2,4,6-collidine.
4. The reaction mixture 24 hours later.
5. The previous solution after adding a few drops of aqueous solution of HCl 2M.

The formation of two products is observed with the addition of disulfide **4**. With the addition of 2,4,6-collidine, compound **12** is obtained, which remains stable for 24 hours. By attempting

to eliminate 2,4,6-collidine with HCl, the unidentified initial products are recovered. This compound is not stable, so benzylamine is not a suitable group. Therefore, the following experiment is performed with *p*-chloroaniline, which is expected to have an activity more similar to that of benzyl alcohol (Figure 23).

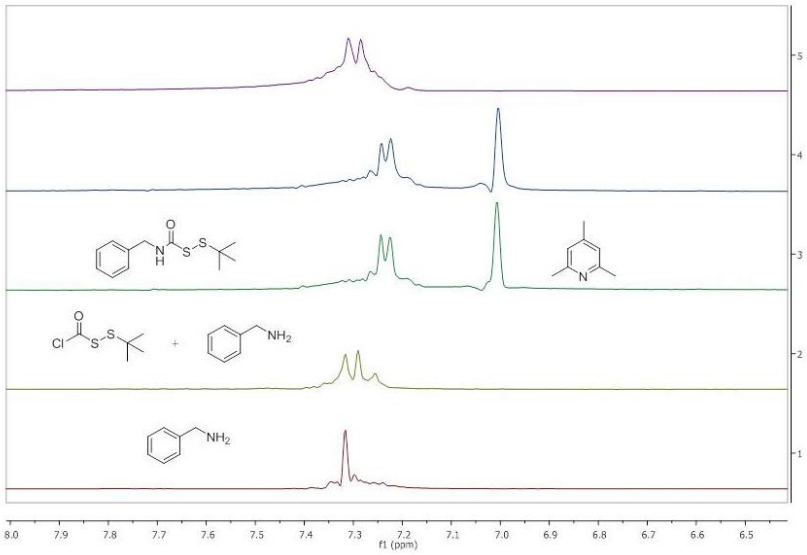


Figure 23. *^{1}H NMR spectra (6.5-8.0 ppm) in deuterochloroform at 20 ºC showing the evolution of reactions for the synthesis of compound **12**.*

III. *S,S-tert*-butyl(4-chlorophenyl)carbame(dithioperoxoate)

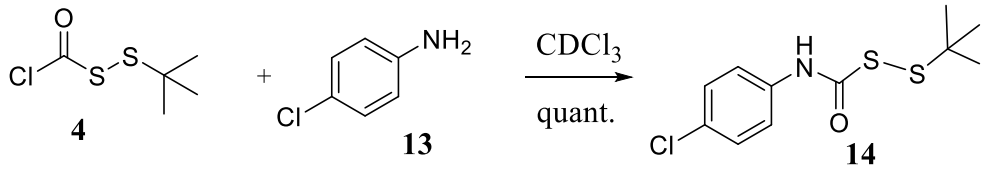


Figure 24. *Synthesis of compound **14**.*

The ^{1}H NMR spectra (aromatic region) for the synthesis of compound **14** (shown in Figure 25) correspond, in ascending order, to:

1. *p*-Chloroaniline.
2. *p*-Chloroaniline with disulfide **4**.
3. The above mixture after the addition of 1 equivalent of 2,4,6-collidine.
4. The reaction mixture 24 hours later.
5. The previous solution after adding a few drops of aqueous solution of HCl 2M.

In this case, it can be seen that it is not necessary to use an auxiliary base to obtain compound **14**. It remains stable for 24 hours and after HCl treatment to remove the excess of 2,4,6-collidine.

p-Chloroaniline is a very promising group, which is why the aim is to find a drug that contains aniline in its structure.

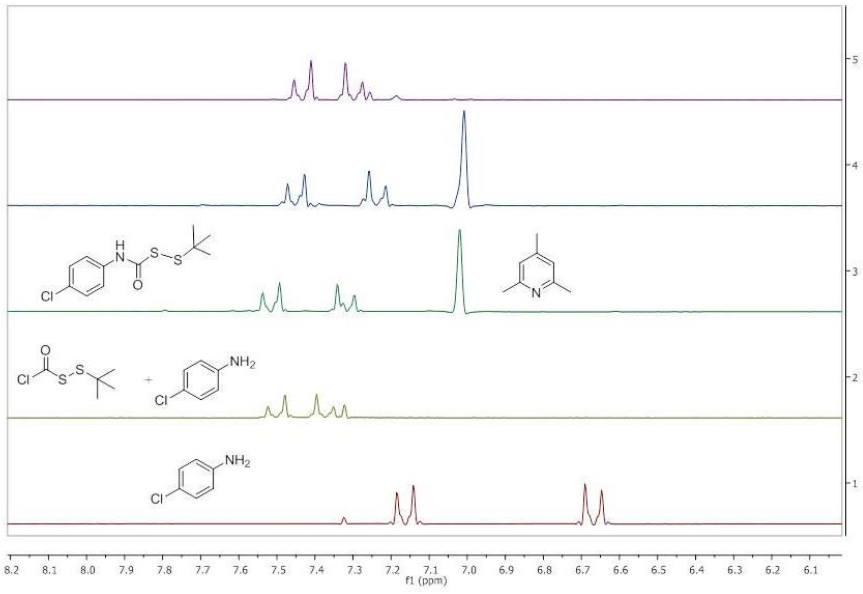


Figure 25. *^{1}H NMR spectra (6.1-8.2 ppm) in deuterochloroform at 20 ºC showing the evolution of reactions for the synthesis of compound **14**.*

We also tested compound **6** with benzyl alcohol (Figure 26).

IV. *O*-benzyl-*S*,*S*-trityl carbon(dithioperoxoate)

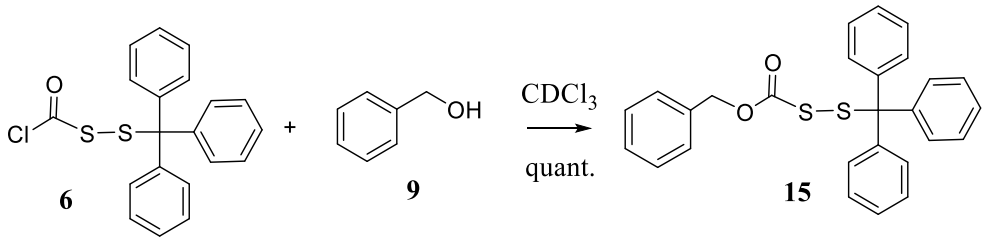


Figure 26. *Synthesis of compound **15**.*

The ^{1}H NMR spectra (aromatic region) for the synthesis of compound **15** (shown in Figure 27) correspond, in ascending order, to:

1. Benzyl alcohol.
2. Benzyl alcohol with the addition of disulfide **4**.
3. The above mixture after the addition of 1 equivalent of 2,4,6-collidine.

4. The product with CD_3OD.

Adding the collidine increases the conversion of the reaction. In this case, it was decided to study its stability by dissolving it in deuterated methanol, to mimic the protic polar environment present in the cells. Methanol was used and not water because the trityl group is too nonpolar to allow the compound to be dissolved in water. The shift of the spectrum signals was observed, which leads to the probable hydrolysis of the compound by methanol.

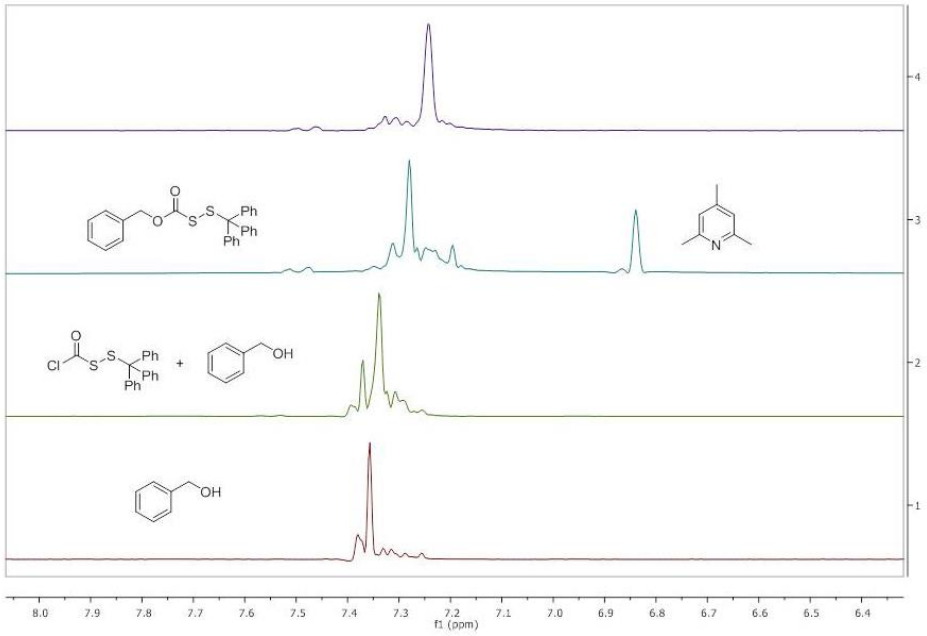


Figure 27. *^{1}H NMR spectra (6.4-8.0 ppm) in deuterochloroform at 20 ºC showing the evolution of reactions for the synthesis of compound **15**.*

Compound **6** was also tested with *p*-chloroaniline (Figure 28).

V. *S,S*-trityl(4-chlorobenzyl)carbame(dithioperoxoate)

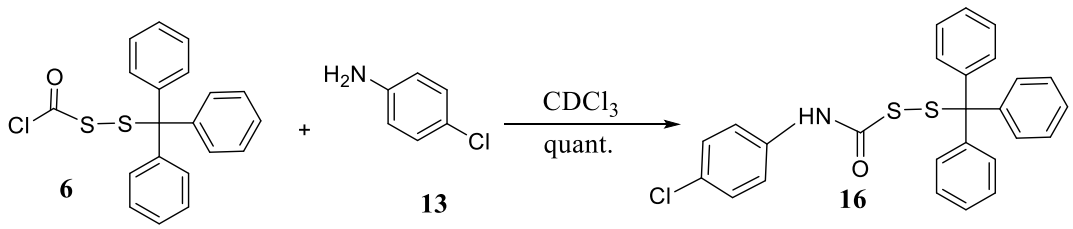


Figure 28. *Synthesis of compound **16**.*

The ^{1}H NMR spectra (aromatic region) for the synthesis of compound **16** (shown in Figure 29) correspond, in ascending order, to:

1. *p*-Chloroaniline.
2. *p*-Chloroaniline with the addition of disulfide **4**.

3. The above mixture after the addition of 1 equivalent of 2,4,6-collidine.
4. The previous solution after adding a few drops of aqueous solution of HCl 2M.

In this case, the auxiliary base would not have been necessary, the compound with the disulfide bond is obtained directly. However, addition of collidine produces the generation of another compound, as it can be observed the appearance of two additional doublets in the ^{1}H NMR spectrum. Then, after the addition of HCl, one compound is obtained. This experiment reiterates the possible effectiveness of aniline on the drug structure.

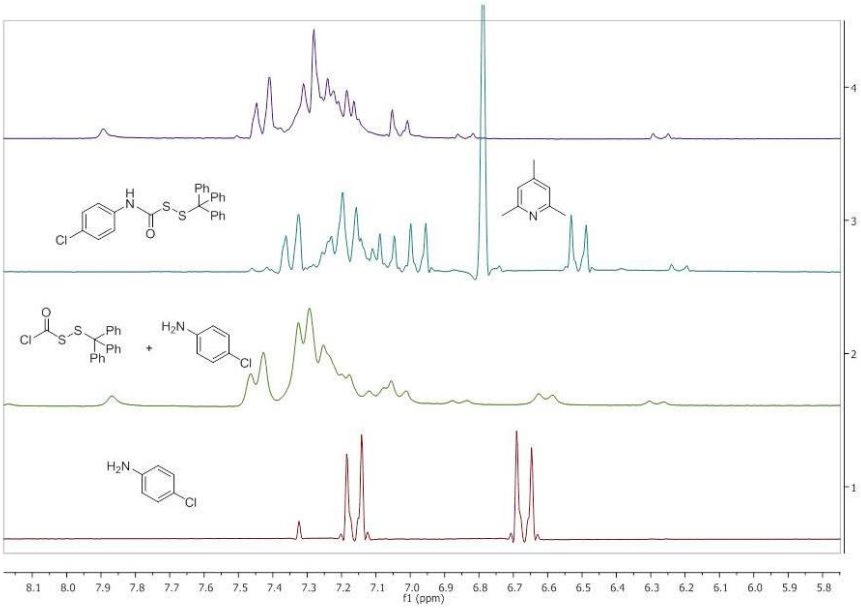


Figure 29. *^{1}H NMR spectra (5.8-8.1 ppm) in deuterochloroform at 20 ºC showing the evolution of reactions for the synthesis of compound **16**.*

Then, the stability of compound **10** was studied in a buffered medium at pH 7 that simulated the cellular environment. In this case, several trials were performed from a stock solution composed of 2.7 mg of compound **10** and 1 ml of MeOD. MeOD was used as a protic solvent to simulate the effect of water, because compound **10** is not soluble in water and does not contain polar groups.

The reducing conditions of the cancerous cells under hypoxia conditions as well as the overexpression of glutathione were simulated with the addition of dithiothreitol (Figure 30).

Two experiments were performed: (i) 3.94 mg of dithiothreitol and 5 mg of a buffer solution of K_2HPO_4 and KH_2PO_4 were added in a vial with 0.5 ml of the stock solution of compound **10** in MeOD and (ii) in another vial with 0.5 ml of stock solution of compound **10** only 5 mg of the buffered solution of phosphates was added.

The result of the experiment showed that compound **10** was stable in the buffered medium until dithiothreitol was added, breaking the disulfide bond. Therefore, benzyl alcohol is reiterated as a good functional group that can be contained in the structure of the drug.

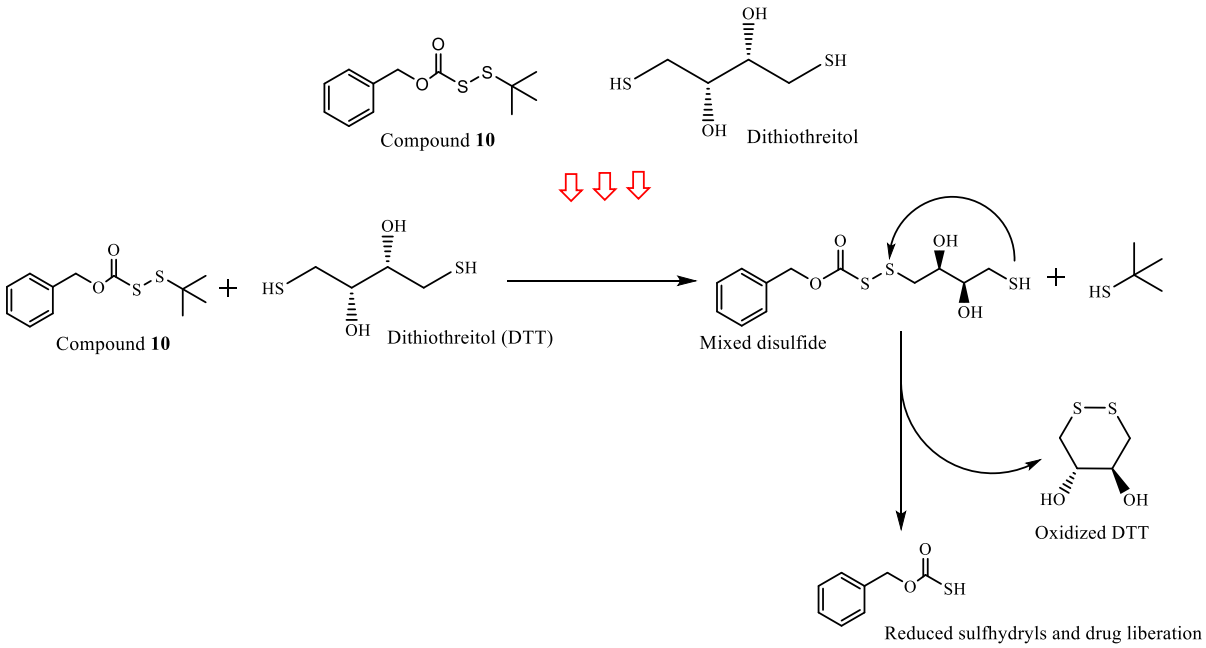


Figure 30. *Above: Dithiothreitol and compound **10** structure. Below: Dithiothreitol mechanism of action to break the disulfide bond.*

3.3. Synthesis of Tacedinaline

The good results that *p*-chloroaniline offered in the previous reactivity tests with acid chloride **4** led to the search for a drug that contains an aniline group in its structure. Among several possibilities, Tacedinaline was chosen (**21**).

As it is known Tacedinaline is primarily an investigational compound rather than a widely commercialized drug, to carry out its synthesis, the retrosynthetic route in figure 31 was proposed.

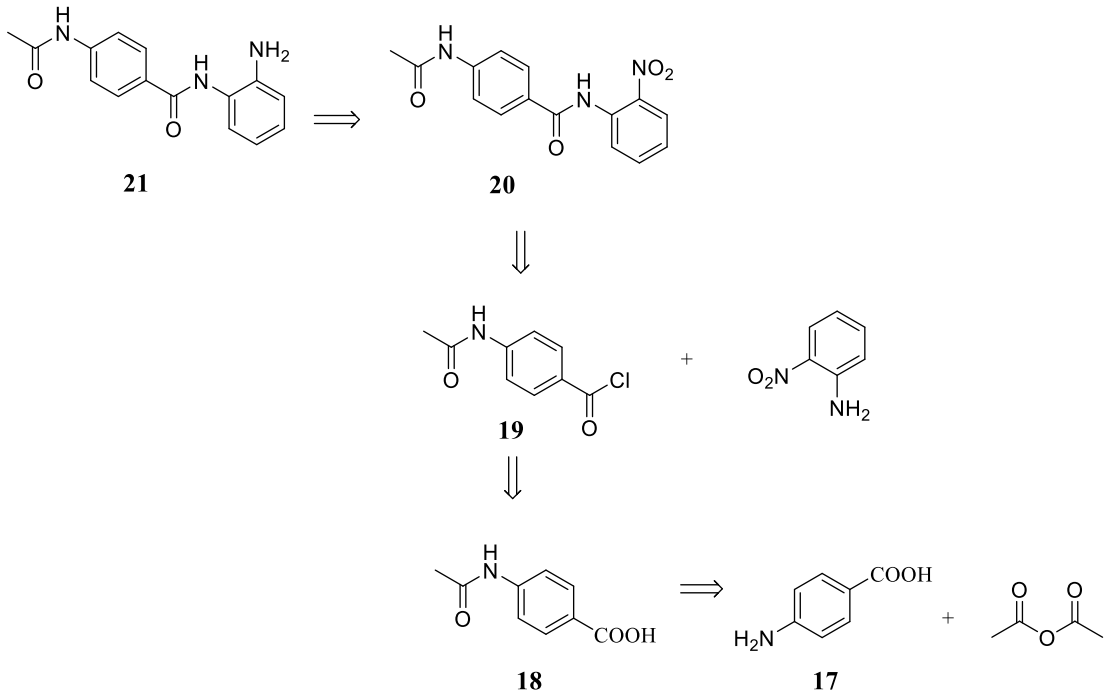


Figure 31. *Retrosynthesis of compound **21**.*

Compound **18** was obtained in good yield (68%) by dissolving compound **17** in Ac_2O and pyridine (Figure 32).

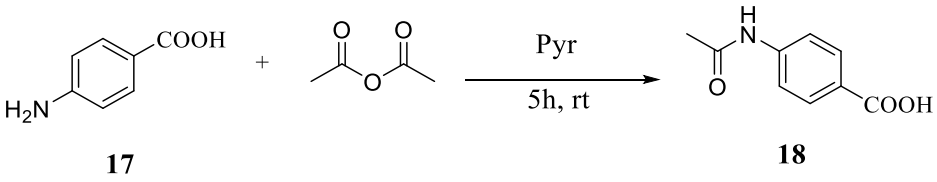


Figure 32. *Synthesis of compound **18**.*

Obtaining acid chloride (**19**) was more complicated, and different reaction conditions were studied.

The first reaction was carried out refluxing compound **18** with thionyl chloride until the HCl and SO_2 bubbles disappeared. Under these conditions, the solution turned orange and analysis of the reaction mixture by ^1H NMR showed that the desired acid chloride **19** had not been obtained.

In a second experiment, oxalyl chloride was tested on dichloromethane (DCM) and a few drops of dimethylformamide (DMF) as a catalyst. After 24 hours of reacting, it was observed that the compound had not dissolved, so it was decided to add more DCM, oxalyl chloride and DMF, until the compound was dissolved. After evaporating the solvents under reduced pressure, and analysing the crude by ^{1}H NMR, the desired reaction product was not observed.

The third experiment was carried out with phosphorus pentachloride (PCl_5), in excess, and DCM. When all the starting material had been dissolved, the volatiles were evaporated under reduced pressure at 70 °C to remove all excess of $POCl_3$. However, analysis by ^{1}H NMR showed unexpected shielding of acetamide methyl group. We believe that under these reaction conditions the iminochloride depicted in figure 33 is obtained.

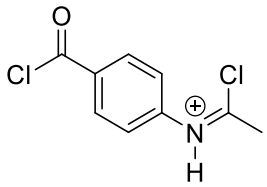


Figure 33. *Representation of the iminochloride.*

To increase the nucleophilia of carboxylic acid and promote the formation of the acid chloride over that of imininochloride, carboxylate was first synthesized by dissolving the acid in DCM and adding triethylamine (TEA) (Figure 34).

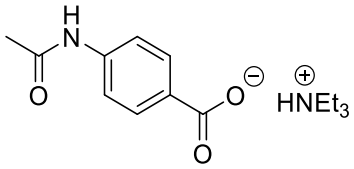


Figure 34. *Representation of triethylammonium carboxylate*.

The solvent and excess of triethylamine were then evaporated under reduced pressure, the residue was dissolved in DCM and cooled down with an ice bath, and an equivalent of PCl_5 was added, stirring the solution until the compound was dissolved, finally obtaining the acid chloride (Figure 35).

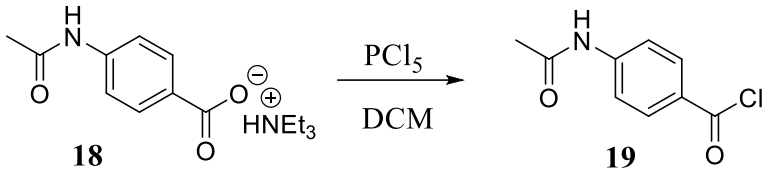


Figure 35. *Synthesis of compound **19**.*

Due to the low nucleophilia of 2-nitroaniline, different reaction conditions were studied to perform the coupling with acid chloride **19**: (1) with DCM and TEA, (2) with THF and (3) with pyridine (Figure 36). In all three cases, compound **20** was obtained.

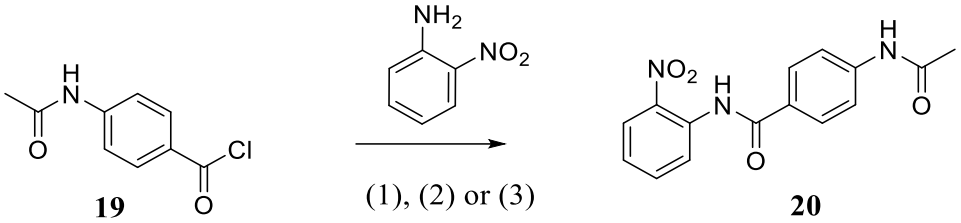


Figure 36. *Synthesis of compound **20**.*

In all three cases, once the reaction was complete, an aqueous solution of 2M HCl was added, and the desired compound was extracted with ethyl acetate. Column purification on silica gel was necessary. Due to the low yield obtained of compound **20,** subsequently, its synthesis was optimized by melting compound **19** with excess of 2-nitroaniline, maintaining agitation for 12 hours. In this case, compound **20** was obtained with 61% yield (Figure 37)

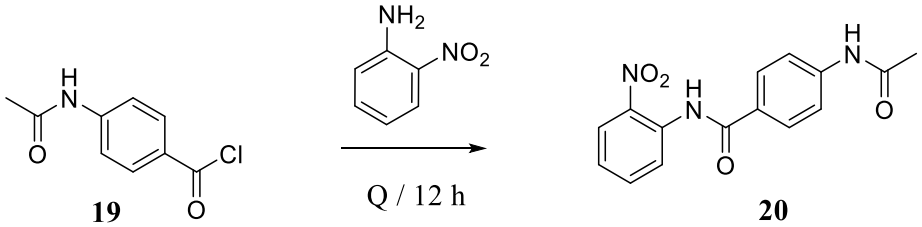


Figure 37. *Compound synthesis **20**.*

The last step in the synthesis of Tacedinaline **21** is hydrogenation with palladium on carbon (Figure 38).

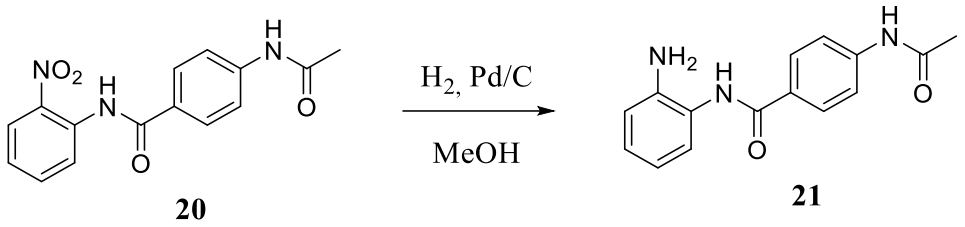


Figure 38. *Synthesis of compound **21**.*

3.4. Functionalization of Tacedinaline with acid chloride 4

In figure 40 it can be seen the evolution of the reactions for the synthesis of compound **22** by ^{1}H NMR, following the previous methodology (Figure 39). Compound **4** has been chosen to be attached to compound **21** (Tacedinaline) due to its ease of attachment.

I. S,S-tert-butyl(2-(4-acetamidobenzamide)phenyl)carbame(dithioperoxoate)

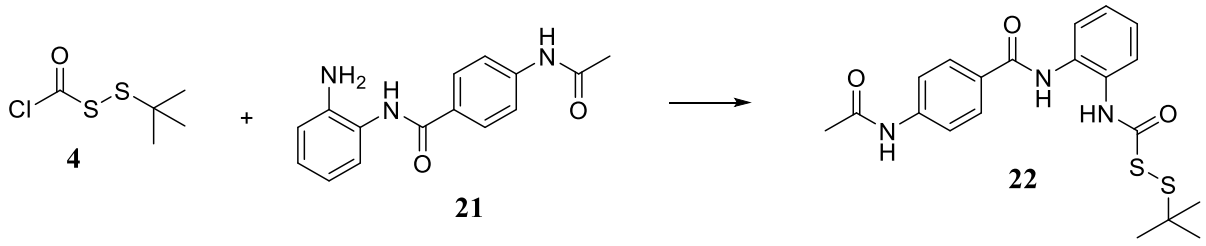


Figure 39. *Synthesis of compound **22**.*

The ^{1}H NMR spectra (aromatic region) for the synthesis of compound **22** performed in deuterochloroform (shown in Figure 40), correspond, in ascending order, to:

1. Tacedinaline.
2. Tacedinaline with the addition of disulfide **4**.
3. The above mixture after the addition of 1 equivalent of 2,4,6-collidine.
4. The previous solution after adding a few drops of aqueous solution of HCl 2M.
5. The organic phase after washing with H_2O.

In the second spectrum, the signals of Tacedinaline are not easy to identify due to its poor solubility in $CDCl_3$. The addition of an auxiliary base is necessary to dissolve the compound, as can be seen in the third spectrum. The subsequent removal of the collidine signals, with an aqueous solution of 2M HCl, allows the better observation of the signals of compound **22**. It

can be seen how the signals from 6.8-6.9 ppm to 7.5-7.6 ppm have been deshielded. Finally, the removal of traces of collidine hydrochloride, with H_2O, keeps compound **22** stable.

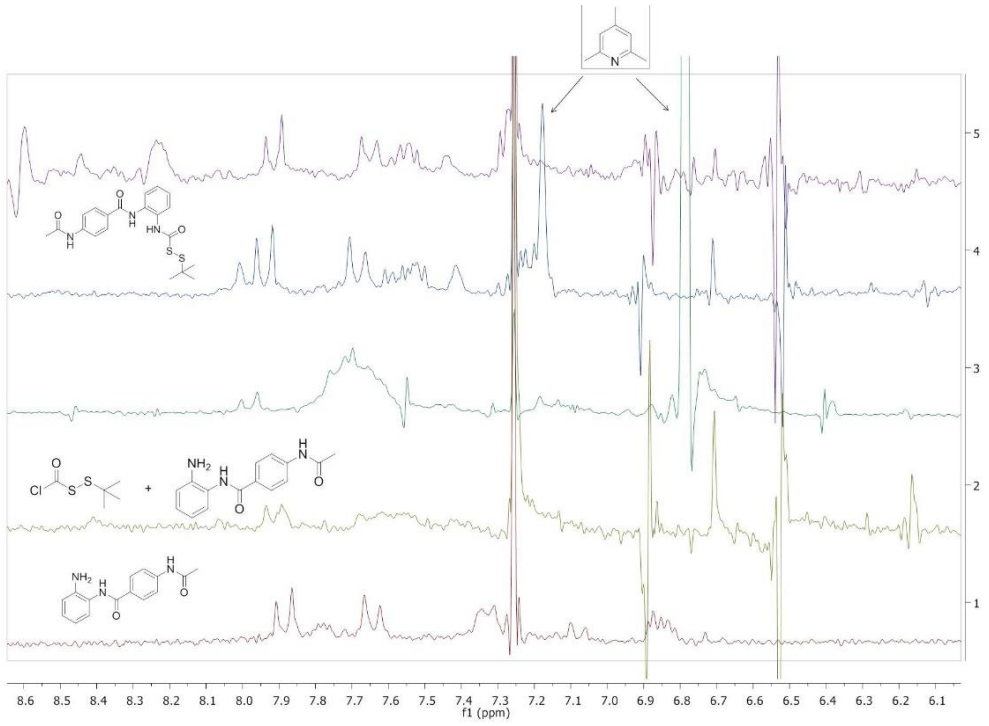
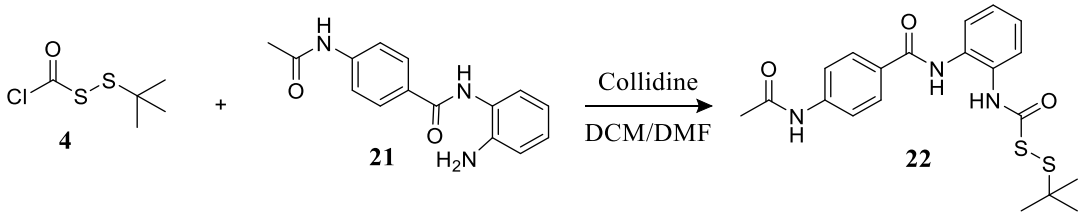


Figure 40. *^{1}H NMR spectra (6.1-8.6 ppm) in deuterochloroform at 20 ºC showing the evolution of reactions for the synthesis of compound **22**.*

However, due to the difficulty to analyse the reaction mixture, it was decided to carry out the synthesis of the prodrug on a larger scale. DMF was added as a cosolvent to increase the solubility of Tacedinaline.

3.5. Prodrug synthesis

I. S,S-tert-butyl(2-(4-acetamidobenzamide)phenyl)carbame(dithioperoxoate)



4 **21** **22**

Figure 41. *Synthesis of compound **22**.*

To synthesize compound **22** at the scale of 100 mg, compound **21** is added to compound **4**, dissolved in DCM, maintaining the reaction at 0 ºC. Because compound **21** is not completely dissolved, DMF and 2 equivalents of 2,4,6-collidine are added as an auxiliary base, and the reaction is left to stir overnight.

After this time, the reaction mixture is washed with an aqueous solution of 2M HCl and purified by chromatographic column on silica gel. However, a low yield is obtained in this reaction, obtaining 6 mg (7%) of the product.

3.6. Cell assays

Finally, both Tacedinaline "compound X" and prodrug **22** "compound X-S2" (Figure 42 and 43) were tested on healthy (fibroblast-HS-5) and colon cancer cells (HCT-116), both under hypoxia conditions. Cell viability was measured at 24 h and 48 h. The results of these tests are shown in figures 42 and 43.

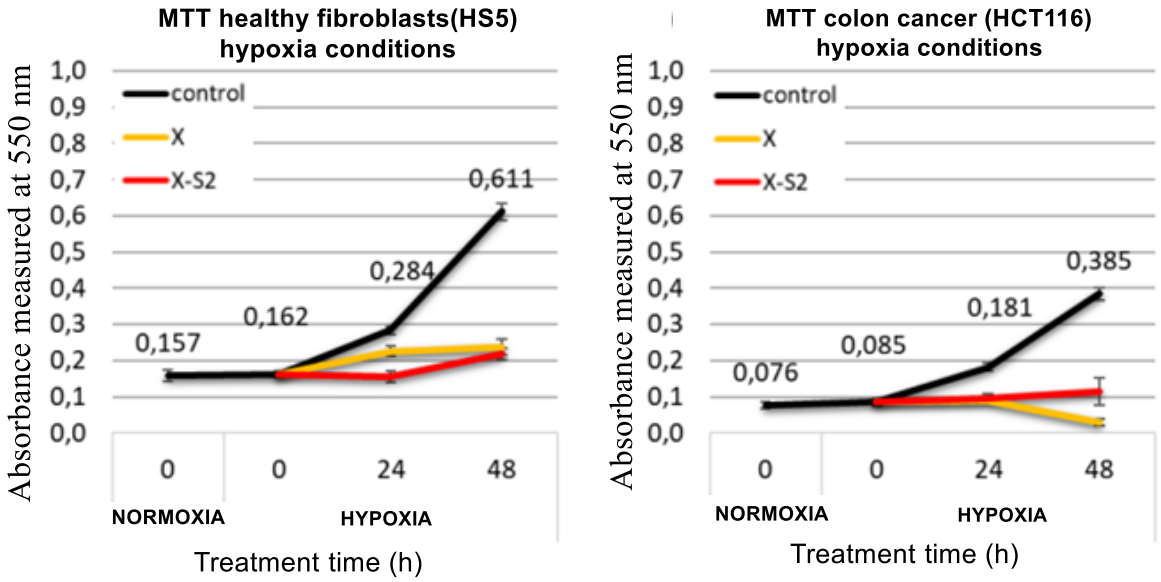


Figure 42. *Left: Effect of Tacedinaline and prodrug **22** on healthy fibroblasts under hypoxia conditions. Right: effect of Tacedinaline and prodrug **22** on colon cancer cells under hypoxia conditions.*

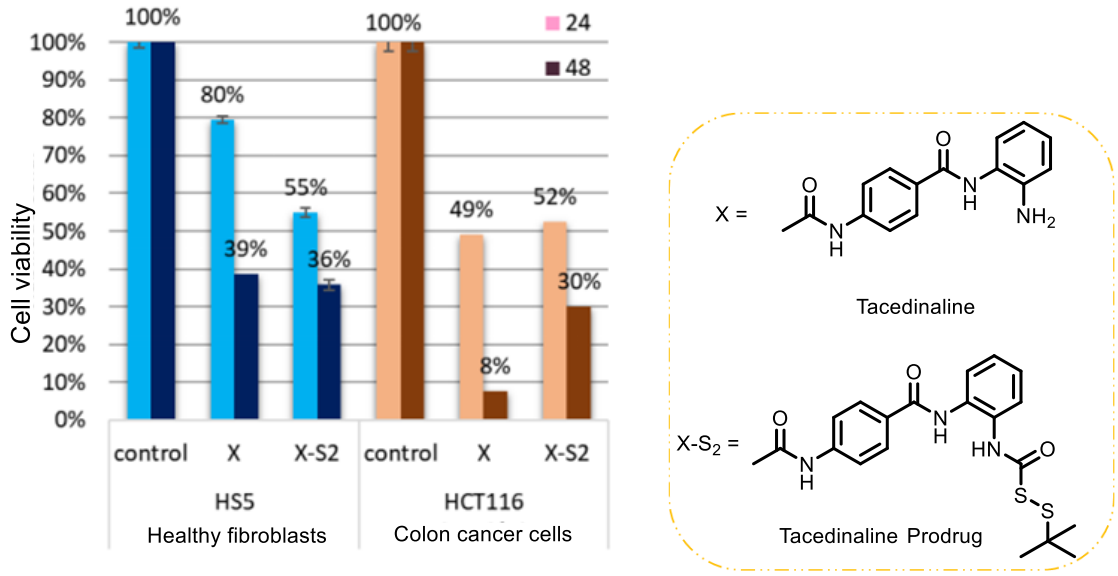


Figure 43. *Comparative graph of the cell viability of both compounds in healthy and cancerous cells under hypoxia conditions.*

Figure 43 shows the percentage of living cells that remain 24 and 48 hours after treatment with the drug and prodrug, both in healthy (HS-5) and cancer (HCT-116) cells under hypoxia conditions. The following information can be obtained from this graph:

- In healthy cells, Tacedinaline is not highly cytotoxic during the first 24 hours, unlike the prodrug which has reduced the viability to 55 %. After 48 hours, an increase in cytotoxicity is observed, with this activity being very similar in Tacedinaline and the prodrug (36-39%).

- In cancer cells, the cytotoxic effect of Tacedinaline is significantly increased compared to healthy cells at both 24 and 48 hours after treatment (49% and 8%, respectively). On the other hand, the prodrug maintains practically the same cytotoxicity, being less effective than Tacedinaline (52% vs 49% after 24 h and 30% vs 8% after 48 h) and slightly more effective respect to healthy cells.

These results are not as expected, as the prodrug compound has a cytotoxicity higher than Tacedinaline in healthy cells than cancer cells under hypoxia conditions. In addition, it seems that the prodrug releases the drug under the reducing conditions that hypoxia implies.

However, more experiments need to be conducted on cells to compare the effect of Tacedinaline and the prodrug in healthy and cancer cells under normoxia and in hypoxia

conditions. In this case, if the initial hypothesis is correct, the prodrug should be less cytotoxic than Tacedinaline in the cells under normoxia conditions. In this case to match the launch theory with the obtained results, more studies will be carried out with new molecular conception, the integration of novel anticancer agents and biological tests of validation.

4. Conclusions

Based on the background in the research group, the literature and the results obtained in this work, several conclusions are obtained:

- Previous experiments in the group had shown that the derivatization of compounds, such as pregnenolone and farnesol, with disulfide bonds with polar groups without steric hindrance leads to structures that are excessively reactive and undergo premature hydrolysis.
- The choice of the *tert*-butyl group as a group adjacent to the disulfide has been a good option to be able to synthesize these compounds and make them stable in water.
- Several studies have been carried out to find the most suitable drug structure to bind to disulfide. It has been observed that aniline and benzyl alcohol moieties are compatible with the designed disulfide **4**, their coupling is easy and the product stable.
- Tacedinaline drug has been synthesized in good yield after optimizing some reaction conditions, such as the formation of the acid chloride and the coupling with 2-nitroaniline.
- It has been possible to synthesize a prodrug containing Tacedinaline, as a cytotoxic compound, derivatized with a disulfide bond that is stable in water at cellular pH.
- The synthesis of the drug and the prodrug has been complicated, so that very little product has been obtained, which has made characterization difficult.
- The synthesized prodrug has been studied in trials with healthy (HS-5) and cancerous (HCT-116) cells under hypoxia conditions. The results have not been as expected, as Tacedinaline has shown more toxicity than the prodrug, also no selectivity for cancer cells has been found. However, the hypothesis that the prodrug is activated under hypoxia conditions could be valid.

- Further cell trials are needed, as it is necessary to check whether or not the prodrug is activated in healthy cells without hypoxia. If the prodrug works, it will not be activated under those conditions. This would be a major advance in the synthesis of more selective and targeted drugs that eliminate the side effects of current anti-cancer drugs.
- The development of HDACi will lead to cancer drugs that are safer and more effective than 'non-targeted' drugs. These types of compounds would be capable of inducing the death of cancer cells from a large number of neoplasms, although their mechanisms of action need to be further studied.

5. Experimental Section

5.1. Materials and instrumentation

Several methods were used to characterize the different compounds obtained (IR, ^{1}H NMR, ^{13}C NMR, HRMS and M.p.).

A *Nicolet IR100* spectrophotometer was used for infrared (IR) spectra, and they were performed neat or as a film, over a NaCl mount, expressing the bands in cm^{-1}.

^{1}H NMR and ^{13}C NMR spectra were recorded at room temperature using a Bruker Avance NEO 400 MHz with a Prodigy CPPBBO BB-H&F z-gradient cryo-probe spectrometers (NMR Service, NUCLEUS, University of Salamanca) and Bruker WP-200-SY (200 MHz for ^{1}H NMR) from the Department of Organic Chemistry of the Faculty of Chemical Sciences at USAL. Chemical shifts (δ) are given in ppm with the solvent signal as internal standard unless otherwise stated ($CHCl_3$ 7.26 ppm for ^{1}H NMR, $CDCl_3$ 77.0 ppm for ^{13}C NMR; CH_3OD 3.31 ppm for ^{1}H NMR, CD_3OD 49.0 ppm for ^{13}C NMR; DMSO 2.50 for ^{1}H NMR, DMSO-d_6 39.52 for ^{13}C NMR).

The coupling constants (*J*) are expressed in hertz (Hz) and the following abbreviations will be used to explain the multiplicities of the signals: s (singlet), d (doublet), t (triplet), c (quartet), dd (double doublet), dt (double triplet), dc (double quartet) and m (multiplet).

Melting points (M.p.) were performed under a *Kofler* hot stage microscope.

The mass spectra were performed at the Mass Spectrometry Service of the University of Salamanca by Dr. César Raposo Funcia and Dr. Juan F. Boyero Benito, where they were recorded with Waters ZQ 4000 and Thermo Q Exactive Focus spectrometers.

5.2. Cell lines and culture conditions

In order to assess our antitumoral prodrugs validity, MTT assays were carried out on two different cell lines (normal and tumour), in which they were selected for in vitro studies: normal fibroblast HS-5 (ATCC® CRL11882™) and colorectal carcinoma HCT-116 (ATCC® CCL247™). All were obtained from the American Tissue Collection.

Cells were cultured in Dulbecco's modified Eagle's medium (DMEM) supplemented with 1 % penicillin-streptomycin (P-S) and 10 % fetal bovine serum (FBS), referred to as DMEM+ . They were maintained at 37 °C in a 5 % CO_2 atmosphere at 70 - 90 % confluency and subcultured using 0.05 % EDTA 1x trypsin.

5.3. Cell viability determination

To determine the toxicity of the compounds, cells were seeded in quadruplicate in 24-well plates at an initial concentration of 16000 cells per well. After 24 hours in a humidified incubator with 5% CO_2, the medium was removed from the wells, and new medium containing the study treatments was added (50 µM) under hypoxia (2 % of oxygen). In all tests, the plates included medium control (medium without cells), to check for contamination, and cell control (medium without treatment) as a 100% viability value. Finally, cell viability was quantified by MTT assays after 24 and 48 hours of treatment. The MTT assay is a colorimetric assay used to determine the cytotoxicity of certain drugs (by measuring cell viability). It consists of adding thiazolyl blue tetrazolium bromide dissolved in PBS (5 mg/ml) to the cell medium at a concentration of 20 µl/well and incubating at 37 ˚C for 1 h. During this time, the live cells are incubated at 37 ˚C for 1 h. Meantime, live cells react with the compound to produce violet formazan crystals. Afterwards, the medium is removed and 0.5 mL of DMSO is added to dissolve the crystals, forming a purple solution, the absorbance of which is proportional to the quantity of live cells after each treatment. The absorbance was measured with ultraviolet light (λ = 550 nm) using an EZ Read 2000 microplate reader (Biochrom) and cell viability (Vc) was calculated according to the equation mentioned below:

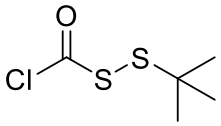
$$\textbf{Viable cells (\%)} = \frac{\text{Total number of viable cells per mL of aliquot}}{\text{Total number of cells per mL of aliquot}} \times 100$$

Once the cell viability data was obtained, a statistical analysis was performed using Statgraphics Centurion XVI Version 16.1.03(StatPoint Technologies).

The MTT assays were performed at the Chemical Engineering Department by Dr. Inmaculada De Dios Pérez under the direction of Prof. Eva María Martín del Valle.

5.4. Synthetic details and characterization

***S,S-tert*-butylcarbonchloride(dithioperoxoate)(4):**



4

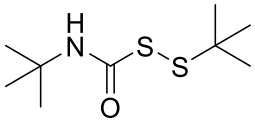
In a 50 ml round-bottom flask, compound **1** (1.6 g, 12.3 mmol) was added. Then, compound **3** (1.2 g, 13.3 mmol) was included and dissolved by continuous stirring. Once the mixture was homogenized, the crude residue was obtained by evaporating the reaction mixture under reduced pressure using a bleach trap. Compound **4** is obtained as a colourless liquid quantitatively.

M.p. Oily

^{1}H NMR (400 MHz, $CDCl_3$) δ (ppm): 1.43 (s, 9H).

^{13}C NMR (101 MHz, $CDCl_3$) δ (ppm): 167.5 (C), 50.8 (C), 29.80 (3 CH_3).

***S,S-tert*-butyl *tert*-butylcarbame(dithioperoxoate) (8):**



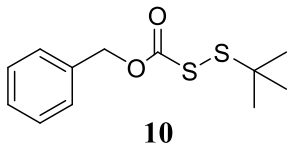
8

In 1 mL of CH_2Cl_2 compound **4** (285 mg, 1.54 mmol) was dissolved under an inert argon atmosphere at -78 °C with continuous stirring. Compound **7** (0.5 g, 6.8 mmol) was added very slowly, resulting in a white solid.

Then, the reaction mixture was diluted in 10 mL CH_2Cl_2 and poured over a 100 mL Erlenmeyer flask containing ice and 5 mL of 2M HCl. The mixture was transferred to a separatory funnel,

then the organic phase was separated, the aqueous phase was washed twice using CH_2Cl_2 and combined with the previous organic phase. To remove water, the organic phase is added on an Erlenmeyer with anhydrous sodium sulfate, filtered with a funnel and cotton, and the salts were washed with CH_2Cl_2. Then under a reduced pressure the organic solvent was evaporated, using a vacuum trap with bleach, affording 260 mg (76%) of compound **8**.

***O*-benzyl *S,S*-*tert*-butylcarbon(dithioperoxoate) (10)**:

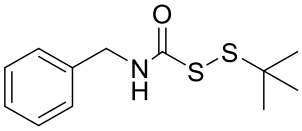


10

In a 25 mL round-bottom flask equipped with magnetic stirrer, compound **4** (17.10 mg, 0.1 mmol) was dissolved in 500 µL of $CDCl_3$, then compound **9** (11.35 mg, 0.1 mmol) was added with continuous stirring, resulting in compound **10**. Then, 1 equivalent of 2,4,6-collidine (14.30 mg, 0.12 mmol) was poured at (-78 °C) for 10 minutes affording a pale yellow solid quantitatively.

Compounds **12-16** were not characterized since their synthesis was carried out on a small scale in an NMR tube with the sole objective of testing the reactivity of compound **4**.

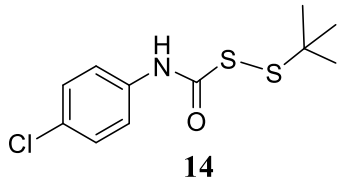
***S,S*-*tert*-butylbenzylcarbame(dithioperoxoate)** (**12**):



12

In a 25 mL round-bottom flask, compound **4** (17.10 mg, 0.1 mmol) and compound **11** (10 mg, 0.1 mmol) were dissolved in 0.5 mL of $CDCl_3$, a rapid formation of a white precipitate was observed. Then, the mixture was centrifugated, once two layers were obtained the solid was analysed by ^1H NMR, appearing two unidentified products. 1 equivalent of 2,4,6-collidine (11.22 mg, 0.1 mmol) was added without obtaining the expected product, hence without being able to identify it. The tube contents were washed with 2M HCl so that the 2,4,6-collidine signal disappears, with the impossibility to obtain compound **12**.

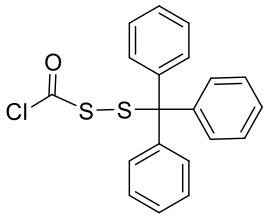
***S,S-tert*-butyl(4-chlorophenyl)carbame(dithioperoxoate) (14):**



14

In 0.5 mL of $CDCl_3$, 4-chloroaniline **13** (10.22 mg, 0.08 mmol) was dissolved, then compound **4** (14.48 mg, 0.08 mmol) was added. A white precipitate was quickly formed. The reaction mixture was centrifuged and a yellow product crystallized. In the ^1H NMR spectrum, it was observed that compound **14** had been obtained. For the stability validation, 1 equivalent of 2,4,6-collidine (9.53 mg, 0.08 mmol) was added, as a result, the compound was kept stable.

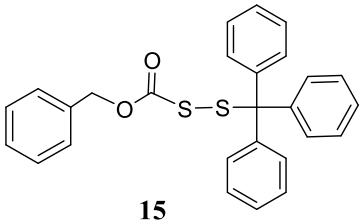
***S,S*-tritylcarbonchloride(dithioperoxoate) (6):**



6

In a 25 mL round-bottom flask, compound **1** (0.5 g, 3.8 mmol) was dissolved in 5 mL of CH_2Cl_2. Then, compound **5** (1.1 g, 3.8 mmol) was added and dissolved by agitation. Once the reaction mixture was homogenized, the volatiles were evaporated under reduced pressure using a vacuum trap with bleach to afford a pale yellow solid, which was used without further purification in the following step.

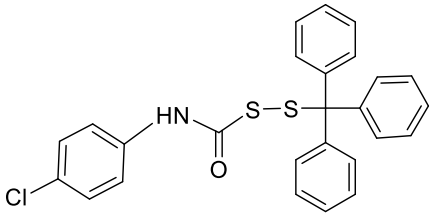
_O_-benzyl-_S,S_-tritylcarbon(dithioperoxoate) (15):



15

In a 25 mL round bottom flask equipped with a magnetic stirrer compound **6** (44 mg, 0.12 mmol) was dissolved in 0.5 mL of $CDCl_3$, then compound **9** (13 mg, 0.12 mmol) was added while stirring. Compound **15** was obtained. Then, 1 equivalent of 2,4,6-collidine (20.75 mg, 0.17 mmol) was added. It was observed that the product was stable.

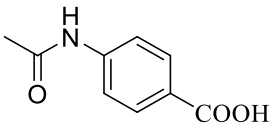
_S,S_-trityl(4-chlorobenzyl)carbamo(dithioperoxoate) (16):



16

In a 25 mL round-bottom flask, compound **6** (34.92 mg, 0.09 mmol) was dissolved in 0.5 mL of $CDCl_3$, compound **13** (10.81 mg, 0.08 mmol) was added by keeping the continuous stirring. Compound **16** was obtained. Then, 2 equivalents of 2,4,6-collidine (24.49 mg, 0.2 mmol) were added. The product remains stable.

4-Acetamidobenzoic acid (18):



18

In a 50 mL round-bottom flask, 4-aminobenzoic acid, compound **17** (1 g, 7.3 mmol), was dissolved in a mixture of 0.83 mL of Ac_2O and 3.65 mL of pyridine. The reaction was stirred at room temperature for 5 hours.

Once the reaction was over, it was added carefully to an Erlenmeyer flask containing a mixture of 2M HCl aqueous solution and ice, and the pH of the mixture was checked. Then, a white precipitate was filtered under reduced pressure, using a Büchner funnel, obtaining 0.887 g (68%) of compound **18** as a white solid.

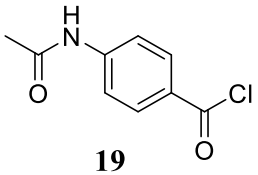
M.p.: > 200 ºC

IR (nujol, υ, $cm^{-1)}$: 3312, 1664.

^{1}H NMR (400 MHz, CD_3OD) δ (ppm): 7.95 (d, *J* = 8.4 Hz, 2H), 7.65 (d, *J* = 8.4 Hz, 2H), 2.13 (s, 3H).

^{13}C NMR (101 MHz, CD_3OD) δ (ppm): 171.9 (C), 169.5 (C), 144.4 (C), 131.8 (2 CH), 126.9 (C), 120.0 (2 CH), 24.0 (CH_3).

4-acetamidobenzoyl chloride (19):



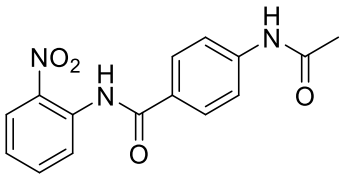
19

In 15 mL CH_2Cl_2, compound **18** (600 mg, 3.35 mmol) was dissolved and triethylamine (339 mg, 467 µL, 3.35 mmol) was added (1 equivalent). Then, a homogenous mixture was obtained and evaporated under vacuum, forming the triethylammonium salt.

The triethylammonium salts were dissolved in 10 ml of DCM and 1 equivalent of PCl_5 (696 mg, 3.35 mmol) was included, by maintaining the reaction at 0 °C. The organic solvent was eliminated under reduced pressure once the reaction was over, affording compound **19**, which was used without further purification in the next reaction.

Characterisation of compound **19** was not realized due to its instability.

4-acetamido-*N*-(2-nitrophenyl)benzamide (20)



20

Compound **19** was melted with an excess of 2-nitroaniline (5 eq, 2.31 g, 16.75 mmol) and stirred for 12 hours. After this time, the mixture was dissolved in methanol, generating a precipitate which was filtered under reduced pressure, obtaining 615 mg (61%) of compound **20** as a pale yellow solid, which was used without further purification in the next step.

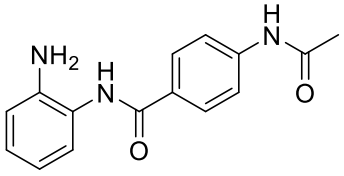
M.p.: > 200 ºC

IR (nujol, υ, cm^{-1}): 3306, 1671, 1606.

^{1}H NMR (400 MHz, CD_3OD) δ (ppm): 8.35 (d, *J* = 8.3 Hz, 2H), 8.18 (d, *J* = 8.3 Hz, 2H), 7.96 (d, *J* = 7.8 Hz, 1H), 7.78 – 7.72 (m, 2H), 7.37 (t, *J* = 7.8 Hz, 1H), 2.17 (s, 3H).

^{13}C NMR (101 MHz, CD_3OD) δ (ppm): 171.6 (C), 167.0 (C), 144.1 (C), 141.5 (C), 135.9 (CH), 134.5 (C), 129.9 (C), 129.6 (2 CH), 126.5 (CH), 125.7 (CH), 125.4 (2 CH), 120.3 (CH), 24.0 (CH_3).

4-acetamide-*N*-(3-aminophenyl) benzamide (21):



21

In a mixture of 30 mL of EtOAc and 5 mL of MeOH, compound **20** (600 mg, 2.62 mmol) was dissolved, and Pd/C (100 mg, 0.047 mmol) was added, the reaction mixture was carried out under 4 atm of H_2 for 12 hours with continuous stirring.

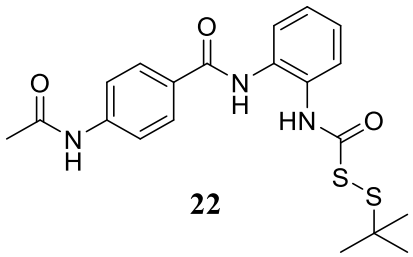
Once hydrogenation process was complete, the Pd/C was filtered, then the product was washed with MeOH, obtaining 420 mg (60%) of compound **21** as a white solid (Tacedinaline).

M.p.: > 200 ºC

IR (nujol, υ, cm^{-1}): 3293, 1638, 1599.

^{1}H NMR (400 MHz, CD_3OD) δ (ppm): 7.95 (d, *J* = 8.5 Hz, 2 H), 7.71 (d, *J* = 8.5 Hz, 2H), 7.18 (d, *J* = 7.6 Hz, 1H), 7.07 (t, *J* = 7.6 Hz, 1H), 6.90 (d, *J* = 7.6 Hz, 1H), 6.78 (t, *J* = 7.6 Hz, 1H), 2.15 (s, 3H).
^{13}C NMR (101 MHz, CD_3OD) δ (ppm): 171.9 (2 C), 143.5 (2 C), 130.4 (C), 129.8 (2 CH), 128.5 (CH), 127.7 (CH), 125.6 (C), 120.2 (2 CH), 119.9 (CH), 118.9 (CH), 24.0 (CH_3).

***S,S-tert*-butyl(2-(4-acetamidobenzamide)phenyl)carbamo(dithioperoxoate) (22):**



22

In a 25 mL round-bottom flask, compound **4** (40 mg, 0.22 mmol) was dissolved in 4 mL of CH_2Cl_2, then compound **21** (100 mg, 0.37 mmol) was added, the reaction was cooled down at 0 ºC. To dissolve the compound, DMF (2 ml) and 2 equivalents of 2,4,6-collidine (53.2 mg, 0.44 mmol) was added as an auxiliary base, the reaction mixture was stirred overnight.

Once the reaction had finished, it was transferred to a separatory funnel, washed with an aqueous solution of 2M HCl, dried over anhydrous Na_2SO_4, filtered and evaporated at reduced pressure. The reaction crude was purified by chromatography column on silica gel, using CH_2Cl_2/EtOAc as eluents, affording 6 mg of compound **22** (7% yield) as an oil.

IR (nujol, υ, cm^{-1}): 1742, 1664, 1521.
^{1}H NMR (400 MHz, $CDCl_3$) δ (ppm): 7.86 (d, *J* = 8.6 Hz, 2 H), 7.60 (d, *J* = 8.4 Hz, 2 H), 7.29 (d, *J* = 7.6 Hz, 2 H), 7.18 (t, *J* = 6.3 Hz, 2 H), 2.09 (s, 3 H), 1.18 (s, 9 H).
^{13}C NMR (101 MHz, $CDCl_3$) δ (ppm): 177.9 (C), 168.6 (C), 165.5 (C), 144.7 (C), 141.6 (C), 130.1 (C), 129.1 (2 CH), 128.8 (C), 127.0 (CH), 126.9 (CH), 126.5 (CH), 124.2 (CH), 119.3 (2 CH), 49.3 (C), 34.6 (3 CH_3), 31.2 (CH_3).
MS (ESI): 418.1247 ($M+H^+$); the calculated value for $C_{20}H_{24}O_3N_3S_2^+$ is 418.1254.

6. References

(1) Cacciatore, I.; Cornacchia, C.; Pinnen, F.; Mollica, A.; Di Stefano, A. Prodrug Approach for Increasing Cellular Glutathione Levels. *Molecules* **2010**, *15* (3), 1242–1264. https://doi.org/10.3390/molecules15031242.

(2) Liu, P.; Hao, L.; Liu, M.; Hu, S. Glutathione-Responsive and -Exhausting Metal Nanomedicines for Robust Synergistic Cancer Therapy. *Front. Bioeng. Biotechnol.* **2023**, *11*. https://doi.org/10.3389/fbioe.2023.1161472.

(3) Forman, H. J.; Zhang, H.; Rinna, A. Glutathione: overview of its protective roles, measurement, and biosynthesis. *Mol. Aspects Med.* **2009**, *30* (1-2), 1-12, https://doi.org/10.1016/j.mam.2008.08.006.

(4) Lee, M. H.; Sharma, A.; Chang, M. J.; Lee, J.; Son, S.; Sessler, J. L.; Kang, C.; Kim, J. S. Fluorogenic Reaction-Based Prodrug Conjugates as Targeted Cancer Theranostics. *Chem. Soc. Rev.* **2018**, *47* (1), 28–52. https://doi.org/10.1039/C7CS00557A.

(5) Wang, Q.; Guan, J.; Wan, J.; Li, Z. Disulfide Based Prodrugs for Cancer Therapy. *RSC Adv.* **2020**, *10* (41), 24397–24409. https://doi.org/10.1039/D0RA04155F.

(6) Chakraborty, A.; Sharma, A.; Albericio, F.; de la Torre, B. G. Disulfide-Based Protecting Groups for the Cysteine Side Chain. *Org. Lett.* **2020**, *22* (24), 9644–9647. https://doi.org/10.1021/acs.orglett.0c03705.

(7) Marks, P.; Rifkind, R. A.; Richon, V. M.; Breslow, R.; Miller, T.; Kelly, W. K. Histone Deacetylases and Cancer: Causes and Therapies. *Nat. Rev. Cancer* **2001**, *1* (3), 194–202. https://doi.org/10.1038/35106079.

(8) Tabraue-Chávez, M.; Panadero-Fajardo, S.; Arévalo-Ruiz, M.; Domínguez-Seglar, J. F.; Gómez-Vidal, J. A. Síntesis y evaluación de nuevos inhibidores de las HDAC. *Ars. Pharm.* **2010**, *51* (supl.3), 541–548. http://hdl.handle.net/10481/26621.

(9) Bolden, J. E.; Peart, M. J.; Johnstone, R. W. Anticancer Activities of Histone Deacetylase Inhibitors. *Nat. Rev. Drug Discov.* **2006**, *5* (9), 769–784. https://doi.org/10.1038/nrd2133.

(10) Dokmanovic, M.; Clarke, C.; Marks, P. A. Histone Deacetylase Inhibitors: Overview and Perspectives. *Mol. Cancer Res.* **2007**, *5* (10), 981–989. https://doi.org/10.1158/1541-7786.MCR-07-0324.

(11) Marks, P. A.; Xu, W.-S. Histone Deacetylase Inhibitors: Potential in Cancer Therapy. *J. Cell. Biochem.* **2009**, *107* (4), 600–608. https://doi.org/10.1002/jcb.22185.

(12) Ma, X.; Ezzeldin, H. H.; Diasio, R. B. Histone Deacetylase Inhibitors: Current Status and Overview of Recent Clinical Trials. *Drugs* **2009**, *69* (14), 1911–1934. https://doi.org/10.2165/11315680-000000000-00000.

(13) Miller, T. A.; Witter, D. J.; Belvedere, S. Histone Deacetylase Inhibitors. *J. Med. Chem.* **2003**, *46* (24), 5097–5116. https://doi.org/10.1021/jm0303094.

(14) Eckschlager, T.; Plch, J.; Stiborova, M.; Hrabeta, J. Histone Deacetylase Inhibitors as Anticancer Drugs. *Int.J. Mol Sci* **2017**, *18* (7), 1414. https://doi.org/10.3390/ijms18071414.

(15) Hubeek, I.; Comijn, E. M.; Van der Wilt, C. L.; Merriman, R. L.; Padron, J. M.; Kaspers, G. J. L.; Peters, G. J. CI-994 (N-Acetyl-Dinaline) in Combination with Conventional Anti-Cancer Agents Is Effective against Acute Myeloid Leukemia in Vitro and in Vivo. *Oncol. Rep.* **2008**, *19* (6), 1517–1523. https://doi.org/10.3892/or.19.6.1517.

(16) McClarty, B.; Rodriguez, G.; Dong, H. Dose Effects of Histone Deacetylase Inhibitor Tacedinaline (CI-994) on Antipsychotic Haloperidol-Induced Motor and Memory Side Effects in Aged Mice. *Front. Neurosci.* **2021**, *15*, 674745. https://doi.org/10.3389/fnins.2021.674745.

(17) Autin, P.; Blanquart, C.; Fradin, D. Epigenetic Drugs for Cancer and microRNAs: A Focus on Histone Deacetylase Inhibitors. *Cancers* **2019**, *11* (10), 1530. https://doi.org/10.3390/cancers11101530.

(18) Iqbal Choudhary, M.; Shahab Alam, M.; Rahman, A.-u.; Yousuf, S.; Wu, Y.-C.; Lin, A.-S.; Shaheen, F. Pregnenolone Derivatives as Potential Anticancer Agents. *Steroids* **2011**, *76* (14), 1554–1559. https://doi.org/10.1016/j.steroids.2011.09.006.

(19) Ghasemi, M.; Turnbull, T.; Sebastian, S.; Kempson, I. The MTT Assay: Utility, Limitations, Pitfalls, and Interpretation in Bulk and Single-Cell Analysis. *Int. J. Mol. Sci.* **2021**, *22* (23), 12827. https://doi.org/10.3390/ijms222312827.

(20) Berridge, M. V.; Herst, P. M.; Tan, A. S. Tetrazolium Dyes as Tools in Cell Biology: New Insights into Their Cellular Reduction. In *Biotechnology Annual Review*; Elsevier, 2005; Vol. 11, pp 127–152. https://doi.org/10.1016/S1387-2656(05)11004-7.

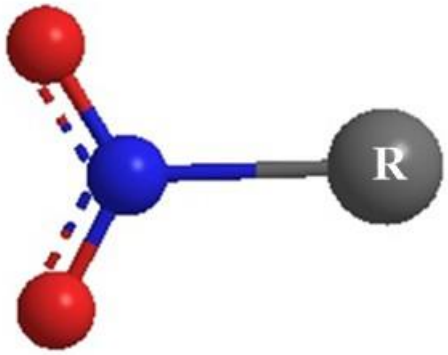
(21) Kumar, P.; Nagarajan, A.; Uchil, P. D. Analysis of Cell Viability by the MTT Assay. *Cold Spring Harb Protoc* **2018**, *2018* (6), pdb.prot095505. https://doi.org/10.1101/pdb.prot095505.

(22) Chen, C. H.; Campbell, P. A.; Newman, L. S. MTT Colorimetric Assay Detects Mitogen Responses of Spleen but Not Blood Lymphocytes. *Int. Arch. Allergy Appl. Immunol.* **1990**, *93* (2–3), 249–255. https://doi.org/10.1159/000235309.

(23) Stockert, J. C.; Blázquez-Castro, A.; Cañete, M.; Horobin, R. W.; Villanueva, Á. MTT Assay for Cell Viability: Intracellular Localization of the Formazan Product Is in Lipid Droplets. *Acta Histochemica* **2012**, *114* (8), 785–796. https://doi.org/10.1016/j.acthis.2012.01.006.

(24) Mani, S.; Singh, M.; Kumar, A. *Animal Cell Culture: Principles and Practice*, 1st ed. 2023 edition.; Springer: Cham, 2023.

CHAPTER 2: PRODRUGS FUNCTIONALIZED WITH NITRO GROUPS



In chapter 2 the design and synthesis of prodrugs functionalized with nitro groups will be discussed.

1. Objectives

The general objective of this chapter is the design and synthesis of a molecule which contains a nitroaromatic moiety which can be attached to a cytotoxic drug (specifically a nitrogen mustard) the latter can be released under hypoxia conditions to increase the parent ingredient biodistribution, selectivity, and an efficient attack *in situ* against cancer cells.

In order to reach the main goal, specific objectives are listed below:

Objective 1: Design and synthesis of a nitroaromatic moiety for the purpose of attaching it to a cytotoxic anti-cancer drug.

Objective 2: The right selection of the drug: easy linkage, stability and efficacy against cancer cells

Objective 3: To include a specific property in the nitroaromatic fraction (linker) in order to fulfil its theranostic features such as the fluorescence.

Objective 4: Functionality validation of the proposed molecule by carrying out series of biological tests on cancerous and healthy cells.

2. Introduction

Despite the advanced progresses made to fight against cancer, which is responsible for millions of deaths worldwide every year, the latter has become one of the greatest concerns for the scientific community.

To improve new strategies for cancer therapy, the study of the tumour microenvironment has allowed the design of new drugs that are more effective and have fewer adverse effects.

Specifically, in this chapter we focus on using the hypoxia environment that exists in tumor tissues for the design of a linker with a nitro group for anti-cancer drugs, exploiting the reducing medium which will convert the nitro to amine group, releasing by that the cytotoxic drug that is capable of killing tumor cells *in situ* without causing side effects.

As mentioned previously prodrugs are pharmacologically inactive substances, which demand a transformation within the body to become a truly active drug.[1]

Tumor hypoxia is an interesting phenomenon in oncology despite its obstacles created during the therapy such as radiotherapy and the multi-drug resistance, it is still an attractive target for several therapeutic designs as nitroaromatics bio- reductively activated[2] (Figure 1).

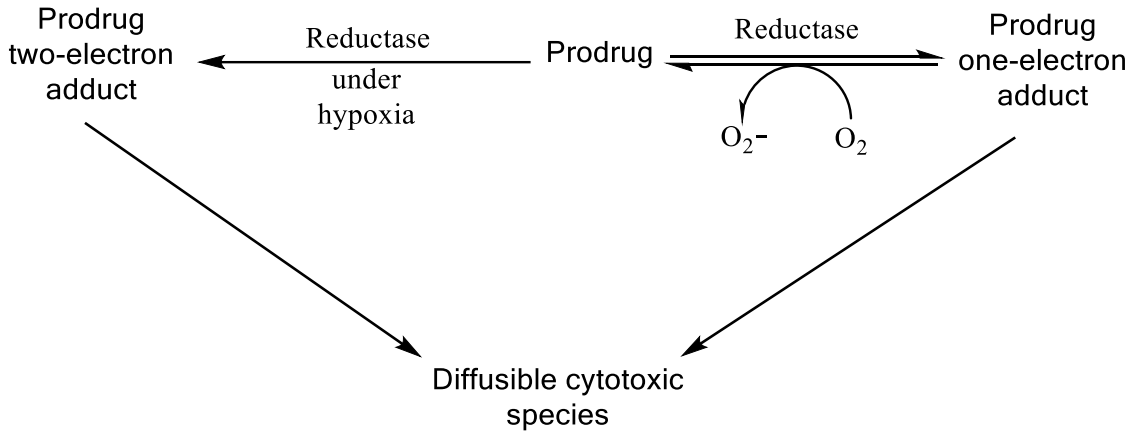


Figure 1. *Hypoxia activated-prodrug mechanism.*[2]

2.1. Nitroaromatics

Nitroaromatics are an organic compounds category that has been examined for its potential use in cancer therapy. Nitroaromatic hypoxia-activated prodrugs are designed to selectively undergo enzyme-based nitro group reduction in hypoxic regions from solid tumors, producing dynamic drugs.[3]

2.1.1. Nitroaromatics attached to mustard gas

Nitrobenzyl mustard quaternary ammonium salts were the primitive category representing current generation of hypoxia selective cytotoxic molecules.[4]

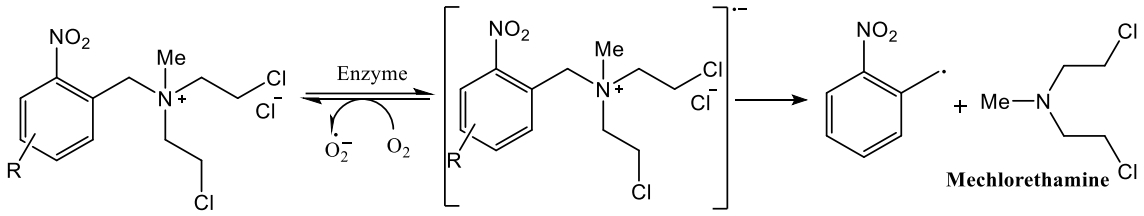


Figure 2. *Proposal of Nitrobenzyl mustard quaternary ammonium salts activation and drug release through bioreduction.*[4]

Seminal contributions about nitroaromatics syntheses which could be cleaved under hypoxic effect have been mentioned in Yu Chen *et al.* review.[4] The strategy is based on drug release through radical cleavage. As a part of drug release study under the hypoxic effect, the same review has dealt another range of prodrug activation and drug release through cyclization based on the modification in electron density and/or nucleophilicity during the process of reduction in order to liberate the active ingredient (the drug) as it is shown in Figure 3.

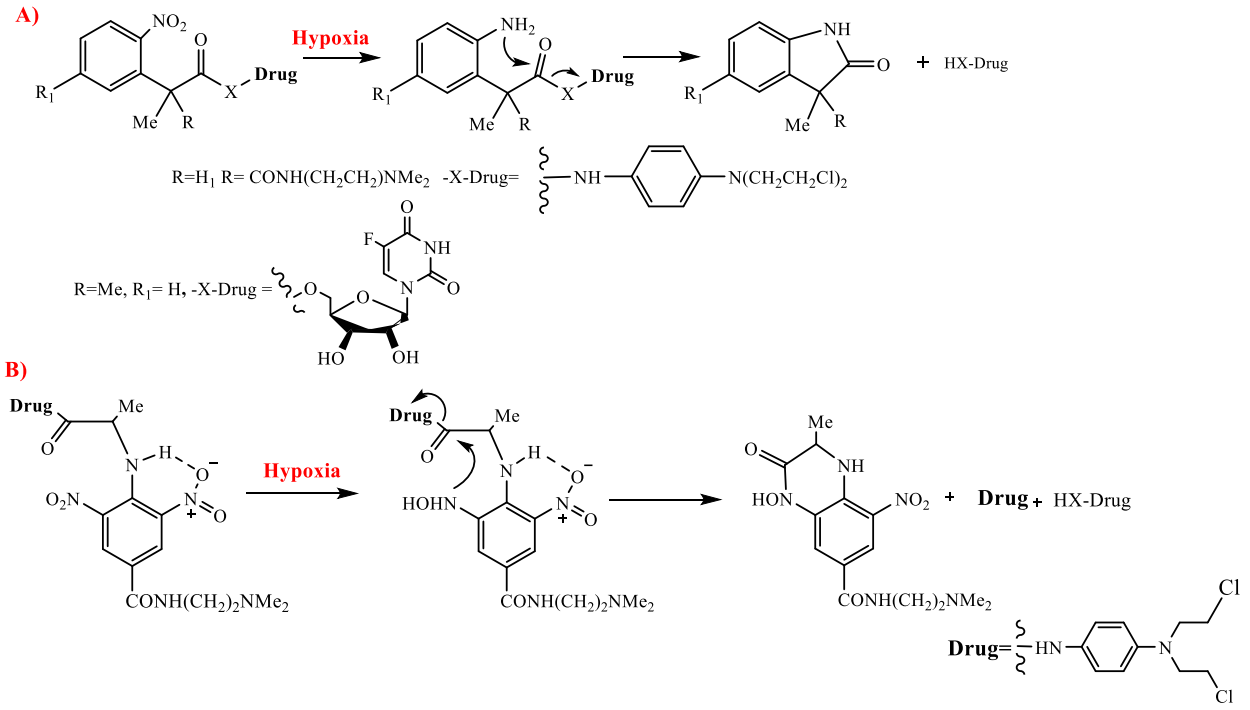


Figure 3. *2-Nitrophenylalkanoyl activation by bioreduction and the subsequent cyclization of conjugates of amine or alcohol containing drugs (modified).*[4]

The exploitation of the bioreduction available in solid tumors has made a qualitative leap in the design of nitroaromatics so that an intramolecular cleavage of an amide or ester group could be realized from the formed amine after the nitro group reduction in the aim of triggering the parent drug liberation.[4]

2.2. Our strategy

In this chapter, new molecular activators with a nitro group in their structure are presented. They will be able of binding to drugs for the treatment of cancer by ester bond, amide or thioester, which within cellular hypoxia environment are capable of releasing these antineoplastic drugs.

In addition, the structure of the molecular activator, thanks to its fluorescence, will make it possible to visualize the internalization of the prodrug inside the cellular tissue and then, the final release of the drug.

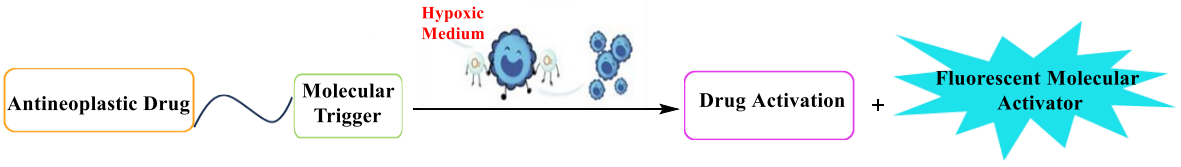


Figure 4. *Outline of the design of the hypoxia-activated prodrug.*

The selection of the right antineoplastic drug and the linker will be a necessity for an effective prodrug production.

2.3. Fluorescence contribution in anti- cancer drugs (ACDs) pharmacokinetics

Due to the ADCs cytotoxicity and their poor control of selectivity, it has become an incentive to take in consideration drugs pharmacokinetics**,** before their validation as drugs, interestingly the establishment of new analytical tools , including them the fluorescence so that the ACDs could be easily detected.[5]

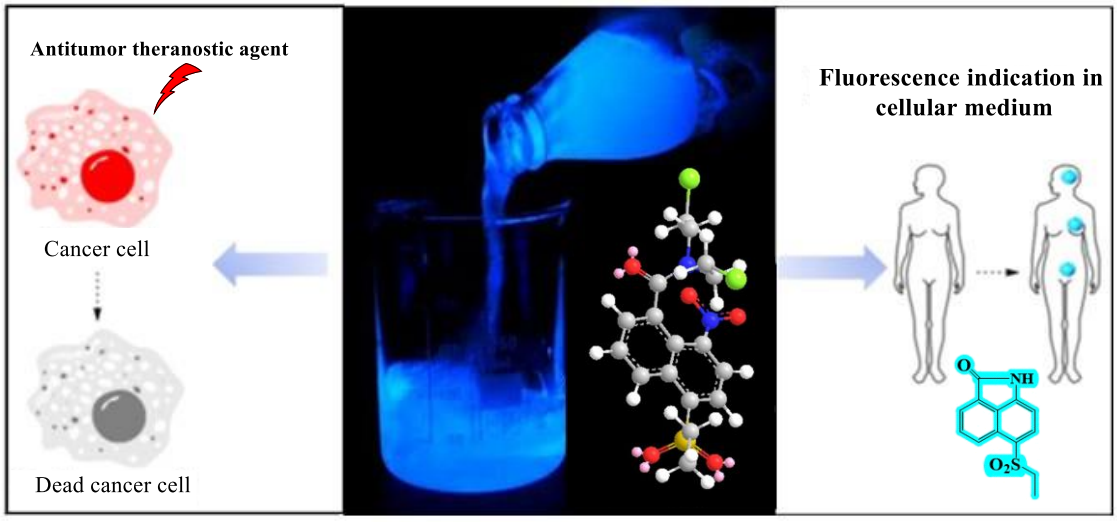


Figure 5. *Theranostic effect: combination of therapeutic and imaging diagnostic techniques (fluorescence).*[6]

Actually, the presence of a 1-naphthoic acid subunit in the trigger is promising to construct theranostic agents since this moiety is natively fluorescent. We will use this skeleton in some of the prodrug structures that will be presented in this chapter.

2.3.1. 1-Naphtoic acid

1-Naphtoic acid is a polycyclic aromatic hydrocarbon with low molecular weight[7] that plays a pivotal role in pharmaceutical and analytic syntheses, and/or could be an intermediate in several organic reactions such as pharmaceuticals, photochemicals, plant growth hormones, dyes, etc.[8] Interesting fluorescence features are displayed by naphthoic acids including their emission and excitation spectra (Figure 6), in particular their derivatives which allows the detection of its path through various samples such as the human serum.[9]

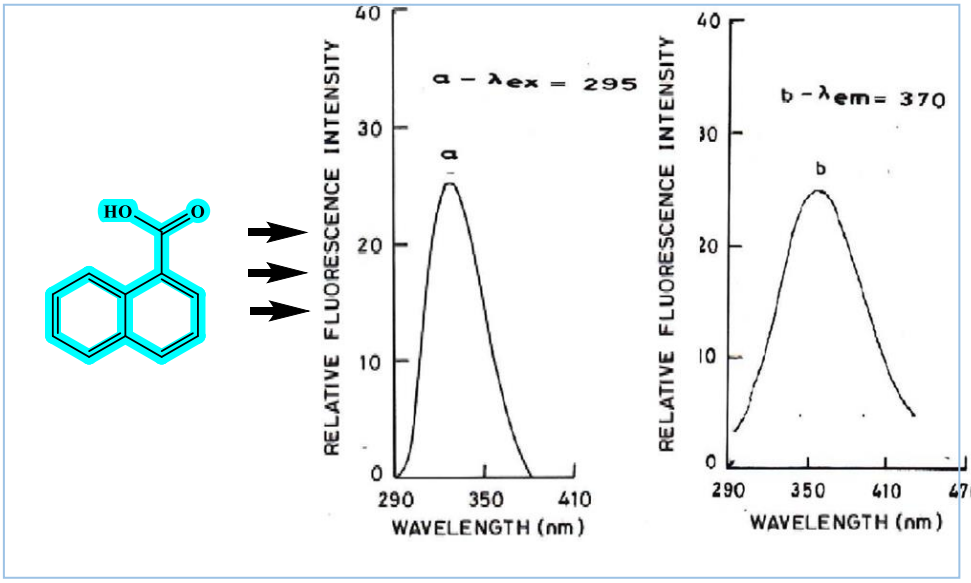


Figure 6. *1-Naphtoic acid excitation and emission spectra (modified).*[8]

2.4. The proposed challenge

As it has been mentioned before, most of the problems related with the adverse effects of current cancer therapies are related with the obstacle of cell selectivity in treatments: the cytotoxic drugs available on the market are not able to differentiate cancer cells from healthy ones, since most of the drugs affect cells that are capable of dividing rapidly, including tumor cells, but also hair, nail´s cells, etc. Therefore, adverse effects may appear including: fatigue, hair loss, infections, anaemia, nausea, vomiting, loss of appetite, diarrhoea, urinary problems, dry skin, mood swings, decreased libido, fertility problems, etc.

Of particular note is the effect of dosage, which assign side effects and the drug's ability to kill cancer cells.

To solve the problem of non-specificity, this work proposes to bind a carrier molecule to the drug so that it selectively targets cancer cells only. This is known as Targeted Cancer Therapy.

In order to exploit the idea, it is necessary to find the metabolic or structural differences between healthy and cancer cells. Thus, molecules could be designed that only work on cancer cells. It is similar to how antibiotics work, which only affect prokaryotic cells and not eukaryotes, because they selectively target a region of the cell (such as the cell wall) that is not present in eukaryotic cells.

2.5. Bioreducible Mustards: New Scope for Exploitation

In fact, hypoxia in tumor populations is contemplated as a double-edged weapon since it can be both: an indirect problem in chemo and radio-therapy resistance, and a possible approach in cancer therapy by the exploitation of its reducible capacities for cytotoxic agents' liberation. Nitroaromatic hypoxia-activated prodrugs (HAPs) are a promising class of anticancer substances (Figure 7), their activation process involves the reduction of the nitro group under hypoxic conditions, or the enzymatic pathway such as nitroreductases, as a result converting the prodrug into its active cytotoxic form[3,10] (Figure 7).

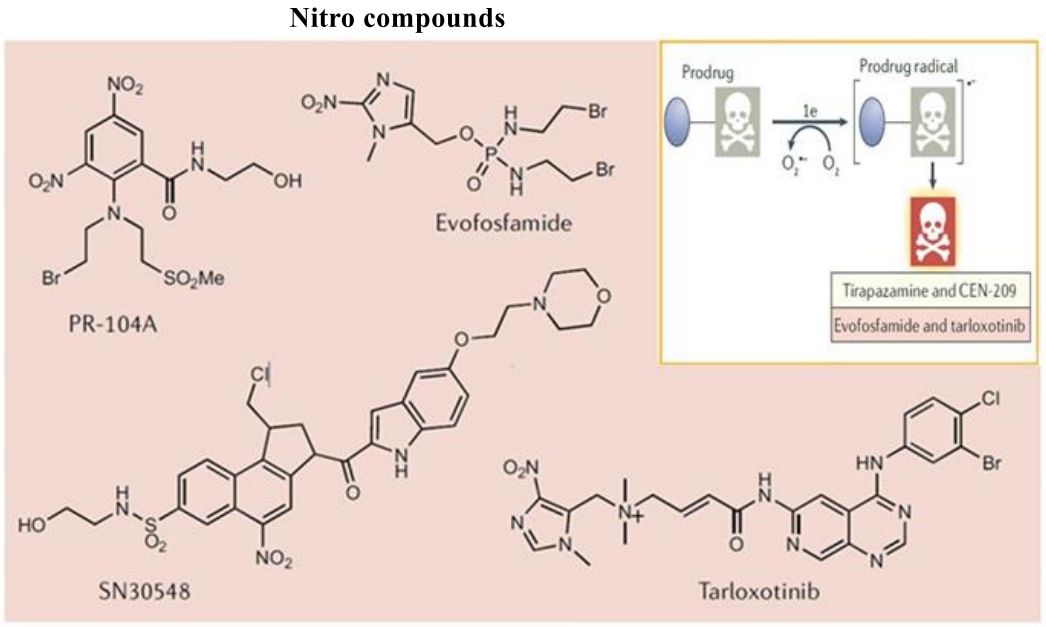


Figure 7. *Hypoxia- activated prodrugs (HAPs) incorporate a latent drug (grey skull and crossbones box) that is activated (red skull and crossbones box) by enzymatic reduction of a conjugated 'trigger' unit (blue circle).*[11]

As discussed earlier, the DNA alkylating agents, in particular the nitrogen mustards, were the first useful anti-cancer compounds, in which the modern chemotherapy veers into the exploitation of molecular abnormalities within the cancer microenvironment by developing prodrugs from subunits of nitrogen mustards and triggers of selectivity.

Quoting Rajesh K. Singh and his colleagues, nitrogen mustards are antineoplastic drugs subclass which acts on DNA by alkylating or /and cross linking of the two strains in order to stop the replication as it is shown in Figure 8.[12]

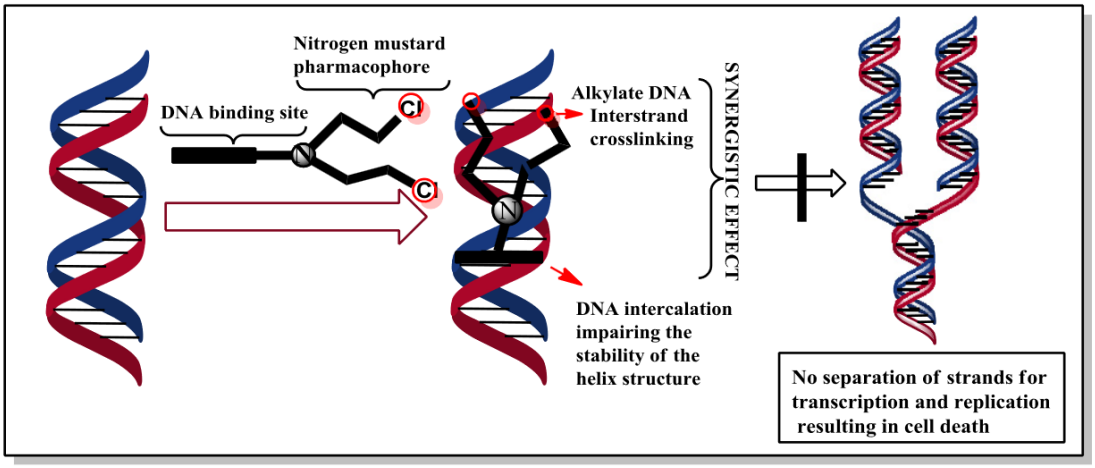


Figure 8. *Nitrogen mustards effects on the DNA double helix.*[12]

2.5.1. Nitrogen Mustards Hybrids

In fact, nitrogen mustard derivatives begun with the development of bis (2-chloroethyl)sulfide as it displayed therapeutic capabilities on leukaemia.

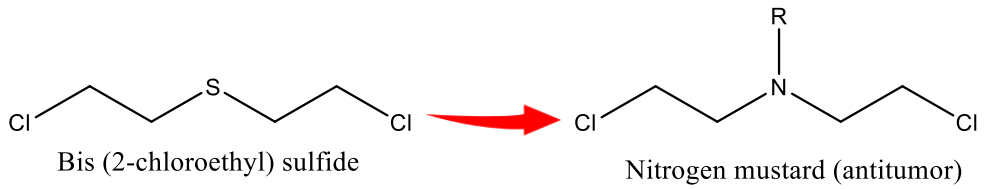


Figure 9. *Nitrogen mustard origin and advancement.*

However, due to its severe toxicity, its clinical application was not approved as an antitumor agent, hence its adaptation with conjugate molecules was necessary to provide novel methods for the antitumor effect, selectivity and the reduction toxicity improvement , consequently the hybridation of nitrogen mustard by binding draggable units was considered as the new generation of multifunctional theranostic agents (Figure 9).[13]

In relation with the purpose of improving nitrogen mustards properties (selectivity, targetability, safety pharmacokinetics and pharmacodynamics), this chapter will treat the linking of *N*,*N*-bis(2-chloroethyl)amine with a molecular trigger , before that a definition of the cytotoxic molecule is required.

2.5.2. *N,N*-bis(2-chloroethyl)amine

N,N-bis(2-chloroethyl)amine also called bis(2-chloroethyl)amine is an organic compound classified as a type of a nitrogen mustard and an alkylating agent with a chemical formula $C_4H_9Cl_2N$ and a molecular weight of 142.02g/mol.[14]

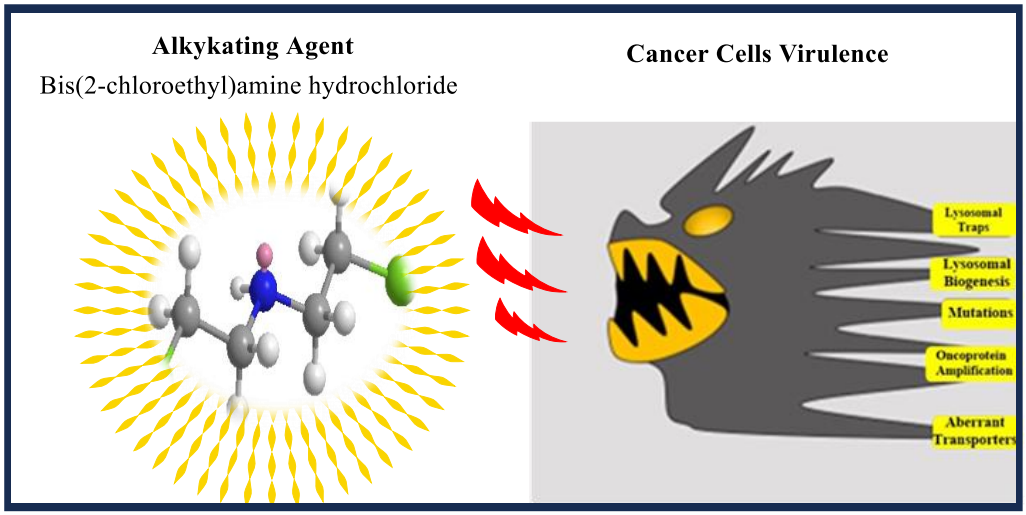


Figure 10.*The effect of bis(2-chloroethyl)amine hydrochloride as an alkylating agent against cancer cells (modified).*[15]

2.6. Nitroaromatics attached to antimetabolites (pyrimidine analogues) 5-Fluorouridine

Our research has been reinforced by a second proposal represented by the linkage of our synthetized nitroaromatics moieties with a pyrimidine analogue (5-Fluorouridine), which makes it possible the reductive power exploitation of nitro group within the tumor microenvironment, to achieve the systemic biodistribution of the drug. The choice of the drug falls within its proven efficacy and cytotoxicity against a group of tumors.

2.6.1. 5-Fluorouridine (5-FUrd)

5-Fluorouridine is a solid organic compound, also known as 5-FUrd, 5-Fluorouracil 1-beta-D-ribofuranoside, 5-Fur, or 5-Fluoro-uridine. The compound is classified as a pyrimidine nucleoside which belongs to the group of pyrimidine nucleosides and analogues, also a metabolite of 5-fluorouracil (5-FU).[16]

According to the literature, 5-fluorouridine as opposed to 5- fluorouracil, which is frequently administered directly as anti-cancer treatment, fluorouridine is used commonly as a valuable compound for investigation and comparison purposes and not for the direct consumption as a

chemotherapy drug, in addition it is considered as more harmful on cancer cells than 5-fluorouracil.[17]

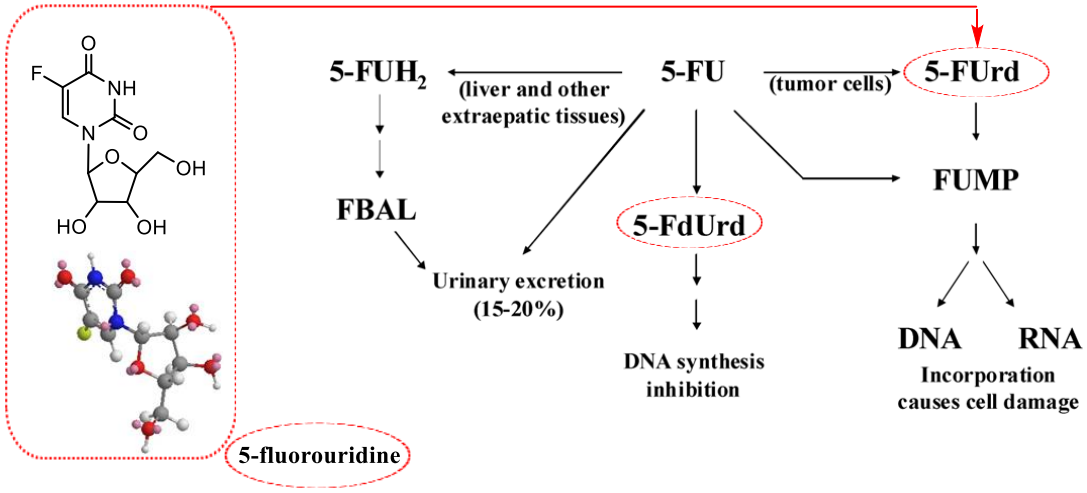


Figure 11. *Left :5-fluorouruidine 2D and 3D structure. Right :5-fluorouracil metabolism within the human body and 5-fluorouridine generation as metabolite (modified figure).*[18]

To overcome the 5-FUrd drawbacks following its use as an anti-cancer therapy, 5-fluorouridine prodrug was synthetized in order to avoid its systemic toxicity, lack of selectivity, and multi-drug resistance (MDR) development.

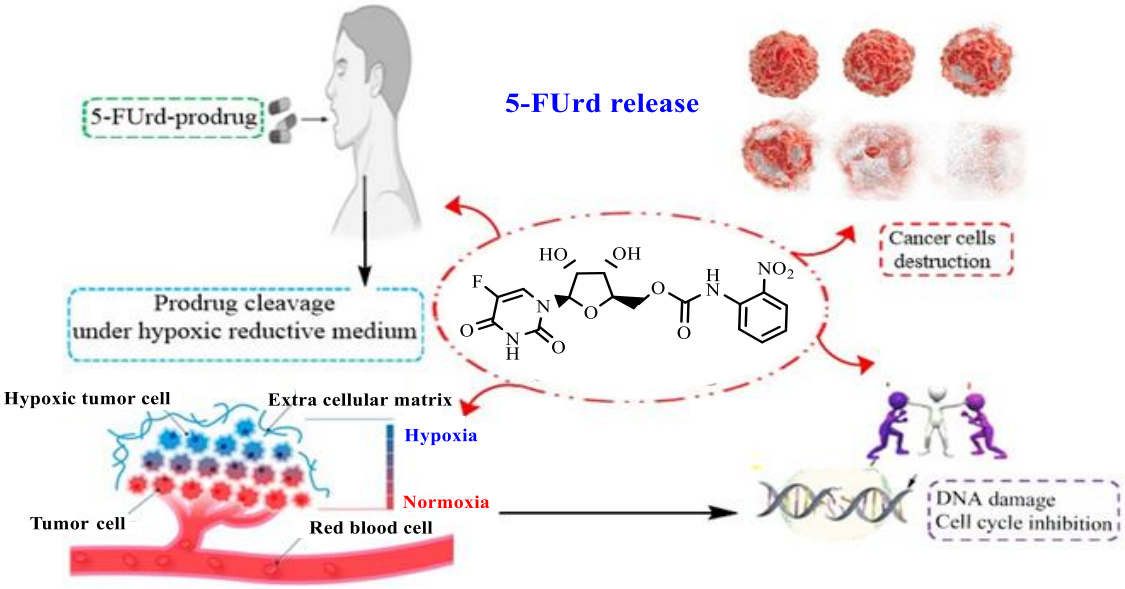


Figure 12. *5-Fluorouridine prodrug pathway, its cleavage under hypoxia medium and DNA attack by 5-FUrd liberation in situ , finally the cellular death (modified).*[19]

As mentioned earlier, 5-FUurd is a 5- fluorouracil metabolite that contributes to damaging the tumor cells by mimicking the pyrimidine structure to interlocate on DNA and RNA scale with more effective process. Based on these data, the theorical advantage of 5-fluorouridine prodrug is the exploitation of cellular medium (hypoxia) and the metabolic signalling to cleave, liberate and activate the parent ingredient directly against the target (cancer cells).

3. Methodology

3.1. Synthesis of nitro-based prodrugs (Nitrogen mustard/bis(2-chloroethyl)amine)

The synthesis of nitro-based prodrugs, particularly those involving nitrogen mustard bis(2-chloroethyl)amine, is a complex process that typically requires several key steps.

The molecule that is intended to be used as a molecular activator is depicted in Figure 13A. This molecule consists of a naphthalene ring that has a carboxylic acid at position 1, a nitro group at position 8 and a sulfone at position 5. The role of the carboxylic acid is to serve as an anchor for drug binding (Figure 13B). The nitro group, being located in *peri* position with respect to the carboxylic acid, suffers from the steric repulsion of the latter and will facilitate the release of the drug once the reduction of nitro to amino occurs under the conditions of hypoxia in which the cancer cells are found. We intend that the amino group at position 8 will displace the ester or amide bond that binds the drug to naphthalene (Figure 13C).

The presence of sulfone in position 5 allows the activating agent to show fluorescent characteristics once the reduction occurs, since the structure generated resembles dansyl-amide, a molecule used as a fluorophore (Figure 13D).

This would allow us to monitor the progress of the reaction and the selectivity of the prodrug by fluorescent spectroscopy.

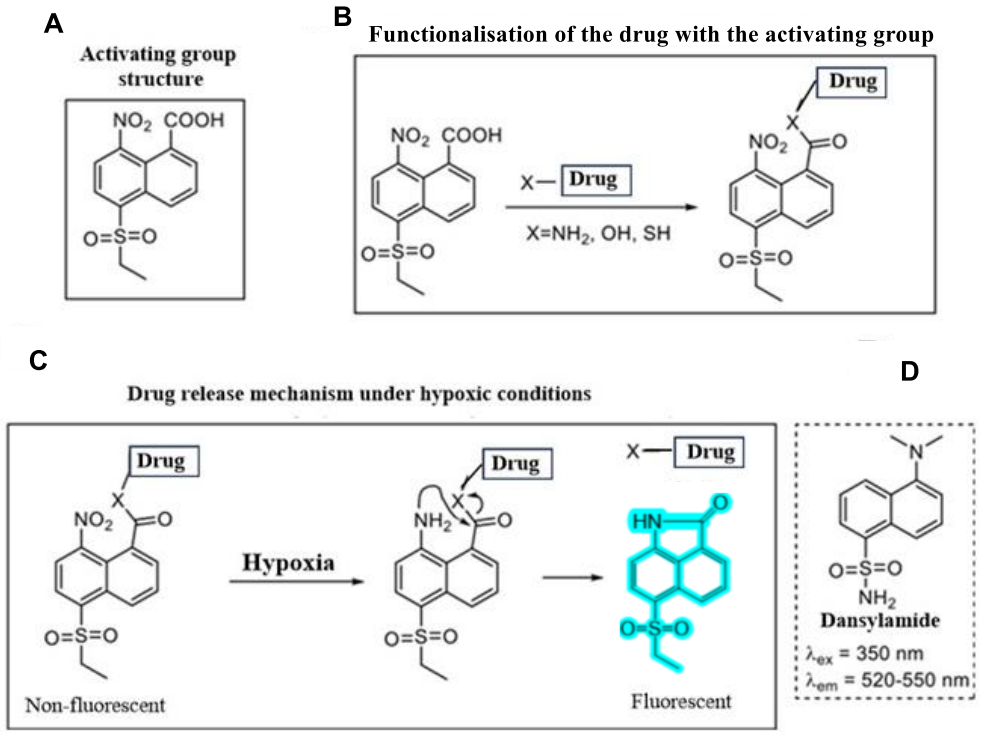


Figure 13. *(A) Structure of the activating group; (B) drug functionalization reaction; (C) mechanism of drug release and (D) structure of dansylamide.*

We decided to use bis(2-chloroethyl)amine as the drug to be attached to the activating group designed in figure 13.

To synthesize the prodrug, the following retrosynthesis was designed (Figure 14):

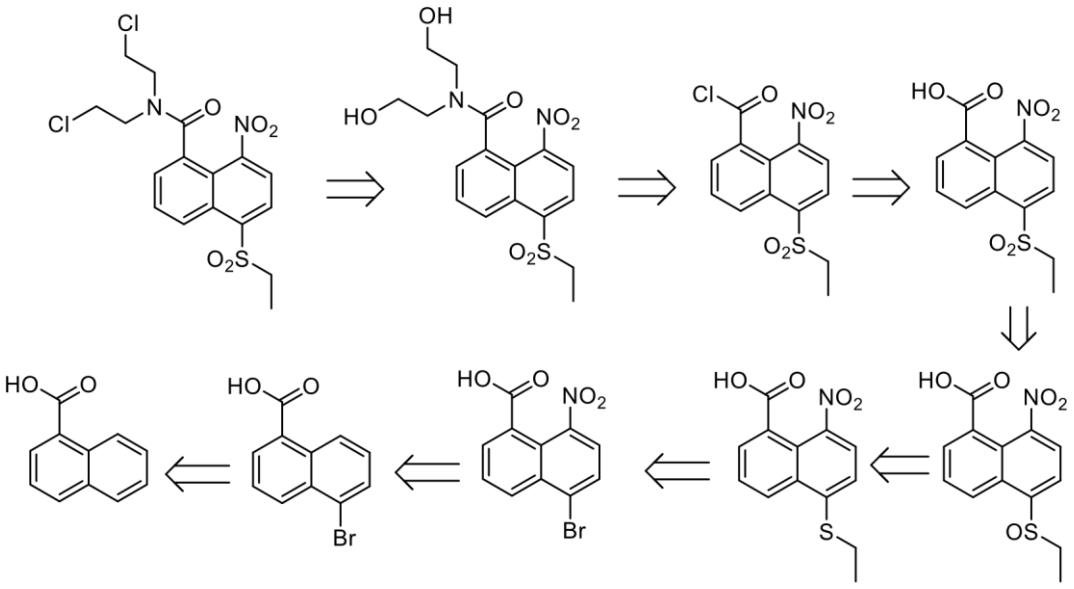


Figure 14. *Retrosynthesis designed for the prodrug.*

Also, the synthesis of prodrugs based on different nitro group triggers will be performed. They will be linked to 5-fluorouridine and their cleavage and liberation will be tested under the reductive conditions inside the tumoral environment by cyclization resulting from the reduction of the nitro to amine group.

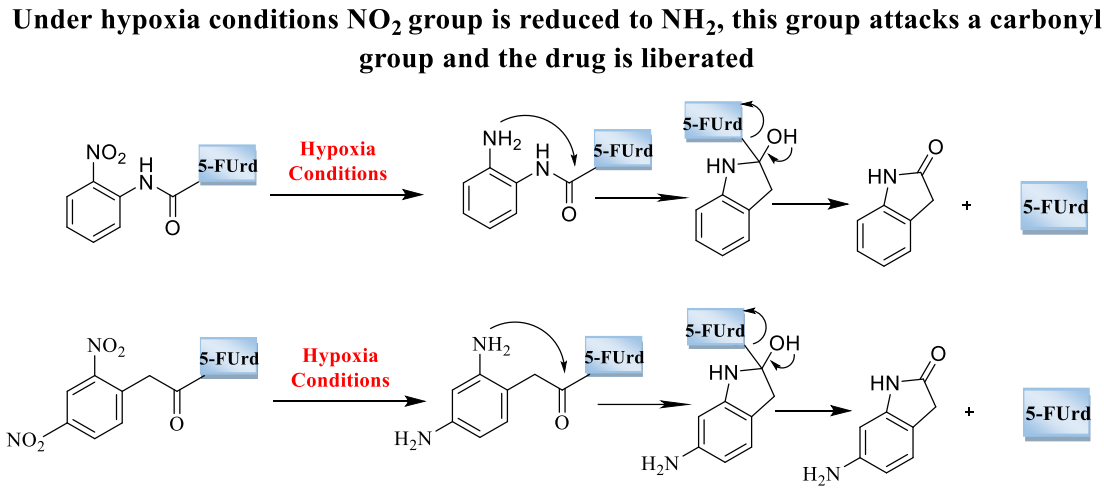


Figure 15. *Prodrugs-based nitro group reduction process under hypoxic conditions and drug liberation.*

3.2. Synthesis of nitro-based prodrugs (5-Fluorouridine)

3.2.1. 5-Fluorouridine prodrug 1

The conception of **5-Fluorouridine prodrug 1** (Figure 16) is based on the coupling of the cytotoxic agent 5-Fluorouridine with 1-isocyanate-2-nitrobenzene, the latter has been selected thanks to the nitro group it contains since it is considered the key factor for drug liberation under the bioreductive action, and the ease with which it can be attached to the drug under mild conditions.

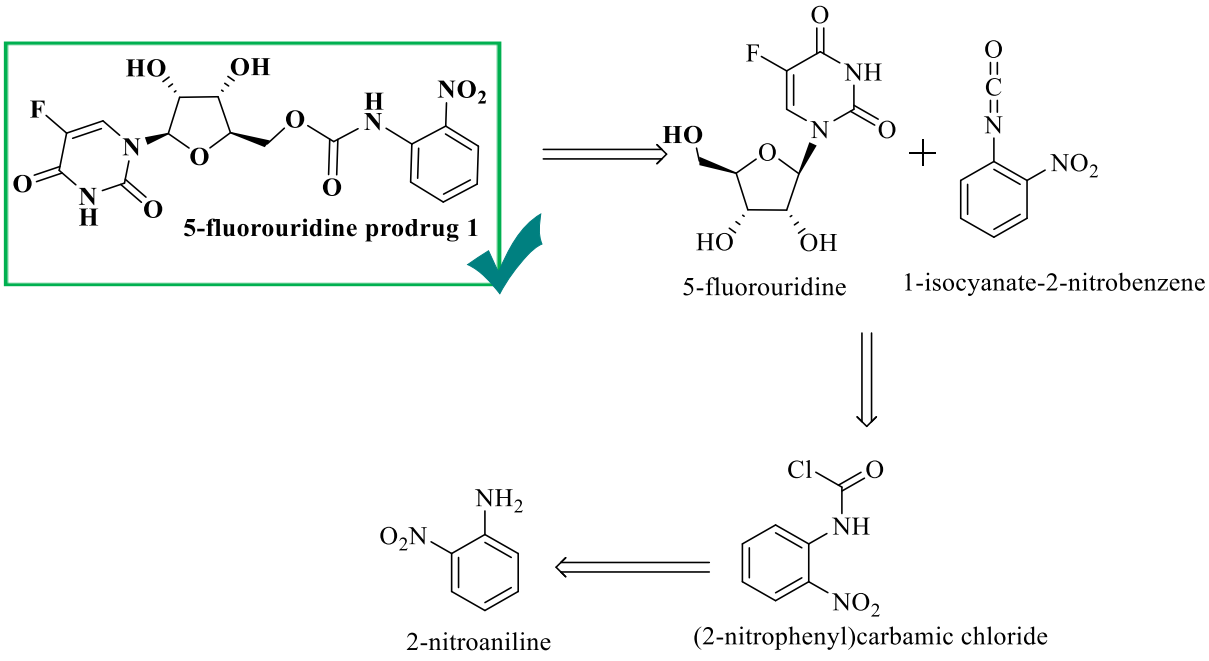


Figure 16. *Retrosynthesis of 5-fluorouridine prodrug **1**.*

3.2.2. 5-Fluorouridine prodrug 2

A second design was proposed in which an ester functional group was employed to attach the trigger to 5-fluorouridine (Figure 17). In this case, the objective of placing two nitro groups was blocking the *para* position to direct the second nitration to the *ortho* position. Then, reduction of the nitro groups to the amine should produce a lactam and the drug liberation at the same time.

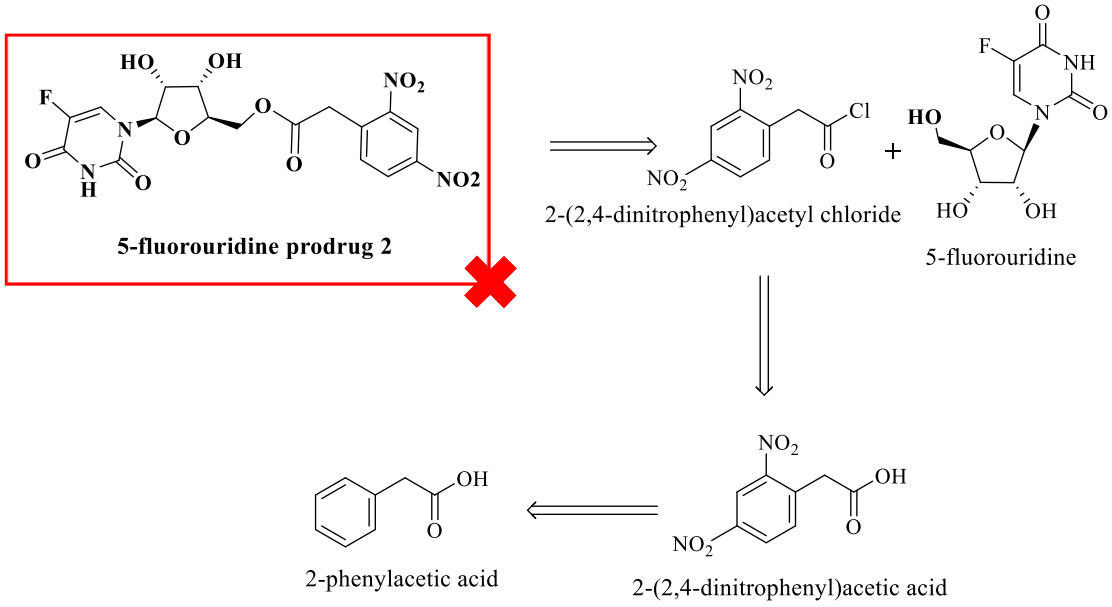


Figure 17. *Retrosynthesis of 5-fluorouridine prodrug **2**.*

Encouraged by the successful synthesis of the prodrug **1** based on nitro group and 5-FUrd (compound **19**), several trials were realized in order to synthetize **5-Fluorouridine prodrug 2**.

The reaction pathway is represented in Figure 17 and describes the synthetic steps in which the procedure started with the nitration of 2-phenylacetic acid in *para* and *ortho* (C-2 and C-4) positions using a mixture of nitric and sulfuric acid (20%/80%) under controlled temperature (not below 60 ºC) to obtain 2-(2,4-dinitrophenyl)acetic acid. The next step was the preparation of the acid chloride 2-(2,4-dinitrophenyl)acetyl chloride, using thionyl chloride with heating (70 ºC).

In order to link 5-FUrd with the acid chloride under milder conditions, the two reagents were mixed in the presence of pyridine, unfortunately the coupling failed.

3.3. Synthesis of the auxiliary group

Compound **1** was obtained according to an optimized published literature procedure, by reacting 1-naphtoic acid with bromine in acetic acid and chloroform as solvents. By controlling the bromine amount, it is possible to obtain only the monobromination product.

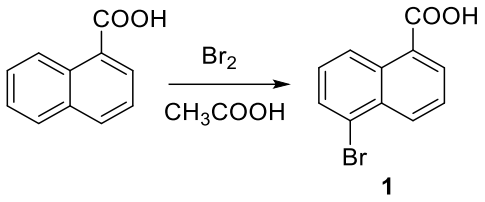


Figure 18. *Synthesis of compound **1**.*

Then nitration of position 8 takes place with nitric acid (Figure 19). The main problem in the synthesis of compound **2** is the risk of explosion due to the presence of nitric acid and the exothermic nature of the reaction. In order to avoid the dangerous consequences of the reaction, it is necessary to keep the temperature below 30 °C, using an ice bath and a thermometer for the temperature control. In this case, the product is obtained with quantitative yield.

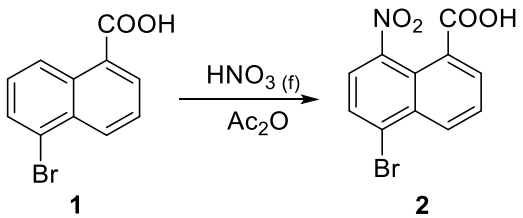


Figure 19. *Synthesis of compound **2**.*

Although compound **2** could be used directly as an auxiliary group, it could certainly not behave as a fluorophore. It also presented solubility problems, so the proposed plan was followed and bromine atom was substituted to a sulfur atom using ethanethiol (90% yield, Figure 20) and oxidized to produce sulfoxide then sulfone (Figures 21, 22).

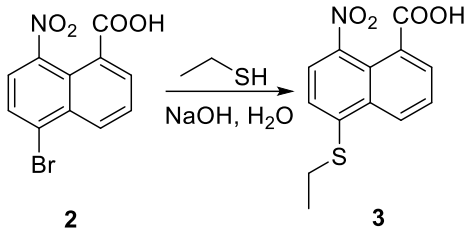


Figure 20. *Synthesis of compound **3**.*

The presence of the ethyl group increases solubility in the reaction medium. Although oxidation with Oxone allowed us to reach the sulfoxide easily (99% yield), we found more difficulties in oxidation to the sulfone, probably due to problems with the solubility of the sulfoxide. In principle, the presence of the carboxyl group allows compound **4** to be dissolved in a basic aqueous solution, but this requires the use of water-soluble oxidants, or the use of a cosolvent.

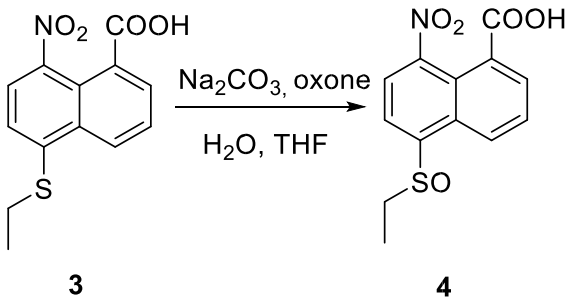


Figure 21. *Synthesis of compound **4**.*

To complete the oxidation to the sulfone, different oxidants were tested to optimize the reaction. In addition, different bases, such as NaOH, K_2CO_3, Cs_2CO_3 or KOH, were used to improve the solubility of the starting material. Solvents were also modified to improve solubility.

Finally, compound **4** was dissolved in methanol and THF, LiOH was added as a base and Oxone as an oxidant, and water as cosolvent. Sulfone **5a** was obtained with 76% yield.

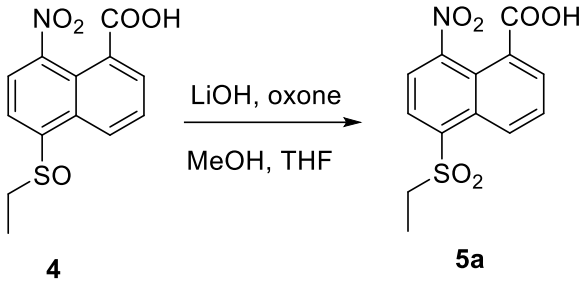


Figure 22. *Synthesis of compound **5a**.*

The synthesis of the acid chloride (compound **5b**) from the acid (compound **5a**) was carried out using PCl_5. The solvent and phosphorus oxychloride were eliminated under reduced pressure. The acid chloride thus obtained was used directly in the next reaction without any additional purification, due to the risk of hydrolysis.

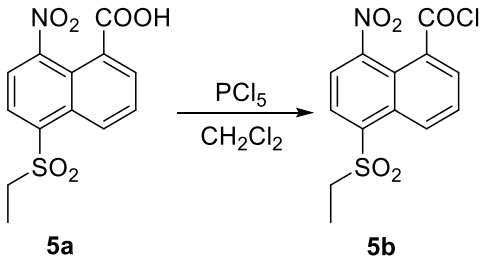


Figure 23. *Synthesis of compound **5b**.*

Once compound **5b** was obtained, its reactivity with amines, alcohols and thiols was studied, with the aim of investigating which functional groups may carry the drugs susceptible to binding to the molecular activator.

Regarding the formation of amide-like bonds, different aliphatic amines, such as butylamine and dibutylamine, were used.

For this, the amine is dissolved in ethyl acetate and added to compound **5b**. Next, 2M HCl is added to neutralize the excess of base, and the product is extracted with ethyl acetate. In principle, the reaction proceeds with good performance, but the main problem with the synthesis was the purification stage.

Several tests were also conducted using different aromatic amines, such as aniline, 4-chloroaniline and toluidine, which required continuous optimization of reaction conditions, changing temperature, solvents, and reaction times. As a result, aliphatic amines have shown a

performance and ease of attachment unlike aromatics, which prompted us to look for drugs containing amines that could be susceptible to be attached to the activator.

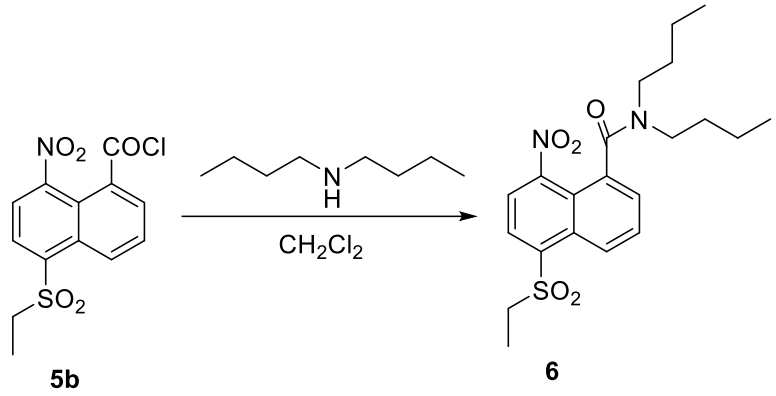


Figure 24. *Synthesis of compound **6**.*

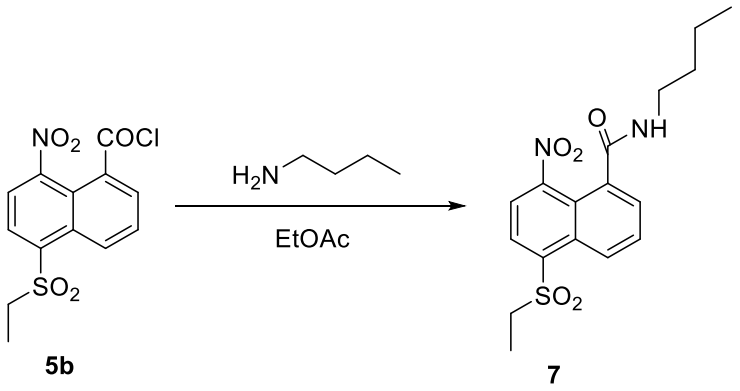


Figure 25. *Synthesis of compound 7.*

The reactivity of **5b** acid chloride with 1-dodecanothiol was also studied. In the case of compound **8** (Figure 26), problems were reported starting with the homogeneity of the starting materials in methylene chloride. The problem was solved by adding THF as a cosolvent. Purification was then performed using a silica gel chromatographic column. It was difficult to find the right eluents, as well as the complication associated with the small amount of the final product available. The synthesis was successful, but the purification of the final product requires future optimization.

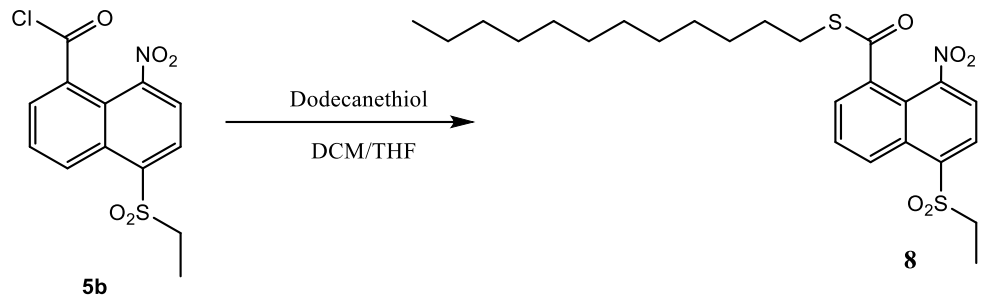


Figure 26. *Synthesis of compound **8**.*

In addition, different alcohols, such as 2-propanol and 1-pentanol, were tested to obtain an ester bond in the final molecule. In the first case, methylene chloride was used as a solvent and kept in agitation for half an hour. The reaction went smoothly, but no optimal procedure was found to purify the final product. In the case of 1-pentanol (compound **9**), a mixture of CH_2Cl_2/THF 4:1 v/v was used as a solvent.

First, purification of the final product by column chromatography on silica gel using DCM and EtOAc as eluents was attempted, although the product was coeluted from silica in the presence of 1-pentanol. Finally, successful purification was carried out by co-evaporating excess pentanol with toluene under reduced pressure.

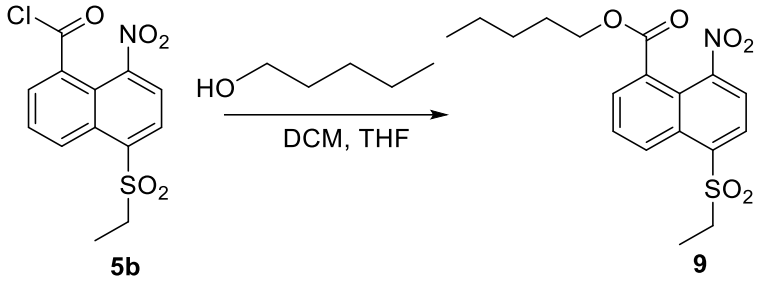


Figure 27. *Synthesis of compound **9**.*

Once the reactivity of the acid chloride **5b** with different functional groups was studied, the binding of bis(2-chloroethyl)amine hydrochloride nitrogen mustard was addressed.

Multiple attempts were made to obtain the prodrug directly by reacting compound **5b** with drug bis(2-chloroethyl)amine hydrochloride. The acid chloride **5b** was reacted with two equivalents of compound **1**, in the presence of triethylamine, and DCM as a solvent, however, the reagents did not react with each other.

The reaction was carried out in an ice bath. Other solvents and bases, such as dimethylformamide and pyridine were studied and the amounts of the reagents were modified, but optimal conditions were not found. In order to not waste reagents, tests were carried out

with an analogue of compound **5b**, benzoyl chloride (Figure 28), but again, no product was obtained.

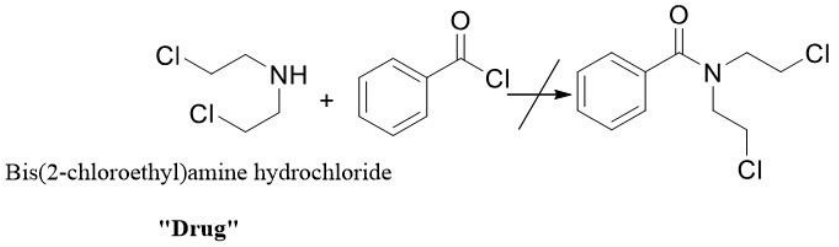


Figure 28. *Unsuccessful reaction between the drug and benzoyl chloride.*

In order to not waste bis(2-chloroehtyl)amine drug in test reactions, reaction with diethanolamine was tested. To do this, it was dissolved in an aqueous solution of Na_2CO_3 saturated with solid Na_2CO_3. Benzoyl chloride was added to ethyl acetate, then the reaction mixture was kept in stirring for 45 minutes (Schotten-Baumann conditions). After recovering the organic phase, it was treated with an aqueous solution of 2M HCl to remove the excess of diethanolamine, and extraction with ethyl acetate was performed, obtaining compound **11**.

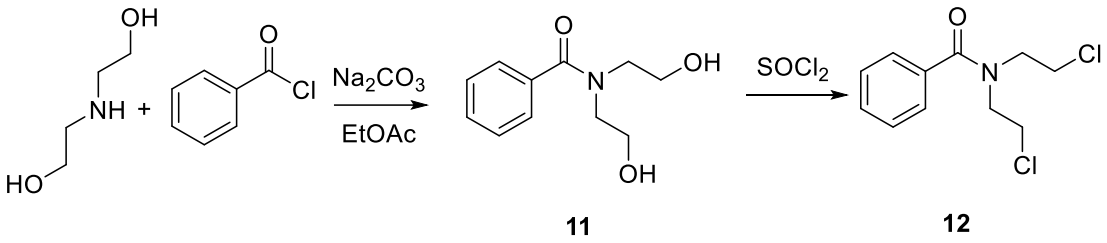


Figure 29. *Reaction between diethanolamine and benzoyl chloride.*

The hydroxyl groups were then replaced by chlorine atoms using thionyl chloride to obtain the desired product (compound **12**).

Once the reaction conditions with benzoyl chloride were optimized, the same conditions were applied for compound **5b**. Compound **13** was obtained by reacting compound **5b** in ethyl acetate with diethanolamine dissolved in a saturated aqueous solution of Na_2CO_3.

Again, 2M HCl was used to remove excess base and extracted with EtOAc, obtaining a quantitative yield. Compound **14** was obtained by reacting compound **13** with thionyl chloride.

For its purification, a preparatory column was used, using a 1:1 v/v hexane/EtOAc mixture as an eluent, obtaining compound **14** with a 31% yield.

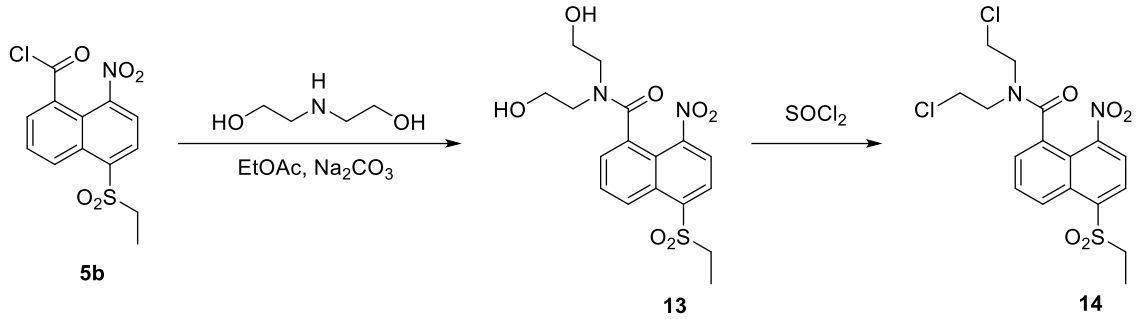


Figure 30. *Synthesis of compounds **13** and **14**.*

Once the prodrug was synthesized, its ability to release the drug under reducing conditions was studied. To do this, compound **14** was dissolved in deuterated methanol, Zn and a drop of acetic acid were added. The progress of the reaction was followed by ^{1}H NMR.

The reduction of the nitro group to amine was confirmed by the shielding of aromatic signals from naphthalene ring, especially the doublet of position 2. The amino group, being sterically hindered, attacks the carbonyl group at position 1, producing lactam **15a** and releasing nitrogen mustard. Although the ^{1}H NMR spectra showed the release of nitrogen mustard, mass spectrometry did not detect the formation of lactam **15a**, but the mass obtained matched that of heterocycle **15b**. Despite this, the release of the drug was successful.

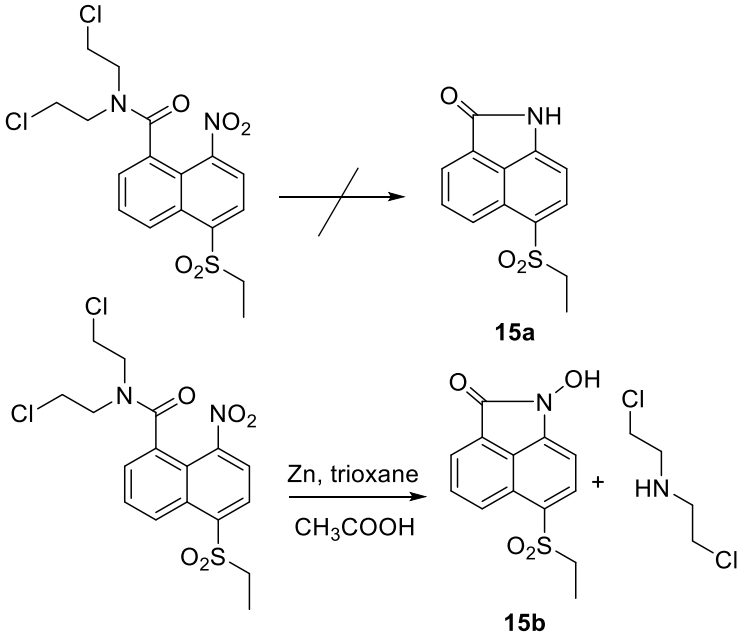


Figure 31. *Reduction of the prodrug **14**.*

An attempt was also made to functionalize some of the intermediates used in the preparation of compound **5a** with the drug, with the intention of saving synthesis steps in the preparation of the prodrug.

To do this, compound **3** was reacted with PCl_5 to obtain the acid chloride. However, during synthesis, the sulfide group was replaced by a chlorine atom. In any case, the synthesis of the prodrug continued, obtaining compound **16**. In this way, the influence of sulfone on the reduction rate of the nitro group to amino in the cellular hypoxia environment will be analysed, as well as on the nucleophilic properties of the amino group when attacking the carbonyl group and releasing the drug.

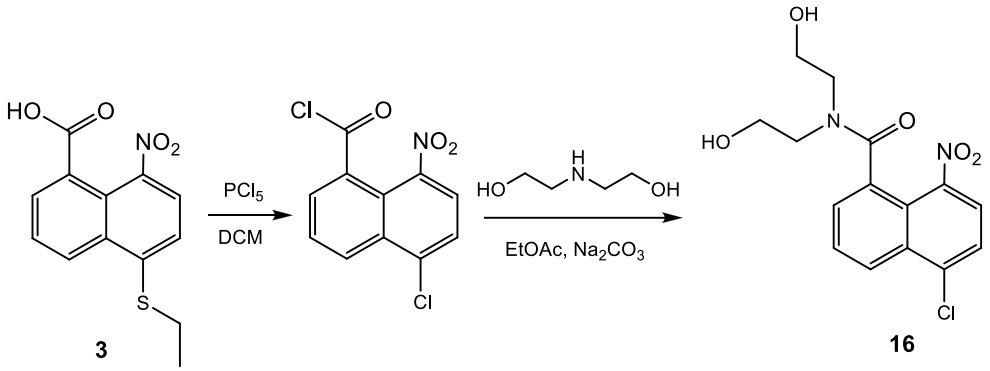


Figure 32. *Synthesis of compound **16**.*

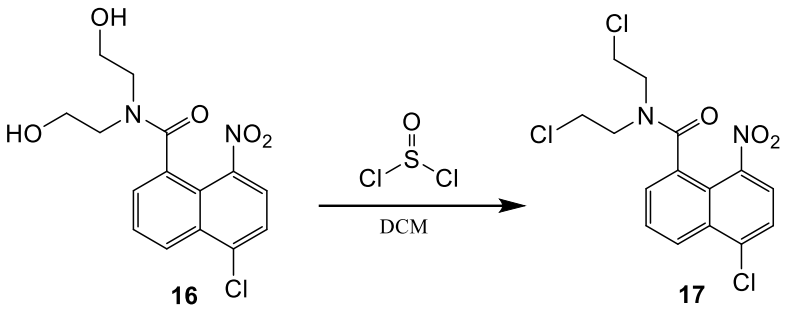


Figure 33. *Synthesis of compound **17**.*

3.4. Synthesis of other auxiliary groups

We also studied other nitro derivatives which could be used as a molecular trigger to release a drug under hypoxia conditions. They are designed to make a cyclization reaction after nitro reduction and release the drug (Figure 15).

For the synthesis of compound **18**, 2-nitroaniline was treated with phosgene solution in toluene. The reaction was carried out under two temperatures (0 ºC/15 min) and (100 ºC/30min) in which (2-nitrophenyl)carbamic chloride was obtained as an intermediate, triethylamine was added to the acid chloride by maintaining the continuous stirring for two hours. The final compound was obtained by extraction with hexane, its validity was confirmed with ^{1}H NMR spectroscopy, then incorporated in the next step without further purification and characterization.

***N.B*:** 1-isocyanate-2-nitrobenzene could be obtained commercially and the full description can be obtained from literature.[20]

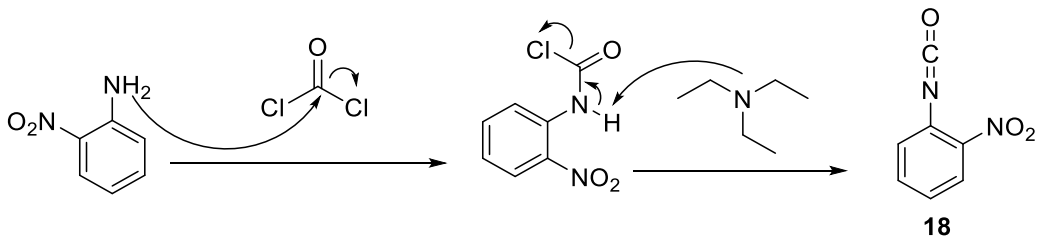


Figure 34. *Synthesis of compound **18**.*

Actually, before compound **19** synthesis, the coupling between compound **18** and benzyl alcohol was tested, mimicking by that the functional group included in the drug (5-flourouridine). This coupling was realized aimed at assessing the ability of linking the drug with1-isocyanato-2-nitrobenzene as a kind of validation since 5-fluorouridine is expensive.

Compound **19** was synthetized by coupling compound **18** with 5-fluorouridine using DMF as a solvent for the obtention of a homogenous mixture. Once the reaction was over at room temperature, compound **19** was obtained by filtration, then it was purified by column chromatography over silica gel, eluting with EtOAc/DCM mixtures of increasing polarity, hence a yellow solid was obtained with 24% yield.

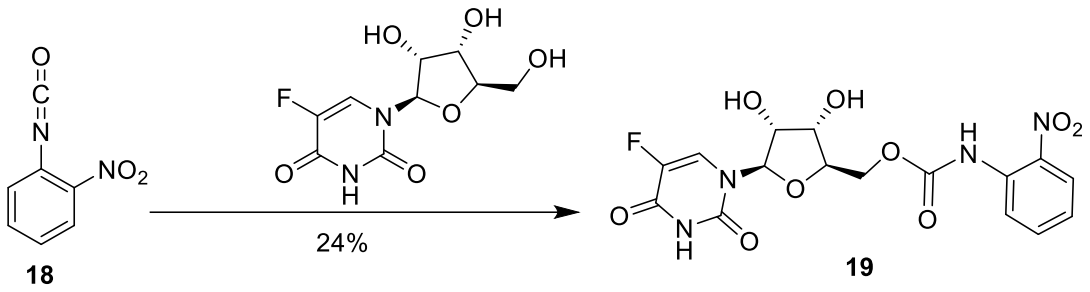


Figure 35. *Synthesis of compound **19**.*

3.5. Fluorescence properties

Since one of the research objectives is the ability of using the compound generated after the drug release as a fluorophore, the fluorescence spectrum of compounds **14** and **15b** were measured. To this end, an excitation and emission wavelength scan was performed to determine the wavelength that generated the maximum fluorescence intensity for both compounds **14** and **15b**. It was found that, by exciting both compounds at 269 nm, **14** was barely fluorescent while **15b** generated a band with a maximum at 405 nm (Figure 36). This behaviour is ideal for using the drug as a theranostic compound, as it would allow the cells in which the drug has been released to be identified by fluorescence microscopy. As can be seen in the figure below, the product obtained after the release of the drug (Pr) has shown remarkable fluorescence. Its intensity is the highest recorded.

On the other hand, there is a clear absence of fluorescence in the starting material (SM). This fact is compatible with the expectation of the design of the molecule.

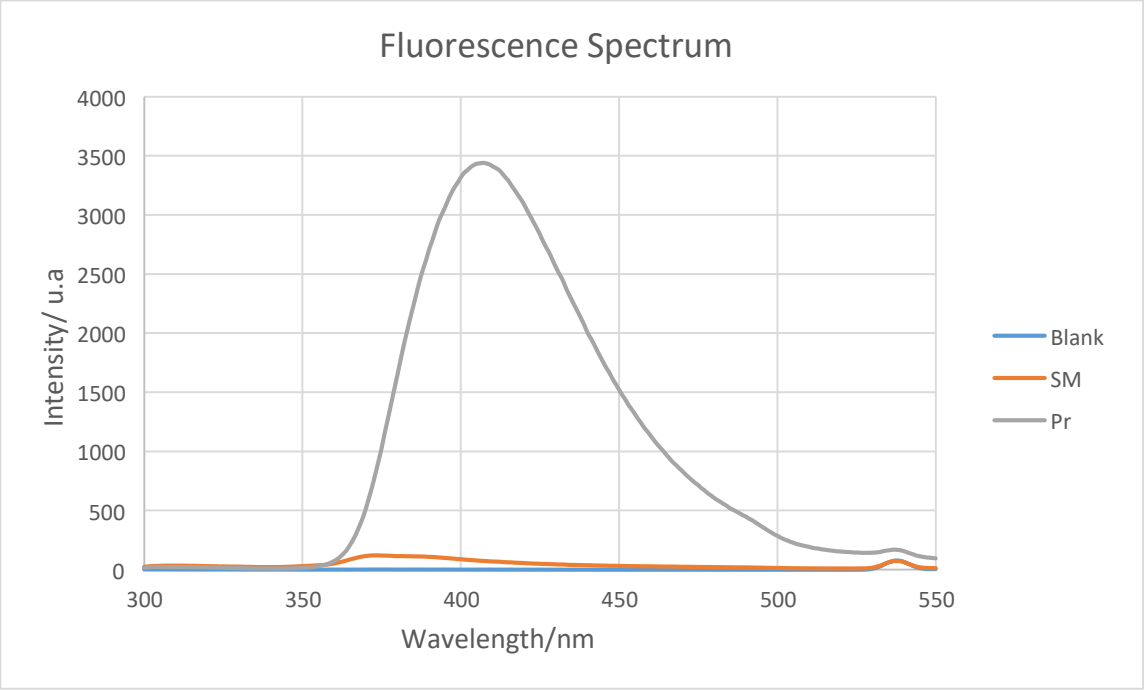


Figure 36. *Fluorescence spectrum with λ_{Ex} = 269 nm / λ_{Em} = 405 nm.*

In addition to the initial objective of the synthesis, which is the release of the drug into the hypoxia microenvironment (in this case simulated), fluorescence has been confirmed in the compound generated after the drug released. This will allow the tracking and localization of the compound within tumour tissues, which can help detect the correct positioning of the cytotoxic molecule. With this, the tracking capacity of the prodrug is proven.

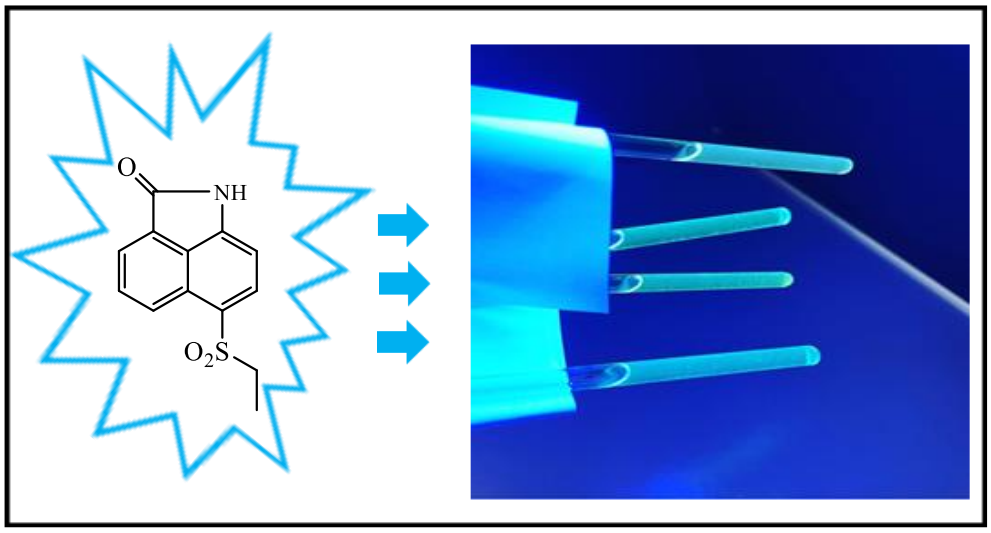


Figure 37. *Fluorescence of compound **15b.***

3.6. Biological trials: MTT assay

Based on the initial hypothesis of our investigation, whose concept reflected in the objective of targeted and selective therapy for cancer, *in vitro* cell assays were carried out for the purpose of testing, validating or optimising our prodrugs synthetized previously.

To achieve the aim, the MTT assay was performed to detect the cytotoxicity level of compounds **14** and **17**. Also, nitrogen mustard gas, bis-(2-chloroethyl)-amine, was used as drug control. The results are shown in figure 38. Cultures of colon cancer cells and fibroblasts (healthy cells) were grown in two different oxygen conditions (5% and 18% oxygen), by treating them with the drugs control, compound **14** and **17**.

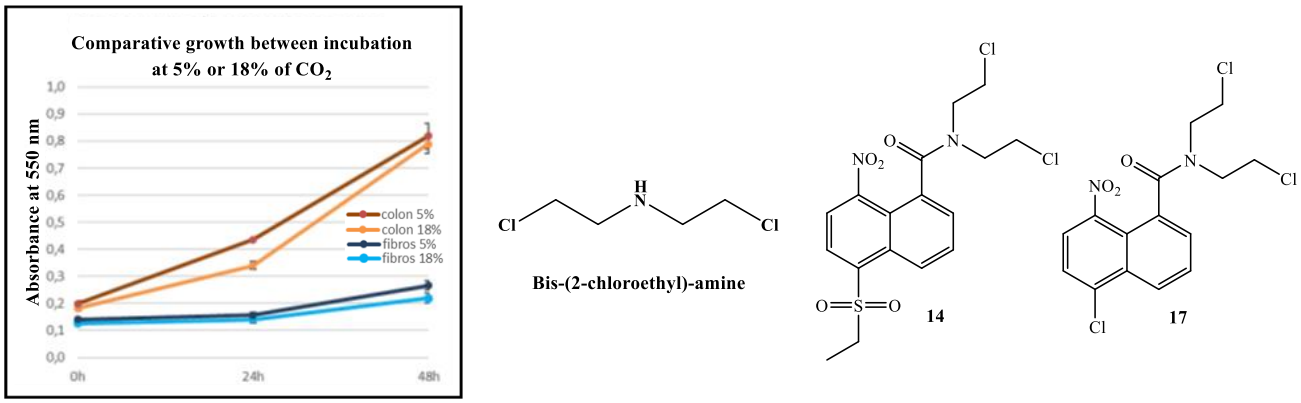


Figure 38. *Left: Growth curve of the two lines used (fibroblasts and colon cancer cells) incubated at 5% and 18% O_2. Right: prodrugs **14** and **17** and nitrogen mustard bis-(2-chloroethyl)-amine.*

Actually, during the research carried out on IC_{50} of bis(2-chloroethyl)amine, it has been only found one thesis from the University of Zaragoza, in which they determined that the IC_{50} of fibroblasts exposed for 1 hour to nitrogen mustard gas (ref. B38503, Sigma) was 3.77 mM. This dose is very high, although it must be taken into account that they did it for a very short exposure time. That means that to reach the IC_{50} in 48 hours we would need a concentration of approximately 80 µM. So, we decided to treat the cells with two different concentrations of bis-(2-chloroethyl)-amine. (100 and 200 µM) and one concentration of compound **14** (100 µM).

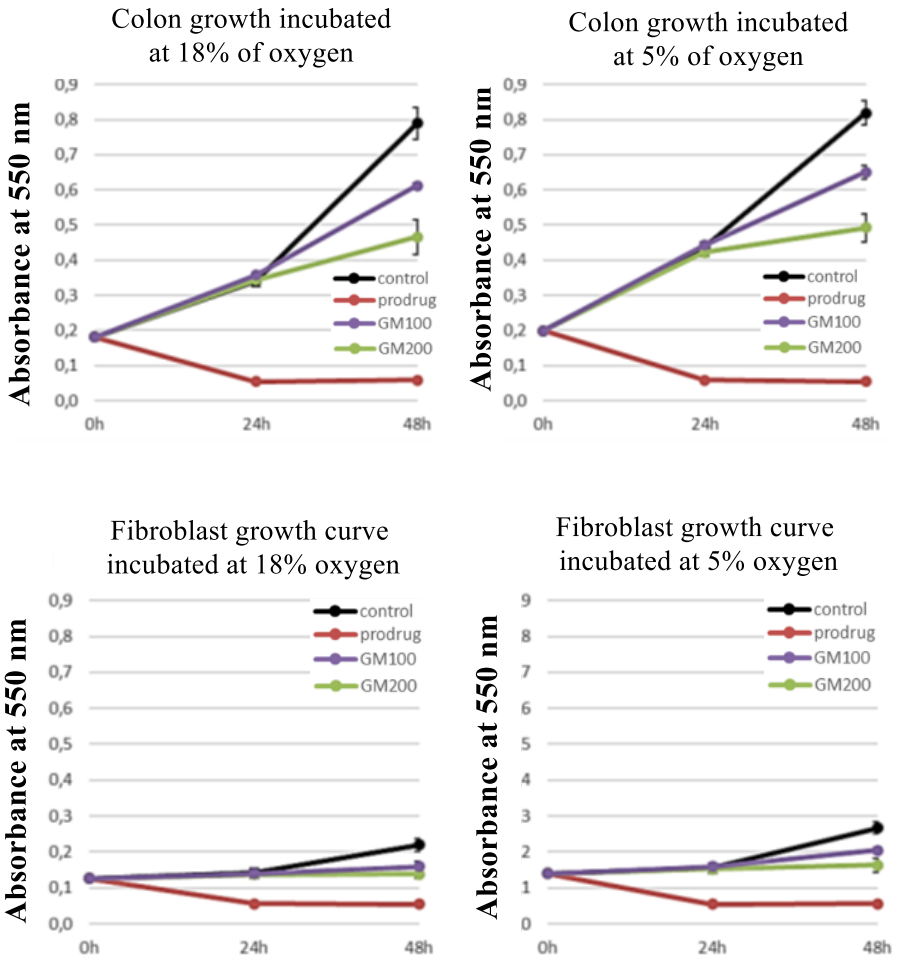


Figure 39. *Absorbance results of the two cell lines under hypoxia and hyperoxia conditions after treatment with prodrug **14** and the nitrogen mustard agent Bis-(2-chloroethyl)-amine.*

Surprisingly, the prodrug results were unpredictable, because of its precipitation when added to the cell medium at that concentration. So, solubility tests were carried out indirectly with the lethal effect study.

Solutions from the two prodrugs in DMEM+ were prepared and divided on 6 falcons, with a final concentration of 50 µM, admitting in each case a different concentration of DMSO to help to solubilise each drug, which is indicated below:

50 µM of Prodrug **14**	**50 µM** of Prodrug **17**
0.05 % DMSO	**0.05 %** DMSO
0.5 % DMSO	**0.5 %** DMSO
1 % DMSO	**1 %** DMSO

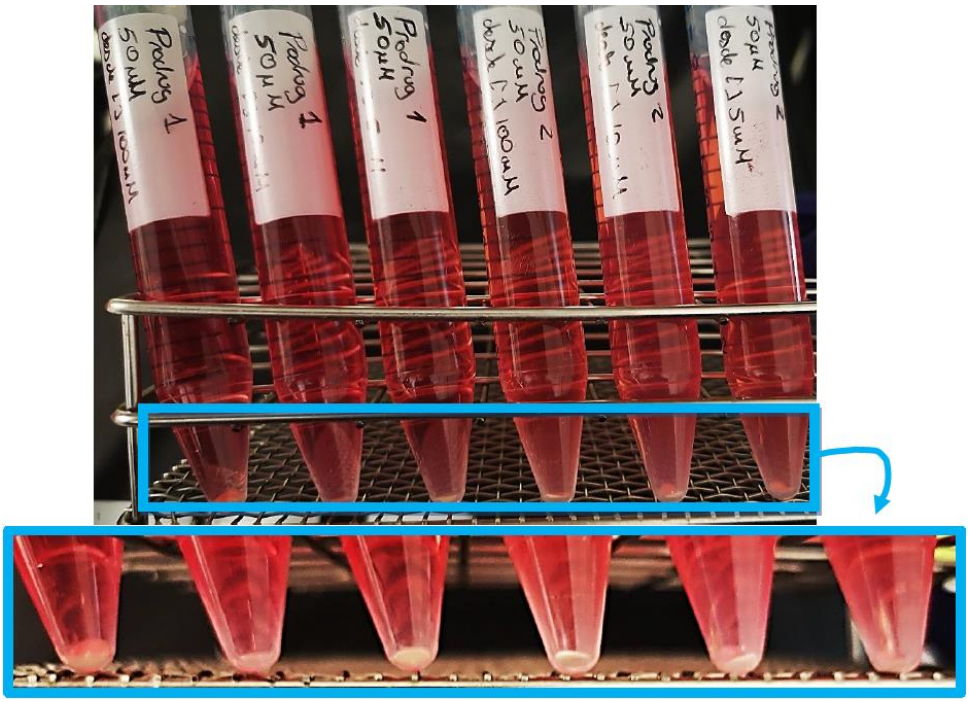


Figure 40. *Compounds **14** (from left to right: Falcon 1, 2 and 3) and **17** (Falcon 4, 5 and 6) added at a final concentration of 50 µM in DMEM from different concentrations of stock solution in DMSO.*

As can be seen, the two prodrugs precipitate in all cases. Thus, they kill and prevent cell growth when added to the cell medium at this concentration. The problem is that prodrug precipitation inhibits cell growth in both healthy cells and cancer cells, and the reason is precipitation, and not drug release under hypoxia conditions. Therefore, our hypothesis could not be tested with prodrugs **14** and **17** under these conditions.

The assay has opened up new horizons for the study of solubility. Thus, in order to study the effectiveness of the drug proposed in this chapter, it will be necessary to modify the design and the chemical structure in order to obtain theranostic prodrugs with better solubility in cellular media.

4. Conclusions

In this chapter several nitroaromatics derivatives have been designed and synthesized by attaching them to cytotoxic anticancer drugs: bis(2 chloroethyl)amine and 5-fluorouridine, as a result two antineoplastic prodrugs have been produced.

In addition, different functional groups have been studied so that they could be attached to the anticancer agents respecting the design modification and its ability to be triggered under the bioreductive media in the absence of oxygen.

Bis(2 chloroethyl)amine prodrug (compound **14)** is able to be used as a theranostic thanks to the fluorescence of its byproduct (compound **15b**) following the prodrug cleavage under hypoxic conditions which allows the compound monitoring within the tumour tissues, and on the other hand to check its cytotoxicity in reducing cancer cells viability. The expected liberation was tested first in an NMR tube by mimicking the tumoral reductive microenvironment, using chemical reducing agents (zinc).

The limitations of the work lie in performing the MTT assays (*in vitro* assays), which were realized in order to verify the prodrugs cytotoxicity by its cleaving and activation inside the cancerous hypoxic environment according to the theoretical strategy.

Contrary to what was expected, thanks to the MTT assays a solubility issue has been detected in which precipitations of compound **14** were observed within the falcons of cell buffer (Figure 40), in this case the understanding of organic moieties dissolution has become a priority to guarantee prodrugs structural adaptability and design inside the cellular media then the human body. Consequently, since solubility is an important factor in synthesising prodrugs and aiming to enhance prodrugs physicochemical and pharmacological characteristics, promising modulations will be discussed in the next chapters.

5. Experimental Section

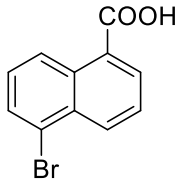
5.1. Materials and instrumentation

Fluorescence Spectroscopy

Fluorescence spectra were performed on a Jasco FP-8300 spectrofluorometer with a 150W Xe lamp.

5.2. Synthetic details and characterization

5-bromo-1-naphthoic acid (1)



1

This compound was prepared according to a modified published literature.[21]

1-naphthoic acid (20.0 g, 116.2 mmol) was placed in a 250 mL round bottom flask equipped with a reflux condenser, and $CHCl_3$ (80.0 mL) and acetic acid (10.0 mL) were added. The suspension was refluxed until a homogeneous solution was obtained. Bromine (12.0 mL, 234 mmol) was then added dropwise and after 3 minutes the brominated compound **1** started to precipitate. The thick solution was further refluxed for 2 hours. Cooling down and filtering the precipitate yielded the brominated compound (**1**) (26.0 g, 90% yield) as a white powder.

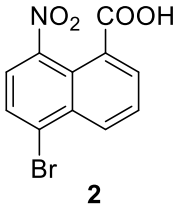
M.p. >200 ºC

^{1}H NMR (DMSO-d_6, 400 MHz): 8.87 (d, 1H, J = 8.8 Hz), 8.42 (d, 1H, J = 8.5 Hz), 8.22 (dd, 1H, J = 7.2, 0.8 Hz,), 7.99 (dd, 1H, J = 7.3, 0.8 Hz), 7.77 (dd, 1H, J = 8.5, 7.2 Hz), 7.57 (dd, 1H, J = 8.8 ,7.3 Hz).

^{13}C NMR (DMSO-d_6, 100 MHz): 168.3 (C), 131.9 (C), 131.4 (C), 130.9 (CH), 130.6 (CH), 130.4 (CH), 128.9 (C), 128.1 (CH), 126.8 (CH), 125.8 (CH), 122.4 (C).

MS (ESI$^-$): chemical formula $C_{11}H_6O_2Br$, theorical mass 248.9557; experimental mass [M - H $^-$] 248.9559.

5-bromine-8-nitro-1-naphtoic acid (2)



2

5-bromo-1-naphthoic acid, **1** (20.0 g, 79.7 mmol) was placed in a round bottom flask with acetic anhydride (200 mL), *p*-toluene sulfonic acid (4.0 g) and P_2O_5 (5.0 g). Fuming nitric acid (20.0 mL) was carefully added to this suspension, keeping the temperature below 30ºC. After 30 minutes the reaction was poured over water and ice. Once the acetic anhydride was hydrolysed (2 hours), the precipitate was filtered to yield, after drying, the nitro compound (**2**). This crude compound can be further purified by recrystallization from THF/EtOH, affording pure compound **2** in 86% yield (20.3 g) as a pale cream crystalline solid.

M.p.: 211-214 ºC.

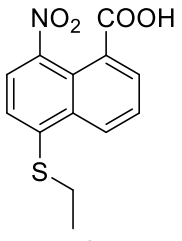
IR (neat, ν in cm^{-1}): 3351, 2929, 2843, 1670, 1521, 1346.

^{1}H NMR (DMSO-*d*$_6$, 400 MHz): 8.50 (dd, 1H, *J* = 8.4, 1.2 Hz), 8.20 (dd, 1H, *J* = 7.2, 1.2 Hz,), 8.16 (ABq, 2H, J_{AB} = 8.4 Hz), 7.91 (dd, 1H, *J* = 8.4,7.2 Hz).

^{13}C NMR (DMSO-*d*$_6$, 100 MHz): 167.6 (C), 146.8 (C), 132.3 (C), 131.8 (CH), 130.5 (CH), 130.0 (CH), 129.6 (C), 128.7 (CH), 128.5 (C), 125.4 (CH), 122.1 (C).

MS (ESI$^-$): chemical formula $C_{11}H_5O_4NBr$, theorical mass 293.9407; experimental mass [M-H$^-$]: 293.9410.

5-(ethylthio)-8-nitro-1-naphtoic acid (3)



3

In a 100 mL round-bottom flask, ethanethiol (2.5 mL, 3.0 g, 0.048 mol) was added over a solution of NaOH (4.5 g, 0.1 mol) in 45 mL of water and stirred for 10 minutes. Compound **2** (3.0 g, 0.01 mol) was then added. After 3 hours stirring at room temperature, 2M HCl and ice

were added, obtaining an orange precipitate, which was filtered into a Büchner funnel (2.69 g, 90%).

M.p.: 188.5 – 189 ºC.

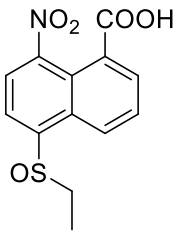
IR (nujol, ν in cm^{-1}): 3397, 2949, 2852, 1677, 1300.

^{1}H NMR (400 MHz, DMSO-*d_6*) δ 8.44 (d, *J* = 8.6, 1.2 Hz, 1H), 8.18 (d, *J* = 8.2 Hz, 1H), 8.13 (d, *J* = 1.2 Hz, 1H), 8.12 (d, *J* = 1.2 Hz, 1H), 7.80 (t, *J* = 8.5, 7.2 Hz, 1H), 3.27 (q, *J* = 7.3 Hz, 4H), 1.37 (t, *J* = 7.3 Hz, 3H*)*.

^{13}C NMR (101 MHz, DMSO-*d_6)* δ 167.9 (C), 143.9 (C), 143.7 (C), 131.1 (CH), 131.0 (C), 129.5 (C), 127.1 (CH), 126.7 (CH), 124.8 (CH), 121.2 (CH), 121.0 (C), 25.3 (CH_2), 13.1 (CH_3).

MS (ESI^+): chemical formula: $C_{13}H_{12}NO_4S^+$; theoretical mass: 278.0591; experimental mass [$M\text{-}H^+$]: 278.0913.

5-(ethylsulfinyl)-8-nitro-1-naphthoic acid (4)



4

Compound **3** (3.98 g ,0.01 mol) and Na_2CO_3 (7.0 g, 0.06 mol) were dissolved in 10 mL of water, 2 equivalents of Oxone were added to the mixture with a continuous stirring for 10 minutes. Next, 10 mL of tetrahydrofuran was poured, the mixture was kept at 40 ºC for 1 h 30 min. After this time, aqueous 2M HCl was added and the reaction mixture was filtered under vacuum, obtaining a grey solid (3.48 g, 99%).

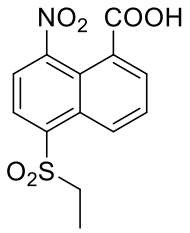
Mp: 200- 205 ºC.

IR (neat, ν in cm^{-1}): 2929, 2845, 1723, 1541, 1353, 1255.

^{1}H NMR (400 MHz, CD_3OD) δ 8.38 (d, *J* = 7.9 Hz, 1H), 8.30 (dd, *J* = 8.5, 1.1 Hz, 1H), 8.24 (dd, *J* = 7.3, 1.1 Hz, 1H), 8.22 (d, *J* = 8.0 Hz, 1H), 7.85 (t, 1H), 3.31 (dt, *J* = 3.3, 1.6 Hz, 2H), 1.22 (t, *J* = 7.4 Hz, 3H).

^{13}C NMR (101 MHz, CD_3OD) δ 169.8 (C), 151.1 (C), 146.62 (CH), 132.9 (C), 131.7 (C), 131.5 (C), 129.2 (CH), 126.5 (CH), 125.3 (CH), 124.2 (CH), 123.2 (C), 50.0 (CH_2), 6.2 (CH_3). **MS (ESI$^+$) :**chemical formula: $C_{13}H_{12}O_5N^{32}S$, theorical Mass: 294,04307, experimental mass [M+H+]: 294,0429

5-(ethylsulfonyl)-8-nitro-1-naphtoic acid (5a)



5a

LiOH (600 mg, 200 mmol) was dissolved in 220 mL of water and added dropwise over a solution of compound **4** (1.00 g, 3.41 mmol) in 66 mL of MeOH:THF 2.3:1 v/v. Oxone (5.0 g, 8.0 mmol) was then added. After 1 hour, the reaction mixture was concentrated at reduced pressure, up to about 10 mL. Next, the reaction mixture was added over 50 mL of 2M HCl and ice, compound **5** was filtered under vacuum affording a pale yellow solid (0.8 g, 76%).

M.p.: 203 – 205 ºC.

IR (film, ν in cm $^{-1}$): 3743, 3643, 3118, 2343, 1723, 1534, 1275, 1132.

^{1}H NMR (400 MHz, CD_3OD) δ 9.07 (dd, *J* = 8.8, 1.1 Hz, 1H), 8.47 (d, *J* = 8.0 Hz, 1H), 8.32 (d, *J* = 8.0 Hz, 1H), 8.28 (dd, *J* = 7.2, 1.1 Hz, 1H), 7.93 (t, *J* = 8.8, 7.2 Hz, 1H), 3.46 (q, *J* = 7.4 Hz, 2H), 1.23 (t, *J* = 7.4 Hz, 3H).

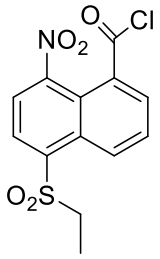
^{13}C NMR (101 MHz, CD_3OD) δ 169.7 (C), 153.0 (C), 140.3 (C), 132.8 (CH), 132.3 (C), 131.7 (CH), 131.6 (C), 130.0 (CH), 128.9 (CH), 124.4 (CH), 124.0 (C), 51.6 (CH2), 7.4 (CH3).

MS (ESI$^+$): chemical formula: $C_{13}H_{11}O_6N_{23}Na_{32}S^+$; theorical mass: 332.0199; experimental mass [M+Na^+]: 332.0196.

5-(ethylsulfonyl)-8-nitro-1-naphthoyl(5b) chloride

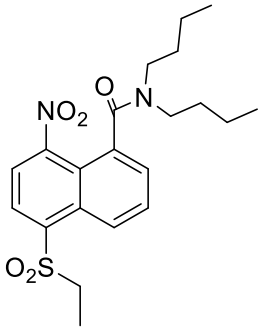
Acid activation using PCl_5.

Acid **5a** (330 mg, 1.0 mmol) was slowly added to a 10% w/v solution of PCl_5 (330 mg, 1.1 mmol) in CH_2Cl_2. It remained in agitation for 30 minutes. The reaction mixture was concentrated at reduced pressure, and the product was used in the next step without any further purification.



5b

***N*,*N*-dibutyl-5-(ethylsulfonyl)-8-nitro-1-naphthamide(6)**



6

Di-*N*-butylamine (300 µL, 1.78 mmol) was added to compound **5b** (150 mg, 0.45 mmol) using EtOAc as a solvent. The mixture was kept in stirring for 10 minutes at room temperature and extracted using 2M HCl and EtOAc. The organic phase was washed with aqueous 2M HCl and an aqueous solution of 1% H_2SO_4, dried over anhydrous Na_2SO_4, filtered and evaporated at reduced pressure. It was then purified using a silica gel chromatographic column, with methylene chloride and EtOAc (10:1 v/v) as the eluent. After evaporating the solvents at reduced pressure, compound **6** was obtained as a brown oil (90 mg, 46%).

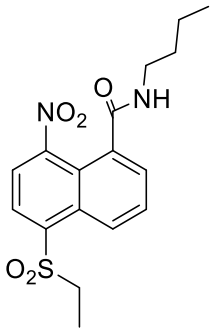
IR (film, ν in cm^{-1}): 2962, 2929, 2877, 1736, 1638, 1534, 1327, 1145.

^{1}H NMR (400 MHz, $CDCl_3$) δ 8.96 (dd, *J* = 8.7, 1.0 Hz, 1H), 8.43 (d, *J* = 8.0 Hz, 1H), 8.05 (d, *J* = 8.0 Hz, 1H), 7.80 (dd, *J* = 8.7, 7.2 Hz, 1H), 7.69 (dd, *J* = 7.1, 1.0 Hz, 1H), 3.60 – 3.24 (m, 7H), 1.81 – 1.58 (s, 3H), 1.52 – 1.34 (s, 3H), 1.36 – 1.19 (m, 7H), 1.08 – 0.95 (s, 3H).

^{13}C NMR (101 MHz, $CDCl_3$) δ 169.2 (C), 151.8 (C), 138.7 (C), 134.0 (C), 131.7 (C), 130.4 (CH), 128.7 (CH), 128.7 (CH), 125.9 (CH), 123.4 (CH), 122.3 (CH), 50.9 (CH_2), 49.9 (CH_2), 45.1 (CH_2), 30.5 (CH_2), 29.3 (CH_2), 20.7 (CH_2), 20.4 (CH_2), 14.1 (CH_3), 13.9 (CH_3), 7.5 (CH_3).

MS (ESI$^+$): chemical formula: $C_{21}H_{29}N_2O_5S^+$;theorical mass: 421.1792; experimental mass [M+H$^+$]: 421.1788.

***N*-butil-5-(ethylsulfonyl)-8-nitro-1-naphthamide (7)**



7

A solution of butylamine (50 µL, 0.51 mmol) dissolved in 2 mL of EtOAc was added dropwise over a solution of compound **5b** (50 mg, 0.16 mmol) in 3 mL of EtOAc at -78 °C under argon atmosphere. After ten minutes, aqueous 2M HCl was added to remove excess of butylamine. The organic phase was dried over anhydrous Na_2SO_4, filtered, and evaporated at reduced pressure. Finally, purification was performed in a silica gel column, using CH_2Cl_2 as an eluent at the beginning. In order to increase polarity, CH_2Cl_2/ EtOAc (1:1 v/v) was then used. Finally, after evaporation of the solvents at reduced pressure, compound **9** was obtained in the form of a white solid (25 mg, 40%).

M.p.: 214.5-215 ºC.

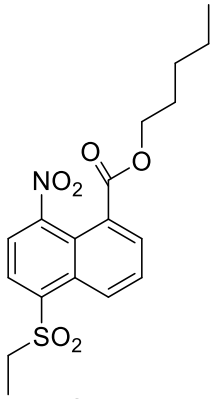
IR (film, ν in cm^{-1}): 3260, 2923, 2351, 1638, 1541, 1456, 1366, 1314, 1132.

^{1}H NMR (400 MHz, $CDCl_3$) δ 9.01 (dd, *J* = 8.8, 1.1 Hz, 1H), 8.46 (d, *J* = 8.0 Hz, 1H), 8.13 (d, *J* = 8.0 Hz, 1H), 7.84 (dd, *J* = 40.8, 1.4 Hz, 2H), 3.48 (td, *J* = 7.3, 5.8 Hz, 2H), 3.32 (q, *J* = 7.4 Hz, 2H), 1.68 (m, 2H), 1.48 (dd, *J* = 15.1, 7.4 Hz, *2H*), 1.31 (m, 3H), 1.00 (t, *J* = 7.3 Hz, 3H).

^{13}C NMR (101 MHz, $CDCl_3$) δ 168.4 (C), 152.7 (C), 138.5 (C), 134.3 (C), 131.4 (C), 130.5 (CH), 129.0 (CH), 128.8 (CH), 126.7 (CH), 122.7 (C), 122.7 (CH), 50.8 (CH_2), 40.1 (CH_2), 31.5 (CH_2), 20.2 (CH_2), 13.8 (CH_3), 7.3 (CH_3).

MS (ESI$^+$) : chemical formula: $C_{18}H_{21}NNaO_6S^+$; theorical mass: 402.0987; experimental mass [M + Na^+]: 402.0977.

Pentyl 5-(ethylsulfonyl)-8-nitro-1-naphthoate (9)



9

1-pentanol (1 mL, 9.25 mmol) was added to compound **5b** (50 mg, 0.15 mmol). The mixture was then dissolved in 200µL of methylene chloride and stirred for 30 min. The excess of 1-pentanol was removed by azeotropic distillation using toluene, obtaining compound **9** in the form of oil (20 mg, 33%).

Mp.: Oily.

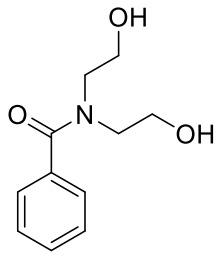
^{1}H NMR (400 MHz, $CDCl_3$) δ 9.06 (dd, *J* = 8.8, 1.1 Hz, 1H), 8.46 (d, *J* = 2.0 Hz, 1H), 8.21 (dd, *J* = 7.2, 1.1 Hz, 2H), 7.85 (dd, *J* = 8.7, 7.2 Hz, 1H), 4.30 (t, *J* = 6.9 Hz, 2H), 3.32 (q, *J* = 7.4 Hz, 2H), 1.73 (ddd, *J* = 21.1, 10.6, 6.4 Hz, 2H), 1.43 – 1.32 (m, 4H), 1.32 (m, 3H), 0.90 (t, *J* = 7.0 Hz, 3H).

^{13}C NMR (101 MHz, $CDCl_3$) δ 166.8 (C), 151.6 (C), 139.0 (C), 132.1 (CH),131.2 (C), 130.5 (CH), 130.0 (CH), 129.1 (C), 128.9 (C), 127.6 (CH), 123.1 (CH), 66.5 (CH_2), 51.0 (CH_2), 28.3 (CH_2), 28.2 (CH_2), 22.5 (CH_2), 14.1 (CH_3), 7.5 (CH_3).

IR (film, ν in cm^{-1}): 3314, 2955, 2936, 2865, 1723, 1463, 1054.

MS (ESI$^+$): chemical formula: $C_{18}H_{21}NNaO_6S^+$; theorical mass: 402.0987; experimental mass [M + Na^+]: 402.0977.

***N,N-bis*(2-hydroxyethyl)benzamide (11)**

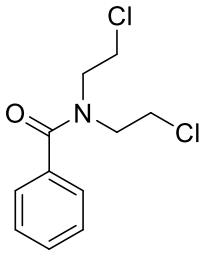


11

In a 50 mL round-bottomed flask, diethanolamine (1.0 g, 9.5 mmol) is added followed by a saturated aqueous solution of Na_2CO_3 (1.0 g, 9.5 mmol). The mixture is stirred for 5 minutes. Benzoyl chloride (200 µL, 1.7 mmol) is then dissolved in 2 mL of EtOAc. The solution is incorporated into the previous reaction mixture. After 30 minutes, the organic phase is treated with 2M HCl/ EtOAc, then dried over anhydrous Na_2SO_4, filtered and after evaporation of the organic solvent at reduced pressure, compound **11** was obtained as a colourless oil (60 mg, 17%), which was used in the next reaction without further purification.

The spectral properties match with the commercial compound.[22]

***N,N-bis*(2-chloroethyl)benzamide (12)**

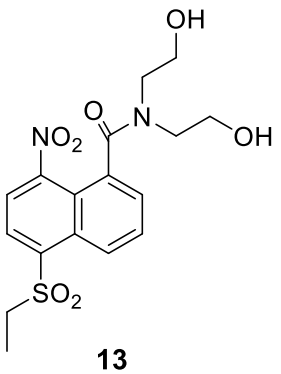


12

500 µL of $SOCl_2$ was added to *N*,*N*-bis(2-hydroxyethyl)benzamide (60 mg, 0.29 mmol). The reaction was performed at 0 ºC for 1 hour with continuous agitation [21]. The excess of $SOCl_2$ was evaporated at reduced pressure, and compound **12** was obtained as a yellow oily liquid (60 mg, 84%).

The spectral properties match with the commercial compound.[23]

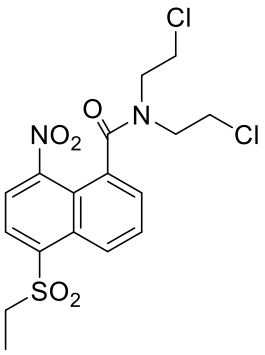
5-(ethylsulfonyl)-*N*,*N*-bis(2-hydroxyethyl)-8-nitro-1-naphthamide (13)



13

Diethanolamine (1.0 g, 9.5 mmol) was dissolved in 3 mL of a 4% w/v solution of Na_2CO_3 for 10 min. Compound **5b** (50 mg. 0.15 mmol) was then dissolved in 1 mL of EtOAc and transferred to the previous solution. After 1 hour stirring the reaction mixture at room temperature, the two phases were separated, and the organic phase was washed with an aqueous solution of 2M HCl, dried over anhydrous Na_2SO_4, filtered and evaporated at reduced pressure, obtaining 60 mg (99%) of an oily yellow liquid, which was used for the next reaction without additional purification.

***N*,*N*-bis(2-chloroethyl)-5-(ethylsulfonyl)-8-nitro-1-naphthamide (14)**



14

Thionyl chloride (400 µL, 5.5 mmol) was added over a solution of compound **13** (60 mg, 0.15 mmol) in 2 mL of CH_2Cl_2 at 0°C and the solution was stirred at that temperature for one hour. It was then evaporated under reduced pressure and purified by column chromatography on silica gel, using CH_2Cl_2/EtOAc (100:3 v/v) as the eluent. As impurities were still remaining, a preparative chromatography was performed using a 1:1 hexane/EtOAc mixture as eluent. After scraping the silica and leaching the product using EtOAc and evaporating the solvent, pure compound **14** was obtained as a brown oil (20 mg, 31%).

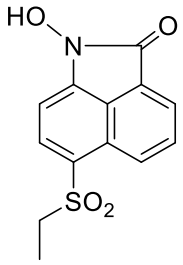
IR (film, ν in cm^{-1}): 2929, 1645, 1529, 1431, 1366, 1320, 1139, 743.

^{1}H NMR (400 MHz, $CDCl_3$) δ 9.04 (dd, *J* = 8.3, 1.3 Hz, 1H), 8.47 (d, *J* = 8.0 Hz, 1H), 8.10 (d, *J* = 8.0 Hz, 1H), 7.87 (m, 2H), 3.86 (m, 8H), 3.33 (m, 2H), 1.31 (t, *J* = 6.6 Hz , 3H).

^{13}C NMR (101 MHz, $CDCl_3$) δ 170.2 (C), 151.1 (C), 139.0 (C), 131.84 (C), 131.6 (C), 130.5 (CH), 129.6 (CH), 128.7 (CH), 126.6 (CH), 123.1 (C), 122.7 (CH), 52.0 (CH_2), 50.9 (CH_2), 47.7 (CH_2), 40.9 (CH_2), 40.2 (CH_2), 7.3 (CH_3).

MS (ESI): chemical formula: $C_{17}H_{19}Cl_2N_2O_5S^+$; theorical mass: 433.0392; experimental mass: [M+H^+]: 433.0385.

7-(ethylsulfonyl)-1*H*,3*H*-naphtho[1,8-*cd*][1,2]oxazin-3-one(15b)



15b

In a closed vial, compound **14** (40 mg, 0.09 mmol) was dissolved in 5 mL of CD_3OD and trioxane (15 mg, 0.17 mmol) was added as an internal standard. The solution was shaken for 5 minutes and then Zn (30 mg, 0.17 mmol) and 5 drops of acetic acid were added. After two hours of magnetic stirring, the ^{1}H NMR spectrum showed that the compound had been reduced and the drug was released.

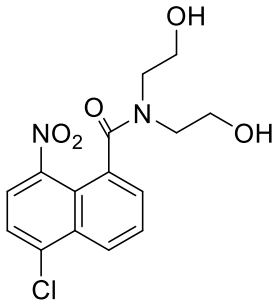
According to the results of mass spectrometry and NMR, the final structure of the reduced product is that corresponding to compound **15b**.

^{1}H NMR (400 MHz, DMSO) δ 8.52 (d, *J* = 8.5 Hz, 1H), 8.11 (t, *J* = 7.0 Hz, 1H), 8.05 (d, *J* = 7.0 Hz, 1H), 7.87 (d, 1H), 7.27 (d, *J* = 7.6 Hz, 1H), 3.39 (s, 2H), 1.13 (s, 3H).

^{13}C NMR (101 MHz, DMSO) δ 176.6 (C), 142.8 (C), 134.6 (CH), 132.3 (C),131.0 (C) ,130.7 (CH), 128.8 (CH), 127.3 (C), 125.2 (CH), 123.5 (C), 104.4 (CH), 50.8 (CH_2), 7.4 (CH_3).

MS (ESI^+): chemical formula: $C_{13}H_{11}NO_4S^-$; theorical mass: 276.04; experimental mass: [M-H^+]: 275.94.

5-chloro-*N*,*N*-bis(2-hydroxyethyl)-8-nitro-1-naphthamide (16)

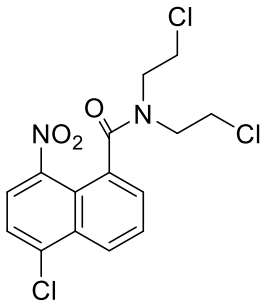


16

Compound **3** (500 mg, 1.8 mmol) was dissolved in CH_2Cl_2 and PCl_5 (750 mg, 3.6 mmol) was added. The reaction mixture was stirred for 30 minutes and then evaporated at reduced pressure to remove the solvent and phosphorus oxychloride generated. It was then dissolved in 3 mL of EtOAc (mixture I).

Next, in a 250 mL round-bottom flask, diethanolamine (5.0 g, 47.6 mmol) was dissolved in 17 mL of EtOAc and a saturated aqueous solution of Na_2CO_3 (15 mL of 4% Na_2CO_3 and 800 mg of Na_2CO_3) was added with continuous stirring (mixture II). Mixture (I) was transferred over mixture (II) and stirred. After 20 minutes, the reaction was transferred to a separatory funnel, the organic phase was separated, washed with an aqueous solution of 2M HCl, dried over anhydrous Na_2SO_4, filtered and evaporated under reduced pressure. An oily yellow compound (370 mg, 61%) was obtained and used in the next step without additional purification.

***N*,*N*-bis(2-chloroethyl)-5-(ethyltium)-8-nitro-1-naphthamide (17)**



17

Compound **16** (370.0 mg, 1.1 mmol) was dissolved in 3 mL of methylene chloride. On the other hand, $SOCl_2$ (1.6 mL, 22.1 mmol) was added to 3 mL of methylene chloride. The second mixture was added on top of the first, and the reaction was kept in stirring at 0 ºC for 1 hour. The mixture was then purified by column chromatography on silica gel, using CH_2Cl_2 as the eluent, and the pure compound was obtained as a brown oil (32 mg, 8%).

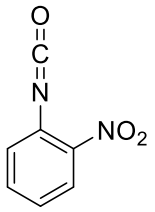
IR (film, ν in cm $^{-1}$): 3747,3916, 3650, 3098, 2955, 2916, 2845.04, 2371, 1645, 1573, 1469, 1424, 1359.

^{1}H NMR (400 MHz, $CDCl_3$) δ 8.49 (dd, *J* = 8.5, 1.3 Hz, 1H), 7.95 (d, *J* = 8.2 Hz, 1H), 7.80 (dd, *J* = 7.2, 1.3 Hz, 1H), 7.74 (t, *J* = 8.5, 7.2 Hz, 1H), 7.68 (d, *J* = 8.2 Hz, 1H), 4.05 – 3.62 (m, 8H).

^{13}C NMR (101 MHz, $CDCl_3$) δ 170.5 (C), 146.1 (C), 138.2 (C), 132.3 (C), 130.6 (C), 129.7 (CH), 127.4 (CH), 127.2 (CH), 125.5 (CH), 124.4 (CH), 123.2 (C), 52.0 (CH_2), 47.8 (CH_2), 41.0 (CH_2), 40.2 (CH_2).

MS (ESI$^+$): chemical formula: $C_{15}H_{14}Cl_3N_2O_3^+$; theorical mass 375.07; experimental mass: [M+H$^+$]: 375.07.

1-isocyanato-2-nitrobenzene (18)

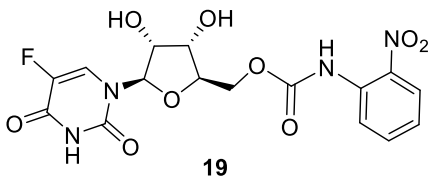


18

In a round bottom flask equipped with argon gas and a magnetic stirrer, 2-nitroaniline (500 mg, 3.7 mmol) in 21.2 mL of toluene was added over 1 hour to 1.8 mL of phosgene solution in toluene (20%: v/v). The reaction mixture was cooled down at -0 ºC for 15 minutes, then heated for 30 minutes at 100 ºC, triethylamine was added and kept reacting with continuous stirring at room temperature for 2 hours. The reaction mixture was evaporated under reduced pressure, the compound was extracted with hexane and then used in the next step without further purification or characterization.

The spectral properties match with the commercial compound.[24]

((2R,3S,4R,5R)-5-(5-fluoro-2,4-dioxo-3,4-dihydropyrimidin-1(2*H*)-yl)-3,4-dihydroxytetrahydrofuran-2-yl)methyl 2-(2-nitrophenyl)acetate (19)



19

Compound **23** (100 mg, 0.60 mmol) was mixed with 5-fluorouridine (160 mg, 0.60 mmol) in a 50 mL round bottom flask, 3 mL of DMF were poured to homogenize the reaction with continuous stirring at room temperature for 15 minutes. Once the reaction had finished, the mixture was filtered under reduced pressure. The residue was purified by column chromatography on silica gel using 50% EtOAc in DCM yielding compound **24** (60 mg, 24 %) as a yellowish solid.

M.p.:127-130 ºC

IR (nujol, υ, cm^{-1}): 3753, 3371, 1366, 1346, 1093.

^{1}H NMR (400 MHz, CD_3OD) δ 8.28 (td, *J* = 8.2, 2.8 Hz, 1H), 8.17 (t, *J* = 8.4 Hz, 1H), 7.83 (dt, *J* = 9.8, 4.9 Hz, 1H), 7.71 (ddd, *J* = 7.8, 6.8, 3.2 Hz, 1H), 7.32 – 7.24 (m, 1H), 5.90 – 5.85 (m, 1H), 4.57 (dd, *J* = 12.1, 3.0 Hz, 1H), 4.48 (dd, *J* = 12.1, 4.9 Hz, 1H), 4.27 – 4.17 (m, 3H), 3.35 (s, 2H).

^{13}C NMR (101 MHz, CD_3OD) δ 159.5 (C), 159.4 (C), 154.4 (C), 150.8 (C), 143.0 (C), 140.6 (C), 136.2 (CH), 126.7 (CH), 126.1 (CH), 125.7(CH), 124.6 (CH), 91.4 (CH), 83.1 (CH), 74.9 (CH), 71.1 (CH), 65.8 (CH_2).

MS (ESI$^+$): chemical formula $C_{16}H_{15}FN_4O_9Na$, theorical mass 449.0715 experimental mass$[M+Na]^+$: 449.0711.

5.3. NMR spectra

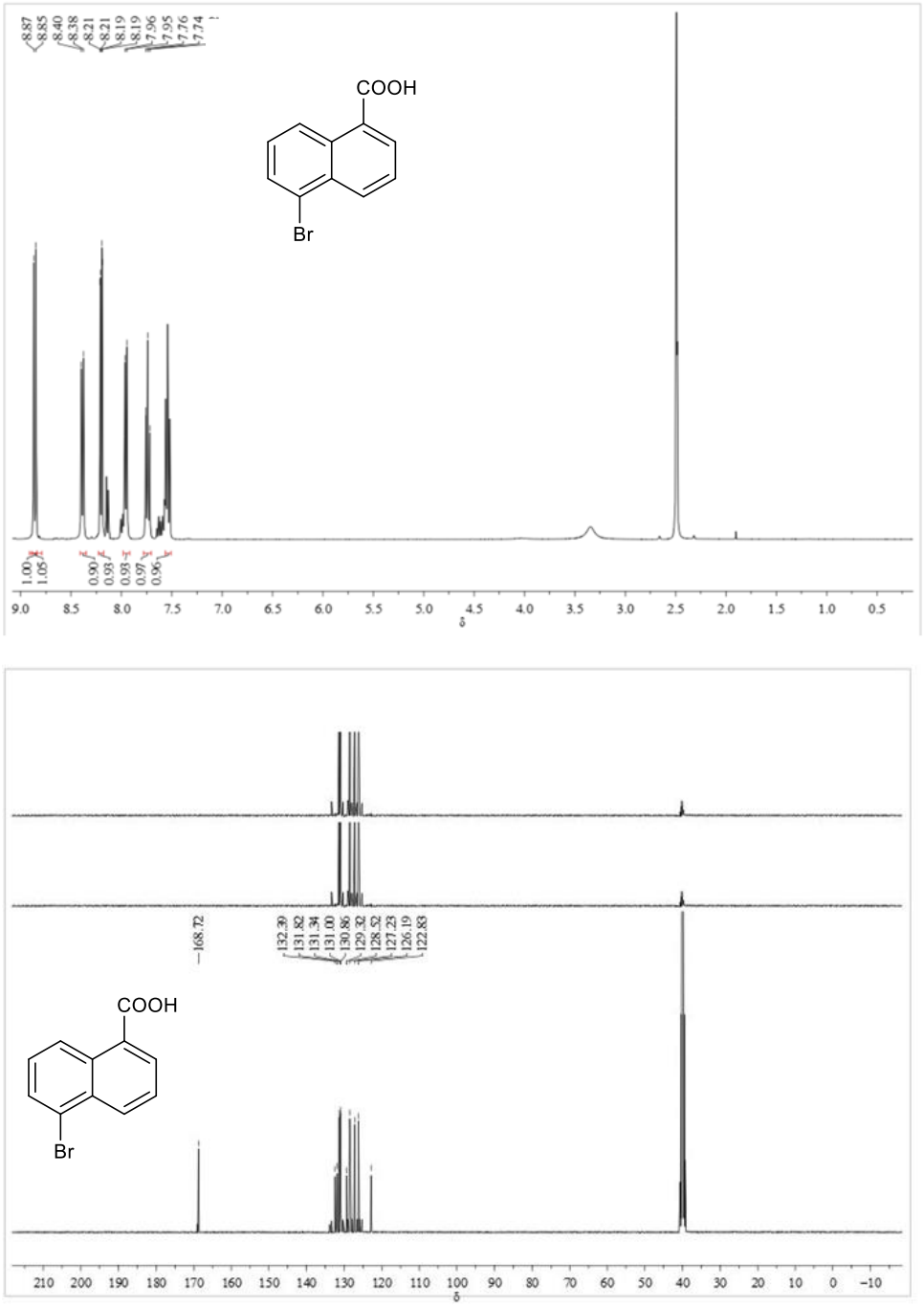


Figure S1. *^{1}H NMR (DMSO-d_6, 400 MHz) and ^{13}C (DMSO-d_6, 100 MHz) spectra of compound **1**.*

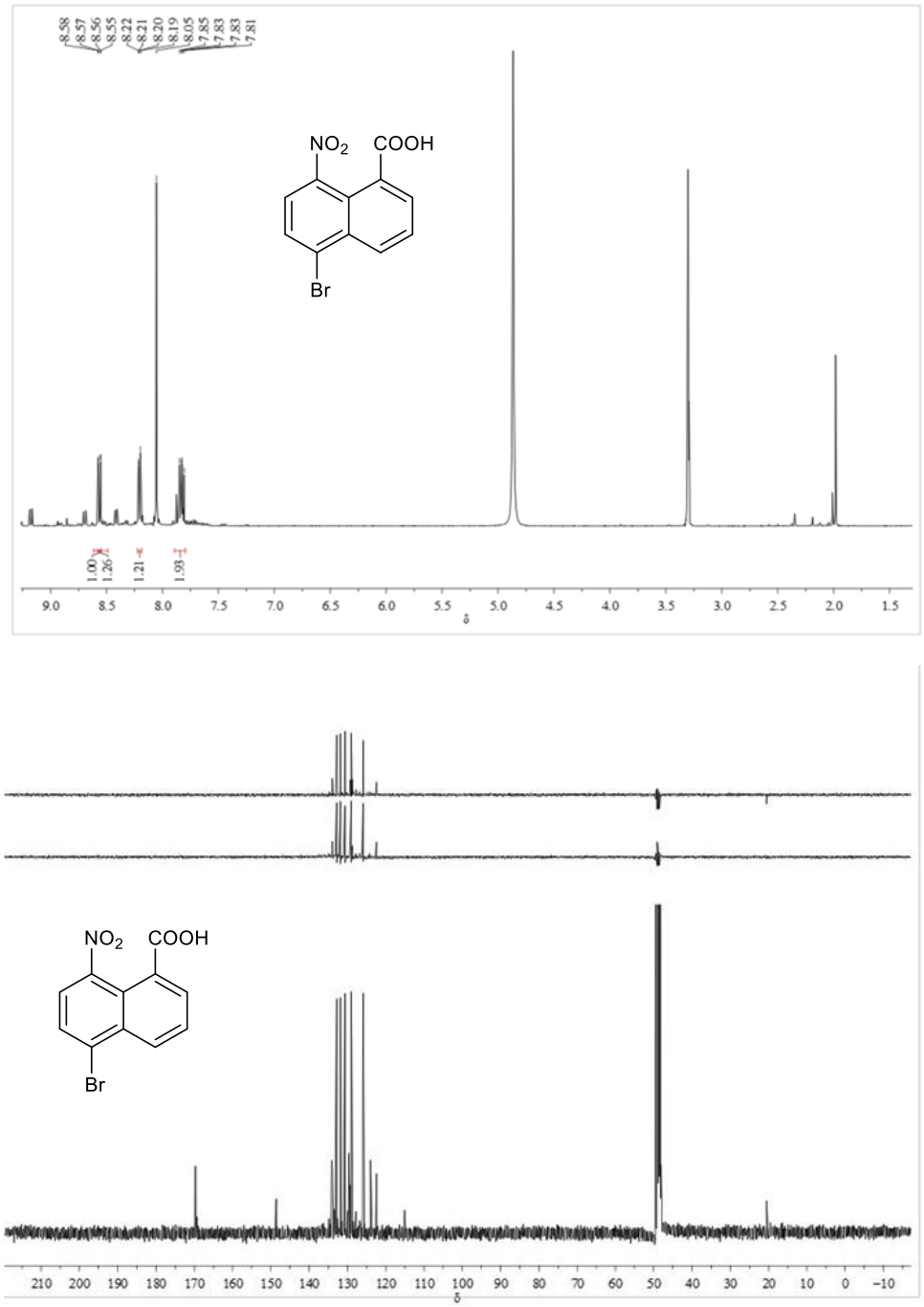


Figure S2. *^{1}H NMR (CD_3OD, 400 MHz) and ^{13}C (CD_3OD, 100 MHz) spectra of compound* ***2****.*

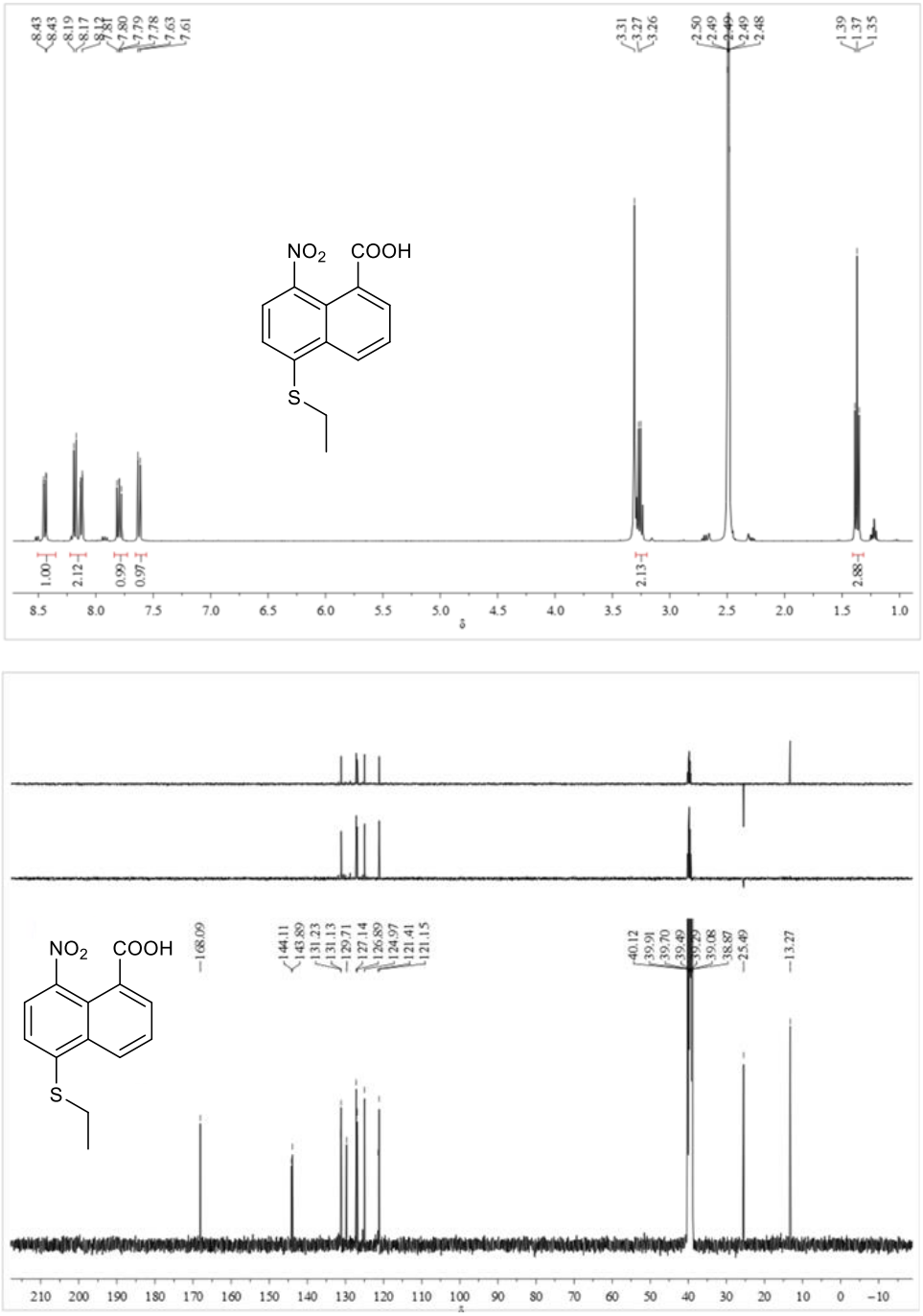


Figure S3. *^{1}H NMR (DMSO-d_6, 400 MHz) and ^{13}C (DMSO-d_6, 100 MHz) spectra of compound **3**.*

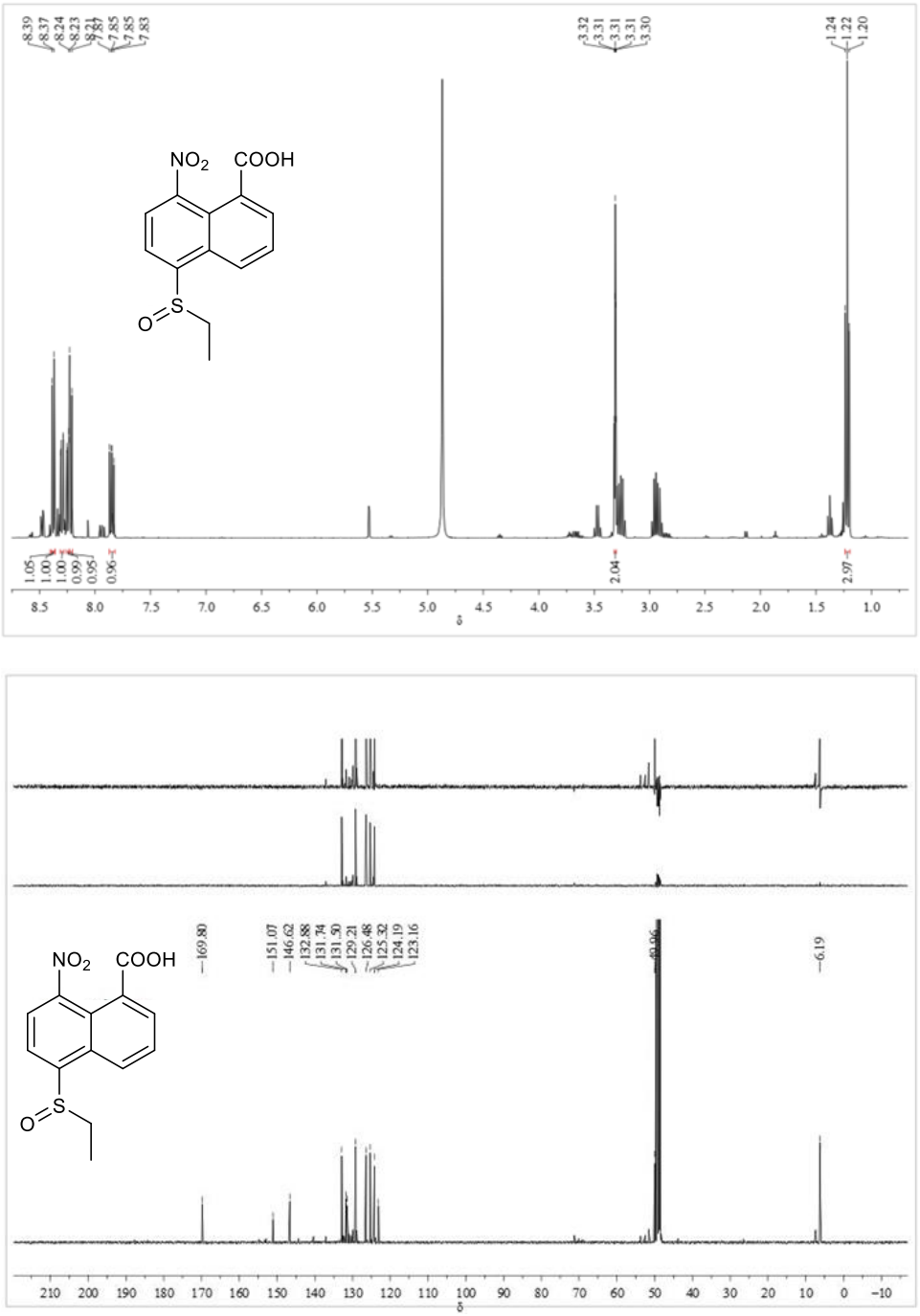


Figure S4. *^{1}H NMR (CD_3OD, 400 MHz) and ^{13}C (CD_3OD, 100 MHz) spectra of compound **4**.*

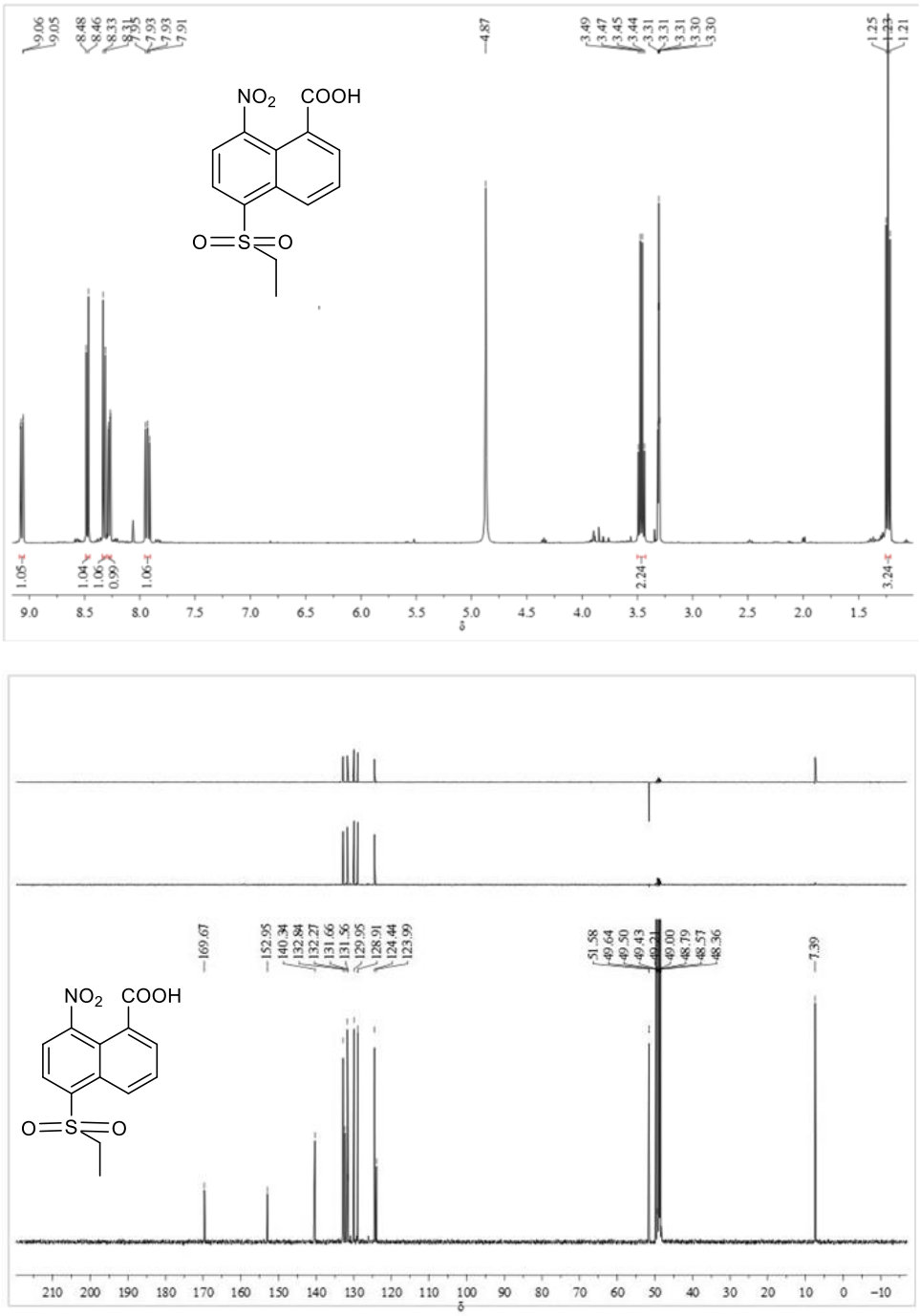


Figure S5. *^{1}H NMR (CD_3OD, 400 MHz) and ^{13}C (CD_3OD, 100 MHz) spectra of compound* ***5****.*

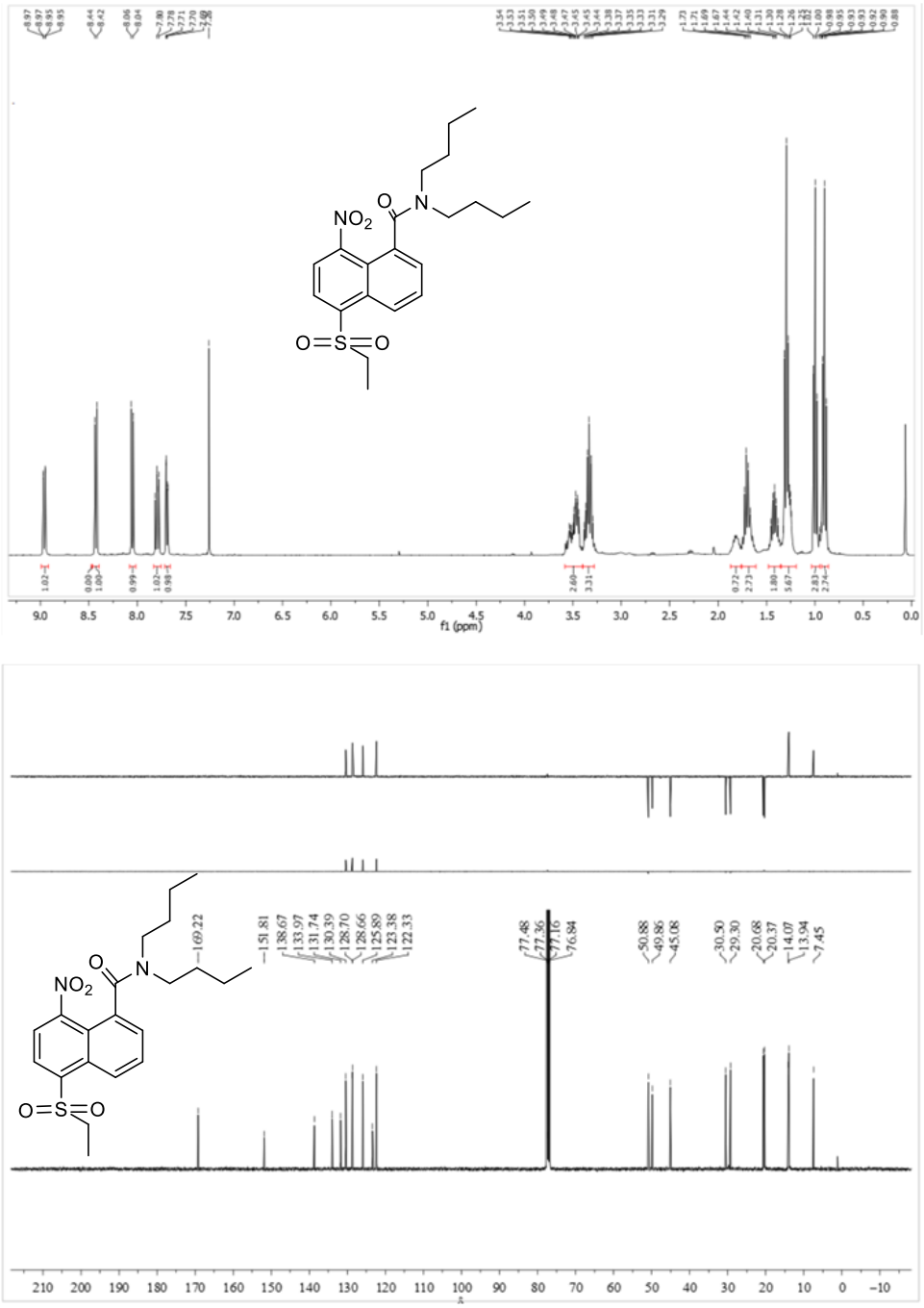


Figure S6. *^{1}H NMR ($CDCl_3$, 400 MHz) and ^{13}C ($CDCl_3$, 100 MHz) spectra of compound* ***6***.

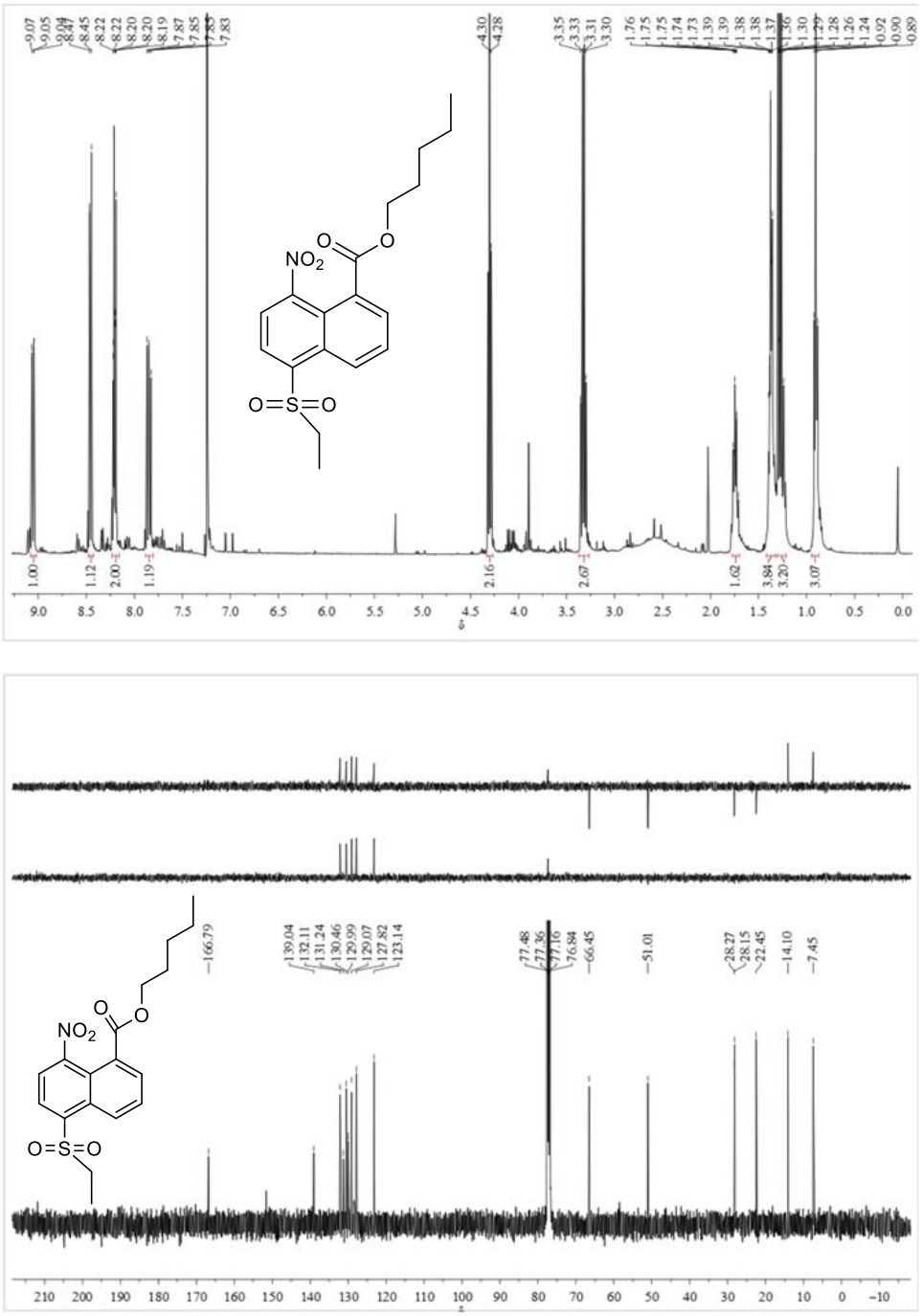


Figure S7. *^{1}H NMR ($CDCl_3$, 400 MHz) and ^{13}C ($CDCl_3$, 100 MHz) spectra of compound 7.*

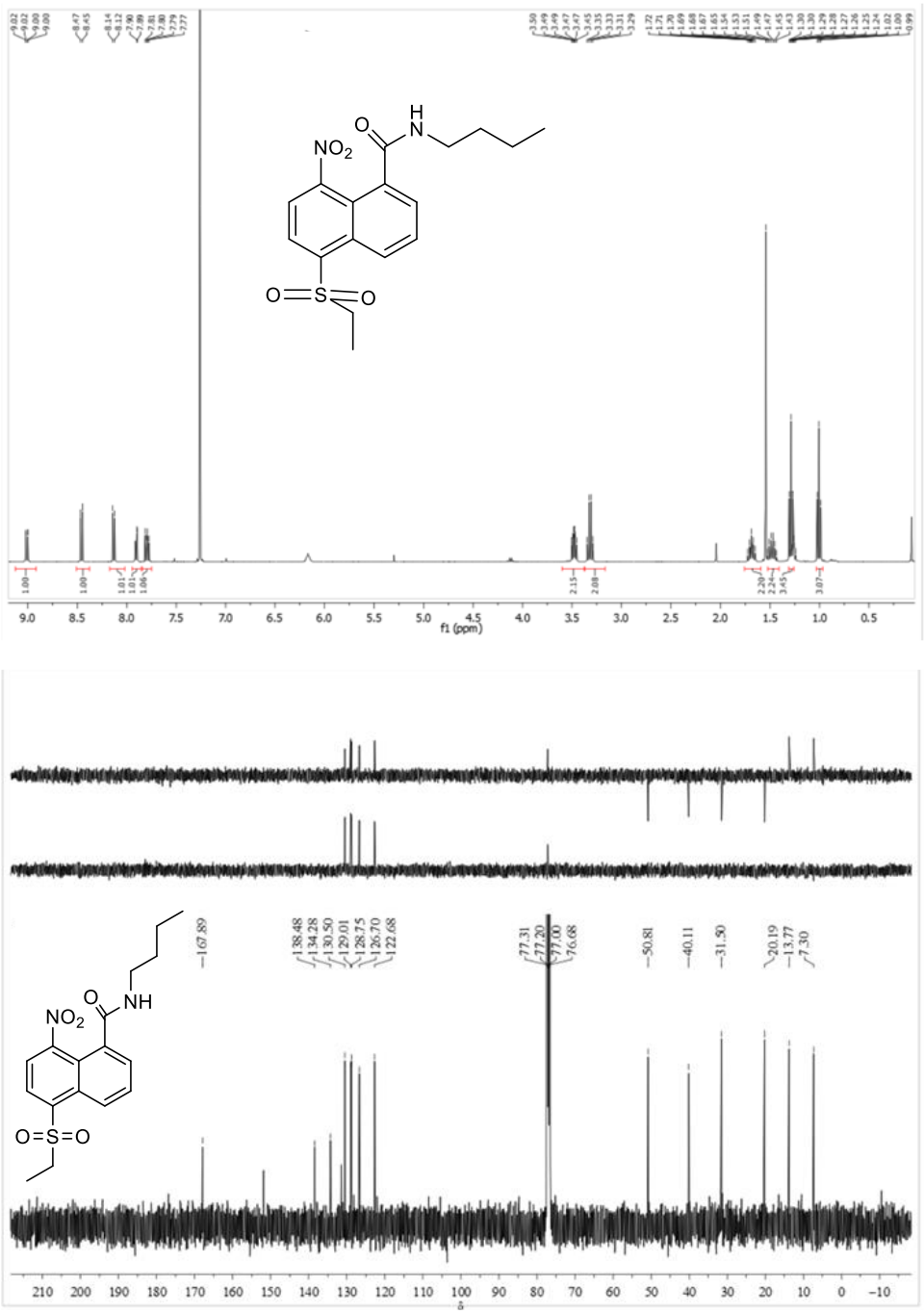


Figure S8. *^{1}H NMR ($CDCl_3$, 400 MHz) and ^{13}C ($CDCl_3$, 100 MHz) spectra of compound* **9**.

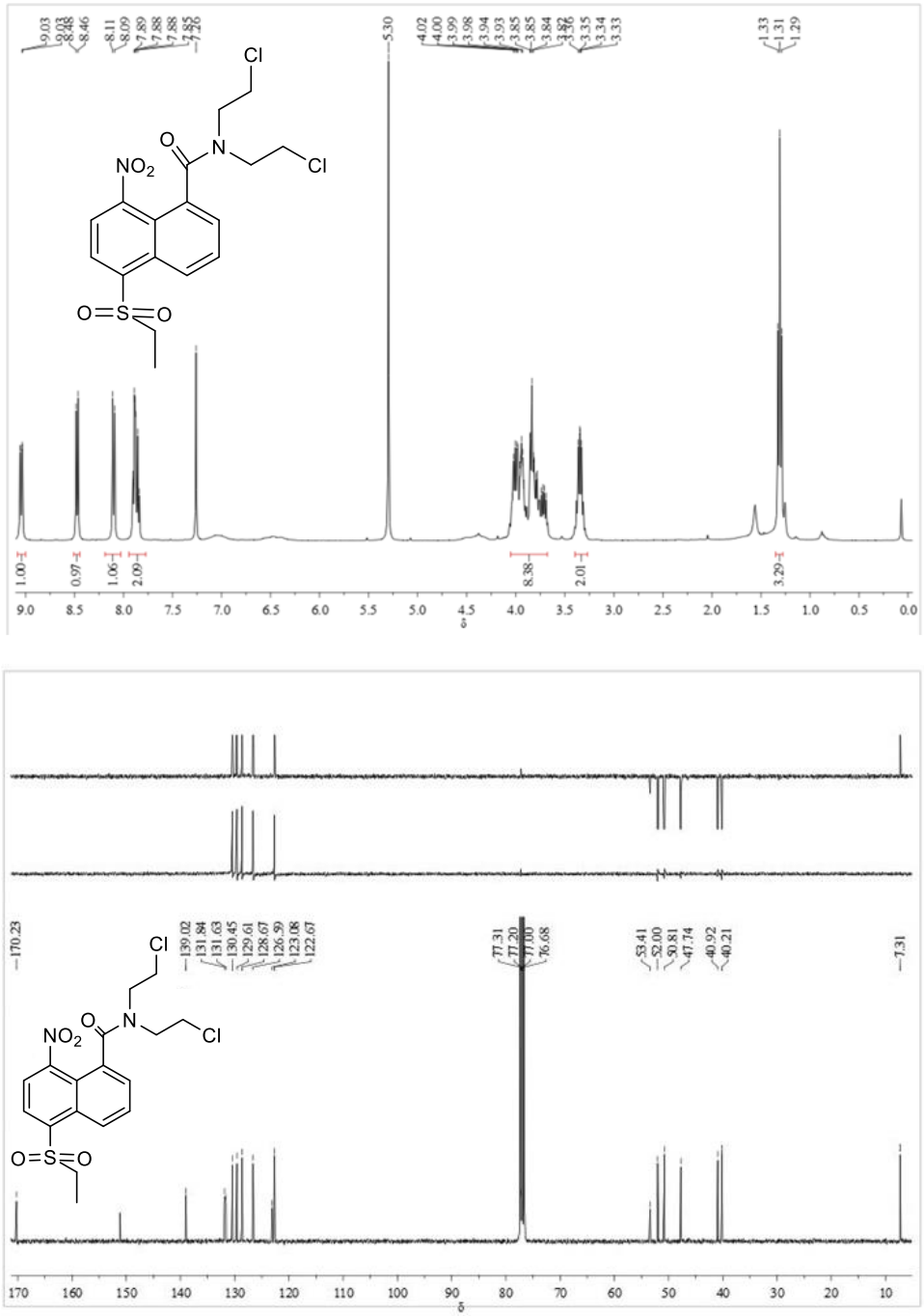


Figure S9. *^{1}H NMR ($CDCl_3$, 400 MHz) and ^{13}C ($CDCl_3$, 100 MHz) spectra of compound **14**.*

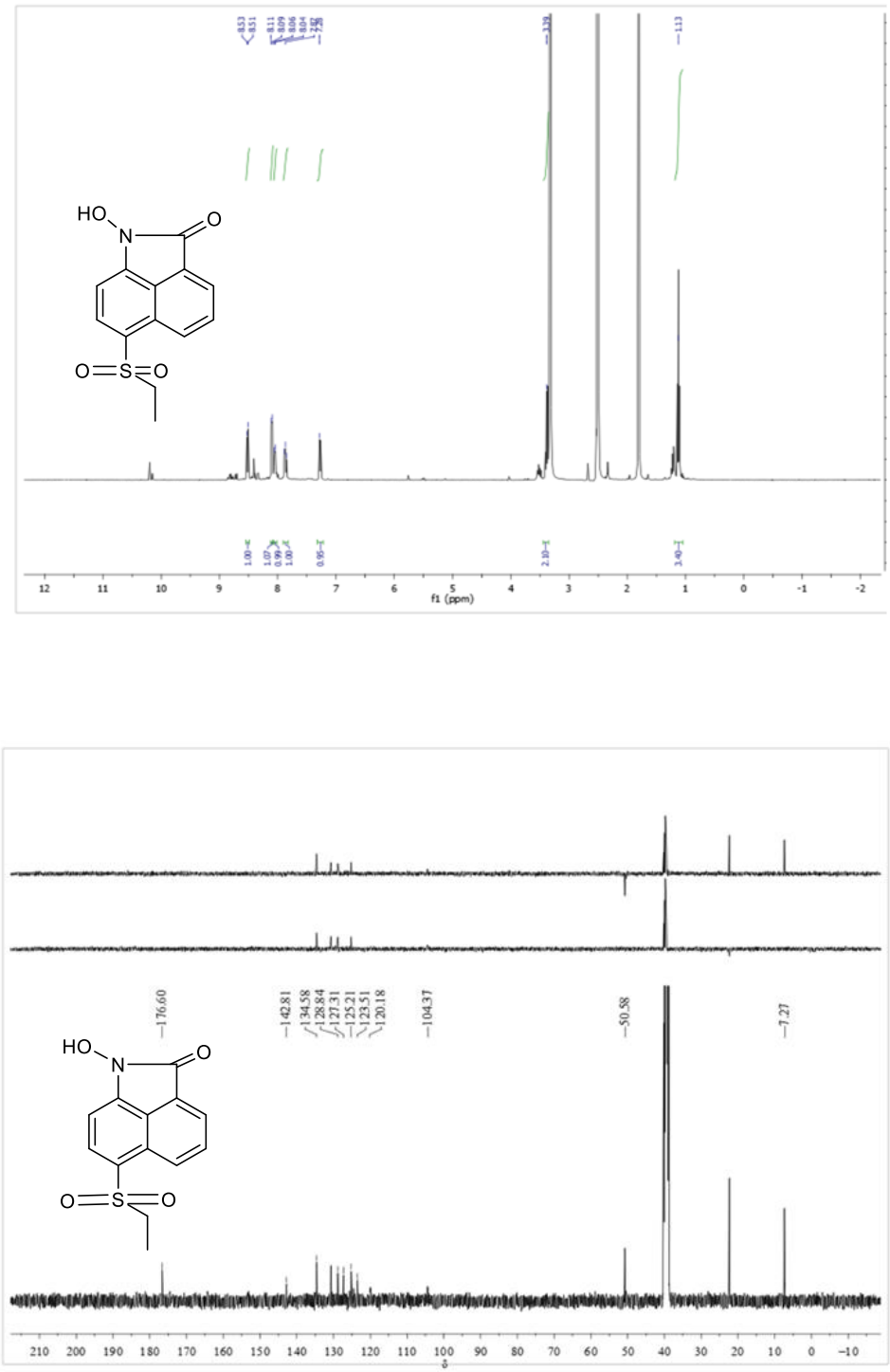


Figure S10. *^{1}H NMR (CD_3OD, 400 MHz) and ^{13}C (CD_3OD, 100 MHz) spectra of compound **15b**.*

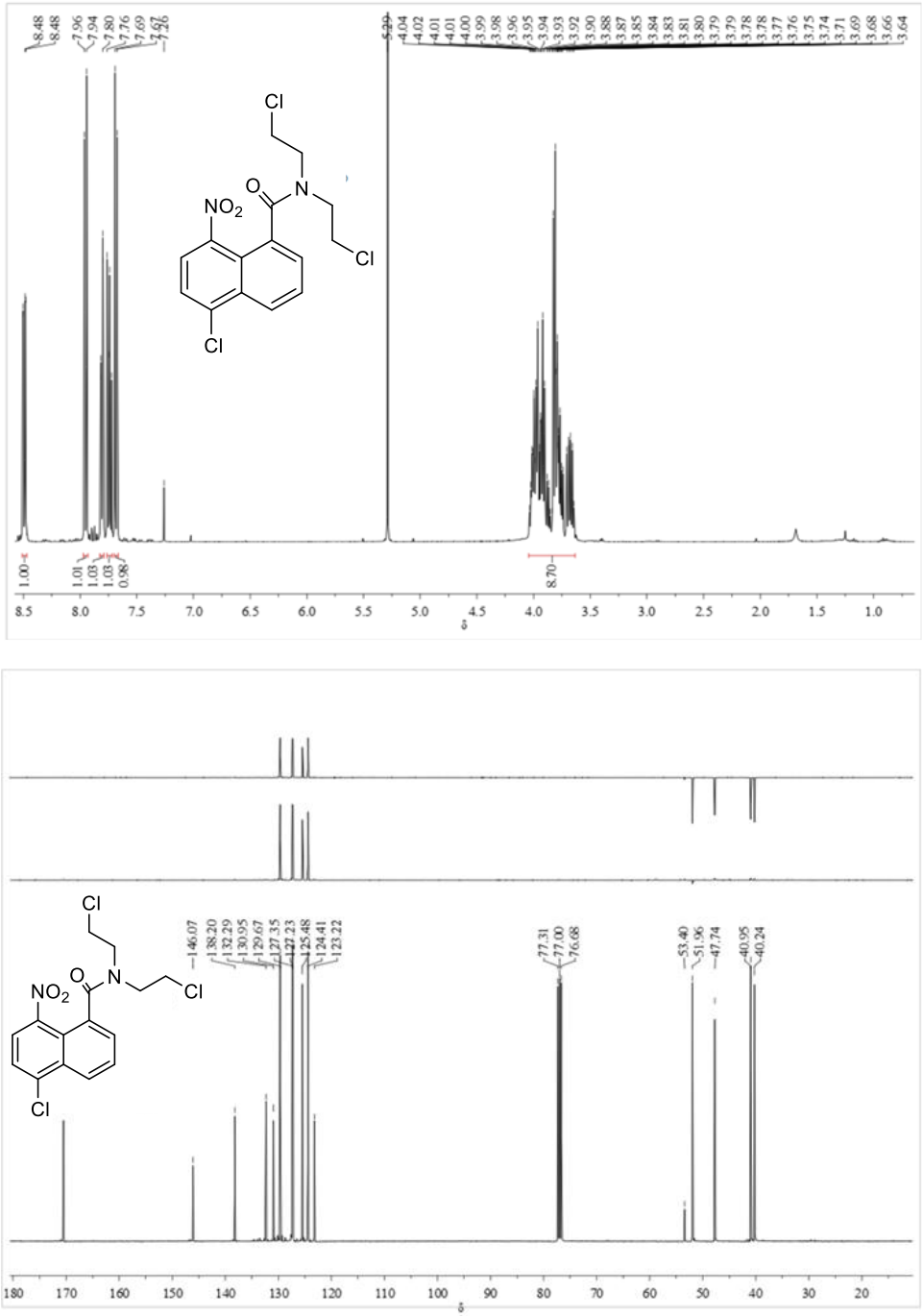


Figure S11. *^{1}H NMR ($CDCl_3$, 400 MHz) and ^{13}C ($CDCl_3$, 100 MHz) spectra of compound **17**.*

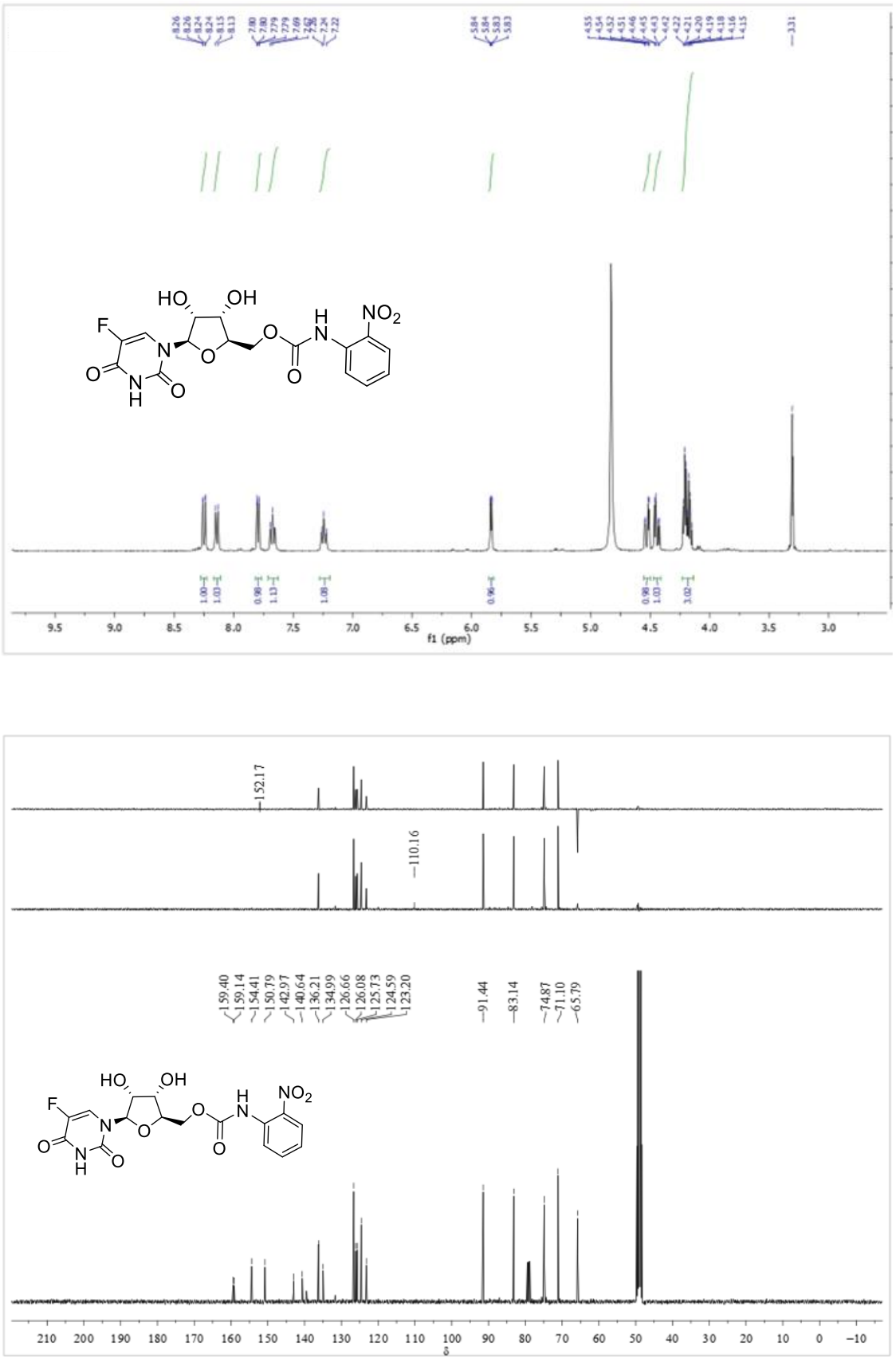


Figure S12. *^{1}H NMR (CD_3OD, 400 MHz) and ^{13}C (CD_3OD, 100 MHz) spectra of compound **19**.*

6. ferences

(1) Stella, V. J.; Charman, W. N. A.; Naringrekar, V. H. Prodrugs: Do They Have Advantages in Clinical Practice? *Drugs* **1985**, *29* (5), 455–473. https://doi.org/10.2165/00003495-198529050-00002.

(2) Denny, W. A. The Role of Hypoxia-Activated Prodrugs in Cancer Therapy. *The Lancet Oncology* **2000**, *1* (1), 25–29. https://doi.org/10.1016/S1470-2045(00)00006-1.

(3) Denny, W. A. Nitroaromatic Hypoxia-Activated Prodrugs for Cancer Therapy. *Pharmaceuticals* **2022**, *15* (2), 187. https://doi.org/10.3390/ph15020187.

(4) Chen, Y.; Hu, L. Design of Anticancer Prodrugs for Reductive Activation. *Med. Res. Rev.* **2009**, *29* (1), 29–64. https://doi.org/10.1002/med.20137.

(5) Aaron, J.-J.; Trajkovska, S. Fluorescence Studies of Anti-Cancer Drugs--Analytical and Biomedical Applications. *Curr. Drug Targets* **2006**, *7* (9), 1067–1081. https://doi.org/10.2174/138945006778226633.

(6) Santos, V. L. dos A.; Gonsalves, A. de A.; Guimarães, D. G.; Simplicio, S. S.; Oliveira, H. P. de; Ramos, L. P. S.; Costa, M. P. da; Oliveira, F. de C. E. de; Pessoa, C.; Araújo, C. R. M. Naphth[1,2-d]Imidazoles Bioactive from β-Lapachone: Fluorescent Probes and Cytotoxic Agents to Cancer Cells. *Molecules* **2023**, *28* (7), 3008. https://doi.org/10.3390/molecules28073008.

(7) Mohapatra, B.; Phale, P. S. Microbial Degradation of Naphthalene and Substituted Naphthalenes: Metabolic Diversity and Genomic Insight for Bioremediation. *Front. Bioeng. Biotechnol.* **2021**, *9*, 602445. https://doi.org/10.3389/fbioe.2021.602445.

(8) Jangir, S. K.; Acharya, S. Spectrofluorimetric Study of 1-Naphthoic Acid in Micellar Surfactant Solution. *J. Chem. Pharm. Res.* **2014**, *6* (4), 1107-1112. https://www.jocpr.com/articles/spectrofluorimetric-study-of-1naphthoic-acid-in-micellar-surfactant-solution.pdf

(9) Feng, J.; Zhong, J.; Tang, X. Selective and Sensitive Detection of Cyanate Using 3-Amino-2-Naphthoic Acid-Based Turn-on Fluorescence Probe. *Anal. Bioanal. Chem.* **2019**, *411* (16), 3613–3619. https://doi.org/10.1007/s00216-019-01843-w.

(10) Wang, Q.; Song, Y.; Yuan, S.; Zhu, Y.; Wang, W.; Chu, L. Prodrug activation by 4,4'-bipyridine-mediated aromatic nitro reduction. *Nat. Commun.* **2024**, *15,* 8643. https://www.nature.com/articles/s41467-024-52604-y.

(11) Singleton, D. C.; Macann, A.; Wilson, W. R. Therapeutic Targeting of the Hypoxic Tumour Microenvironment. *Nat. Rev. Clin. Oncol.* **2021**, *18* (12), 751–772. https://doi.org/10.1038/s41571-021-00539-4.

(12) Singh, R. K.; Kumar, S.; Prasad, D. N.; Bhardwaj, T. R. Therapeutic Journery of Nitrogen Mustard as Alkylating Anticancer Agents: Historic to Future Perspectives. *Eur. J. Med. Chem.* **2018**, *151*, 401–433. https://doi.org/10.1016/j.ejmech.2018.04.001.

(13) Chen, Y.; Jia, Y.; Song, W.; Zhang, L. Therapeutic Potential of Nitrogen Mustard Based Hybrid Molecules. *Front. Pharmacol.* **2018**, *9*, 1453. https://doi.org/10.3389/fphar.2018.01453.

(14) *Bis(2-chloroethyl)amine hydrochloride | CAS 821-48-7 | SCBT - Santa Cruz Biotechnology*. https://www.scbt.com/p/bis-2-chloroethyl-amine-hydrochloride-821-48-7 (accessed 2024-02-13).

(15) Zhai, X.; El Hiani, Y. Getting Lost in the Cell–Lysosomal Entrapment of Chemotherapeutics. *Cancers* **2020**, *12* (12), 3669. https://doi.org/10.3390/cancers12123669.

(16) *5-fluorouridine*. https://go.drugbank.com/drugs/DB01629 (accessed 2024-02-26).

(17) PubChem. *5-Fluorouridine*. https://pubchem.ncbi.nlm.nih.gov/compound/9427 (accessed 2024-02-26).

(18) Farquharson, S.; Gift, A.; Shende, C.; Inscore, F.; Ordway, B.; Farquharson, C.; Murren, J. Surface-Enhanced Raman Spectral Measurements of 5-Fluorouracil in Saliva. *Molecules* **2008**, *13* (10), 2608–2627. https://doi.org/10.3390/molecules13102608.

(19) Alzahrani, S. M.; Al Doghaither, H. A.; Al-Ghafari, A. B.; Pushparaj, P. N. 5-Fluorouracil and Capecitabine Therapies for the Treatment of Colorectal Cancer (Review). *Oncology Reports* **2023**, *50* (4). https://doi.org/10.3892/or.2023.8612.

(20) PubChem. *2-Nitrophenyl isocyanate*. https://pubchem.ncbi.nlm.nih.gov/compound/76834 (accessed 2024-10-22).

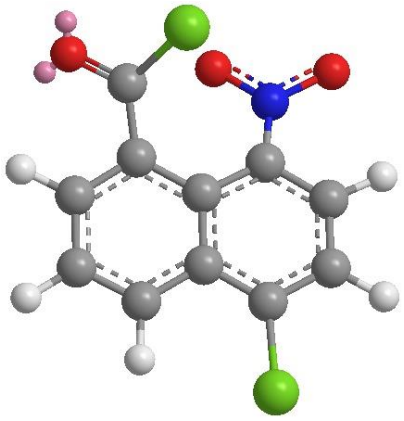
(21) Repine, J. T.; Johnson, D. S.; White, A. D.; Favor, D. A.; Stier, M. A.; Yip, J.; Rankin, T.; Ding, Q.; Maiti, S. N. Synthesis of Monofluorinated 1-(Naphthalen-1-Yl)Piperazines. *Tetrahedron Lett.* **2007**, *48* (31), 5539–5541. https://doi.org/10.1016/j.tetlet.2007.05.156.

(22) PubChem. *N,N-Bis(2-hydroxyethyl)benzamide*. https://pubchem.ncbi.nlm.nih.gov/compound/94109 (accessed 2024-10-23).

(23) PubChem. *N,N-bis(2-chloroethyl)benzamide*. https://pubchem.ncbi.nlm.nih.gov/compound/315322 (accessed 2024-10-23).

(24) Kiselev, V. D.; Malkov, V. B.; Murzin, D. G.; Shakirov, I. M.; Konovalov, A. I. Thermochemical Study of the Reaction of Isocyanate with Amines. *Dokl. Phys. Chem. (Engl. Transl.)* **1989**, *308*, 711–713.

CHAPTER 3: 5-CHLORO-8-NITRO-1-NAPHTHOYL (NNAP): A SELECTIVE PROTECTIVE GROUP FOR AMINES AND AMINO ACIDS



In chapter 3 the synthesis of a selective protective group for amines and amino acids 5-Chloro-8-Nitro-1-Naphthoyl (NNapCl) will be discussed.

1. Objectives

The main objective of this chapter is to explore the properties of 5-chloro-8-nitro-1-naphthoyl (NNapCl) as a protecting group with orthogonal properties, which implies an easiest protection and deprotection for amines and amino acids. Spectroscopic and structural studies will be afforded as well as modelling and crystallographic analysis to fulfil the structural requirements.

To achieve this goal, the specific objectives shown below are proposed:

Objective 1 Design, modelling, and synthesis of 5-chloro-8-nitro-1-naphthoyl (NNapCl).

Objective 2 To study and optimize the reaction conditions for protection and deprotection.

Objective 3 To test the substrates that are able to be protected with NNapCl (amines, amino acids, amino alcohols, etc.) and check the compatibility with other protecting groups (alcohols, esters, etc.).

Objective 4 To test the orthogonality of NNap in the presence of other protecting groups such as Boc, etc. and apply this protecting group in peptide synthesis.

2. Introduction

Over the years, organic synthesis, and the understanding about biological physiology of living organisms, have formed an effective synergy in producing biomimetic molecules, in an attempt to create a functional simulation of nature, in order to achieve a range of objectives including the therapeutic one.

In general, organic design strategy is based usually on satisfying many challenges such as chemoselectivity, regioselectivity and stereoselectivity.[1]

To selectively carry out a chemical reaction at a reactive site in a polyfunctional compound other reactive sites must be temporarily inactive, for this aim, protecting groups have been and are currently being developed. Protecting groups must meet a range of prerequisites,[2] so what are protecting groups?

2.1. Protecting groups

Protecting or protective groups are synthetic derivatives made reversibly from an existing functional group within a molecule.

With the aim of creating a temporary inactivation of the principal functional group under synthetic or biological conditions, protective groups are attached to drop the reactivity, so that a provisional stability of the protected functional group will be insured, avoiding undesirable side reactions and bonds formation.[3,4]

In the light of the thesis proposal, the synthesis of a selective protecting group will be discussed fulfilling by that the main objective of targeting new synthetic strategies under the name of an orthogonal protective group for amines. Amino acids on the other hand will also be included.

Inspired by the naphthalene derivative developed in the previous chapter as a molecular trigger of cytotoxic drugs, we envisioned that, following a similar strategy, the same molecule could be used as a protective group in organic synthesis. Although the integration of protecting groups in a polyfunctional molecule may bring additional steps by incorporating the adequate protective group with specific requirements, it allows to carry out reactions without affecting more sensitive protective groups. In our case, it allows to protect many functionalities including amines.[6]

2.2. Amino groups protection

Amines are generally nucleophilic basic compounds which confers them vulnerability to react with a wide range of elements in nature such as oxidizing, alkylating, and carbonyl compounds.[6] Therefore, by protecting the amine as a carbamate, other functional groups can react selectively with electrophiles, leaving the carbamate (protected amino group) intact[3].

In fact, the amine protection is necessary during the peptide synthesis in which the connection of amino acids can produce unwanted products when their amino groups are not protected (Figure 1).[7]

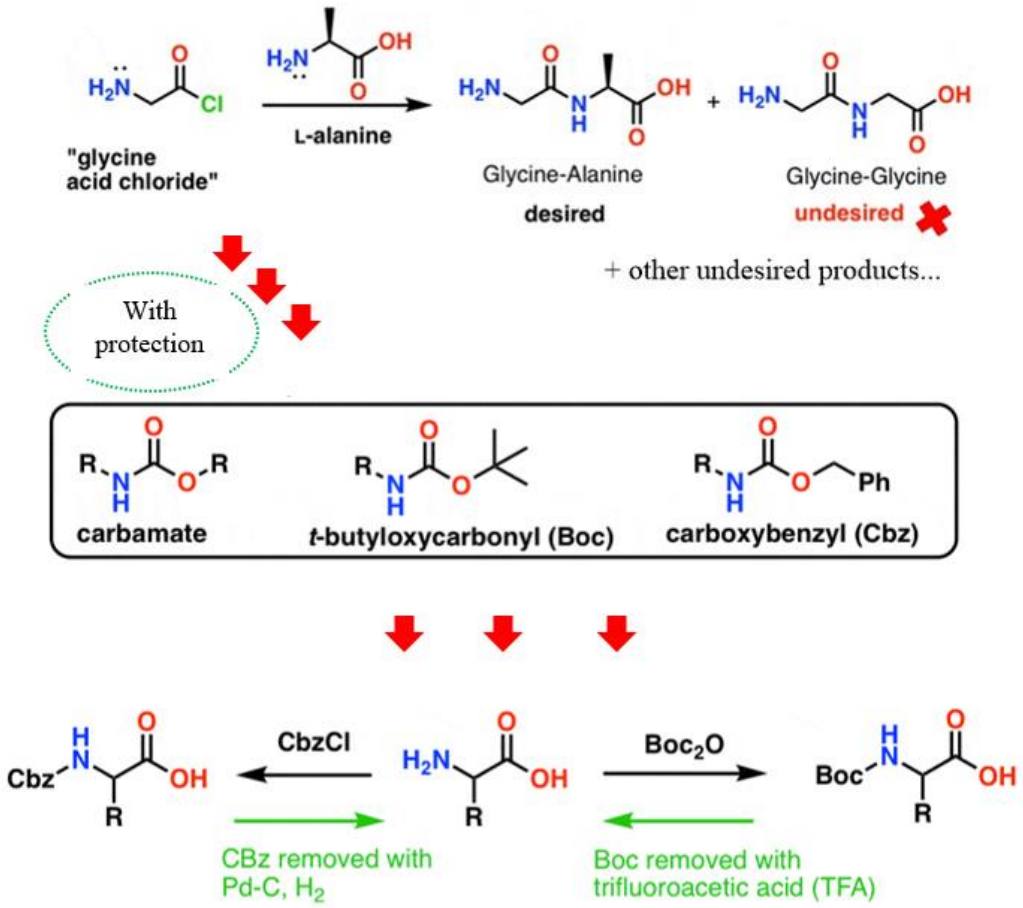
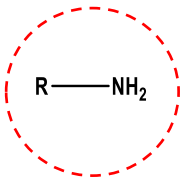
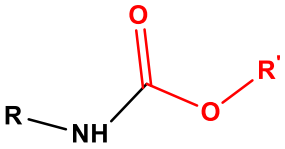
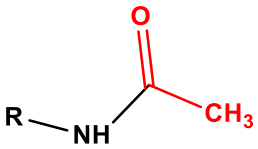
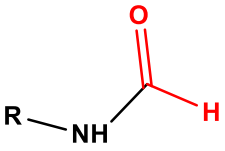


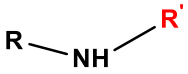
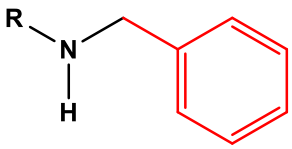
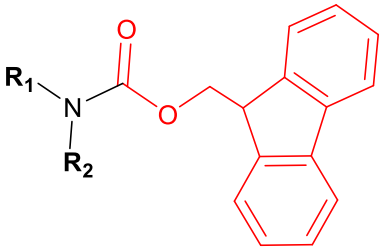
Figure 1. *Comparative illustration showing the crucial role of protective groups in amine reactivity for the desirable product obtention (modified illustration).*[7]

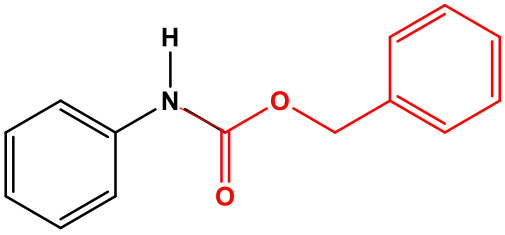
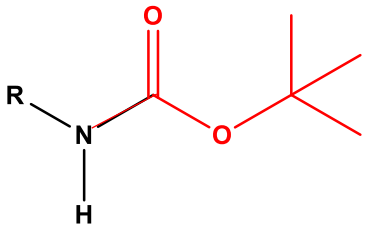
2.2.1. Protection varieties

Numerous processes are available to protect the amino groups as it is shown in the table below.

Table 1. *Protective group ranges for amines.*[8]

	Protection type	Structure	Characteristics
	Carbamoylation		A famous choice in protecting groups for amines, due to the non nucleophility and the stability of their nitrogen under a variety of reaction conditions, including them Boc, Cbz, and Fmoc.
	Acylation		A well-known option of protective groups, used in multistep synthetic routes, for the production of bioactive compounds. Several acylating agents are reported till date for N-acylation using the following reagents: -Acetic anhydride -Acetic acid/acetyl chloride -*N*, *N*-Dimethyl acetamide -Acetamide -Miscelleneous samples
	Formylation		Another famous choice in protective groups for amines with a significant application in organic and pharmaceutical syntheses using the following reagents: -Formic acid -CO_2 / polyhydromethylsiloxane (PHMS) -*N*, *N*-Dimethylformamide -Formaldehyde/ Formamide -Miscellaneous samples

	Alkylation		*N*-Alkylation protection in amines plays a crucial role in organic synthesis within the commercial and pharmaceutical formation products, it can be carried out using the following ways: -Alkylation using methanol. - CO_2 /polyhydromethylsiloxane (PHMS). - Formic acid/Formaldehyde. -Dimethyl carbonate. - CO_2+H.
	Benzylation		*N*-Benzyl amine is present in a wide variety of organic synthesis. The pharmacologically and biologically active compounds use essentially the aldehyde in amines benzylation.
	Fmoc		9-Fluorenylmethyloxycarbonyl is a protective group for organic molecules selected essentially for the orthogonal protection and its important characteristics of lability in basic medium and stability in the acidic conditions.

	Cbz		Carbobenzyloxy is used for amines protection thanks to its stability in basic and aqueous acidic media with an easiest detachment by catalytic hydrogenation.
	Boc		*Tert*-butyloxycarbonyl group has become most frequently and largely used protective group for amines thanks to its ease in protection and deprotection and its orthogonal properties.

2.3. Background

Several examples show the large steric tension between the substituents of the 1,8-disubstitued naphthalenes,[9] this steric strain is usually relieved by bond bending with the substituents twisted out of the plane of the aromatic rings.

According to a previous work shown in Figure 2, the X-ray crystal structure of 8-(dimethylamino)1-naphthyl methyl ketone,[13] illustrates the Burgi-Dünitz trajectory in which the combination of the steric compression and the bonding interaction between the lone pair of the amine and the carbonyl group deforms the molecule (Figure 2B).[14]

Another example is the high reactivity of 8-dimethylamino-1-naphthaldehyde, in which its treatment with benzoyl chloride,[15] leads to benzoylation of the aldehyde oxygen and addition of the *peri*-dimethylamino group to the former carbonyl group, setting a new N−C bond (Figure 2C).

Thus, 1,8-bis(dimethylamino)naphthalene (pK_a= 12.1)[10] is a stronger base than dimethylaniline (pK_a = 5.15), because protonation reduces the electrostatic and steric strain.

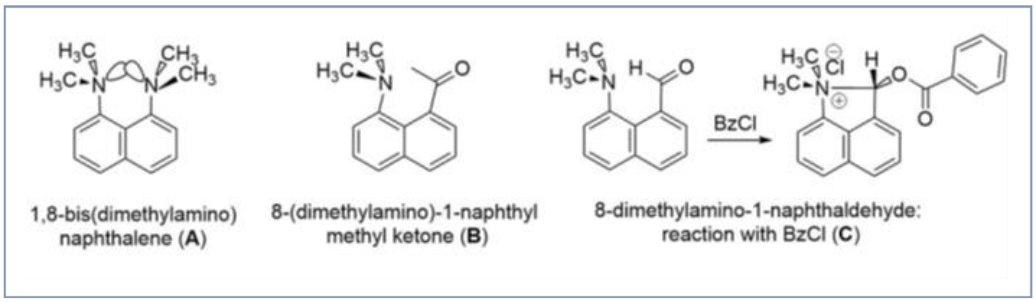


Figure 2. *Unusual reactivity of 1,8-substituted naphthalenes*.

A similar method in our work which consists of the reduction of the 8-nitro group to amine (**E**) leads to a decrease in the steric strain, due to the formation of a N−C bond between the *peri* substituents, the amine nitrogen at C-8, and the amide carbonyl group at C-1.
Thus, formation of the five-membered lactam (**F**) is accompanied by release of the protected amine (Figure 3).

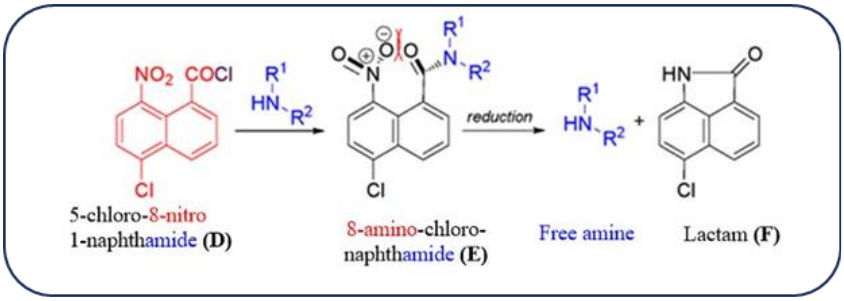


Figure 3. *Steric hindered amides synthesis using NNap and deprotection.*

To solve the numerous problems and obstacles related with the protecting groups in organic chemistry such as orthogonality disequilibrium, little yield, not inert towards reaction conditions…etc., carbamates were always the best option for amines protection.[11] In fact the amine liberation is trigged by CO_2 release as a deprotection force, nevertheless, carbamates can present a range of drawbacks such as their high toxicity as well as the presence of two different conformations.[12]

In this chapter an alternative solution will be explored which involves the synthesis of a sterically stressed amide with an unusual deprotection under mild reductive conditions (Figure 4). The latter is based on a large release of steric hindrance.

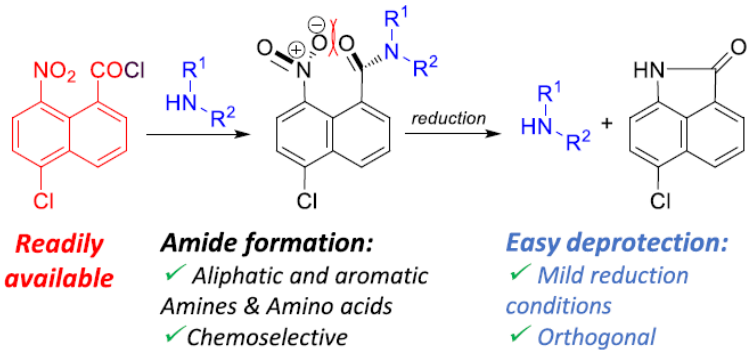


Figure 4. *NNap: Amines protecting group.*

As mentioned previously, the molecule synthesized in the previous chapter, the 5-chloro-8-nitro-1-naphthoyl (NNap), will be used as a protective group of amines and amino acids. It can be easily introduced in the presence of Schotten-Baumann conditions, generating the corresponding amides in high yields.

3. Methodology

3.1. Amine's protection using the protective group NNap

Amine protection was carried out under Schotten-Baumann conditions in a two-phase reaction using methylene chloride and aqueous sodium carbonate solution; easy work-up using liquid-liquid extraction and acid washing was enough to obtain the amides (**D**, Table 2) with high purity and usually no chromatography was needed.

Thus, reaction of the amine with 1.0 equiv. of the acyl chloride **4** and in the presence of Na_2CO_3 (5.0 equiv.) afforded the corresponding amide in good to excellent yields (Table 2, entries 1-6). Primary and secondary amines were tested: *n*-octylamine (**5**), *n*-decylamine (**6**) and benzylamine (**7**) afforded, in 30 minutes, a quantitative NMR yield of the desired amides (86-95% isolated yields). The more hindered primary amine *tert*-octylamine (**8**) and the secondary amine di-*n*-butylamine (**9**) also gave the corresponding amides in high yields (87-90% isolated yields).

To further explore the substrate scope, an aromatic amine, 4-*tert*-butylaniline (**10**), was tested; as shown in Table 2 (entry 6), the aniline **10** was easily transformed into the target amide in 91% isolated yield under the same reaction conditions.

The protection was carried out essentially by using the following reaction.

a) Amine (1 equiv) in CH_2Cl_2 was added dropwise to a solution of the acid chloride NNapCl, **4** (1.0 equiv) in CH_2Cl_2 at 0 °C. After stirring 5 min, an aqueous Na_2CO_3 (5.0 equiv) solution was added and the mixture was allowed to warm to room temperature, stirring for additional 25 minutes.



Figure 5. *Acylation of Amines with 5-chloro-8-nitro-1-naphthoyl chloride 4 (NNapCl).*

Table 2. *Isolated yields from amines acylation using (NNapCl).*

entry	amine	amide (%)
1	*n*-octylamine (**5**)	**12** (86%)
2	*n*-decylamine (**6**)	**13** (95%)
3	benzylamine (**7**)	**14** (87%)
4	*tert*-octylamine (**8**)	**15** (90%)
5	di-*n*-butylamine (**9**)	**16** (87%)
6	4-*tert*-butylaniline (**10**)	**17** (91%)
7	(1*S*,2*S*)-(+)-*trans*-1-amino-2-indanol (**11**)	**18** (86%)

The yields analysis after acylating the amines using the NNapCl confirmed the performance of our protective group, giving the highest possible yields with simple reaction conditions.
5-chloro-8-nitro-1-naphthoyl (NNap) organic synthesis and different modelling, structural and analytical studies will be discussed in the next section.

3.2. The NNap protective group formation

The protective group synthesis starts from the commercially available 1-naphthoic acid **1** as shown below in Figure 6. The synthetic scheme is the same as described previously in Chapter 2, although some steps have been optimized.

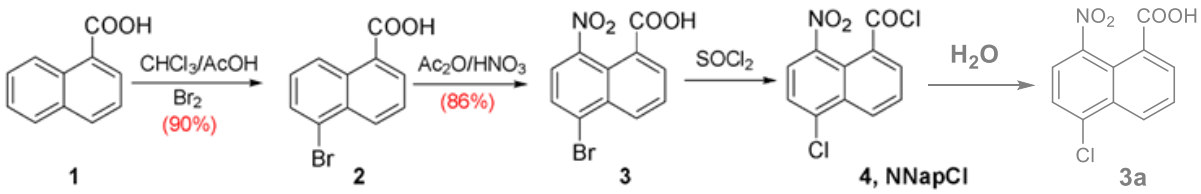


Figure 6. *The Protective Group (NNapCl) synthesis process.*

In fact, a direct nitration of compound **1** takes place in the C-5 position; therefore, previous bromination was carried out to block that position. Then, nitration in acetic anhydride using *p*-TsOH as catalyst yielded a clean reaction in the expected C-8 position.

Treatment of the acid **3** with thionyl chloride afforded the acid chloride **4** with concomitant halogen exchange in C-5 position.

The replacement of bromine by chlorine was experimentally confirmed: hydrolysis of the acid chloride **4** with water produced a carboxylic acid (**3a**), whose spectral properties (NMR and MS) showed that chlorine had replaced the C-5 bromine atom.

Both the carboxylic acid **3** and its potassium salt are highly crystalline compounds.

Slow evaporation of an aqueous equimolar solution of potassium hydroxide and the acid **3** allowed us to obtain high-quality crystals suitable for X-ray diffraction analysis (Figure 7).

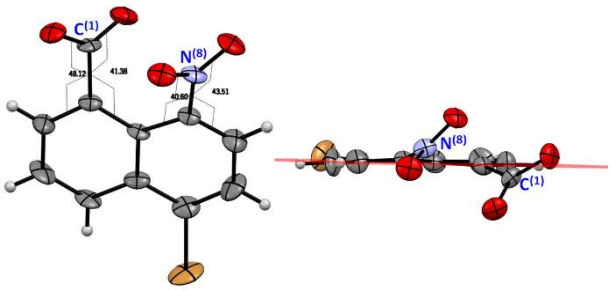


Figure 7. *ORTEP diagram of the potassium salt of the carboxylic acid (**3**). K^+ counterion and a crystallization water molecule have been omitted for clarity. Displacement ellipsoids are drawn at 50 % probability level. Hydrogen atoms are shown as spheres of arbitrary radius.*

The structure shows a strong steric interaction between substituents at C-1 and C-8 positions that are placed outside the plane of the naphthalene ring with torsion angles of 40°−48°.

3.3. Amide crystallographic study

Gratifyingly, single crystals of the amide **17** (Figure **5b**) were obtained by slow evaporation of a methanol solution.

The X-ray structure showed the same features to that of the potassium salt of acid **3**; the nitro and the amide groups are twisted out of the plane of the naphthalene ring, lying on opposite sides of this plane. Additionally, the replacement of bromine by chlorine at C-5 position was corroborated (Figure 8).

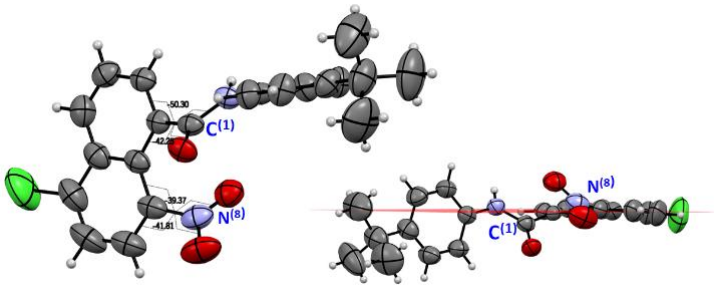


Figure 8. *ORTEP diagram of amide **17**. The crystallization methanol molecule has been omitted for clarity. Displacement ellipsoids are drawn at 50 % probability level. Hydrogen atoms are shown as spheres of arbitrary radius.*

3.4. Deprotection study of NNap

The protective group removal was studied using a diversity of reducing conditions with amide **16** as model substrate (Table 3).

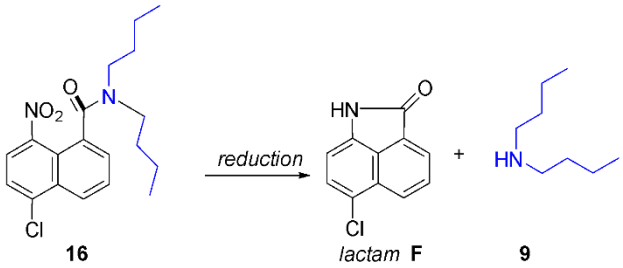
The reduction of the nitro group is a widely used transformation and many methods are available.[16]

In our case, due to the unique reactivity of the *peri*-disubstituted naphthalenes, the reduction of the nitro group occurs under mild conditions producing cleanly the desired amine in high yields, along with the expected lactam **F** (Table 3).

Although our attempts to grow single crystals of the lactam **F** were not successful, the crystal structure of the closely related 1,8-naphtholactam is known.[17]

The steric hindrance between *peri* positions in compounds **3** and **16**, twisted on either side of the naphthalene plane, is no longer present in the 1,8-naphtholactam, that possesses a nearly absolute planar configuration.

Table 3. *Reduction of the protecting group NNap.*



Entry	Conditions	yield of **9** (%)
1	Zn/AcOH; 60ºC, 10 min	95%
2	$SnCl_2$/MeOH; 60ºC, 10 min	80%
3	H_2/Pd (C)/AcOEt; 20ºC, 12 h	90%

The best results obtained from the reduction reaction were using Zn/AcOH (Table 3, entry 1):

A solution of the amide **16** in acetic acid was added to a preheated suspension of Zn in acetic acid (60º) affording di-*n*-butylamine **9** in 95% yield and lactam **F**.

The reaction conditions optimization allows a significative scope for the deprotection steps with the amides **12** (*n*-octylamide), **15** (*tert*-octylamide) and **17** (4-*tert*-butylanilide) deprotected in excellent yields (>90%).

The progress of the reduction could be monitored in an NMR tube (Figure 9).

Starting from the 5-chloro-8-nitro-1-naphthamide **16** (spectrum at the bottom), nitro group reduction to amine (**E16)** took place immediately following mixing (second spectrum from the bottom); however, in these dilute solution (CD_3OD as solvent), intramolecular cyclization to lactam **F** required heating in a water bath at 60ºC for several hours.

Thus, ^{1}H NMR signals corresponding to both the amine (**E16**) and lactam (**F**) could be easily identified in the different spectra until total conversion was achieved (lactam **F** spectrum at the top).

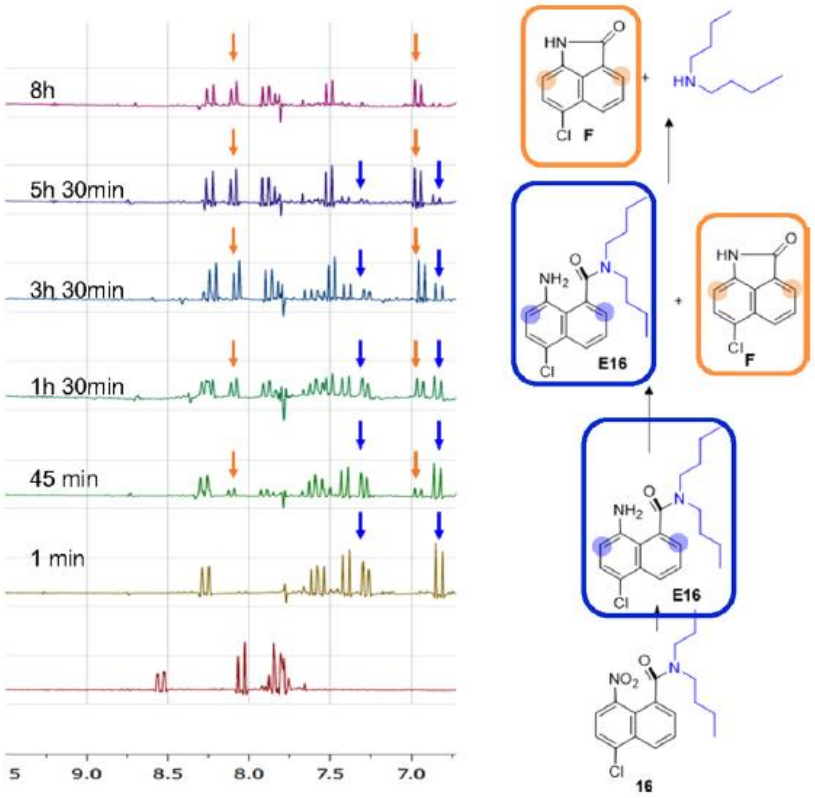


Figure 9. *^{1}H NMR spectra (aromatic region) of the reduction progress for amide **16** from the intermediate amine **E16** to the lactam **F** using Zn/AcOH.*

Reaction conditions of the deprotection are as follows: amide **16** (10.0 mg), Zn (80.0 mg) and acetic acid (20 mg) were dissolved in 1.0 mL of CD_3OD at 20ºC. (The deprotection progress was followed in an NMR tube).

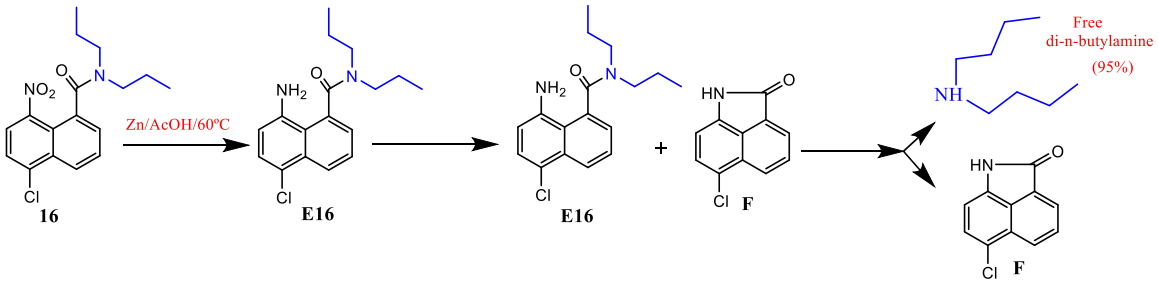


Figure 10. *Amide **16** reduction process with amine (**di-n-butylamine**) and lactam **F** liberation.*

3.5. Isolation of intermediate amines produced in the deprotection process

The endeavours to isolate the intermediate aromatic amine (**E16**) were unsuccessful, but when the reaction mixture was treated with acetic anhydride, the amine (**E16**) was trapped as the acetamide (**Ac16**).

Notably, one of the butyl chains of the acetamide **Ac16** is highly shielded: methyl triplet (4-Bu) at 0.53 ppm, probably because it is over the naphthalene ring as shown in figure 11.

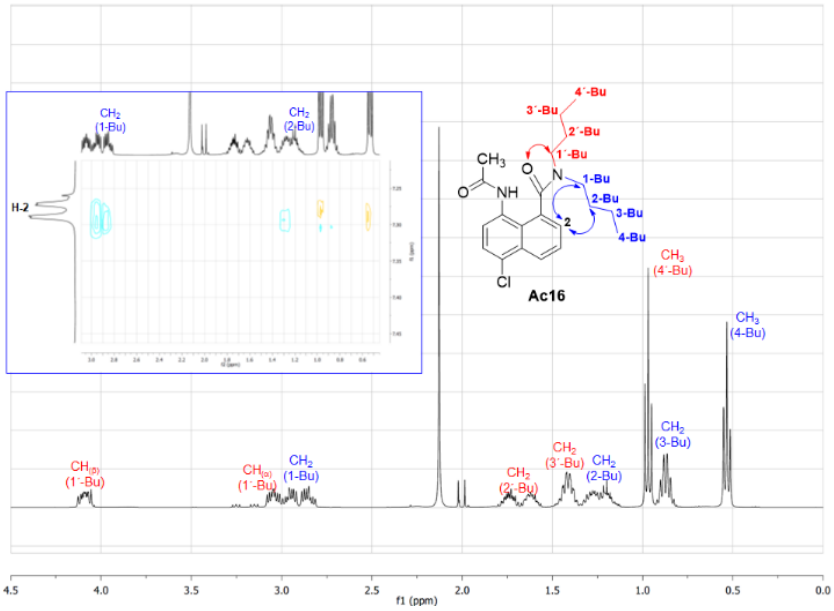


Figure 11. *^{1}H NMR spectra (aliphatic region) of acetamide **Ac16** in $CDCl_3$ at 20ºC and ROESY spectrum (inset) showing correlations between naphthalene C-2 proton and methylenes (1-Bu and 2-Bu).*

The correlation of the methylene protons (1-Bu and 2-Bu) with the aromatic C-2 proton (7.28 ppm) of the naphthalene ring (Figure 11, inset) was also shown with the ROESY spectra.

The absorption of the C-2 proton at 7.28 ppm is also very unusual, since it is *ortho* to a carboxylic group: twist of the amide carbonyl group from the plane of the aromatic ring explains this unusual shift.

On the other hand, one of the methylene protons of the other butyl chain (1´-Bu) is strongly deshielded (4.10 ppm) due to the proximity with the amide carbonyl group.

These effects show a rigid conformation in this part of the molecule, probably due to an angular H-bond between the acetamide and the amide carbonyl group (Figure 11).

A proposal for a possible geometry was allowed to be established thanks to the 2D NMR spectra and molecular modelling studies, the proposed geometry consists on the hypothesis of

a molecule with one butyl chain pointing towards the shielding zone of the naphthalene ring. A similar effect was observed for the non-acetylated compound, the amine **E16**.

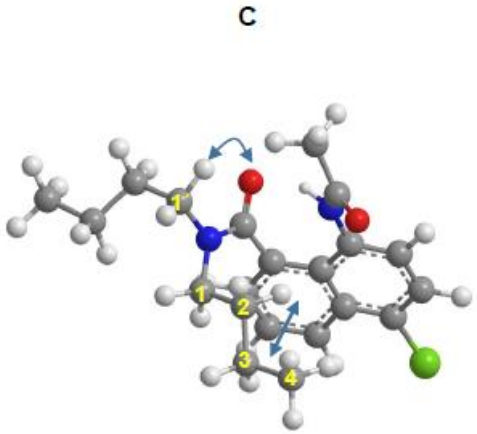


Figure 12. *Possible geometry for compound **Ac16**, obtained by computational methods (GAMESS interface for Chem3D 19.1 software using the RHF/3-21G).*

3.6. Deprotection using Hantzsch Ester

Eventually, reduction was studied with the Hantzsch ester to mimic physiological conditions and in particular NADPH.

Hantzsch ester reduced successfully the nitro group of amide **12** in the presence of eosin Y under 40W white light irradiation.

While the amine **5** (70% yield) is nicely liberated from the protecting group, curiously the lactam **F** was not obtained.

Analysis of the reaction products showed 8-amino-5-chloro-1-naphthoic acid as the main product, since this is not the expected compound the structure was confirmed through comparison with a synthesized compound obtained from the reduction of the nitro derivative **3a** under basic conditions.

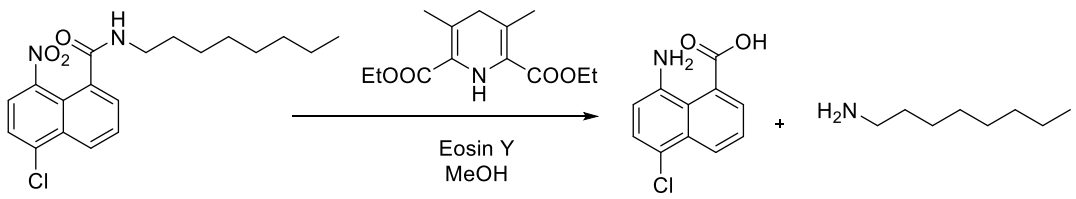


Figure 13. *Amide **12** reduction process with unexpected product using Hantzsch ester and eosin Y.*

3.7. NNap a multi-applicable protective group

3.7.1. Peptides synthesis using NNap

Since the amino functionality protection plays a crucial role in peptide synthesis, we explored the utility of NNap protective group in the synthesis of L-leucyl-L-leucine. Thus, L-leucine was first reacted with NNapCl **4** affording amide **19** in high yield (Figure 14).

The synthesis of the dipeptide **20** was completed by *i*-Pr_2NEt/DCC mediated coupling between H-Leu-O*t*Bu • HCl and **19** (Figure 14), no racemization was observed.

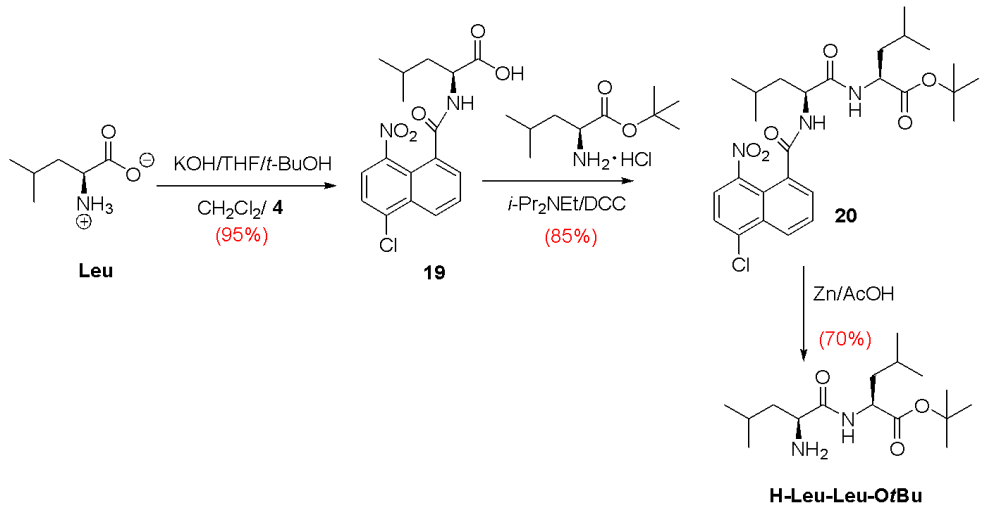


Figure 14. *NNap´s scope of application in peptide synthesis:* ***H-Leu-Leu-OtBu*** *synthesis.*

3.7.2. Orthogonal protection of L-lysine using NNap

One of the main challenges in peptide synthesis is related to selective protection of the ε and α-amino groups of L-lysine.[18] Common protective groups as benzyloxycarbonyl (Cbz) or fluorenylmethoxycarbonyl (Fmoc) are not selective and protection of the ε-amino lysine usually requires blocking the α-amino group using copper salts.[19] Likewise, benzyloxy carbonylation of the α-amino group involves temporary blocking of the ε-amino by condensation with benzaldehyde.[20]

These procedures are time consuming and imply the use of additional reagents, so the development of new methods for orthogonal selective protection of the amino groups of lysine is highly desirable.

A supramolecular approach using cyclodextrins (β-CD) has shown strong regioselectivity and good yields in the Cbz protection of the ε and α amino groups.[21] The reaction has been

performed on 1 mmol scale (1 mmol Lys; 0.1 mmol β-CD) and its selectivity appears to be limited to the Cbz group and the β-CD.

To exploit our previous results, the reaction was explored with lysine; after finding the optimal conditions, to our delight, treatment of the L-lysine methyl ester dihydrochloride (H-Lys-OMe 2HCl) with NNapCl **4** resulted in selective and high yield protection of the ε-amino group (Figure 15).

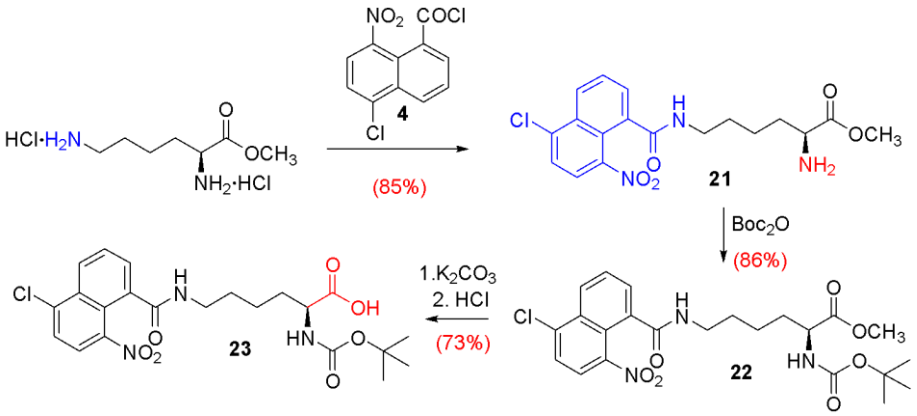


Figure 15. *Orthogonal protection of L-lysine using NNap´s protective group properties.*

The regioselectivity in favour of the ε-amino group yielding compound **21** might be justified due to the highly sterically hindered naphthoyl chloride **4**.

The amino ester **21** was amenable to further synthetic elaborations, such as protection of the α-amino group (**22**) or hydrolysis to carboxylic acid (**23**).

Applying the strategy of orthogonal functional group protection, the free α-amino group was acylated with Boc_2O to afford **22** in good yield.

Ultimately, the deprotected acid **23** was obtained by hydrolysis of the methyl ester under extremely mild conditions: aqueous potassium carbonate in methanol at room temperature.

The absence of racemization was confirmed.

3.7.3. NNap application to indanolamines

Another example showing the potential of this protecting group is demonstrated, using indanolamines.

First, indanolamine **11** was chemoselectively protected by treatment with NNapCl **4** (Figure **5b**, Table 2 "entry 7"), and next, the less nucleophilic hydroxyl group was esterified with benzoyl chloride.

Finally, compound **24** was reacted with Zn/AcOH and the amine functionality was deprotected without affecting the more sensitive ester group, with no transposition to the amino group, neither racemization, was observed in compound **25** (Figure 16).

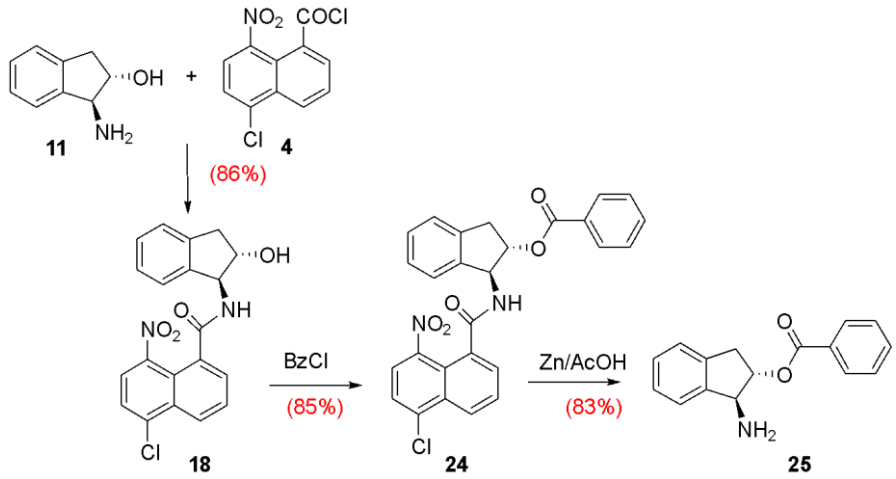


Figure 16. *The NNap application to indanolamines.*

4. Conclusions

Considering all of the facts, an available and efficient protective group for amines has been developed, the 5-chloro-8-nitro-1-naphthoyl (NNap). The steric hindrance between *peri* positions in the naphthalene ring allows deprotection under mild reduction conditions and selectivity in the case of lysine.

The steric hindrance has been proved thanks to X-ray diffraction studies that show that the nitro- and carboxyl groups are twisted from the plane of the naphthalene ring.

NNapCl is readily installed in amines, both aliphatic and aromatic, under Schotten-Baumann conditions, with good yields. It is selective for amines in the presence of alcohols; hence, this protective group is also suitable for aminoalcohols. It is remarkable that NNap allows the selective protection of the NH_2 group of the lateral chain of lysine without previous protection of the alfa amino group.

Deprotection takes place under mild reduction conditions with Zn. This allows its selective deprotection in the presence of other protecting groups such as Boc and proves its orthogonal properties. The applicability of NNap has been tested in the synthesis of H-Leu-Leu-OtBu dipeptide.

These promising results suggest that this new protective group has great potential to be further developed and included as alternative and complementary protecting group in the amine protection groups arsenal.

5. Experimental Section

5.1. Materials and instrumentation

X-ray diffraction studies

• *Procedure for the single crystal preparation*

Potassium carboxylate **(K•3)**. Single crystals suitable for X-ray diffraction measurements were obtained by slowly evaporating aqueous solutions of stoichiometric mixtures of the carboxylic acid **3** (50 mg) and the equimolar amount of potassium hydroxide in 3 mL of water in a clean and dry 10 mL glass vial. The mouth of the glass vial was covered with a cap having a small hole and kept it for slow evaporation at room temperature. At the end of the process, single crystals were obtained after 5-6 days.

Amide **17**. Single crystals suitable for X-ray diffraction measurements were obtained by slowly evaporating solutions of the amide **17** (50 mg) in 2 mL of methanol in a clean and dry 10 mL glass vial. The mouth of the glass vial was covered with a cap having a small hole and kept it for slow evaporation at room temperature. At the end of the process, single crystals were obtained after 5-6 days.

● *X-Ray Crystallography*

Suitable single crystals of **K•3** and **17** were mounted on glass fibre for data collection on a Bruker Kappa APEX II diffractometer. Data were collected at 298(2) K using Cu Kα radiation (λ = 1.54178 Å) and ω scan technique and were corrected for Lorentz and polarization effects. The detector was placed at approximately 37.5 mm from the crystal.
A series of narrow frames of data were collected with a scan width of 0.5º in ω and an exposure time of 10 s per frame.
The data were integrated with SAINT[24]to a resolution of 0.78 Å using a narrow-frame algorithm.
Data were corrected for absorption effects using the multi-scan method using SADABS.[25]
Subsequent structure solution and refinement were carried out with SHELXT and SHELXL, respectively.[26,27] The structures were solved by direct methods combined with difference

Fourier synthesis and refined by full-matrix least-squares procedures, with anisotropic thermal parameters in the last cycles of refinement for all non-hydrogen atoms.

The refinement was based on F2 for all reflections, weighted R factors (*wR*) and goodness-of-fit (GoF) values are based on F2, while conventional R factors (R) are based on F.

The Fo2 > 2σ(Fo2) criterion was used only for calculating R factors and it is not relevant to the choice of reflections for the refinement.

The R factors based on F2 are about twice as large as those based on F. Scattering factors were taken from the International Tables for Crystallography.[28] Hydrogen atom positions were calculated by geometrical methods and refined as a riding model.

The potassium salt of the carboxylic acid (**3**) crystallizes with one molecule of water; it should be noticed that hydrogen atoms of water molecules are not shown in the structural formula of the complex, as they were not located by X-ray diffraction. The amide **17** crystallizes with one molecule of methanol.

Mercury 4.2.0 program was used for analysis and molecular and crystal structure drawings preparation. [29]

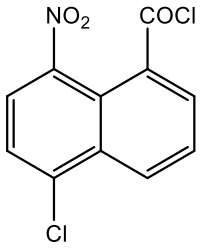
The CCDC numbers assigned for the crystal structures are: 2252216 (**K•3**, potassium salt of carboxylic acid **3**) and 2252212. (amide **17**).

Modelling studies

Theorical studies were carried out using GAMESS interface for Chem3D 19.1 software[30] using the RHF/3-21G.

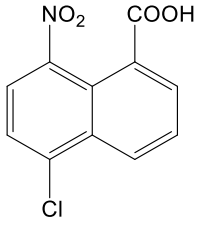
5.2. Synthetic details and characterization

5-chloro-8-nitro-1-naphthoyl chloride (4, NNapCl)



5-bromo-8-nitro-1-naphthoic acid (1.0 g, 3.38 mmol) was placed in a round bottom flask and thionyl chloride (5.0 mL) and a trace of pyridine were added. The round bottom flask was equipped with a condenser and a paraffin bubbler. The reaction mixture was stirred and heated in a water bath at 40ºC until a homogeneous solution was obtained. Once the acid was completely dissolved, the reaction was finished and the thionyl chloride was removed under vacuum. The crude acid chloride was used without further purification in the next step.
Due to its instability, the acid chloride **4** is not characterized.

5-chloro-8-nitro-1-naphthoic acid (3a)



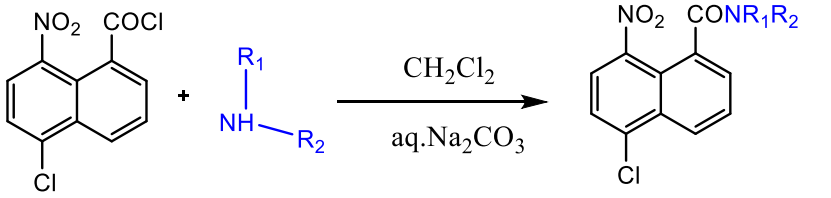
5-bromo-8-nitro-1-naphthoyl chloride **4** (500 mg, 1.85 mmol) was stirred in a 1:1 mixture of THF and water overnight. The solvent was evaporated under vacuum yielding the acid **3a** (440 mg, 95% yield) as a yellow crystalline solid.

M.p.>200 ºC.
IR (neat, ν in cm^{-1}) 3303, 2953, 1678, 1530, 1391, 730.
^{1}H NMR (DMSO-d_6, 400 MHz,) δ 8.55 (dd, 1H, J = 8.5 , 1.2 Hz), 8.24 (d, 1H, J = 8.2 Hz), 8.23 (dd, 1H, J = 7.2 ,1.2 Hz, 1H), 8.00 (d, 1H, J = 8.2 Hz), 7.94(dd, 1H, J = 8.5 , 7.2 Hz).

^{13}C NMR (DMSO-*d*$_6$, 100 MHz): 167.8 (C), 146.2 (C), 136.8 (C), 131.8 (CH), 131.1(C), 129.5 (C) 128.5 (CH), 127.7 (CH), 126.2 (CH), 125.3 (CH), 122.1 (C).

HRMS (ESI) m/z: [M - H] $^-$ Calculated for $C_{11}H_5ClNO_4$ 249.9902; Found 249.9913.

5.3. General Procedure (A) for amine (5-11) protection using NNapCl



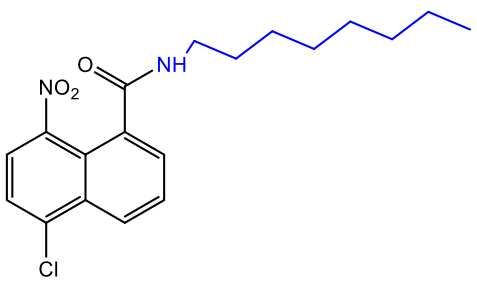
amines **(5-11)** amides **D (12-18)**

4 was prepared according to the above-described procedure by reacting 5-bromo-8-nitro-1-naphthoic acid **3** (500 mg; 1.69 mmol; 1 eq.) with thionyl chloride (5 ml; 69 mmol; 40 eq.). The crude acid chloride **4** was dissolved in methylene chloride (15 mL) and cooled down in an ice bath.

Then, a solution of the amine (1.69 mmol; 1 eq.) dissolved in CH_2Cl_2 (3.0 mL) was added dropwise. After stirring for 5 minutes, a solution of Na_2CO_3 (8.45 mmol, 890 mg) in water (4 mL) was added and the mixture was allowed to warm to room temperature, stirring for an additional 25 minutes.

Water (20 mL) was then added, and the layers were separated in a separatory funnel. The organic layer was washed with HCl 2M and dried over anhydrous Na_2SO_4. The solvent was removed by vacuum and the crude residue was purified.

5-chloro-8-nitro-*N*-octyl-1-naphthamide (12)



Purified by crystallization: 530 mg (86% yield) of a pale cream crystalline solid.

M.p. 182ºC-184ºC.

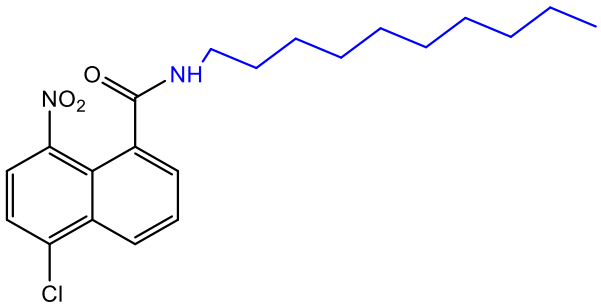
IR (neat, ν in cm^{-1}) 3249, 3100,2919, 1519, 1424, 836, 759.

^{1}H NMR ($CDCl_3$, 400 MHz): 8.47 (dd, 1H, *J* = 8.4 ,1.2 Hz,), 7.97 (d, 1H, *J* = 8.2 Hz,), 7.84 (dd, 1H, *J* = 7.2 , 1.2 Hz,), 7.68 (dd, 1H, *J* = 8.4 , 7.2 Hz), 7.67 (d, 1H, *J* = 8.2 Hz), 6.18 (m, 1H), 3.46 – 3.41 (m, 2H), 1.70 – 1.63 (m, 2H), 1.43 – 1.23 (m, 10H), 0.90 – 0.87 (m, 3H).

^{13}C NMR ($CDCl_3$, 100 MHz): 168.2 (C), 146.8 (C), 137.7 (C), 133.5 (C), 132.2 (C), 129.3 (CH), 127.5 (CH), 127.4 (CH), 125.5 (CH), 124.3 (CH), 123.0 (C), 40.3 (CH_2), 31.8 (CH_2), 29.5 (CH_2), 29.3 (CH_2), 29.2 (CH_2), 27.0 (CH_2), 22.6 (CH_2), 14.1 (CH_3).

HRMS (ESI) m/z: $[M+H]^+$ Calculated for $C_{19}H_{24}O_3N_2Cl$ 363.1470; Found 363.1464.

5-chloro-*N*-decyl-8-nitro-1-naphthamide (13)



Purified by crystallization: 630 mg (95% yield) of a pale crystalline solid.

M.p. 149ºC-151ºC.

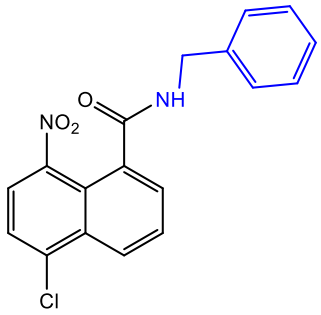
IR (neat, ν in cm^{-1}) 3243, 3095, 2921,1579,1465, 722.

^{1}H NMR ($CDCl_3$, 400 MHz): 8.47 (dd, 1H, *J* = 8.4, 1.2 Hz,), 7.97 (d, 1H, *J* = 8.0 Hz), 7.84 (dd, 1H, *J* = 7.0, 1.2 Hz), 7.68 (dd, 1H, *J* = 8.4, 7.0 Hz), 7.67 (d, 1H, *J* = 8.0 Hz), 6.18 (m, 1H), 3.46 – 3.41 (m, 2H), 1.70 – 1.62 (m, 2H), 1.43 – 1.27 (m, 14H), 0.90 – 0.86 (m, 3H).

^{13}C NMR ($CDCl_3$, 100 MHz): 168.2 (C), 146.9 (C), 137.7 (C), 133.5 (C), 132.2 (C), 129.3 (CH), 127.5 (CH), 127.4 (CH), 125.5 (CH), 124.3 (CH), 122.9 (C), 40.3 (CH_2), 31.9 (CH_2), 29.6 (CH_2), 29.5 (CH_2), 29.5 (CH_2), 29.3 (CH_2), 29.3 (CH_2), 27.0 (CH_2), 22.7 (CH_2), 14.1 (CH_3).

HRMS (ESI) m/z: $[M+H]^+$ Calculated for $C_{21}H_{28}O_3N_2Cl$ 391.1793; Found 391.1777.

_N_-benzyl-5-chloro-8-nitro-1-naphthamide (14)



Purified by crystallization: 500 mg (87% yield) of a pale cream crystalline solid.

M.p.>200ºC

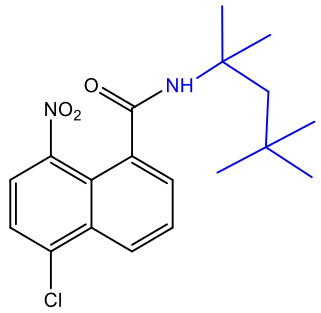
IR (neat, ν in cm^{-1}) 3257, 3089, 1530, 1357, 845, 756, 700.

^{1}H NMR (DMSO-d_6, 400 MHz): 9.37 (t, 1H, J = 5.6 Hz), 8.48 (dd, 1H, J = 8.4 , 1.2 Hz,), 8.17 (d, 1H, J = 8.4 Hz,), 8.03 (dd, 1H, J = 7.2 , 1.2 Hz), 7.95 (d, 1H, J = 8.4 Hz), 7.91 (dd, 1H, J = 8.4 , 7.2 Hz), 7.41 (d, 2H, J =7.2Hz), 7.35 (t, 2H, J = 7.2 Hz), 7.26 (t, 1H J = 7.2 Hz), 4.46 (d, 2H, J = 5.6 Hz).

^{13}C NMR (DMSO-d_6, 100 MHz): 167.3 (C), 146.7 (C), 139.1 (C), 136.4 (C), 132.8 (C), 131.1 (C), 130.5 (CH), 128.4 (CH), 128.3 (2CH), 127.5 (2CH), 126.9 (CH), 126.6 (CH), 126.0 (CH), 124.8 (CH), 122.1 (C), 42.6 (CH_2).

HRMS (ESI) m/z: $[M+H]^+$ Calculated for $C_{18}H_{14}O_3N_2Cl$ 341.0688; Found 341.0683.

5-chloro-8-nitro-_N_-(2,4,4-trimethylpentan-2-yl)-1-naphthamide (15)



Purified by crystallization: 550 mg (90% yield) of a pale cream powder.

M.p. 150ºC-152ºC.

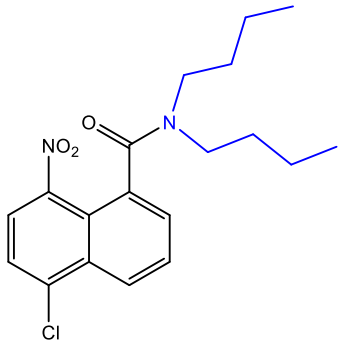
IR (neat, ν in cm^{-1}) 3306, 3066, 2953, 1539, 1351, 836, 753.

^{1}H NMR ($CDCl_3$, 400 MHz): 8.44 (dd, 1H, *J* = 8.4 , 1.2 Hz,), 7.96 (d, 1H, *J* = 8.4 Hz,), 7.80 (dd, 1H, *J* = 7.2 , 1.2 Hz), 7.65 (d, 1H, *J* = 8.4 Hz), 7.65 (dd, 1H, *J* = 8.4 , 7.2 Hz), 6.07 (s, 1H), 1.83 (s, 2H), 1.57 (s, 6H), 1.09 (s, 9H).

^{13}C NMR ($CDCl_3$, 100 MHz): 166.8 (C), 147.0 (C), 137.5 (C), 134.7 (C), 132.3 (C), 128.9 (CH), 127.4 (CH), 127.1 (CH), 125.4 (CH), 124.1 (CH), 123.0 (C), 56.4 (C), 52.8 (CH_2), 31.7 (C), 31.6 ($2CH_3$) 28.7 ($3CH_3$).

HRMS (ESI) m/z: $[M+H]^+$ Calculated for $C_{19}H_{24}O_3N_2Cl$ 363.1470; Found 363.1465.

***N, N*-dibutyl-5-chloro-8-nitro-1-naphthamide (16)**



Purified by chromatography: 530 mg (87% yield) of a deep orange oil.

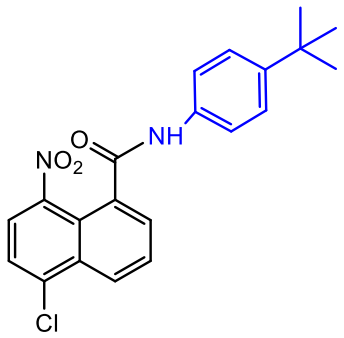
IR (neat, ν in cm^{-1}) 3754, 2961, 2872, 1633, 1465, 762.

^{1}H NMR ($CDCl_3$, 400 MHz): 8.45 (dd, 1H, *J* = 8.4 ,1.2 Hz,), 7.92 (d, 1H, *J* = 8.0 Hz,), 7.73 – 7.63 (m, 3H), 3.58 – 3.31 (m, 4H), 1.82 – 1.64 (m, 4H), 1.47 – 1.36 (m, 2H), 1.31 – 1.21 (m, 2H), 0.99 (t, 3H, *J* = 7.2 Hz) 0.89 (t, 3H, *J* = 7.2 Hz).

^{13}C NMR ($CDCl_3$, 100 MHz): 169.5 (C), 146.7 (C), 137.7 (C), 133.0 (C), 132.4 (C), 128.8 (CH), 127.2 (CH), 126.4 (CH), 125.2 (CH), 123.9 (CH), 123.5 (C), 49.7 (CH_2), 44.8 (CH_2), 30.4 (CH_2), 29.2 (CH_2), 20.5 (CH_2), 20.2 (CH_2), 14.0 (CH_3), 13.8 (CH_3).

HRMS (ESI) m/z: $[M+H]^+$ Calculated for $C_{19}H_{24}O_3N_2Cl$ 363.1470; Found 363.1463.

▪ ***N*-(4-(*tert*-butyl)phenyl)-5-chloro-8-nitro-1-naphthamide (17)**



Purified by crystallization: 586 mg (91% yield) of an orange crystalline solid.

M.p.>200 ºC.

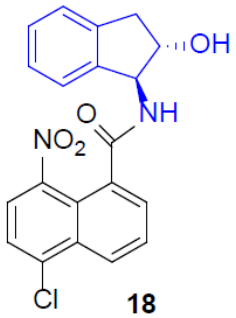
IR (neat, ν in cm^{-1}) 3749, 2961, 1595, 1527, 1348, 836.

^{1}H NMR ($CDCl_3$, 400 MHz): 8.49 (d, 1H, *J* = 8.4 Hz), 8.01 (d, 1H, *J* = 8.4 Hz), 7.96 (d, 1H, *J* = 7.2 Hz), 7.91 (broad s, 1H), 7.72 – 7.68 (m, 2H), 7.54 (d, 2H, *J* = 8.4 Hz), 7.38 (d, 2H, *J* = 8.4 Hz), 1.33 (s, 9H).

^{13}C NMR ($CDCl_3$, 100 MHz): 166.0 (C), 148.0 (C), 146.7 (C), 137.9(C), 134.8 (C), 133.4 (C), 132.1 (C), 129.3 (CH), 127.7 (CH), 127.5 (CH), 126.0 (2CH), 125.7 (CH), 124.6 (CH), 122.8 (C), 120.4 (2CH), 34.4 (C), 31.4 ($3CH_3$).

HRMS (ESI) m/z: $[M+H]^+$ Calculated for $C_{21}H_{20}O_3N_2Cl$ 383.1157; Found 383.1150.

5-chloro-*N*-((1*S*,2*S*) -2-hydroxy-2,3-dihydro-1*H*-inden-1-yl) -8-nitro-1-naphthamide (18)



18

Purified by crystallization: 550 mg (86% yield) of a yellow powder.

M.p.>200 ºC.

IR (neat, ν in cm^{-1}) 3502, 3285 ,2920, 1737 ,1634 ,1514, 1353, 1277, 1079.

^{1}H NMR ($CDCl_3$, 400 MHz): 8.56 (dd, 1H, *J* = 8.4 , 1.2 Hz), 8.05 (d, 1H, *J* = 8.2 Hz), 7.99 (dd, 1H, *J* = 7.2 , 1.2 Hz), 7.76 (dd, 1H, *J* = 8.4 , 7.2 Hz), 7.74 (d, 1H, *J* = 8.2 Hz), 7.38 – 7.36 (m, 1H), 7.32 – 7.28 (m, 3H), 6.57 (d, 1H, *J* = 6.4 Hz), 5.40 (t, 1H, *J* = 6.4 Hz), 4.69 (td, 1H, *J* = 8.0 , 6.4 Hz), 3.38 (dd, 1H, *J* = 16 , 8.0 Hz), 3.03 (dd, 1H, *J* = 16 , 8.0 Hz).

^{13}C NMR ($CDCl_3$, 100 MHz): 170.0 (C), 146.6 (C), 140.8 (C), 139.0 (C), 138.2 (C), 132.4 (C), 132.3 (C), 129.6 (CH), 128.8 (CH), 128.1 (CH), 127.5 (CH), 127.3 (CH), 125.8 (CH), 125.4 (CH), 124.7 (CH), 123.1 (CH), 123.0 (C), 81.6 (CH), 64.3 (CH), 38.3 (CH_2).

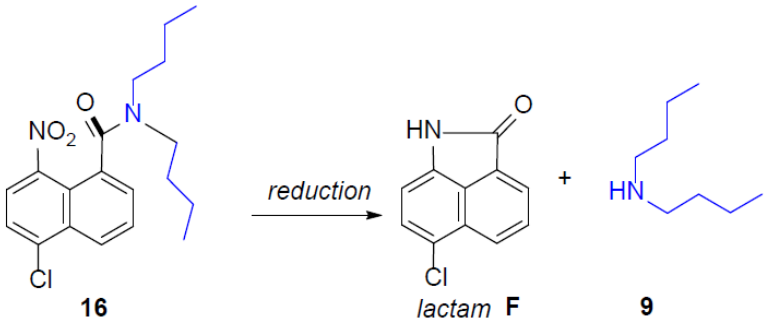
HRMS (ESI) m/z: $[M+H]^+$ Calculated for $C_{20}H_{16}O_4N_2Cl$ 383.0793; Found 383.0792.

$[\alpha]_D^{20}$ +78.4 (c 0.25, MeCN).

5.4. Procedure for deprotection

Removal of the protective group was explored using a variety of reducing conditions: Zn/AcOH, $SnCl_2$/MeOH, and H_2/Pd (C)/EtOAc. Next, the different procedures are described for amide **16**.

Reduction of amines (**12**, **15**, **17** and **18**) proceeded under similar conditions. Lactam **F** was purified by column chromatography on silica gel using 100% CH_2Cl_2 to a mixture CH_2Cl_2: EtOAc (9:1).



16 *lactam* **F** **9**

Zn/AcOH (B)

A solution of the amide **16** (300 mg, 0.83 mmol, 1 eq.) in acetic acid (3 mL) was added to an Erlenmeyer flask containing a preheated (60ºC) and well-stirred suspension of Zn (3.0 g, 46 mmol, 55 eq.) in acetic acid (6 mL). The reaction mixture was stirred for 10 minutes, and ethyl acetate (20 mL) and water (20 mL) were then added. Zn was removed by filtration (or careful decantation), the two phases separated, and the organic layer acidified with 2N HCl. The acidic

aqueous layer and the ethyl acetate layer (containing the lactam **F**) were separated, and the acidic extract basified with solid Na_2CO_3. The basic aqueous layer was finally extracted with ethyl acetate, the combined organic layers dried over anhydrous Na_2SO_4, filtered, and the ethyl acetate was evaporated under reduced pressure, to afford di-n-butylamine **9** in 95% yield (160 mg).

$SnCl_2$/MeOH (C)

The amide **16** (140 mg, 0.39 mmol, 1 eq.) was dissolved in methanol (10 mL) and excess of $SnCl_2$ was added (300 mg, 1.58 mmol, 4 eq.).

The reaction mixture was heated in a water bath at 60ºC for 10 minutes. Next, 2.0 mL of an aqueous 2M Na_2CO_3 solution, solid Na_2CO_3 (500 mg, 4.72 mmol) and ethyl acetate (20 mL) were added, and the reaction mixture was stirred for additional 10 minutes, until a basic pH was obtained.

The reaction mixture was filtered, the phases separated, and the combined organic layers acidified with 2M HCl. Lactam **F** could be isolated from the organic layer, after drying over anhydrous Na_2SO_4, filtering and evaporating the solvent under reduced pressure.

The acidic extracts (containing the protonated amine) were basified with solid Na_2CO_3 and extracted with ethyl acetate, dried over anhydrous Na_2SO_4, filtered, and evaporated under reduced pressure to afford di-*n*-butylamine **9** in 80% yield (63 mg).

H_2/Pd (C)/ EtOAc (D)

The amide **16** (140 mg, 0.39 mmol, 1eq.) was dissolved in ethyl acetate (7.0 mL). Then 100 mg of Pd/C 5% were added, and the mixture was reacted with hydrogen under pressure (3.5 atm) overnight at 20ºC.

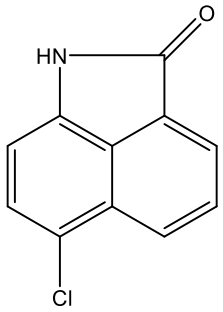
The catalyst was removed by filtration and the solvent was evaporated under reduced pressure, but lactam cyclization was incomplete according to ^{1}H NMR spectrum. The crude residue was then dissolved in acetic acid and heated for 2 minutes at 100ºC to complete the amine liberation. The reaction mixture was worked up with ethyl acetate and water as described previously to afford di-*n*-butylamine **9** in 90% yield (71 mg).

Hantzsch Ester / eosin Y.

Amide **12** (96 mg, 0.26 mmol) was dissolved in 14 mL of methanol. Hantzsch ester (846 mg, 3.34 mmol) and Eosin Y (42 mg, 0.06 mmol) were added. The solution was bubbled with argon for 30 minutes and then it was stirred under argon atmosphere and irradiated with white light (Kessil lamp) at room temperature for 17 hours.

Then, the solid was filtered under reduced pressure and the mother liquors were concentrated and the residue purified by silica gel chromatography column using EtOAc-MeOH as eluent, yielding 50 mg of the compound as a red solid which was further purified by crystallization in MeOH.

6-chlorobenzo[*cd*]indol-2(1H)-one (F)



Orange crystalline solid.

M.p.> 200ºC.

IR (neat, ν in cm^{-1}) 3755, 2927, 2859, 2369, 2338, 1354.

^{1}H NMR (CD_3OD, 400 MHz): 8.26 (dd, 1H, *J* = 8.4 , 0.4 Hz), 8.10 (d, 1H, *J* = 6.8 Hz,), 7.88 (dd, 1H, *J* = 8.4 , 6.8 Hz), 7.51 (d, 1H, *J* = 7.2 Hz), 6.94 (d, 1H, *J* = 7.2 Hz).

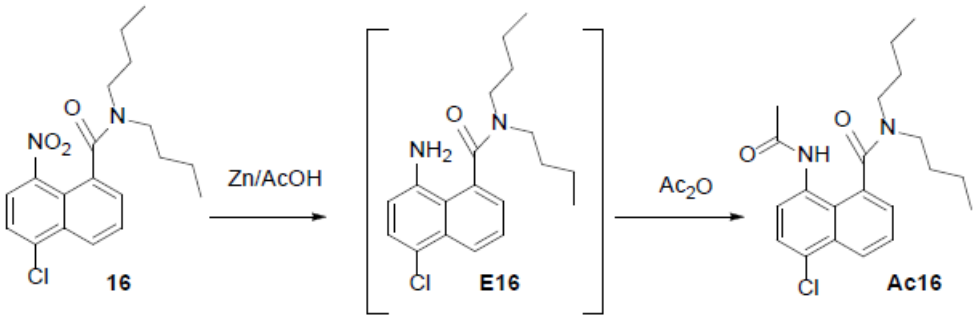
^{13}C NMR (CD_3OD, 100 MHz): 171.4 (C), 138.4 (C), 130.9 (CH), 129.4 (CH), 129.3 (CH), 129.0 (C), 128.7 (C), 128. 3 (C), 126.1 (CH), 125.6 (C), 108.5 (CH).

HRMS (ESI) m/z: $[M+H]^+$ Calculated for $C_{11}H_7ONCl$ 204.0210; Found 204.0210.

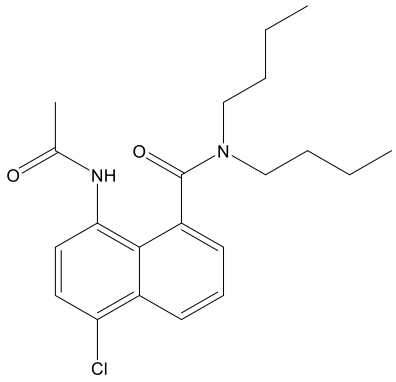
5.5. Capture of the intermediate amine

Amide **16** (0.83 mmol, 300 mg) in acetic acid (3 mL) was added to a suspension of Zn (46 mmol, 3.0 g) in acetic acid (6 mL). The reaction mixture was stirred for 10 minutes, then, acetic anhydride (10 mL) was added, and the reaction mixture was stirred at room temperature until acetylation was complete. Ethyl acetate (20 mL) and 4% (w/v) aqueous solution of Na_2CO_3 (20 mL) were then added and Zn was removed by filtration (or careful decantation).

The two phases were separated, and the organic layer dried over anhydrous Na_2SO_4 and filtered. The solvent was evaporated under reduced pressure and the crude residue was purified by silica gel column chromatography using CH_2Cl_2: EtOAc (95:5) to afford 255 mg (82%) of the desired compound **Ac16**.



8-acetamido-*N*,*N*-dibutyl-5-chloro-1-naphthamide (Ac16)

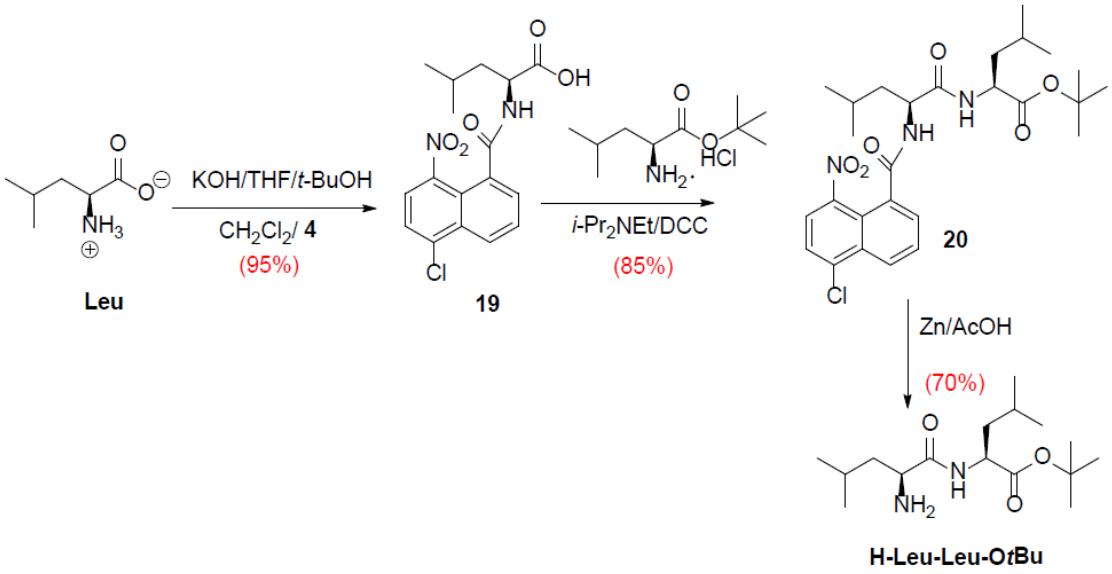


^{1}H NMR ($CDCl_3$, 400 MHz): 8.75 (s, 1H), 8.31 (dd, 1H, *J* = 8.4 , 1.2 Hz), 7.69 (d, 1H, *J* = 8.0 Hz), 7.55 (d, *J* = 8.0 Hz, 1H), 7.50 (dd, 1H, *J* = 8.4 ,7.2 Hz), 7.28 (dd, 1H, *J* = 7.2 ,1.2 Hz,), 4.13 – 4.01 (m, 1H), 3.08 – 2.99 (m, 1H), 2.98 – 2.81 (m, 2H), 2.13 (s, 3H), 1.82 – 1.56 (m, 2H), 1.48– 1.35 (m, 2H), 1.35 – 1.11 (m, 2H), 0.97 (t, 3H, *J* = 7.2 Hz), 0.92 – 0.83 (m, 2H), 0.53 (t, 3H *J* = 7.2 Hz).

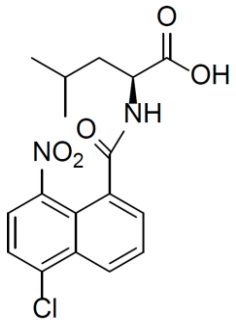
^{13}C NMR ($CDCl_3$, 100 MHz): 173.8 (C), 168.7 (C), 131.8 (2C), 131.6 (C), 129.5 (C), 126.8 (CH), 126.5 (CH), 126.5 (CH), 125.8 (CH), 125.2 (C), 124.4 (CH), 49.6 (CH_2), 45.3 (CH_2), 30.3 (CH_2), 30.1 (CH_2), 24.1(CH_3), 20.4 (CH_2), 19.6 (CH_2), 13.9 (CH_3), 13.3 (CH_3).

HRMS (ESI) m/z: $[M+H]^+$ Calculated for $C_{21}H_{28}O_2N_2Cl$ 375.1834; Found 375.1831.

5.6. Synthesis of H-Leu-Leu-O*t*Bu



(5-chloro-8-nitro-1-naphthoyl)-L-leucine (19)



19

The acid chloride **4** was prepared according to the described procedure by reacting 5-bromo-8-nitro-1-naphthoic acid **3** (500 mg, 1.69 mmol) with thionyl chloride (5 mL). Meanwhile, L-Leucine (540 mg, 4.12 mmol) was suspended in 10 mL of a tetrahydrofuran-*tert*-butanol (1:1) mixture containing potassium hydroxide (230 mg, 4.12 mmol) and ultrasonic treatment was applied until total dissolution. Next, the leucine solution was added to a solution of the acid chloride **4** in CH_2Cl_2 (10 mL) at 0ºC and the reaction was stirred for 15 minutes. The reaction mixture was then poured onto a 2M HCl solution and extracted with CH_2Cl_2, dried over anhydrous Na_2SO_4, filtered, and evaporated under reduced pressure to afford the protected L-leucine **19** as a cream coloured solid (585 mg, 95%). No further purification was required.

M.p. 142ºC-144ºC.

IR (neat, ν in cm^{-1}) 3294, 2961, 1724, 1641, 1530, 1350, 765.

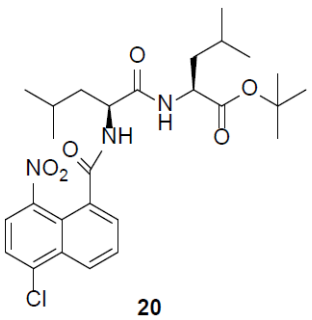
^{1}H NMR ($CDCl_3$, 400 MHz): 8.50 (d, 1H, *J* = 8.4 Hz,), 7.99 (d, 1H, *J* = 8.0 Hz), 7.95 (d, 1H, *J* = 6.8 Hz), 7.73 – 7.68 (m, 1H), 7.69 (d, 1H, *J* = 8.0 Hz), 6.60 (d, 1H, *J* = 8.0 Hz), 4.86 (td, 1H, *J* = 8.4 ,5.2 Hz), 1.98 – 1.74 (m, 3H), 1.06 (d, 3H, *J* = 6.4 Hz), 1.03 (d, 3H, *J* = 6.4 Hz).

13C NMR ($CDCl_3$, 100 MHz): 176.1 (C), 168.0 (C), 146.7 (C), 137.9 (C), 132.5 (C), 132.2 (C), 129.8 (CH), 127.9 (CH), 127.5 (CH), 125.7(CH), 124.5 (CH), 122.8 (C), 51.1 (CH), 41.4 (CH_2), 24.8 (CH), 22.8 (CH_3), 21.6 (CH_3).

HRMS (ESI) m/z: $[M+Na]^+$ Calculated for $C_{17}H_{17}O_5N_2ClNa$ 387.0718; Found 387.0713.

$[\alpha]_D^{20}$ - 44.3 (c 1, $CHCl_3$).

***tert*-butyl (5-chloro-8-nitro-1-naphthoyl)-L-leucyl-L-leucinate (20)**



20

The protected L-leucine **19** (105 mg, 0.30 mmol), H-Leu-O*t*Bu• HCl (67 mg, 0.30 mmol) and *i*-Pr_2NEt (51 µL, 0.30 mmol) were dissolved in methylene chloride (10.0 mL) under stirring. Then DCC (64 mg, 0.30 mmol) was added, and the reaction mixture was stirred at room temperature for 30 minutes. The dicyclohexyl urea was removed by filtration, and the reaction mixture was poured into a dilute solution of 2M HCl. The two phases were separated, the combined organic layers dried over anhydrous Na_2SO_4, filtered, and concentrated under reduced pressure. The crude residue was purified by silica gel column chromatography using methylene chloride/ethyl acetate (9:1 to 7:3) to afford 135 mg of the desired dipeptide **20** as a brown oil in 85% yield.

IR (neat, ν in cm^{-1}) 3280, 2958, 1638, 1536, 1351, 1155.

^{1}H NMR ($CDCl_3$, 400 MHz): 8.51 (dd, 1H, *J* = 8.4 , 1.2 Hz,), 7.99 (d, 1H, *J* = 8.0 Hz,), 7.90 (dd, 1H, *J* = 7.2 , 1.2 Hz), 7.71 (dd, 1H, *J* =8.4 , 7.2 Hz), 7.70 (d, 1H, *J* =8.0 Hz), 6.70 (d, 1H,

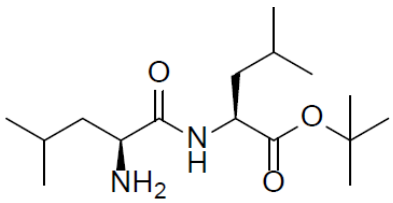
J = 8.4 Hz), 6.30 (d, 1H, *J* = 8.4 Hz), 4.66 (td, 1H, *J* = 8.4 ,5.9 Hz), 4.50 (td, 1H, *J* = 8.4 , 5.7 Hz), 1.90 – 1.76 (m, 6H), 1.47 (s, 9H), 1.03 (d, 3H, *J* = 6.0 Hz), 1.02 (d, 3H, *J* = 6.0 Hz), 0.92 (t, 6H, *J* = 6.0 Hz).

^{13}C NMR ($CDCl_3$, 100 MHz): 171.6 (C), 171.3 (C), 167.9 (C), 146.8 (C), 137.8 (C), 132.7 (C), 132.2 (C), 129.6 (CH), 127.8 (CH), 127.5 (CH), 125.6 (CH), 124.4 (CH), 122.8 (C), 81.8 (C), 52.0 (CH), 51.6 (CH), 41.5 ($2CH_2$), 27.9 ($3CH_3$), 24.8 (2CH), 23.0 (CH_3), 22.7 (CH_3), 22.3 (CH_3), 22.0 (CH_3).

HRMS (ESI) m/z: $[M+Na]^+$ Calculated for $C_{27}H_{36}O_6N_3ClNa$ 556.2184; Found 556.2183.

$[\alpha]_D^{20}$ - 71.3 (c 1, $CHCl_3$).

***Tert*-butyl L-leucyl-L-leucinate (H-Leu-Leu-O*t*Bu)**



H-Leu-Leu-O*t*Bu

The protected dipeptide **20** (106 mg, 0.20 mmol) was dissolved in acetic acid (1.0 mL) and added to a preheated and well-stirred suspension of Zn (1.0 g) in AcOH (3.0 mL). Following the above-described procedure for deprotection (B), 45 mg of the dipeptide H-Leu-Leu-O*t*Bu was obtained as a colourless oil in 70% yield. The spectroscopic properties agreed with those published.[31]

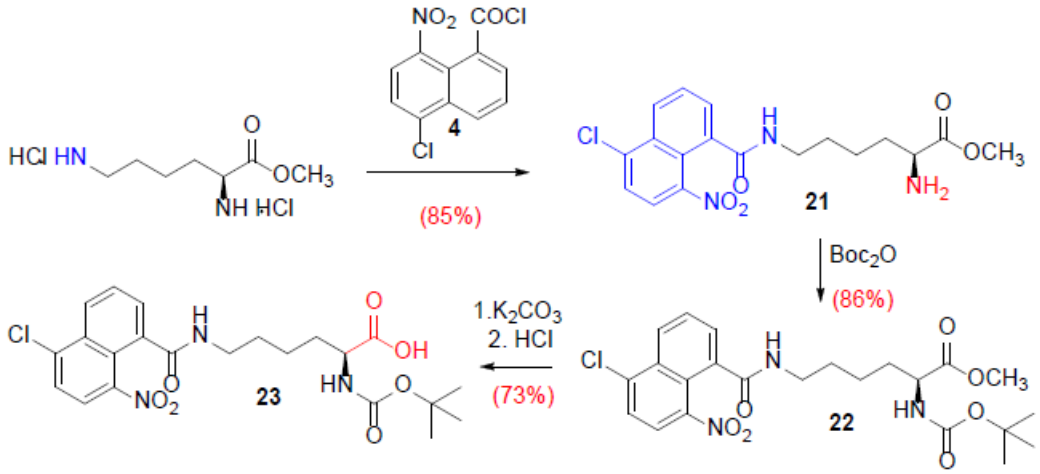
^{1}H NMR ($CDCl_3$, 400 MHz): 7.58 (d, 1H, *J* = 8.0 Hz), 4.48 (dt, 1H, *J* = 8.8, 5.2 Hz) 3.40 (d, 1H, *J* = 8.0 Hz), 1.76-1.22 (m, 8H), 1.45 (s, 9H), 0.97-0.92 (m, 12H).

^{13}C NMR ($CDCl_3$, 100 MHz):175.1 (C), 172.4 (C), 81.8 (C), 53.5(CH), 50.8 (CH), 44.1 (CH2), 41.7 (CH2), 28.0 (3CH3), 25.0 (CH), 24.9 (CH), 23.4 (CH3), 22.9 (CH3), 22.1 (CH3), 21.3 (CH3).

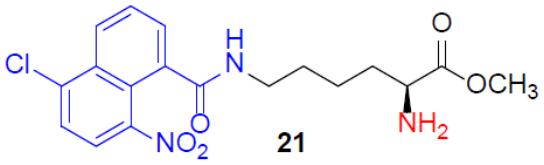
HRMS (ESI) m/z: $[M+H]^+$ Calculated for $C_{16}H_{33}O_3N_2$ 301.2486; Found 301.2480.

$[\alpha]_D^{20}$ -21.5 (c 1, $CHCl_3$).

5.7. Orthogonal protection of lysine



Methyl *N*-6-(5-chloro-8-nitro-1-naphthoyl)-L-lysinate (21)



H-Lys-OMe•2HCl (2.20 g, 10.2 mmol) was suspended in a dichloromethane-*tert*-butanol (5:1) solvent mixture (60 mL) containing *i*-Pr$_2$Et (7.0 mL, 40.1 mmol) and stirred at room temperature until total dissolution. Next, a solution of the acid chloride **4** (920 mg, 3.4 mmol) in CH_2Cl_2 (10 mL) was added. The reaction mixture was stirred for 10 minutes until it was completed. Then, the reaction mixture was worked-up, extracting with ethyl acetate (50 mL) and aqueous sodium carbonate 4% (w/v). The combined organic layers were dried over anhydrous Na_2SO_4, filtered, and concentrated under reduced pressure.

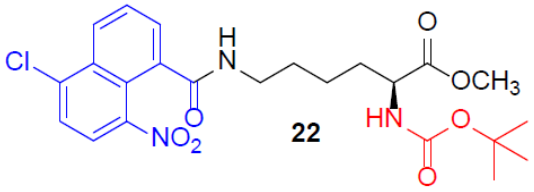
The crude residue (1.3 g) was purified by crystallization to yield 1.1 g of the desired compound **21** in 85% yield as a pale yellow crystalline solid.

M.p. 155ºC-157ºC. IR (neat, ν in cm^{-1}) 3260, 2952, 1636, 1533, 1351, 1179.

^{1}H NMR (CD_3OD, 400 MHz): 8.55 (dd, 1H, J = 8.4 , 1.2 Hz), 8.08 (d, 1H, J = 8.0 Hz,), 7.97 (dd, 1H, J = 7.2, 1.2 Hz), 7.83 (dd, 1H, J = 8.4 ,7.2 Hz), 7.83 (d, 1H, J = 8.0 Hz), 4.08 (t, 1H, J = 6.4 Hz), 3.83 (s, 3H), 3.37 (t, 2H, J = 6.8 Hz), 2.08 – 1.91 (m, 2H), 1.76 – 1.68 (m, 2H), 1.67 – 1-49 (m, 2H).

^{13}C NMR (CD_3OD, 100 MHz): 171.0 (C), 170.9 (C),148.3 (C), 138.6 (C), 134.1 (C), 133.2 (C), 131.5 (CH), 129.1 (CH), 128.3 (CH), 127.0 (CH), 125.8 (CH), 123.9 (C), 53.9 (CH3), 53.7 (CH), 40.40 (CH2), 31.2 (CH2), 39.8 (CH2), 23.4 (CH2).
HRMS (ESI) m/z: $[M+H]^+$ Calculated for $C_{18}H_{21}O_5N_3Cl$ 394.1164; Found 394.1161.
$[\alpha]_D^{20}$ +7.9 (c 1, MeOH).

Methyl *N*2-(*tert*-butoxycarbonyl)-*N*6-(5-chloro-8-nitro-1-naphthoyl)-L-lysinate (22)

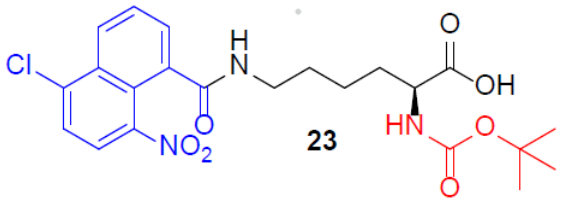


22

The lysine derivative **21** (1.30 g, 3.30 mmol) was dissolved in CH_2Cl_2 (30 mL) and a solution of Boc_2O (720 mg, 3.30 mmol) in 5 mL CH_2Cl_2 was added. The reaction mixture was stirred for 20 minutes, and the solvent was removed under vacuum. The crude residue was purified by column chromatography on silica gel using CH_2Cl_2/EtOAc mixtures of increasing polarity (9/1 to 7/3) to afford 1.4 g (86% yield) of the desired compound **22** as a yellow powder.

IR (neat, ν in cm^{-1}) 3306, 2981, 1644, 1528, 1359, 1211, 1169.
^{1}H NMR (CD_3OD, 400 MHz): 8.49 (dd, 1H, *J* = 8.4 , 1.2 Hz), 8.02 (d, 1H, *J* = 8.0 Hz,), 7.89 (dd, 1H, *J* = 7.2 , 1.2 Hz), 7.84 – 7.78 (m, 2H), 4.09 (dd, 1H, *J* = 8.8 , 5.2 Hz), 3.67 (s, 3H), 3.28 – 3.25 (m, 2H), 1.85 – 1.71 (m, 1H), 1.55 – 1.43 (m, 3H), 1.85 – 1.71 (m, 2H), 1.37 (s, 9H).
^{13}C NMR (CD_3OD, 100 MHz): 175.0 (C), 171.0 (C),158.2 (C), 148.3 (C), 138.4 (C), 134.4 (C), 133.4 (C), 131.6 (CH), 129.3 (CH), 128.2 (CH), 127.0 (CH), 125.7 (CH), 123.9 (C), 80.4 (C), 55.1 (CH), 52.6 (CH3), 40.5 (CH2), 31.4 (CH2), 29.6 (CH2), 28.7 (3CH3), 24.3 (CH2).
HRMS (ESI) m/z: $[M+Na]^+$ Calculated for $C_{23}H_{28}O_7N_3ClNa$ 516.1508; Found 516.1506.
$[\alpha]_D^{20}$ -31 (c 0.5, $CHCl_3$).

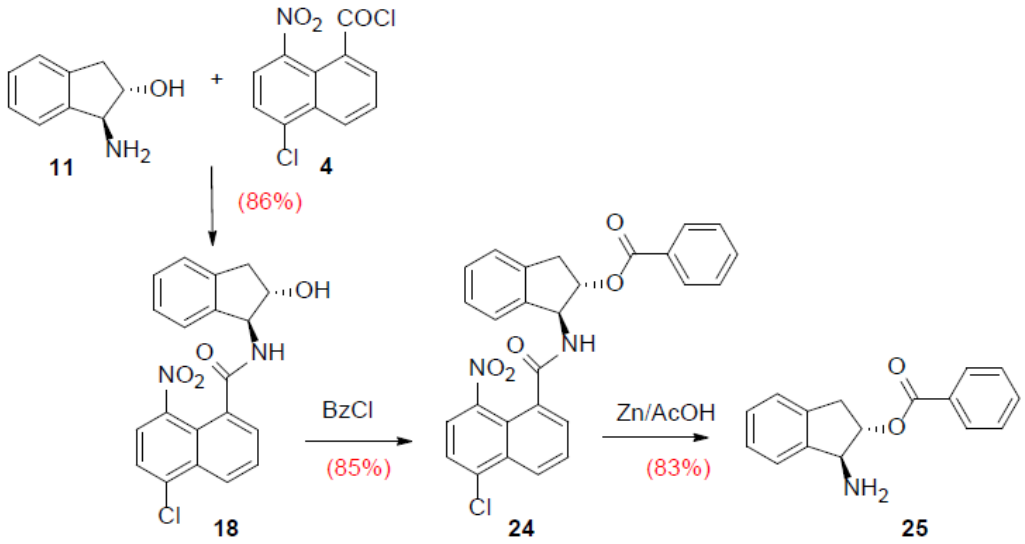
N^2-(*tert*-butoxycarbonyl)-N^6-(5-chloro-8-nitro-1-naphthoyl)-L-lysine (23)



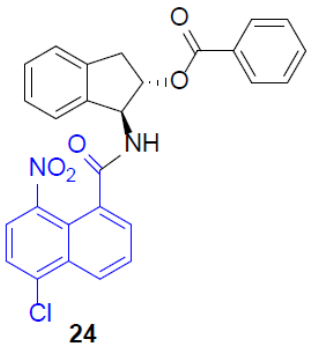
The methyl ester **22** (210 mg, 0.43 mmol) was dissolved in methanol (5 mL) containing water (500 mg). Potassium carbonate (210 mg, 1.52 mmol) was added, and the reaction mixture was heated in a water bath at 35ºC for 4 hours. The reaction mixture was then poured on 2M HCl and a solid precipitated. The solid product was then filtered and recrystallized to give 150 mg of the compound **23** in 73% yield as a pale yellow crystalline solid.

^{1}H NMR (CD_3OD, 400 MHz): 8.54 (dd, 1H, J = 8.4 ,1.2 Hz), 8.07 (d, 1H, J = 8.0 Hz,), 7.94 (dd, 1H, J = 7.2, 1.2 Hz), 7.86 – 7.78 (m, 2H), 4.12 – 4.08 (m, 1H), 3.34 (t, 2H, J = 6.8 Hz), 3.28 – 3.25 (m, 2H), 1.92 – 1.47 (m, 6H), 1.42 (s, 9H).
^{13}C NMR (CD_3OD, 100 MHz): 176.3 (C), 170.9 (C),158.2 (C), 148.3 (C), 138.5 (C), 134.3 (C), 133.2 (C), 131.4 (CH), 128.9 (CH), 128.0 (CH), 127.1 (CH), 125.7 (CH), 123.8 (C), 80.45 (C), 54.9 (CH), 40.8 (CH2), 32.6 (CH2), 29.8 (CH2), 28.6 (3CH3), 24.6 (CH2).
HRMS (ESI) m/z: $[M+Na]^+$ Calculated for $C_{22}H_{26}O_7N_3ClNa$ 502.1352; Found 502.1347.
$[\alpha]_D^{20}$ -34.6 (c 1, $CHCl_3$).

5.8. Reaction with 1-amino-2-indanol (11)



(1*S*,2*S*)-1-(5-chloro-8-nitro-1-naphthamido)-2,3-dihydro-1*H*-inden-2-yl benzoate (24)



24

Compound **18** (500 mg, 1.31 mmol) was dissolved in a mixture of benzoyl chloride (155 µL, 1.31 mmol) and pyridine (4 mL) and the reaction mixture were stirred vigorously for 1 hour at room temperature. Then, water (around 5 drops) was added and stirring was maintained, the reaction mixture was treated with ethyl acetate (40 mL) and 2M HCl (50 mL) and the two phases were separated. The organic layer was dried over anhydrous Na_2SO_4, filtered, and the solvent evaporated under reduced pressure.

The crude residue was purified by silica gel column chromatography, with methylene chloride: diethyl ether (99:1) as eluent, to afford 540 mg (85% yield) of the compound **24** as a white powder.

M.p.>200ºC.

IR (neat, ν in cm^{-1}) 3261, 1722, 1642 ,1517, 1462, 1353 ,1269 ,1114.

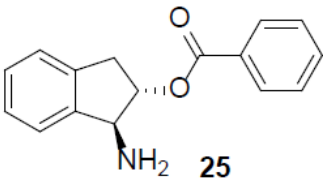
^{1}H NMR (DMSO-*d*$_6$, 400 MHz): 9.50 (d, 1H, *J* = 8.0 Hz), 8.49 (dd, 1H, *J* = 8.0 , 1.2 Hz), 8.17 (d, 1H, *J* = 8.0 Hz), 8.07 (dd, 1H, *J* = 7.2 , 1.2 Hz,), 8.02 (dd, 2H, *J* = 8.4 , 1.2 Hz), 7.95 (d, 1H, *J* = 8.0 Hz), 7.92 (dd, 1H, *J* = 8.0 , 7.2 Hz), 7.68 – 7.63 (m, 1H), 7.53 – 7.48 (m, 3H) 7.34 – 7.30 (m, 3H), 5.72 – 5.64 (m, 2H), 3.57 (dd, 1H, *J* = 16 , 6.8 Hz), 3.05 (dd, 1H, *J* = 16 , 6.8 Hz).

^{13}C NMR (DMSO-*d*$_6$, 100 MHz): 167.2 (C), 165.7 (C), 146.6 (C), 140.0 (C), 139.0 (C), 136.4 (C), 133.3 (CH), 132.6 (C), 131.1 (C), 130.7 (CH), 129.6 (C), 129.3 (2CH), 128.6 (2CH), 128.3 (CH), 128.3 (CH), 127.2 (CH), 126.7 (CH), 126.0 (CH), 124.9 (CH), 124.8 (CH), 124.3 (CH), 122.1 (C), 80.4 (CH), 58.5 (CH), 36.1 (CH_2).

HRMS (ESI) m/z: $[M+H]^+$ Calculated for $C_{27}H_{20}O_5N_2Cl$ 487.1055; Found 487.1055.

$[\alpha]_D^{20}$ +11.6 (c 1, $CHCl_3$).

(1*S*,2*S*)-1-amino-2,3-dihydro-1*H*-inden-2-yl benzoate (25)



25

Compound **24** (90 mg, 0.19 mmol) was dissolved in acetic acid (3.0 mL) and a preheated (60ºC) suspension of Zn (1.0 g) in acetic acid (4.0 mL) was added under vigorous stirring. The reaction mixture was stirred for 20 minutes, and the Zn removed by filtration or careful decantation. Following the above-described procedure for deprotection **B**, 40 mg of the compound **25** was obtained in 83% yield.

^{1}H NMR ($CDCl_3$, 400 MHz): 7.88 (dd, 2H *J* = 8.4 , 1.2 Hz), 7.38 (t, 1H, *J* = 7.6 Hz), 7.29 – 7.19 (m, 3H), 7.13 – 7.03 (m, 3H), 5.17 – 5.11 (m, 1H), 4.35 (d, 1H, *J* = 5.2 Hz), 3.38 (dd, 1H, *J* = 16.4 , 7.6 Hz), 2.83 (dd, 1H, *J* = 16.4, 6.4 Hz).
^{13}C NMR ($CDCl_3$, 100 MHz): 166.8 (C), 143.1 (C), 138.9 (C), 133.0 (CH), 130.0 (C), 129.6 (2CH), 128.3 (2CH), 128.1 (CH), 127.3 (CH), 124.8 (CH), 124.0 (CH), 84.7 (CH), 62.4 (CH), 36.4 (CH2).
HRMS (ESI) m/z: $[M+H]^+$ Calculated for $C_{16}H_{16}O_2N$ 254.1176; Found 254.1174.
$[\alpha]_D^{20}$ +20.5 (c 1, $CHCl_3$).

5.9. NMR spectra

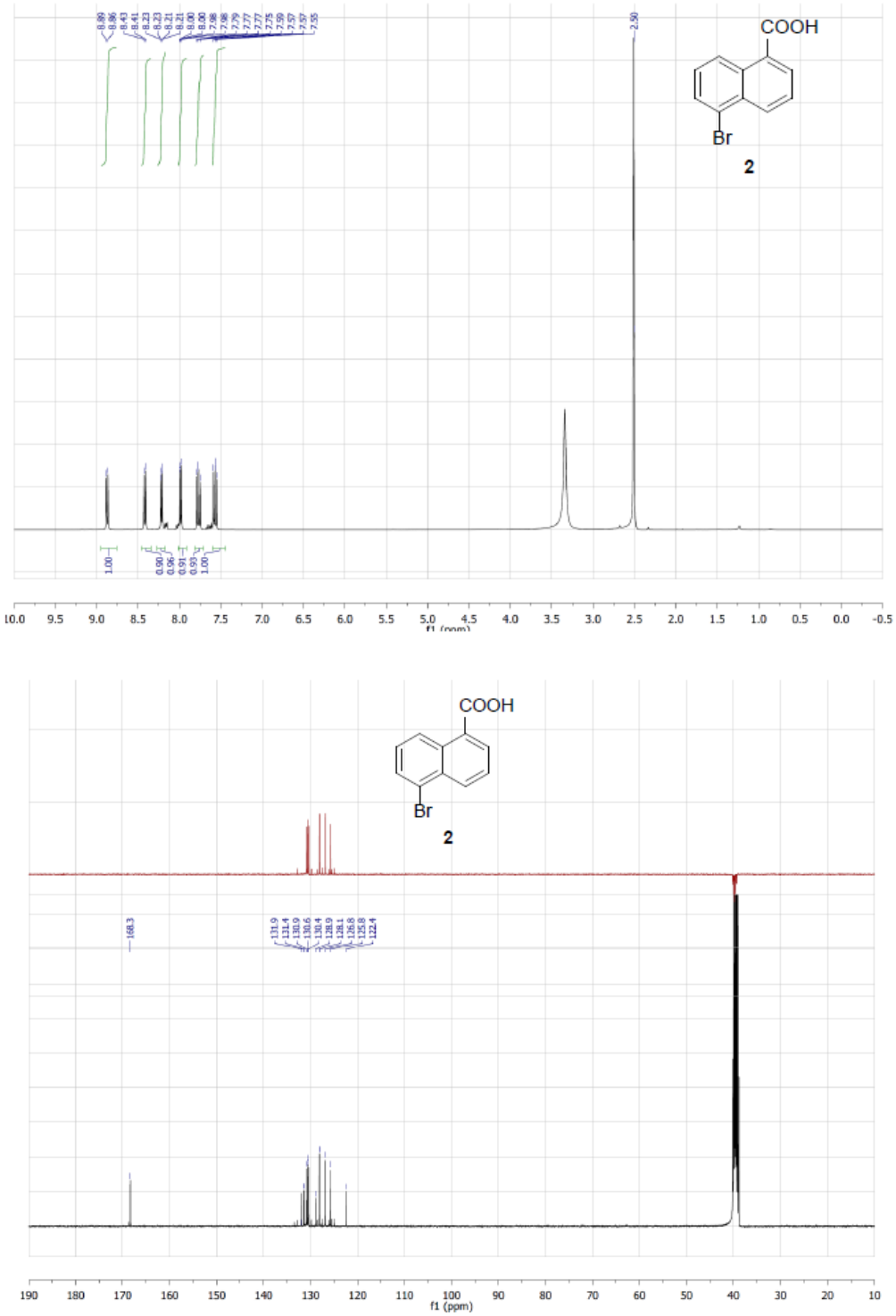


Figure S1. *^{1}H NMR (DMSO-d_6, 400 MHz) and ^{13}C (DMSO-d_6, 100 MHz) spectra of (**2**).*

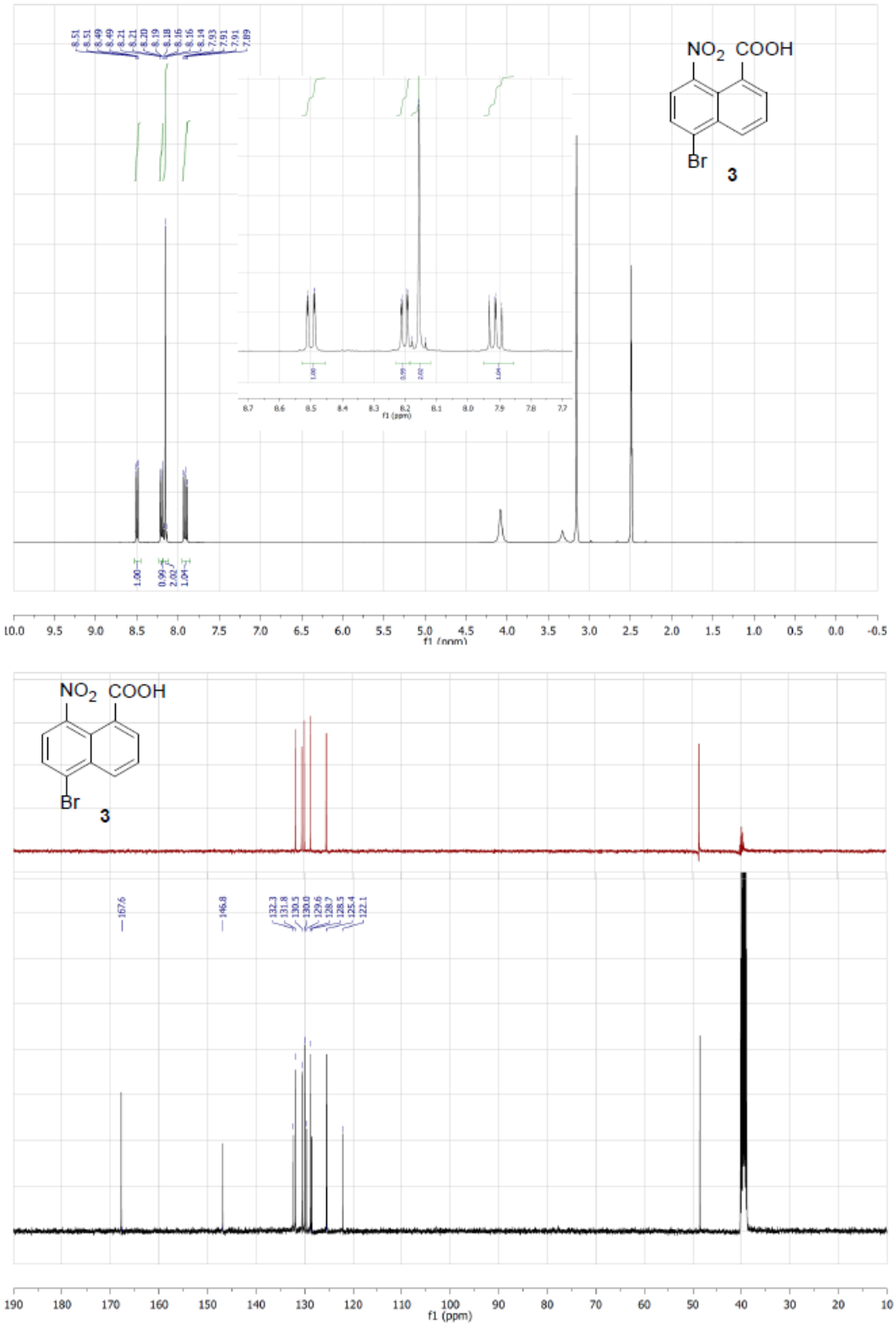


Figure S2. *^{1}H NMR (DMSO-d_6, 400 MHz) and ^{13}C (DMSO-d_6, 100 MHz) spectra of (**3**). Signals corresponding to traces of MeOH are visible.*

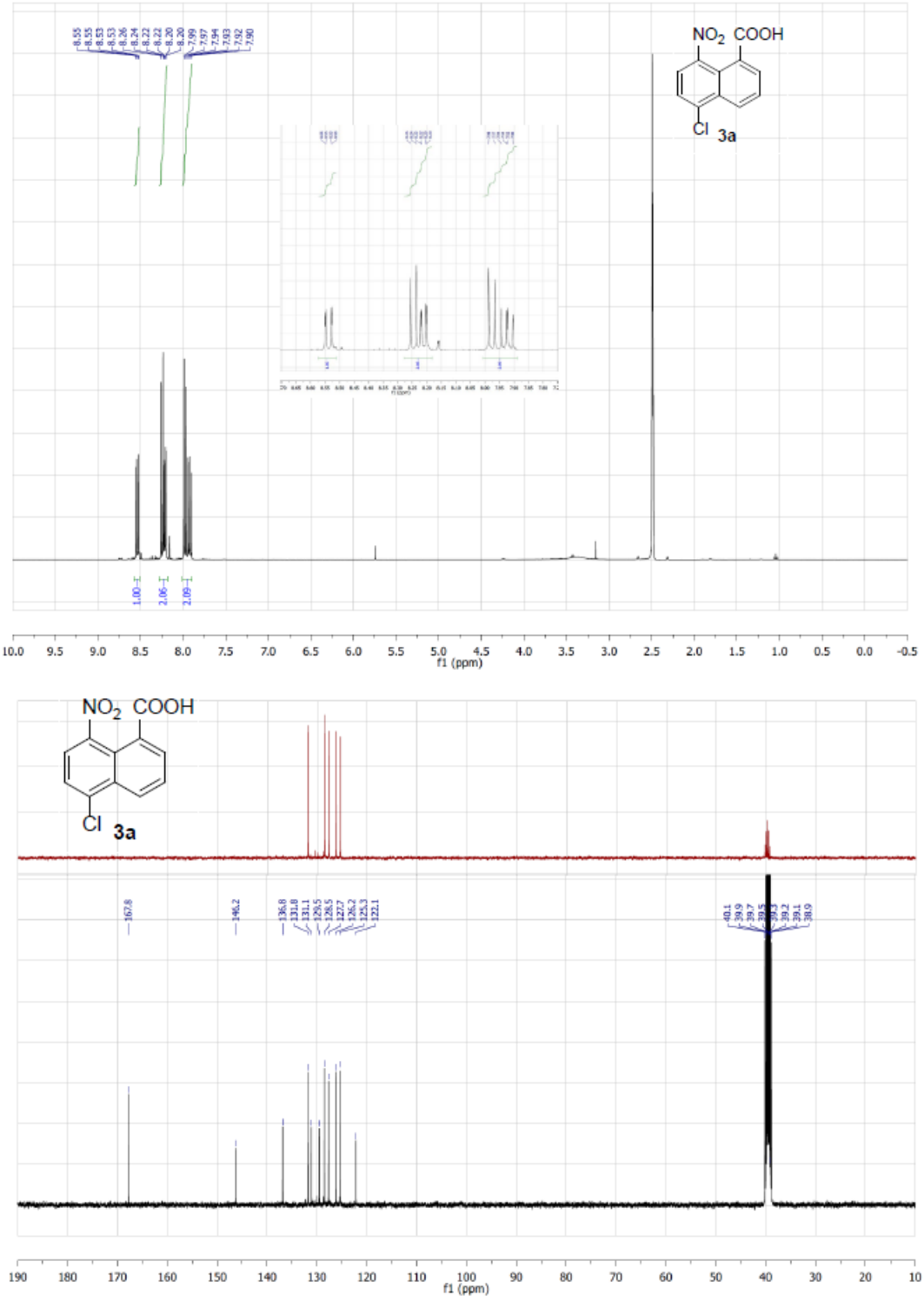


Figure S3. *^{1}H NMR (DMSO-d_6, 400 MHz) and ^{13}C (DMSO-d_6, 100 MHz) spectra of (**3a**).*

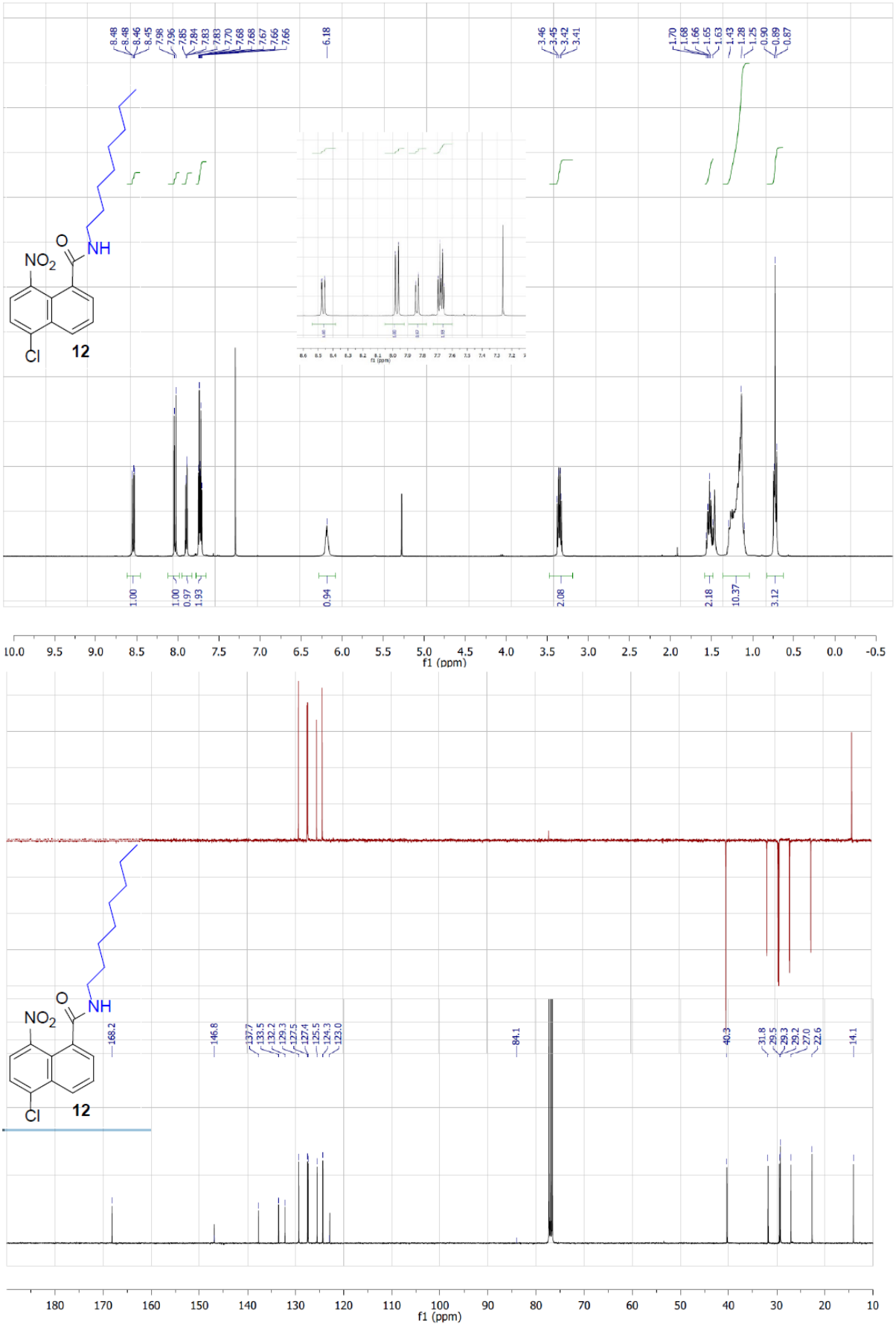


Figure S4. *^{1}H NMR ($CDCl_3$, 400 MHz) and ^{13}C ($CDCl_3$, 100 MHz) spectra of (**12**).*

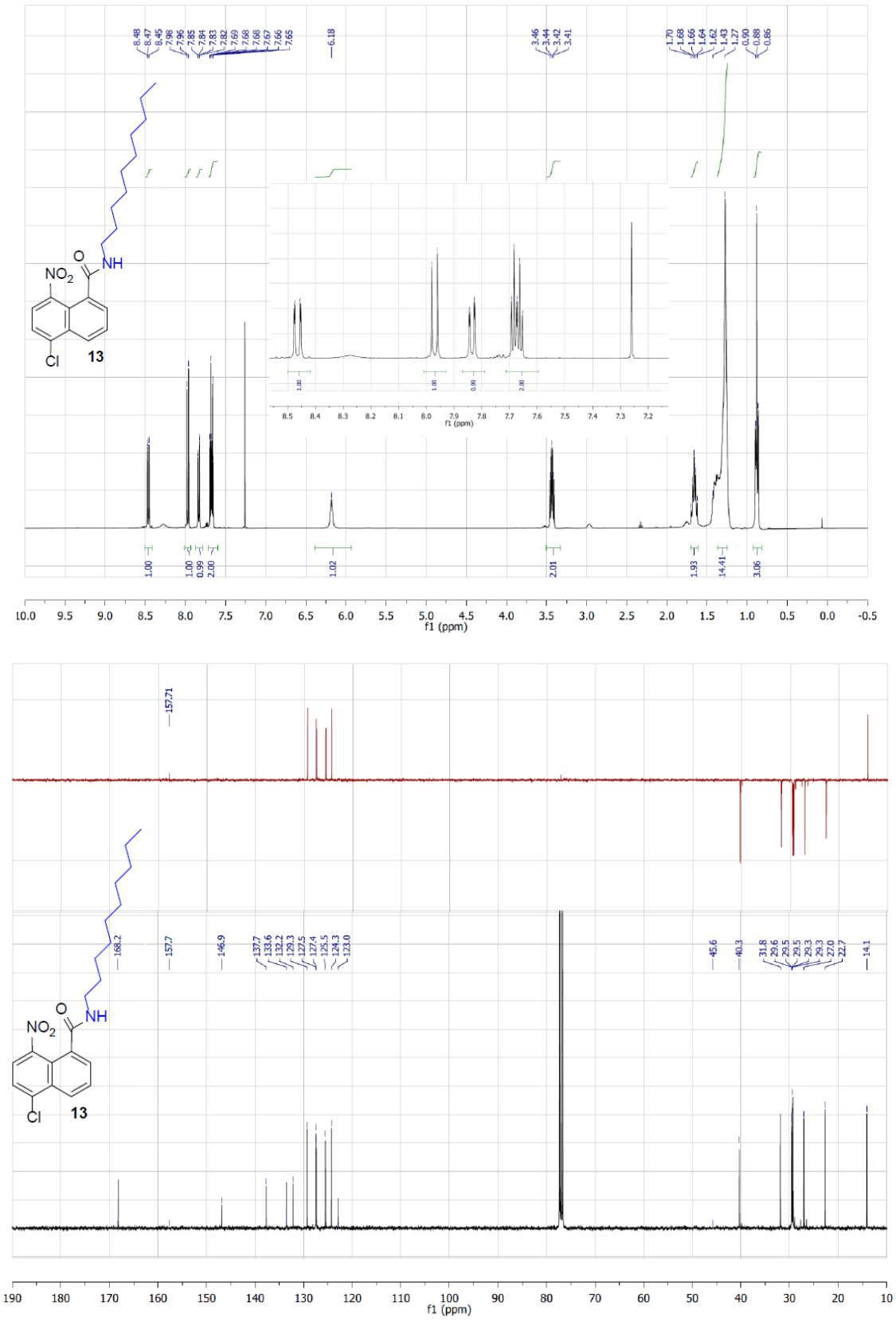


Figure S5. *^{1}H NMR ($CDCl_3$, 400 MHz) and ^{13}C ($CDCl_3$, 100 MHz) spectra of (**13**).*

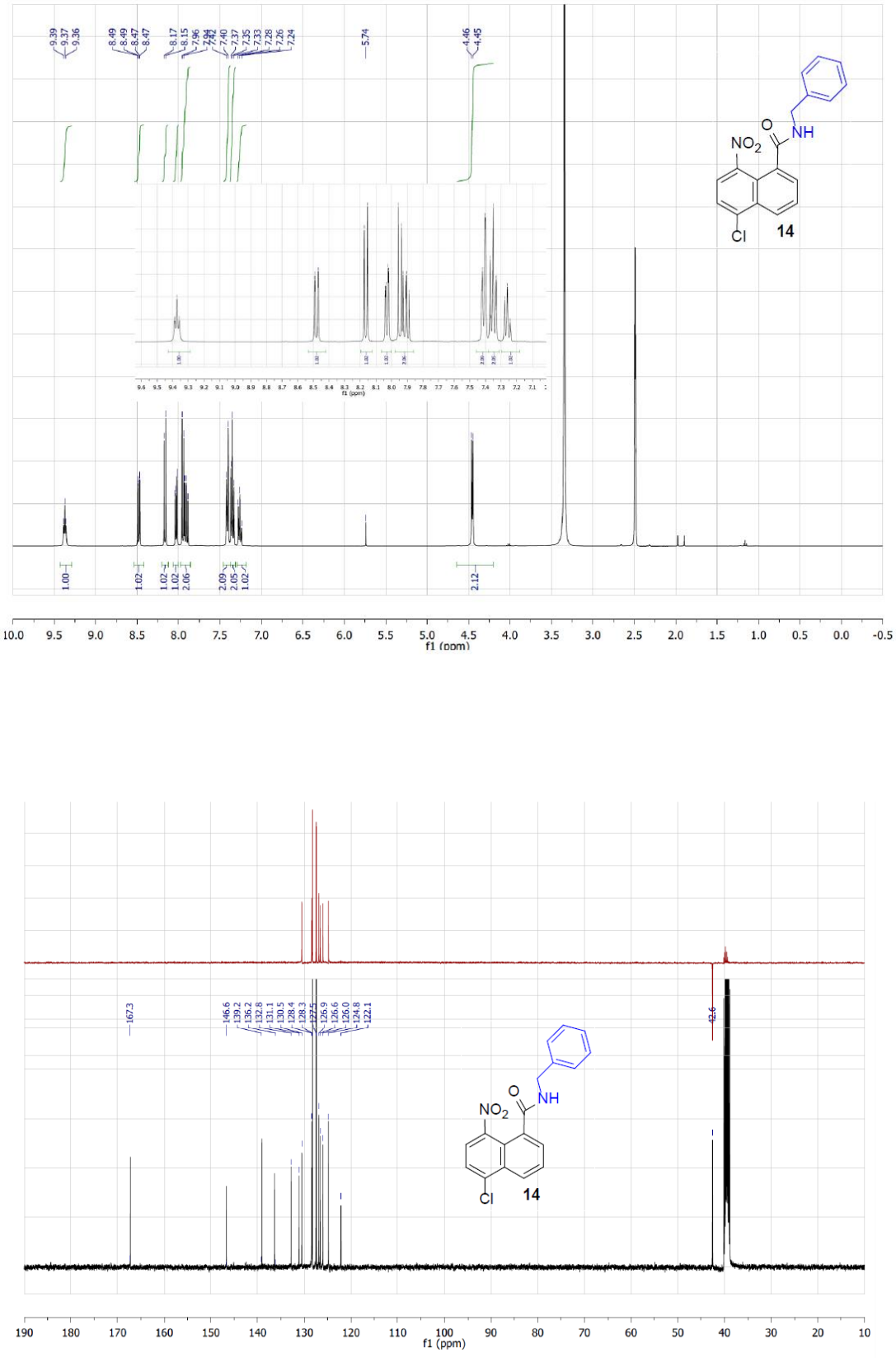


Figure S6. *^{1}H NMR (DMSO-d_6, 400 MHz) and ^{13}C (DMSO-d_6, 100 MHz) spectra of (**14**).*

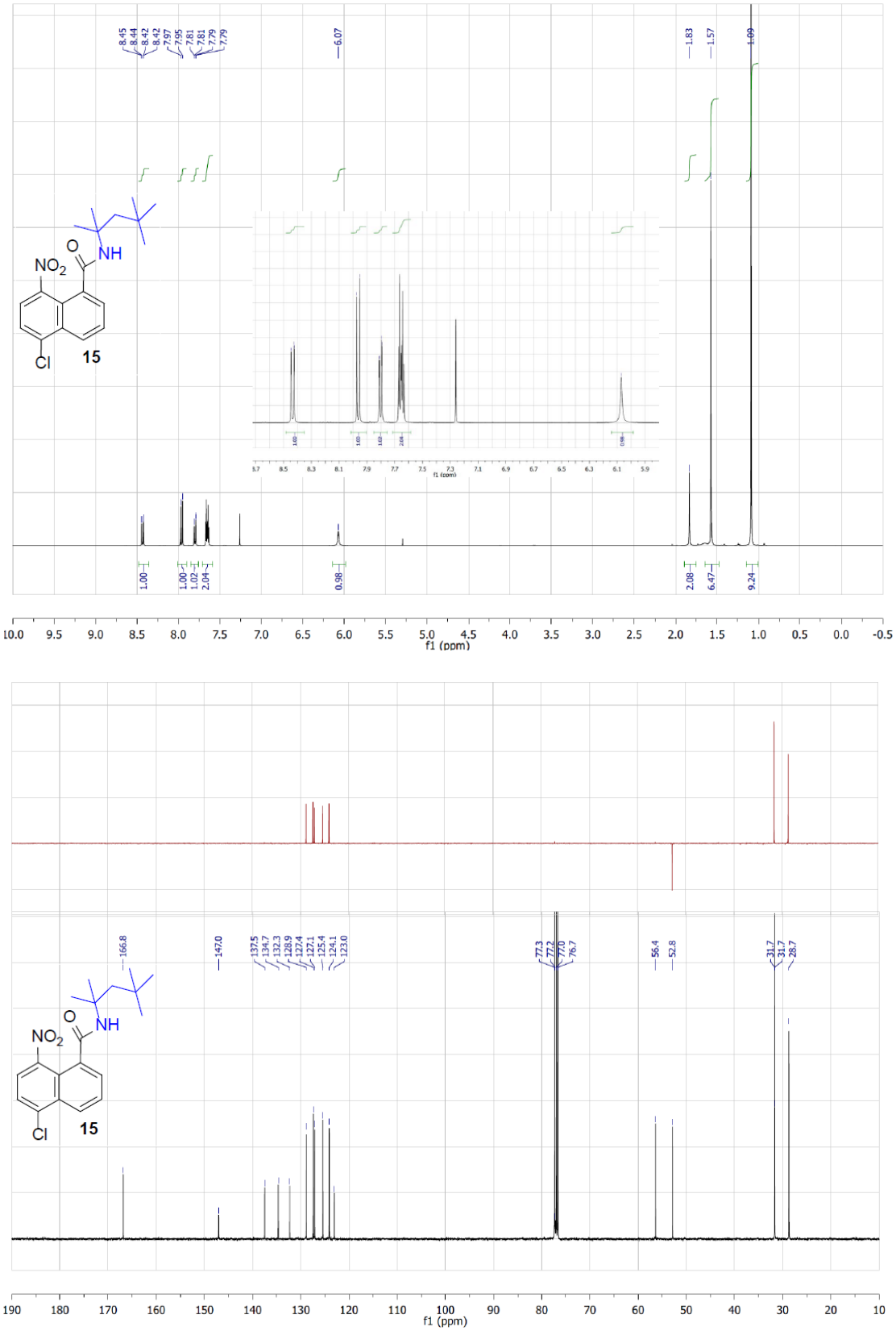


Figure S7. *^{1}H NMR ($CDCl_3$, 400 MHz) and ^{13}C ($CDCl_3$, 100 MHz) spectra of (**15**).*

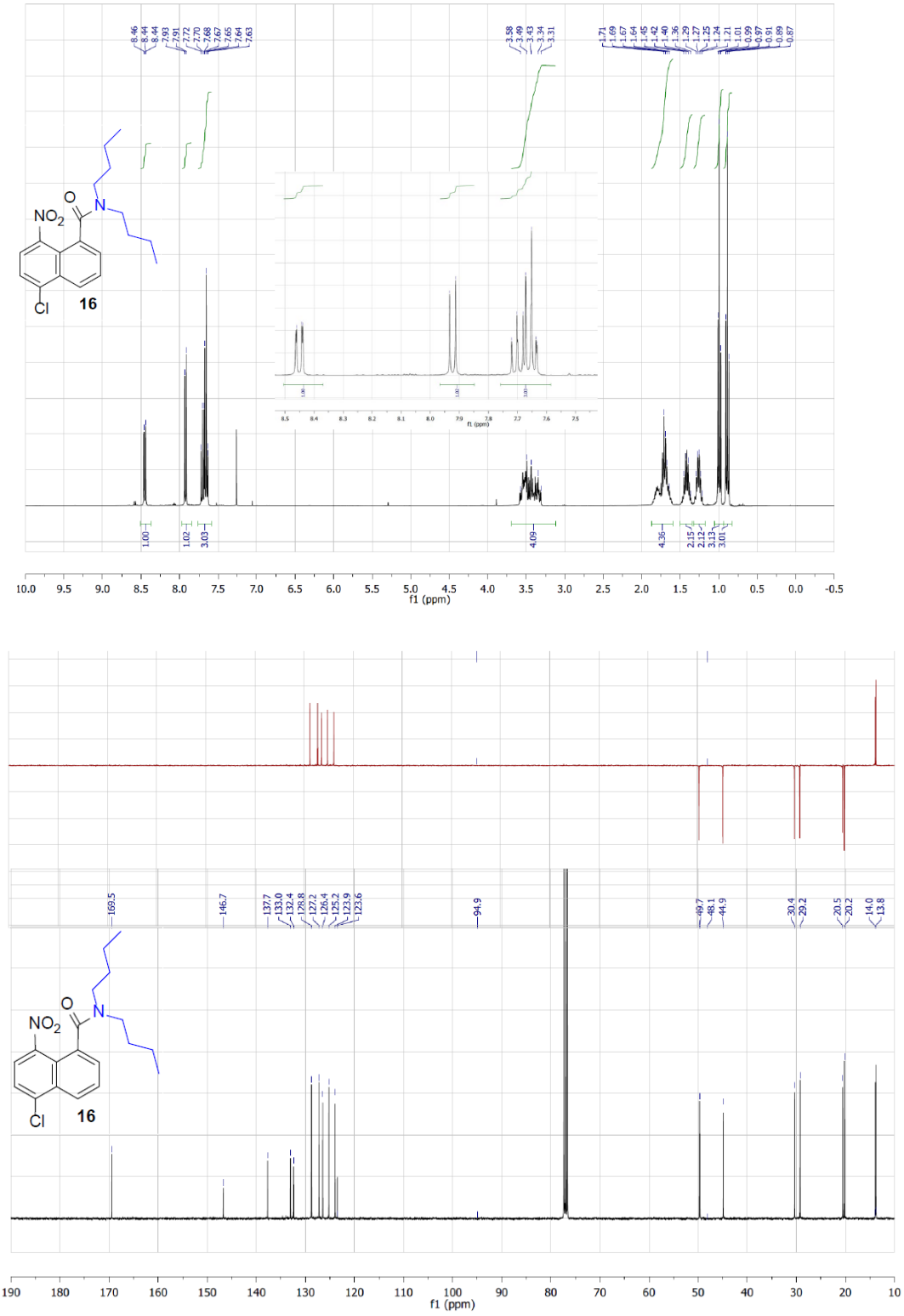
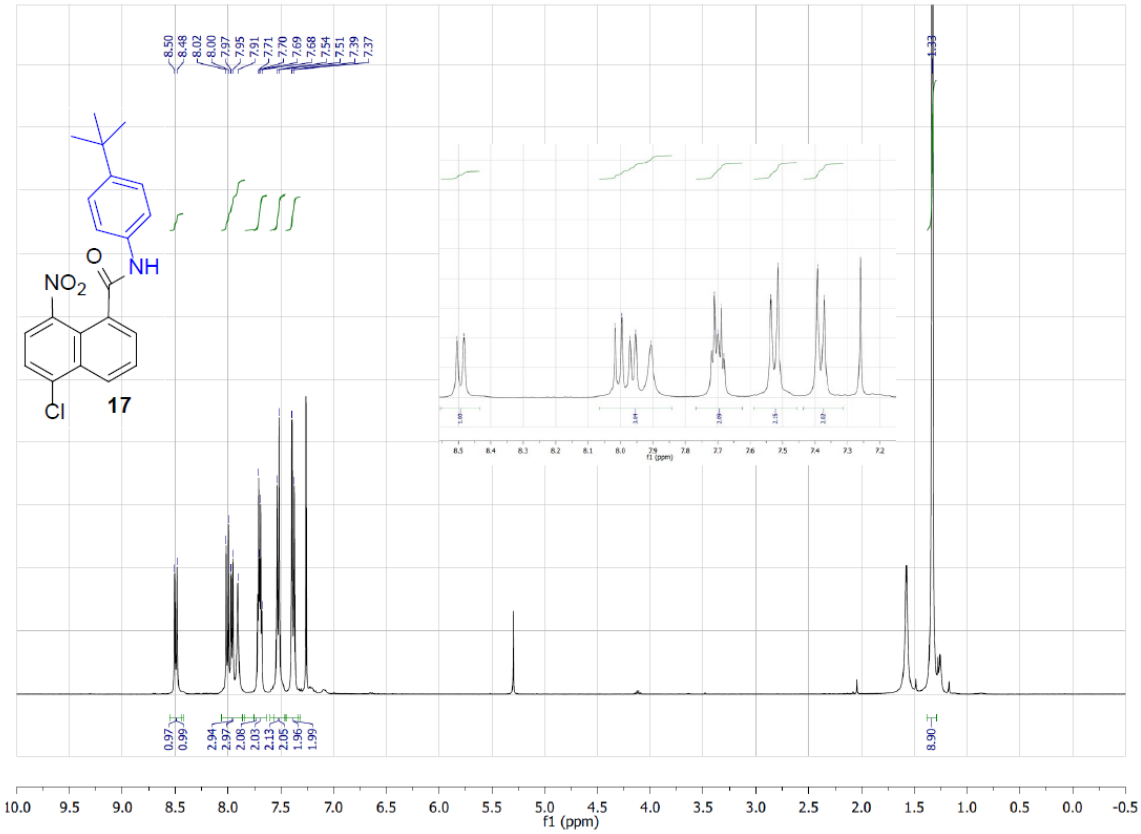


Figure S8. *^{1}H NMR ($CDCl_3$, 400 MHz) and ^{13}C ($CDCl_3$, 100 MHz) spectra of (**16**).*



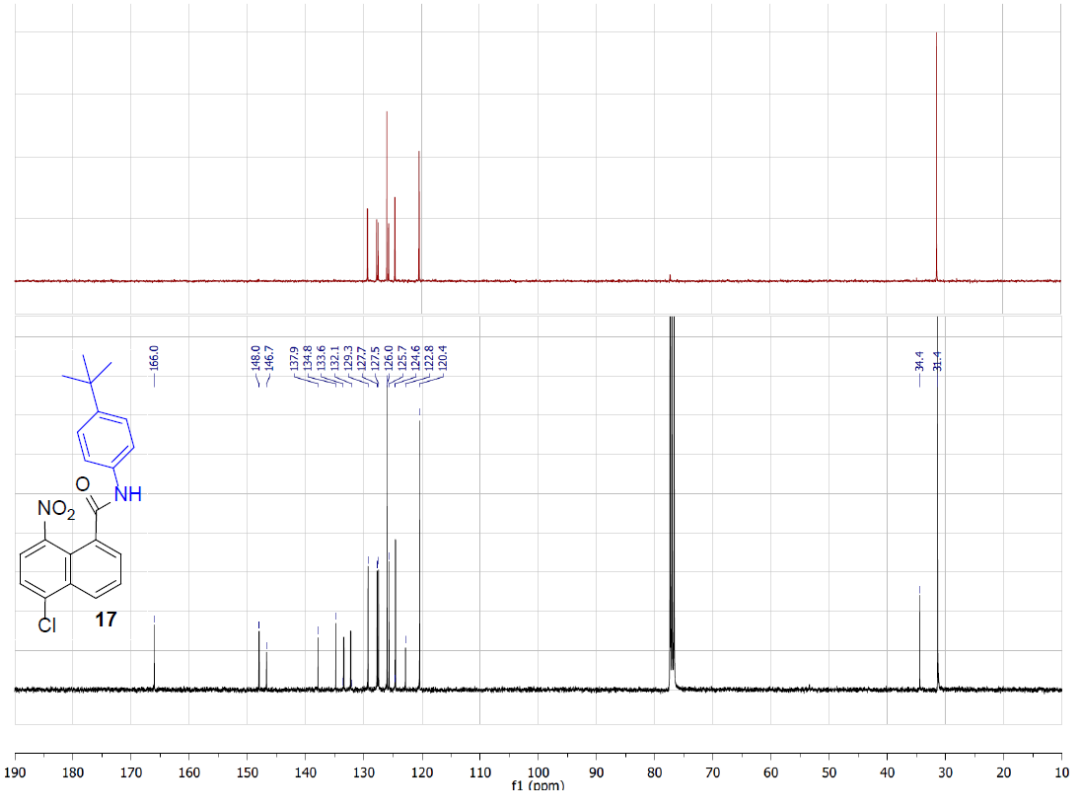


Figure S9. *^{1}H NMR ($CDCl_3$, 400 MHz) and ^{13}C ($CDCl_3$, 100 MHz) spectra of (**17**).*

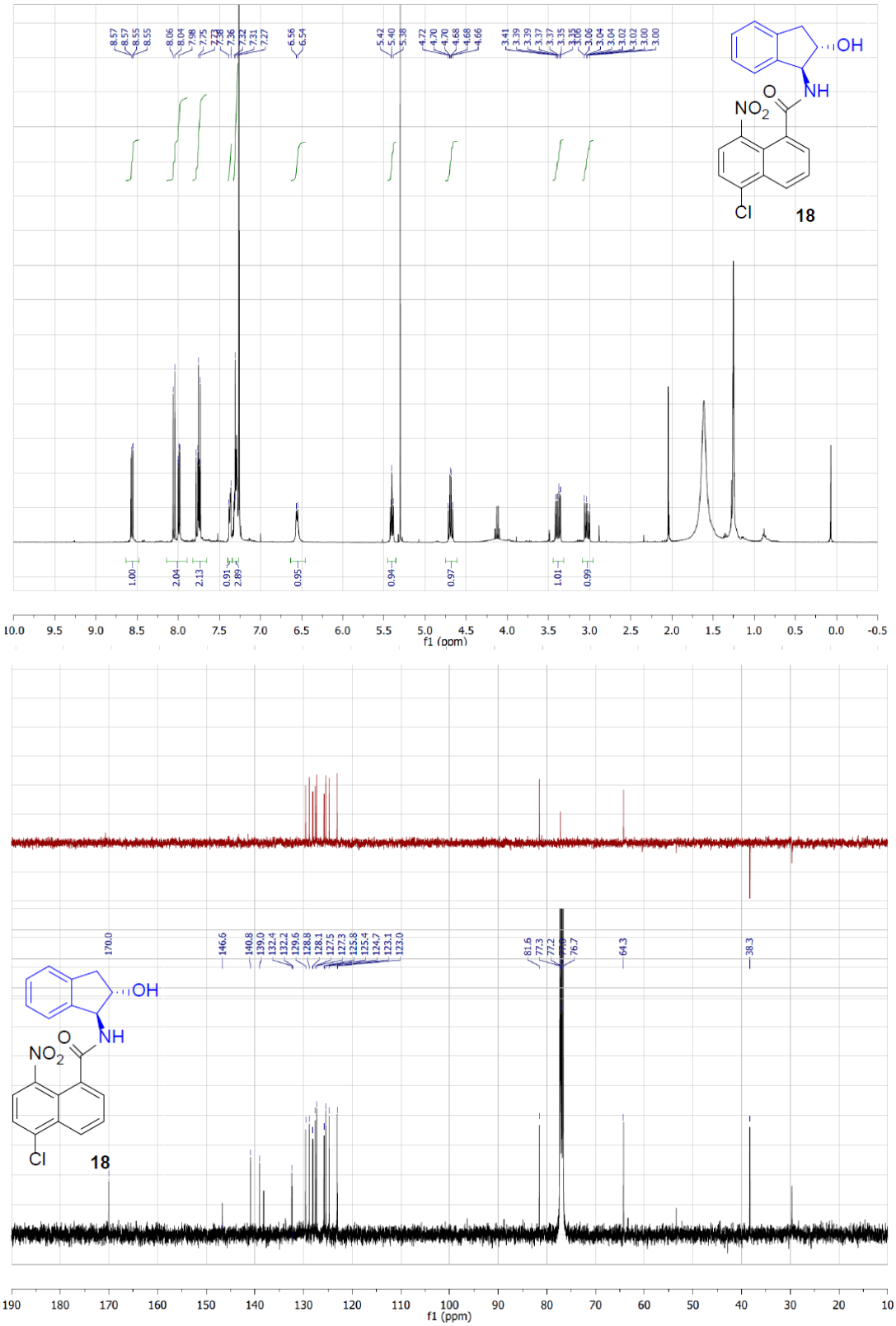


Figure S10. *^{1}H NMR ($CDCl_3$, 400 MHz) and ^{13}C ($CDCl_3$, 100 MHz) spectra of (**18**). Signals corresponding to traces of ethyl acetate are visible.*

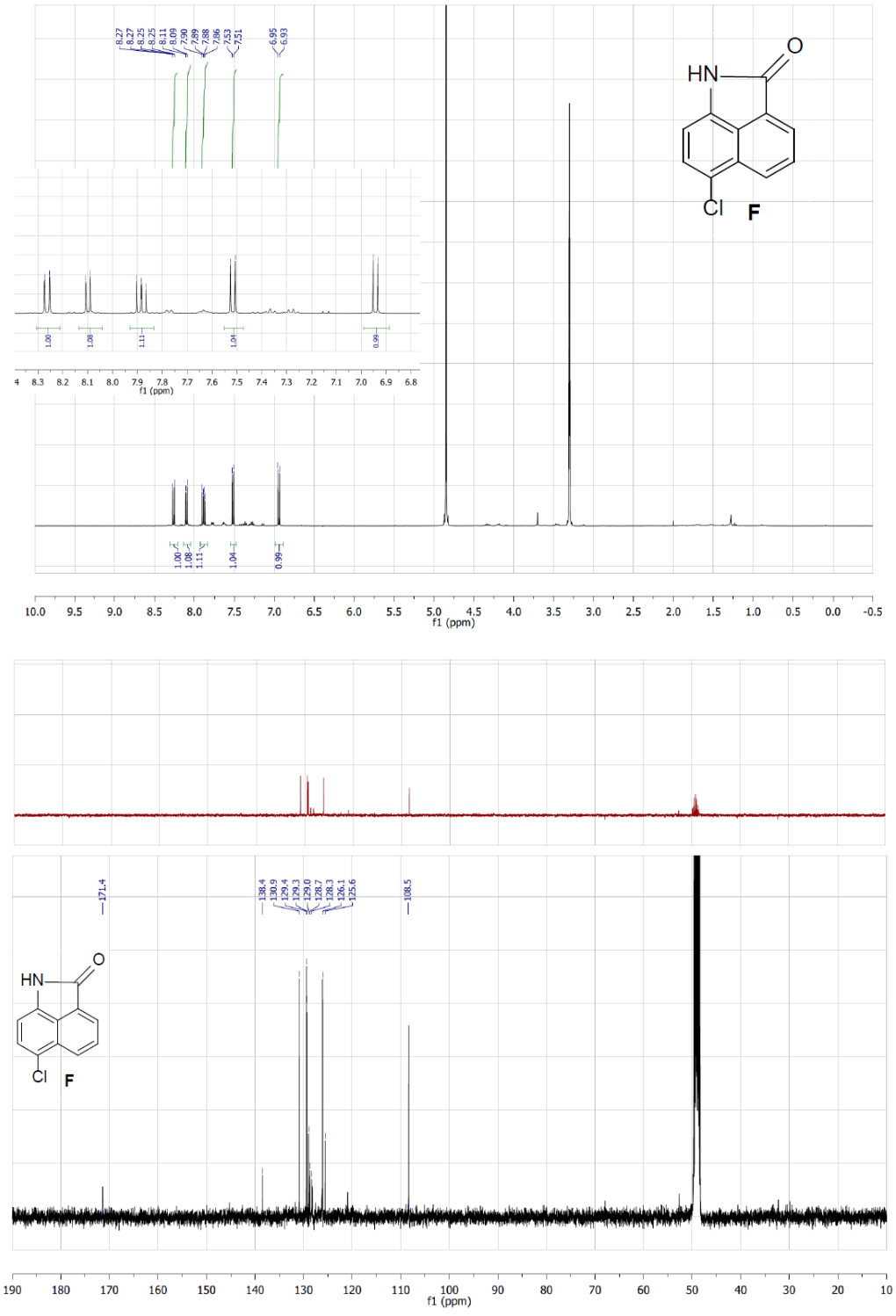


Figure S11. *^{1}H NMR (CD_3OD, 400 MHz) and ^{13}C (CD_3OD, 100 MHz) spectra of (**F**).*

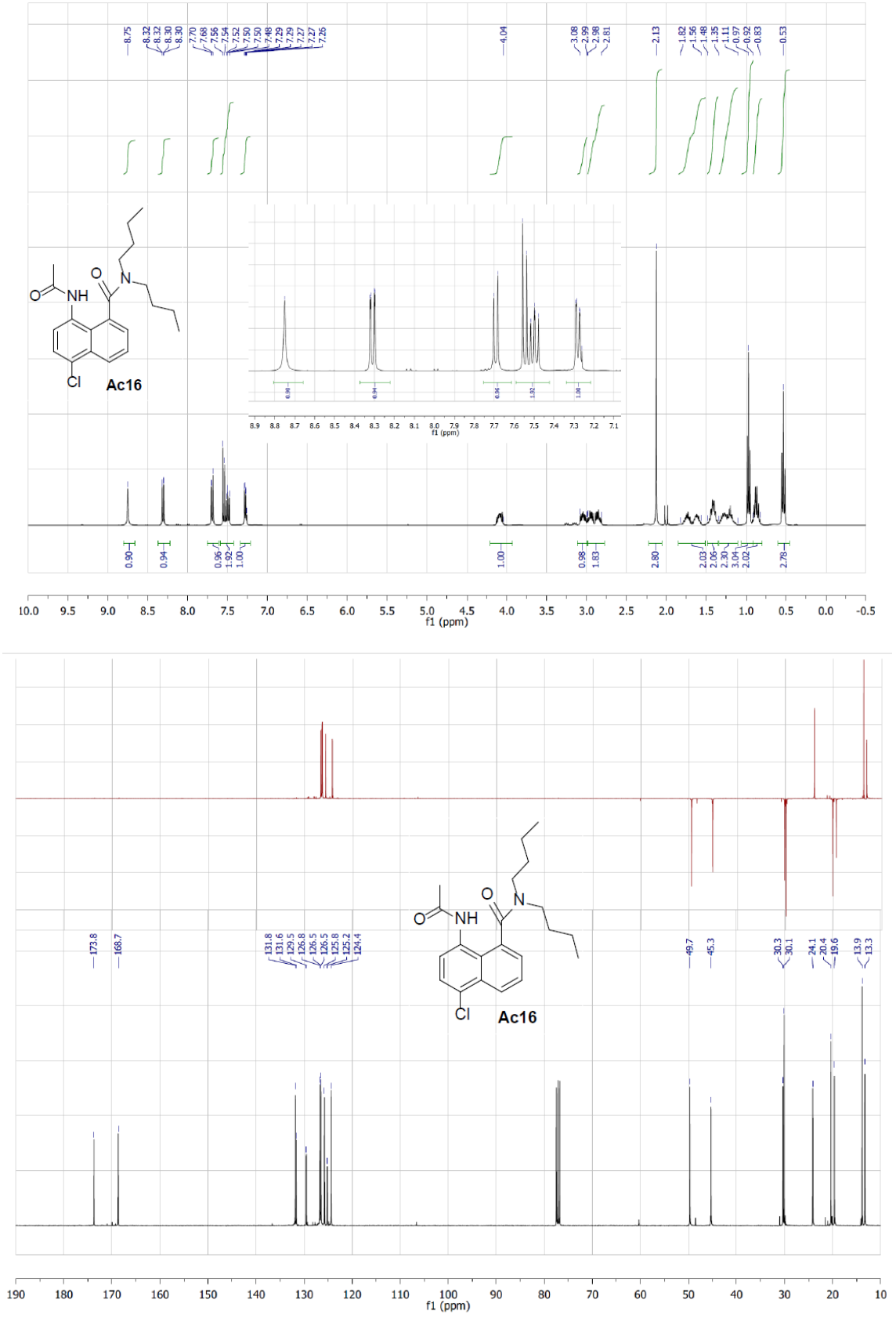


Figure S12. *^{1}H NMR ($CDCl_3$, 400 MHz) and ^{13}C ($CDCl_3$, 100 MHz) spectra of (**Ac16**).*

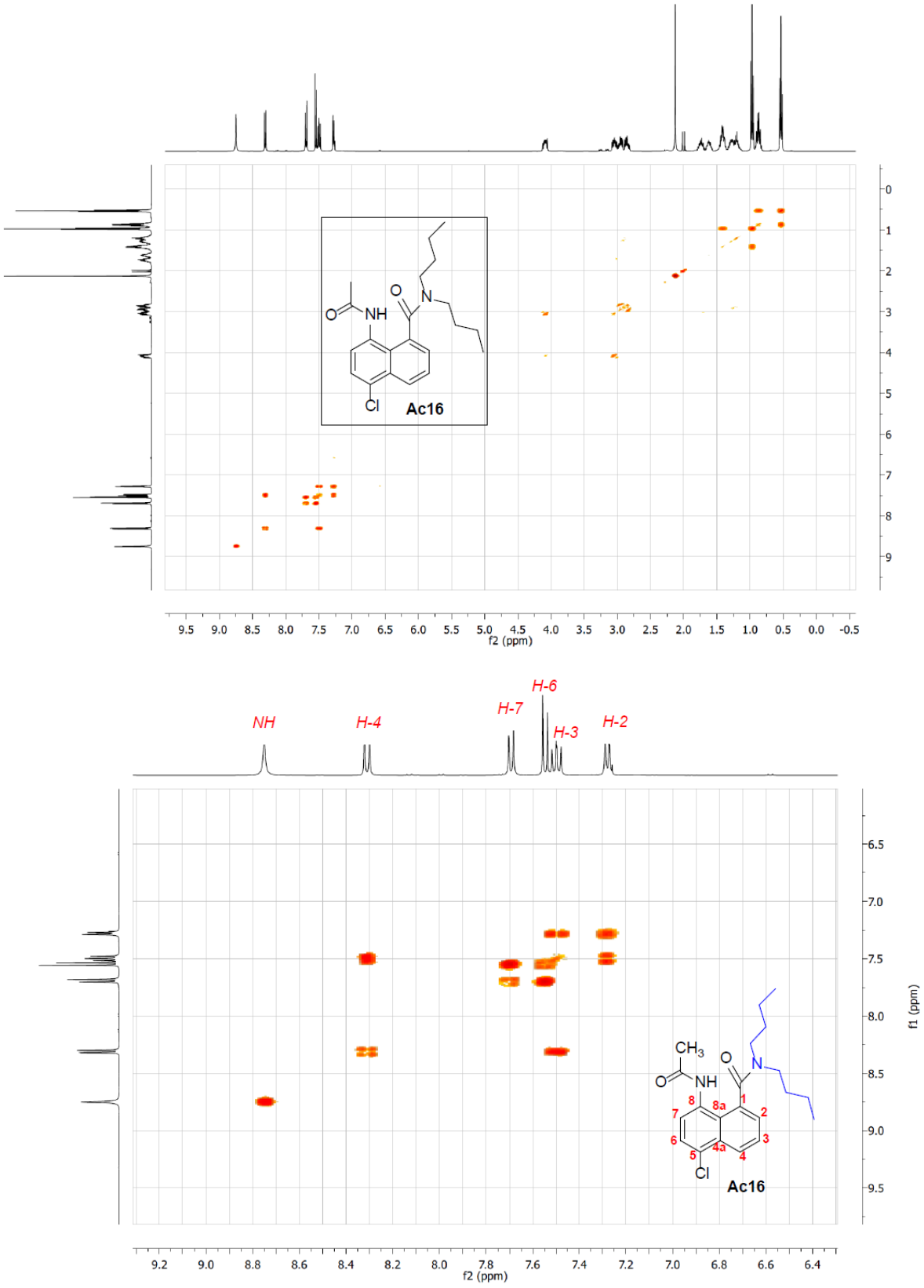


Figure S13. *COSY ($CDCl_3$, 400 MHz) spectrum (and expansion of the aromatic region) of (**Ac16**).*

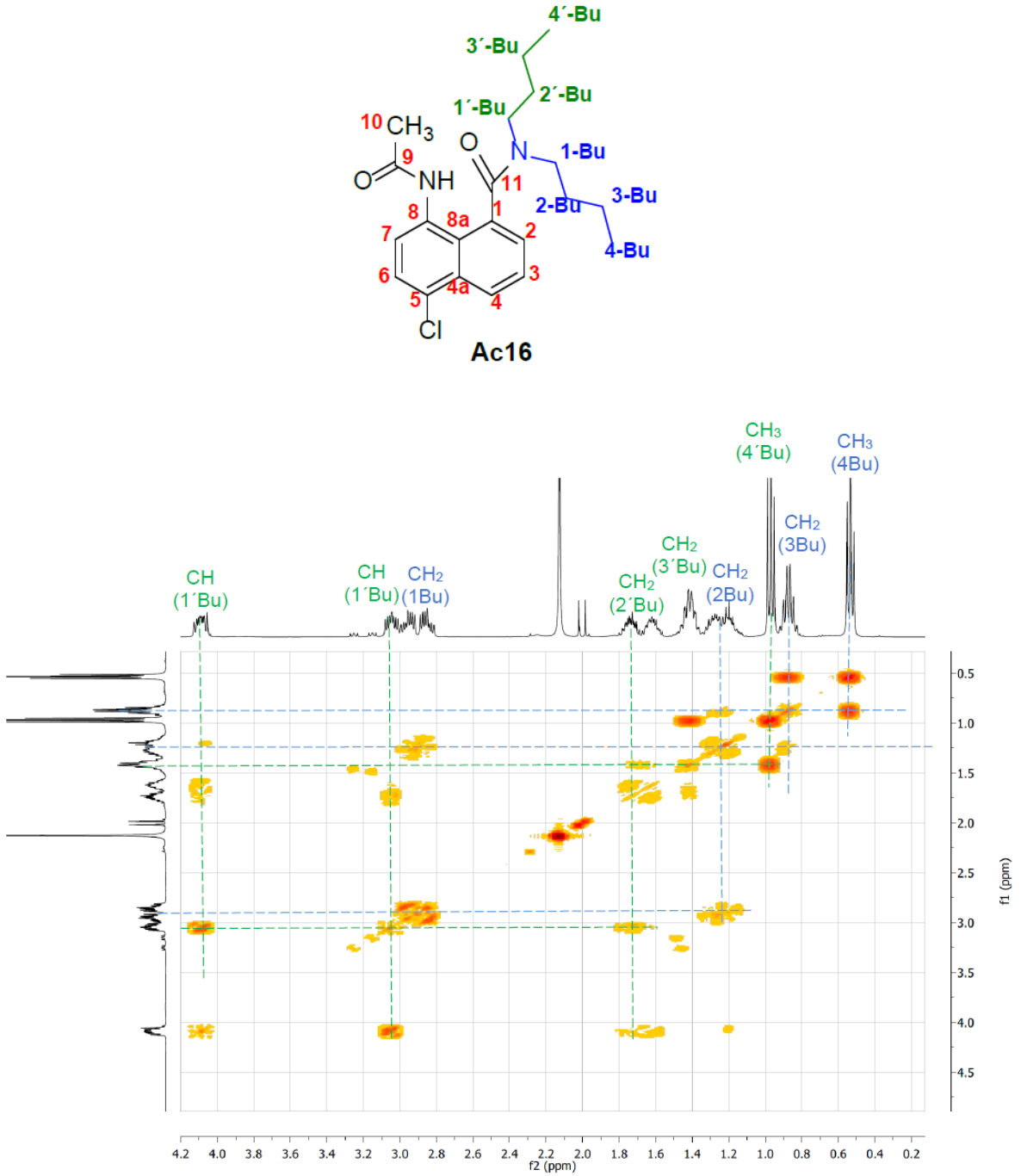


Figure S14. *COSY ($CDCl_3$, 400 MHz) spectrum (and expansion 0 - 4.2 ppm) of (**Ac16**).*

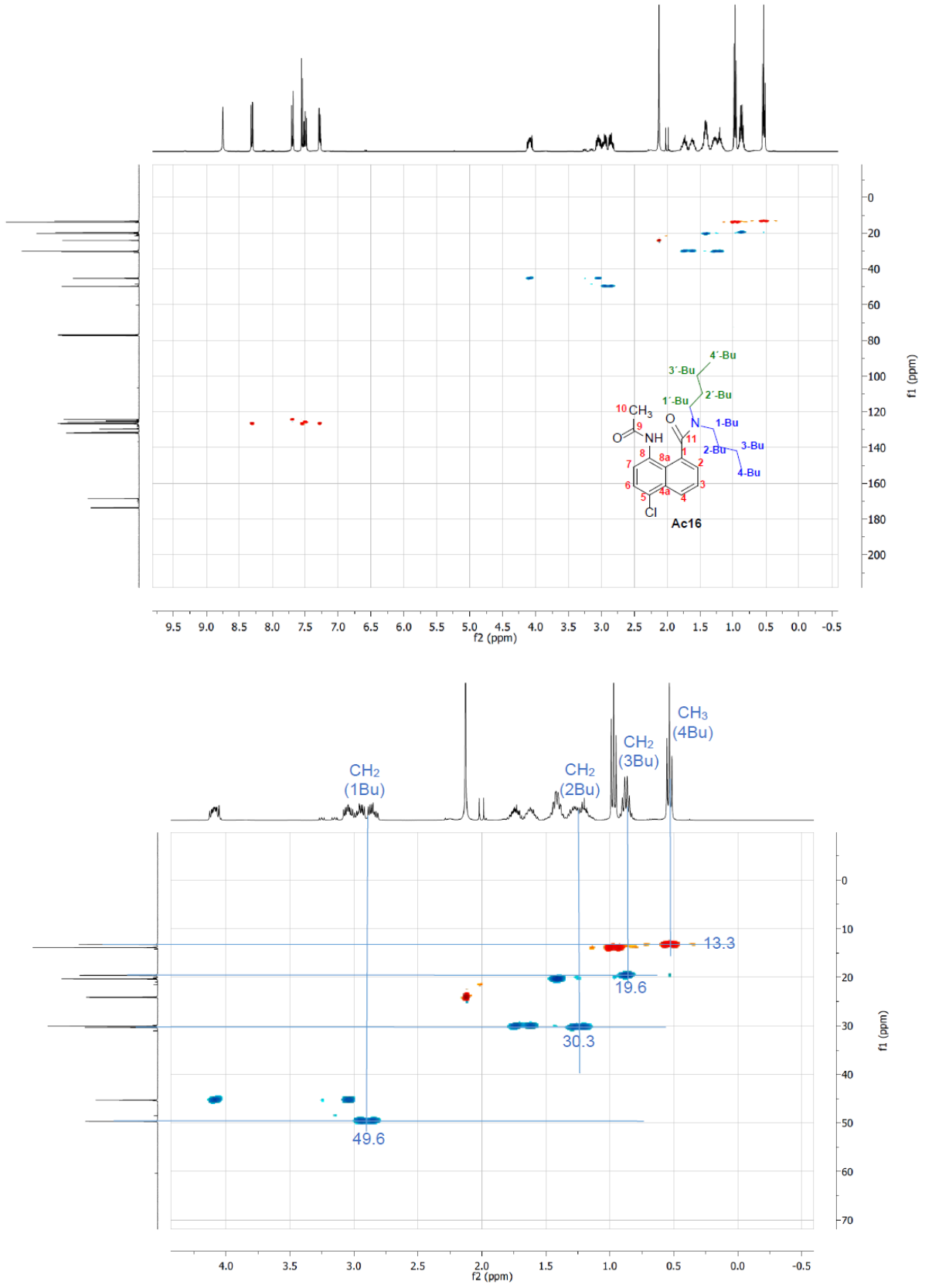


Figure S15. *HSQC 145 Hz (and expansion) of (**Ac16**) in $CDCl_3$.*

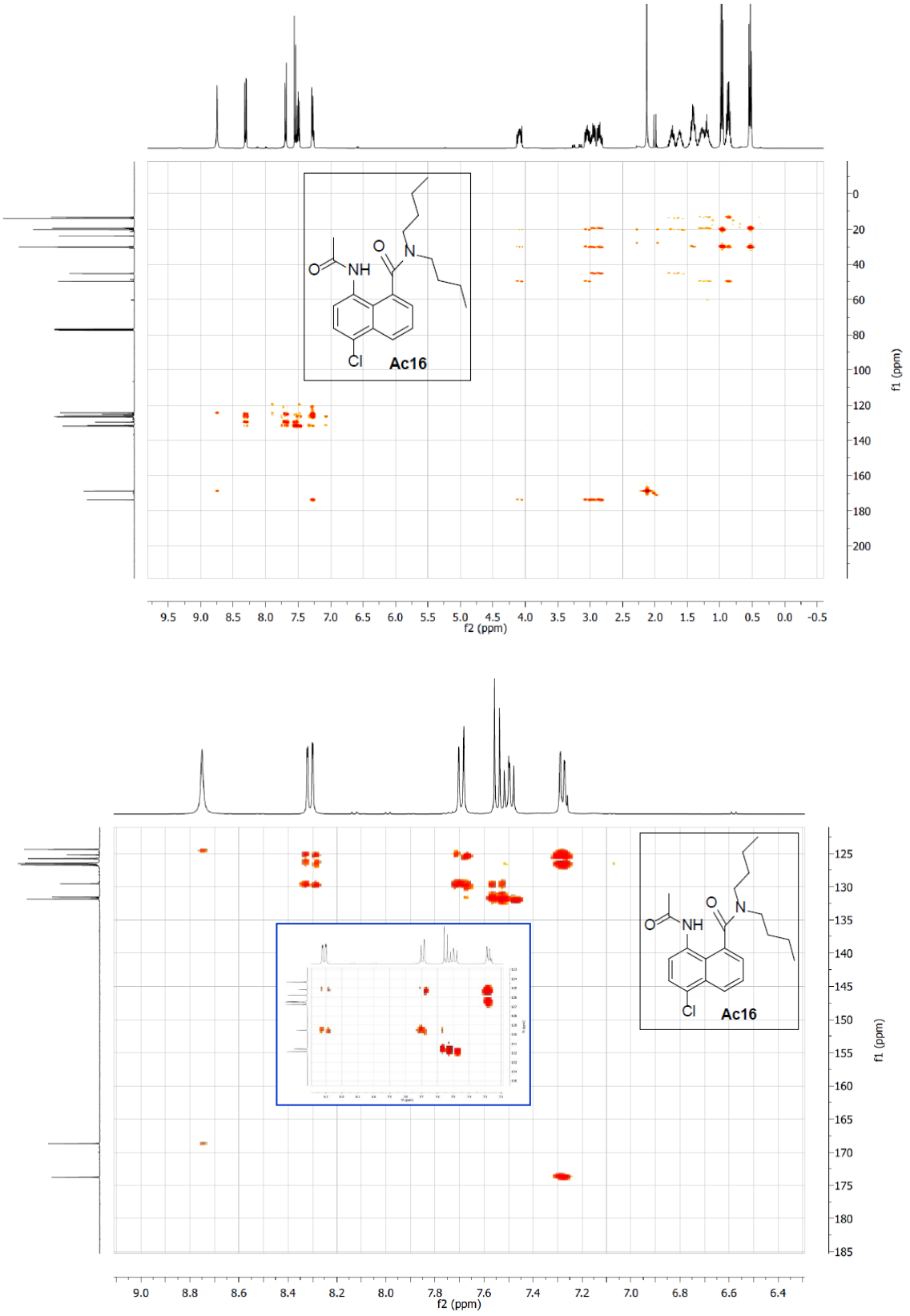
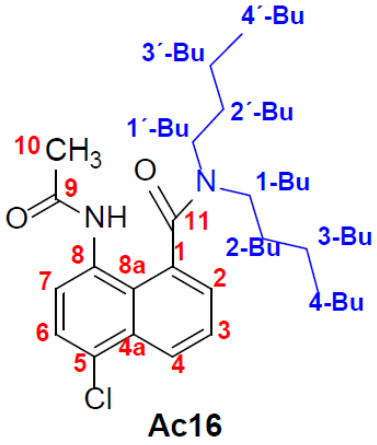


Figure S16. *HMBC CIGAR (and expansion) of (**Ac16**) in $CDCl_3$.*

Table S1. *^{1}H NMR ($CDCl_3$, 400 MHz) and ^{13}C ($CDCl_3$, 100 MHz) chemical shift assignments for* ***Ac16***



Ac16

	^{1}H NMR (δ)		**^{13}C NMR (δ)**
NH	8.75 (s, 1H)	C-9	168.7 (C)
H-4	8.31 (dd, 1H, *J* = 8.4, 1.2 Hz)	C-4	126.5 (CH)
H-7	7.69 (d, 1H, *J* = 8.0 Hz)	C-7	124.4 (CH)
H-6	7.55 (d, *J* = 8.0 Hz, 1H)	C-6	126.8 (CH)
H-3	7.50 (dd, 1H, *J* = 8.4, 7.2 Hz),	C-3	125.8 (CH)
H-2	7.28 (dd, 1H, *J* = 7.2, 1.2 Hz,)	C-2	126.5 (CH)
H-1´-Bu$_{(\alpha)}$	4.13 – 4.01 (m, 1H)	C-1´-Bu	45.3 (CH_2)
H-1´-Bu$_{(\beta)}$	3.08 – 2.99 (m, 1H)		
H-1- Bu	2.98 – 2.81 (m, 2H)	C-1-Bu	49.6 (CH_2)
H-CH_3	2.13 (s, 3H)	C-10	24.1(CH_3)
H-2´-Bu	1.82 – 1.56 (m, 2H)	C-2´-Bu	30.1(CH_2)
H-3´-Bu	1.48– 1.35 (m, 2H)	C-3´-Bu	20.4 (CH_2)
H-2-Bu	1.35 – 1.11 (m, 2H)	C-2-Bu	30.3 (CH_2)
H- 4´- Bu	0.97 (t, 3H, *J* = 7.2 Hz)	C-4´- Bu	13.9 (CH_3)
H-3-Bu	0.92 – 0.83 (m, 2H)	C-3-Bu	19.6 (CH_2)
H-4-Bu	0.53 (t, 3H *J* = 7.2 Hz).	C-4-Bu	13.3 (CH_3)
		C-11	173.8 (C)
		C-1	131.8 (C)
		C-4a	131.8 (C)
		C-5	129.5 (C)
		C-8	131.6 (C)
		C-8a	125.2 (C)

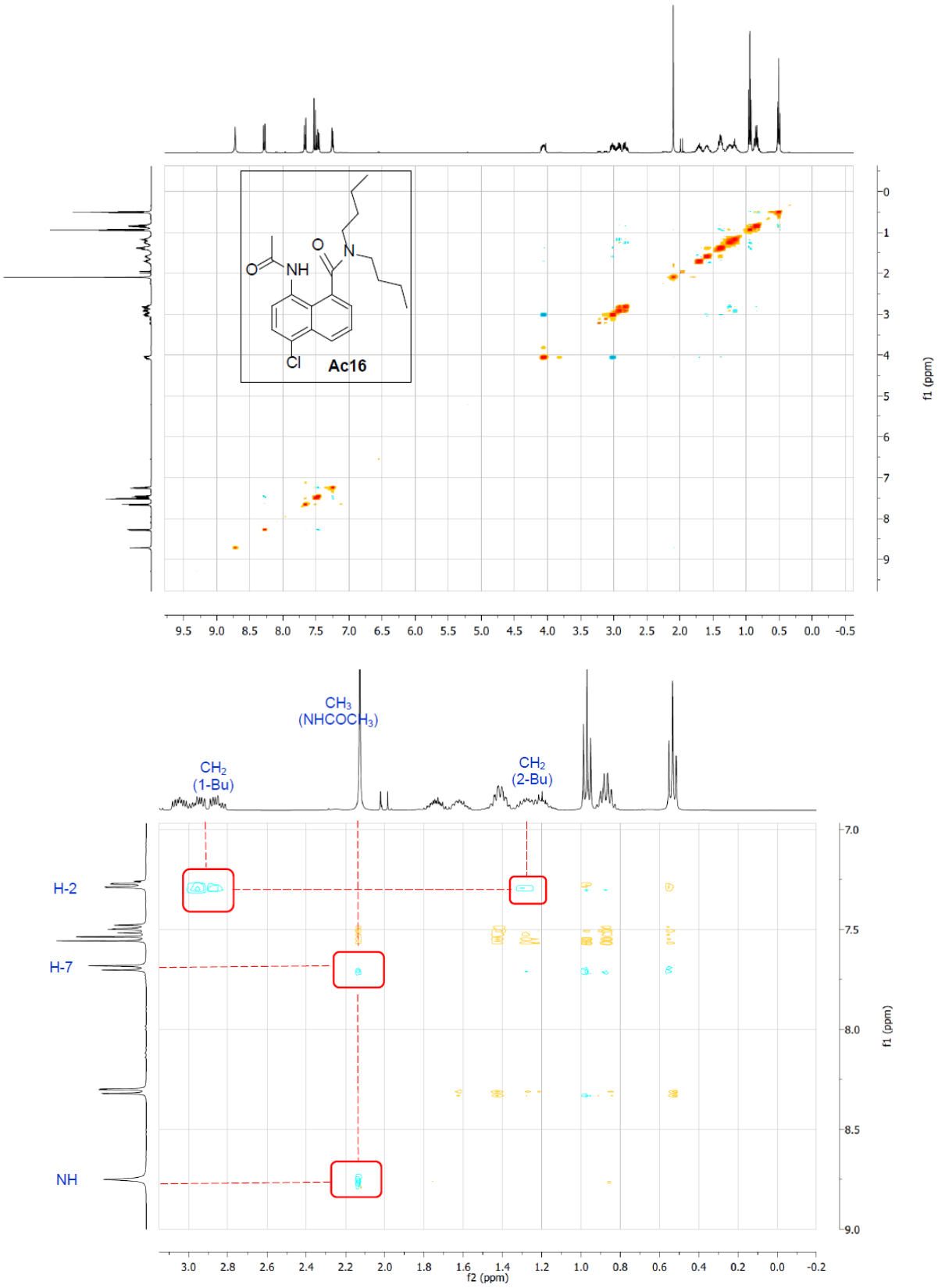


Figure S17. *ROESY (of (**Ac16**) in $CDCl_3$ showing the main correlations.*

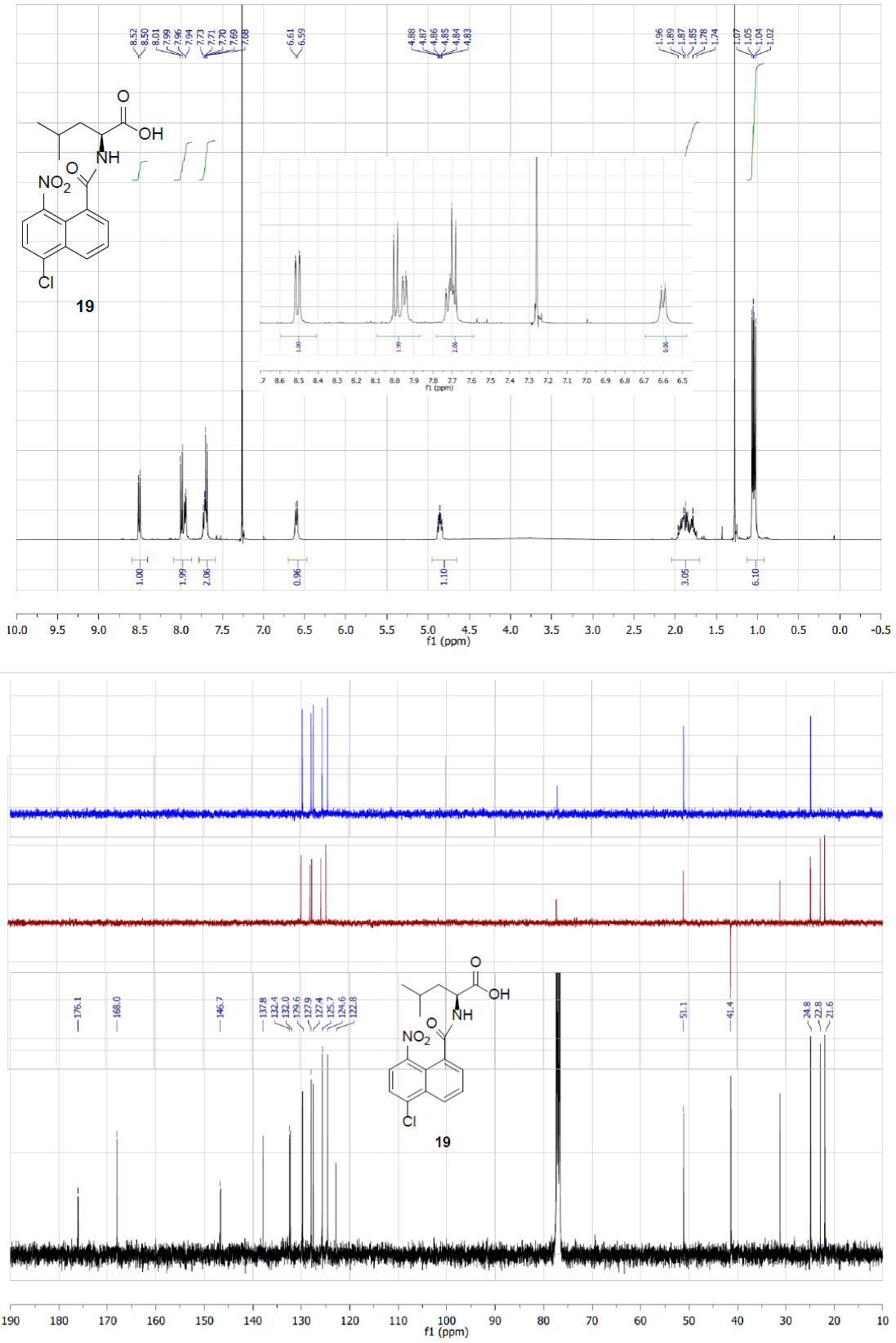


Figure S18. *^{1}H NMR ($CDCl_3$, 400 MHz) and ^{13}C ($CDCl_3$, 100 MHz) spectra of (**19**). Signals corresponding to traces of tBuOH are visible.*

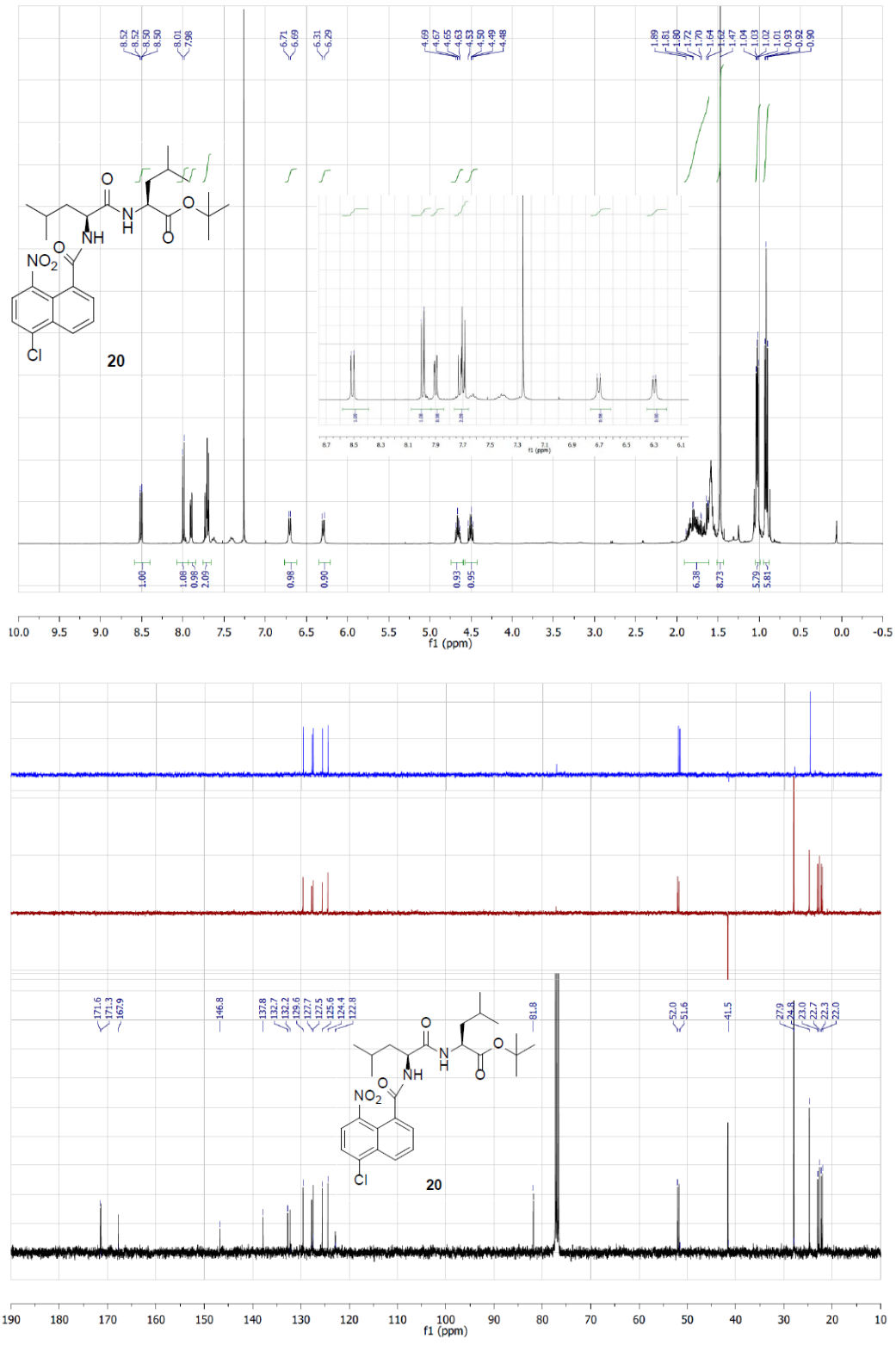


Figure S19. *^{1}H NMR ($CDCl_3$, 400 MHz) and ^{13}C ($CDCl_3$, 100 MHz) spectra of (**20**).*

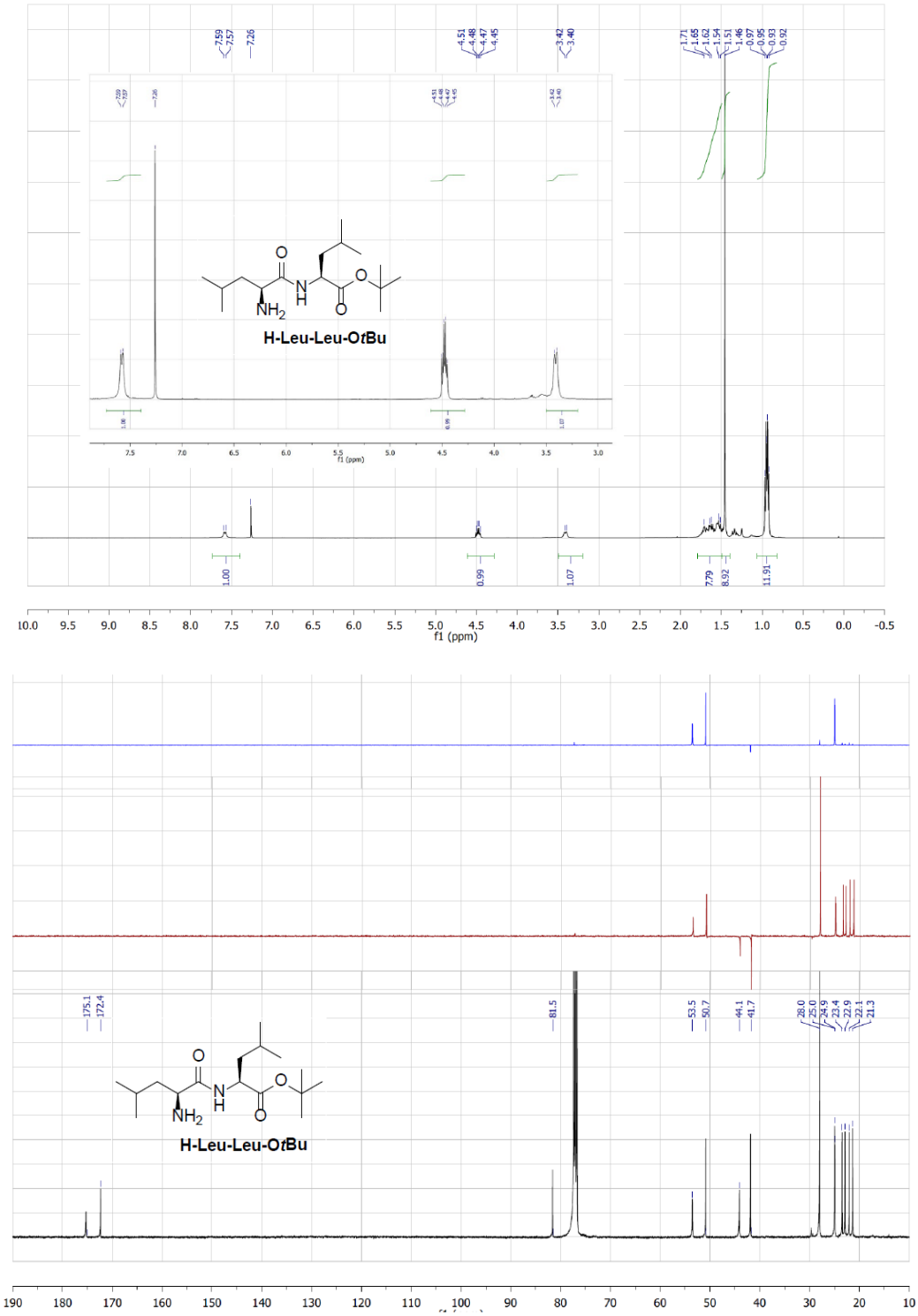


Figure S20. *^{1}H NMR ($CDCl_3$, 400 MHz) and ^{13}C ($CDCl_3$, 100 MHz) spectra of (**H-Leu-Leu-OtBu**).*

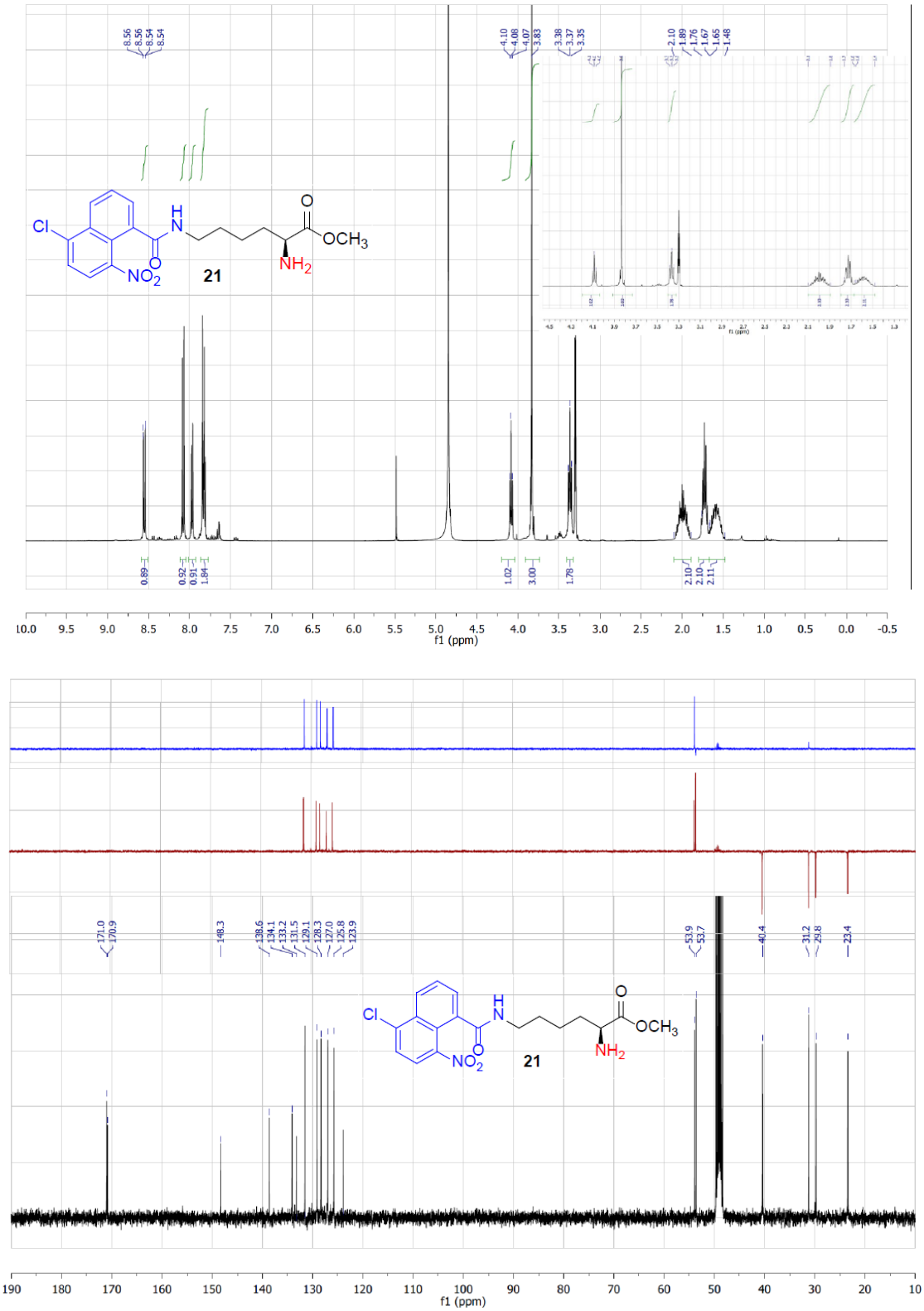


Figure S21. *^{1}H NMR (CD_3OD, 400 MHz) and ^{13}C (CD_3OD, 100 MHz) spectra of (**21**).*

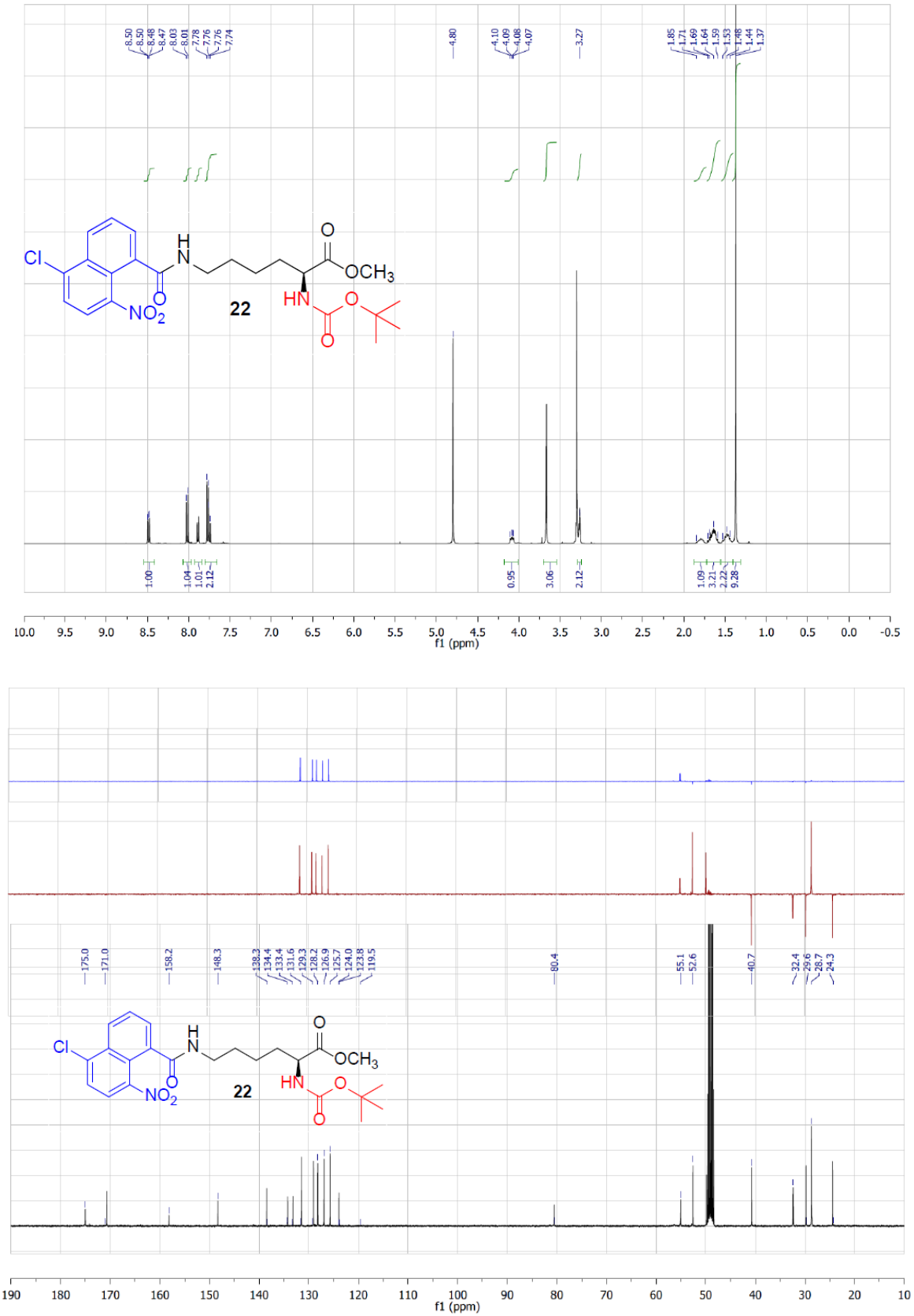


Figure S22. *^{1}H NMR (CD_3OD, 400 MHz) and ^{13}C (CD_3OD, 100 MHz) spectra of (**22**).*

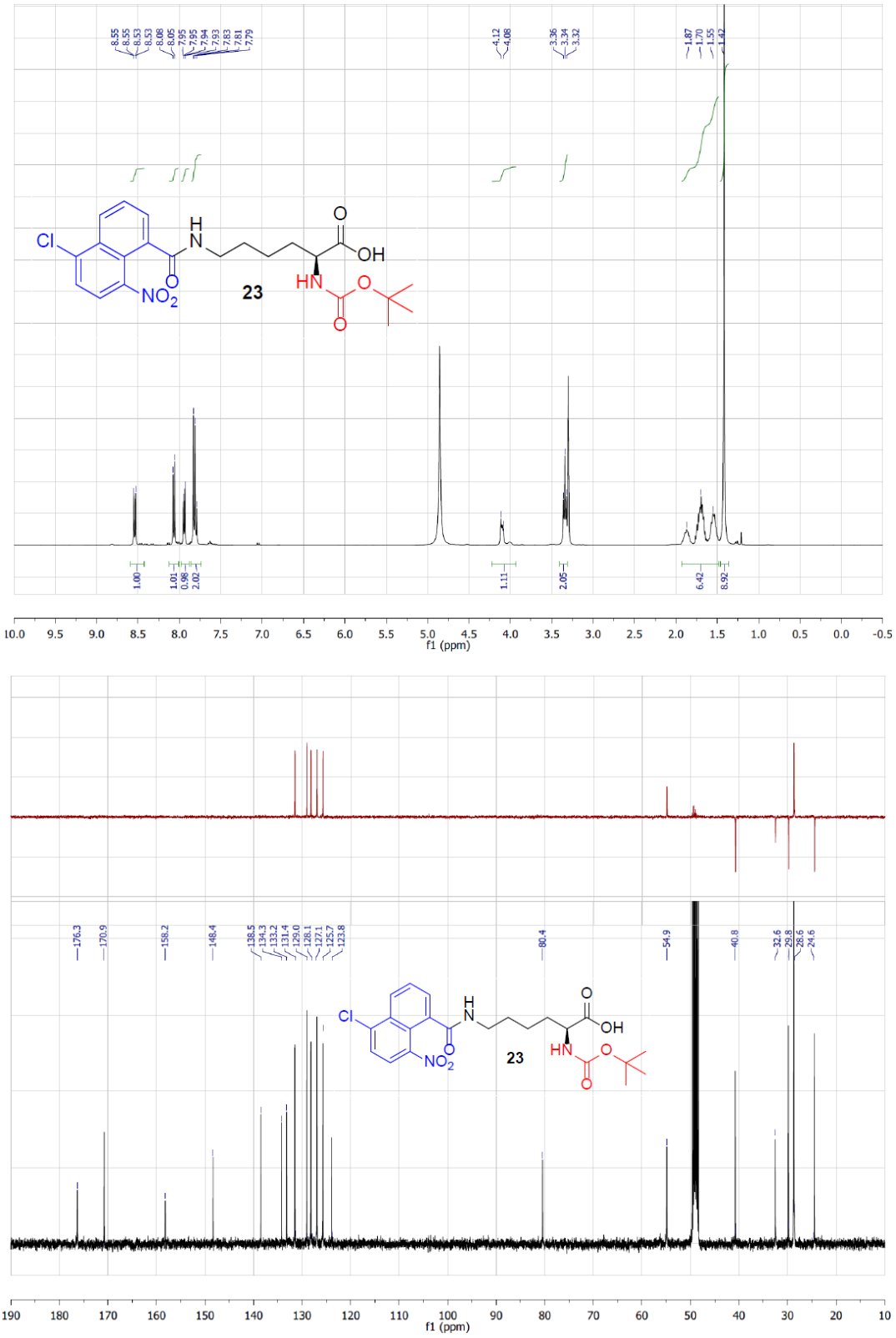


Figure S23. *^{1}H NMR (DMSO-d_6, 400 MHz) and ^{13}C (DMSO-d_6, 100 MHz) spectra of (**23**).*

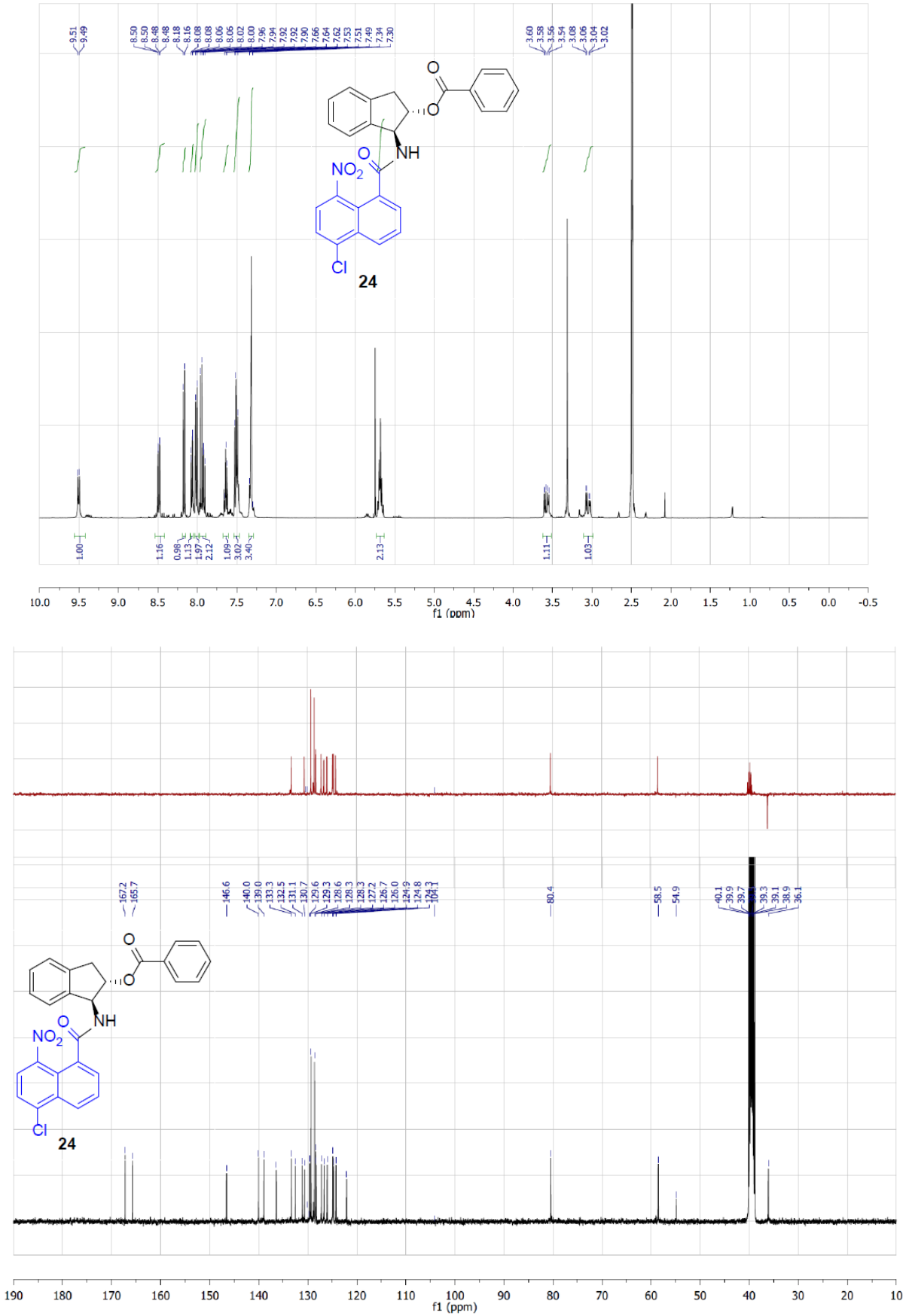
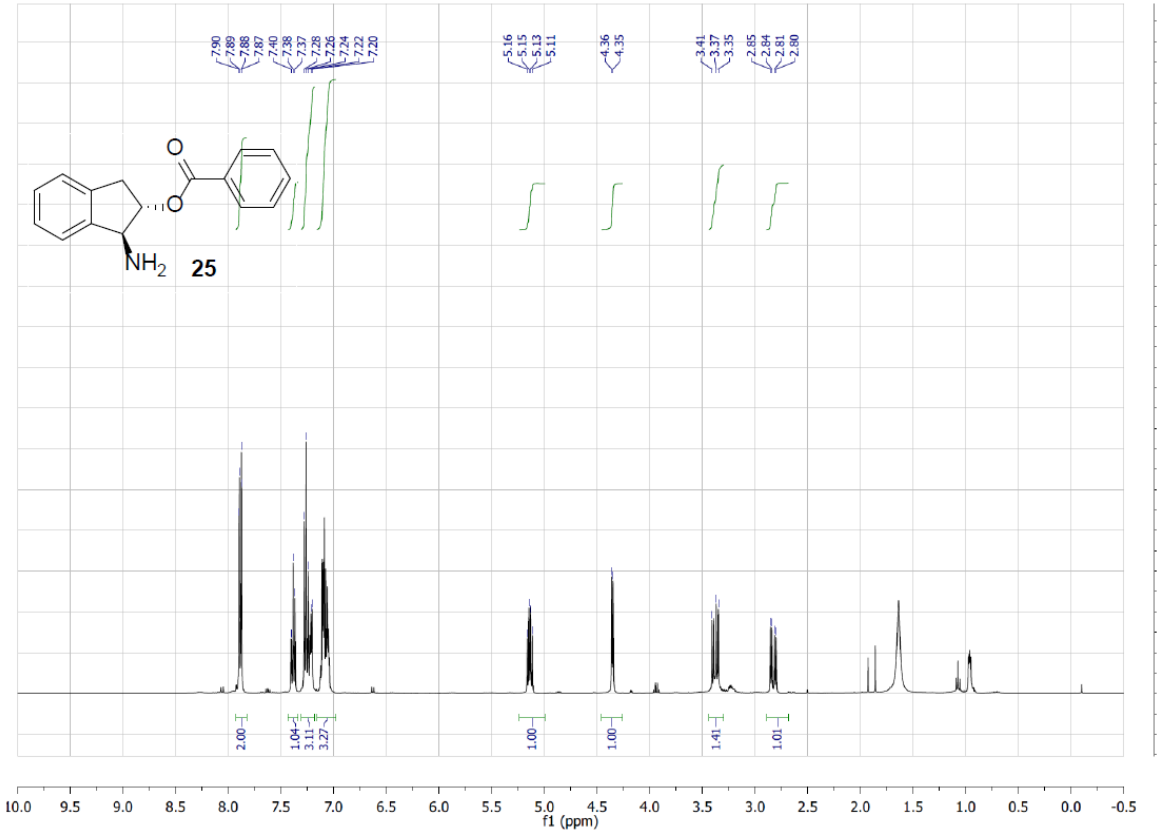


Figure S24. *^{1}H NMR (DMSO-d_6, 400 MHz) and ^{13}C (DMSO-d_6, 100 MHz) spectra of (**24**).*



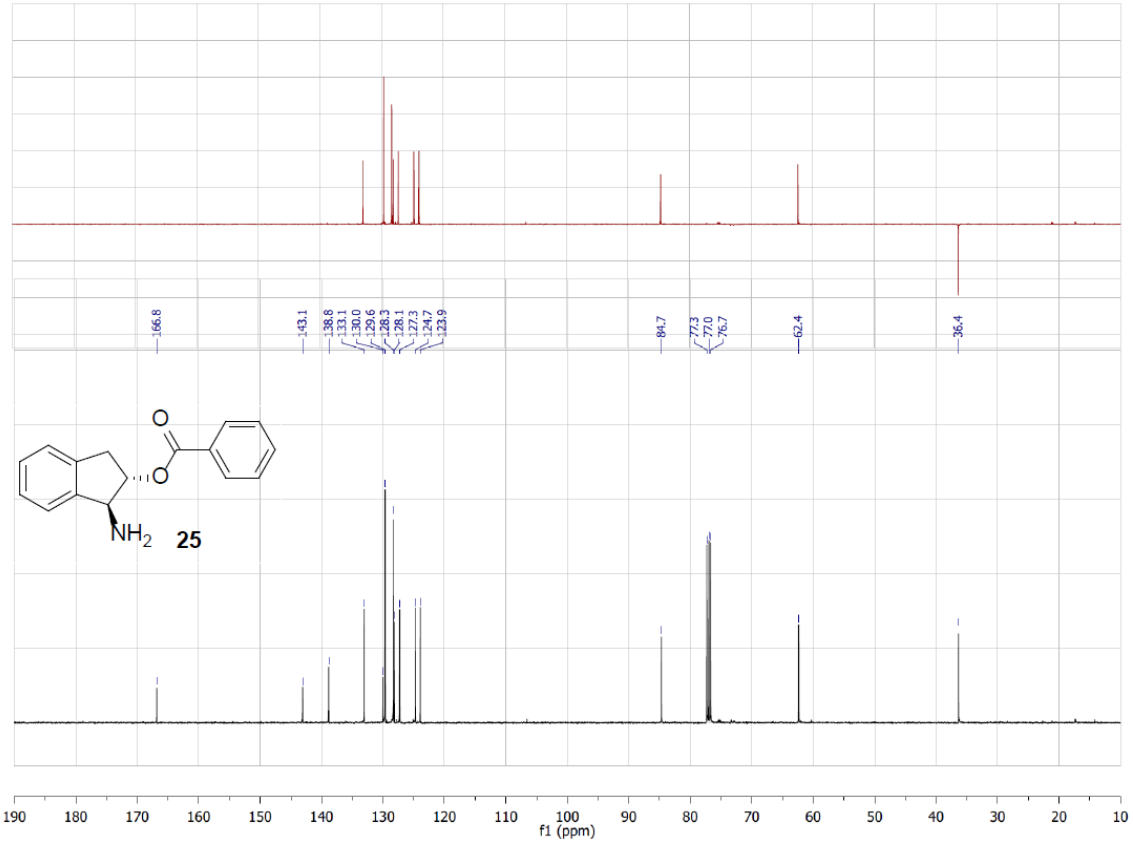


Figure S25. *^{1}H NMR ($CDCl_3$, 400 MHz) and ^{13}C ($CDCl_3$, 100 MHz) spectra of (**25**).*

5.10. Crystallographic data

5.10.1. Potassium carboxylate (K•3)

Table S2. *Crystal data and structure refinement for Potassium carboxylate* (**K•3***) (CCDC 2252216)*

Empirical formula	C11H5BrKNO5
Formula weight	350.17
Temperature (K)	298(2)
Wavelength (Å)	1.54178
Crystal system	Monoclinic
Space group	P21/c
Unit cell dimensions:	
a (Å)	17.5678(7)
b (Å)	6.0655(3)
c (Å)	12.3732(6)
α [°], β[°], γ[°]	90.00,107.532(2), 90.00
Volume	1257.21(10)
Z, Density (calculated) (Mg/m3)	4, 1.850
Absorption coefficient (mm-1)	7.599
F (000)	688
Crystal size (mm)	0.20 x 0.18 x 0.14
2Θ range for data collection (°)	7.17 to 66.78
Limiting indices	-19≤ h ≤20, -7≤ k ≤6, -14≤ l ≤14
Reflections collected / Independent	7547/2032 (Rint = 0.0602)
Refinement method	Full-matrix least-squares on F2
Data / restraints / parameters	2032 / 0 / 173
Goodness-of-fit on F2	2.342
Final R indices [I>2σ(I)]	R1 = 0.1322, wR2 = 0.2947
R indices (all data)	R1 = 0.1363, wR2 = 0.2987
Largest diff. peak and hole (eÅ-3)	2.048 and -3.878

$C_{11}H_5BrKNO_5$

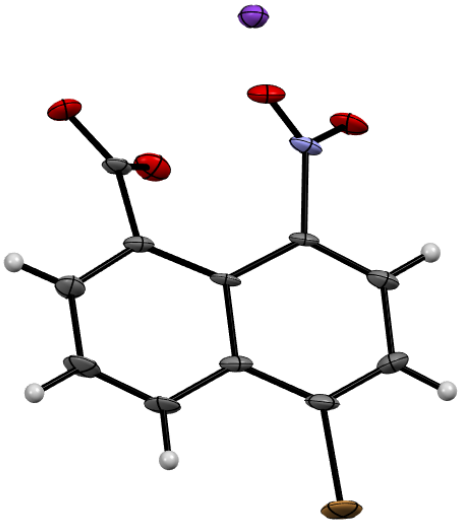


Figure S26. *Molecular structure of compound* **K•3**. *Displacement ellipsoids are drawn at 50 % probability level. Hydrogen atoms are shown as spheres of arbitrary radius.*

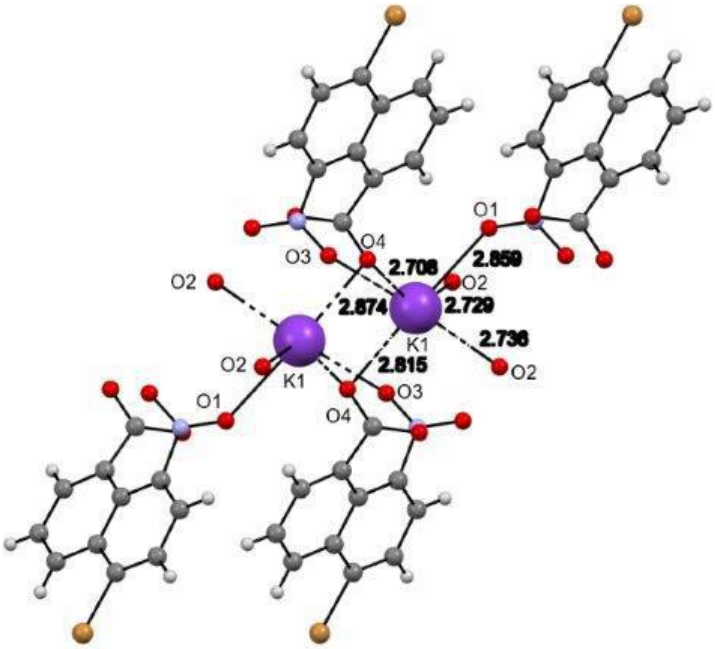


Figure S27. *Views showing the octahedral coordination of the K atom, with the K-O distances (in Å).*

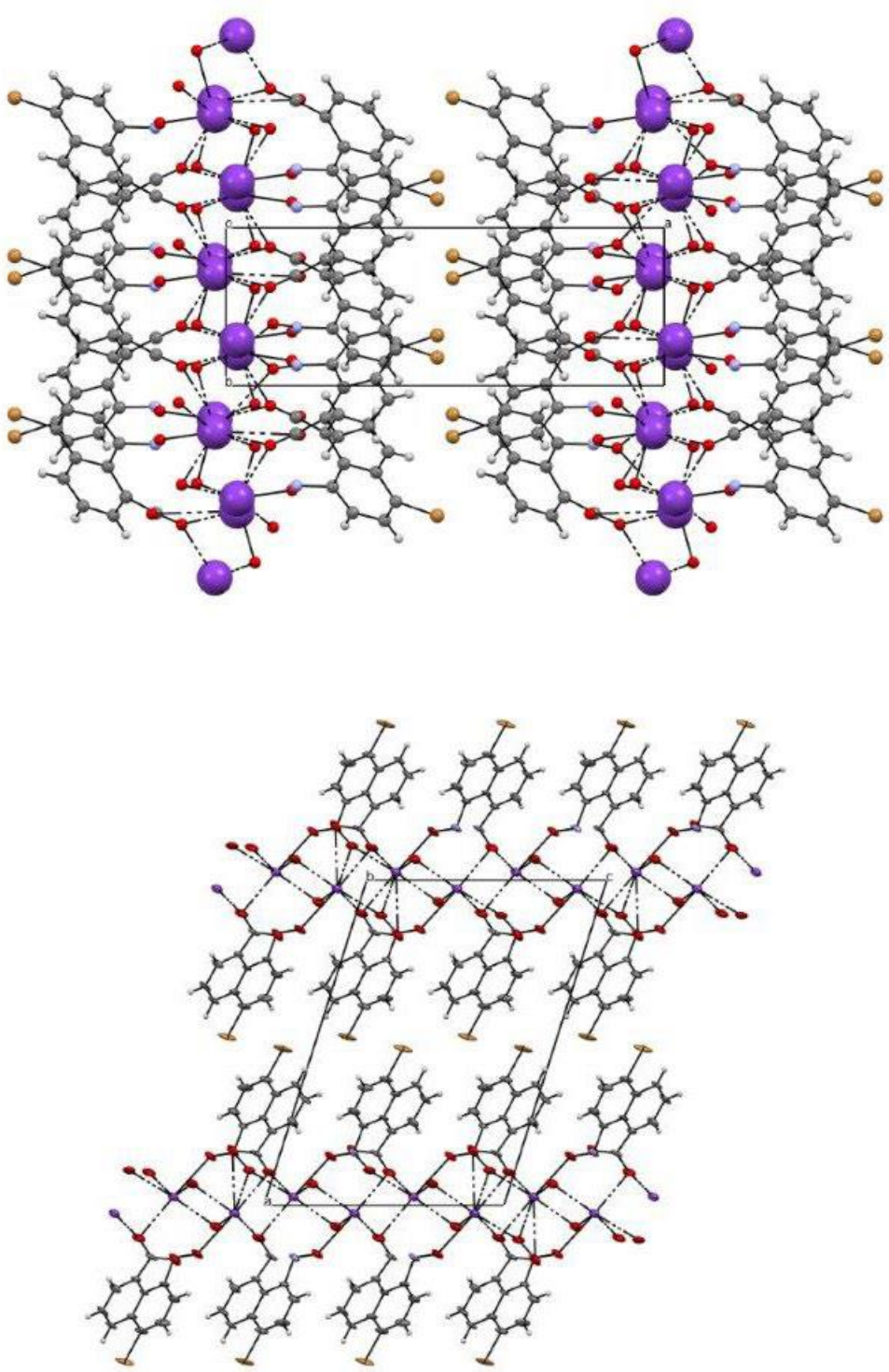


Figure S28. *Crystal packing along b and c axes.*

5.11.2. Amide 17

Table S3. *Crystal data and structure refinement for amide **17** (CCDC 2252212)*

Empirical formula	$C_{43}H_{42}Cl_2N_4O_7$
Formula weight	797.71
Temperature (K)	298(2)
Wavelength (Å)	1.54178
Crystal system	Monoclinic
Space group	$P2_1/c$
Unit cell dimensions:	
a (Å)	17.1860(5)
b (Å)	14.3114(5)
c (Å)	35.0105(10)
α [º], β[º], γ[º]	90.00,103.027(2), 90.00
Volume	8389.4(5)
Z, Density (calculated) (Mg/m^3)	8, 1.263
Absorption coefficient (mm^{-1})	1.830
F(000)	3344
Crystal size (mm)	0.16 x 0.12 x 0.10
2Θ range for data collection(°)	2.64 to 67.57
Limiting indices	$-20\leq h \leq 16$, $-15\leq k \leq 16$, $-41\leq l \leq 41$
Reflections collected / Independent	53709/14182 (Rint = 0.0576)
Refinement method	Full-matrix least-squares on F^2
Data / restraints / parameters	14182/ 0 / 1026
Goodness-of-fit on F^2	1.020
Final R indices[$I>2\sigma(I)$]	R1 = 0.0660, wR2 = 0.1751
R indices (all data)	R1 = 0.0973, wR2 = 0.1975
Largest diff. peak and hole ($eÅ^{-3}$)	0.435 and -0.327

$C_{43}H_{42}Cl_2N_4O_7$

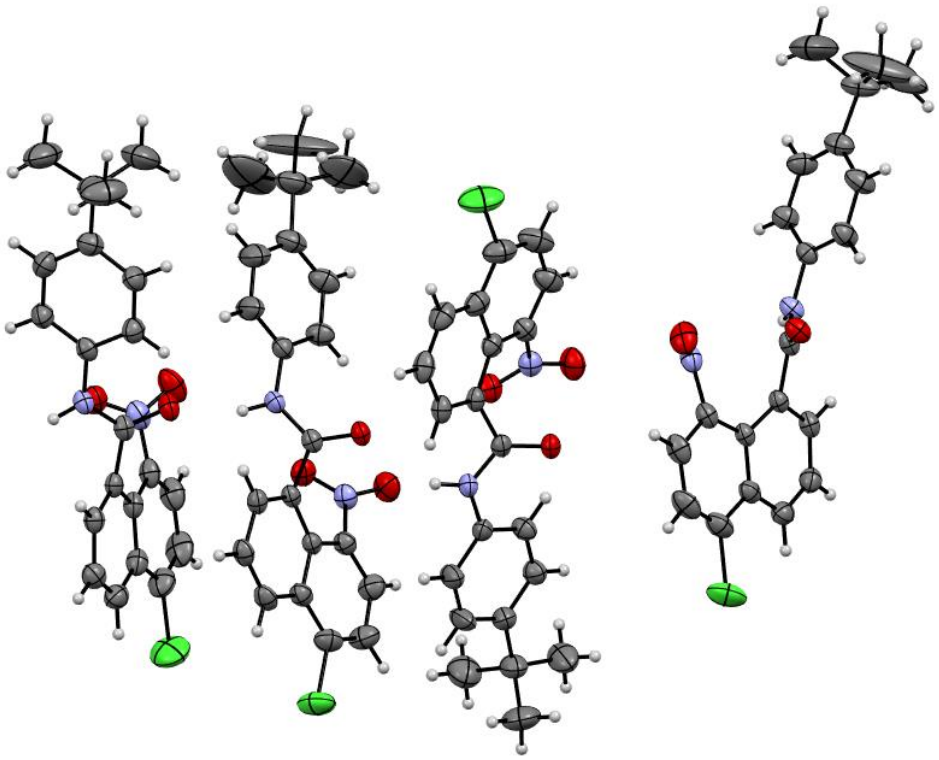


Figure S29. *Molecular structure of amide **17**. Displacement ellipsoids are drawn at 50 % probability level. Hydrogen atoms are shown as spheres of arbitrary radius. Solvent molecules have been omitted for clarity.*

5.12. Modelling studies

Theorical studies were carried out using GAMESS interface for Chem3D 19.1 software [30] using the RHF/3-21G. No imaginary frequencies were observed, and the calculated total energy was - 954413.1802 kcal/mol.

The figure shows a possible geometry for the compound **Ac16**, considering the information from the NMR spectra.

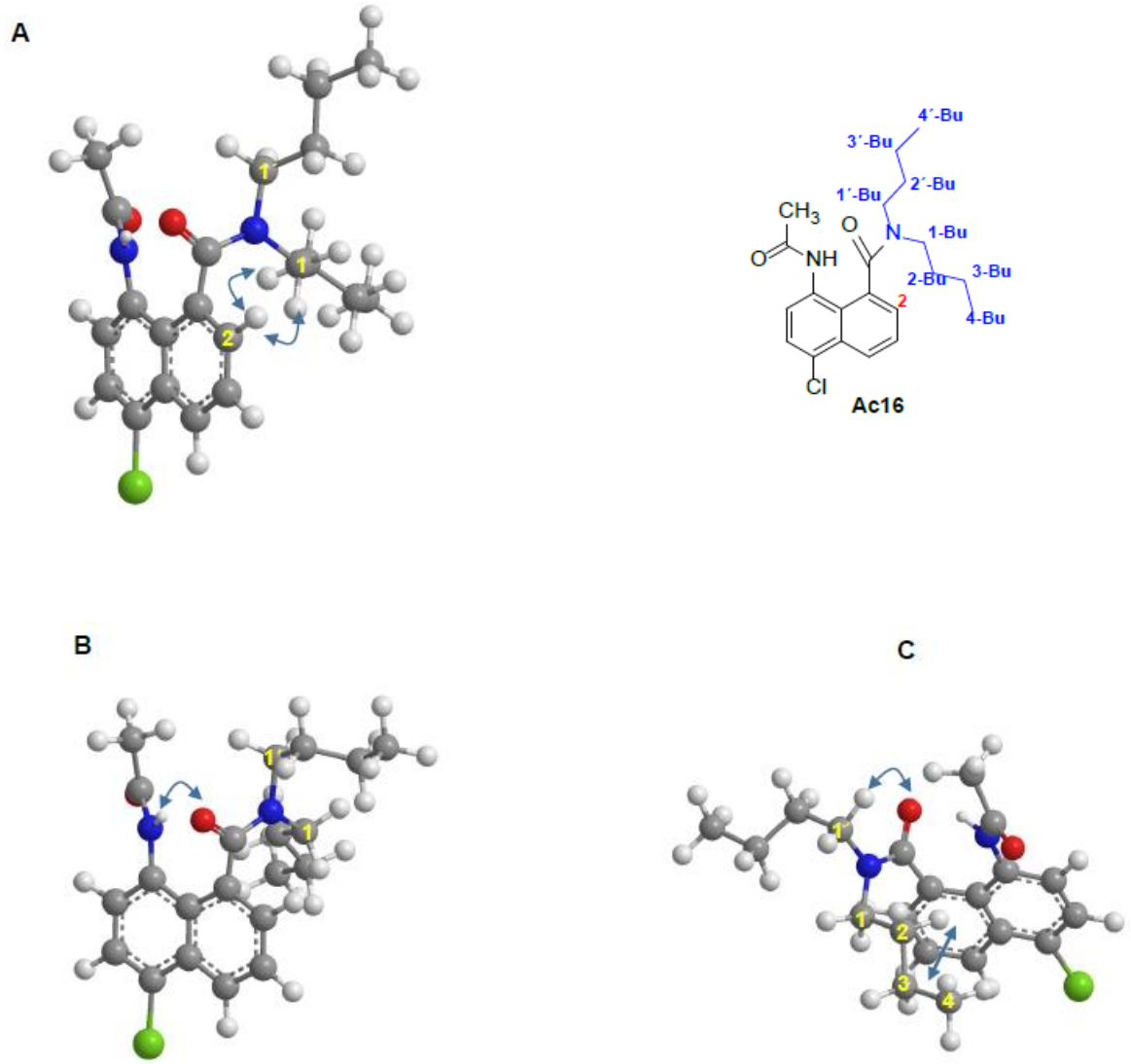


Figure S30. *Methylene protons (1-Bu and 2-Bu) are close to aromatic proton C-2 (**A**). An angular intramolecular H-bond is set between acetamide NH and dibutylamide carbonyl group (**B**). One of the H of the methylene group (1´-Bu) is highly deshielded due to proximity to dibutylamide carbonyl group. Methylene 3-Bu and methyl 4-Bu are over the naphthalene ring.*

Coordinates for the model of **Ac16**
C(1) -6.028 0.651 1.787
C(2) -6.263 -0.083 2.877
C(3) -5.233 -0.489 3.630
C(4) -3.962 -0.217 3.257
C(5) -3.704 0.511 2.135
C(6) -4.771 0.980 1.441
C(7) -2.940 -0.696 3.994
C(8) -1.666 -0.521 3.627
C(9) -1.405 0.134 2.493
C(10) -2.405 0.633 1.745
N(11) -4.641 1.816 0.395
C(12) -5.355 1.944 -0.755
C(13) -5.026 3.203 -1.534
O(14) -6.138 1.109 -1.130
C(15) -1.972 1.199 0.582
O(16) -1.942 2.401 0.458
N(17) -1.634 0.349 -0.459
C(18) -1.378 0.844 -1.820
C(19) -1.520 -1.111 -0.321
C(20) -2.611 -1.918 -1.043
C(21) -2.352 -3.428 -0.873
C(22) -3.413 -4.293 -1.567
C(23) 0.036 0.549 -2.353
C(24) 0.297 1.250 -3.698
C(25) 1.700 0.932 -4.233
Cl(26) -5.660 -1.398 5.047
H(27) -6.904 1.031 1.237
H(28) -7.309 -0.305 3.154
H(29) -3.086 -1.283 4.916
H(30) -0.843 -0.947 4.225
H(31) -0.350 0.225 2.176
H(32) -3.824 2.374 0.492
H(33) -5.071 4.096 -0.867
H(34) -3.999 3.134 -1.960
H(35) -5.749 3.361 -2.365
H(36) -2.130 0.416 -2.520
H(37) -1.541 1.942 -1.885
H(38) -0.512 -1.437 -0.665
H(39) -1.538 -1.440 0.737
H(40) -3.609 -1.650 -0.619
H(41) -2.627 -1.687 -2.133
H(42) -1.349 -3.680 -1.298
H(43) -2.327 -3.691 0.212
H(44) -3.183 -5.377 -1.439
H(45) -4.426 -4.107 -1.142
H(46) -3.450 -4.082 -2.661
H(47) 0.792 0.884 -1.604
H(48) 0.178 -0.545 -2.513
H(49) -0.464 0.928 -4.449

H(50) 0.194 2.354 -3.571
H(51) 1.885 1.441 -5.207
H(52) 2.482 1.272 -3.516
H(53) 1.831 -0.163 -4.394

6. References

(1) Rodney A. Fernandes. *Protecting-Group-Free Organic Synthesis*, John Wiley&Sons Ltd.; Indian Institute of Technology Bombay Mumbai, India, 2018.

(2) Greene's Protective Groups in Organic Synthesis, 1st ed.; Wuts, P. G. M., Ed.; Wiley, 2014. https://doi.org/10.1002/9781118905074.

(3) *Protective Groups*. https://www.organic-chemistry.org/protectivegroups/ (accessed 2024-01-08).

(4) Isidro-Llobet, A.; Álvarez, M.; Albericio, F. Amino Acid-Protecting Groups. *Chem. Rev.* **2009**, *109* (6), 2455–2504. https://doi.org/10.1021/cr800323s.

(5) Dunkel, P. Photoremovable Protecting Groups. *Encyclopedia* **2022**, *2* (3), 1225–1236. https://doi.org/10.3390/encyclopedia2030082.

(6) Omprakash Rathi, J.; Subray Shankarling, G. Recent Advances in the Protection of Amine Functionality: A Review. *ChemistrySelect* **2020**, *5* (23), 6861–6893. https://doi.org/10.1002/slct.202000764.

(7) Ashenhurst, J. *Protecting Groups for Amines - Carbamates*. Master Organic Chemistry. https://www.masterorganicchemistry.com/2018/06/07/protecting-groups-for-amines-carbamates/ (accessed 2024-01-12).

(8) Omprakash Rathi, J.; Subray Shankarling, G. Recent Advances in the Protection of Amine Functionality: A Review. *ChemistrySelect* **2020**, *5* (23), 6861–6893. https://doi.org/10.1002/slct.202000764.

(9) Antonov, A. S.; Tupikina, E. Y.; Karpov, V. V.; Mulloyarova, V. V.; Bardakov, V. G. Sterically Facilitated Intramolecular Nucleophilic NMe_2 Group Substitution in the Synthesis of Fused Isoxazoles: Theoretical Study. *Molecules* **2020**, *25* (24), 5977. https://doi.org/10.3390/molecules25245977.

(10) Ozeryanskii, V. A.; Pozharskii, A. F.; Antonov, A. S.; Filarowski, A. Out-Basicity of 1,8-Bis(Dimethylamino)Naphthalene: The Experimental and Theoretical Challenge. *Org. Biomol. Chem.* **2014**, *12* (15), 2360–2369. https://doi.org/10.1039/C3OB41986J.

(11) Ragnarsson, U.; Grehn, L. Dual Protection of Amino Functions Involving Boc. *RSC Adv.* **2013**, *3* (41), 18691–18697. https://doi.org/10.1039/C3RA42956C.

(12) Sonntag, N. O. V. The Reactions of Aliphatic Acid Chlorides. *Chem. Rev.* **1953**, *52*, 237−401. https://doi.org/10.1021/cr60162a001.

(13) Schweizer, W. B.; Procter, G.; Kaftory, M.; Dunitz, J. D. Structural Studies of 1,8-Disubstituted Naphthalenes as Probes for Nucleophile-Electrophile Interactions. *Helv. Chim. Acta* **1978**, *61* (8), 2783–2808. https://doi.org/10.1002/hlca.19780610806.

(14) Bürgi, H. B.; Dunitz, J. D.; Lehn, J. M.; Wipff, G. Stereochemistry of Reaction Paths at Carbonyl Centres. *Tetrahedron* **1974**, *30* (12), 1563–1572. https://doi.org/10.1016/S0040-4020(01)90678-7.

(15) Wannebroucq, A.; Jarmyn, A. P.; Pitak, M. B.; Coles, S. J.; Wallis, J. D. Reactions and Interactions Between Peri Groups in 1- Dimethylamino-Naphthalene Salts: An Example of a "Through Space" Amide. *Pure Appl. Chem.* **2016**, *88*, 317−331. https://doi.org/10.1515/pac-2015-1103.

(16) Orlandi, M.; Brenna, D.; Harms, R.; Jost, S.; Benaglia, M. Recent Developments in the Reduction of Aromatic and Aliphatic Nitro Compounds to Amines. *Org. Process Res. Dev.* **2018**, *22* (4), 430–445. https://doi.org/10.1021/acs.oprd.6b00205.

(17) Zhou, C.; Wang, M.; Guo, W.; Ye, G.; Wang, Y.; Yang, Y.; Xia, G.; Wang, H. Lactam Node as a Two-Fold Functional Unit for Achieving Highly Efficient and Tunable Dual-State Emitters. *Dyes Pigm.* **2023**, *213*, 111198. https://doi.org/10.1016/j.dyepig.2023.111198.

(18) Su, J.; Sheng, X.; Li, S.; Sun, T.; Liu, G.; Hao, A. Effective Regioselective Protection of Amino Groups of Lysine Achieved by a Supramolecular Enzyme-Mimic Approach. *Org. Biomol. Chem.* **2012**, *10* (47), 9319–9324. https://doi.org/10.1039/C2OB27021H.

(19) Pícha, J.; Buděšínský, M.; Macháčková, K.; Collinsová, M.; Jiráček, J. Optimized Syntheses of Fmoc Azido Amino Acids for the Preparation of Azidopeptides. *J. Pept. Sci.* **2017**, *23* (3), 202–214. https://doi.org/10.1002/psc.2968.

(20) Amatuni, A.; Shuster, A.; Abegg, D.; Adibekian, A.; Renata, H. Comprehensive Structure–Activity Relationship Studies of Cepafungin Enabled by Biocatalytic C–H Oxidations. *ACS Cent. Sci.* **2023**, *9* (2), 239–251. https://doi.org/10.1021/acscentsci.2c01219.

(21) Su, J.; Sheng, X.; Li, S.; Sun, T.; Liu, G.; Hao, A. Effective regioselective protection of amino groups of lysine achieved by a supramolecular enzyme-mimic approach. *Org. Biomol. Chem.* **2012**, *10*, 9319−9324. https://doi.org/10.1039/C2OB27021H.

(22) Armarego, W. L. F.; Armarego, W. L. F.; Perrin, D. D. *Purification of Laboratory Chemicals*, 4. ed., reprint.; Butterworth-Heinemann: Oxford, 2002.

(23) Gottlieb, H. E.; Kotlyar, V.; Nudelman, A. NMR Chemical Shifts of Common Laboratory Solvents as Trace Impurities. *J. Org. Chem.* **1997**, *62* (21), 7512–7515. https://doi.org/10.1021/jo971176v.

(24) SAINT-NT Version 6.0, Madison, Wisconsin, USA: Bruker–AXS, 2001.

(25) Krause, L.; Herbst-Irmer, R.; Sheldrick, G. M.; Stalke, D. Comparison of Silver and Molybdenum Microfocus X-Ray Sources for Single-Crystal Structure Determination. *J. Appl. Cryst.* **2015**, *48* (1), 3–10. https://doi.org/10.1107/S1600576714022985.

(26) Sheldrick, G. M. Crystal Structure Refinement with SHELXL. *Acta Cryst. C* **2015**, *71* (1), 3–8. https://doi.org/10.1107/S2053229614024218.

(27) Sheldrick, G. M. SHELXT – Integrated Space-Group and Crystal-Structure Determination. *Acta Cryst. A* **2015**, *71* (1), 3–8. https://doi.org/10.1107/S2053273314026370.

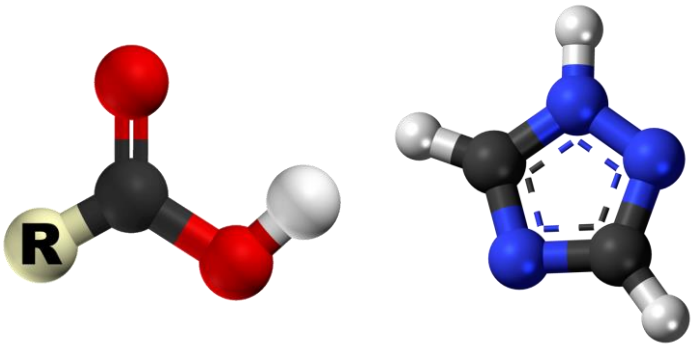
(28) International Tables for Crystallography. Springer. https://www.springer.com/series/6995 (accessed 2024-01-21).

(29) Macrae, C. F.; Edgington, P. R.; McCabe, P.; Pidcock, E.; Shields, G. P. Taylor, R.; Towler, M.; Van de Streek, J. *J. Appl. Cryst.* **2006**, *39*, 453-457. https://doi.org/10.1107/S002188980600731X.

(30) Barca, G. M. J.; Bertoni, C.; Carrington, L.; Datta, D.; De Silva, N.; Deustua, J. E.; Fedorov, D. G.; Gour, J. R.; Gunina, A. O.; Guidez, E.; Harville, T.; Irle, S.; Ivanic, J.; Kowalski, K.; Leang, S. S.; Li, H.; Li, W.; Lutz, J. J.; Magoulas, I.; Mato, J.; Mironov, V.; Nakata, H.; Pham, B. Q.; Piecuch, P.; Poole, D.; Pruitt, S. R.; Rendell, A. P.; Roskop, L. B.; Ruedenberg, K.; Sattasathuchana, T.; Schmidt, M. W.; Shen, J.; Slipchenko, L.; Sosonkina, M.; Sundriyal, V.; Tiwari, A.; Galvez Vallejo, J. L.; Westheimer, B.; Włoch, M.; Xu, P.; Zahariev, F.; Gordon, M. S. Recent Developments in the General Atomic and Molecular Electronic Structure System. *J. Chem. Phys.* **2020**, *152* (15), 154102. https://doi.org/10.1063/5.0005188.

(31) Linden, W. A. van der; Willems, L. I.; Shabaneh, T. B.; Li, N.; Ruben, M.; Florea, B. I.; Marel, G. A. van der; Kaiser, M.; Kisselev, A. F.; Overkleeft, H. S. Discovery of a Potent and Highly B1 Specific Proteasome Inhibitor from a Focused Library of Urea-Containing Peptide Vinyl Sulfones and Peptide Epoxyketones. *Org. Biomol. Chem.* **2012**, *10* (1), 181–194. https://doi.org/10.1039/C1OB06554H.

CHAPTER 4: SYNTHESIS OF WATER-SOLUBLE PRODRUGS



In Chapter 4 hydro-solubility of prodrugs will be discussed.

1. Objectives

The **main objective** of this chapter is the synthesis of a series of prodrugs with water solubility enhancement. These antineoplastic prodrugs will obey a design modification by integrating a polar functional group through an aromatic nucleophilic substitution or using click chemistry. To achieve this goal, the specific objectives shown below are proposed:

- **Objective 1**: Addressing the solubility challenges of poorly water-soluble drugs using innovative formulation approaches as click chemistry.
- **Objective 2**: Synthesis and characterization of the antineoplastic drugs by integrating a polar functional group (carboxylic group) to improve the hydro-solubility.
- **Objective 3**: Carrying out a series of cell trials to test the validation of the synthesized prodrugs in terms of solubility and efficacy towards cancer cells.

2. Introduction

Organic syntheses of biologically active compounds have been always surrounded by solubility issues, in which their absorption inside the body is obstructed by many factors. Since the hydro-solubility of a drug is considered as an important feature in confirming new drugs validity, researchers have developed new methods to prevent the crystallization of active compounds, thereby increasing their formulation development and bioavailability.[1]

Actually, in spite of the successful drug developments and their promising pharmacological activities various hurdles such as poor solubility, high first pass and metabolism by cytochrome enzymes still constituting a notable problem for new organic entities completion, bioequivalence and validation.[2] Before tackling the anticancer prodrugs lack of solubility, we define first what is solubility in chemistry.

2.1. What is solubility?

The solubility term can be defined as the maximum quantity of a solute that dissolves in a certain volume of a determined solvent at a specified pH, temperature and pressure.[3] In general, a compound having a solubility of at least 0.1 g/L is considered as adequately soluble and a compound having a solubility of ≤ 0.01 g/L is considered as poorly soluble (Figure 1).[4]

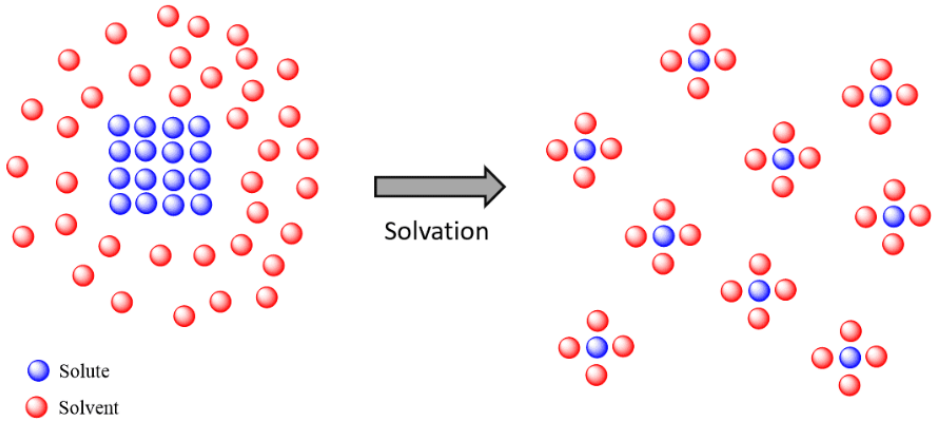


Figure 1. *Solubility process interpreted by intramolecular fragmentation and clusters formation via the solvent interaction.*[5]

2.2. Hydro-solubility improvement in prodrugs

Literature survey demonstrates that about 70% of active pharmaceutical ingredients and new chemical entities are considered as poorly soluble.[6] In recent decades, new anticancer molecules designers and researchers have faced several challenges in cancer therapy in which their delivery to tumor cells without interacting with the normal cells was a promising objective in targeted therapy.[7] Since the majority of antineoplastic drugs are insoluble in water medium, their carriage could be realized through an attachment of anticancer drug and a hydrophilic part to ensure absorption, permeability and pharmacokinetic properties.[7,8]

Prodrugs moieties are considered as safe and constructive strategy in solving poor aqueous solubility problems, since their design could be controlled by adding a hydrophilic part which facilitate the solubility and permeability even if the principal drug has low solubility in water medium (anticancer drugs).[8] These promoieties can be carbonates, carbamates, phosphates, imines, ethers, esters or amides (Figure 2).

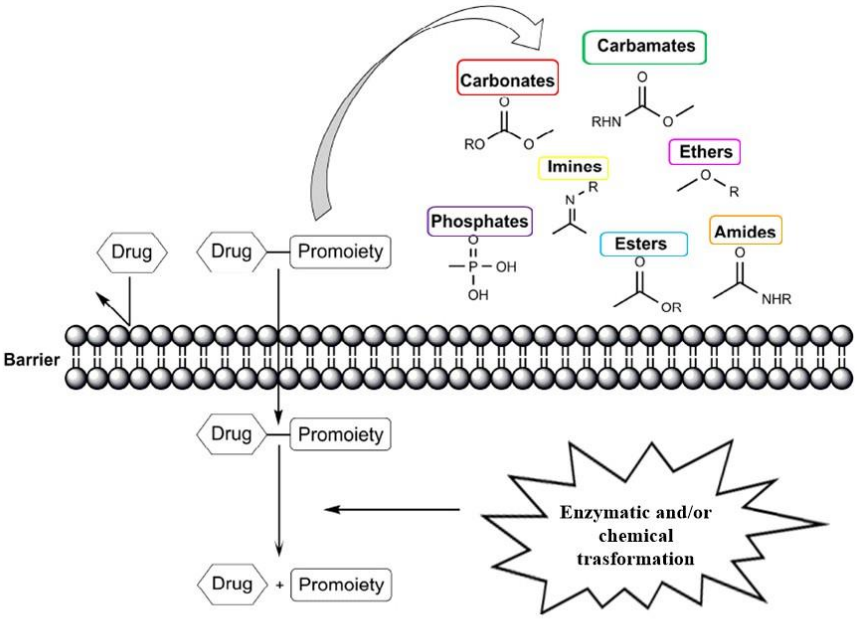


Figure 2. *Prodrugs activation pathways through hydro-solubility approach*.[8]

2.3. Background: Examples of solubilizing anticancer prodrugs from poorly-soluble drugs

In fact, due to the poor solubility of anticancer prodrugs many issues can result during *in vitro* assays, such as precipitation and crystallisation which leads to a lack of solubility and permeability which bias the results.[8]

We take the example of Etoposide drug or known as the podophyllotoxin Etoposide (glycoside of podophyllotoxin) with a broad range of clinical activities (Figure 3). It has been used for the treatment of small tumor cells such as lung cancer and testicular intraepithelial neoplasia, nevertheless it is confronted by several complications such as notably toxicity, and precipitation when diluting.[9,10]

Due to the Etoposide bulky gelatine capsulation and several issues during its oral dosage, Etoposide absorption as a powder suspension has proved as unstable and erratic with low to negligible bioavailability from an *in situ* rat model, these problems could be due to various issues as well as the gradual dissolution, variations in acidic media and the low aqueous solubility.[9,11,12]

In this case, Etoposide solubility enhancement was carried via the prodrug approach "Etopophos" prodrug in which Etoposide drug was linked with a phosphate ester (Figure 3).[9]

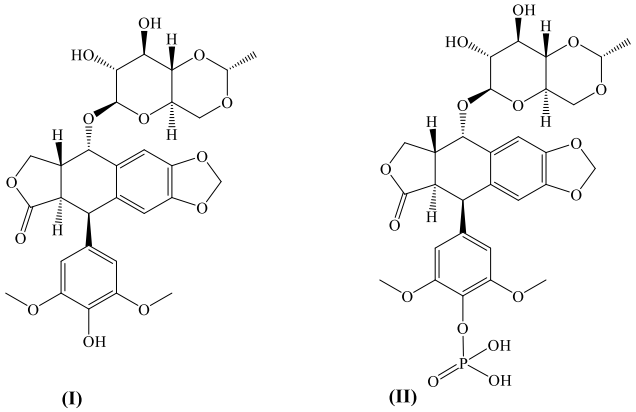


Figure 3. *Etoposide chemical structure (I) and Etopophos (II), its phosphate ester prodrug.*[9]

In light of the results obtained through *in vitro* and *in vivo* assays the phosphate prodrug has experimented a rapid conversion to Etoposide (parent drug) in 5 minutes with a dose of 70 % from Etopophos through IV administration in rates (animal model).[9,13]

Another example of antineoplastic drug whose solubility has been increased by chemical modification is Taxol (Figure 4), the latter is used usually in treating some types of cancer particularly ovarian, breast, lung cancer and melanoma owing to its high toxicity against tumor properties and its potential as antileukemic agent.

Taxol is characterized by a high hydrophobicity and low solubility (0.25 μg/mL). Using the same strategy used with Etoposide, Taxol phosphate ester prodrug was synthetized in order to improve the solubility (> 10 mg/mL). This ester has shown a light stability for 24 hours in deionized water, as well as in the presence of alkaline phosphatase (bovine intestinal mucosa) at pH ≈ 7, a cleavage *in vitro* was reported liberating the parent drug (Taxol) in 25 min at 37 ºC with a conversion level above 90%. According to the authors, Taxol prodrug has met two key requirements: high solubility and satisfactory reconversion and cleavage.[9]

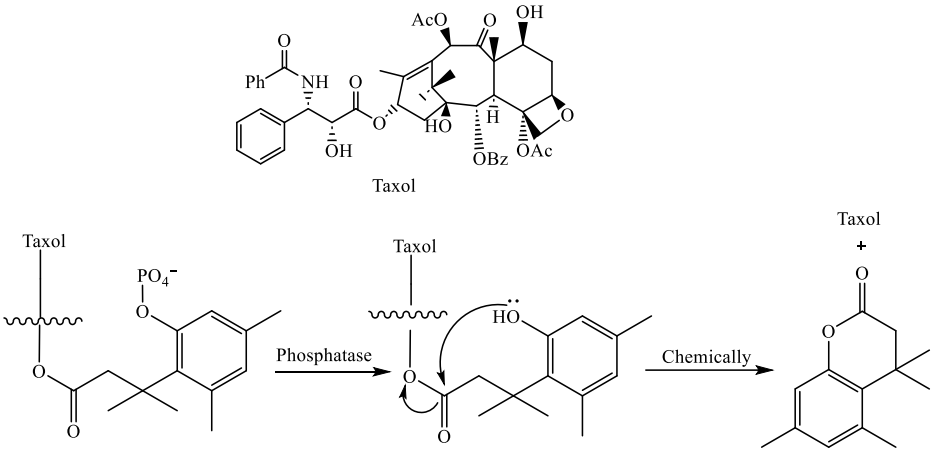


Figure 4. *Enzymatic and chemical cleavage of Taxol prodrug and release of the Taxol parent drug[9](adapted).*

2.4. Carboxylic acid functional group

With the increase in the understanding of organic chemistry, carboxylic acid group has become a common functional group in many drugs, since its structure is integrated (-COOH) [14] in all living systems, and considered as an essential component of the amino acid structure. Therefore, it is not surprising that the carboxylic acid moiety can be found in the pharmacophore of about 450 commercial drugs, such as fibrates, statins, β-lactam antibiotics, and non-steroidal anti-inflammatory drugs (NSAIDs).[15,16]

2.4.1. Pharmaceutical applications

Due to its pivotal role in the large scope of organic chemistry, and its beneficial properties, carboxyl group has been used in several chemo-pharmaceutical syntheses in which it contributes in the stimulation and the bioactivity of large drugs range.

In fact, the polar characteristics of the carboxyl group increases its ability to dissolve in polar solvents such as water. The carboxyl-containing molecules are able to form hydrogen bonds with water molecules thanks to the induced polarity, which gives them greater solubility when

compared to nonpolar molecules hence, the capacity of carboxyl groups to engage in hydrogen bonding is one such use. Since most biological activities occur in aqueous media, a drug's capacity to generate hydrogen bonds can have a big impact on how soluble it is and how easily it is absorbed and distributed.[14]

For these reasons, two strategies have been employed: click chemistry and the integration of thioglycolic acid.

2.4.2. *First strategy*: Click reaction

Click chemistry is a versatile concept exclusively employed for the most viable and dependable chemical reactions. It was introduced in 2001 and culminated in 2022 when Sharpless, Meldal and Bertozzi were awarded with the Nobel prize of chemistry due to their contribution in recognition of the transformative effect that click and bioorthogonal chemistry have had in research and drug development.

This is a significant advancement for drug development research as well as biomedicine which relies on the ability to obtain new structures, by inducing highly selective reactions.

In recent years, it has been witnessed experimentally that click reactions have an extremely quick chemical transformation rate as well as their performance in terms of developing in water, which is an essential element in click reactions, not only for selectivity reasons but also because it is the most effective heat sink to operate the enormous heat production when click reactions are performed on large scales.[17,18,19]

One of the most important reactions is the reaction of an azide with a terminal alkyne to give the corresponding triazole.

Azides are very common in organic synthesis; it is a good group to introduce a nitrogen into the molecule. Usually, the reaction between an azide and an alkyne takes place directly, however, in the absence of any catalyst, a high temperature is needed for the formation of the triazole cycloaddition, and it generates two possible regioisomers 1,4 and 1,5 (Figure 5).

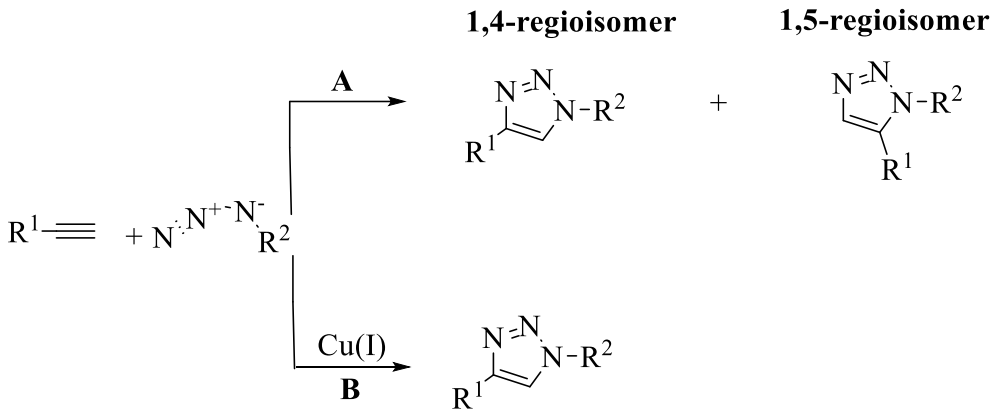


Figure 5*: Cycloaddition of an azide with an alkyne and the two possible regioisomers obtained: (A) inactivated azide-alkyne cycloaddition yielding a mixture of the 1,5- and the 1,4-triazole regioisomers and (B) copper (I) (Cu(I)) catalysis in alkyne-azide coupling reactions favouring the formation of only the 1,4-regioisomer.*[20]

The use of copper (I) allows the reaction to work at room temperature, becoming a regioselective reaction, since it generates a 1,4-disubstituted triazole, whereas when a ruthenium complex is used as a catalyst, the 1,5-disubstituted heterocycle is formed.[21]

2.4.2.1. Click chemistry: a powerful tool in hydro-solubility enhancement of antitumor prodrugs

Exploiting the click reaction`s insensitivity towards water and oxygen, and due to the ease of eliminating the byproducts resulting from the reactions without using purification procedures (chromatographic methods), click chemistry has gotten the attention of medicinal chemists to integrate it in the pharmacologically valuable drugs syntheses.[22]

In fact, prodrugs are intelligent transporters that respond simultaneously to the tumour microenvironment and/or the intracellular components through an extracellular stability and an intracellular activation by liberating their payload inside the targeted cell (cancer cell). Hence unlike the conventional formulations, the approach of hydro-solubilizing prodrugs has been accomplished with the integration of click chemistry into the synthesis procedure in several studies. For example, Y. Hayashi *et al.* (2013) have mentioned in their article based on previous studies that the employment of anti-microtubule (e.g. Plinabulin) was a promising concept for the water-solubility enhancement via prodrug and click chemistry approaches by preserving the mother skeleton of the molecule.[23]

Plinabulin (Figure 6) is a small molecule that has shown powerful anti-tumour activity[24] (e.g. lung cancer). Nevertheless, its lack of solubility (<0.1 μg/mL, H_2O) has pushed the researchers

to improve its design by enhancing the solubility property in order to increase its pharmaco-kinetics and dynamic characteristics.

Y. Hayashi and his colleagues affirm in their article that after several investigations, and through click chemistry, an efficient method incorporating esterase hydrolysis was created.[17, 23] They used copper-catalysed alkyne azide coupling (CuAAC) in a purpose of obtaining high yields and considerable chemoselectivity, so that the incorporation of non-protected water-solubilizing fragment under mild conditions was possible.[23,25]

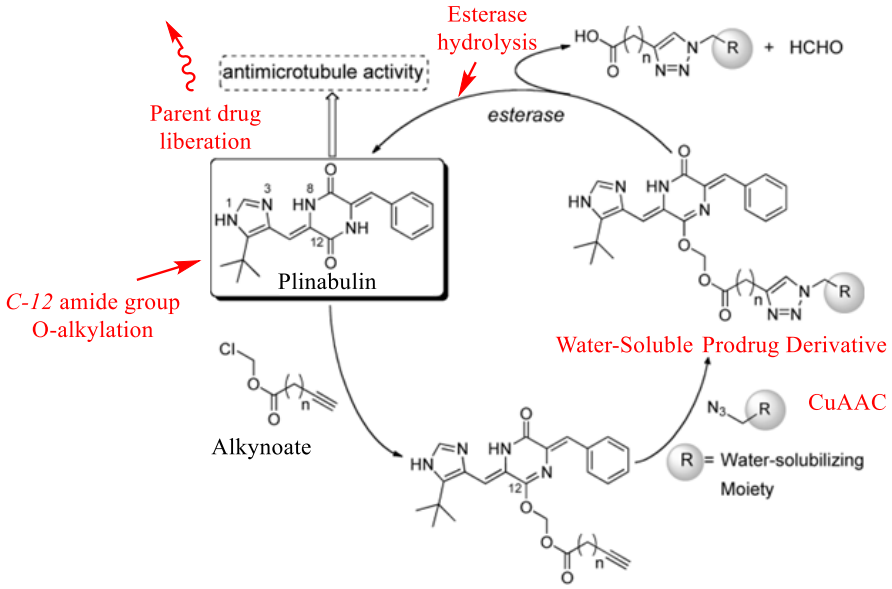
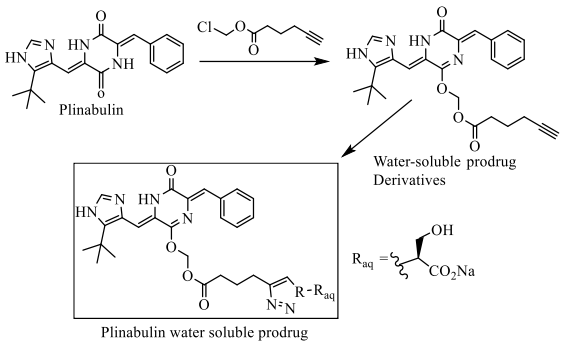


Figure 6. *Plinabulin prodrug synthesis and cleavage pathway using click chemistry for hydro-solubility properties enhancement (modified illustration).*[23]

By applying the click chemistry strategy via the prodrug approach Y. Hayashi and his research team were able to synthesise a moiety with hydro solubilisation potential, so that the linkage of the modified Plinabulin with serine-like water solubilizing moieties has afforded a prodrug with a high solubility capacity in which the Plinabulin low solubility in H_2O has been improved from <0.1 μg/mL to 6.38 mg/mL. The compound was tested *in vivo* in the presence of the esterase (extracted from liver pork), consequently under this condition the parent drug was liberated with a half-life of 59.9 min, as it is shown in figure 7 below.



Compound	Water solubility (mg/mL)	Half-life ($t_{1/2}$) (min)
Plinabulin water soluble prodrug	6.38	59.9
Plinabulin	<0.1 μg/mL	not tested

Figure 7. *Plinabulin prodrug synthesis (Left), and summarizing table of half-lives and the water-solubility of the prodrug and the parent drug Plinabulin (Right).*[23]

2.4.2.2. Click chemistry employment in synthesising our prodrug with high solubility potential

In light of previous studies and inspired by the idea of projecting and integrating the click reaction in the synthesis of our antineoplastic prodrugs that activate under hypoxic conditions with the aim of improving the prodrug solubility, different processes were carried out in order to obtain the appropriate final molecule matched to the main theoretical strategy.

Because aliphatic sp^3 nitrogens are a very bad leaving group in amides, in this work, we set out to look for a drug that had a more electronegative nitrogen, which could be released from the transporter at room temperature.

In this chapter Tacedinaline is used to bind to an acid chloride that in turn binds an azide and with the terminal alkyne through this reaction the corresponding triazole would be formed.[15]

The literature search led us to the previously mentioned Tacedinaline, in which the aromatic nitrogen must be rapidly expelled from the transporter once the nitro group has been reduced to the corresponding amine (Figure 8).

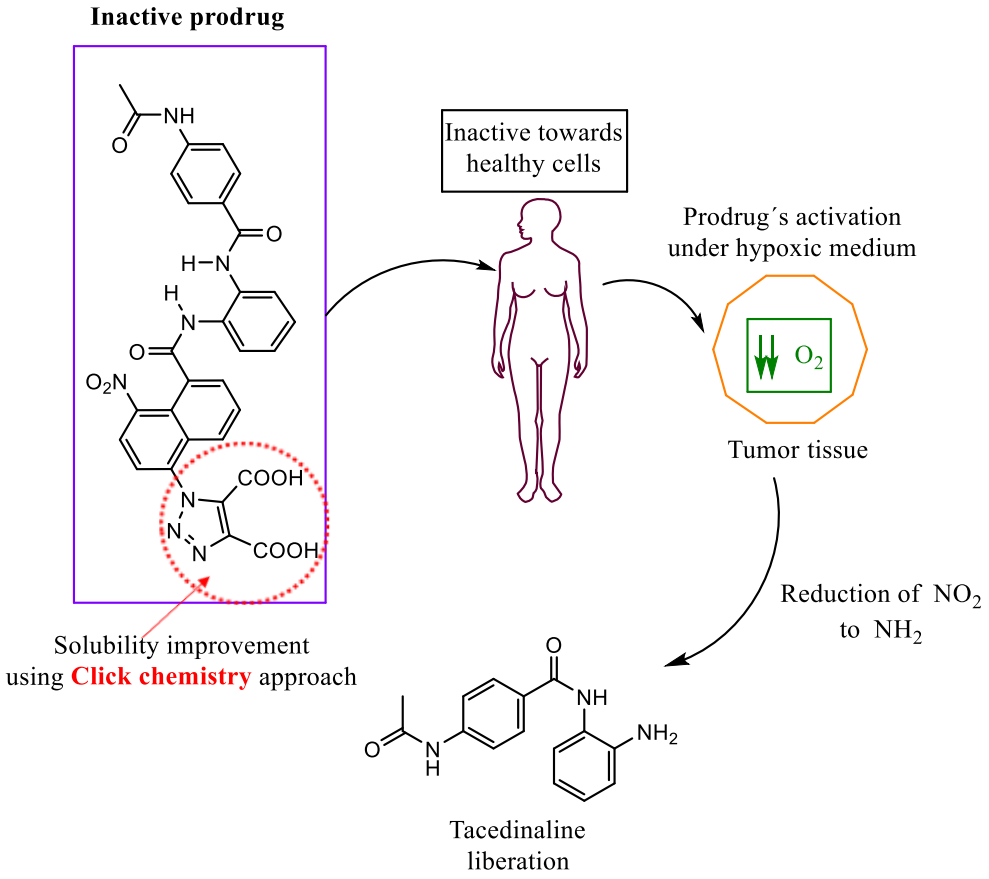


Figure 8. *Idea of prodrug activation inside the cancer cell (prodrug derived from click chemistry approach for solubility properties enhancement).*

To avoid the toxicity in healthy cells, Tacedinaline was linked to the transporter, which in this case is the ***5-bromo-8-nitro-1-naphtoic*** fragment (Figure 9). In this case, the presence of NO_2 under reducing tumor microenvironment (e.g. Hypoxia), will be reduced to the corresponding NH_2, releasing Tacedinaline.

In addition, the trigger was modified using an azide by nucleophilic aromatic substitution of the bromo atom which must subsequently allow the solubilization of the prodrug in the physiological environment after pertinent modification *via* click chemistry. The reaction of the azide with a suitable dipolarophile must generate the right prodrug, so that it can cross the physiological barriers. In this section, acetylenedicarboxylic has been chosen as a dipolarophile (Figure 9). The reaction of the azide with this compound must generate a triazole that supports two carboxylic acids.

Since these two acids must be in their carboxylate form under physiological environments, we expect the prodrug to have adequate water solubility for transport.

For Tacedinaline to be a cytotoxic compound, it must have a free aromatic amino group, since this amino is acylated in the prodrug, it is expected that there will be no longer cytotoxicity, at least related to histones.

Only in the reducing interior of the cancer cell, Tacedinaline must be released, and consequently DNA replication is prevented, because histones can no longer perform their function.

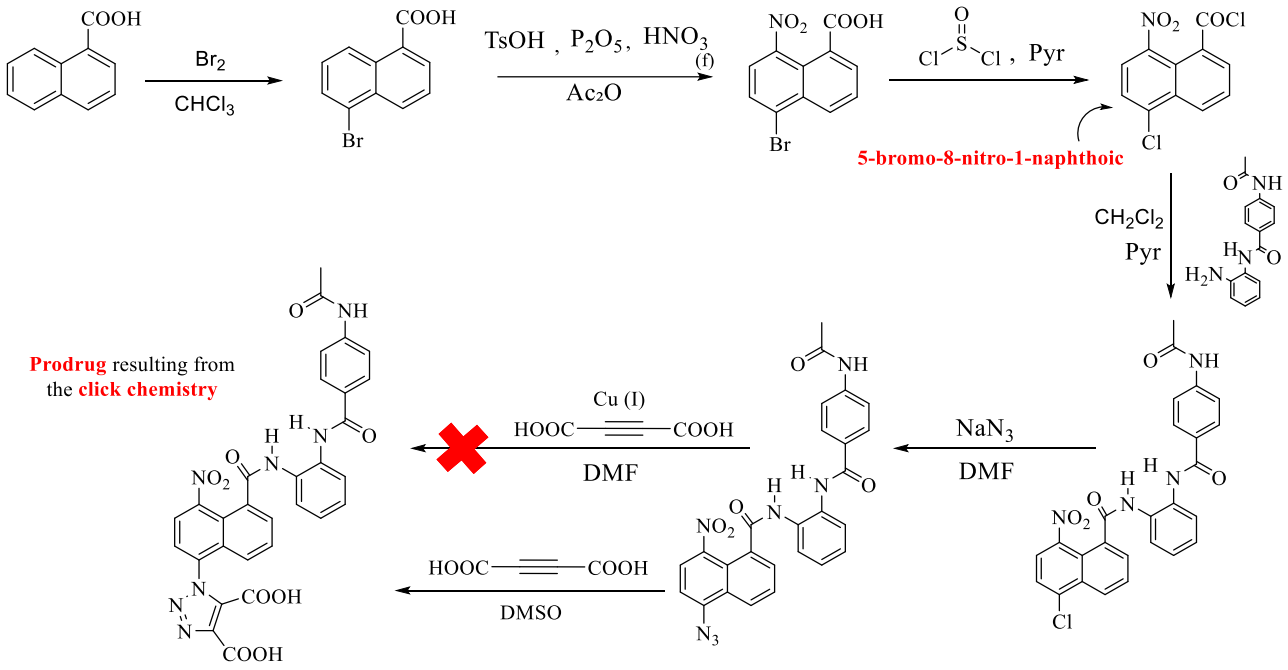


Figure 9. *Tacedinaline prodrug synthesis route using click chemistry.*

Surprisingly, the use of copper was ineffective, as its addition has affected the nitro group (decomposition), in which after finalizing all the synthesis steps arriving to the final one which is a simple click chemistry that takes the form of mixing the azide with acetylenedicarboxylic in the presence of copper (I) to give the expected triazole. Unfortunately, that was not the case since the copper has degraded the nitro, also a slightly high temperature was required to produce the coupling which has affected negatively the reaction product due to the sensitivity of the nitro.

For these reasons, the reaction was carried out in the absence of copper, then the expected prodrug linked to the triazole was obtained successfully. However, the complexity of its purification was a strong factor which has prompted us to look for a change in the molecular

design, in the strategy, and even diversifying the range of the used antineoplastic drugs (the parent drugs suspected of being released).

2.4.3. *Second strategy*: Thioglycolic acid integration

In order to improve solubility, a carboxylic group (have been installed directly in the structure of the prodrug consequently thioglycolic acid was selected to fulfil the strategy plan.

2.4.3.1. Thioglycolic acid (TGA)

Thioglycolic acid also known as mercaptoacetic acid is an organic compound which affiliate to thiols group with the formula $C_2H_4O_2S$, it is characterized by the fact that it contains both mercaptan and carboxylic functional groups[26] (Figure 10).

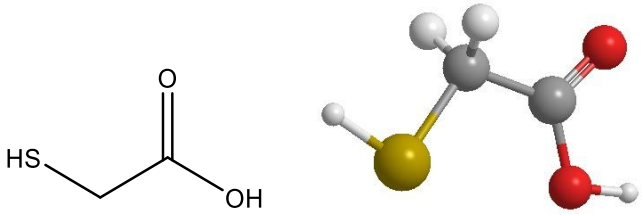


Figure 10. *2D and 3D representation of thioglycolic acid.*

2.4.3.2. Involvement of thioglycolic acid as an example belonging to carboxylic group in antineoplastic prodrugs solubilization

In order to achieve our goal in enhancing solubility for our moieties, the key chart was the design modification by the integration of thioglycolic acid and substituting the bromine atom from ***5-bromo-8-nitro-1-naphthoic acid*** aromatic ring by replacing it with a sulfur atom from the mercaptoacetic acid. Once the thioglycolic acid is attached, the resulting molecule is esterified, the desired antineoplastic drug (the cytotoxic molecule) is attached then the obtained compound is hydrolysed affording the last version of the expected selective, cytotoxic and water-soluble prodrugs (Figure 11).

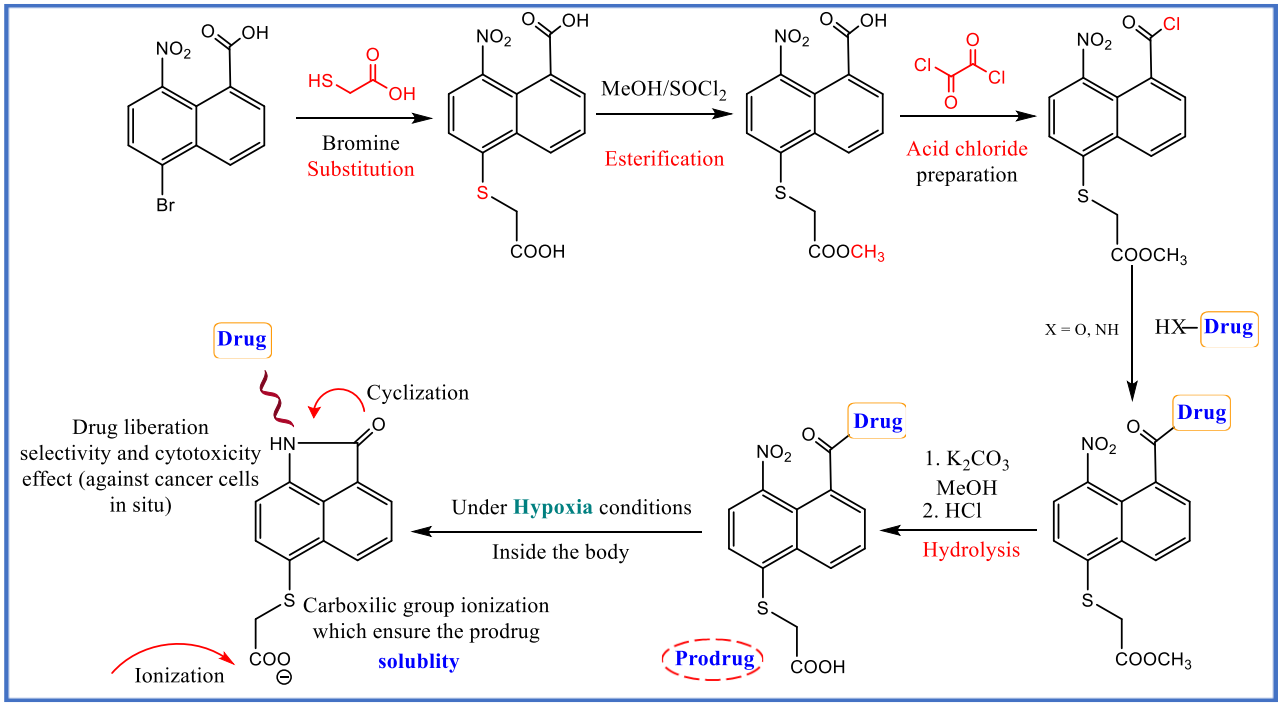


Figure 11. *The strategy of synthetizing the antineoplastic drugs with the selectivity, cytotoxicity and solubility properties (own elaboration).*

In fact, the improvement of prodrug solubility has been accompanied by a diversification in the range of cytotoxic substances that can be linked to the protective group, in this case four anti-cancer substances have been selected for the accomplishment of the master plan, cited as follows:

Farnesol, Pregnenolone, bis(2-chloroethyl)amine, Tacedinaline.
Since the bis(2-chloroethyl)amine "nitrogen mustard gas" and Tacedinaline were identified earlier, we address now the Farnesol and Pregnenolone definitions.

2.5. What is Farnesol?

Farnesol is a natural 15-carbon organic compound, uncoloured liquid oil with a sweet, soft and delicate smell, it has a chemical formula of $C_{15}H_{25}OH$ and a molecular mass of 222.372 g/mol, classified as an acyclic primary sesquiterpene alcohol which exists in essential oils of plants, in particular citronella, sandalwood, tuberose blossom, etc.[27,28,29] Even though Farnesol could be generated endogenously by the enzymatic dephosphorylation of farnesyl pyrophosphate (FPP), a catabolite of the cholesterol biosynthetic pathway in mammalian cells[30] (Figure 12).

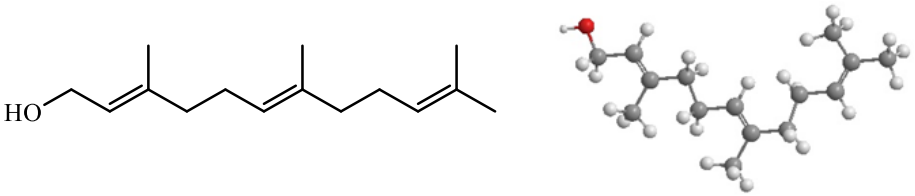


Figure 12. *2D and 3D representation of Farnesol.*[31]

2.5.1. Anticancer chemotherapeutic properties of Farnesol

Due to its anti tumor activity, Farnesol has been considered one from the natural compounds that gained a significant attention from years ago[28], in which it has been identified as an extracellular inducer of apoptosis[32], according to previous investigations. Farnesol anticancer capacities are represented by the tumorigenic proteins and signal transduction cascades in various tumor cell lines.

Additionnally, it is capable of decrease cancer cell proliferation, angiogenesis and survival while triggering apoptosis.[33,34,35]

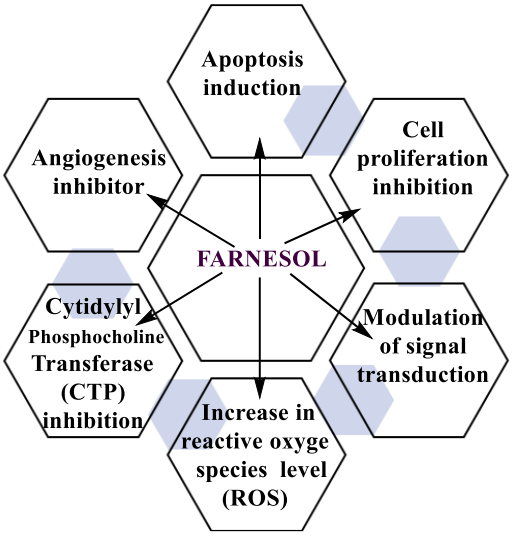


Figure 13. *Farnesol´s different signalling pathway and cytotoxic modes of action towards cancer cells (own elaboration).*

Beside its regulation of inflammatory responses and its benific efficiency on allergic asthma, Farnesol significantly affects a variety of human malignancies such as breast cancer, prostate cancer, pancreatic cancer, lung cancer, and multiple myeloma.[28] Despite the effect of farnesol is considered as unknown in inducing apoptosis in mammalian cells, several studies asserted that Farnesol inhibit Choline-Phosphate Cytidylyltransferase (CTP), consequently block the biosynthesis of phosphatidylcholine (PC) which is implicated at 50% in the eukaryotic phospholipid cell membrane formation, as a result, since cancer cells proliferate rapidly, the

mechanism require an accelerated membrane synthesis, as Farnesol acts by preventing phosphatidylcholine (PC) formation, thereby inhibiting cell progression[36] (Figure 14).

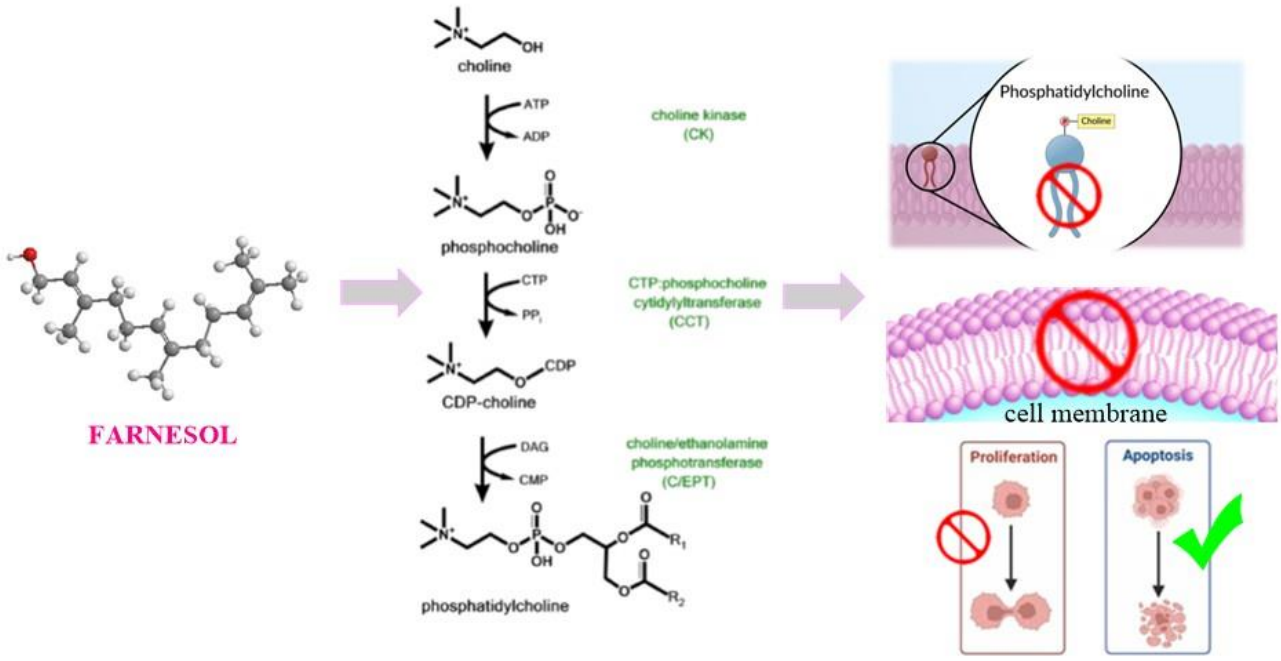


Figure 14. *Left: Biosynthesis pathway of phosphatidylcholine (PC). Right: Farnesol mode of action on cancer cells proliferation (own elaboration).*

Another substance which has been investigated as curative agent for cancer is pregnenolone. This compound is a hormone, and it has been proposed also for our prodrugs synthesis.

2.6. What is pregnenolone?

Pregnenolone also known as P5 or pregn - 5 -en-3β-ol-20-one is a naturally occurring steroidal estrogen, and cholesterol metabolite, it is identified as a pioneer for multiple range of hormones, such as estrogen, cortisone, testosterone, and progesterone (Figure 15).[37,38,39]

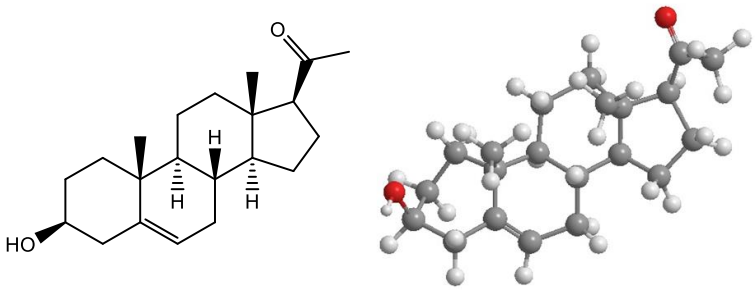


Figure 15. *2D and 3D representation of Pregnenolone.*

2.6.1. Anticancer chemotherapeutic properties of Pregnenolone

According to numerous studies Pregnenolone can be employed as an antitumoral substance in both *in vitro* and *in vivo* tests in which it can inhibit mammalian glucose-6-phosphate dehydrogenase activity (G6PD) at the concentration of 10^{-6} or even less.[40] This enzyme plays a crucial role for the pentose phosphate pathway (PPP) which is responsible of producing NADH that contributes in protecting the cell proliferation against the oxidative stress by stimulating the anabolic mechanism then cell growth.[41,42] Consequently high levels of G6PD contributes in cancer cells activity as well as resistance to apoptosis.[43] For these reasons G6PD dificiency approach has demonstrated a promissing outlooks for pregnenolone as an anticancer agent, since G6PD enzyme inhibition can lead to an oxidative stress in cancer cells which consequently cause their death[41,43] (Figure 16).

Specifically, some steroid derivatives have been shown to have anticancer properties; additionally, their superior capacity to cross cell membranes enhances their bioavailability.[44] Pregnenolone has been used as a model to synthetize steroid derivatives with enhanced anticancer properties.[44,45]

Formerly, Pregnenolone has been used and assessed for a range of biological fuctions in which when applied on different cancer cell lines such as PC-3, prostatic adenocarcinoma; MCF-7, mammary adenocarcinoma and SKLU-1, lung adenocarcinoma, they have exhibited strong cytotoxic action and high cell permeability.[46,47,48]

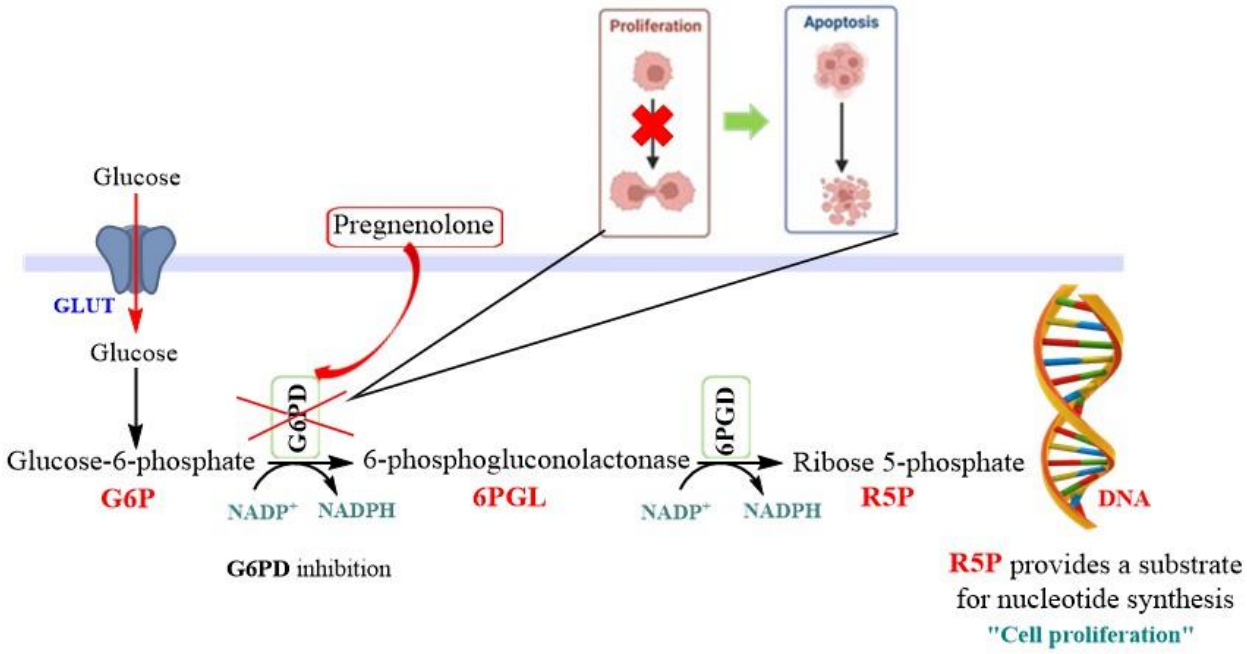


Figure 16. *Pregnenolone mode of action against cell proliferation by inhibiting the action of the G6PD enzyme in the Pentose Phosphate pathway (PPP) own elaboration.*

As a result of applying the second strategy, 4 prodrugs were supplied as it is mentioned below (Figure 17).

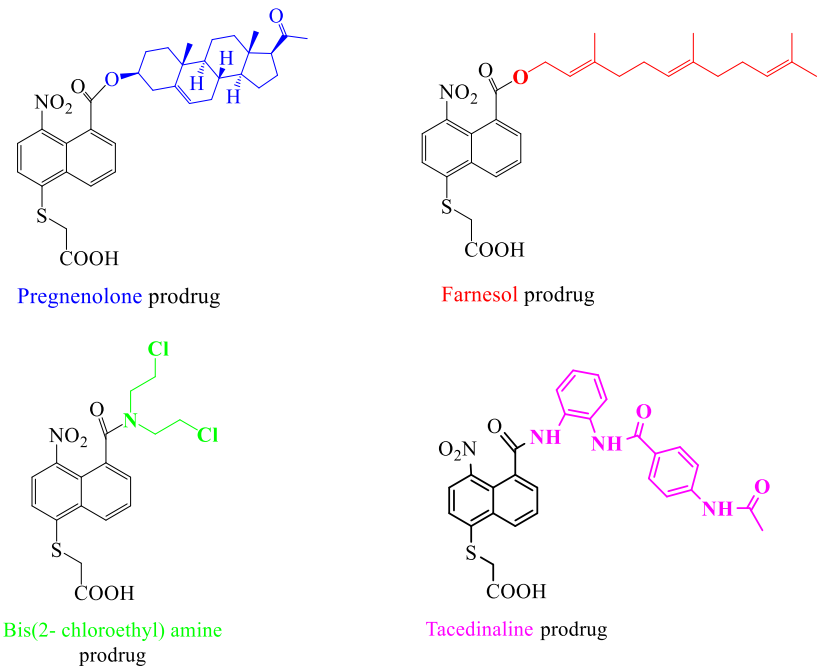


Figure 17. *The synthetized antineoplastic prodrugs with the hydro-solubility enhancement property (carboxylic acid functional group).*

3. Methodology

3.1. Synthesis of 5-azide-8-nitro-1-naphtoic acid

Compound **3** was synthesized following the procedure described in Chapter 2. The substitution of bromine in the aromatic ring is hampered by the low solubility of naphthoic acid in organic solvents. To find a suitable solvent, experiments were done in EtOH, MeOH and DMF. Of these three solvents, DMF was chosen because it proved to be the best solvent for naphthoic acid. Because sodium azide is an ionic compound that is highly insoluble in organic solvents, water was included in the reaction medium, as the hydrogen bonds in the water should favour the solubilization of the azide.

In a first experiment, the reaction at room temperature was attempted. After an hour of stirring, a ^{1}H-NMR spectrum was performed to study the progress of the reaction because a color change from yellow to dark brown had been observed. The ^{1}H-NMR spectrum showed that despite the change in coloration, no appreciable amounts of the azide **4** had been generated (Figure 18), since only the signals of the original bromide were observed.

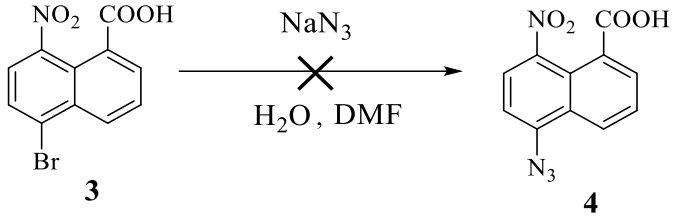


Figure 18. *Synthesis of compound **4**.*

In a second experiment, we avoided the presence of water. Hydrogen bonds with azide reduce its reactivity, as these interactions must be broken to attack the aromatic ring. The same amounts of the reagents were used, but in this case without adding water. To obtain a homogeneous reaction mixture, the reaction was heated in a silicone oil bath at 60ºC, and the color change was observed again. It should be noted that as it is a prodrug, it is preferable to have light colors, it is a very important characteristic to achieve an adequate performance, since the dark color is usually associated with obtaining resins.

In this case, after four hours, it was verified with a ^{1}H-NMR spectrum that we had obtained the substitution of bromine for azide (Figure 19).

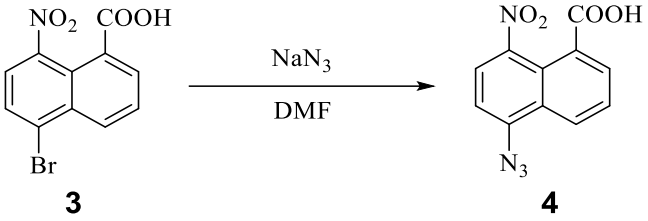


Figure 19. *Synthesis of compound **4**.*

3.2. Optimisation: Synthesis of Tacedinaline

Tacedinaline is not a commercial compound, so it has been necessary to carry out its synthesis. Figure 23 shows a logical retrosynthesis to carry out the preparation of this drug. Some steps have been improved from the synthesis carried out in Chapter 1.

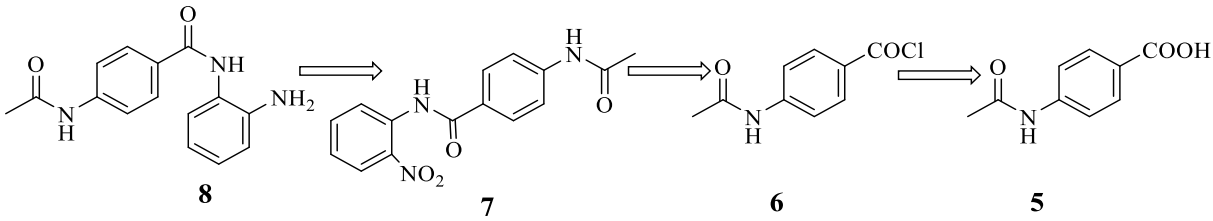


Figure 20. *Retrosynthesis of Tacedinaline preparation.*

Synthesis began with acetylation of 4-aminobenzoic acid. This compound is commercial and very economical because it has industrial utility. Acetic anhydride was used for acetylation. The addition of small portions of 4-aminobenzoic acid to acetic anhydride initially generates a rapid increase in temperature of the reaction mixture that remains homogeneous. Subsequently, the addition of more 4-aminobenzoic leads to precipitation of the corresponding acetate. The addition of water allows the hydrolysis of the acetic anhydride, and the filtration of the reaction mixture leads to quantitative yield of the expected acetate.

The mechanism of this reaction consists of the nucleophilic attack of the amine on the carbon of the carbonyl of acetic anhydride, then the double bond of oxygen is re-established and the acetate as the leaving group, acting in turn as a base and abstracts a proton from the amide generating the reaction product (Figure 21).

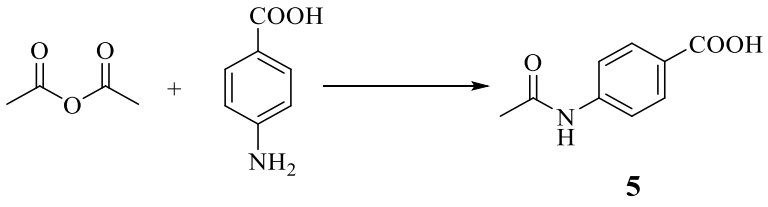


Figure 21. *Para-aminobenzoic acid acetate formation.*

To obtain the *para*-aminobenzoic acid chloride, thionyl chloride and phosphorus pentachloride were studied. In either case, complex mixtures were obtained. We believe that the reason is the lack of solubility of *para*-aminobenzoic acid acetate in thionyl chloride or in the chloroform used as a solvent in the phosphorus pentachloride reaction. Because it has to be heated, not only the acid reacts, but also the acetate group, finally generating the aforementioned mixtures. In order to be able to work at low temperatures and in milder conditions that do not involve the reaction of acetate, we consider using the triethylammonium salt of the aforementioned acid. Triethylammonium salt was obtained by adding a molar excess of triethylamine to a suspension of methylene chloride acid (Figures 22 and 23).

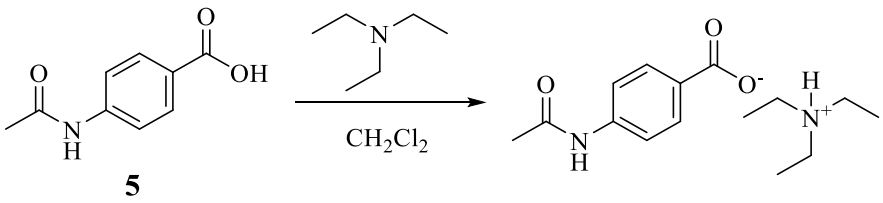


Figure 22. *Triethylamine utilization.*

The evaporation of methylene chloride and the excess of triethylamine generates the corresponding triethylammonium salt, which is a colorless solid. The addition of methylene chloride generates a suspension of the triethylammonium salt, and the addition of thionyl chloride to this suspension allows, after heating to 40ºC, to obtain a homogeneous solution of the acid chloride, but this solution strongly colors and the final yield of the acid chloride is low. The mechanism of the acid chloride formation reaction is shown in figures 23 and 24.

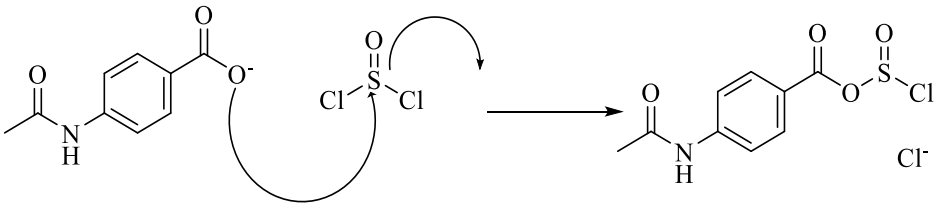


Figure 23. *Attack on sulfur from thionyl chloride releasing chloride.*

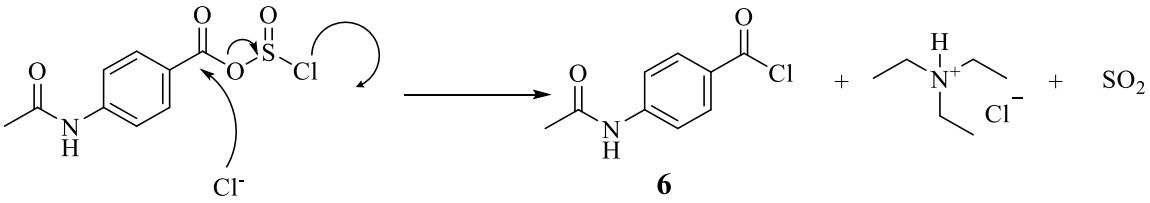
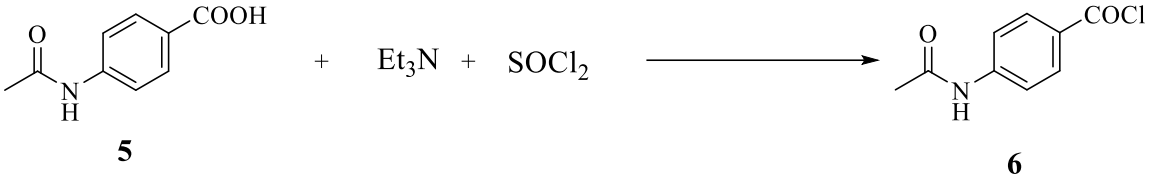


Figure 24. *Rearrangement to obtain compound **5**.*

In turn, the chloride attacks the carbonyl and forms acid chloride since it is a more active and electrophilic form, so that the corresponding acid chloride is subsequently formed.



5 **6**

Figure 25. *Reaction of compound **6** formation.*

To avoid loss of performance in the formation of acid chloride, it was necessary to work under milder conditions, where no heating of the reaction mixture took place. To achieve these conditions, a solution of the triethylammonium salt of *para*-aminobenzoic acid was prepared. Because *para*-aminobenzoic acid is not very soluble in methylene chloride, it was necessary to add a large amount of methylene chloride to reach a homogeneous solution. Under these conditions, the addition of one equivalent of thionyl chloride rapidly generates the acid chloride and only methylene chloride needs to be evaporated to obtain the reaction product with a high yield and a pale-yellow color.

To avoid the use of a high amount of methylene chloride, we develop other conditions, in which a fair equivalent of triethylamine is added to the suspension of *para*-aminobenzoic acid, and before the precipitation of the triethylammonium salt occurs, a small molar excess of thionyl chloride is added.

The evaporation of methylene chloride again generates colored acid chlorides because methylene chloride (boiling point = 39.6ºC) is more volatile than thionyl chloride (76ºC) which is used in excess, so at the end of evaporation the excess thionyl chloride must react with the acetamide reducing the performance of the reaction. To destroy the excess thionyl chloride, the solution of acid chloride in methylene chloride was washed with water. This procedure allows the triethylammonium hydrochloride to be removed, as this compound is very soluble in water. While the hydrochloride of triethylamine was successfully removed, the solution now showed a precipitate that turned out to be the starting para-acetamido benzoic acid., which was produced by hydrolysis of the acid chloride.

To avoid the hydrolysis of the acid chloride, the reaction was carried out at 0ºC using water and ice, and even using brine to lower the temperature of the ice bath further, but in all cases, mixtures of acid chloride with the corresponding acid were obtained, so this procedure was discarded.

An alternative solution was to add toluene to the reaction mixture. Because toluene boils at 111°C, evaporation of the solvent under vacuum must allow the distillation of thionyl chloride while the acid chloride is still diluted in the toluene, thus avoiding the strong coloration of the reaction.

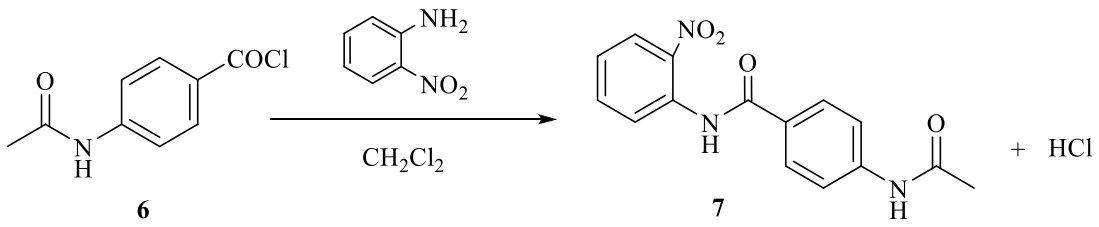
Next, the acid chloride is treated with an amine, in our case it will be 2-nitroaniline.

The general reaction of amides with acid chlorides usually takes place in the presence of a non-nucleophilic auxiliary amine. The reason is that the reaction generates hydrochloric acid that protonates the starting amine. In general, the protonated amine is no longer reactive, so the performance of the reaction would have ended in the absence of the auxiliary base at 50% at most. For this reason, the reaction of 2-nitroaniline with *para*-acetamido benzoic acid chloride was initially carried out in pyridine.

The results were not satisfactory, as the reaction was very slow. Non-nucleophilic pyridines, such as collidine and lutidine, were also tried, but again slow reactions were obtained in which the reaction mixture needed to be heated, obtaining strongly colored compounds that showed partial resinification.

Surprisingly, the reaction in methylene chloride of acid chloride in the presence of a small excess of 2-nitroaniline gave very good results. The reaction mixture is heated in a water bath (60ºC) and the methylene chloride evaporates. After 2 hours, when there is no methylene chloride left, the reaction is complete.

We believe that this surprising effect occurs because 2-nitroaniline is a very weak base, since it is conjugated with the aromatic nitro group and therefore resembles an alcohol. The hydrochloric acid that is generated in the reaction is likely to generate general acid catalysis, which accelerates the process, while the distillation of methylene chloride must partially wash away the acid that is generated, as hydrogen chloride is a gas.



6 **7**

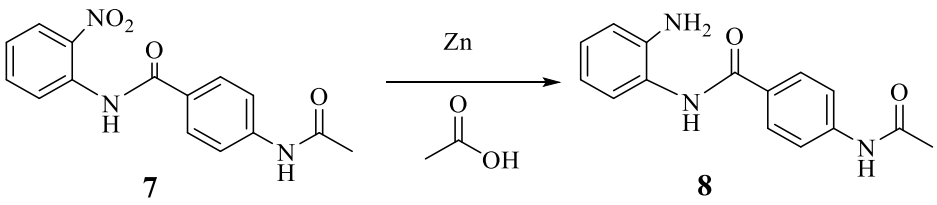
Figure 26. *Acylation of 2-nitroaniline in which HCl is generated which surprisingly does not inhibit the reaction of 2-nitroaniline with acid chloride.*

Finally, in order to obtain Tacedinaline, the NO_2 has to be reduced to NH_2.

The reaction of the nitro group to transform it into the amino of Tacedinaline was carried out using Zn dust.

This reaction only proceeds well if it is very fast, otherwise the amine obtained can react with the starting nitro group or with the reduction intermediates, which are the derived nitrous and hydroxylamine, these reactions generate azobenzene, azoxybenzenes and other products. To ensure that the reduction reaction is as fast as possible, powdered Zn is used and heated by stirring in a bath at 60ºC with acetic acid until a paste-like solution remains.

Under these conditions, the Zn oxide layer that prevents reduction had to be transformed into Zn acetate, leaving the metal surface active to transfer electrons rapidly to the nitro group of the substrate.



7 **8**

Figure 27. *Reduction for the formation of Tacedinaline.*

Once the reaction has been carried out, ethyl acetate is added, and the metallic Zn and Zn acetate generated are filtered. The evaporation of the solvent generated the desired phenylenediamine. It should be noted that at a temperature greater than 60ºC, the corresponding benzimidazole is partially formed. This structure is shown in figure 28 and is the logical product of the attack of the free amino group on the carbonyl of acetamido benzoic.

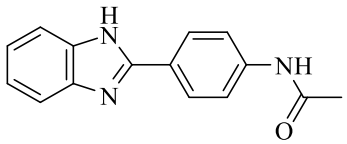


Figure 28. *Structure of N-(4-(1H-benzo[d]imidazole-2-yl)phenyl) acetamide.*

Small amounts of the benzimidazole can be separated from Tacedinaline easily by crystallization into methanol, since the benzimidazole is a much more soluble compound in this medium.

3.3. Coupling of Tacedinaline with the protective group

The first proposal was to add 5-azide-8-nitro-1-naphtoic acid, methylene chloride, HATU (Hexafluorophosphate Azabenzotriazole Tetramethyl Uronium), a reagent used in peptide coupling chemistry to generate an active ester from a carboxylic acid and DIPEA (base). This reaction took place at 0ºC. After about 25 minutes, the reaction mixture was analysed by ^{1}H-NMR and the result was the formation of the acyl triazolopyridine obtained in figure 29.

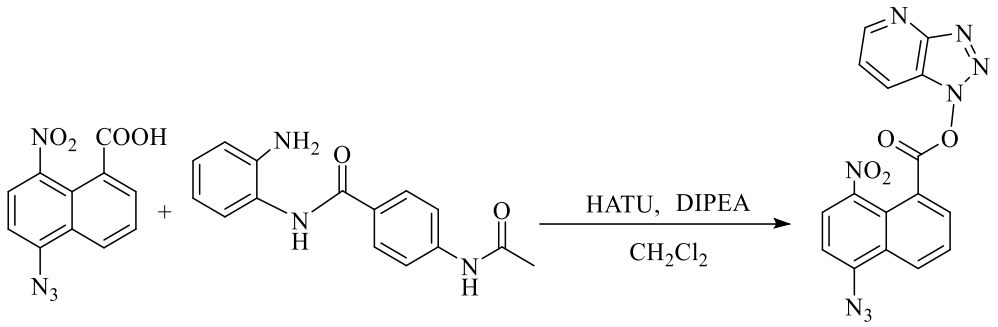


Figure 29. *Acyl triazolopyridine synthesis using HATU reaction.*

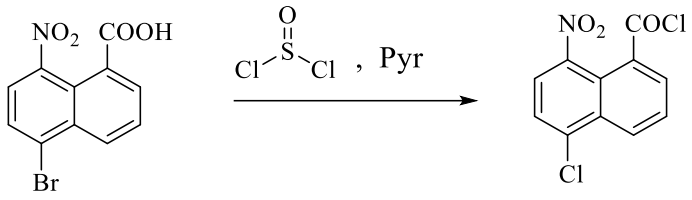
Because acyl triazolopyridine did not react readily with the amino group of Tacedinaline, we decided to transform naphthoic acid **3** into the corresponding acid chloride.

To do this, we initially use thionyl chloride. The naphthoic acid turned out to be insoluble in thionyl chloride, so it was necessary to reflux for two hours to carry out the reaction. At the end of this time the reaction becomes homogeneous, but the yield of the acid product is very poor, as resinification products appear, probably due to the reaction of thionyl chloride with the nitro group.

Looking for a gentler procedure, we added pyridine to the reaction medium. The presence of pyridine catalyzes the formation of naphthoic acid chloride. By heating the reaction mixture to 60ºC for 10 minutes, the acid chloride is slightly yellow, and a high yield is obtained.

A subsequent study of the products of the reaction showed that the bromine atom has been replaced by a chlorine in the acid chloride. This reaction is unexpected, but we were able to confirm it, as the hydrolysis of acid chloride in water/THF generates a different naphthoic acid than the original bromo-naphthoic acid (see Chapter 3).

The spectroscopic data for compounds **3** and **9** coincide with those described in the literature.[18]



3 **9**

Figure 30. *Compound **9** reaction.*

The coupling of Tacedinaline with naphthoic acid chloride also proved to be a problematic reaction. On the one hand, naphthoic acid chloride is not very stable, and decomposes over time, even at room temperature, while Tacedinaline is poorly soluble in organic solvents.

Because Tacedinaline has a basic nitrogen, an auxiliary base is also required, and in general, acid chloride breaks down in the presence of basic compounds. The first conditions to be tested to carry out the coupling were of the Schotten-Baumann type. As a base, a concentrated solution of sodium carbonate in water was used and the chloride of naphthoic acid was dissolved in ethyl acetate and solid Tacedinaline was added.

Since Tacedinaline is not very soluble in ethyl acetate, the reaction is slow. Over time it becomes colored and finally the yield is very low due to the formation of resins. To prevent the reaction from being heterogeneous, pyridine solvent was used. Pyridine does dissolve Tacedinaline well and serves as an auxiliary base. The addition of naphthoic acid chloride to the solution of Tacedinaline in pyridine at room temperature rapidly generates a very dark color, which reveals extensive resinification of the reagents.

Analysis of the ^{1}H-NMR reaction, on the other hand, showed that a small amount of the desired coupling product had been produced.

To find milder reaction conditions, the addition of the solution of Tacedinaline in pyridine on a dilute solution of acid chloride in methylene chloride was carried out.

Again, the first drops of the Tacedinaline solution led to a strong coloration of the acid chloride solution, but the analysis of the reaction by ^{1}H-NMR showed that the yield of the desired product *N*-(2-(4-acetamidobenzamide)phenyl)-5-chloro-8-nitro-1-naphthamide had been superior.

In another test, the same conditions were repeated, but by cooling the acid chloride solution to 0ºC. Again, a lot of coloration was obtained, but the yield improved again.

Following this same strategy, the reaction was repeated by cooling the acid chloride solution to -70ºC. Although coloration is generated again, it is much weaker than in the previous cases and, on the other hand, the addition of aqueous hydrochloric acid to the reaction medium strongly discolors it.

In addition, under these conditions the coupling product precipitates, so the simple filtration of the reaction medium has allowed us to isolate the crude coupling product.

Crystallization in methanol makes it possible to obtain this pure compound with an acceptable yield.

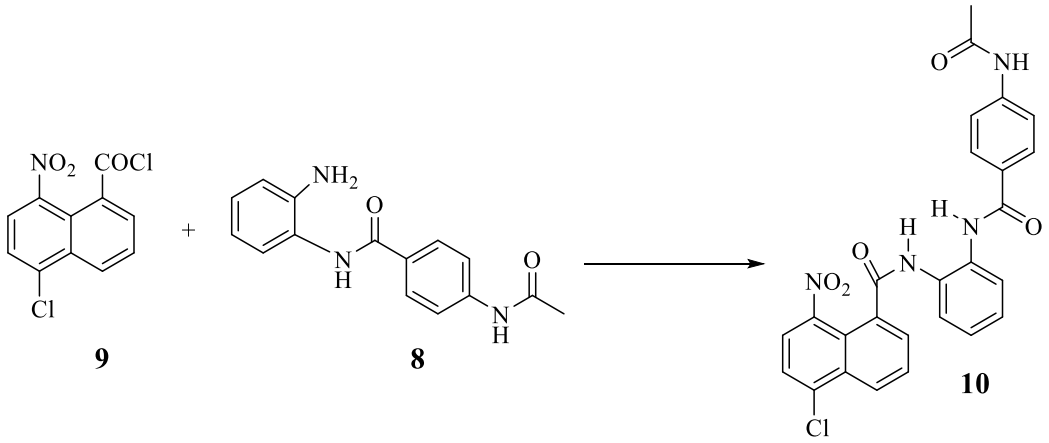


Figure 31. *Protected Tacedinaline synthesis.*

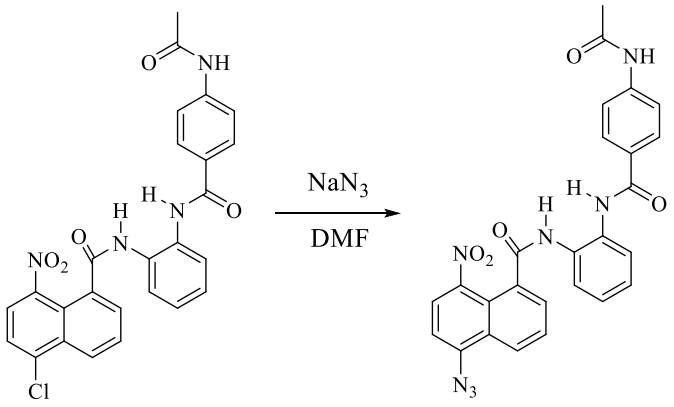
Tacedinaline, protected with naphthoate, is a compound that is very insoluble in water, and for this reason physiological activity must be very poor. Drugs must be able to cross both polar and nonpolar barriers, so if we want to transport Tacedinaline into the cells, we must develop a compound that is more water-soluble. In order to improve the water solubility of protected Tacedinaline, we plan to introduce polar groups such as carboxylates, polyols or ammonium groups into the structure.

Fortunately, the presence of the chlorine atom, a good leaving group, should allow some of these groups to be easily introduced into naphthalene in our molecule.

An attractive solution for introducing carboxylates is the use of a click reaction as shown in figure 33.

To carry out the click reaction, it is necessary to have an azide group in the molecule. This group was introduced into naphthalene using sodium azide and DMF solvent. Because DMF is an aprotic polar solvent, it dissolves sodium azide well without reducing the reactivity of the azide group, as it does not form hydrogen bonds with it. To reduce the reaction time and work at as low a temperature as possible, a high concentration of sodium azide was used.

Under these conditions the reaction is completed in 1 hour and a quarter at 60ºC. Again, the reaction product is purified by crystallization into methanol.



10 **11**

Figure 32. *Compound **11** synthesis.*

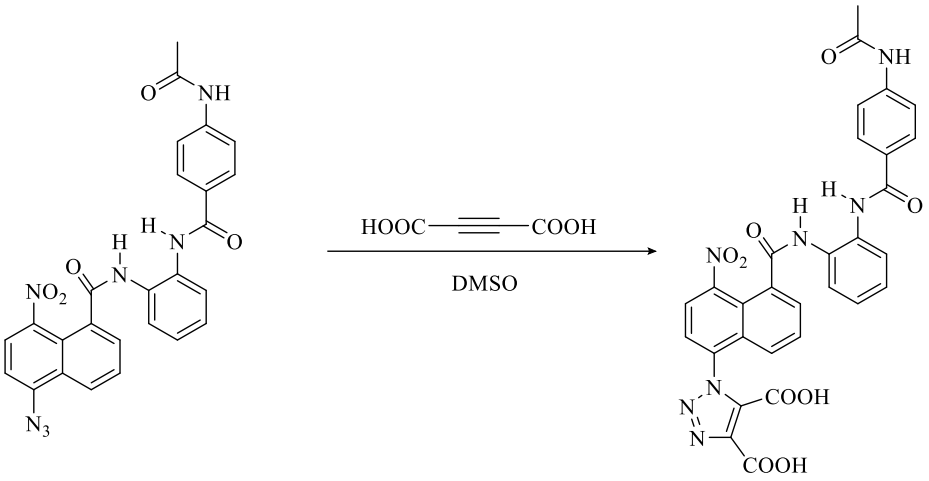
3.4. Synthesis based on click reaction

The last step is supposed to be a simple click reaction, in which mixing the azide with the acetylenedicarboxylic acid in the presence of Cu(I) generates the corresponding triazole, but in our case, the addition of Cu(I) led to a strong staining and decomposition of the azide.

Because it is possible for Cu(I) to generate radicals in the nitro group, by transferring an electron, we tried to carry out the reaction in the absence of copper. We were unable to get the azide to react with the dipolarophile at room temperature, so it was necessary to heat the reaction to 90ºC for four hours. At the end of this time, the presence of the starting material in ^{1}H-NMR did not seem evident, so the reaction was worked out by adding water and filtration. From 200 mg of the azide, 230 mg of the coupling product was obtained, so initially it could be thought that the reaction had been successful.

Due to the complexity of the ^{1}H-NMR spectrum, silica gel column chromatography was carried out, eluting with chloroform/methanol mixtures of increasing polarity, in which it was possible to separate two different products.

The ^{1}H-NMR of the less polar fraction (90mg) showed the presence of a compound that we have not been able to identify and the starting material, while in the more polar fractions (80mg) the desired triazole could be identified (Figure 33).



11 **12**

Figure 33. *Compound **12** synthesis using Click reaction.*

The spectroscopic properties of triazole agree with the expected structure.

The mass spectrum shows the molecular peak at 623.13 uma, again confirming the expected structure.

Compound **12** is not soluble in water directly, but the addition of potassium carbonate, which deprotonates the carboxylic acid, does allow the solubilization of our compound by the formation of potassium salts.

The ^{1}H-NMR spectrum allows the identification of all prodrug signals and is shown in figure 34.

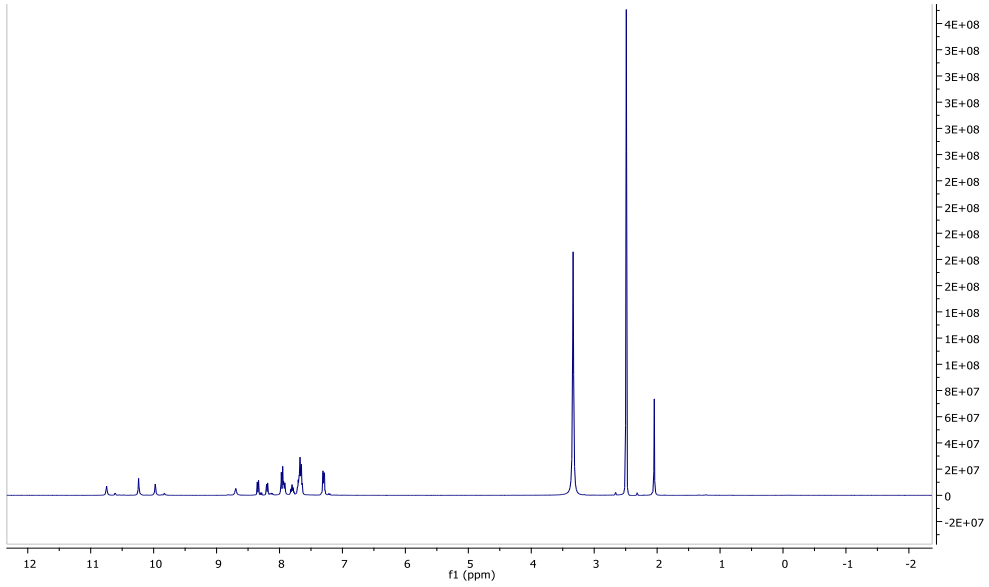


Figure 34. *^{1}H-NMR spectrum of the obtained prodrug (compound **12**) from click chemistry reaction.*

3.5. Bioreductive medium mimicry

Actually, once the definitive version of the prodrug was obtained, a mimicking of the hypoxic conditions (reductive medium) was necessary to approve the parent drug liberation under the expected conditions and the desired site. To accomplish the process zinc and acetic acid were employed to carry out the reduction in collaboration with ^{1}H NMR control for the chemical validation.

In order to confirm that the reduction of the nitro group releases the real drug, Tacedinaline, the solution of the potassium salt of the prodrug and excess zinc dust was added to an NMR tube. After stirring the solution (1 minute), the ^{1}H-NMR spectrum was recorded, in which the signals from the Tacedinaline protons could be observed.

It should be noted that the chemical displacements of these protons do not correspond to those of free Tacedinaline, we believe that a complex must have formed with Zn that we have not been able to break up so far. In addition, the reduction with Zn has not allowed us to observe the protons of the lactam expected after the attack of the amino to the carbonyl of the naphthoic acid.

It is possible that the Zn salt of the reduction product is insoluble in the aqueous medium and therefore its protons do not appear in the ^{1}H-NMR spectrum.

To confirm that the release of Tacedinaline did occur after the reduction of the nitro group, the reaction in acetic acid was carried out at 60ºC, which are the same conditions in which we have previously obtained Tacedinaline, by reduction of the corresponding nitro group.

This reaction was worked up by the usual method, adding ethyl acetate to the acetic acid of the reaction mixture and filtering the Zn and the corresponding salts. The evaporation of the solvents allowed us to obtain in a mixture of chloroform/methanol a spectrum superimposable with that of Tacedinaline, thus confirming the release of the drug.

Again, the absence of lactam signals associated with drug release is surprising. Looking for where the lactam had gone, the Zn and its salts were extracted with dimethyl sulfoxide and the corresponding ^{1}H-NMR spectrum was carried out.

In this spectrum, large signals of Tacedinaline could be observed, which still presented the Zn salts, as well as small signals assignable to lactam, so we believe that indeed the Zn salts of lactam must be very insoluble.

Because the reduction inside the tumor cell does not require the use of Zn, we have not looked further for lactam, as we consider it not relevant for the therapeutic effect of this prodrug.

3.6. Synthesis of prodrugs soluble in water using a thioglycolic acid fragment

Following the second strategy plan, a new design was created starting by the protective group modification (TGA integration) as mentioned in Figure 35.

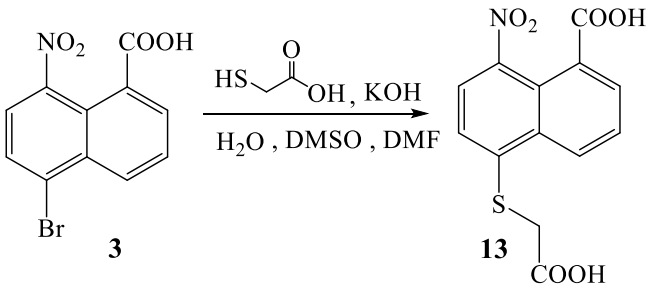


Figure 35. *Synthesis of compound **13**.*

Direct nucleophilic substitution of the bromine atom from the 5-bromo-8-nitro-1-naphthoic acid was realized by using thioglycolic acid potassium salt dissolved in water, however since the naphthalene derivative has a lack of solubility, the problem was solved by using the combination of two solvents DMSO and DMF to dissolve it, the two fractions were mixed by

stabilizing the temperature (below 10ºC). The final compound was obtained by treating the mixture with hydrochloric acid (2M) then filtered.

3.6.1. Fischer Esterification

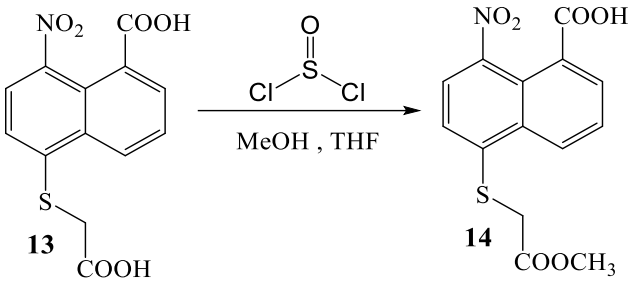


Figure 36. *Synthesis of compound **14.***

Once compound **13** was obtained, Fischer esterification was realized using methanol, THF and thionyl chloride as a catalyst for HCl production within the reaction mixture, the reaction lasted almost 1 hour. The reaction was worked up following the usual method removing the excess of the solvents under vacuum, then the concentrated mixture was crystallized using methylene chloride to obtain the pure compound with an acceptable yield (88%).

Actually, the esterification step was made in order to block or protect the carboxylic group of the thioglycolic acid from any cross-interaction in the next chemical reaction.

3.6.2. Acid activation using $C_2O_2Cl_2$

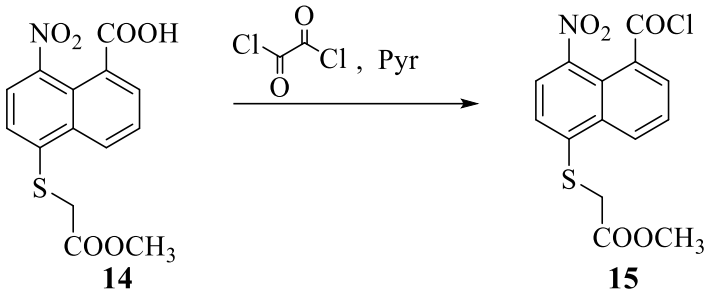


Figure 37. *Naphthoic acid chloride formation (compound **15**).*

Carboxylic acid was transformed into carboxylic acid chloride using oxalyl chloride to produce the naphthoic acid chloride and to facilitate the subsequent antitumor drugs linkage under given conditions.

However, the preparation of the naphthoic acid chloride is complicated since it is sensitive and instable even at room temperature and can generate other byproducts (see chapter 5).

Also, the addition of pyridine traces within the reaction mixture was necessary due to the naphthoic acid insolubility nature and the heterogenicity of the reaction which can affect the reactivity rate, then the obtained final compound has been used in some of the following reactions without further purification (unstable).

3.6.3. Antineoplastic agents' attachment

3.6.3.1. *Pregnenolone Prodrug*

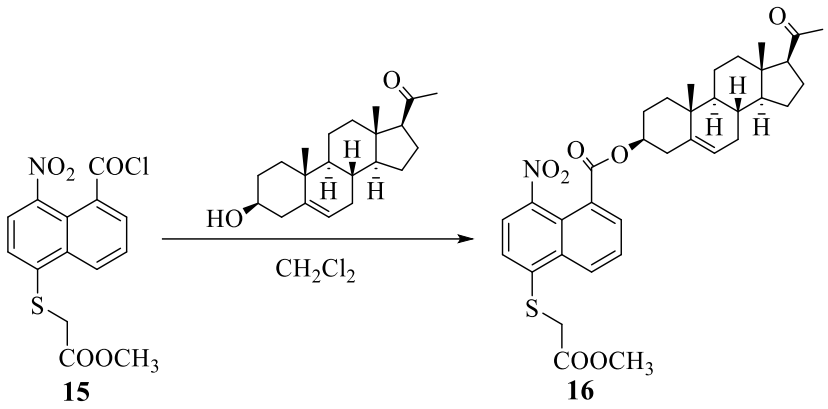


Figure 38. *Synthesis of compound **16**.*

Because Pregnenolone is known as sparingly soluble compound in the aqueous media and in order to increase its solubility, pregnenolone was attached to compound **15** thanks to the presence of the chlorine atom which is a good leaving group that enables the pregnenolone to be simply linked to the naphthalene acid chloride.

For these reasons compound **15** was prepared according to the general procedure of acid activation using $C_2O_2Cl_2$, then diluted in CH_2Cl_2, the commercial pregnenolone was poured over the reaction mixture under milder conditions, next the crude final compound was obtained evaporating the organic solvents and purified by silica gel column using CH_2Cl_2 as eluent.

3.6.3.2. *Farnesol prodrug*

Due to its interesting anticancer properties, Farnesol was selected to be employed in the synthesis of an antineoplastic prodrug, however because of its hydrophobicity, the solubility enhancement was indispensable. First and foremost, the naphthalene acid chloride was prepared according to acid activation using $C_2O_2Cl_2$ in order to attach the farnesol, several modifications of the temperature (0 ºC, -78 ºC, rt) and the solvents (CH_2Cl_2, THF, DMF, TOPO, etc) have been employed in order to improve the reaction process, unfortunately the results were not good enough because of the inability to produce the final molecule.

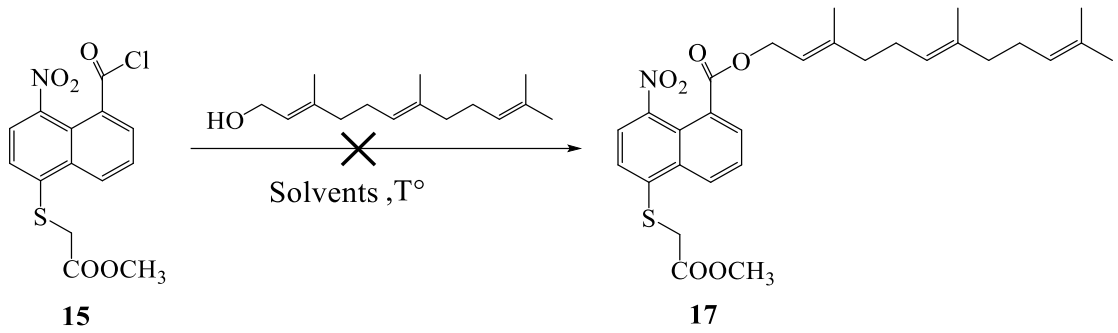


Figure 39. *Defective synthesis of Farnesol prodrug.*

For these reasons the strategy has been modified by synthetizing farnesol iodide, and attach it to compound **14** directly under milder conditions by the employment of a base which is in this case DIPEA (*N*,*N*-Diisopropylethylamine) and chloroform as solvent (Figure 40).

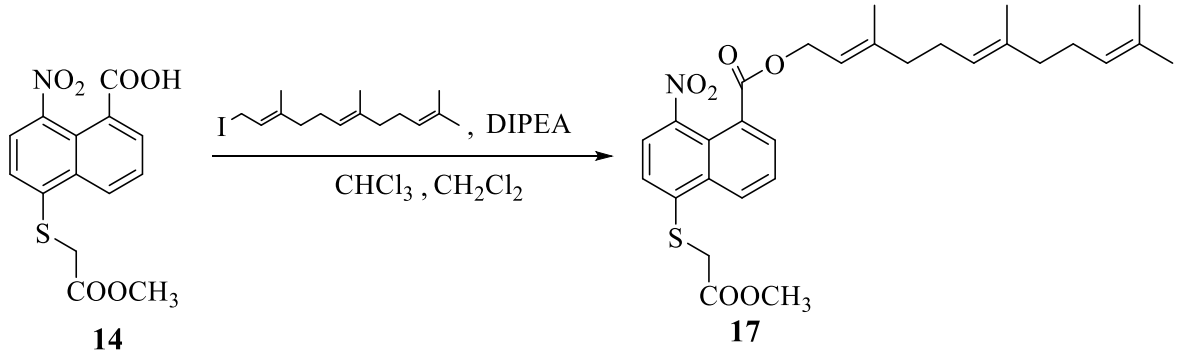


Figure 40. *Synthesis of compound **17**.*

3.6.3.3. *Bis(2-chloroethyl)amine prodrug*

Actually, in the majority of cases, the antitumour drugs coupling with our protective group always requires the naphthoic acid chloride synthesis, also in the case of bis(2-chloroethyl)amine "nitrogen mustards" (NMs) which are bifunctional alkylating agents extensively employed in the clinical treatment of cancers.

The first idea for the attachment was to liberate the free amine from the commercial bis(2-chloroethyl)amine hydrochloride using sodium hydroxide and water then extracting it with ether.

The putative acid chloride of compound **14** was prepared dissolving it in oxalyl chloride. Then, Schotten-Baumann conditions with Na_2CO_3 and EtOAc were used to anchor bis(2-chloroethyl)amine. Surprisingly, a new compound was obtained in 70% yield and the expected

amide was only obtained in traces amount (Figure 41). To explain the obtention of compound **14B**, we propose the formation of compound **14A** instead of the acid chloride of compound **14**. Then, a rearrangement generates **14B**, as it will be explained in Chapter 5.

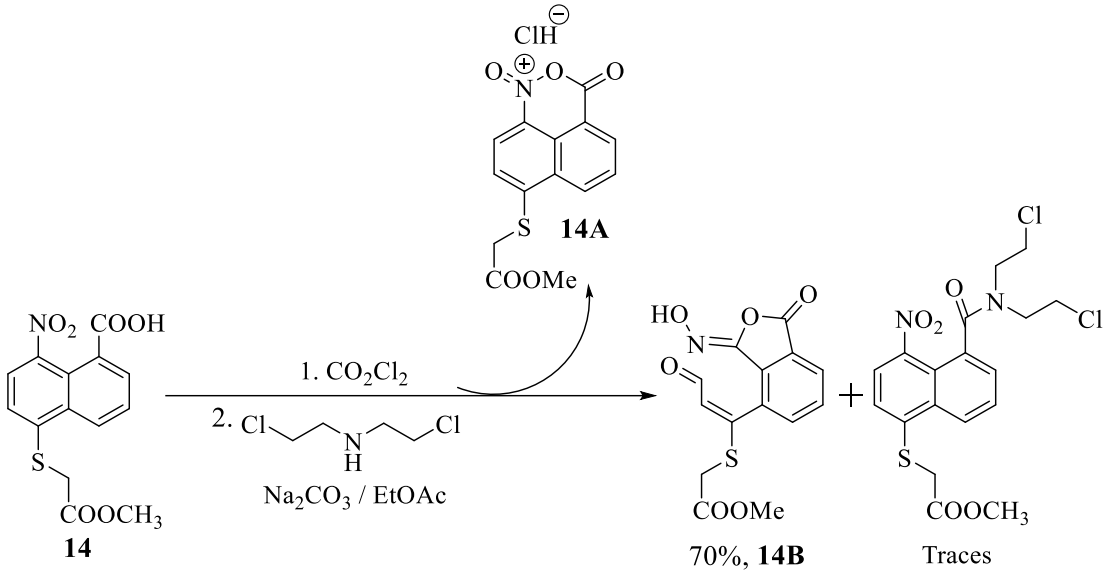


Figure 41. *Bis(2-chloroethyl)amine prodrug defective synthesis.*

However, the master plan has been modified on the basis of a new attachment procedure, in which compound **14A** was prepared according to the general procedure of acid activation using $C_2O_2Cl_2$ then dissolved in CH_2Cl_2 and poured over a mixture of diethanolamine and CH_2Cl_2 at 0ºC.

The reaction mixture has been washed twice with HCl (2M) and sulfuric acid, then the organic phase was recovered with EtOAc. The crude reaction mixture was purified using column chromatography over silica gel and CH_2Cl_2/ EtOAc as eluents. In this case, we obtained amide **18** as the main product (Figure 42).

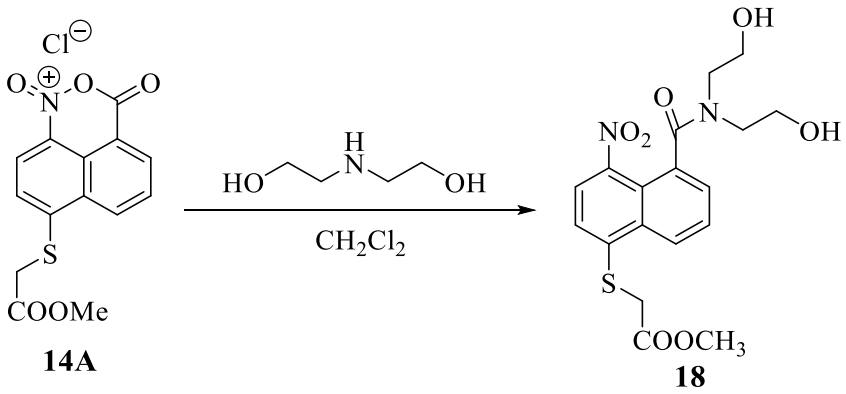


Figure 42. *Compound **19** synthesis.*

In order to obtain the desired dichloride, compound **18** has been dissolved in CH_2Cl_2 and then thionyl chloride and toluene have been added and the reaction mixture has been refluxed for 1 hour. Finally, the desired linkage has been successfully obtained according to the ^{1}H-NMR spectrum. Purification was carried out using silica gel column chromatography and CH_2Cl_2, EtOAc as eluents to afford the pure compound **19** (Figure 43).

The displacement of the -OH from the diethanolamine with chlorine atoms from the thionyl chloride has given the expected antineoplastic drug attached safely.

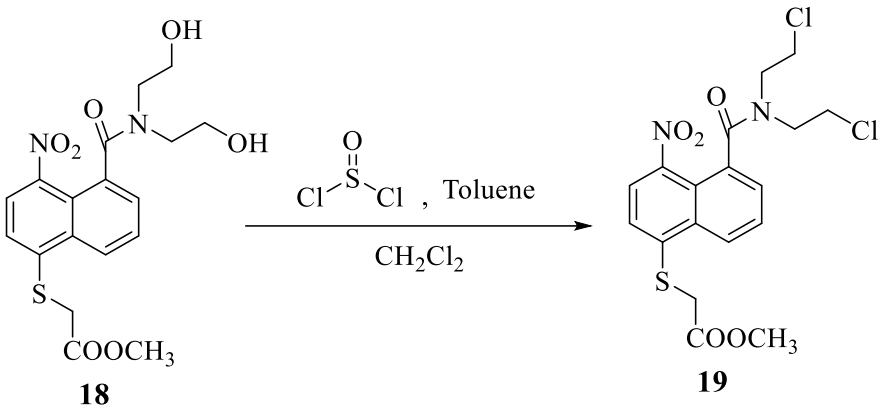


Figure 43. *Synthesis of compound **19**.*

3.6.3.4. *Tacedinaline prodrug*

Tacedinaline selection was due to its cytotoxic nature towards tumor cells. Despite its higher hydro-solubility (Tacedinaline presents an amino group which is protonated under physiological pH), we tried to link it directly to compound **15**, since the latter contains a carboxylic group (introducing a polar group) for water-solubility improvement according to our new strategy described above.

Surprisingly, even if the reaction was carried out under mild conditions, the result was a complex mixture.

For this reason, an alternative solution was proposed, reversing the synthetic steps, attaching Tacedinaline to the acid chloride **9** to yield the amide **10** (Figure 44).

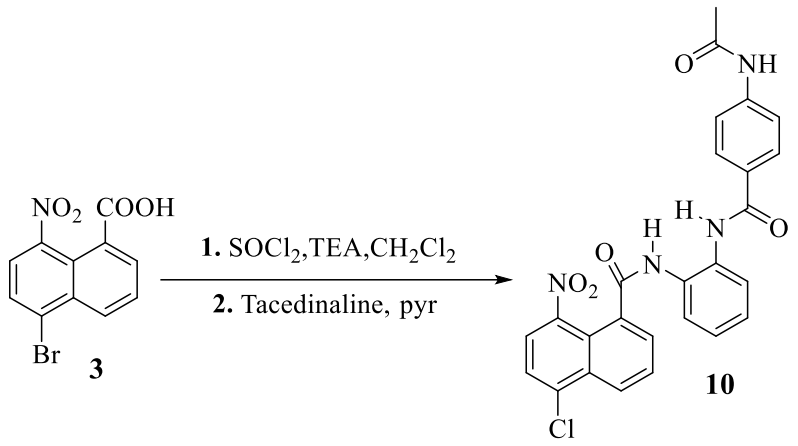


Figure 44. *Compound **10** synthesis (first step).*

In a second step, the naphthalene C5 chlorine atom in compound **10** was substituted with thioglycolic acid as shown in Figure 45 to yield the prodrug **20**.

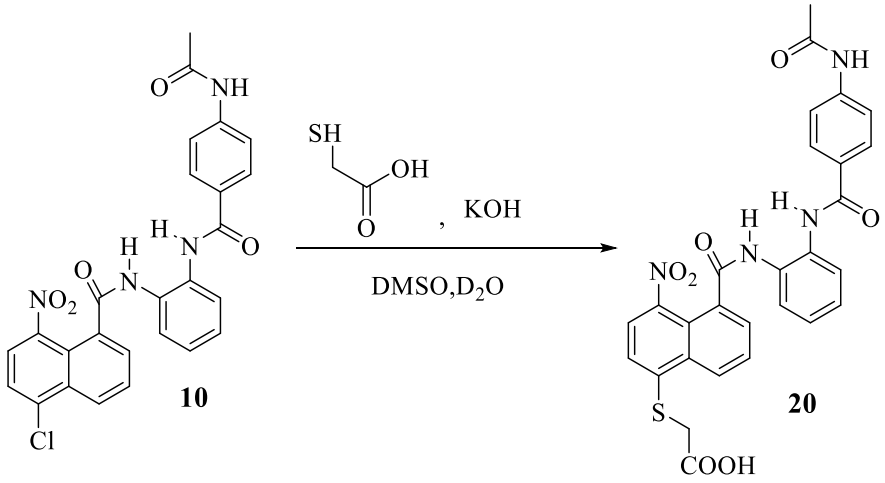


Figure 45. *Tacedinaline prodrug synthesis.*

3.6.4. The hydrolysis of the prodrug's esters

Actually, the use of Fischer esterification for compound **13** was essential as a protection for the carboxylic group of the thioglycolic acid from reacting when linking the drug, obtaining by that the compound **14** which was the safest way to launch the protective group with the drug (Figure 46).

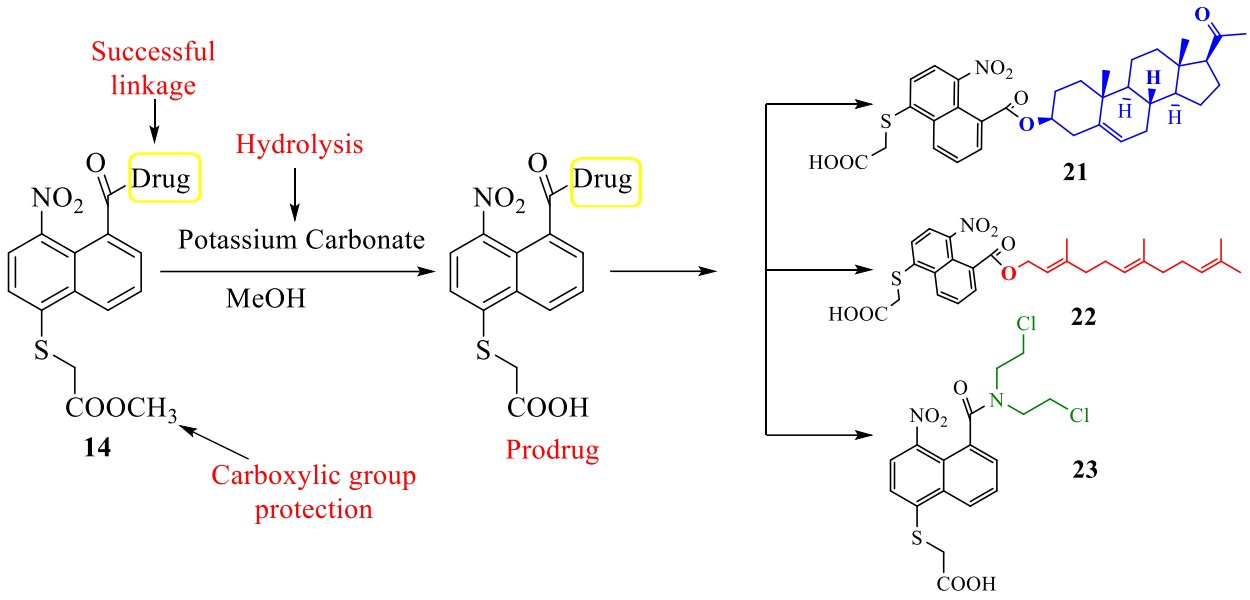


Figure 46. *General procedure of prodrugs hydrolysis.*

3.6.5. Hydrolysis general procedure

In general, the hydrolysis was carried out in the same way in order to obtain the prodrugs in their final state. The synthesised molecules were dissolved in methanol, then potassium carbonate was added, the hydrolysis progress was monitored by TLC, once it finished the reaction mixture was treated with HCl (2M) and the organic layer was extracted using EtOAc. The organic solvent was separated, evaporated under reduced pressure, yielding the final prodrugs which were characterized recording the ^{1}H-NMR spectra.

3.7. Biological trials

3.7.1. Cell lines and culture conditions

In order to assess our antitumoral prodrugs validity, MTT assays were realized in order to confirm their cytotoxicity and ability to dissolve in the cellular medium after following the novel design strategy.

MTT assays were carried out on two different cell lines (normal and tumour), in which they were selected for *in vitro* studies: normal fibroblast HS-5 (ATCC® CRL11882™) and colorectal carcinoma HCT-116 (ATCC® CCL247™). All were obtained from the American Tissue Collection.

Cells were cultured in Dulbecco's modified Eagle's medium (DMEM) supplemented with 1 % penicillin-streptomycin (P-S) and 10 % fetal bovine serum (FBS), referred to as DMEM+ .

They were maintained at 37 °C in a 5 % CO_2 atmosphere at 70 - 90 % confluency and subcultured using 0.05 % EDTA 1x trypsin.

3.7.2. Cell viability determination

To determine the toxicity of the compounds, cells were seeded in quadruplicate in 24-well plates at an initial concentration of 16000 cells per well. After 24 hours in a humidified incubator with 5% CO_2, the medium was removed from the wells, and new medium containing the study treatments was added (50µM) under normoxia and hypoxia (2 % of oxygen). In all tests, the plates included medium control (medium without cells), to check for contamination, and cell control (medium without treatment) as a 100% viability value. Finally, cell viability was quantified by MTT assays after 24 and 48 hours of treatment. The MTT assay is a colorimetric assay used to determine the cytotoxicity of certain drugs (by measuring cell viability). It consists of adding thiazolyl blue tetrazolium bromide dissolved in PBS (5 mg/ml) to the cell medium at a concentration of 20 µL/well and incubating at 37 ˚C for 1 h. During this time, the live cells are incubated at 37 ˚C for 1 h. Meantime, live cells react with the compound to produce violet formazan crystals. Afterwards, the medium is removed and 0.5 mL of DMSO is added to dissolve the crystals, forming a purple solution, the absorbance of which is proportional to the quantity of live cells after each treatment. The absorbance was measured with ultraviolet light (λ = 550 nm) using an EZ Read 2000 microplate reader (Biochrom) and cell viability (Vc) was calculated according to the equation mentioned below:

$$\textbf{Viable cells (\%)} = \frac{\text{Total number of viable cells per mL of aliquot}}{\text{Total number of cells per mL of aliquot}} \times 100$$

Once the cell viability data was obtained, a statistical analysis was performed using Statgraphics Centurion XVI Version 16.1.03 (StatPoint Technologies).

Table 1. *Concentrations, weights and volumes used in the preparation of stock solutions.*

In DMSO	In DMEM				
I [ ] Prodrug (mM)	**F[ ] Prodrug (µM)**	**V DMEM (mL)**		**V Prodrug (mL)**	**percentage DMSO**
5	50	25		0.25	1%
Treatments	**NAME**	**MOLECULAR WEIGHT (g/mol)**	**PRODRUGS WEIGHTS (g)**	**INITIAL CONCENTRATION (g/L)**	**VOLUME DMSO (mL)**
Treat.1	Compound **21**	605.746	0.01600	3.03	5.28
Treat.2	Compound **22**	511.633	0.08158	2.56	31.89
Treat.3	Compound **23**	431.284	0.01107	2.16	5.13
Treat.4	Compound **20**	558.565	0.02119	2.79	7.59
Treat.5	Compound**13**	307.276	0.03000	1.54	19.53
Treat.6	Compound **3**	296.076	0.03000	1.48	20.27

The table above represents prodrugs with their weights, molecular weights, concentrations and the volumes of DMSO used to prepare the solutions.

The compounds abbreviations and structures are represented in figure 47, in which from **1** to **4** are the anti-cancer prodrug**s, 5** is the triggering moiety and **6** is the triggering moiety without the solubilizing group, they were used as prodrugs control behaviour under hypoxia.

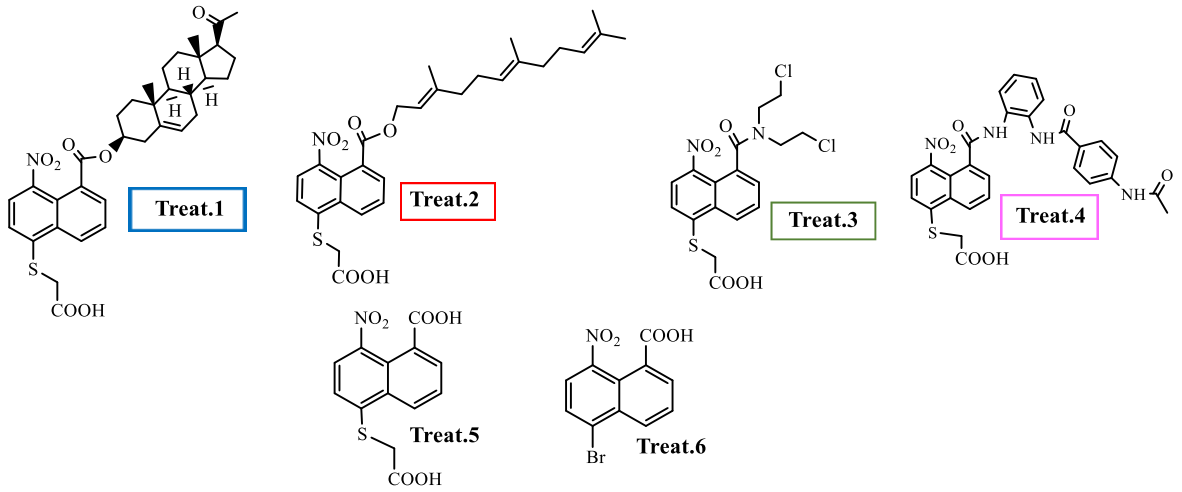


Figure 47. *The structures of prodrugs used in cell essays for their validation.*

With the aim of checking out the cells of interest state, microscopic observation was carried out at 20X magnification using an optical microscope (Figure 48).

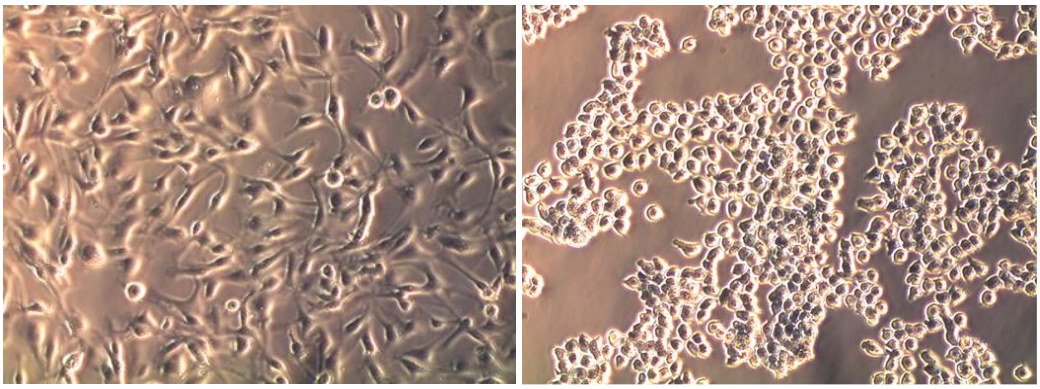


Figure 48. *Microscopic observation of fibroblasts (Left)* ***HS-5*** *and colon cancer cells* ***HCT-116*** *(Right) with magnification 20X.*

Also, the preparation of a stock solution from our cytotoxic compounds was made in a soluble medium (DMSO + PBS), (Figure 49).

The following day the culture medium in the wells was replaced with fresh DMEM containing the treatments of interest by adding as much volume as necessary in the cell medium to achieve the required concentrations for each treatment, leaving some wells with untreated medium as a cell control.



Figure 49. *Prodrugs stock solution with an observable solubility of the compounds.*

Cells were then incubated again for 24 and 48 h at 37°C under normoxia (20 % O_2) and hypoxia (2% O_2). Next, MTT solution (5 mg mL^{-1}) was added to each well, plates were incubated for an additional hour at 37 °C and formazan crystals were dissolved by replacing the culture medium with DMSO. Optical density values of the wells were determined with a microplate reader (Zetasizer Nano ZS90, Malvern Instruments Inc., Royston, UK), with absorbance at 550 nm. MTT assays were performed in duplicate for each treatment.

3.7.3. Results

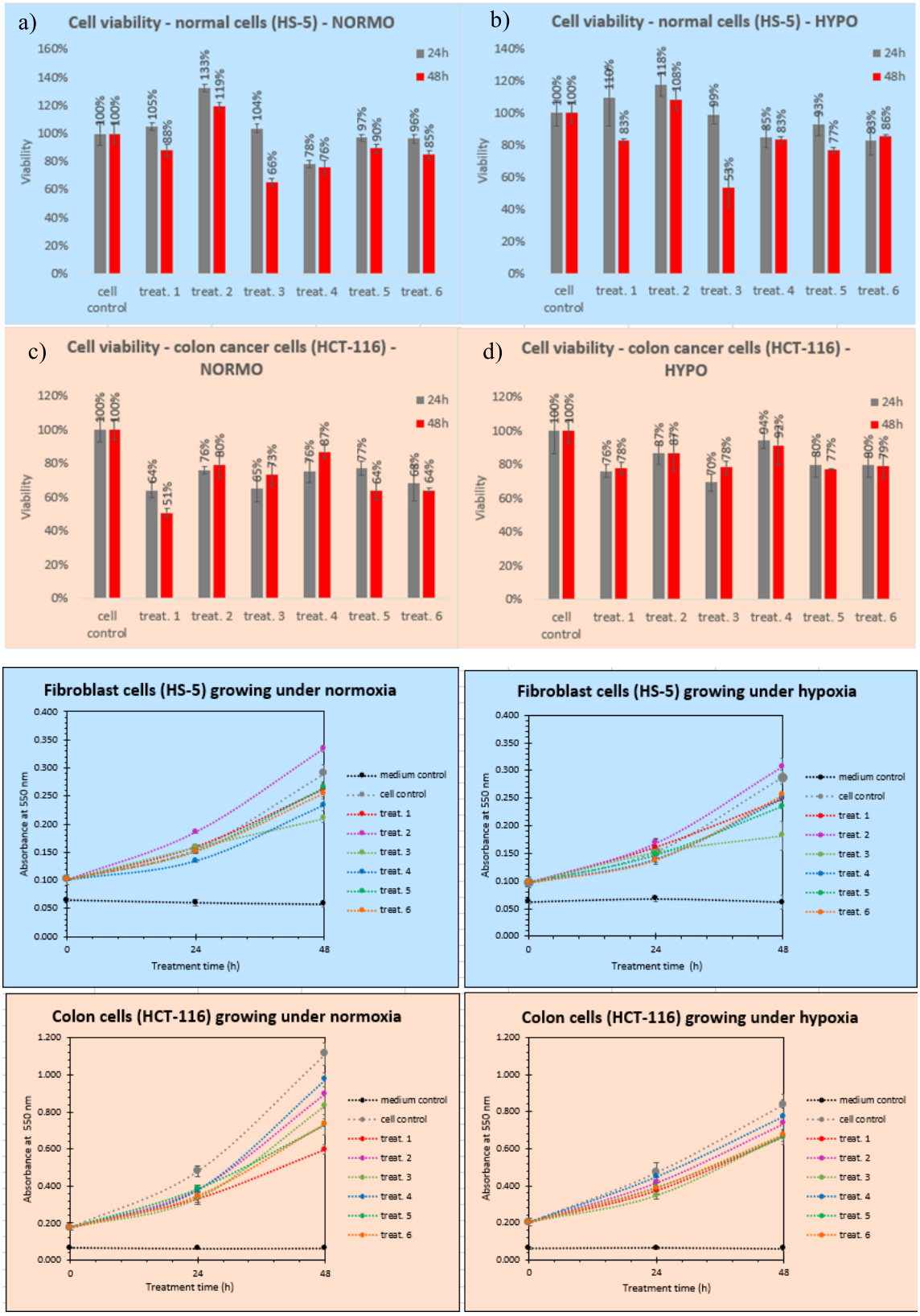


Figure 50. *Prodrugs effects on fibroblasts and colorectal cancer cells growth under hypoxic and normoxic conditions measured by optical density over the time (represented by curves and graphs).*

Graphics **(a)** and **(b)** correspond to the cell's growth measured by optical density for fibroblasts (normal cells) after treating them with our compounds after 24h and 48h in normoxia and hypoxia.
Graphics **(c)** and **(d)** correspond to the cell's growth measured by optical density for colon cancer cells, after treating them with our compounds after 24h and 48h in normoxia and hypoxia.

It should be noted that cell monitoring revealed cell growth variance for the different treatments tested (prodrugs) and the conditions applied (hypoxia/normoxia) after 24 and 48 hours. The results are interpreted according to the results mentioned in figure 50 (graphs) as follows:

➢ **Pregnenolone prodrug (21)**: For this prodrug we observe that its effect is more noticeable in normoxia than in hypoxia, so that after 24 hours of treatment cancer cells viability under normoxia was reduced to 64% in comparison to those under hypoxic condition 76%. Interestingly, the viability has been reduced by up to 51% after 48h under normoxia with respect to that in hypoxia 78% and the control. Normal cells viability remained preserved after 24 hours under normoxia and hypoxia with a slight reduction in growth after 48 hours under the two previously mentioned conditions normoxia-hypoxia, respectively 88%-83%.
These results indicate that the prodrug exerted a considerable cytotoxicity on cancer cells under normoxic conditions after 48 hours, as well as under hypoxic conditions.

➢ **Farnesol prodrug (22)**: The effect of this prodrug was that cancer cell viability has been reduced similarly under normoxic and hypoxic media during 24 and 48 hours with a growth interval of [76%-80%.]. However, the normal cells viability under all the conditions mentioned above remained intact 100% or even more.
On the basis of these results and whatever the conditions applied (normoxia/ hypoxia) the prodrug was able to make a slightly differentiation between colon cancer cells and healthy cells, this fact is proved by keeping the percentage of healthy cells preserved while the colon cancer cells growth was reduced lightly and similarly in the presence and the absence of oxygen.

➢**Bis(2-chloroethyl)amine prodrug (23)**: Regarding this prodrug we observe that after 24 hours of treatment under normoxia conditions, healthy cells viability remained stable, however

it has been reduced to 65% in colon cancer cells. After 48 hours of treatment normal cells viability was reduced to 66% whereas the viability percentage of colon cancer cells was similar to the value obtained after 24 hours. Also, the results are quite similar in the case of hypoxic conditions so that healthy cells viability was 99% while for colon cancer cells was 70% under the same condition after 24 hours and 53% for normal cells and 78% for cancer cells after 48 hours.

This means that the reduction of oxygen concentration did not affect to cell viability, however the prodrug shows some degree of discrimination between cancer and normal cells after 24 hours of treatment affecting mostly colon cancer cells.

➢ **Tacedinaline prodrug (20)**: Concerning Tacedinaline prodrug we can observe that regardless the medium conditions (normoxia/hypoxia), the cell types (healthy/cancerous) or even the duration of treatment, the latter showed cytotoxicity reflected by a variance in cell viability as shown in graphs a, b, c and d in figure 50. After 24 hours its efficacy in reducing colon cancer cells and healthy cells viability was quite similar under normoxia conditions, 76 and 78%, respectively.

After 48 hours under the same medium condition, normal cells viability has been affected more than colon cancer cells. However, under different growth conditions which is hypoxia for 24/48 hours of treatment, the effect was almost identical with the same ratio of reducing the viability, so that for colon cancer cells under hypoxia the difference of their viability reduction between 24 and 48 hours is virtually negligible, respectively 94% and 92%, which is also the case for the normal cells under the same condition (85%-83%)

These results indicate the prodrug did not show a great lethal effect towards colon cancer cells under hypoxia conditions, hence it showed a lack of discrimination to a greater extent.

➢**Compounds 3 and 13**: In fact, compounds **3** and **13** were included in the test to check their cytotoxicity against cancer and normal cells.

In fact, the two compounds have shown some degree of cytotoxicity towards cancer and healthy cells by reducing their viability under normoxia and hypoxia, even without being attached to an antitumor drug. It can be observed that the cytotoxicity was higher in the case of cancer cells under normoxia conditions (64% of viability after 48 hours for both compounds **3** and **13** for HCT-116 colon cancer cells). This means that the molecular trigger can increase the cytotoxicity of the drug itself.

The results mentioned above are summarized as follow in figure 51.

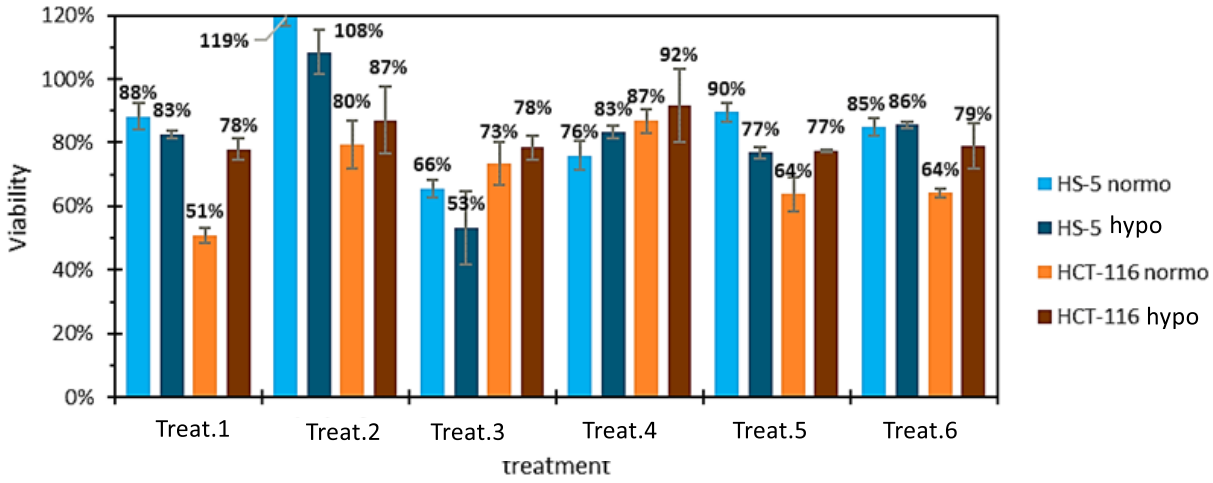


Figure 51. *Summary of the graphical representation of prodrugs tests on **(HS-5)** healthy fibroblast and **(HCT-116)** colorectal cancer cells, and their viability after 48 hours of treatment.*

After having observed the previous MTT results, it was necessary to know which concentration from the pure cytotoxic compounds would match with the concentrations used from the prodrugs.

Hence, by exploiting the literature data, we realized that we were working with low concentrations. For instance, the IC_{50} of free Farnesol is 113 µM for colon cancer cells and 71 µM for fibroblasts. In addition, since compound **21** (Pregnenolone prodrug) was the most promising and effective substance against cancer cells, it was studied deeper. The MTT assays have been performed for this prodrug during 48 hours at different concentrations using different flasks of cell lines (just in case the cells are in different growth phases), the obtained results are mentioned as follow (Figure 52).

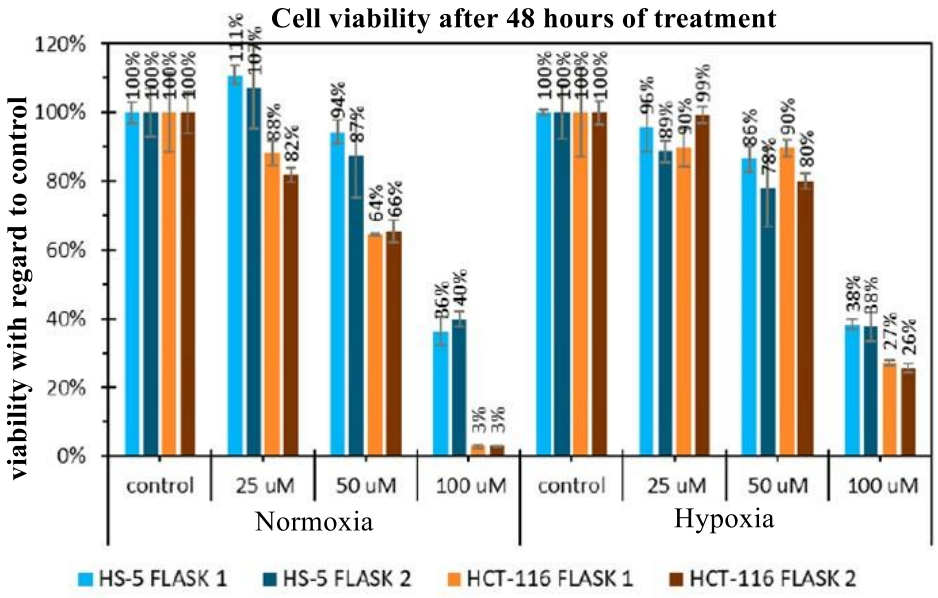


Figure 52. *Cell viability with regard to control, after 48 hours of treatment using different concentrations from the prodrug **21**.*

The graphs shown in figure 52 represent the percentage of cell viability in function of the treatment applied at different concentrations for 48 hours, in which we observe a variation of viability under normoxia and hypoxia conditions. However, there is not much difference between flask 1 and 2.

Under normoxia conditions: we can observe that the cellular viability of colon cancer cells has been reduced to 82% when working with the concentration 25 µM, this value decreased to 64% at 50 µM and 3% at 100 µM. The cell viability of healthy cells was much higher moving from 100% viability at 25 µM to 87% at 50 µM and then to 36% at 100 µM. These results indicate that the prodrug has affected both cell lines by increasing the drug´s concentrations, however it is clear that the treatment has reduced mostly the cancerous cells viability even under normoxia medium unlike the healthy cells, which remained more or less with a higher viability the those of colon cancer.

Under hypoxia conditions: under the hypoxic medium it can be seen that cancer cell viability decreased in function of cell concentration, so that by working at low concentration 25 µM, viability percentage was 90%, this value changed by increasing the concentration at 50 µM to 80%. However, a decline was observed when a higher concentration was applied 100 µM, with viability falling to 26% for colon cancer cells.

On the other hand, for healthy cells viability with regard to the control it has not affected clearly at 25 µM of the treatment (96%), otherwise the viability percentage has been shrunk to 78% at 50 µM to reach 38% at 100 µM.

From these results we can conclude that the compound **21** has affected the colon cancer cells with a great extent than the healthy ones under hypoxia medium by increasing the concentration level of the treatment, these promising results prompted us to investigate its lethal effect by realising a cell counting test.

3.7.4. Cell counting

For the purpose of studying the prodrug (compound **21**) effect further (to assess the percentage of cell viability by enumeration), a cell culture was carried out by treating the two cell lines (fibroblasts and colon cancer cells) for 24 hours under normoxic and hypoxic medium using the concentration of 50 µM.

After 24 hours of incubation under treatment, the supernatant was collected and stored it in centrifuge tubes (the medium that has been in contact with the cells). On the other hand, the cells were lifted and quantified by resuspending them in 2 mL of PBS. 10 µL of each sample was mixed with 10 µL of trypan blue and counted using the cell counter, the results are shown in Table 2.

Table 2. *Counting of healthy and cancerous cells treated with compound **21**.*

	Control		Treated	
	$[\ ]_{cel}$ (c/mL)	Living cells	$[\ ]_{cel}$ (c/mL)	Living cells
HCT-116 (Normoxia)	4,96E+06	84%	2,09E+06	88%
HCT-116 (hypoxia)	3,76E+06	92%	2,03E+06	93%
HS-5 (Normoxia)	1,43E+06	95%	1,05E+06	88%
HS-5 (hypoxia)	1,29E+06	92%	8,21E+05	92%

Based on these data, the total number of cells was quantified in each case and the percentage of viability was determined relative to the control in each case. The results are shown in Table 3.

Table 3. *Viability percentage of cancer and healthy cells after being treated with compound **21** comparing to the control under normoxia and hypoxia conditions.*

	Total cell count		Viability percentage	
	control	treated	control	treated
HCT-116 (Normoxia)	4,17E+06	1,84E+06	100%	44%
HCT-116 (hypoxia)	3,46E+06	1,89E+06	100%	55%
HS-5 (Normoxia)	1,36E+06	9,24E+05	100%	68%
HS-5 (hypoxia)	1,19E+06	7,55E+05	100%	64%

According to the counting results (Table 3), both cell lines showed a variance in the percentage of proliferation subject to two different conditions (normoxia/hypoxia), after having treated with pregnenolone prodrug (compound **21**). From comparing the viability percentage between cancer cells under hypoxia and fibroblasts under normoxia and by taking in consideration that the hypoxic medium condition is a specific feature of cancerous cell clusters, we can observe clearly that the treatment was able to reduce cell viability to 55% under the desired condition (hypoxia) while the viability percentage of fibroblasts was quite higher (68%) under normoxia. However, the efficacy of the treatment can be observed also under the normoxic conditions towards the cancerous cell population in which it has reduced its viability under the normoxic medium to 44%.

These results indicate that the compound **21** has affected the cell viability of colon cancer cells to a greater extent under both conditions especially under normoxic conditions, where viability is reduced to below 50% .

On the other hand, as compound **21** has shown a promising result in attacking the cellular population by reducing its viability which is confirmed by MTT assays and counting cell results, we decided to study the mechanism that we proposed for the drug liberation was taken place inside the cells. A mass spectrometry analysis was proposed to examine the supernatant and the lysed cells after treating them with the prodrug, to check whether it is actually soluble and if it penetrates cancer cells more precisely in order to exert its cytotoxic effect. Also, for an in-depth confirmation study we decided to couple the mass spectrometry study with HPLC analysis to detect the presence of pregnenolone prodrug and/or its derivatives resulting from the expected cleavage, pure pregnenolone and lactam (Figure 53).

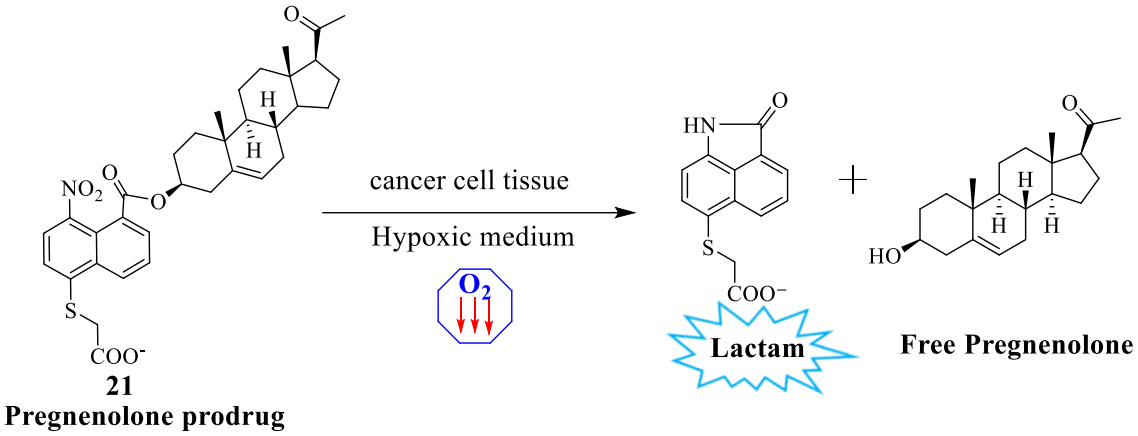


Figure 53. *Pregnenolone prodrug cleavage under hypoxic conditions.*

Accordingly, the supernatant was removed and kept separately for analysis, then 2 mL of RIPA buffer was added to the treated cell samples in PBS in order to lyse them. Lysed cells and supernatant were analysed separately by mass spectroscopy.

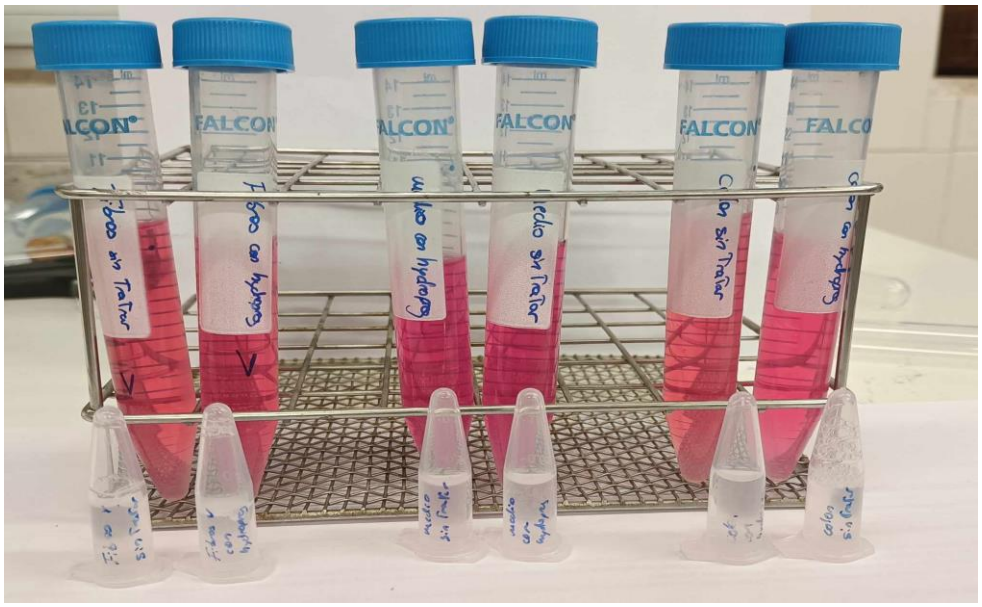


Figure 54. *Separated cellular medium (Redish pink/Falcons) and lysed cells (colorless/Eppendorf).*

The samples were organised as shown in Table 4 for mass spectrometry analysis.

Table 4. *Separation of cells from medium and their lysis using RIPA buffer.*

Medium which has been in contact with cells			**Lysed cells**		
			Blank of PBS:RIPA (1:1)		
Control	Normoxia	Medium Fibroblasts Colon	Control	Normoxia	Fibroblasts Colon
	Hypoxia	Medium Fibroblasts Colon		Hypoxia	Fibroblasts Colon
Treated	Normoxia	Medium Fibroblasts Colon	Treated	Normoxia	Fibroblasts Colon
	Hypoxia	Medium Fibroblasts Colon		Hypoxia	Fibroblasts Colon

3.7.5. Mass spectrometry results

HPLC-mass spectrometry analysis showed the presence of the prodrug and pure pregnenolone in both the supernatant and lysed cells. However, the lactam was not observed in some cases. Figures 55 and 56 represent the abundance of each compound for each treatment.

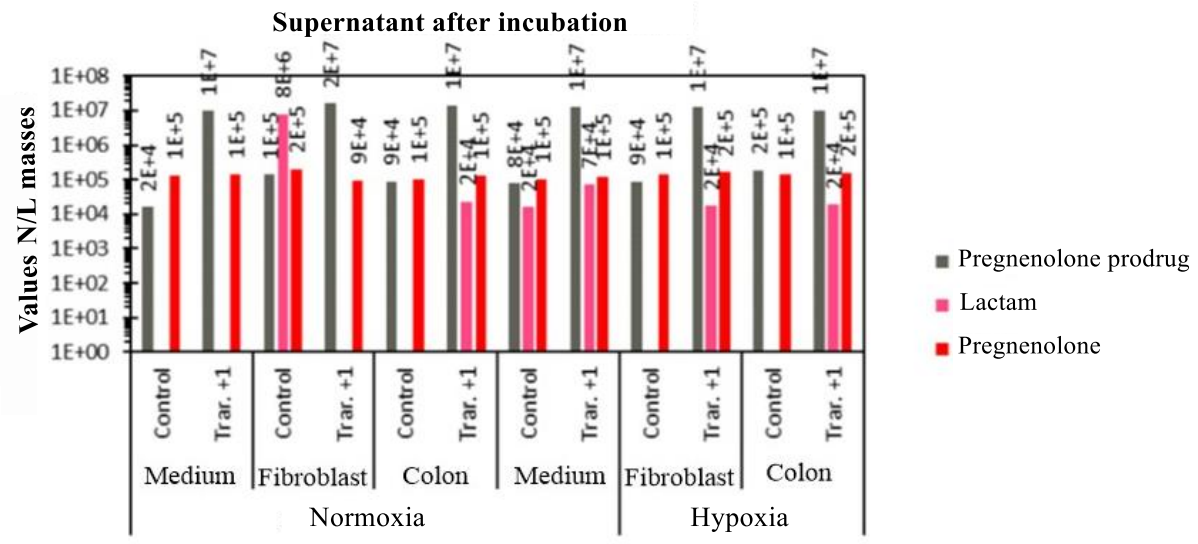


Figure 55. *Obtained values of compound **21**(Pregnenolone prodrug) and its derivates by MS of the supernatant after incubating the two cell lines (fibroblasts and colon cancer cells) inside the cells for 24 hours under normoxic and hypoxic conditions.*

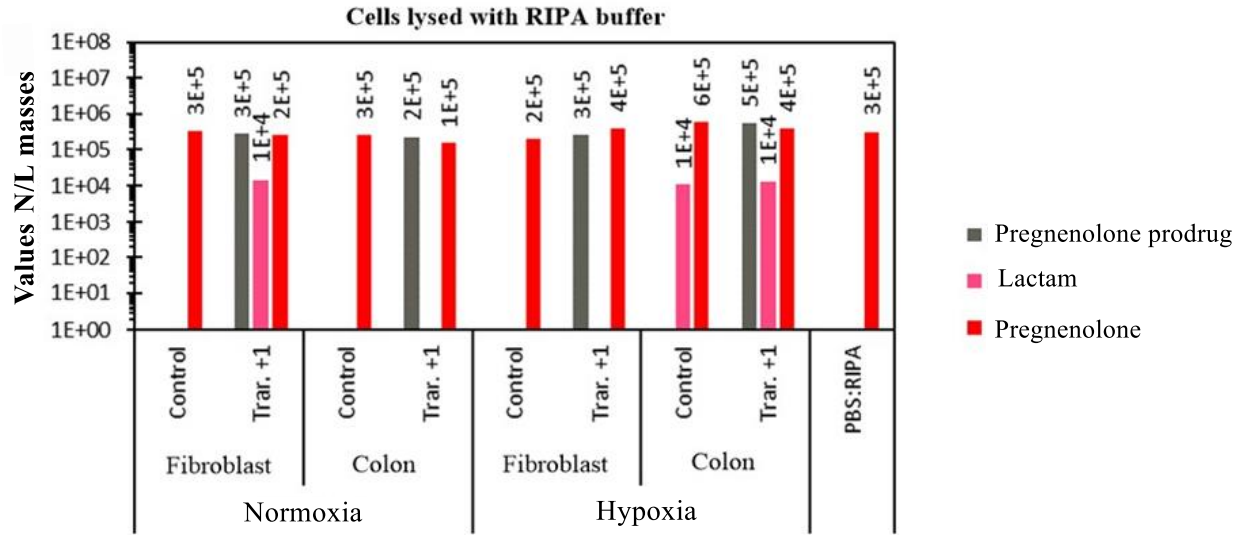


Figure 56. *Obtained values of compound **21** (Pregnenolone prodrug) and its derivates by MS of the lysed cells (fibroblasts and colon cancer cells) using RIPA buffer.*

Actually, the target of this analysis is the detection of the prodrug **21** presence or its derivatives within the cells, especially colon cancer cells to confirm its solubility and internalization. According to the mass spectrometry analysis results of the supernatant (medium which was in contact with both treated cell lines, Figure 55), and the lysed cells with RIPA buffer (Figure 56), we can observe the abundance of compound **21** in both cases. Interestingly, its value is higher in lysed cancer cells that have undergone the treatment in the absence of oxygen "hypoxia" (Figure 56), this result can confirm that the prodrug has been able to penetrate inside cells, in addition the presence of the pure pregnenolone (free parent drug) and lactam which is generated from the prodrug detachment.

Considering these encouraging and promising results, additional investigations were performed to follow the drug's pathway and confirm its intracellular passage and behaviour under the given conditions.

However, direct injection of an aliquot of lysed cells into the HPLC equipment allowed us to detect the prodrug (compound **21**) in very small amounts but not the lactam. Therefore, we decided to include a step before injecting the samples to increase the concentration of the prodrug and /or its derivatives, by extracting them to an organic solvent (Figure 57).

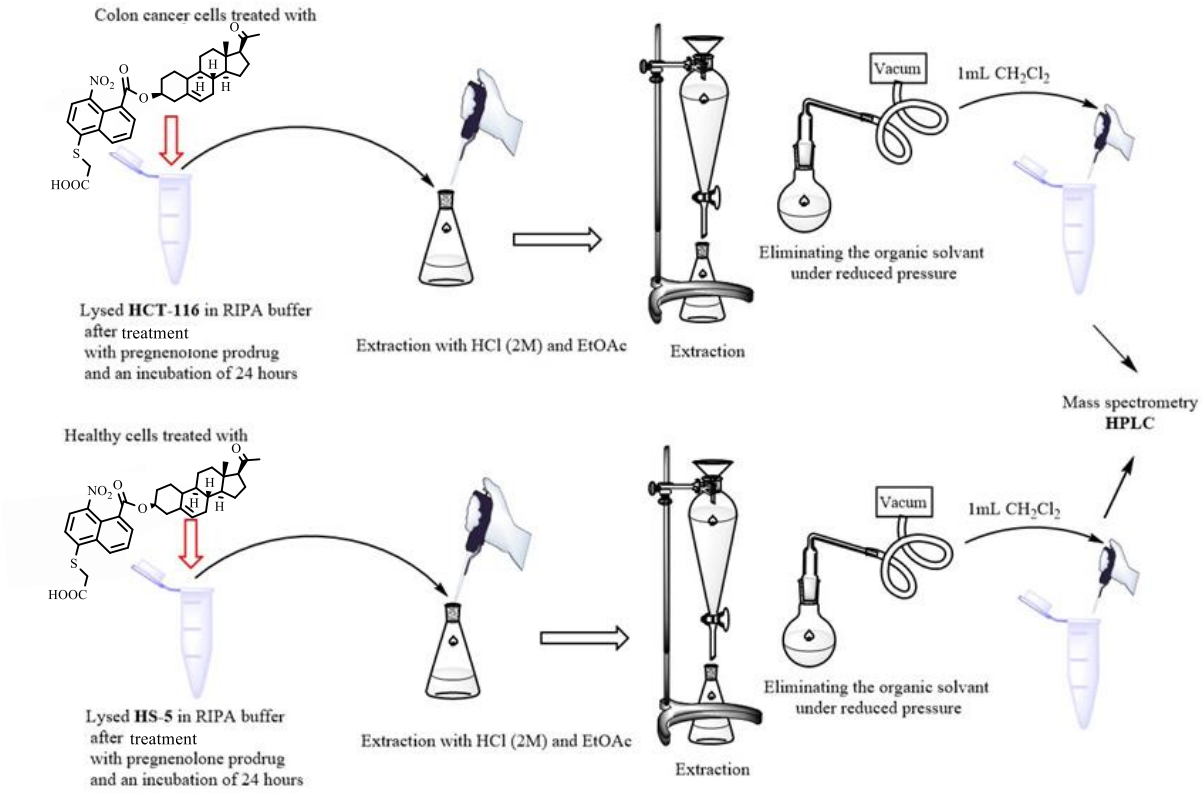


Figure 57. *The followed protocol to reveal the presence of pregnenolone prodrug or one of its derivatives inside the cells (own elaboration).*

As it is mentioned in figure 57, the lysed and lifted cells in RIPA/PBS buffers from the two cell lines (fibroblasts and colon cancer cells) were acidified using aqueous HCl (2M) to protonate the carboxylate group of the prodrug and lactam and extracted using ethyl acetate. The organic solvent was evaporated and the crude dissolved in 1 mL of CH_2Cl_2 and analysed by HPLC. Lactam (Figure 56) and the pure pregnenolone were used as references. Lysed colon cancer cells and healthy cells were analysed (Figures 58 and 59).

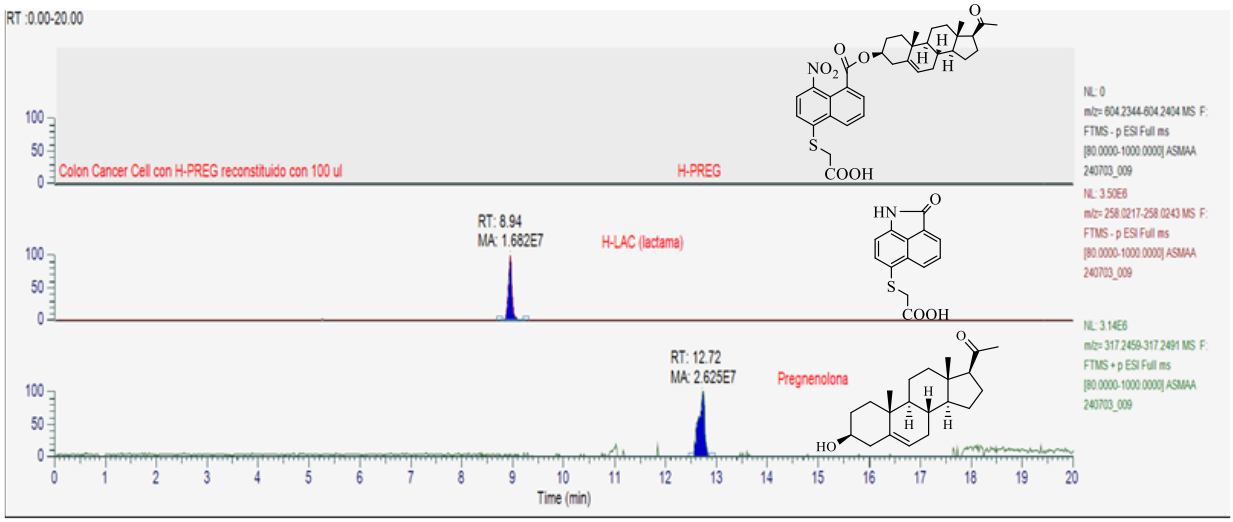


Figure 58. *HPLC traces of lysed colon cancer cells. Top: pregnenolone prodrug; medium: lactam; bottom: pregnenolone.*

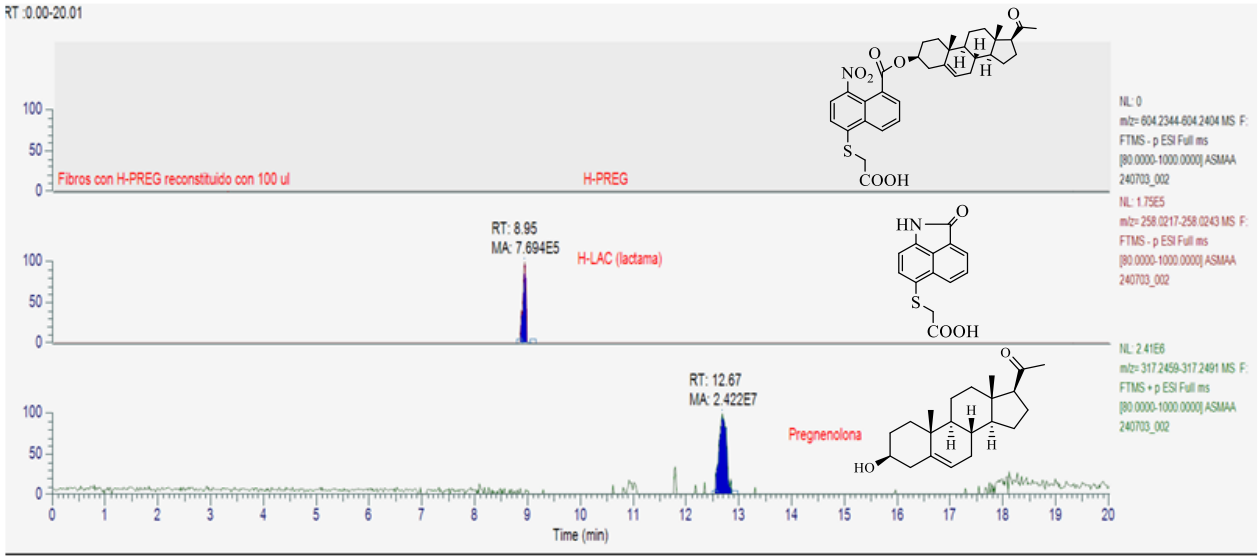


Figure 59. *HPLC traces of lysed healthy cells (fibroblasts). Top: pregnenolone prodrug; medium: lactam; bottom: pregnenolone.*

Based on the results showed above (Figures 58 and 59), the lactam has been detected in both cancer cells and fibroblasts, and also pregnenolone. This means, that the prodrug has released the drug inside the cells. Curiously, the retention time of pregnenolone (control) varies from the pregnenolone detected inside lysed cells, while the mass is the same. This could mean that a pregnenolone isomer is obtained instead of the initial pregnenolone attached to the prodrug. Further investigation is needed to confirm this isomerization. However, pregnenolone prodrug could not be detected inside the cells which is probably explained by a fast liberation of the

internalised prodrug under the required conditions proved by the lactam and pregnenolone detection

On the other side, only the prodrug has been detected within the supernatant medium of both colon cancer cells and fibroblasts. This indicates the prodrug stability inside the medium, hence it could be considered as a positive sign, in this case the breaking up of the bonds could be realized only inside the cells and this is what makes it compatible with the launch hypothesis from the point of view of solubility, targeting, cleavage and even *in situ* cytotoxicity.

Hence, according to HPLC results, it is indicated that the prodrug has been internalised within the cells, that could be explained by the efficacy of the novel design applied for the solubility enhancement of our moieties by the integration of a polar functional group (carboxylic group). In this case, one of the main objectives of structural modification in order to ensure the solubility of our syntheses have been achieved.

Also, the objective of releasing the drug inside the cell has been proved.

4. Conclusions

The following conclusions are extracted from this chapter:

- Regarding prodrug **12** synthesis:

In this chapter, it has been possible to improve compound **8** (Tacedinaline) synthesis. It was attached to a triggering moiety to generate prodrug **12**, which was able to be cleaved under a reducing medium mimicking the hypoxic conditions of cancer cells, to release the cytotoxic compound **8**.

- Regarding the *click* reaction:

It was observed that the addition of Cu(I) led to strong coloration and decomposition of the nitro group and the azide, since it is possible for Cu(I) to generate radicals in the nitro group by transferring an electron. Then, an attempt was made to carry out the reaction in the absence of copper, although it was necessary to heat the reaction between the azide and the dipolarophile at 90ºC for four hours to obtain the desired prodrug.

- Regarding the polar functional group integration for hydro-solubility enhancement:

Also, in this chapter, a new strategy has been employed by modifying the molecular design of compound **3** (5-bromo-8-nitro-1-naphthoic acid), so that thioglycolic acid has been attached to

compound **3**, then antineoplastic agents were linked with the latter, synthesizing four anti-tumor prodrugs which are compounds: **20**, **21**, **22** and **23**.

- Regarding the synthesized anti-tumoral prodrugs (Compounds **20**, **21**, **22** and **23**) and MTT assays:

  The expected prodrugs were synthetised successfully by attaching the selected anticancer agents to the modified protective group (compound **14A**).

  These compounds were tested by MTT assays applied on two cell lines: healthy fibroblasts **HS-5** and colorectal carcinoma **HCT-116**, to validate the prodrugs efficacy from the point of view of solubility in the cellular media and cytotoxicity towards cancer cells. The results of MTT assays have shown a variance of cytotoxic effect towards cells viability regarding each compound under both conditions (hypoxia/normoxia). From the 4 compounds tested, compound **21** (Pregnenolone prodrug) was the more effective followed by compound **23** (Bis(2-chloroethyl)amine prodrug), while compounds **20** and **22** (Tacedinaline and Farnesol prodrugs) have shown a limited effect in reducing the viability of cancer cells population.

  The efficacy of compound **21** required repetition of MTT assays with different concentrations of the prodrug under the same conditions as above, consequently the prodrug has shown satisfactory results when increasing its concentration to 100 µM by reducing the viability of cancer cells to 26 % under hypoxic conditions and under normoxia.

- Regarding the counting cells test and spectrometry analysis (HPLC/MS)

  Further confirmation steps were realised by counting the treated cells with compound **21** from both cell lines. The counting test was carried out following a separation of cells and supernatant (the contact medium) by centrifugation, in which the counting results indicated a considerable positive effect in reducing the viability cell percentage under normoxia and hypoxia.

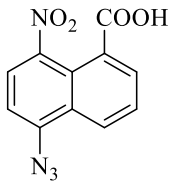
  The treated cells (fibroblasts and cancer cells) were separated from the supernatant and were lysed using RIPA buffer and analysed with HPLC-MS in order to examine their content. The prodrug internalisation was confirmed. Surprisingly the results indicated the total absence of pregnenolone prodrug in the lysed cells, and the presence of lactam and an isomer of pregnenolone. This proves the prodrug undergone cleavage inside the cells,

which shows that it has been successfully internalized thanks to the solubility enhancement and its cytotoxic effect has been verified.

5. Experimental Section

5.1. Synthetic details and characterization

5-azido-8-nitro-1-naphthoic acid (4)



4

In 50 mL round bottom flask equipped with stirring magnet, in 50 ml round bottom flask, 5-bromo-8-nitro-1-naphthoic acid, compound **3** (1g, 3.373mmol), and sodium azide (500 mg, 7.69 mmol) were dissolved in 5 mL of DMF, the resulting mixture was stirred at room temperature for 4 hours. The product was collected by adding water to the mixture then a filtration under reduced pressure was done affording a pale brown solid (800 mg, 83%).

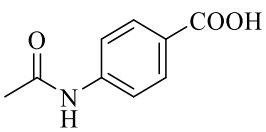
Mp: 192-196ºC

^{1}H NMR (400 MHz, MeOD) δ 9.97 (d, *J* = 8.5 Hz, 1H), 9.80 (d, *J* = 8.3 Hz, 1H), 9.73 (d, *J* = 7.2 Hz, 1H), 9.28 (dd, *J* = 8.5, 7.2 Hz, 1H), 9.08 (d, *J* = 8.3 Hz, 1H).

^{13}C NMR (101 MHz, MeOD) δ 170.3 (C), 145.4 (C), 144.2 (C), 140.4 (C), 133.1 (CH), 130.5 (C), 127.8 (CH), 127.2 (CH), 126.9 (CH), 124.3 (C), 114.2 (CH).

HRMS (ESI+)[M+Na]+ calculated for $C_{11}H_6O_4N_4{}^{23}Na$ 281.0287, found 281.0279.

4-Acetamidobenzoic acid (5)

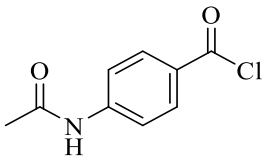


5

In a 500 mL round-bottom flask, 4-aminobenzoic acid (20 g, 148.84 mmol) was dissolved in 200 mL of acetic anhydride. The resulting mixture was heated gently to make it well

homogenized. Once the reaction mixture was dissolved the reagent excess was evaporated under reduced pressure affording compound **5** (25 g, 97%) as a white solid. The obtained crude product has been used without further purification in the next step.

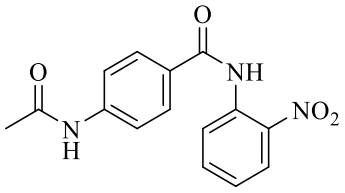
4-Acetamidobenzoyl chloride (6)



6

In a 500 mL round-bottomed flask, compound **5** (5 g, 28.38 mmol) was poured in a mixture of 250 mL of CH_2Cl_2 and 2.82 mL of Et_3N, the obtained suspension was gently heated for two minutes in water bath at 70ºC and, once a homogeneous mixture was observed; 5 mL of thionyl chloride and 30 mL of toluene were added (toluene was added to improve the thionyl chloride evaporation). Finally, the volatiles were evaporated under reduced pressure to yield the acid chloride (4.65 g, 83%), which was used without further purification in the next step.

4-Acetamide-*N*-(2-nitrophenyl) benzamide (7)



7

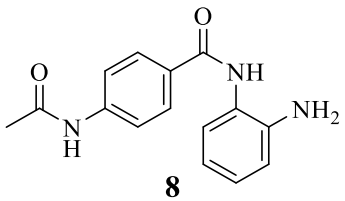
The previous acid chloride (4.65 g, 23.53 mmol) was reacted with a mixture of 2-nitroaniline (3.85 g, 25.9 mmol) and 5 mL of CH_2Cl_2 for 2 hours. After this time, 10 mL of THF is added and evaporated under reduced pressure. The crude reaction was purified by crystallization in MeOH. Filtration was carried out washing the solid with water (it helps remove the remaining Et_3N hydrochloride). Compound **7** (8 g, 88%) was obtained as a golden yellow solid.

M.p.: > 200 ºC

IR (nujol, υ, cm^{-1}): 3306, 1671, 1606.

^{1}H NMR (400 MHz, CD_3OD) δ (ppm): 8.35 (d, *J* = 8.3 Hz, 2H), 8.18 (d, *J* = 8.3 Hz, 2H), 7.96 (d, *J* = 7.8 Hz, 1H), 7.78 – 7.72 (m, 2H), 7.37 (t, *J* = 7.8 Hz, 1H), 2.17(s, 3H).
^{13}C NMR (101 MHz, CD_3OD) δ (ppm): 171.6 (C), 167.0 (C), 144.1 (C), 141.5 (C), 135.9 (CH), 134.5 (C), 129.9 (C), 129.6 (2 CH), 126.5 (CH), 125.7 (CH), 125.4 (2 CH), 120.3 (CH), 24.0 (CH_3).

4-Acetamido-*N*-(2-aminophenyl)benzamide (8)

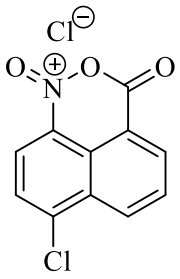


8

The reduction of compound **7** was carried out in a 100 mL Erlenmeyer flask. 30 g of Zinc and 35 mL of acetic acid were mixed and heated in a bath at 60 ºC until a pasty texture (zinc activation) was obtained. Once the zinc is active, compound **7** (3 g, 10 mmol) was added by keeping a constant stirring for 10 minutes. Once the reaction was finished, it was filtered by adding EtOAc (100 mL) and concentrated under reduced pressure affording a beige solid. The crude was purified by crystallization in MeOH yielding a white precipitate. 2.2 g of compound **8** were obtained with a yield of 82 %.

M.p.: > 200 ºC
IR (nujol, υ, cm^{-1}): 3293, 1638, 1599.
^{1}H NMR (400 MHz, CD_3OD) δ (ppm): 7.95 (d, *J* = 8.5 Hz, 2 H), 7.71 (d, *J* = 8.5 Hz, 2H), 7.18 (d, *J* = 7.6 Hz, 1H), 7.07 (t, *J* = 7.6 Hz, 1H), 6.90 (d, *J* = 7.6 Hz, 1H), 6.78 (t, *J* = 7.6 Hz, 1H), 2.15 (s, 3H).
^{13}C NMR (101 MHz, CD_3OD) δ (ppm): 171.9 (2 C), 143.5 (2 C), 130.4 (C), 129.8 (2 CH), 128.5 (CH), 127.7 (CH), 125.6 (C), 120.2 (2 CH), 119.9 (CH), 118.9 (CH), 24.0 (CH_3).

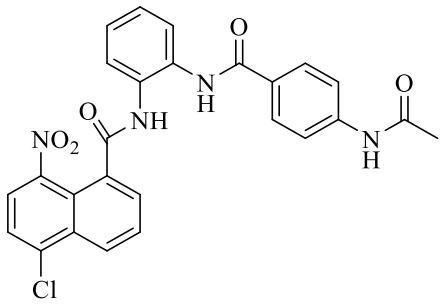
7-chloro-1,3-dioxo-1*H*,3*H*-naphtho[1,8-*cd*][1,2]oxazin-1-ium chloride (9)



9

5-Bromo-8-nitro-1-naphthoic acid **(3)** (1.0 g, 3.38 mmol) was placed in a round bottom flask and thionyl chloride (5.0 mL) and a trace of pyridine were added. The round bottom flask was equipped with a condenser and a paraffin bubbler. The reaction mixture was stirred and heated in a water bath at 40ºC until a homogeneous solution was obtained. Once the acid was completely dissolved, the reaction was finished and the thionyl chloride was removed under vacuum. The crude acid chloride was used without further purification in the next step. Due to its instability, the acid chloride **9** is not characterized.

***N*-(2-(4-acetamidobenzamide)phenyl)-5-chloro-8-nitro-1-naphthamide (10)**



10

In a 100 mL round bottom flask, compound **9** (320 mg, 1.19 mmol) was dissolved in 40 mL of CH_2Cl_2. The resulting mixture was transferred into a two necks flask equipped with an argon gas balloon, thermometer and stirring bar, and immersed in a cold bath at -78 ºC. Tacedinaline (640 mg, 2.38 mmol) was dissolved in 10 mL of pyridine, the resulting mixture was poured within an addition funnel.

Then, the dissolved Tacedinaline in pyridine was added dropwise for 2 minutes to the dissolved acid chloride in CH_2Cl_2. The reaction was allowed to stand for 5 minutes, then poured in a 250 mL Erlenmeyer flask, which contains 100 mL of (2M) HCl and 50 mL of hexane, the mixture

was stirred, and the formed precipitate was filtered and washed using water affording (1.1 g, 92 %) of compound **10** as a beige solid.

M.p. 150-153ºC.

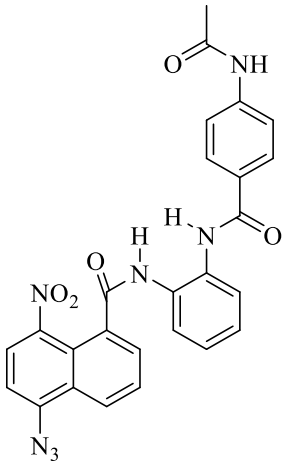
IR (film, υ in cm^{-1}): 3753, 3624, 1670, 1528, 1307, 1158.

^{1}H NMR (400 MHz, DMSO-d_6): δ 10.57 (s, 1H), 10.24 (s, 1H), 9.85 (s, 1H), 8.93 – 8.81 (m, 1H), 8.54 – 8.47 (m, 1H), 8.20 (dd, J = 9.9, 3.0 Hz, 2H), 8.02 – 7.89 (m, 5H), 7.67 (d, J = 8.5 Hz, 2H), 7.32 – 7.21 (m, 2H), 2.06 (s, 3H).

^{13}C NMR (101 MHz, DMSO-d_6): δ 168.7 (C), 167.8 (C), 166.2 (C), 164.9 (C), 146.3 (C), 144.8 (CH), 143.0 (CH), 142.4 (C), 136.6 (C), 132.6 (C), 131.8 (CH), 131.5 (C), 131.1 (C), 130.8 (C), 130.7 (CH), 128.5 (CH), 128.5 (C), 128.3 (CH), 127.0 (CH), 126.7 (CH), 126.2 (CH), 125.8 (CH), 125.8 (CH), 125.6 (CH), 125.2 (CH), 24.0 (CH_3).

HRMS (ESI+) [M+Na]+ Calculated for $C_{26}H_{19}ClN_4O_5Na^{23}$ 525.0933, found 525.0936.

***N*-(2-(4-acetamidobenzamide) phenyl)-5-azide-8-nitro-1-naphthamide (11)**



11

In a 50 mL round-bottom flask, DMF (4 mL) was added followed by sodium azide (1 g, 0.015 mol) and compound **10** (1 g, 2 mmol). The reaction was heated at 60ºC with a continuous stirring for 1 hour and 15 minutes. Once the reaction has finished, water was added and compound **11** precipitated. Filtration was carried out under reduced pressure and the crude was recrystallized from MeOH. Compound **11** (640 mg, 63%) was obtained as a yellow solid.

M.p. 201-202ºC.

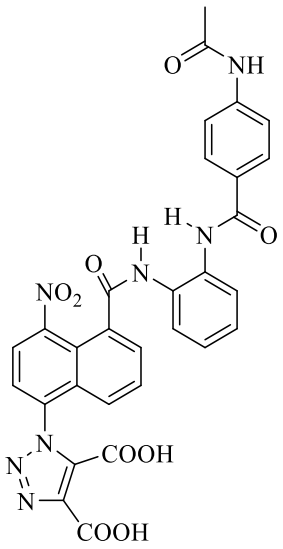
IR (film, υ in cm^{-1}): 3760, 3319, 1606, 1521, 859.

^{1}H NMR (400 MHz, DMSO-d_6): δ 10.45 (s, 1H), 10.18 (s, 1H), 9.78 (s, 1H), 8.32 (dd, *J* = 8.5, 0.9 Hz, 1H), 8.25 (d, *J* = 8.3 Hz, 1H), 8.13 (dd, *J* = 7.1, 0.9 Hz, 1H), 7.91 (d, *J* = 8.7 Hz, 2H), 7.78 (dd, *J* = 8.5, 7.3 Hz, 1H), 7.65 (dd, *J* = 11.7, 8.6 Hz, 5H), 7.29 *(dd, J* = 6.0, 3.5 Hz, 2H), 2.06 (s, 3H).

^{13}C NMR (101 MHz**,** DMSO-d_6**):** δ 168.7 (C), 166.6 (C), 164.9 (C), 146.3 (C), 143.4 (C), 142.3 (C), 142.2 (C), 136.7 (C), 132.2 (C), 131.5 (C), 130.9 (C), 130.6 (CH), 128.5 (CH), 127.0 (CH), 126.4 (C), 125.8 (CH), 125.7 (CH), 125.6 (CH), 125.6 (CH), 125.2 (CH), 125.0 (CH), 122.0 (CH), 122.0 (CH), 118.1 (CH), 114.0 (CH), 24.0 (CH_3).

HRMS (ESI+): $[M+Na]^+$calculated $C_{26}H_{19}N_7NaO_5$ 532.1336; found 532.4712.

1-(5-((2-(4-Acetamidobenzamide)phenyl)carbamoyl)-4nitronaphthalene-1-yl)-1H-1,2,3-triazol-4,5-dicarboxylic acid (12)



12

In a 10mL round-bottomed flask, compound **11** (200 mg, 0.39 mmol), acetylenedicarboxylic acid (400 mg, 3.49 mmol) and 700 μL of DMSO were added. The flask was immersed in a bath at 90ºC for 4 hours. Once the reaction was finished, water was poured to the reaction flask and compound **12** precipitated. The formed solid was filtered. Recrystallization in MeOH yielded 230 mg of compound **12** as brownish solid with 94% yield.

M.p. > 215ºC.

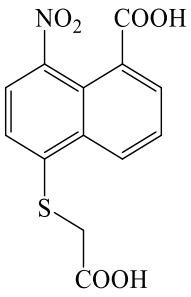
IR (film, υ in cm^{-1}): 3293, 1774, 1735, 1450, 1313.

^{1}H NMR (400 MHz, DMSO-d_6): δ 10.74 (s, 1H), 10.23 (s, 1H), 9.97 (s, 1H), 8.34 (d, *J* = 8.1 Hz, 1H), 8.19 (d, *J* = 7.0 Hz, 1H), 7.96 (d, *J* = 8.7 Hz, 2H), 7.92 (d, *J* = 8.0 Hz, 1H), 7.83 – 7.75 (m , 1H), 7.71 – 7.63 (m, 5H), 7.29 (dq, *J* = 7.3, 3.7 Hz, 2H*)*, 2.04 (s,3H).

^{13}C NMR (101 MHz, DMSO-d_6)**:** δ 168.8 (C), 166.2 (C), 164.9 (C), 163.9 (2C), 147.8 (C), 147.4 (C), 142.4 (C), 137.3 (C), 132.3 (C), 131.6 (C),131.4 (C), 130.8 (C), 130.5 (CH), 129.7 (CH), 129.3 (C), 129.2 (CH), 128.6 (CH), 128.5 (CH), 128.5 (C),127.8 (C), 125.9 (CH), 125.8 (CH), 125.6 (CH), 125.5 (CH), 125.2 (CH), 124.6 (CH), 123.8 (CH), 121.6 (C), 118.2 (CH), 24.0 (CH_3).

HRMS (ESI+):$[M+H]^+$ Calculated for $C_{30}H_{22}N_7O_9^+$ 624.5380; found 624.1474.

5-((Carboxymethyl)thio)-8-nitro-1-naphthoic acid (13)



13

In a round bottom flask, the thioglycolic acid (8 g, 86.85 mmol), potassium hydroxide (4 g, 71.29 mmol) and water (2 ml) were placed and stirred until a homogeneous solution was obtained. The naphthalene derivative compound **3** (4 g, 13.51 mmol) was dissolved in DMSO (25 ml) and DMF (5 ml). Both solutions were cooled down to 5 ºC then, the naphthalene solution was poured over the thioglycolic acid salt, keeping the temperature below 10 ºC. After 10 minutes the reaction was added over aqueous 2M hydrochloric acid (100 ml) and filtered to yield 5-((carboxymethyl)thio)-8-nitro-1-naphthoic acid **13** as a yellow solid (3.7 g, 89% yield).

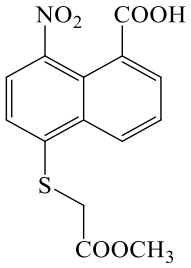
M.p.: >200 ºC

IR (nujol, ν in cm^{-1}): 3760, 3650, 3617, 1697, 1560, 1521, 1385, 1340, 1262, 1191, 899.

^{1}H NMR (400 MHz, DMSO-d_6) δ 8.50 (dd, *J* = 8.5, 0.9 Hz, 1H), 8.22 (d, *J* = 8.2 Hz, 1H), 8.16 (dd, *J* = 7.2, 1.1 Hz, 1H), 7.84 (dd, *J* = 8.5, 7.3 Hz, 1H), 7.62 (d, *J* = 8.3 Hz, 1H), 4.21 (s, 2H).

^{13}C NMR (101 MHz, DMSO-d_6) δ 169.6 (C), 168.0 (C), 144.6 (C), 142.7 (C), 131.2 (CH), 129.7 (C), 127.3 (CH), 126.9 (CH), 124.9 (CH), 121.9 (CH), 121.3 (2C), 34.2 (CH_2).

5-((2-Methoxy-2-oxoethyl)thio)-8-nitro-1-naphthoic acid (14)



14

Compound **13** 5-((carboxymethyl)thio)-8-nitro-1-naphthoic acid (3.7 g, 12 mmol) was dissolved in MeOH (30 ml) and THF (10 ml). Thionyl chloride was added (0.25 ml) and the reaction was allowed to stand (30 minutes). Evaporation under reduced pressure afforded a crude compound which was crystallized from methylene chloride to liberate a yellow crystalline solid (3.4 g, 88% yield).

M.p.: 170 ºC

IR (ν in cm^{-1}, nujol): 3903, 3747, 3663, 1761, 1690, 1567, 1288, 1132, 827.

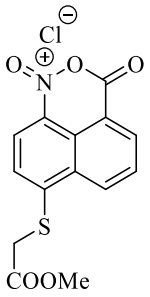
^{1}H NMR (400 MHz, DMSO-d_6) δ 8.49 (dd, *J* = 8.6, 1.1 Hz, 1H), 8.19 (dd, *J* = 8.2, 4.3 Hz, 1H), 8.15 (dd, *J* = 7.2, 1.1 Hz 1H), 7.83 (dd, *J* = 8.6, 7.2 Hz, 1H), 7.62 (d, *J* = 8.3 Hz, 1H), 4.30 (s, 2H), 3.66 (s, 3H).

^{13}C NMR (101 MHz, DMSO-d_6) δ 168.9 (C), 168.0 (C), 144.8 (C), 142.0 (C), 131.3 (C), 131.2 (CH), 129.7 (C), 127.4 (CH), 127.0 (CH), 124.8 (CH), 122.5 (CH), 121.3 (C), 52.6 (CH_3), 33.7 (CH_2).

MS (ESI+)$[M+Na]^+$ calculated for $C_{14}H_{11}O_6N^{23}Na^{32}S$ 344.0205, found 344.0199.

7-((2-methoxy-2-oxoethyl)thio)-1,3-dioxo-1*H*,3*H*-naphtho[1,8-*cd*][1,2]oxazin-1-iumchloride (14A)

General procedure of acid activation using oxalyl chloride



14A

5-((2-methoxy-2-oxoethyl)thio)-8-nitro-1-naphthoic acid (1 g, 3.1 mmol) was suspended in oxalyl chloride (3 ml, 35 mmol) and tetraethyl ammonium chloride (10 mg, 0.06 mmol) was added as a catalyst. The reaction flask was sonicated in an ultrasound bath at 40 ºC for 30 minutes until the starting material was completely dissolved. To the clear solution toluene was added (5 ml) and the solvents were removed under reduced pressure in a water bath at 20 ºC yielding compound **7** as a pale-yellow solid (1 g, 99%).

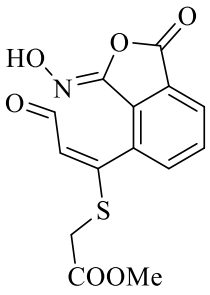
(Melting point and IR were not measured due to the instability of the compound).

^{1}H NMR (400 MHz, $CDCl_3$) δ 8.64 (dd, *J* = 8.6, 1.0 Hz, 1H), 8.36 (dd, *J* = 7.4, 1.0 Hz, 1H), 8.18 (d, *J* = 8.2 Hz, 1H), 7.76 (dd, *J* = 8.6, 7.4 Hz, 1H), 7.61 (d, *J* = 8.2 Hz, 1H), 3.90 (s, 2H), 3.76 (s, 3H).

^{13}C NMR (101 MHz, $CDCl_3$) δ 168.8 (C), 167.7 (C), 144.9 (C), 143.0 (C), 133.1 (CH), 132.7 (C), 130.0 (CH), 126.7 (CH), 125.9 (CH), 124.0 (CH), 121.5 (C), 53.2 (CH_2), 35.3 (CH_3).

HRMS (ESI) ($[M]^+$) calculated. for $C_{14}H_{10}NO_5S^+$ 304.0274, found 304.0273.

Methyl 2-(((*E*)-1-((*Z*)-3-(hydroxyimino)-1-oxo-1,3-dihydroisobenzofuran-4-yl)-3-oxoprop-1-en-1-yl)thio)acetate (4)



14B

Compound **14A** (1 g, 3.1 mmol) was quickly dissolved in methylene chloride (20 ml) and added to a solution of bis(2-chloroethyl)amine (2 g, 14.1 mmol) in an ether solution saturated with water and methylene chloride (100 ml) cooled to -30 ºC. After 30 minutes the reaction mixture

was added over aqueous sulfuric acid (2M, 100 ml), separated in a separatory funnel, and the organic phase was washed again with another portion of aqueous sulfuric acid (50 ml) and water (100 ml). Evaporation of the major part of the methylene chloride induced the crystallization of the aldehyde which was filtered under reduced pressure to yield a pale cream solid (700 mg, 70% yield).

M.p.: 111-113 ºC.

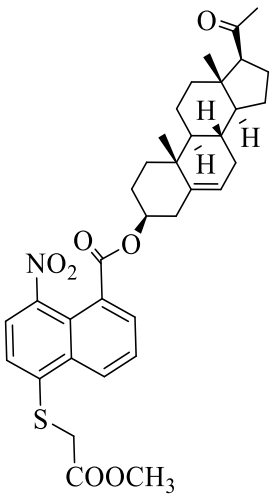
IR (neat, ν in cm^{-1}): 3318, 1785, 1734, 1663, 1573, 1525, 1438, 1283, 1137.

^{1}H NMR (400 MHz, DMSO-*d_6*) δ 11.83 (s, OH), 9.07 (d, *J* = 7.9 Hz, 1H(1)), 8.07 (dd, *J* = 7.0, 1.7 Hz, 1H(7)), 7.85 – 7.76 (m, 2H(5,6)), 6.23 (d, *J* = 7.9 Hz, 1H(2)), 3.95 (d, *J* = 16.0 Hz, 1H(12)), 3.89 (d, *J* = 16.2 Hz, 1H(12)), 3.66 (s, 3H(14)).

^{13}C NMR (101 MHz, DMSO-*d_6*) δ 188.9 (CH(1)), 168.2 (C(13)), 163.2 (C(10)), 159.4 (C(3)), 145.8 (C(11)), 136.5 (CH(5)), 132.9 (C(9)), 131.7 (CH(6)), 128.8 (C(8)), 127.0 (C(4)), 126.7 (CH(7)), 124.5 (CH(2)), 52.6 (CH_3(14)), 34.0 (CH_2(12)).

HRMS (ESI) ([M+Na]$^+$) calculated. for $C_{14}H_{11}NNaO_6S^+$ 344.0199, found 344.0193.

(2*S*,8*R*,10*R*,13*R*,14*S*,17*S*)-17-acetyl-10,13,14-trimethyl-2,3,4,7,8,9,10,11,12,13,14,15,16,17-tetradecahydro-1*H*-cyclopenta[*a*]phenanthren-2-yl 5-((2-methoxy-2-oxoethyl)thio)-8-nitro-1-naphthoate (16)



16

Compound **14** (100 mg, 0.32 mmol) was used to prepare the acid chloride following the procedure explained in *Acid activation using $C_2O_2Cl_2$*.

In a round bottom flask, the crude compound **15** (135 mg,0.40 mmol) was dissolved in 5 mL of CH_2Cl_2 with commercial pregnenolone (133 mg, 42.02 mmol), the reaction mixture was

stirred at room temperature for 10 min. The crude reaction mixture was purified by silica gel column chromatography using CH_2Cl_2 as eluent affording a pale-yellow solid (90 mg, 45%).

Mp:193-196 ºC

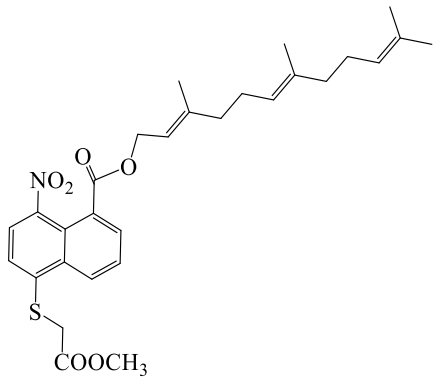
IR (neat, ν in cm $^{-1}$): 3740, 3624, 1690, 1521, 1456, 1385 ,1346 ,788.

^{1}H NMR (400 MHz, $CDCl_3$) δ 8.55 (dd, *J* = 8.6, 1.2 Hz, 1H), 8.13 (dt, *J* = 2.9, 1.5 Hz, 1H), 8.11 (d, *J* = 8.1 Hz, 1H), 7.69 (dt, *J* = 7.9, 5.8 Hz, 1H), 7.57 (d, *J* = 8.2 Hz, 1H), 5.44 (d, *J* = 5.2 Hz, 1H), 4.93 – 4.72 (m, 1H), 3.87 (s, 2H), 3.74 (s, 3H), 2.62 – 2.39 (m, 3H), 2.08 – 1.15 (m, 19H), 1.12 – 0.96 (m, 4H), 0.64 (s, 3H).

^{13}C NMR (101 MHz, $CDCl_3$) δ 209.6 (C), 168.9 (C), 166.6 (C), 145.9 (C), 141.8 (C), 139.6 (C), 132.8 (C), 131.8 (CH), 129.7 (C), 127.8 (CH), 126.9 (CH), 124.7 (CH), 123.6 (CH), 122.6 (CH), 122.4 (C),77.2 (CH) , 76.0 (CH), 63.7 (CH), 56.9 (CH), 53.00 (CH), 49.9 (CH_3), 44.00 (C), 38.9 (CH_2), 37.8 (CH_2), 36.6 (CH_2), 35.3 (CH_2), 31.9 (CH_2), 31.8 (C), 31.5 (CH_3), 27.5 (CH_2), 24.5 (CH_2), 22.9 (CH_2), 21.0 (CH_2), 19.3 (CH_3), 13.2 (CH_3).

MS (ESI-):[M+Na] + : calculated for $C_{35}H_{41}NO_7SNa$ 642.2501 found 642.2489.

(2*E*,6*E*)-3,7,11-trimethyldodeca-2,6,10-trien-1-yl 5-((2-methoxy-2-oxoethyl) thio)-8-nitro-1-naphthoate (17)



17

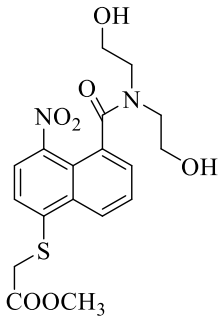
In a round bottom flask compound **15** (100 mg ,0.29 mmol) was dissolved in 3 mL of CH_2Cl_2, the mixture was treated 200µL of *N*, *N*-Diisopropylethylamine. On the other hand, farnesol iodide (200 mg, 0.60 mmol) was dissolved in 500 mg of CH_2Cl_2 in a 50 mL Erlenmeyer flask and transferred to the flask´s mixture, the reaction was stirred for 20 min at room temperature. The crude reaction mixture was purified by silica gel column chromatography using CH_2Cl_2 as eluent yielding a brownish oily compound (150 mg, 98 %).

Mp: Oily

IR (neat, ν in cm $^{-1}$): 3753, 3539, 1580, 1450, 1346,1275, 1100,1009, 821.

^{1}H NMR (400 MHz, $CDCl_3$) δ 8.52 (d, *J* = 8.6 Hz, 1H), 8.12 (d, *J* = 7.2 Hz, 1H), 8.06 (d, *J* = 8.1 Hz, 1H), 7.67 (dd, *J* = 11.5, 4.3 Hz, 1H), 7.55 (d, *J* = 8.1 Hz, 1H), 5.42 (t, *J* = 7.1 Hz, 1H), 5.08 (dt, *J* = 6.9, 3.7 Hz, 2H), 4.80 (t, *J* = 7.4 Hz, 2H), 3.85 (s, 2H), 3.73 (s, 3H), 2.17 – 1.91 (m, 8H), 1.76 (s, 3H), 1.66 (s, 3H), 1.59 (s, 3H).
^{13}C NMR (101 MHz, $CDCl_3$) δ 168.8 (C), 167.1 (C), 145.9 (C), 143.0 (C), 135.3 (C), 132.6 (C), 131.8 (CH), 131.5 (C), 131.2 (C), 129.3 (C), 127.8 (CH), 126.8 (CH), 124.5 (CH), 124.3 (CH), 123.6 (CH), 123.5 (CH), 122.4 (C), 117.7 (CH), 62.4 (CH_2), 52.9 (CH_3), 39.6 (CH_2),35.2 (CH_2), 31.9 (CH_2), 26.7 (CH_2), 26.1 (CH_2), 25.6 (CH_3), 17.6 (CH_3), 16.5 (CH_3), 16.0 (CH_3).
MS (ESI-):[M+Na] +: calculated for $C_{29}H_{35}O_6NNaS$ 548.2083, found 548.2071.

Methyl 2-((5-(bis(2-hydroxyethyl)carbamoyl)-4-nitronaphthalen-1-yl)thio)acetate (18)



18

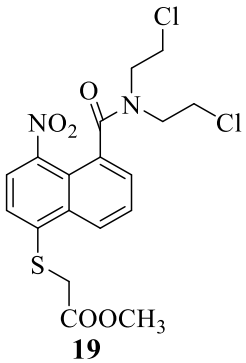
Compound **14A** was synthesized using the procedure for **a*cid activation using*** $C_2O_2Cl_2$.
Compound **14A** (100 mg, 0.29 mmol) was dissolved in 5 mL of CH_2Cl_2 and added over a mixture of diethanolamine (200 mg, 1.90 mmol) dissolved in 3 mL of CH_2Cl_2 and cooled down in an ice bath to 0ºC. The organic phase was diluted with EtOAc and washed twice: once with 20 ml of 2M HCl, and the second with diluted sulfuric acid, dried over anhydrous Na_2SO_4, filtered and concentrated under reduced pressure, the crude was purified by silica gel column chromatography using CH_2Cl_2 and EtOAc as eluents affording an oily compound (110 mg, 93%).

Mp: Oily
IR (neat, ν in cm $^{-1}$):3864, 3745, 2936, 2877, 1748, 1463,1521,1307, 1256, 911, 827, 730.
^{1}H NMR (400 MHz, $CDCl_3$) δ 8.45 (dt, *J* = 10.1, 5.0 Hz, 1H), 8.05 – 7.89 (m, 2H), 7.78 – 7.59 (m, 1H), 7.58 – 7.47 (m, 1H), 4.12 – 3.86 (m, 6H), 3.85 (d, *J* = 5.2 Hz, 2H), 3.74 (s, 2H), 3.47 – 3.32 (s, 3H).

^{13}C NMR (101 MHz, $CDCl_3$) δ 171.8 (C), 169.0 (C), 146.0 (C), 141.5 (C), 138.2 (C), 133.1 (C), 132.0 (C), 130.3 (CH), 127.5 (CH), 126.8 (CH), 125.2 (CH), 123.7 (CH), 60.7 (CH_2), 59.7 (CH_2), 53.6 (CH_2), 53.0 (CH_3), 48.6 (CH_2), 35.2 (CH_2).

MS (ESI-):[M-H+]: calculated value for $C_{18}H_{20}N_2O_7S$ is 408.0991, found 409.1064.

Methyl 2-((5-(bis(2-chloroethyl) carbamoyl)-4-nitronaphthalen-1-yl) sulfonyl) acetate (19)



19

In a 50 mL round bottom flask compound **18** (100 mg, 0.24 mmol) was dissolved in 5 mL CH_2Cl_2, 1mL of thionyl chloride and 2 mL of toluene were added, then the mixture was refluxed for one hour, the obtained crude product was purified over silica gel column chromatography using CH_2Cl_2-EtOAc 80%-20% as eluents yielding an oily compound (75 mg, 70%).

Mp: Oily

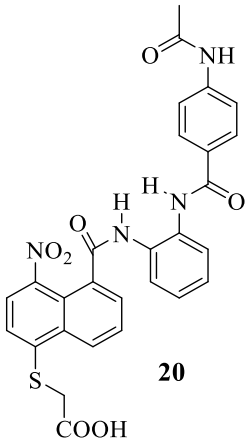
IR (neat, ν in cm $^{-1}$): 3903, 3753, 3630,2936,1567, 1418, 1158, 1015, 918, 827.

^{1}H NMR (400 MHz, $CDCl_3$) δ 8.53 (dd, *J* = 8.5, 1.2 Hz, 1H), 7.99 (d, *J* = 8.1 Hz, 1H), 7.78 (dd, *J* = 7.1, 1.2 Hz, 1H), 7.70 (dd, *J* = 8.5, 7.2 Hz, 1H), 7.58 (d, *J* = 8.1 Hz, 1H), 4.15 – 3.89 (m, 4H), 3.87 (s, 2H), 3.85 – 3.76 (m, 3H), 3.75 (s, 3H), 3.72 – 3.61 (m, 1H).

^{13}C NMR (101 MHz, $CDCl_3$) δ 171.0(C), 168.9 (C), 145.7 (C), 141.8 (C), 133.2 (C), 131.3 (C), 129.4 (CH), 126.9 (CH), 126.7 (CH), 124.4 (CH), 123. 9 (CH), 122.7 (C), 53.0 (CH_3), 52.1 (CH_2), 48.0 (CH_2), 41.1 (CH_2), 40.3 (CH_2), 35.3 (CH_2).

MS (ESI-) [M+H]+: calculated for $C_{18}H_{18}Cl_2N_2O_5S$ 444.0313, found 445.0381.

2-((5-((2-(4-Acetamidobenzamido)phenyl)carbamoyl)-4-nitronaphthalen-1-yl)-l3-sulfaneyl)acetate (20)



20

In three necks round bottom flask finely powdered 5-bromo-8-nitro-1-naphthoic acid (compound **3**) (200 mg, 0.68 mmol) was dissolved in 5 mL of CH_2Cl_2 and treated with 200 µL of triethylamine, a homogenous mixture has been afforded, then the organic solvent was evaporated. The precipitate obtained was dissolved in diluted thionyl chloride (10%) and stirred for 10 min.

After 10 min at room temperature thionyl chloride was evaporated, then the crude reaction mixture was dissolved in CH_2Cl_2 and cooled down at – 70 ºC for 20 min (the flask should be equipped with thermometer, argon ballon connected to an additional funnel and a stopper).

In parallel, Tacedinaline **8** (200 mg, 0.74 mmol) was dissolved in 4 mL of pyridine, this mixture was placed in the addition funnel and added all at once to the previous cold mixture. Then, the stirred reaction was treated with aqueous HCl (2M), a solid was obtained and filtered under vacuum, the crude product **10** was used in the next step without further purification.

In a 50 mL round bottom flask compound **10** (100 mg, 0.19 mmol) was dissolved in 3 mL of DMSO, an aqueous solution of anhydrous thioglycolate (100 mg, 1.10 mmol) and KOH (50 mg, 0.89 mmol) were dissolved in 100 mg of water and added over the mixture, reacting for 10 min at room temperature.

The reaction mixture was washed with aqueous HCl (2M) and the organic layer was extracted with EtOAc, dried over anhydrous sodium sulfate, then the organic solvent was removed under reduced pressure affording (70 mg, 65%) of a grey solid.

Mp: > 200 ºC

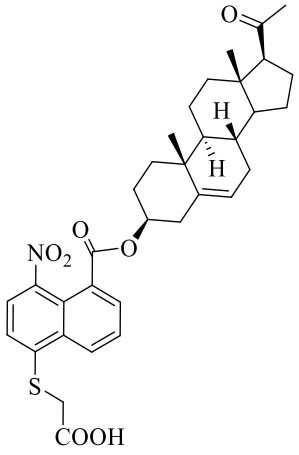
IR (nujol, υ, cm^{-1}): 3903, 3753,3643, 1314, 1165, 970, 743.

^{1}H NMR (400 MHz, DMSO-d_6) δ 10.50 (s, 1H), 10.23 (s, 1H), 9.82 (s, 1H), 8.47 (d, *J* = 8.5 Hz, 1H), 8.15 (dd, *J* = 14.8, 7.6 Hz, 2H), 7.94 (t, *J* = 8.5 Hz, 2H), 7.86 – 7.79 (m, 1H), 7.73 – 7.64 (m, 4H), 7.61 (d, *J* = 8.3 Hz, 1H), 7.29 (dd, *J* = 5.8, 3.6 Hz, 2H), 4.20 (s, 2H), 2.08 (d, *J* = 9.6 Hz, 3H).

^{13}C NMR (101 MHz, DMSO-d_6) δ 169.7 (C), 168.8 (C), 166.7 (C), 164.9 (C), 144.7 (C), 142.5 (C), 142.4 (C), 132.8 (C), 131.5 (C), 131.3 (C), 130.9 (C), 130.0 (2CH), 128.5 (CH), 127.2 (CH), 126.3 (CH), 125.8 (CH), 125.7 (CH), 125.6 (CH), 125.2 (CH), 124.8 (CH), 122.0 (2CH), 121.2 (C), 118.2 (CH), 34.2 (CH_2), 24.1 (CH_3).

MS (ESI+):$[M+Na]^+$: calculated for $C_{28}H_{22}N_4NaO_7S$ 581.1107, found 581.1097.

2-((5-((((2*R*,8*S*,9*S*,10*R*,13*S*,17*S*)-17-acetyl-10,13-dimethyl-2,3,4,7,8,9,10,11,12,13,14,15,16,17-tetradecahydro-1*H*-cyclopenta[*a*]phenanthren-2-yl)oxy)carbonyl)-4-nitronaphthalen-1-yl)thio)acetic acid (21)



21

In a 50 mL round bottom flask compound **16** (50 mg, 0.08 mmol) was dissolved in 3 mL of MeOH, potassium carbonate (100 mg, 0.72 mmol) was added over the reaction mixture and the progress of the reaction was monitored by TLC (methylene chloride as eluent). Finally, the reaction mixture was treated with aqueous HCl (2M), the organic phase was extracted with EtOAc, dried over anhydrous Na_2SO_4, then the solvent was evaporated under vacuum, yielding 50 mg (100%) of a pale yellow solid.

Mp: > 200 ºC

IR (nujol, υ, cm^{-1}): 3896, 3753, 3643, 1288, 1152, 736.

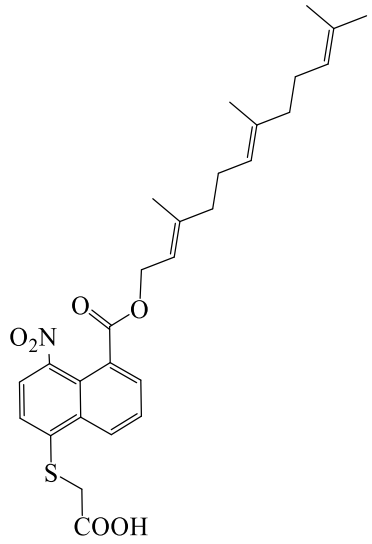
^{1}H NMR (400 MHz, DMSO-d_6) δ 8.52 (dd, *J* = 8.6, 1.1 Hz, 1H), 8.26 (d, *J* = 8.3 Hz, 1H), 8.15 (dd, *J* = 7.2, 1.1 Hz, 1H), 7.85 (dd, *J* = 8.5, 7.3 Hz, 1H), 7.62 (d, *J* = 8.4 Hz, 1H), 5.39 (d, *J* = 3.6 Hz, 1H), 4.62 (ddd, *J* = 11.5, 9.7, 4.3 Hz, 1H), 4.21 (s, 2H), 2.57 (t, *J* = 8.9 Hz, 1H), 2.06 (s, 3H), 2.03 – 1.03 (m, 19H), 0.99 (d, *J* = 8.8 Hz, 4H), 0.54 (s, 3H).

^{13}C NMR (101 MHz, DMSO-d_6) δ 208.5 (C), 169.6 (C), 165.9 (C), 144.0 (C), 143.4 (C), 139.4 (C), 131.8 (CH), 131.1 (C), 128.6 (C), 127.4 (CH), 125.4 (CH), 122.2 (CH), 122.0 (CH), 121.0 (C), 75.3 (CH), 62.5 (CH), 56.0 (CH), 49.2 (CH), 43.2 (C), 37.9 (CH_2), 37.3 (CH_2), 36.4 (CH_2), 36.1 (C), 34.1 (CH_2), 31.5 (CH) 31.3 (CH), 31.2 (CH_2), 31.2 (CH_3),27.0 (CH_2), 24.0 (CH_2), 22.2 (CH_2), 20.5 (CH_2), 18.9 (CH_3), 12.9 (CH_3).

MS (ESI-):[M-H]$^-$: calculated for $C_{34}H_{38}NO_7S$ 604.2447, found 604.2380.

$[\alpha]_D^{20}$ +13.66 (c 1.2, $CHCl_3$).

2-((4-nitro-5-((((2*E*,6*E*)-3,7,11-trimethyldodeca-2,6,10-trien-1-yl)oxy)carbonyl)naphthalen-1-yl)thio)acetic acid (22)



22

In a 50 mL round bottom flask compound **17** (90 mg, 0.17 mmol) was dissolved in 3 mL of MeOH, potassium carbonate (800 mg, 5.78 mmol) was added over the reaction mixture and the progress of the reaction was monitored by TLC (EtOAc as eluent). Finally, the reaction mixture was treated with aqueous HCl (2M), the organic phase was extracted with EtOAc, dried over anhydrous Na_2SO_4 and the solvent was evaporated under vacuum yielding 90 mg (100%) of a brownish oil.

Mp: Oily

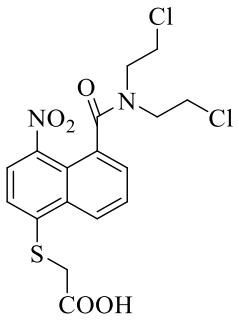
IR (neat, ν in cm $^{-1}$): 3760, 3676,1450 ,1275, 1080, 905, 834.

^{1}H NMR ^{1}H NMR (400 MHz, $CDCl_3$) δ 8.47 (d, *J* = 6.2 Hz, 1H), 8.19 – 7.82 (m, 2H), 7.65 (s, 1H), 7.52 (d, *J* = 5.5 Hz, 1H), 5.42 (s, 1H), 5.10 (s, 2H), 4.80 (s, 2H), 3.85 (s, 2H), 2.20 – 1.90 (m, 8H), 1.75 (s, 3H), 1.66 (s, 3H), 1.58 (s, 6H).

^{13}C NMR (101 MHz, $CDCl_3$) δ 173.0 (C), 167.3 (C), 145.8 (C), 143.2 (C), 141.3 (C), 135.3 (C), 132.5 (C), 131.8 (CH), 131.2 (C), 129.1 (C), 127.7 (CH), 126.8 (CH), 124.6(CH), 124.4 (CH), 124.3 (CH), 123.5 (CH), 122.3 (C), 117.5 (CH), 62.6 (CH_2), 39.6 (CH_2), 35.0 (CH_2), 31.9 (CH_2), 26.7 (CH_2), 26.1 (CH_2), 25.6 (CH_3), 17.6 (CH_3), 16.4 (CH_3), 15.9 (CH_3).

MS (ESI-):[M-H]$^{-}$: calculated for $C_{28}H_{32}NO_6S$ 510.2029, found 510.1958.

2-((5-(bis(2-chloroethyl) carbamoyl) -4-nitronaphthalen-1-yl) thio)acetic acid (23)



23

In a 50 mL round bottom flask compound **19** (50 mg, 0.11 mmol) was dissolved in 3 mL of MeOH, potassium carbonate (500 mg, 3.61 mmol) was added over the reaction mixture, and it was heated gently (below 50 º C) for one hour. The progress of the reaction was monitored by TLC (methylene chloride as eluent). Finally, the reaction mixture was treated with aqueous HCl (2M), the organic phase was extracted with EtOAc, dried over Na_2SO_4 and the solvent was evaporated under vacuum yielding 50 mg (100%) of a brownish oily compound.

Mp: Oily

IR (neat, ν in cm $^{-1}$):3864, 3909, 3747, 3682, 2942, 2851, 1638, 1515, 1359, 1288, 1177, 924, 736.

^{1}H NMR (400 MHz, $CDCl_3$) δ 8.50 (d, *J* = 8.4 Hz, 1H), 7.96 (d, *J* = 8.0 Hz, 1H), 7.74 (d, *J* = 6.8 Hz, 1H), 7.67 (d, *J* = 8.4 Hz, 1H), 7.56 – 7.51 (m, 1H), 4.01 – 3.86 (m, 4H), 3.84 (s, 2H), 3.77 (dd, *J* = 15.3, 8.2 Hz, 2H), 3.66 (dd, *J* = 13.1, 6.9 Hz, 2H).

^{13}C NMR (101 MHz, $CDCl_3$) δ 171.2 (C), 170.2 (C), 145.2 (C), 142.5 (C), 132.9 (C), 131.0 (C), 129.3 (CH), 126.9 (CH), 126.5 (CH), 124.5(CH), 123.1 (CH), 122.4 (C), 52.1 (CH_2), 47.8 (CH_2), 40.9 (CH_2), 40.2 (CH_2), 35.2 (CH_2).

MS (ESI-):[M-H]$^{-}$: Calculated for $C_{17}H_{15}Cl_2N_2O_5S$ 429.0157, found 429.0085.

5.2. NMR Spectra

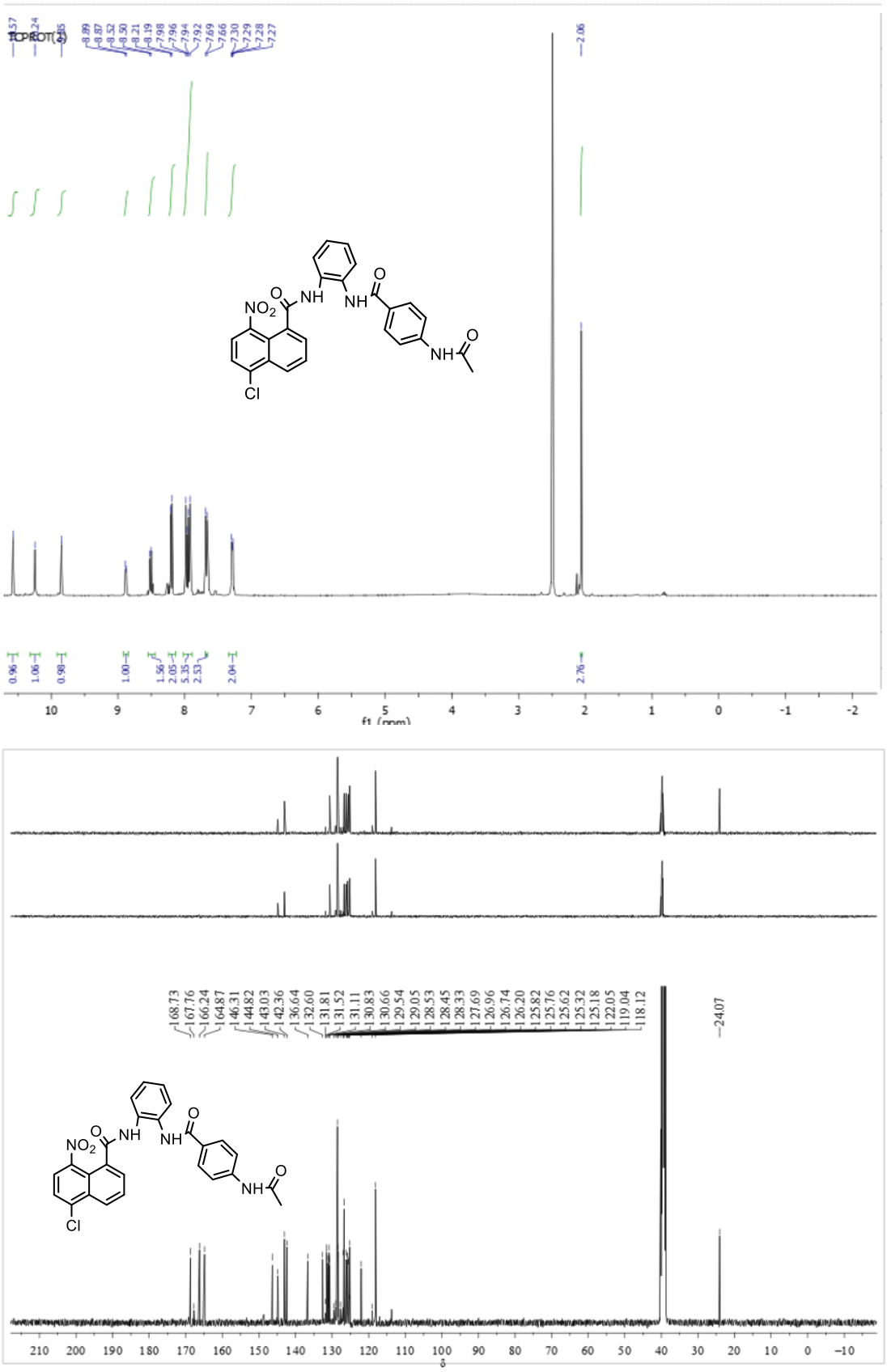


Figure S1. *^{1}H NMR (DMSO-d_6, 400 MHz) and ^{13}C (DMSO-d_6, 100 MHz) spectra of (**10**).*

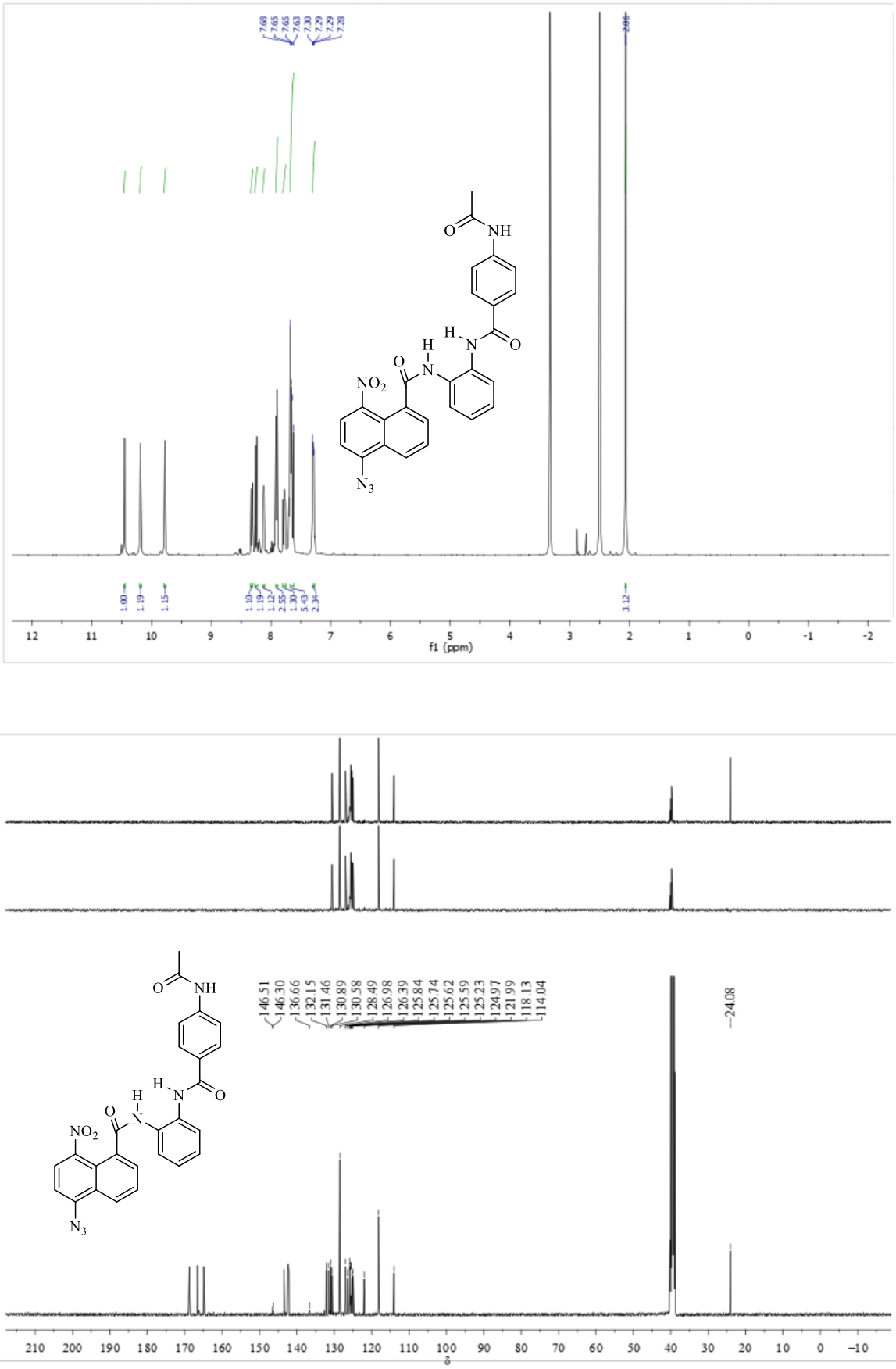


Figure S2. *^{1}H NMR (DMSO-d_6, 400 MHz) and ^{13}C (DMSO-d_6, 100 MHz) spectra of (**11**).*

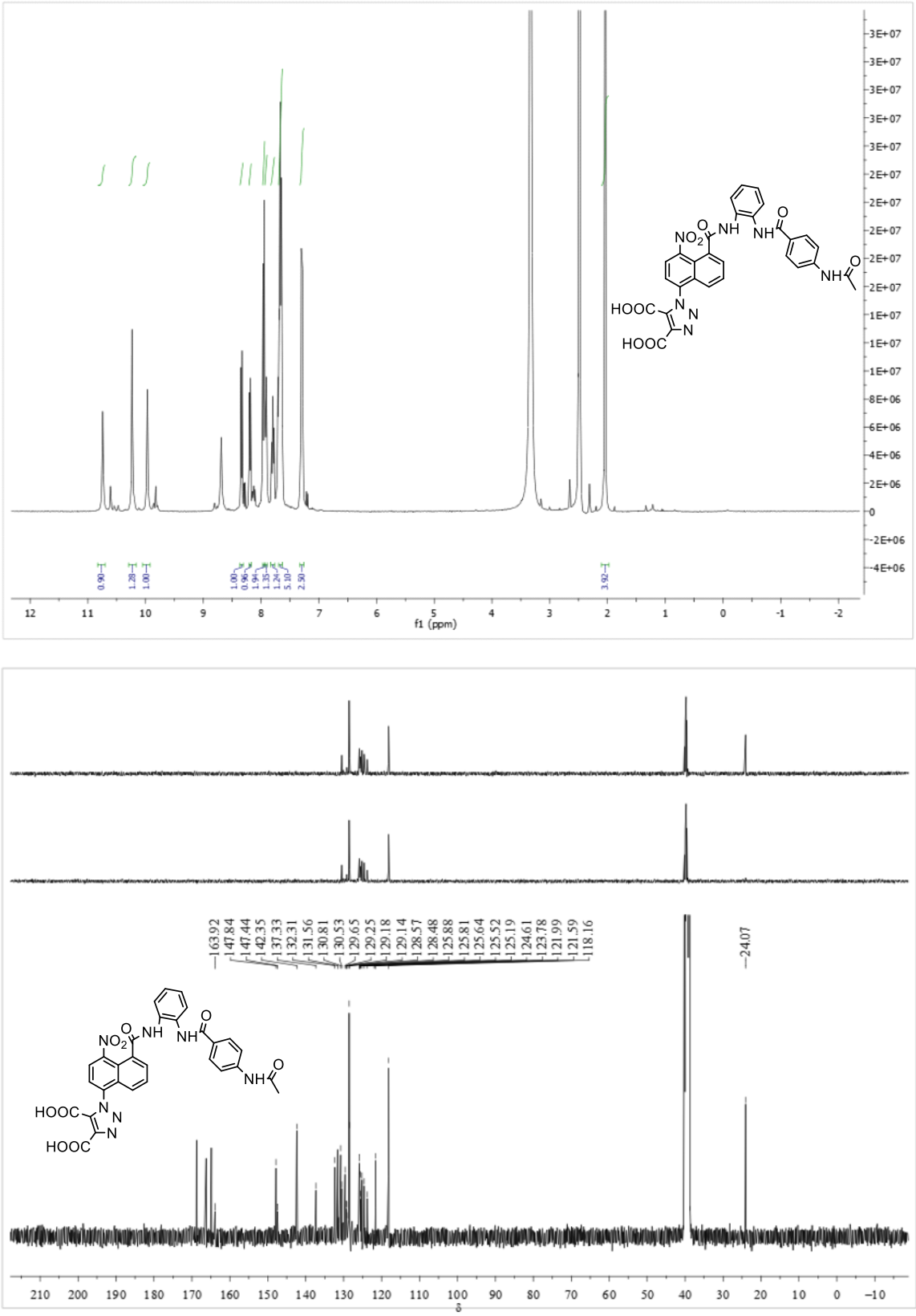


Figure S3. *^{1}H NMR (CD_3OD, 400 MHz) and ^{13}C (CD_3OD, 100 MHz) spectra of (**12**).*

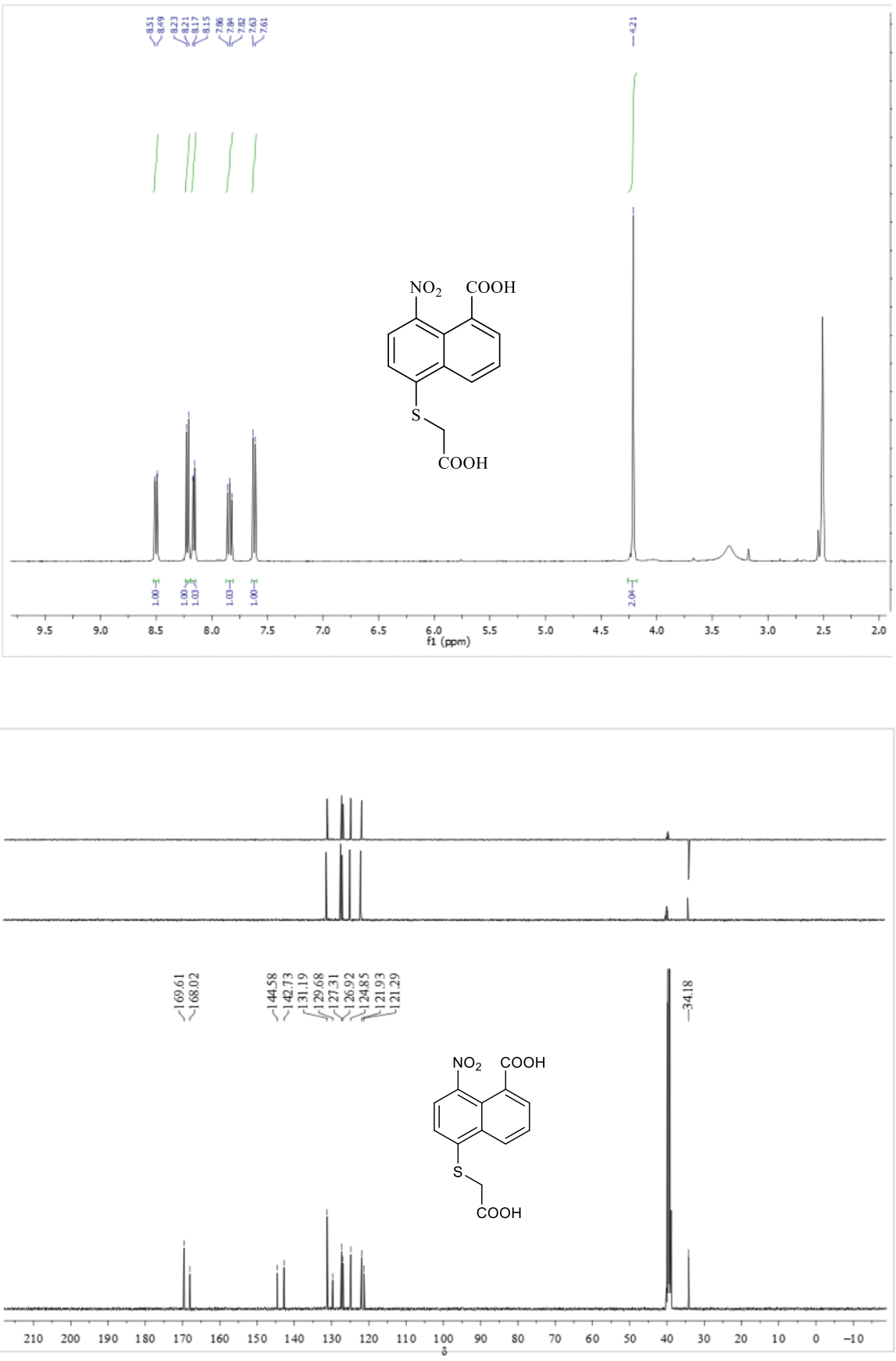


Figure S4. *^{1}H NMR (DMSO-d_6, 400 MHz) and ^{13}C (DMSO-d_6, 100 MHz) spectra of (**13**).*

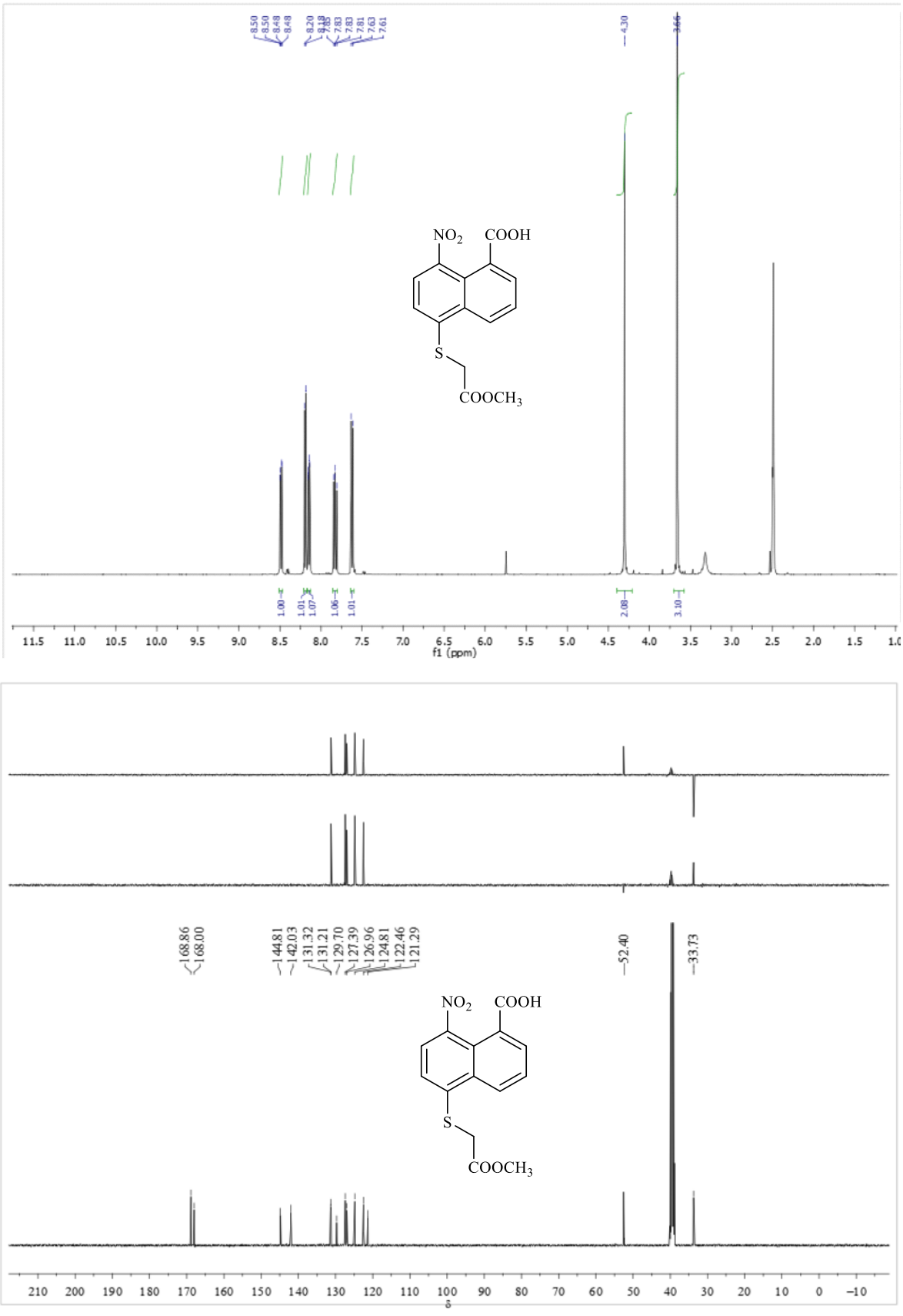


Figure S5. *^{1}H NMR (DMSO-d_6, 400 MHz) and ^{13}C (DMSO-d_6, 100 MHz) spectra of (**14**).*

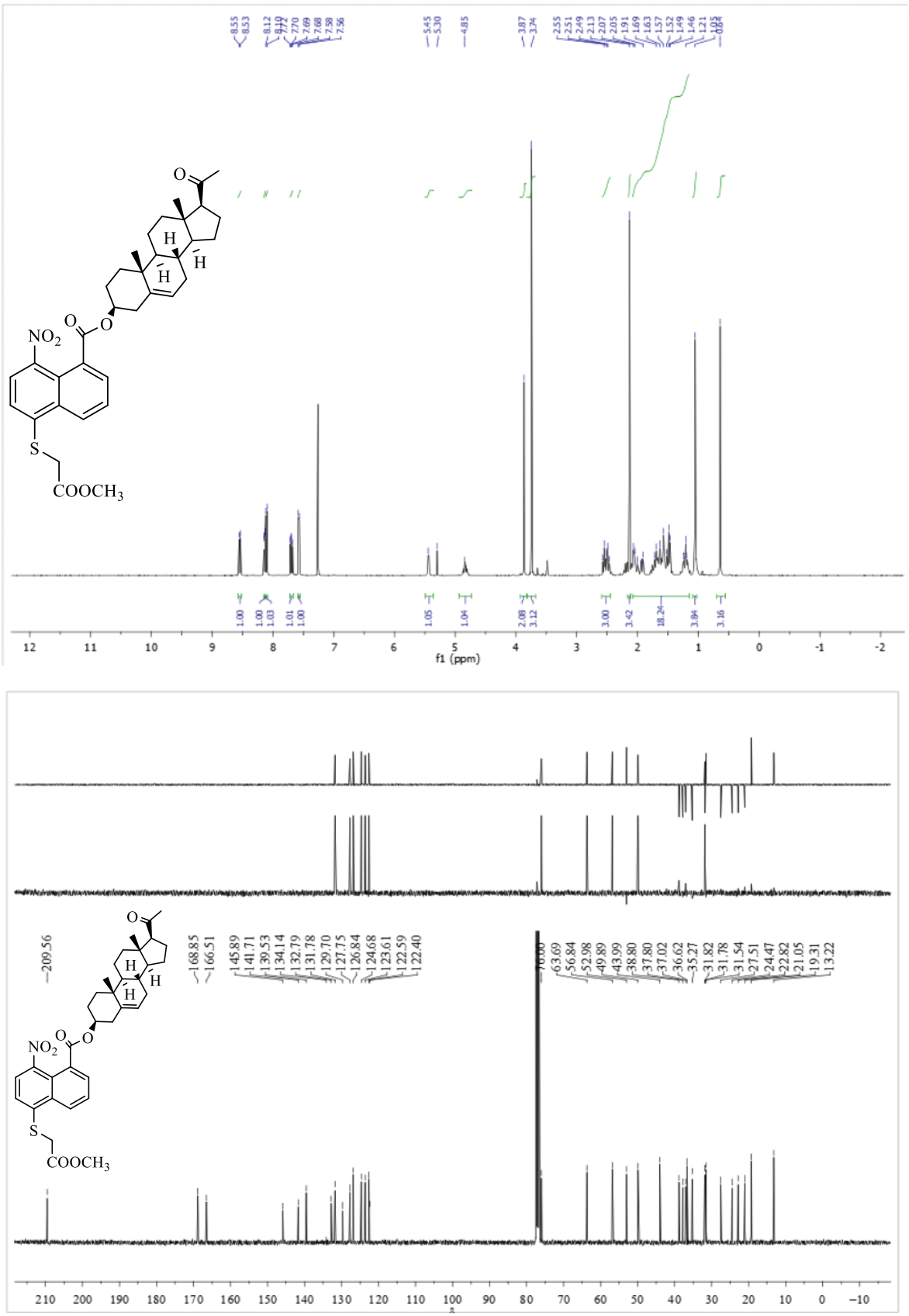


Figure S6. *^{1}H NMR ($CDCl_3$, 400 MHz) and ^{13}C ($CDCl_3$, 100 MHz) spectra of (**16**).*

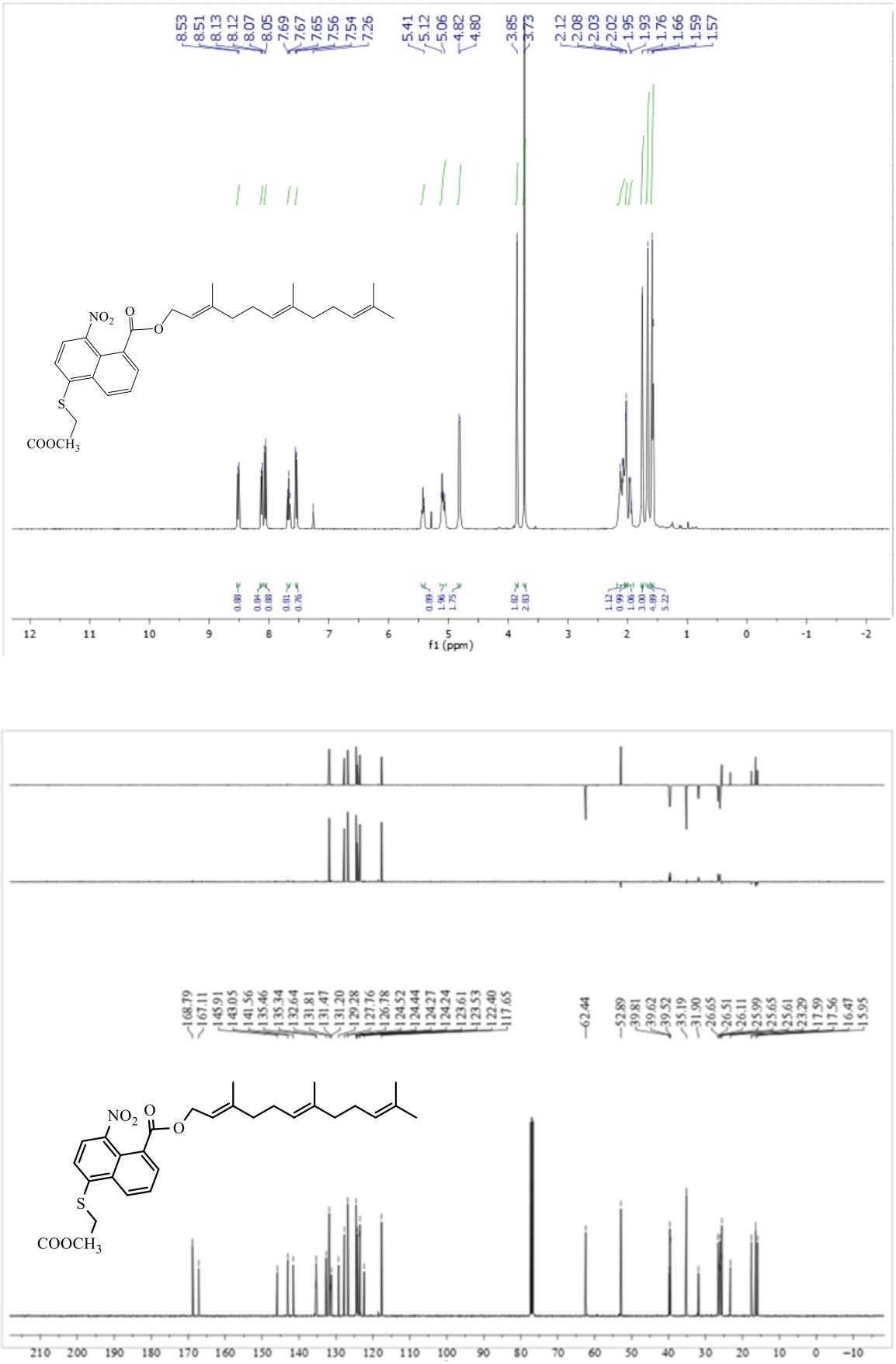
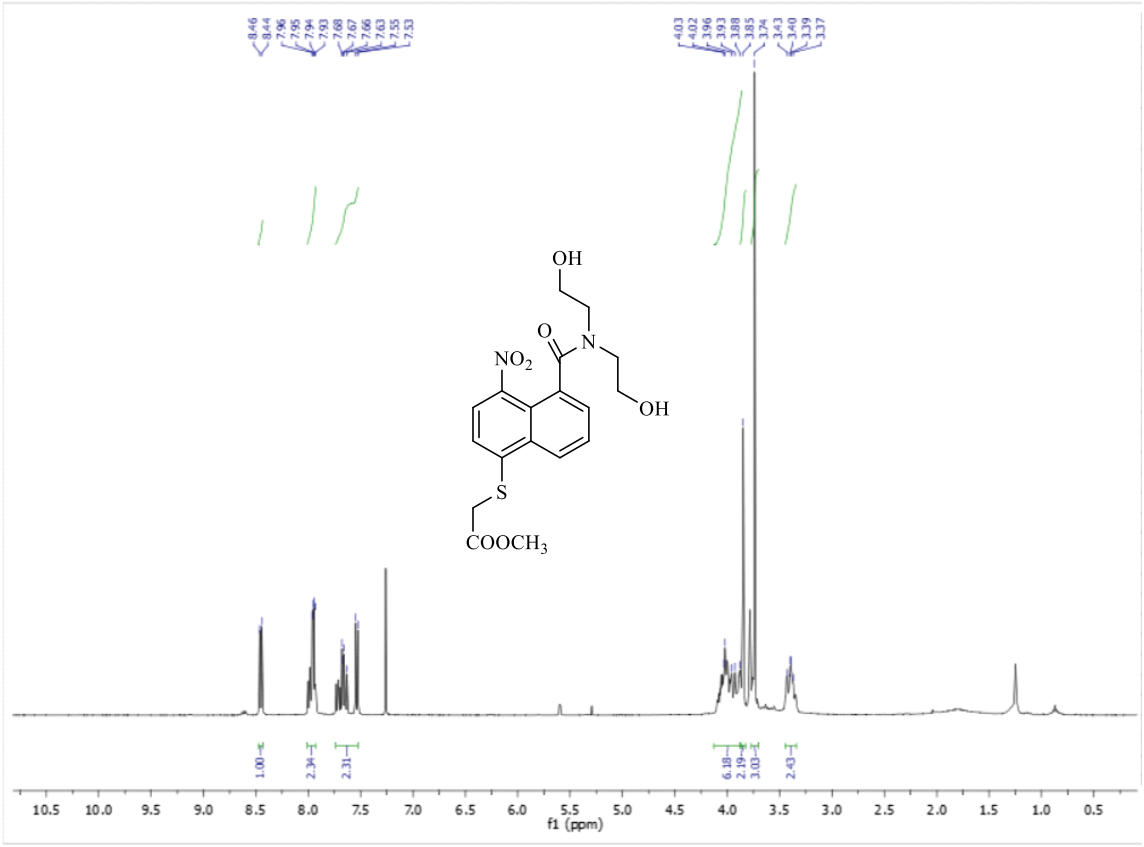


Figure S7. *^{1}H NMR ($CDCl_3$, 400 MHz) and ^{13}C ($CDCl_3$, 100 MHz) spectra of (**17**).*



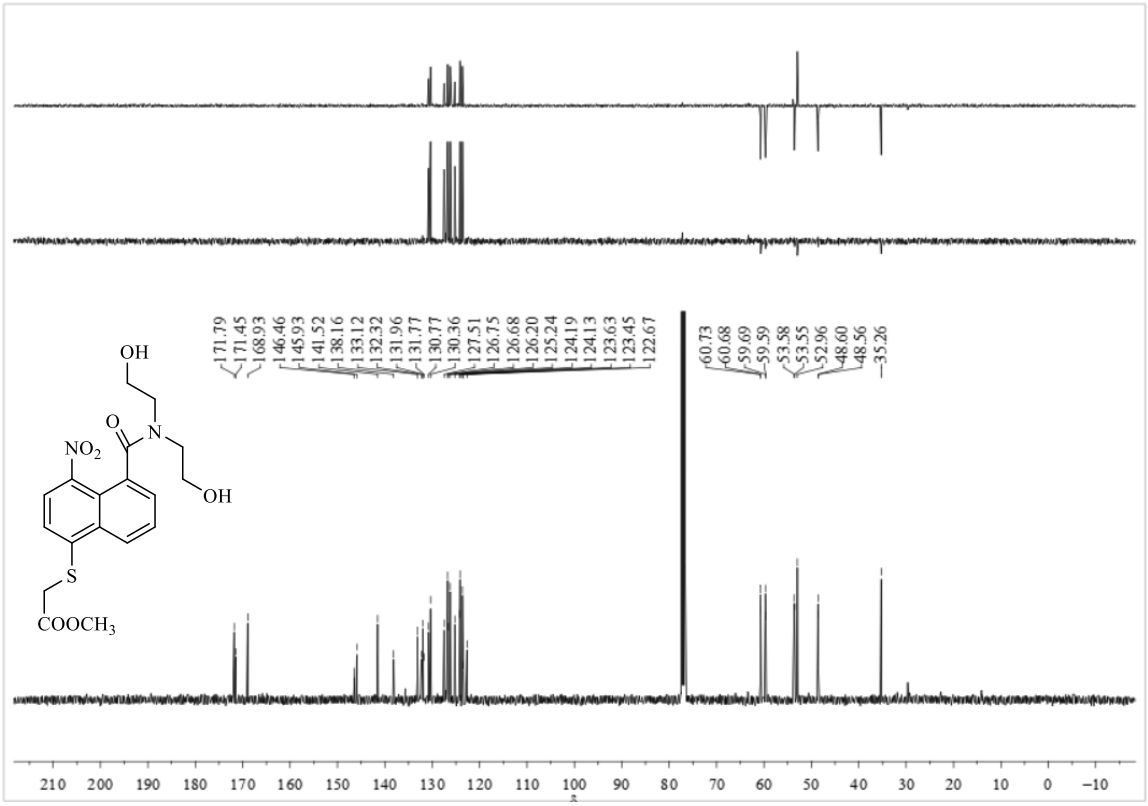


Figure S8. *^{1}H NMR ($CDCl_3$, 400 MHz) and ^{13}C ($CDCl_3$, 100 MHz) spectra of (**18**).*

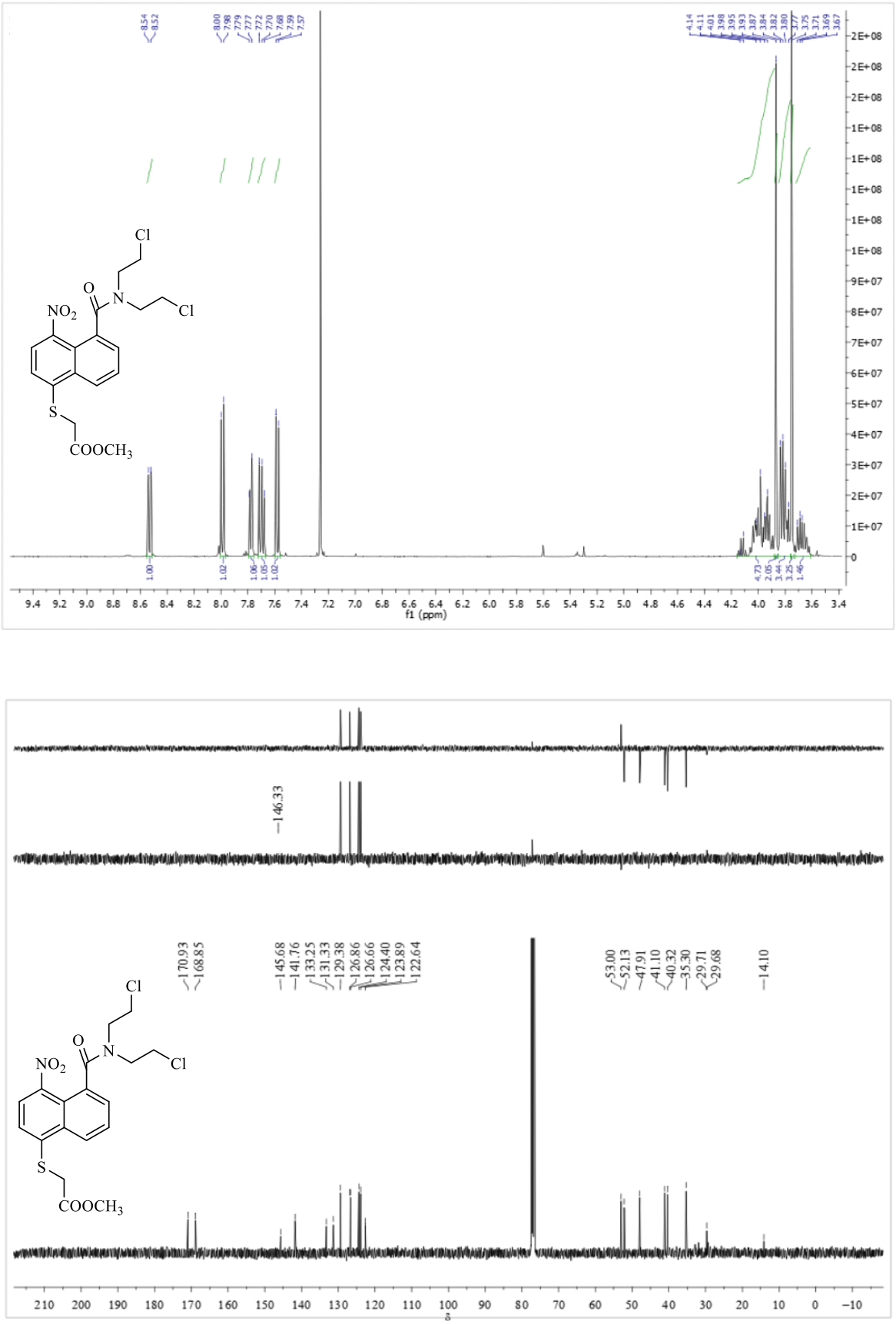


Figure S9. *^{1}H NMR ($CDCl_3$, 400 MHz) and ^{13}C ($CDCl_3$, 100 MHz) spectra of (**19**).*

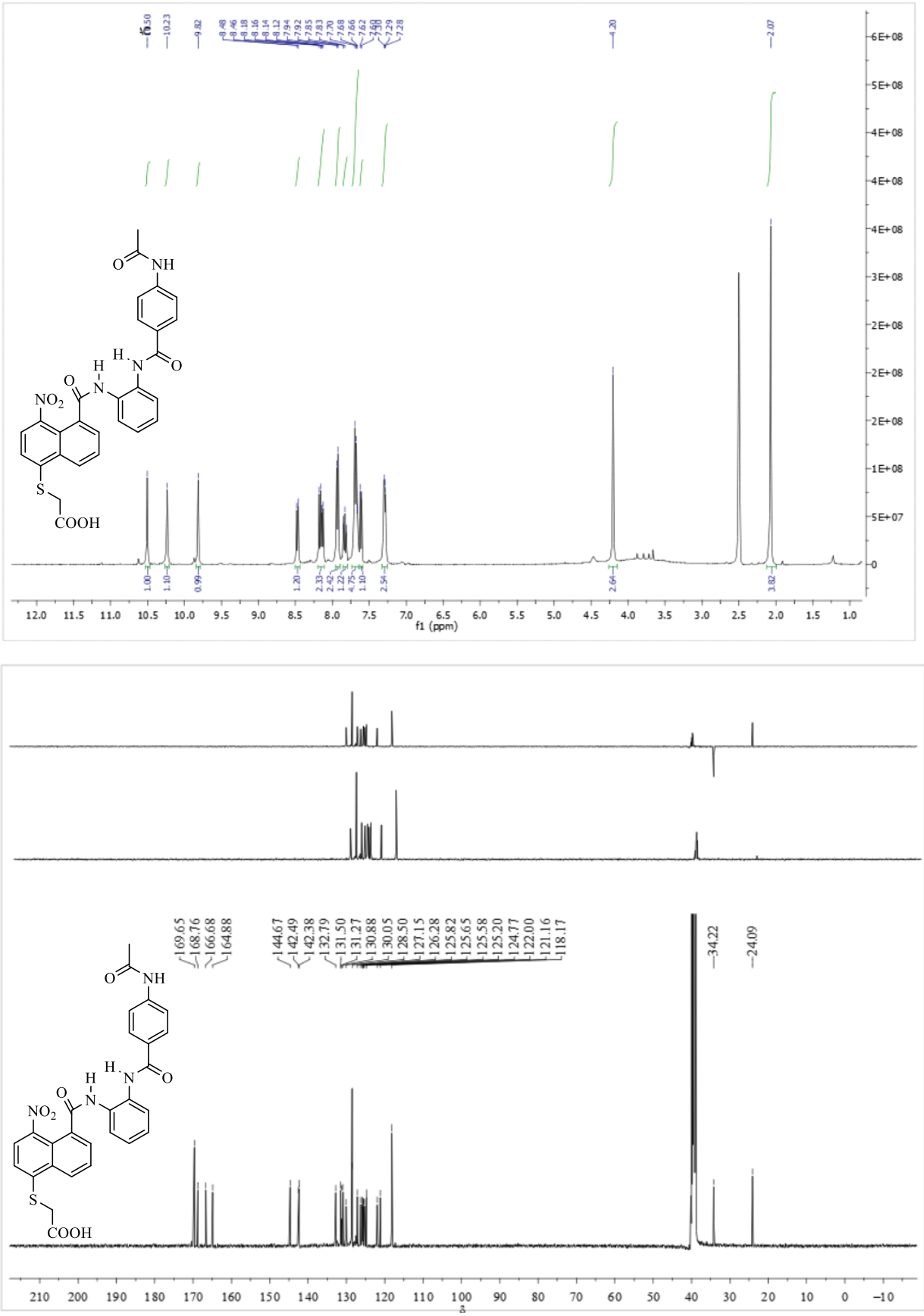


Figure S10. *^{1}H NMR (DMSO-d_6, 400 MHz) and ^{13}C (DMSO-d_6, 100 MHz) spectra of (**20**).*

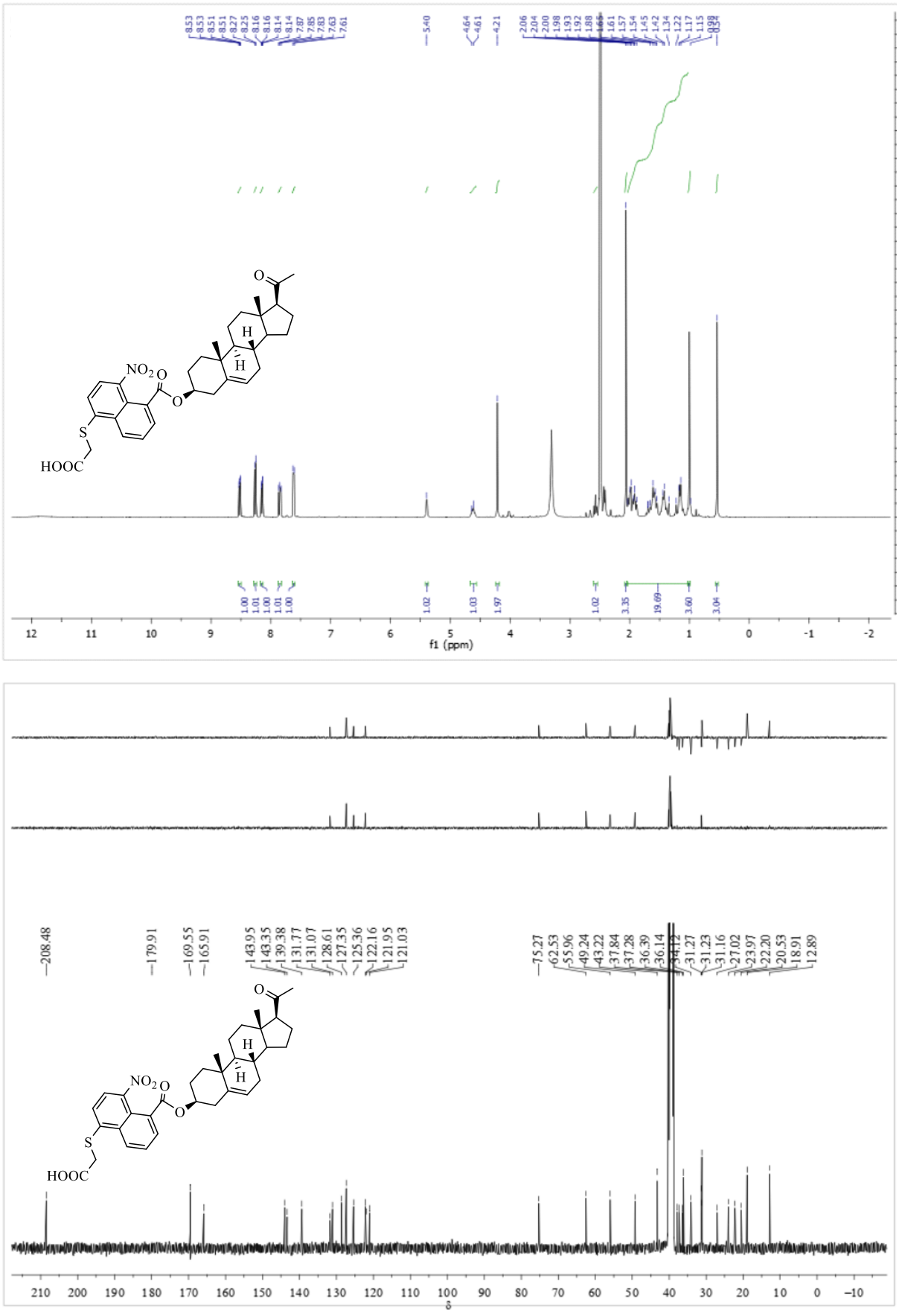


Figure S11. *^{1}H NMR (DMSO-d_6, 400 MHz) and ^{13}C (DMSO-d_6, 100 MHz) spectra of* ***(21)****.*

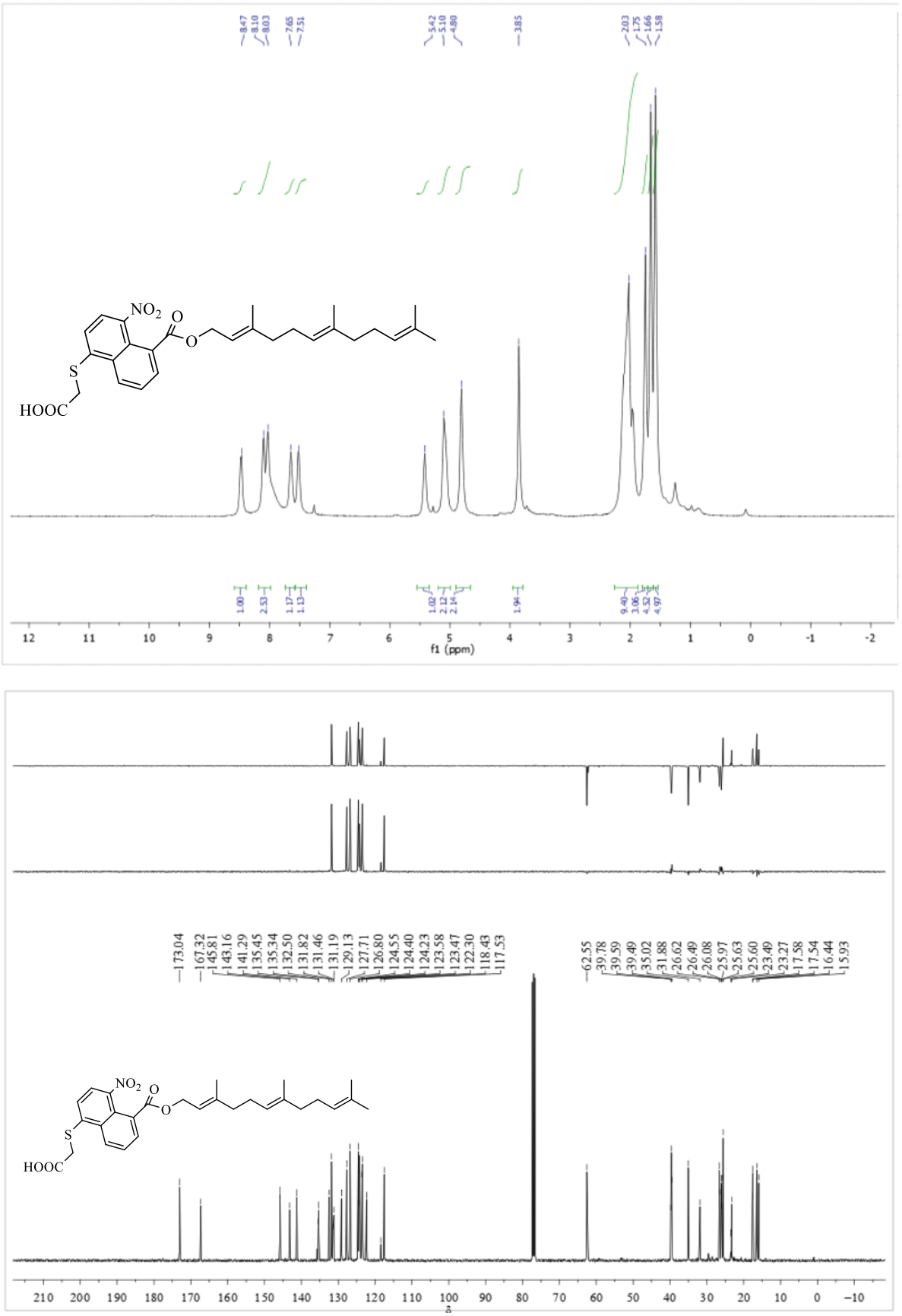


Figure S12. *^{1}H NMR ($CDCl_3$, 400 MHz) and ^{13}C ($CDCl_3$, 100 MHz) spectra of (**22**).*

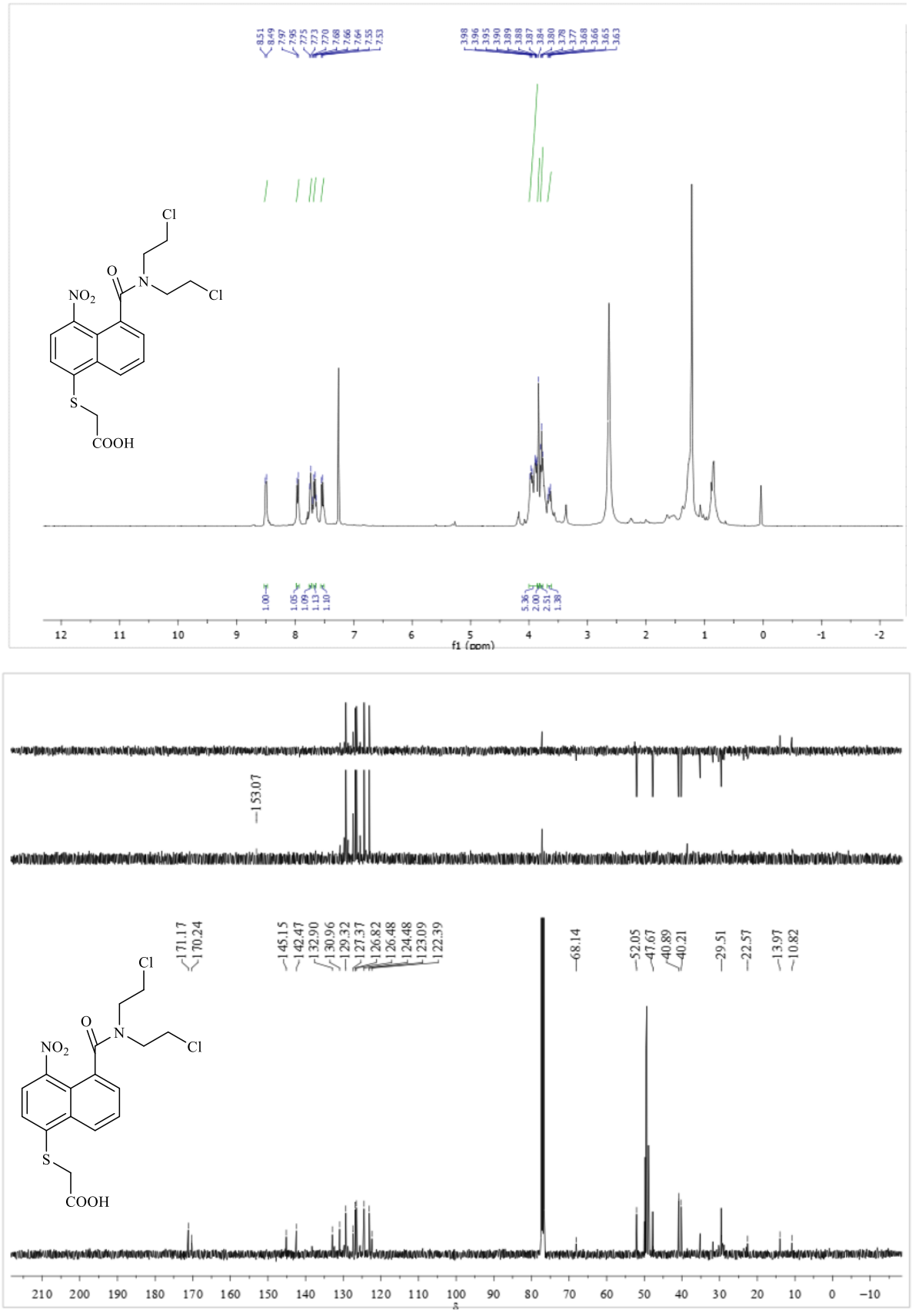


Figure S13. *^{1}H NMR ($CDCl_3$, 400 MHz) and ^{13}C ($CDCl_3$, 100 MHz) spectra of (**23**).*

6. References

(1) Masey, S. *Improving Drug Solubility By Preventing Crystallization*. Xtalks. https://xtalks.com/improving-drug-solubility-051/ (accessed 2024-05-06).

(2) Singh, D.; Bedi, N.; Tiwary, A. K. Enhancing Solubility of Poorly Aqueous Soluble Drugs: Critical Appraisal of Techniques. *J. Pharm. Investig.* **2018**, *48* (5), 509–526. https://doi.org/10.1007/s40005-017-0357-1.

(3) Sanches, B. M. A.; Ferreira, E. I. Is Prodrug Design an Approach to Increase Water Solubility. *Int. J. Pharm.* **2019**, *568*, 118498. https://doi.org/10.1016/j.ijpharm.2019.118498.

(4) Stegemann, S.; Leveiller, F.; Franchi, D.; de Jong, H.; Lindén, H. When Poor Solubility Becomes an Issue: From Early Stage to Proof of Concept. *Eur. J. Pharm .Sci.* **2007**, *31* (5), 249–261. https://doi.org/10.1016/j.ejps.2007.05.110.

(5) Solubility of Organic Compounds - Chemistry Steps. https://www.chemistrysteps.com/solubility-of-organic-compounds/ (accessed 2024-05-09).

(6) Singh, D.; Bedi, N.; Tiwary, A. K. Enhancing Solubility of Poorly Aqueous Soluble Drugs: Critical Appraisal of Techniques. *J. Pharm. Investig.* **2018**, *48* (5), 509–526. https://doi.org/10.1007/s40005-017-0357-1.

(7) Pourjavadi, A.; Amin, S. S.; Hosseini, S. H. Delivery of Hydrophobic Anticancer Drugs by Hydrophobically Modified Alginate Based Magnetic Nanocarrier. *Ind. Eng. Chem. Res.* **2018**, *57* (3), 822–832. https://doi.org/10.1021/acs.iecr.7b04050.

(8) Jornada, D. H.; Fernandes, G. F. dos S.; Chiba, D. E.; Melo, T. R. F. de; Santos, J. L. dos; Chung, M. C. The Prodrug Approach: A Successful Tool for Improving Drug Solubility. *Molecules* **2015**, *21* (1), 42. https://doi.org/10.3390/molecules21010042.

(9) Fleisher, D.; Bong, R.; Stewart, B. H. Improved Oral Drug Delivery: Solubility Limitations Overcome by the Use of Prodrugs. *Adv. Drug Deliv. Rev.* **1996**, *19* (2), 115–130. https://doi.org/10.1016/0169-409X(95)00103-E.

(10) Siderov, J.; Prasad, P.; De Boer, R.; Desai, J. Safe Administration of Etoposide Phosphate after Hypersensitivity Reaction to Intravenous Etoposide. *Br. J. Cancer* **2002**, *86* (1), 12–13. https://doi.org/10.1038/sj.bjc.6600003.

(11) Shah, J. C.; Chen, J. R.; Chow, D. Oral Bioavailability and in Situ Absorption of Etoposide in Rat. *Int. J. Pharm.* **1992**, *84* (3), 223–232. https://doi.org/10.1016/0378-5173(92)90160-4.

(12) Shah, J. C.; Chen, J. R.; Chow, D. Preformulation Study of Etoposide: Identification of Physicochemical Characteristics Responsible for the Low and Erratic Oral Bioavailability of Etoposide. *Pharm. Res.* **1989**, *6* (5), 408–412. https://doi.org/10.1023/a:1015935532725.

(13) Doyle, T. W.; Vyas, D. M. Second Generation Analogs of Etoposide and Mitomycin C. *Cancer Treat. Rev.* **1990**, *17* (2), 127–131. https://doi.org/10.1016/0305-7372(90)90036-F.

(14) *Carboxyl Group: Meaning, Examples, Structure & Applications*. StudySmarter UK. https://www.studysmarter.co.uk/explanations/chemistry/organic-chemistry/carboxyl-group/ (accessed 2024-06-17).

(15) C, Lamberth.; J, Dinges.; Chapter 3. Bioactive Carboxylic Compound Classes: Pharmaceuticals and Agrochemicals, **2016** *Wiley-VCH Verlag GmbH & Co. KGaA*, ISBN:9783527339471. https://doi.org/10.1002/9783527693931.ch1.

(16) Kalgutkar, A. S.; Daniels, J. S., Chapter 3. Carboxylic Acids and their Bioisosteres, In Metabolism, Pharmacokinetics and Toxicity of Functional Groups: Impact of Chemical Building Blocks on Medicinal Chemistry on ADMET, *RSC Drug Discovery* Series 1, Royal Society of Chemistry, **2010**, 99-167. https://doi.org/10.1039/BK9781849730167-00099.

(17) Kolb, H. C.; Finn, M. G.; Sharpless, K. B. Click Chemistry: Diverse Chemical Function from a Few Good Reactions. *Angew. Chem. Int. Ed.* **2001**, *40*, 2004-2021. https://doi.org/10.1002/1521-3773(20010601)40:11<2004::AID-ANIE2004>3.0.CO;2-5.

(18) Kolb, H. C.; Sharpless, K. B. The Growing Impact of Click Chemistry on Drug Discovery. *Drug Discov. Today* **2003**, *8* (24), 1128–1137. https://doi.org/10.1016/s1359-6446(03)02933-7.

(19) McFarland, J. M.; Alečković, M.; Coricor, G.; Srinivasan, S.; Tso, M.; Lee, J.; Nguyen, T.-H.; Mejía Oneto, J. M. Click Chemistry Selectively Activates an Auristatin Protodrug with Either Intratumoral or Systemic Tumor-Targeting Agents. *ACS Cent. Sci.* **2023**, *9* (7), 1400–1408. https://doi.org/10.1021/acscentsci.3c00365.

(20) Barbosa, M.; Martins, C.; Gomes, P. "Click" chemistry as a tool to create novel biomaterials: a short review. *U. Porto Journal of Engineering* **2015**, *1* (1), 22-34. https://doi.org/10.24840/2183-6493_001.001_0004.

(21) Kennedy, D. C.; Mckay, C. S.; Legault, M. C.; Danielson, D. C.; Blake, J. A.; Pegoraro, A. F.; Pezacki. Cellular Consequences of Copper Complexes Used to Catalyze Bioorthogonal Click Re-actions. *J. Am. Chem. Soc.* 2011, 133 (44), 17993–18001 (accessed 2024-06-02).

(22) Ma, N.; Wang, Y.; Zhao, B.-X.; Ye, W.-C.; Jiang, S. The Application of Click Chemistry in the Synthesis of Agents with Anticancer Activity. *Drug Des. Devel. Ther.* **2015**, *9*, 1585–1599. https://doi.org/10.2147/DDDT.S56038.

(23) Hayashi, Y.; Yamazaki-Nakamura, Y.; Yakushiji, F. Medicinal Chemistry and Chemical Biology of Diketopiperazine-Type Antimicrotubule and Vascular-Disrupting Agents. *Chem. Pharm. Bull.* **2013**, *61* (9), 889–901. https://doi.org/10.1248/cpb.c13-00404.

(24) Hayashi, Y.; Takeno, H.; Chinen, T.; Muguruma, K.; Okuyama, K.; Taguchi, A.; Takayama, K.; Yakushiji, F.; Miura, M.; Usui, T.; Hayashi, Y. Development of a New Benzophenone–Diketopiperazine-Type Potent Antimicrotubule Agent Possessing a 2-Pyridine Structure. *ACS. Med .Chem. Lett.* **2014**, *5* (10), 1094–1098. https://doi.org/10.1021/ml5001883.

(25) Rostovtsev, V. V.; Green, L. G.; Fokin, V. V.; Sharpless, K. B. A Stepwise Huisgen Cycloaddition Process: Copper(I)-Catalyzed Regioselective "Ligation" of Azides and Terminal Alkynes. *Angew. Chem. Int. Ed. Engl.* **2002**, *41* (14), 2596–2599. https://doi.org/10.1002/1521-3773(20020715)41:14<2596::AID-ANIE2596>3.0.CO;2-4.

(26) Labat, Y. Thioglycolic Acid. In *Kirk-Othmer Encyclopedia of Chemical Technology*; John Wiley & Sons, Ltd, 2000. https://doi.org/10.1002/0471238961.2008091512010201.a01.

(27) Goossens, A.; Merckx, L. Allergic Contact Dermatitis from Farnesol in a Deodorant: Contact Dermatitis (01051873). *Contact Dermatitis (01051873)* **1997**, *37* (4), 179–180. https://doi.org/10.1111/j.1600-0536.1997.tb00192.x.

(28) Jung, Y. Y.; Hwang, S. T.; Sethi, G.; Fan, L.; Arfuso, F.; Ahn, K. S. Potential Anti-Inflammatory and Anti-Cancer Properties of Farnesol. *Molecules* **2018**, *23* (11), 2827. https://doi.org/10.3390/molecules23112827.

(29) de Araújo Delmondes, G.; Bezerra, D. S.; de Queiroz Dias, D.; de Souza Borges, A.; Araújo, I. M.; Lins da Cunha, G.; Bandeira, P. F. R.; Barbosa, R.; Melo Coutinho, H. D.; Felipe, C. F. B.; Barbosa-Filho, J. M.; Alencar de Menezes, I. R.; Kerntopf, M. R. Toxicological and Pharmacologic Effects of Farnesol (C15H26O): A Descriptive Systematic Review. *Food and Chemical Toxicology* **2019**, *129*, 169–200. https://doi.org/10.1016/j.fct.2019.04.037.

(30) Rioja, A.; Pizzey, A. R.; Marson, C. M.; Thomas, N. S. Preferential Induction of Apoptosis of Leukaemic Cells by Farnesol. *FEBS Lett* **2000**, *467* (2–3), 291–295. https://doi.org/10.1016/s0014-5793(00)01168-6.

(31) Rao, C. V.; Newmark, H. L.; Reddy, B. S. Chemopreventive Effect of Farnesol and Lanosterol on Colon Carcinogenesis. *Cancer Detection and Prevention* **2002**, *26* (6), 419–425. https://doi.org/10.1016/S0361-090X(02)00119-8.

(32) Yilmaz Öztürk, B.; Feyzullazade, N.; Dağ, İ.; Şengel, T. The Investigation of in Vitro Effects of Farnesol at Different Cancer Cell Lines. *Microscopy Research and Technique* **2022**, *85* (8), 2760–2775. https://doi.org/10.1002/jemt.24125.

(33) Fathima Hinaz, Z. H.; Pragya, S.; Ezhilarasan, D.; Shree Harini, K. Anticancer Potential of Farnesol Against Human Osteosarcoma Saos-2 Cells and Human Colorectal Carcinoma HCT-116 Cells. *Cureus* **2023**, *15* (11), e49372. https://doi.org/10.7759/cureus.49372.

(34) Wang, Z.; Chen, H. T.; Roa, W.; Finlay, W. Farnesol for Aerosol Inhalation: Nebulization and Activity against Human Lung Cancer Cells. *J .Pharm . Sci.* **2003**, *6* (1), 95–100. https://sites.ualberta.ca/~csps/JPPS6(1)/W.Finlay/farnesol.htm.

(35) Park, J. S.; Kwon, J. K.; Kim, H. R.; Kim, H. J.; Kim, B. S.; Jung, J. Y. Farnesol Induces Apoptosis of DU145 Prostate Cancer Cells through the PI3K/Akt and MAPK Pathways. *Int. J. Mol. Med.* **2014**, *33* (5), 1169–1176. https://doi.org/10.3892/ijmm.2014.1679.

(36) Voziyan, P. A.; Goldner, C. M.; Melnykovych, G. Farnesol Inhibits Phosphatidylcholine Biosynthesis in Cultured Cells by Decreasing Cholinephosphotransferase Activity. *Biochem. J.* **1993**, *295* (3), 757–762. https://doi.org/10.1042/bj2950757.

(37) Iqbal Choudhary, M.; Shahab Alam, M.; Atta-Ur-Rahman, null; Yousuf, S.; Wu, Y.-C.; Lin, A.-S.; Shaheen, F. Pregnenolone Derivatives as Potential Anticancer Agents. *Steroids* **2011**, *76* (14), 1554–1559. https://doi.org/10.1016/j.steroids.2011.09.006.

(38) Huang, Y.; Tian, W.; Peng, Z.; Cheng, Y.; Wei, M.; Liu, Z.; Pang, L.; Cui, J. Discovery and Biological Evaluation of Pregnenolone Selenocyanoamides with Potential Anticancer and Antimicrobial Activities. *J. Steroid Biochem. Mol. Biol.* **2023**, *234*, 106388. https://doi.org/10.1016/j.jsbmb.2023.106388.

(39) Park-Chung, M.; Malayev, A.; Purdy, R. H.; Gibbs, T. T.; Farb, D. H. Sulfated and Unsulfated Steroids Modulate Gamma-Aminobutyric acidA Receptor Function through Distinct Sites. *Brain Res* **1999**, *830* (1), 72–87. https://doi.org/10.1016/s0006-8993(99)01381-5.

(40) Marks, P. A., & Banks, J. (1960). Inhibition of mammalian Glucose-6-Phosphate Dehydrogenase by steroids. *PNAS*, *46* (4),447–452. https://doi.org/10.1073/pnas.46.4.447.

(41) Nakamura, M.; Magara, T.; Yoshimitsu, M.; Kano, S.; Kato, H.; Yokota, K.; Okuda, K.; Morita, A. Blockade of Glucose-6-Phosphate Dehydrogenase Induces Immunogenic Cell Death and Accelerates Immunotherapy. *J. Immunother. Cancer* **2024**, *12* (7), e008441. https://doi.org/10.1136/jitc-2023-008441.

(42) R, L.; W, W.; Y, Y.; C, G. Exploring the Role of Glucose-6-phosphate Dehydrogenase in Cancer (Review). *Oncology reports* **2020**, *44* (6). https://doi.org/10.3892/or.2020.7803.

(43) Li, F.; Wang, B.; Li, H.; Kong, L.; Zhu, B. G6PD and Machine Learning Algorithms as Prognostic and Diagnostic Indicators of Liver Hepatocellular Carcinoma. *BMC Cancer* **2024**, *24* (1), 157. https://doi.org/10.1186/s12885-024-11887-6.

(44) György, S.; Athanasia, P.; Kyriakos, C.; Olga,M.; Panagiota, P.; Theodora ,C. Design and synthesis of 21-alkynylaryl pregnenolone derivatives and evaluation of their anticancer activity. *Bioorg .Med .Chem.* **2014**, *22* (24), 6980-6988. https://doi.org/10.1016/j.bmc.2014.10.012.

(45) Shervington, L. A.; Smith, N.; Norman, E.; Ward, T.; Phillips, R.; Shervington, A. To Determine the Cytotoxicity of Chlorambucil and One of Its Nitro-Derivatives, Conjugated to Prasterone and Pregnenolone, towards Eight Human Cancer Cell-Lines. *Eur. J. Med. Chem.* **2009**, *44* (7), 2944–2951. https://doi.org/10.1016/j.ejmech.2008.11.014.

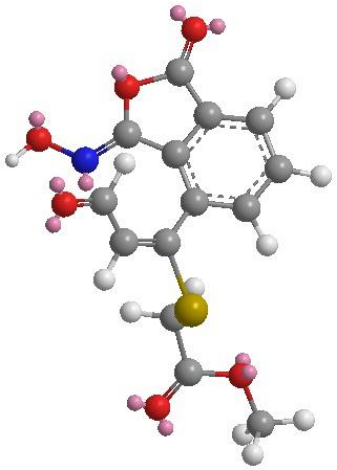
(46) Yadav, P.; Pandey, S. K.; Shama, P.; Kumar, S.; Banerjee, M.; Sethi, A. Experimental and Theoretical Investigation of Synthesized Pregnenolone Derivatives via Palladium Catalyzed Cross Coupling Reactions, Their Anticancer Activity against Lung Cancer Cells. *J. Mol. Struct.* **2021**, *1245*, 131115. https://doi.org/10.1016/j.molstruc.2021.131115.

(47) Huang, L.-J.; Chen, S.-R.; Yuan, C.-M.; Gu, W.; Guo, B.-J.; Wang, Y.-T.; Wang, Y.; Hao, X.-J. C21-Steroidal Pregnane Sapogenins and Their Derivatives as Anti-Inflammatory Agents. *Bioorg. Med. Chem.* **2017**, *25* (13), 3512–3524. https://doi.org/10.1016/j.bmc.2017.04.045.

(48) Sethi, A.; Bhatia, A.; Singh, R.; Srivastava, A. Synthesis and Evaluation of Some Novel Pregnane Derivatives as Anti-Hyperlipidemic and Anti-Oxidant Agents. *Lett. Org. Chem.* **2018**, *15*. https://doi.org/10.2174/1570178615666180806123719.

(49) Repine, J. T.; Johnson, D. S.; White, A. D.; Favor, D. A.; Stier, M. A.; Yip, J.; Rankin, T.; Ding, Q.; Maiti, S. N. Synthesis of Monofluorinated 1-(Naphthalen-1-Yl)Piperazines. *Tetrahedron Lett.* **2007**, *48* (31), 5539–5541. https://doi.org/10.1016/j.tetlet.2007.05.156.

CHAPTER 5: AN UNUSUAL REARRANGEMENT OF A 1,8-NAPHTHALENE DERIVATIVE



In Chapter 5, the rearrangement of a 1,8-nitronaphthalene carboxylate through the fragmentation of a naphthalene ring under mild reaction conditions will be discussed. This reaction was discovered by serendipity in chapter 4, while trying to attach nitrogen mustard to a 1,8-nitronaphthalene derivative.

1. Objectives

The **main objective** of this chapter is the investigation and the study of a 1,8-naphthalene derivative rearrangement obtained from the steric hindrance of the strained aromatic rings from 5-((2-methoxy-2-oxoethyl)thio)-8-nitro-1-naphthoic acid . This novel rearrangement will be explored as the new molecule generated from the initial coupling of a nitrogen mustard moiety and ((2-methoxy-2-oxoethyl)thio)-8-nitro-1-naphthoic acid. To achieve this goal, the specific objectives shown below are proposed:

- **Objective 1**: To identify the structure of the molecule obtained in the rearrangement by characterization by ^{1}H NMR, ^{13}C NMR, bidimensional NMR, IR, HRMS.
- **Objective 2**: To synthesize and characterize intermediate molecules that can help to understand the rearrangement.
- **Objective 3:** To get the X-ray diffraction analysis data of the compound obtained or a derivative in order to confirm the structure of the product obtained.
- **Objective 4:** To propose a plausible reaction mechanism.

2. Introduction

1,8-napthalene derivatives are strained compounds due to the steric hindrance between substituents in 1,8- positions which produce unusual physical properties. In 1975, Anderson studied the rotation-barrier energy of some naphthalene derivatives with *peri* interactions, which strongly depends on the planarity or tetrahedral character of the substituents.[1]

Dünitz in 1978 reported that 8-(dimethylamino)-1-naphthylmethyl ketone has the dimethylamino group tilted towards the ketone group to exploit the binding interactions provided by the Burgi-Dünitz trajectory. In this way, a dihedral angle of 116.65° instead of 120° has been observed (Figure 1A).[2] Also, Wallis has studied the interactions between naphthalene derivatives with substituents in *peri* position.[3,4,5,6,7,8] It is quite remarkable the reaction between dimethylamino-1-naphthaldehyde with benzoyl chloride which produces the dihydro benzolinium compound shown in Figure 1D.[9] Another highlighting example is the reaction reported by Priestap of 8-nitro-1-naphthoic acid which yields a naphthoxazole when treated with Zn and acetic acid (Figure 1B).[10] Both reactions allow to release the steric strain between the groups in 1- and 8- positions. Other chemical properties are also strongly influenced, 1,8-bis(dimethylamino) naphthalene (Proton-sponge®) is a stronger base (pK_a=12.1) than the corresponding dimethylaniline (pK_a= 5.1) since amine protonation releases part of the steric strain between the two amino groups (Figure 1C).[11] Lectka has also studied how NH···F interactions are affected in 1,8-disubstituted naphthalenes (Figure 1E)[12] and Nishiwaki has studied how bulky substituents in *peri* position are able to distort the coplanarity of the naphthalene ring[13], and affect the isomerization of bromine substituents (Figure 1G).[14]

As it has been shown in chapter 4, the attempt to couple the naphthalene fragment with a nitrogenated mustard (a well-known intercrossing DNA molecule) under Schotten-Baumann conditions, led in good yield to an unexpected aldehyde (Figure 1H) accompanying the fragmentation of the naphthalene ring. In this regard, we would like to explain how this reaction takes place and propose a mechanism to explain this unusual rearrangement.

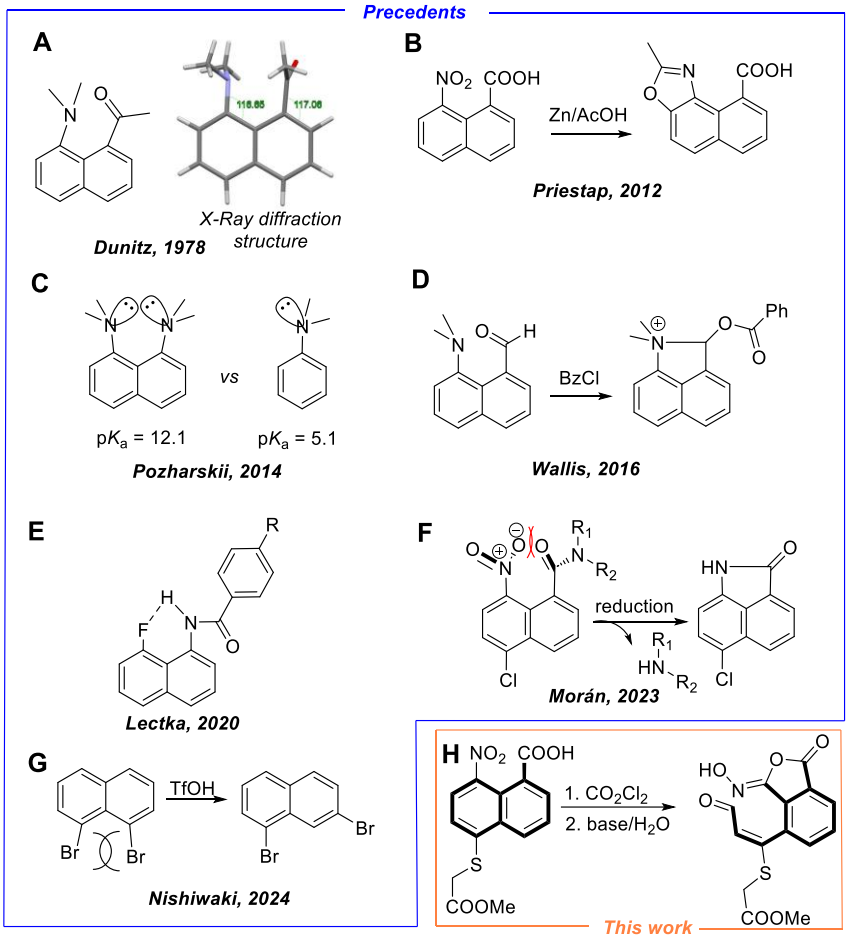


Figure 1. *(A-G) Unusual chemical reactivity and physical properties of 1,8-disubstituted naphthalenes. (H) Unexpected rearrangement obtained in this work.*

3. Methodology

3.1. Compound 4 synthesis

Following the literature procedure[15] compound **1** (Figure 2) was synthesized. Then, thioglycolic acid fragment was introduced by nucleophilic aromatic substitution followed by the carboxylic acid esterification with MeOH and $SOCl_2$. The putative acid chloride of compound **2** was prepared dissolving it in oxalyl chloride. Then, Schotten-Baumann conditions with Na_2CO_3 and EtOAc were used to anchor nitrogen mustard **3**. However, the expected amide was only found at traces amounts, and an unexpected compound was obtained instead in high yield. The same compounds were obtained when the reaction was performed in biphasic reaction mixture with CH_2Cl_2 and aqueous phosphate buffer (Figure 2).

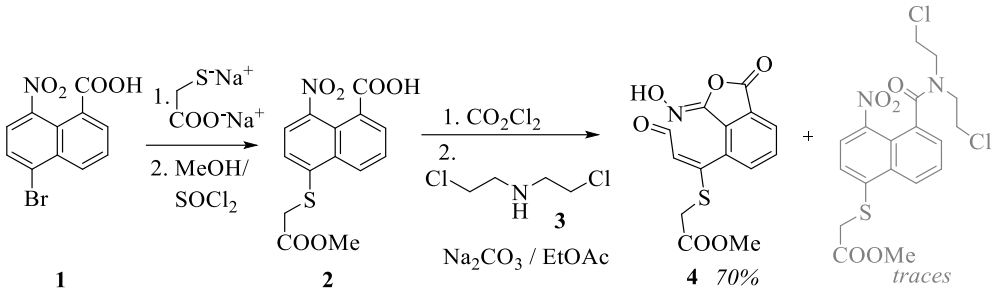


Figure 2. *Synthesis of aldehyde **4** from reported compound **1**.*

Positive electrospray high resolution mass spectrometry showed a peak at 344.0193 corresponding with the molecular formula $C_{14}H_{11}NNaO_6S^+$ ($[M+Na]^+$). This formula is consistent with the protonated aldehyde **4** and also to a structural isomer of the starting naphthoic acid **2**.

The presence of the aldehyde functional group in the rearranged compound **4** was supported by the IR spectrum with characteristic absorptions for aldehydes at 2850 and 2754 cm^{-1}. The stretching carbonyl band is hidden under two other carboxyl bands at 1730 cm^{-1}. ^1H NMR spectrum also supports the aldehyde functional group due to the presence of a 7.9 Hz doublet at 9.08 ppm coupled with an olefinic proton and the ^{13}C NMR spectrum presents a carbonyl carbon CH at 188.9 ppm. The presence of the aldehyde is also supported by the formation of a hemiacetal in CD_3OD after adding a trace of *p*TsOH to a compound **4** CD_3OD solution, showing two doublets at 6.00 and 4.50 ppm with *J*=6.7 Hz. The unusual (*Z*)-3-(hydroxyimino)isobenzofuran-1(3*H*)-one (phthaloxime) structure is consistent with the carboxyl carbon at 163.2 ppm and the imino carbon at 145.7 ppm. HMBC CIGAR long range proton-carbon correlations are also consistent with these assignations, since the hydroxyimino proton singlet at 11.83 ppm showed in the DMSO-d_6 spectrum a three-bond correlation with the hydroxymino carbon at 145.8 ppm, while the aromatic *ortho* proton at 8.07 ppm showed the corresponding correlation with the carboxyl carbon (Figure 3).

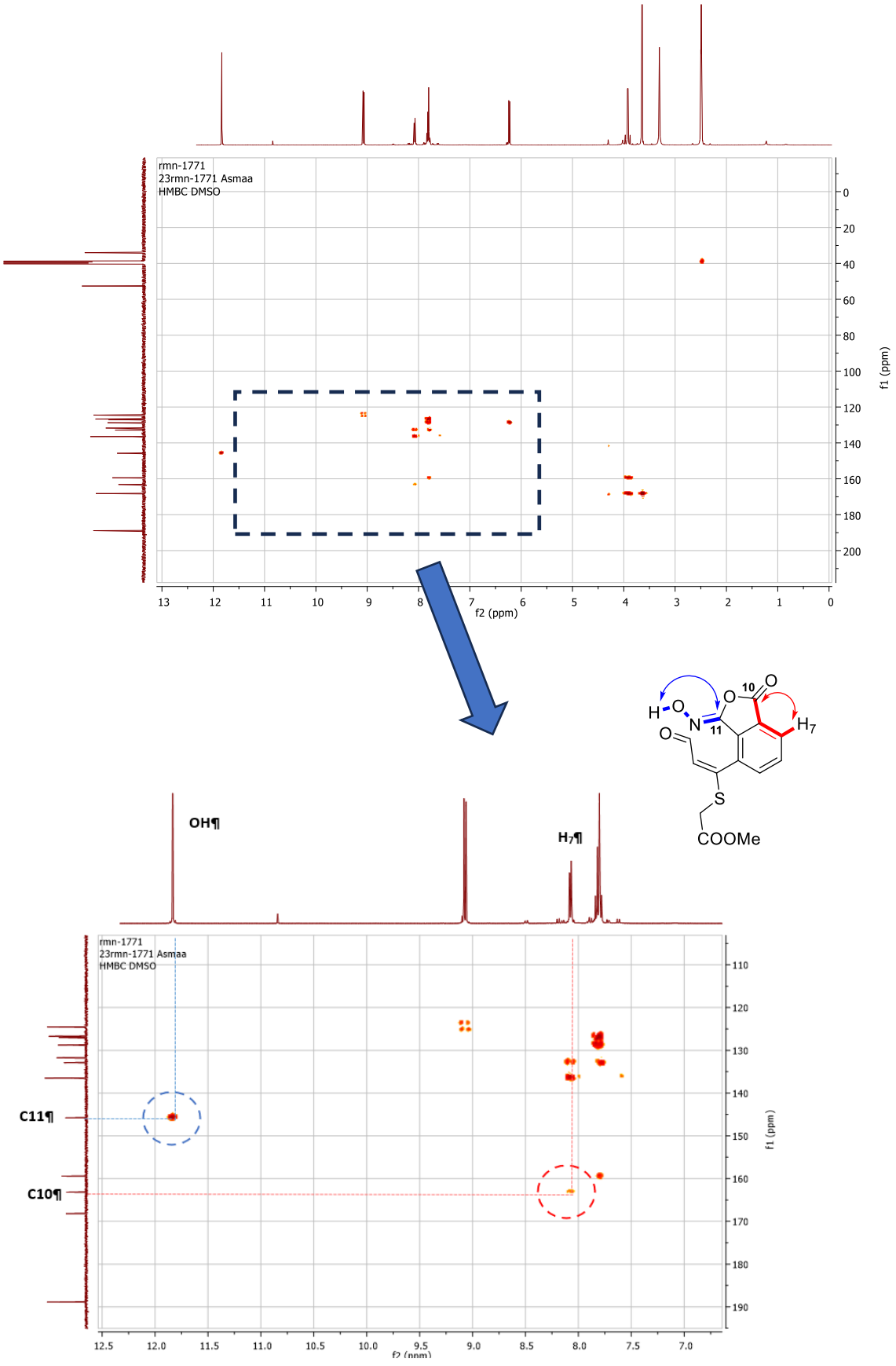


Figure 3. *HMBC CIGAR spectrum of compound **4** in DMSO-d_6.*

All the other correlations are in agreement with the proposed structure. An interesting fact is the splitting of the methylene protons in the ^{1}H NMR spectrum as an AB system at 3.95 and 3.89 ppm. This fact seems not to agree with a planar structure but can be explained due to the presence of atropoisomers. Modelling studies predict a rotational barrier for this structure around 20 kcal/mol (Figure 4). High enough to prevent rotation in the NMR scale.

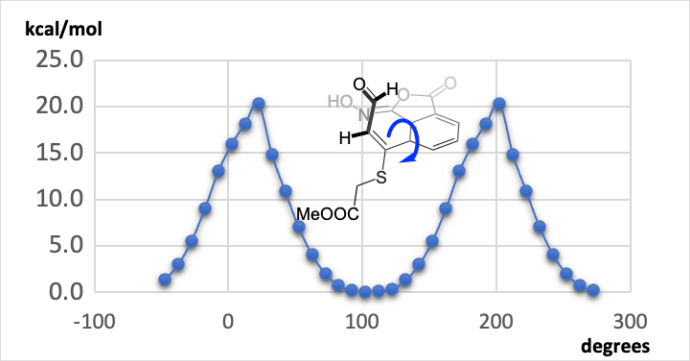


Figure 4. *Modelling studies of the phthaloxime aldehyde showing the twisting between the aromatic ring and the substituent supporting the aldehyde.*

The phthaloxime **I**[16] (Figure 5) has been known for a long time, as the result of the reaction of phthalic anhydride and *O*-benzyl hydroxylamine, followed by hydrogenolysis. It has been reported that this structure is in equilibrium with the hydroxyphthalimide structure **II** thorough a deep red anion intermediate formed under basic conditions (Figure 5) and assignation of the right structure has been a matter of considerable debate.[17,18]

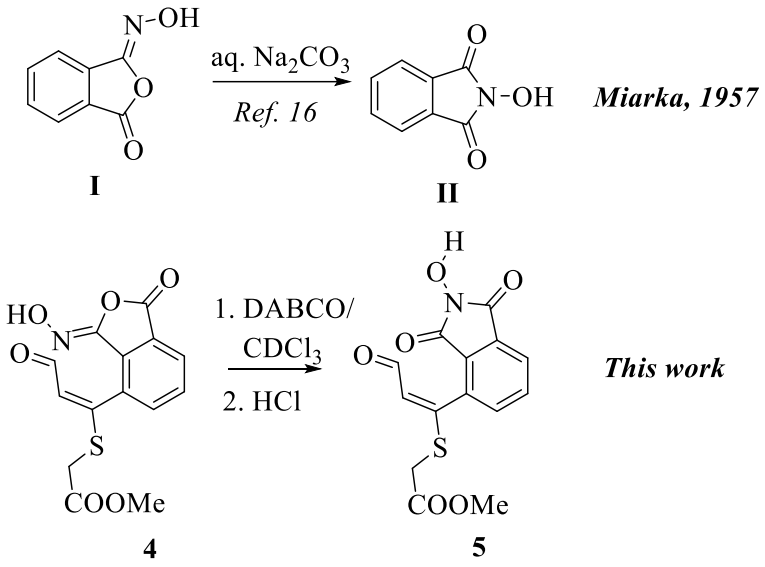
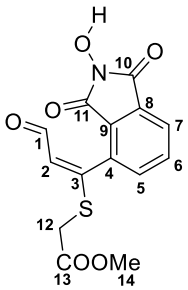


Figure 5. *(Top) Rearrangement of (Z)-3-(hydroxyimino)isobenzofuran-1(3H)-one into N-hydroxyphthalimide under basic conditions reported in literature. (Bottom) Rearrangement found with aldehyde **4**.*

In our case, treatment of a $CDCl_3$ solution of the phthaloxime **4** with DABCO yielded indeed a deep red solution, from which, after acidulation with aqueous 2M HCl, the hydroxyphthalimide compound **5** was obtained. The IR spectrum agreed with the hydroxyphthalimide structure with a characteristic band at 1787 cm^{-1}.[19] The most convincing fact is the appearance of the two carboxyl carbons in the ^{13}C NMR spectrum at 162.4 and 163.0 ppm while the imino carbon at 145.8 ppm has disappeared. All the other spectroscopic properties agree with the structure, therefore in this case there is no structure ambiguity between both compounds.

Table 1. *^{1}H NMR ($CDCl_3$, 400 MHz) and ^{13}C ($CDCl_3$, 100 MHz) chemical shift assignments for compound **5**.*



	^{1}H NMR (δ)		^{13}C NMR (δ)
H1	9.05 (d, *J* = 7.8 Hz, 1H),	C1	188.9 (CH)
H2	6.26 (d, *J* = 7.8 Hz, 1H)	C2	124.7 (CH)
H5	7.67 (dd, *J* = 7.8, 0.9 Hz, 1H)	C3	159.3 (C)
H6	7.79 (t, *J* = 7.6 Hz, 1H)	C4	131.6 (C)
H7	7.90 (dd, *J* = 7.5, 1.0 Hz, 1H)	C5	135.5 (CH)
H12	3.81 (d, *J* = 15.4 Hz, 1H), 3.74 (d, *J* = 15.8 Hz, 1H)	C6	134.5 (CH)
H14	3.77 (s, 3H)	C7	124.9 (CH)
		C8	130.0 (C)
		C9	126.7 (C)
		C10	163.0 (C)
		C11	162.4 (C)
		C12	34.5 (CH_2)
		C13	168.0 (C)
		C14	53.1 (CH_3)

We have been unable to obtain suitable crystals from the previous aldehydes **4** or **5** for X-ray analysis, therefore the 2,4-dinitrophenyl hydrazones of both compounds were prepared with 2,4-dinitrophenyl hydrazine in THF. Both aldehydes rendered the same dinitrophenyl hydrazone which is a deep red crystalline compound from which the X-ray analysis was possible. The structure shown in Figure 6 corresponds to the hydroxyphthalimide compound **6**, since the phthaloxime rearranges under these conditions to the hydroxyphthalimide.

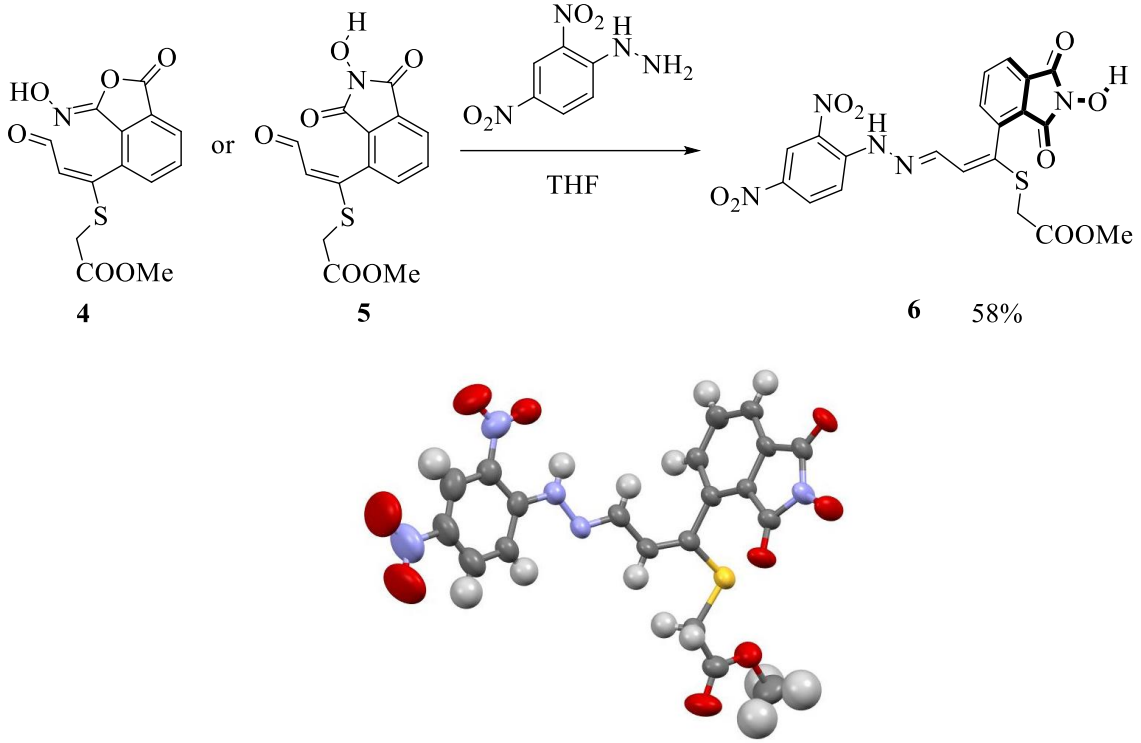


Figure 6. *(Top) Synthesis of compound **6** from either **4** or **5**. (Bottom) ORTEP diagram of compound **6**. Displacement ellipsoids are drawn at 50 % probability level. Hydrogen atoms are shown as spheres of arbitrary radius.*

This structure is in good agreement with the previous modelling of the phthaloxime aldehyde **4** showing an almost 90° torsion angle between the hydroxyphthalimide aromatic ring and the substituent. This fact supports the presence of atropoisomers in these compounds.

A comparison of the ^{13}C-NMR spectra of the hydrazone with both previous aldehydes confirm the structure of the phthaloxime for the reaction of the acylnitronium chloride, since the hydrazone lacks the 145.8 ppm carbon from the imine while it shows the two carboxyl carbons at 162.9 and 163.7 ppm. This result shows that the phthaloxime rearranges to the more stable hydroxyphthalimide in the presence of dinitrophenylhydrazine.

After elucidating the structure of the aldehyde **4** we aimed at investigating the mechanism to explain the unexpected formation of this compound from 1,8-disubstituted naphthalene **2**. We

were suspicious of the reaction between compound **2** and oxalyl chloride to generate the acid chloride, since the reaction of an acid chloride with a secondary amine should obviously yield an amide. In order to explain the low yield of amide we discarded the acid chloride as intermediate, and we propose a naphtho oxazinium chloride **7** instead (Figure 7) as the reaction product of the acid **2** with oxalyl chloride. This intermediate offers a plausible explanation to justify the preference for the nucleophilic attack on the C-7 position of the naphthalene ring instead of the carbonyl group of an acid chloride.

Although the naphtho oxazine chloride **7** is a highly unstable compound it has been possible to carry out a reasonable characterization. High resolution mass spectrometry shows a peak at 304.0273 corresponding to a molecular formula $C_{14}H_{10}NO_5S^+$. The lack of the chloride atom in the molecular formula ruled out the acid chloride structure. IR spectrum showed a broad band at 1728 cm^{-1} inconsistent with an acid chloride which is expected to absorb around 1800 cm^{-1}. ^{13}C NMR showed two carboxyl signals at 168.8 ppm and 167.7 ppm consistent with the expected chemical shifts for the naphtho oxazinium carbon and the ester group.

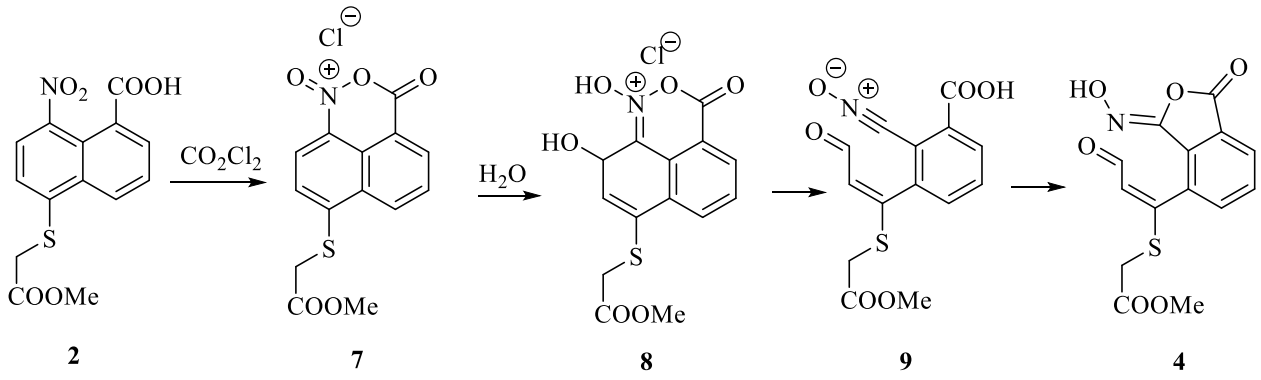
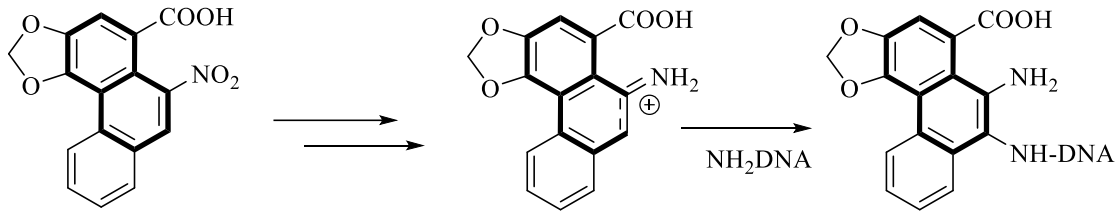


Figure 7. *Key intermediates proposed for the rearrangement of 1,8-disubstituted naphthalene **2**.*

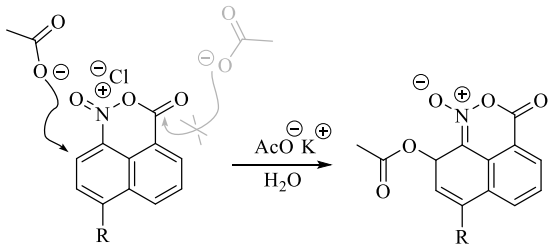
Although the addition of water to the naphthalene skeleton seems a counterintuitive reaction, as it should yield a big loss of aromatic energy, a good precedent can be found in the formation of the naphtho oxazole compound reported by Priestap (Figure 1B). In fact, these compounds also show interesting pharmaceutical and biological properties, since they have similar properties than aristolochic acids which have been proposed to act through a nitrenion ion to couple with DNA through the addition of the amino group of a DNA nucleobase (Figure 8). However, no fragmentation was reported in this case.



E *ref. 10*

Figure 8. *Naphtho oxazole derivatives with cytotoxic activity and the proposed nitrenium intermediate which reacts with the amino group of DNA nucleobases.*

Trying to show that indeed the naphtho oxazinium chloride **7** undergoes nucleophilic attack in C-7, this compound was treated at 0°C with potassium acetate. Two doublets with $J = 5.2$ Hz grow up during the reaction in the ^{1}H NMR spectrum in $CDCl_3$ at 6.67 and 6.15 ppm consistent with the addition of the acetate to C-7 naphthalene ring. However, the compound is unstable, and a further characterization has not been possible. We have been able to perform this study easier with the chloride derivative in position 5 instead of the thioglycolic fragment since a simple washing of the potassium acetate salt with cold water and evaporation of the solvent yielded a crystalline compound easier to handle. The structure of the acetate is shown in figure 9. The physical properties are in good agreement with the addition compound. The HRMS spectrum shows a peak at 315.9976 corresponding to the formula $C_{13}H_8O_5N^{35}Cl^{23}Na$ which matches the proposed acetate. This substitution is known to take place in the presence of oxalyl chloride, as already reported in the literature.[15] The ^{1}H NMR spectrum showed two doublets at 6.72 and 6.41 ppm corresponding to the proton geminal to the acetate group and the vinyl proton, respectively, confirming again the addition of the acetate . This easy nucleophilic addition to the naphthalene C-7 of the dioxo naphtho oxazine may be an interesting clue for the addition of nucleic bases to aristolochic acids as an alternative to the reported nitrenium cation intermediates.



7 R = -SCH$_2$COOMe
10 R = Cl

11 R = -SCH$_2$COOMe
12 R = Cl

Figure 9. *Addition of potassium acetate to the naphthalene compounds **7** and **10** in position C-7.*

While the acetate cannot undergo further reaction, addition of water to C-7 yields an alcohol (**8**) which can evolve to an aldehyde with concomitant ring opening and formation of the nitrile oxide **10** (Figure 6, **7→8→9**). A precedent to this reaction can be found in the Mukaiyama nitrile oxide synthesis from nitroderivatives and isocyanates (Figure 10).[20]

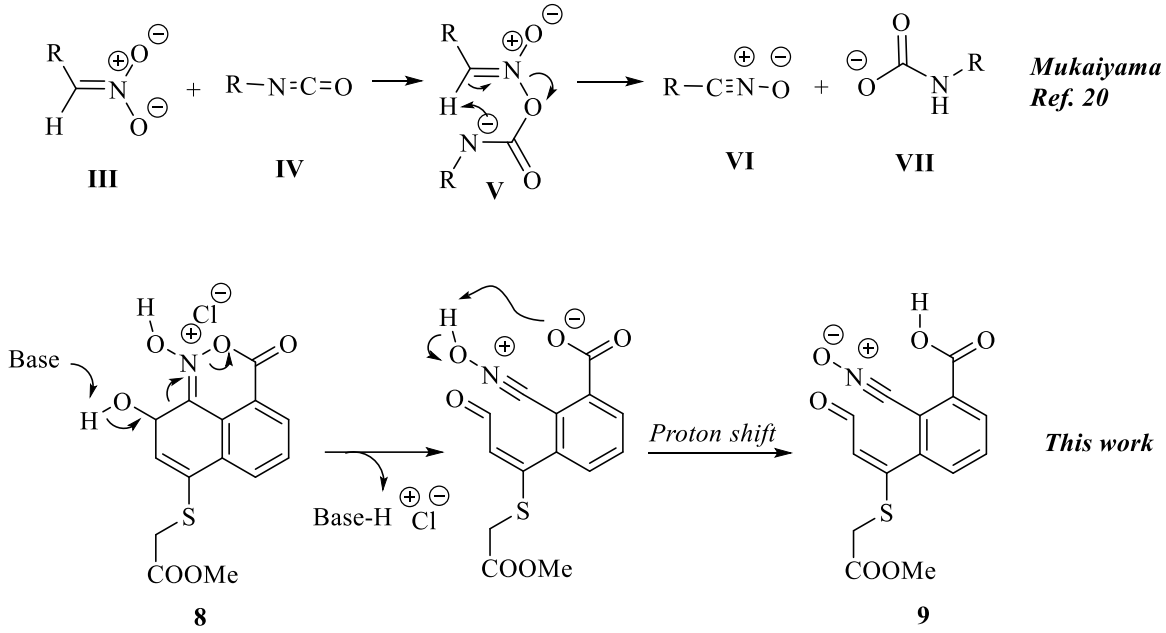


Figure 10. *(Top) Mukaiyama nitrile oxide synthesis. (Bottom) Rearrangement observed in this work.*

The formation of the acyl nitronate is similar in both cases. While in the Mukaiyama reaction a proton is abstracted to yield the nitrile oxide and a carbamate, in our case is the C-C fragmentation which provides the pair of electrons to promote the carboxylate elimination, yielding in this process an aldehyde and a nitrile oxide.

Nitrile oxides are highly reactive species which readily undergo 1,3 dipolar additions.[21] All attempts to trap this intermediate, even with tetracyanoethylene were unsuccessful, probably because the intramolecular reaction with the carboxylic group in C-1 is faster (Figure 7, **9→4**), and the phthaloxime **4** is formed.

To shed light into this unusual rearrangement, DFT calculations were performed by Prof. Luis Simón (Chemical Engineering Department) to understand the reaction mechanism, and specially the preference for the addition of H_2O to the C-7 position of the naphtho oxazinium cation instead of the carboxylic C carbon. To simplify the calculations, the 2-thioacetate group was replaced by a methylsulphane. Dihydrogenphosphate ($H_2PO_4^-$) and dimethylamine were

studied as possible basic catalysts. Solvent effects (chloroform) were included by an implicit solvation model and in the reaction catalyzed by dimethylamine the chlorine counter anion was not included (the net charge of the molecule was +1 in the calculations), while in the case of the $H_2PO_4^-$ catalyzed reaction this group was used as counter anion (the net charge was 0).

An exhaustive search of transition states structures with different orientations of the reacting groups was performed, although some of these orientations collapsed during the optimization to the same structure.

For the reaction catalyzed by dimethylamine, addition to the carboxylic C atom was favoured (≈2.0 kcal/mol energy difference between the most stable Transition states , 95:5 ratio considering all transition states, see ESI). In the case of the reaction catalyzed by $H_2PO_4^-$, the major product corresponds to the addition to C-7 (energy difference of ≈2.5 kcal/mol between most stable transition states, 97:3 ratio, Figure 12). These results agree with experimental observations. Not surprisingly, analogue calculations for the addition of one H_2O molecule to the acyl-chloride show a much larger preference for the addition on the carboxylic C atom (≈8.0 kcal/mol), confirming that the formation of the naphtho oxazinium chloride **A** is necessary to justify the reactivity observed (Figure 12).

The reaction continues with the opening of two of the six-membered rings of intermediate **C**: the C7-C8 bond and the N-O bonds are broken to generate the aldehyde, and the nitrile oxide groups **C**. Transition state structures corresponding to this step (**TS-BC**), catalyzed by an additional dihydrogenphosphate group, were also found. The hydroxy group can adopt a *pseudo-axial* or a *pseudo-equatorial* position, but in the last case it is oriented in an almost planar *s-trans* conformation with respect to the conjugated double bond, an effect that probably contributes to stabilize the equatorial transition state structure. The reaction is concerted but shows some degree of asynchronicity: N-O distance is 2.5 Å while the C-C distance is elongated to 1.9Å. Finally, the reaction proceeds through **TS-CD** and product **D** (corresponding to compound **4**) is formed.

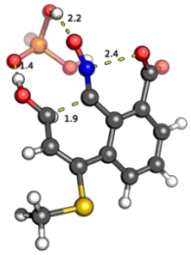


Figure 11. *Minimum energy transition state for the $H_2PO_4^-$ catalyzed fragmentation of C7-C8 and N-O bonds.*

Since the addition of a water molecule to the C-7 (the preceding step) is reversible, the accumulation of the aldehyde product also requires that the transition states corresponding to this second step are also more stable than the transition states (**TS-AE**) of the H_2O addition to the carbonyl C atom. Otherwise, the irreversible formation of the aldehyde from the intermediate would be slower than the protonation and elimination of the C-7 OH group and the addition of the resulting water molecule to the carbonyl C atom to yield the competing reaction towards the carboxylate **E**. However, direct comparison of the energies of these transition states is not possible since they have different number of atoms: the second step transition states are deprotonated with respect to the transition states for the addition of H_2O to the starting materials.

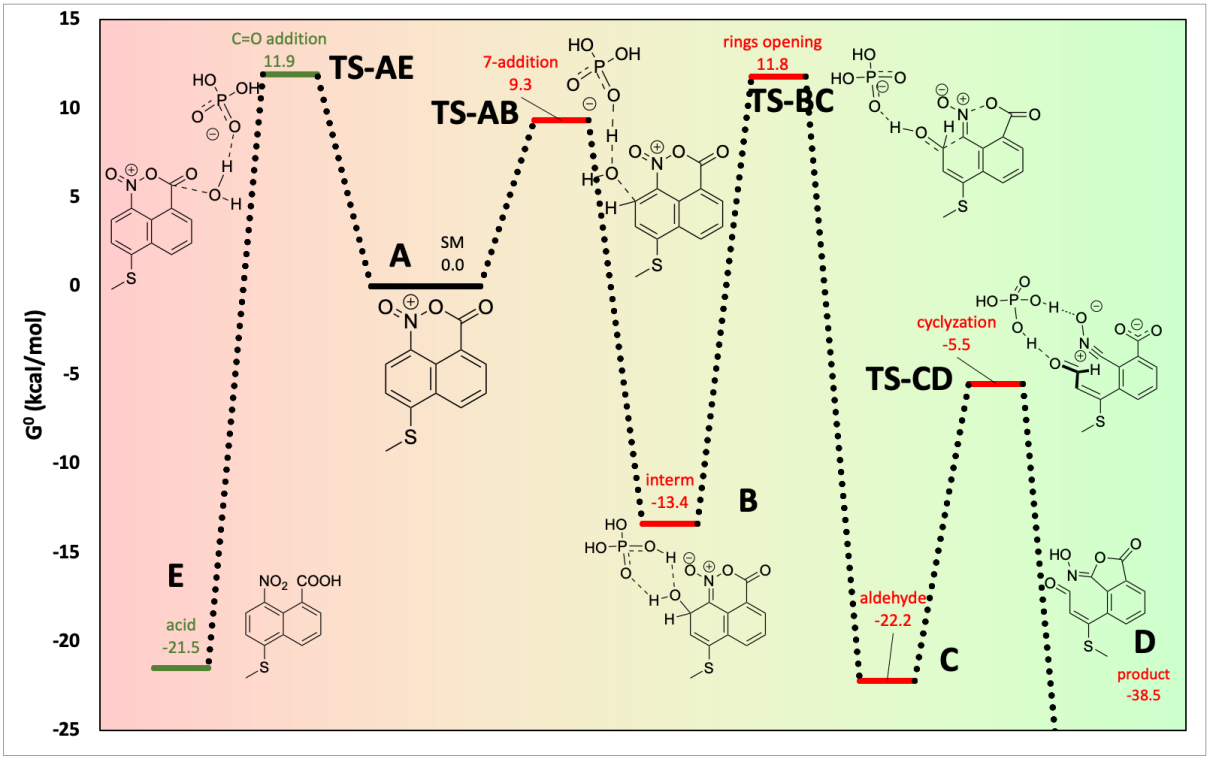


Figure 12. *Computer reaction energy profile for the pathway through the lowest energy transition state structure leading to the rearranged aldehyde (green background) and competing hydrolysis reaction (red background).*

In order to correct for this effect, the energies of a neutral phosphoric acid structure and of a $H_2PO_4^-$ anion were added and subtracted from the energy of the second step TS structure. Formally, this balances the number of atoms under a condition in which the concentrations of phosphoric and dihydrogenphosphate are identical. Curiously, under these assumptions, the energy of the second step most stable transition states is 2.5 kcal/mol[22] higher than the energy of the most stable transition states corresponding to the H_2O addition to the C-7 atom, and very similar to the energy of the transition states for the addition on the carbonyl C atom,

corresponding to the competing path. Under conditions in which the concentration of $H_2PO_4^-$ is higher (basic pK_a), the formation of the aldehyde should be favoured, while, in agreement with experimental results, acid pK_a should increase the effective barrier of the second step and the hydrolysis should follow the competing path.

4. Conclusions

In Chapter 4, an unexpected compound was obtained when the coupling of the molecular trigger and bis(2-chloroethylamine) was attempted. In this chapter, this compound has been isolated and fully characterized by ^{1}H NMR, ^{13}C NMR, bidimensional NMR, IR, HRMS.

The putative acid chloride of the trigger was, in fact, a naphtho oxazinium compound, which has been also isolated and completely characterized.

Attempts to crystallyze compounds **4** or **5** were unsuccessful, however, a 2,4-dinitrophenylhydrazone derivative has allowed us to obtain a crystal from which the X-ray diffraction analysis have been realized. This experiment has confirmed the structure proposed for this unexpected compound.

DFT calculations have been performed in order to understand the mechanism of this reaction. According to them, the steric hindrance between the nitro and carboxylate groups in 1,8 positions promotes the formation of a strained naphtho oxazinium intermediate with reacts with a H_2O molecule and initiates a fragmentation reaction able to break the aromaticity of the naphthalene core and finally generates and aldehyde.

The naphtho oxazinium intermediate could find application as cytotoxic reagent by its similar properties to aristolochic acids which are able to react with DNA nucleobases.

5. Experimental Section

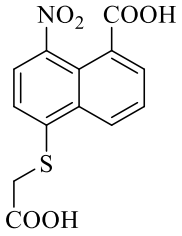
5.1. Materials and instrumentation

Modelling studies

Theorical studies were carried out using Gaussian16 software with w-B97XD functional in combination with 6-31+G(d,p) basis set.

5.2. Synthesis and characterization

5-((carboxymethyl)thio)-8-nitro-1-naphthoic acid (1)



In a round bottom flask thioglycolic acid sodium salt (8 g, 70 mmol), potassium hydroxide (4 g, 0.71 mol) and water (2 ml) were placed and stirred until a homogeneous solution was obtained. Then, 5-bromo-8-nitro-1-naphthoic acid (4 g, 13.5 mmol) was dissolved in DMSO (25 ml) and DMF (5 ml). Both solutions were cooled down to 5 ºC then, the naphthalene solution was poured over the thioglycolic acid salt, keeping the temperature below 10 ºC. After 10 minutes the reaction was added over 2M aqueous hydrochloric acid (100 ml) and filtered to yield 5-((carboxymethyl)thio)-8-nitro-1-naphthoic acid as a yellow solid (3.7 g, 89% yield).

m.p.: >200 ºC

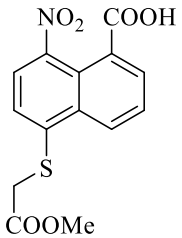
IR (nujol, ν in cm^{-1}): 3760, 3650, 3617, 1697, 1560, 1521, 1385, 1340, 1262, 1191, 899.

^{1}H NMR (400 MHz, DMSO-d_6) δ 8.50 (dd, J = 8.5, 0.9 Hz, 1H), 8.22 (d, J = 8.2 Hz, 1H), 8.16 (dd, J = 7.2, 1.1 Hz, 1H), 7.84 (dd, J = 8.5, 7.3 Hz, 1H), 7.62 (d, J = 8.3 Hz, 1H), 4.21 (s, 2H).

^{13}C NMR (101 MHz, DMSO-d_6) δ 169.6 (C), 168.0 (C), 144.6 (C), 142.7 (C), 131.2 (CH), 129.7 (C), 127.3 (CH), 126.9 (CH), 124.9 (CH), 121.9 (CH), 121.3 (2C), 34.2 (CH_2).

HRMS (ESI) m/z calculated. for $C_{13}H_9O_6N^{23}Na^{32}S$ $[M+Na]^+$ 330.0048, found 330.0043.

5-((2-methoxy-2-oxoethyl)thio)-8-nitro-1-naphthoic acid (2)



5-((carboxymethyl)thio)-8-nitro-1-naphthoic acid (3.7 g, 12 mmol) was dissolved in MeOH (30 ml) and THF (10 ml). Thionyl chloride (0.25 ml, 3.4 mmol) was added, and the reaction was allowed to stand for 1 hour. Evaporation under reduced pressure returned a crude

compound which was crystallized from methylene chloride to yield the methyl ester as a yellow solid (3.4 g, 88% yield).

m.p.: 170 ºC

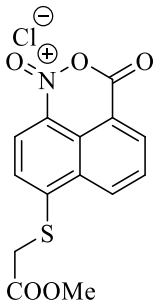
IR (nujol, ν in cm^{-1}): 3903, 3747, 3663, 1761, 1690, 1567, 1288, 1132, 827.

^{1}H NMR (400 MHz, DMSO-*d_6*) δ 8.49 (dd, *J* = 8.6, 1.1 Hz, 1H), 8.19 (dd, *J* = 8.2, 4.3 Hz, 1H), 8.15 (dd, *J* = 7.2, 1.1 Hz 1H), 7.83 (dd, *J* = 8.6, 7.2 Hz, 1H), 7.62 (d, *J* = 8.3 Hz, 1H), 4.30 (s, 2H), 3.66 (s, 3H).

^{13}C NMR (101 MHz, DMSO-*d_6*) δ 168.9 (C), 168.0 (C), 144.8 (C), 142.0 (C), 131.3 (C), 131.2 (CH), 129.7 (C), 127.4 (CH), 127.0 (CH), 124.8 (CH), 122.5 (CH), 121.3 (C), 52.6 (CH_3), 33.7 (CH_2).

HRMS (ESI) m/z calculated. for $C_{14}H_{11}O_6N^{23}Na^{32}S$ $[M+Na]^+$ 344.0205, found 344.0199.

7-((2-methoxy-2-oxoethyl)thio)-1,3-dioxo-1*H*,3*H*-naphtho[1,8-*cd*][1,2]oxazin-1-iumchloride (7)



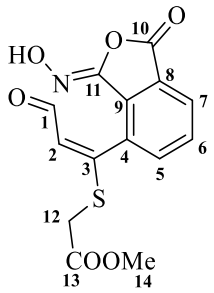
5-((2-methoxy-2-oxoethyl)thio)-8-nitro-1-naphthoic acid (1 g, 3.1 mmol) was suspended in oxalyl chloride (3 ml, 35 mmol) and tetraethyl ammonium chloride (10 mg, 0.06 mmol) was added as a catalyst. The reaction flask was sonicated in an ultrasound bath at 40 ºC for 30 minutes until the starting material was completely dissolved. To the clear solution toluene was added (5 ml) and the solvents were removed under reduced pressure in a water bath at 20 ºC yielding compound **7** as a pale-yellow solid (1 g, 99%).

(Melting point and IR were not measured due to the instability of the compound).

^{1}H NMR (400 MHz, $CDCl_3$) δ 8.64 (dd, *J* = 8.6, 1.0 Hz, 1H), 8.36 (dd, *J* = 7.4, 1.0 Hz, 1H), 8.18 (d, *J* = 8.2 Hz, 1H), 7.76 (dd, *J* = 8.6, 7.4 Hz, 1H), 7.61 (d, *J* = 8.2 Hz, 1H), 3.90 (s, 2H), 3.76 (s, 3H). **^{13}C NMR** (101 MHz, $CDCl_3$) δ 168.8 (C), 167.7 (C), 144.9 (C), 143.0 (C), 133.1 (CH), 132.7 (C), 130.0 (CH), 126.7 (CH), 125.9 (CH), 124.0 (CH), 121.5 (C), 53.2 (CH_2), 35.3 (CH_3).

HRMS (ESI) m/z calculated. for $C_{14}H_{10}NO_5S^+$ ($[M]^+$) 304.0274, found 304.0273.

Methyl 2-(((*E*)-1-((*Z*)-3-(hydroxyimino)-1-oxo-1,3-dihydroisobenzofuran-4-yl)-3-oxoprop-1-en-1-yl)thio)acetate (4)



Compound **7** (1 g, 3.1 mmol) was quickly dissolved in methylene chloride (20 ml) and added to a solution of bis(2-chloroethyl)amine (2 g, 14.1 mmol) in an ether solution saturated with water and methylene chloride (100 ml) cooled to -30 ºC. After 30 minutes the reaction mixture was added over aqueous sulfuric acid (2M, 100 ml), separated in a separatory funnel, and the organic phase was washed again with another portion of aqueous sulfuric acid (50 ml) and water (100 ml). Evaporation of the major part of the methylene chloride induced the crystallization of the aldehyde which was filtered under reduced pressure to yield a pale cream solid (700 mg, 70% yield).

m.p.: 111-113 ºC.

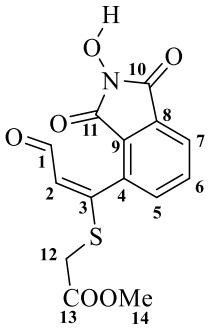
IR (neat, ν in cm^{-1}): 3318, 1785, 1734, 1663, 1573, 1525, 1438, 1283, 1137.

^{1}H NMR (400 MHz, DMSO-d_6) δ 11.83 (s, OH), 9.07 (d, J = 7.9 Hz, 1H(1)), 8.07 (dd, J = 7.0, 1.7 Hz, 1H(7)), 7.85 – 7.76 (m, 2H(5,6)), 6.23 (d, J = 7.9 Hz, 1H(2)), 3.95 (d, J = 16.0 Hz, 1H(12)), 3.89 (d, J = 16.2 Hz, 1H(12)), 3.66 (s, 3H(14)).

^{13}C NMR (101 MHz, DMSO-d_6) δ 188.9 (CH(1)), 168.2 (C(13)), 163.2 (C(10)), 159.4 (C(3)), 145.8 (C(11)), 136.5 (CH(5)), 132.9 (C(9)), 131.7 (CH(6)), 128.8 (C(8)), 127.0 (C(4)), 126.7 (CH(7)), 124.5 (CH(2)), 52.6 (CH_3(14)), 34.0 (CH_2(12)).

HRMS (ESI) m/z calculated. for $C_{14}H_{11}NNaO_6S^+$ ($[M+Na]^+$) 344.0199, found 344.0193.

Methyl (*Z*)-2-((1-(2-hydroxy-1,3-dioxoisoindolin-4-yl)-3-oxoprop-1-en-1-yl)thio)acetate (5)



In a round bottom flask methyl 2-(((*E*)-1-((*Z*)-3-(hydroxyimino)-1-oxo-1,3-dihydroisobenzofuran-4-yl)-3-oxoprop-1-en-1-yl)thio)acetate (100 mg, 0.31 mmol) was dissolved in methylene chloride (20 ml) and DABCO (18 mg, 0.16 mmol) was added. After 20 minutes at room temperature, acetic acid was added, and the reaction mixture was chromatographed over silica gel (20 g) eluting with a mixture of methylene chloride/ethyl acetate 4/1 yielding the isomeric aldehyde as a pale cream oil (17 mg, 17% yield).

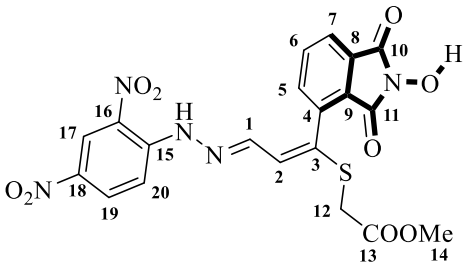
IR (neat, ν in cm^{-1}): 3494, 3280, 1787, 1723, 1664, 1573, 1314.

^{1}H NMR (400 MHz, $CDCl_3$) δ 9.05 (d, *J* = 7.8 Hz, 1H(1)), 7.90 (dd, *J* = 7.5, 1.0 Hz, 1H(7)), 7.79 (t, *J* = 7.6 Hz, 1H(6)), 7.67 (dd, *J* = 7.8, 0.9 Hz, 1H(5)), 6.26 (d, *J* = 7.8 Hz, 1H(2)), 3.81 (d, *J* = 15.4, 1H(12)), 3.77 (s, 3H(14)), 3.74 (d, *J* = 15.8, 1H(12)).

^{13}C NMR (101 MHz, $CDCl_3$) δ 188.9 (CH(1)), 168.0 (C(13)), 163.0 (C(10)), 162.4 (C(11)), 159.3 (C(3)), 135.5 (CH(5)), 134.5 (CH(6)), 131.6 (C(4)), 130.0 (C(8)), 126.7 (C(9)), 124.9 (CH(7)), 124.7 (CH(2)), 53.1 (CH_3(14)), 34.5 (CH_2(12)).

HRMS (ESI) m/z calculated. for calculated. for $C_{14}H_{11}NNaO_6S^+$ ($[M+Na]^+$) 344.0199, found 344.0194.

Methyl2-(((1*Z*,3*Z*)-3-(2-(2,4-dinitrophenyl)hydrazineylidene)-1-(2-hydroxy-1,3-dioxoisoindolin-4-yl)prop-1-en-1-yl)thio)acetate (6)



Either of the aldehydes **4** or **5** (100 mg, 0.31 mmol) were dissolved in THF and 2,4-dinitrophenyl hydrazine was added (100 mg, 0.50 mmol). The reaction mixture was heated to 60 ºC for 30 minutes. Evaporation of the solvent under reduced pressure and chromatography over silica gel (20 g) eluting with CH_2Cl_2/EtOAc (1/1) yielded compound **6** as a deep red solid (90 mg, 58% yield).

m.p.: 123-125 ºC.

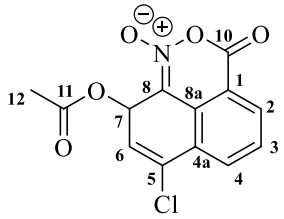
IR (neat, ν in cm^{-1}): 3546, 3280, 1787, 1729, 1599, 1515, 1457, 1320.

^{1}H NMR (400 MHz, $CDCl_3$) δ 10.95 (s, 1H), 9.04 (d, *J* = 2.4 Hz, 1H(17)), 8.30 (dd, *J* = 9.6, 2.4 Hz, 1H(19)), 7.96 – 7.88 (m, 2H (7, 20)), 7.84 (t, *J* = 7.4 Hz, 1H(6)), 7.69 (d, *J* = 7.8 Hz, 1H(5)), 7.39 (d, *J* = 9.6 Hz, 1H(1)), 6.80 (d, *J* = 9.5 Hz, 1H(2)), 3.77 – 3.72 (s, 3H (14)), 3.53 (s, 2H (12)).

^{13}C NMR (101 MHz, $CDCl_3$, CD_3OD) δ 169.2 (C(13)), 163.7 (C(10)), 162.9 (C(11)), 145.2 (CH(1)), 144.3 (C(15)), 141.1 (C(3)), 138.2 (C(18)), 136.0 (CH(5)), 134.5 (CH(6)), 133.2 (C(4)), 130.4 (C(8)), 129.8 (CH(19)), 129.4 (C(16)), 126.8 (C(11)), 124.9 (CH(2)), 124.1 (CH(7)), 123.3 (CH(17)), 116.8 (CH(20)), 52.9 (CH_3(14)), 34.6 (CH_2(12)).

HRMS (ESI) m/z calculated. for $C_{20}H_{14}N_5O_9S^-$ ($[M-H]^-$) 500.0518, found 500.0518.

9-acetoxy-7-chloro-3-oxo-3*H*,9*H*-naphtho[1,8-*cd*][1,2]oxazine 1-oxide (12)



Compound **1** (30 mg, 0.1 mmol) was suspended in oxalyl chloride (1.5 ml, 17.8 mmol) and a trace of triethylammonium bromide was added. The mixture was sonicated for 1 hour at 40-50 ºC until the solution became homogeneous. Bubbles of CO_2 and HCl were observed during the

reaction. Then, the reaction mixture was concentrated under reduced pressure at 20 ºC. The crude reaction mixture was dissolved in 1 ml of $CDCl_3$ and cooled down at 0 ºC under argon atmosphere. Potassium acetate (30 mg, 0.3 mmol) and acetic acid (30 mL, 0.5 mmol) were added. The reaction mixture was stirred for 40 minutes, added over water and extracted twice with CH_2Cl_2. The combined organic phases were dried over Na_2SO_4, filtered and concentrated under reduced pressure to yield compound **12** as a pale-yellow solid (30 mg, 99% yield).

(Melting point and IR were not measured due to the instability of the compound).
^{1}H NMR (400 MHz, $CDCl_3$) δ 8.25 (d, *J* = 7.9 Hz, 1H(2)), 8.14 (d, *J* = 7.8 Hz, 1H(4)), 7.71 (t, *J* = 7.9 Hz, 1H(3)), 6.72 (d, *J* = 5.2 Hz, 1H(7)), 6.41 (d, *J* = 5.2 Hz, 1H(6)), 2.13 (s, 3H(12)).
^{13}C NMR (101 MHz, $CDCl_3$) δ 169.4 (C(11)), 161.9 (C(10)), 133.0 (C(5)), 132.4 (CH(4)), 130.6 (CH(3)), 130.2 (CH(2)), 127.0 (C(4a)), 125.7 (C(8a)), 121.8 (CH(6)), 117.6 (C(1)), 115.5 (C(8)), 63.9 (CH(7)), 20.1 (CH_3(12)).
HRMS (ESI) m/z calculated. for $C_{13}H_8ClNNaO_5^+$ ($[M+Na]^+$) 315.9983, found 315.9976.

5.3. Crystallographic Data

- *Procedure for the single crystal preparation*

Compound **6**. Single crystals suitable for X-ray diffraction measurements were obtained by slowly evaporating a solution of compound **6** in $CHCl_3$/EtOH in a clean and dry 10 mL glass vial. The mouth of the glass vial was covered with a balloon, fastened with a rubber band, and kept it for slow evaporation at 4 °C. At the end of the process, single crystals were obtained after 5-6 days.

- *X-Ray Crystallography*

Suitable single crystals of compound **6** were mounted on glass fibre for data collection on a Bruker Kappa APEX II diffractometer. Data were collected at 298(2) K using Cu K_α radiation (λ = 1.54178 Å) and ω scan technique and were corrected for Lorentz and polarization effects. The detector was placed at a distance of approximately 37.5 mm from the crystal.
A series of narrow frames of data were collected with a scan width of 0.5º in ω and an exposure time of 10 s per frame. The data were integrated with SAINT [23] to a resolution of 0.78 Å using a narrow-frame algorithm. Data were corrected for absorption effects using the multi-scan method using SADABS.[24]

Subsequent structure solution and refinement were carried out with SHELXT and SHELXL, respectively.[25,26] The structures were solved by direct methods combined with difference Fourier synthesis and refined by full-matrix least-squares procedures, with anisotropic thermal parameters in the last cycles of refinement for all non-hydrogen atoms. The refinement was based on F^2 for all reflections, weighted R factors (wR) and goodness-of-fit (GoF) values are based on F^2, while conventional R factors (R) are based on F. The $Fo^2 > 2\sigma(Fo^2)$ criterion was used only for calculating R factors and it is not relevant to the choice of reflections for the refinement. The R factors based on F^2 are about twice as large as those based on F. Scattering factors were taken from the International Tables for Crystallography.[27] Hydrogen atoms were positioned geometrically. Mercury 4.2.0 program was used for analysis and molecular and crystal structure drawings preparation.[28]

- *Crystal Data*

Table 1. Crystal data and structure refinement for compound **6**. CCDC 2351359.

Empirical formula	$C_{23}H_{21}Cl_3N_5O_{10}S$
Formula weight	665.86
Temperature (K)	298(2)
Wavelength (Å)	1.54178
Crystal system	Monoclinic
Space group	$P2_1/c$
Unit cell dimensions:	
a (Å)	17.4129(9)
b (Å)	8.4850(5)
c (Å)	20.4961(8)
α [º], β[º], γ[º]	90.00,100.521(3), 90.00
Volume	2977.4(3)
Z, Density (calculated) (Mg/m^3)	4, 1.485
Absorption coefficient (mm^{-1})	3.987
F(000)	1364
Crystal size (mm)	0.13 x 0.11 x 0.09
2Θ range for data collection(°)	2.58 to 66.98
Limiting indices	$-20\leq h\leq 19$, $-10\leq k\leq 9$, $-21\leq l\leq 23$
Reflections collected / Independent	19491/5021 (Rint = 0.0628)
Refinement method	Full-matrix least-squares on F^2
Data / restraints / parameters	5021/ 0 / 382
Goodness-of-fit on F^2	1.933
Final R indices[I>2σ(I)]	R1 = 0.1010, wR2 = 0.2823
R indices (all data)	R1 = 0.1259, wR2 = 0.2964
Largest diff. peak and hole ($eÅ^{-3}$)	0.780 and -0.857

- *Molecular structure of compound **6***

Compound 6: $C_{23}H_{21}Cl_3N_5O_{10}S$

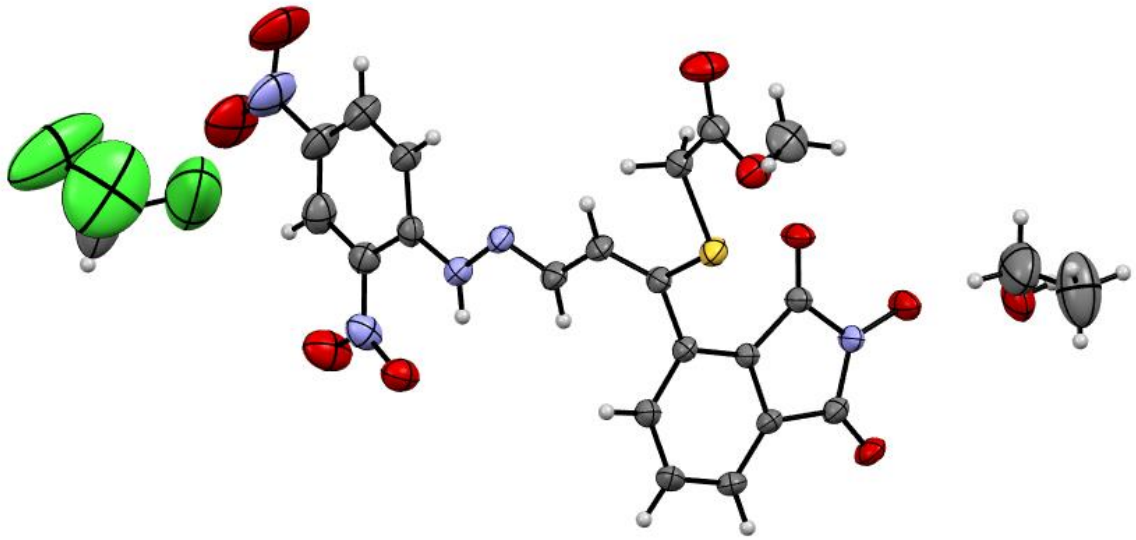


Figure S1. *Molecular structure of compound **6**. Displacement ellipsoids are drawn at 50 % probability level. Hydrogen atoms are shown as spheres of arbitrary radius.*

5.4. Computational Studies

DFT calculations on the reaction mechanism

DFT calculations were done using Gaussian16 software [29]. The functional w-B97XD [30] was used in combination with 6-31+G(d,p) basis set[31]. Solvent effects (chloroform) were introduced by means of implicit SMD solvation model [32], and Gibbs correction to the single point energy was evaluated by the rigid-rotor harmonic approximation[33] as implemented in Good vibes software [34]for a temperature 298 K and a threshold of 100 cm^{-1}.

For each transformation, several transition state structures (corresponding to different conformations) were calculated. The energies in the diagram of figure 12 correspond to the Gibbs free energy of the most stable Transition states , but product distribution was calculated using a Maxwell-Boltzmann average considering the Gibbs free energies of each transition state structure obtained.

5.5. NMR spectra

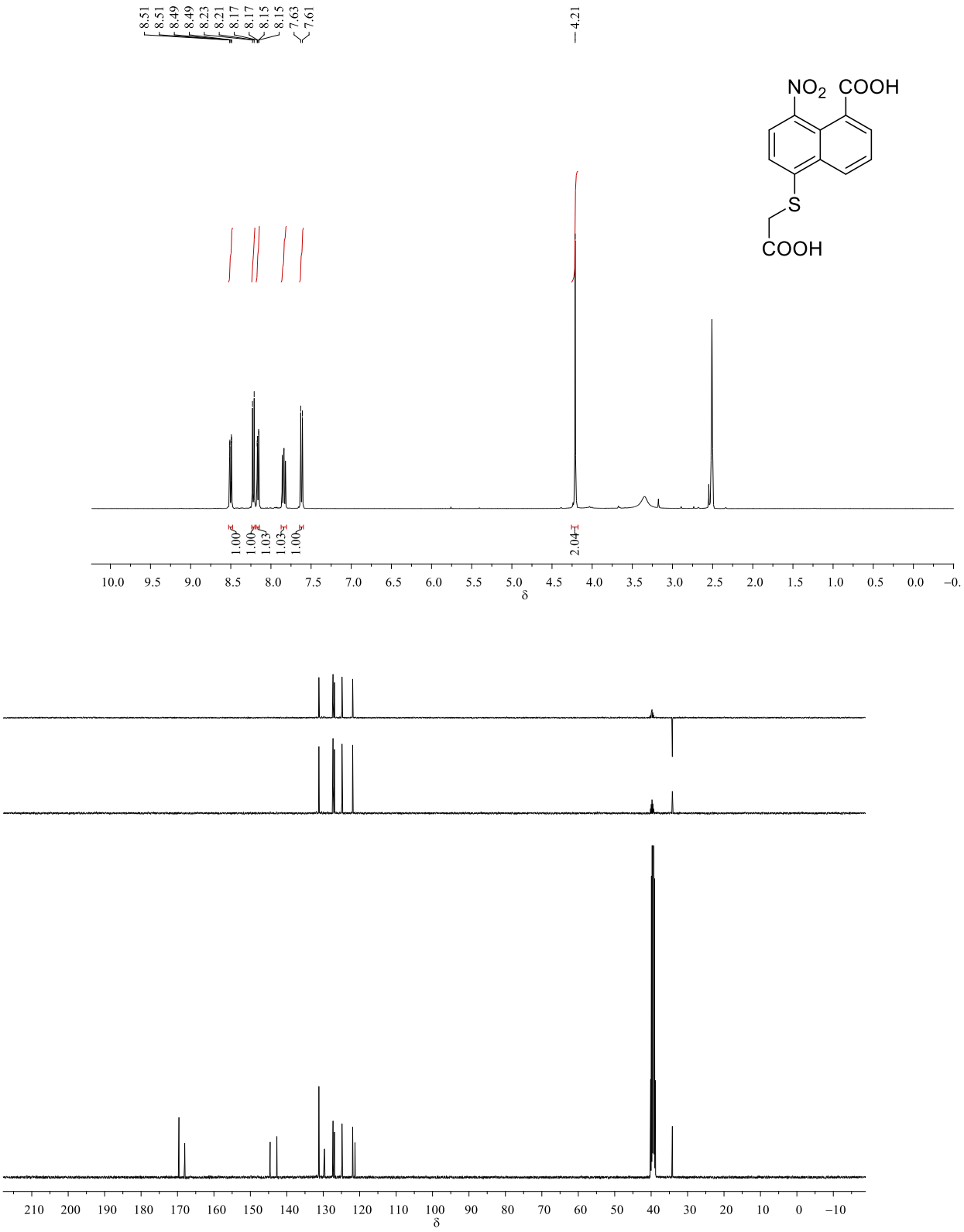


Figure S2. *[1]H NMR (DMSO-d_6, 400 MHz) and [13]C (DMSO-d_6, 100 MHz) spectra of compound **1**.*

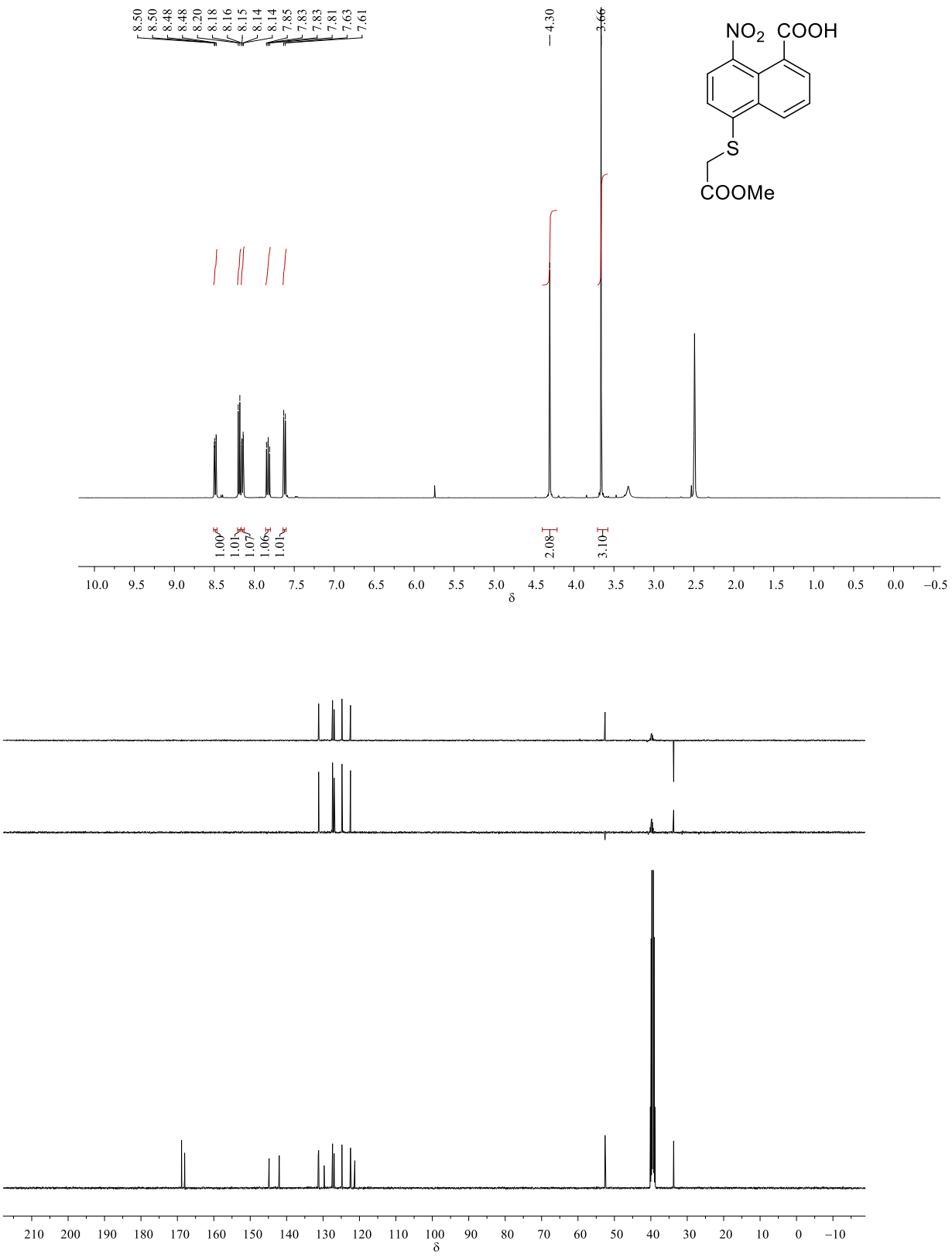


Figure S3. *^{1}H NMR (DMSO-d_6, 400 MHz) and ^{13}C (DMSO-d_6, 100 MHz) spectra of compound **2**.*

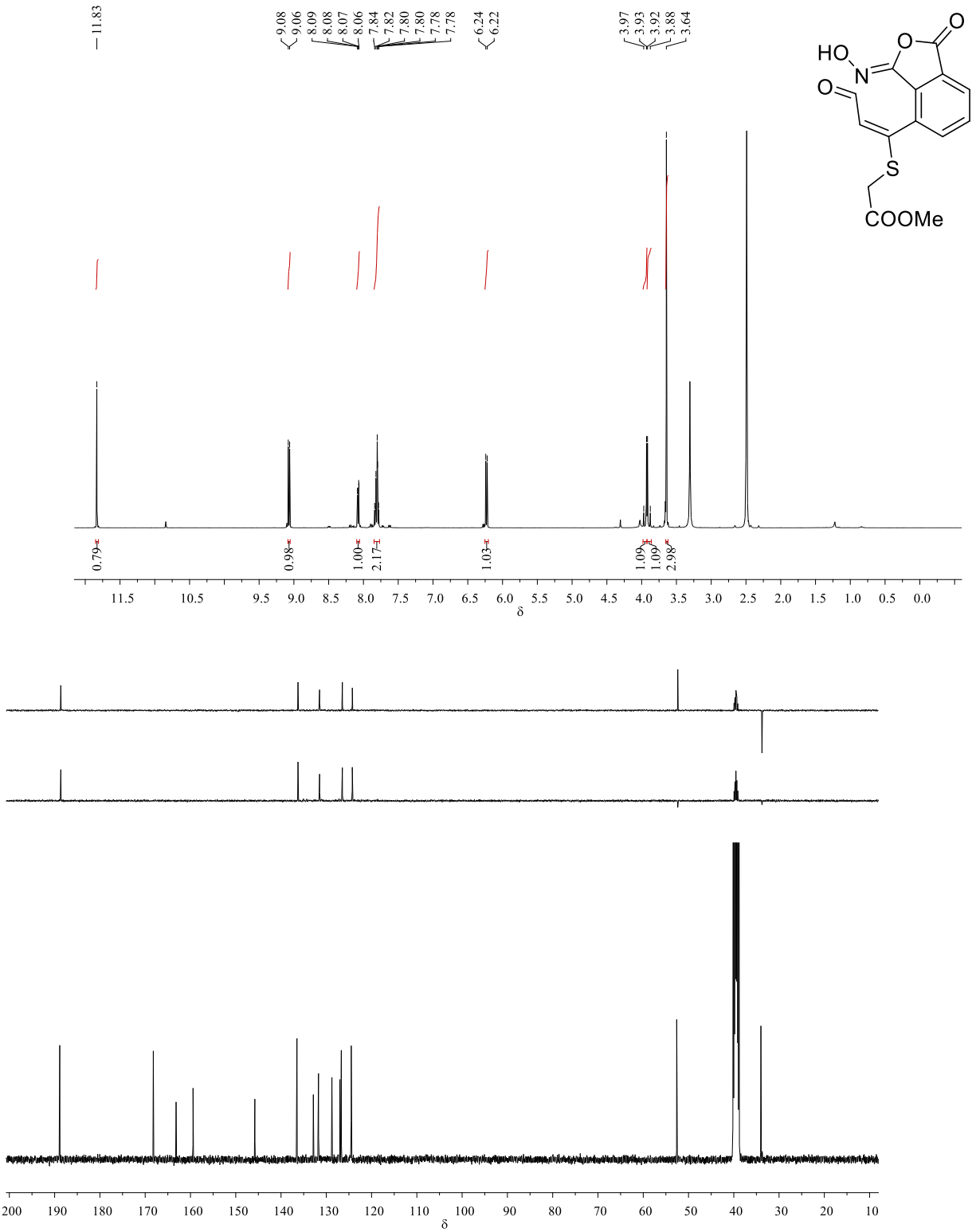


Figure S4. *^{1}H NMR (DMSO-d_6, 400 MHz) and ^{13}C (DMSO-d_6, 100 MHz) spectra of compound **4**.*

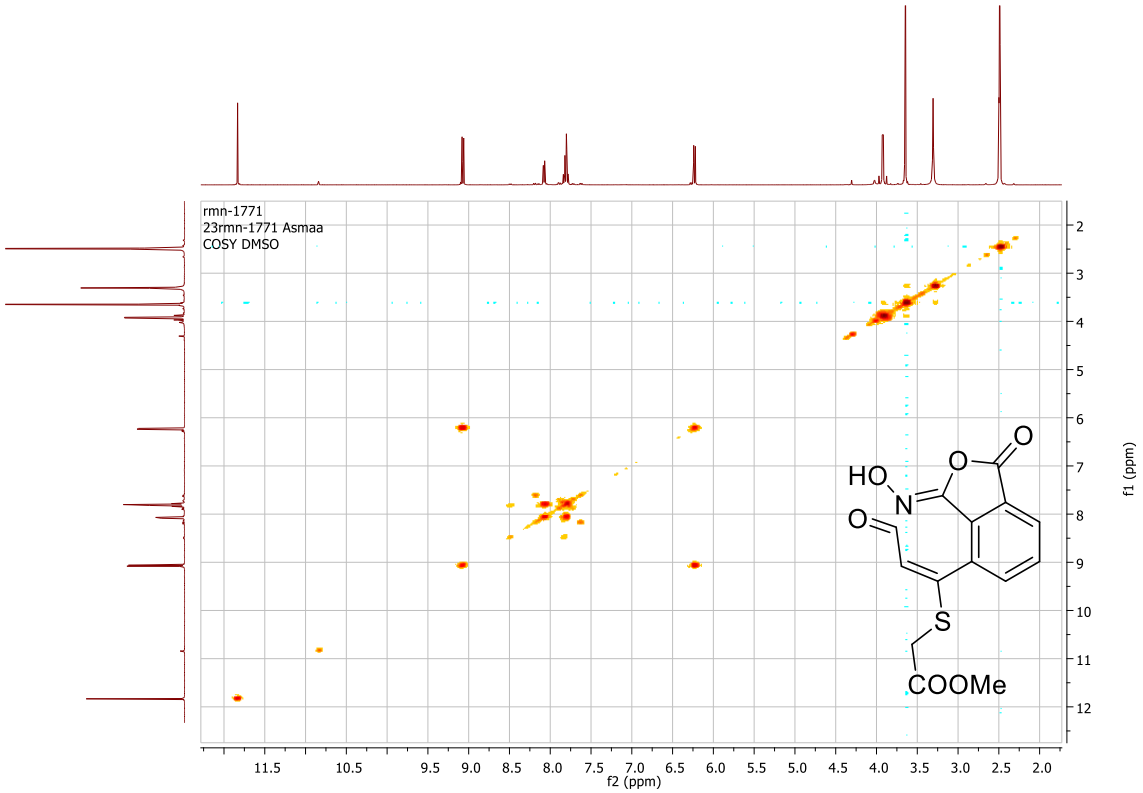


Figure S5. *COSY spectrum of compound **4** in DMSO-d_6.*

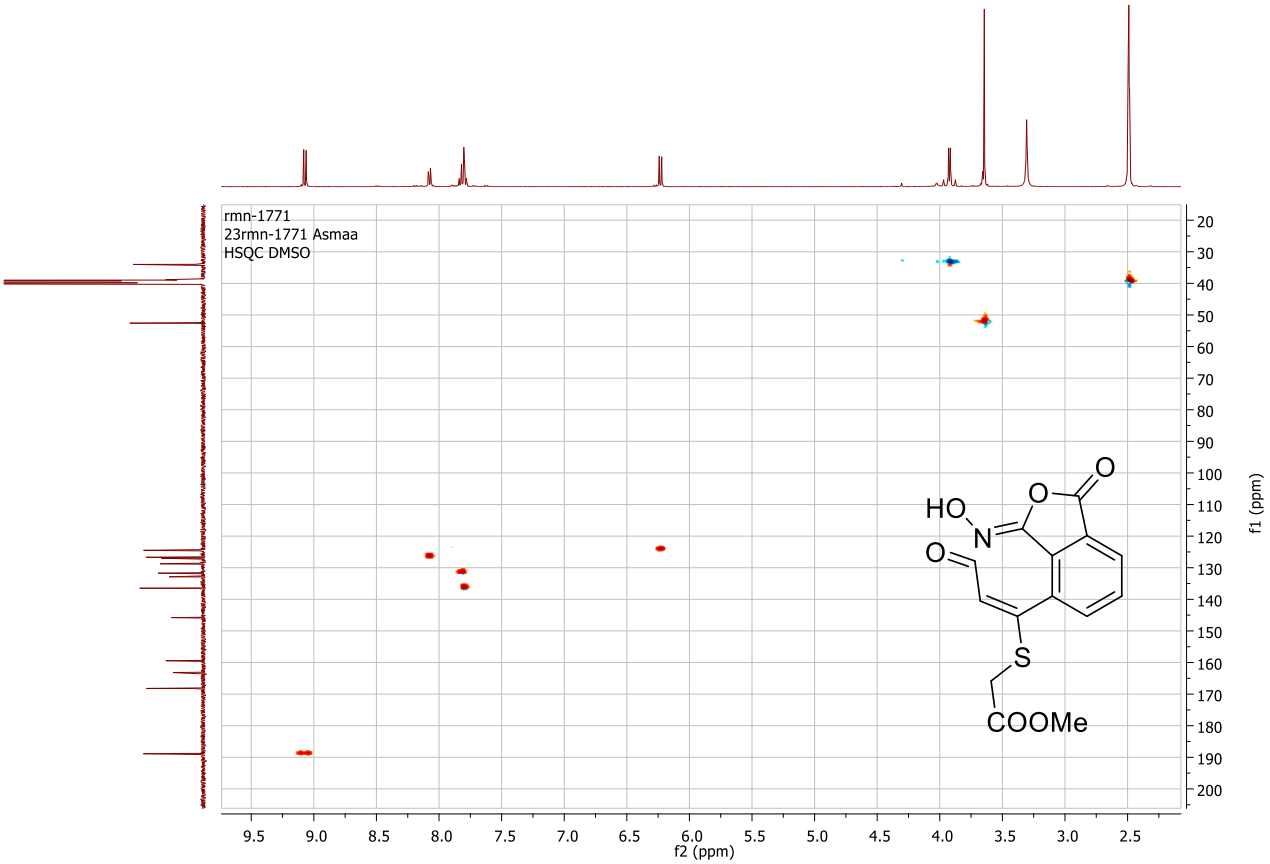


Figure S6. *HSQC 145 Hz spectrum of compound **4** in DMSO-d_6.*

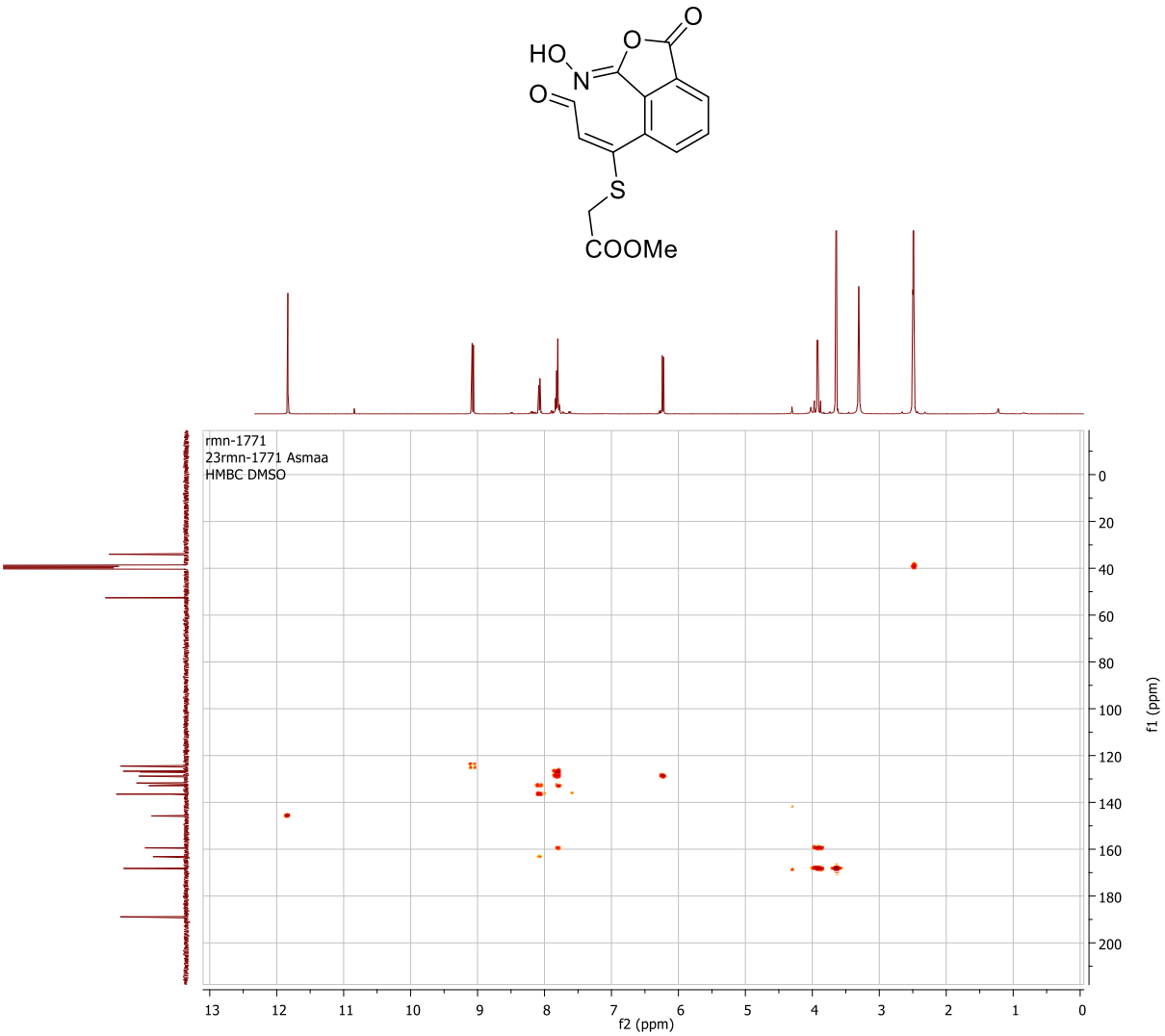


Figure S7. *HMBC CIGAR spectrum of compound **4** in DMSO-d_6.*

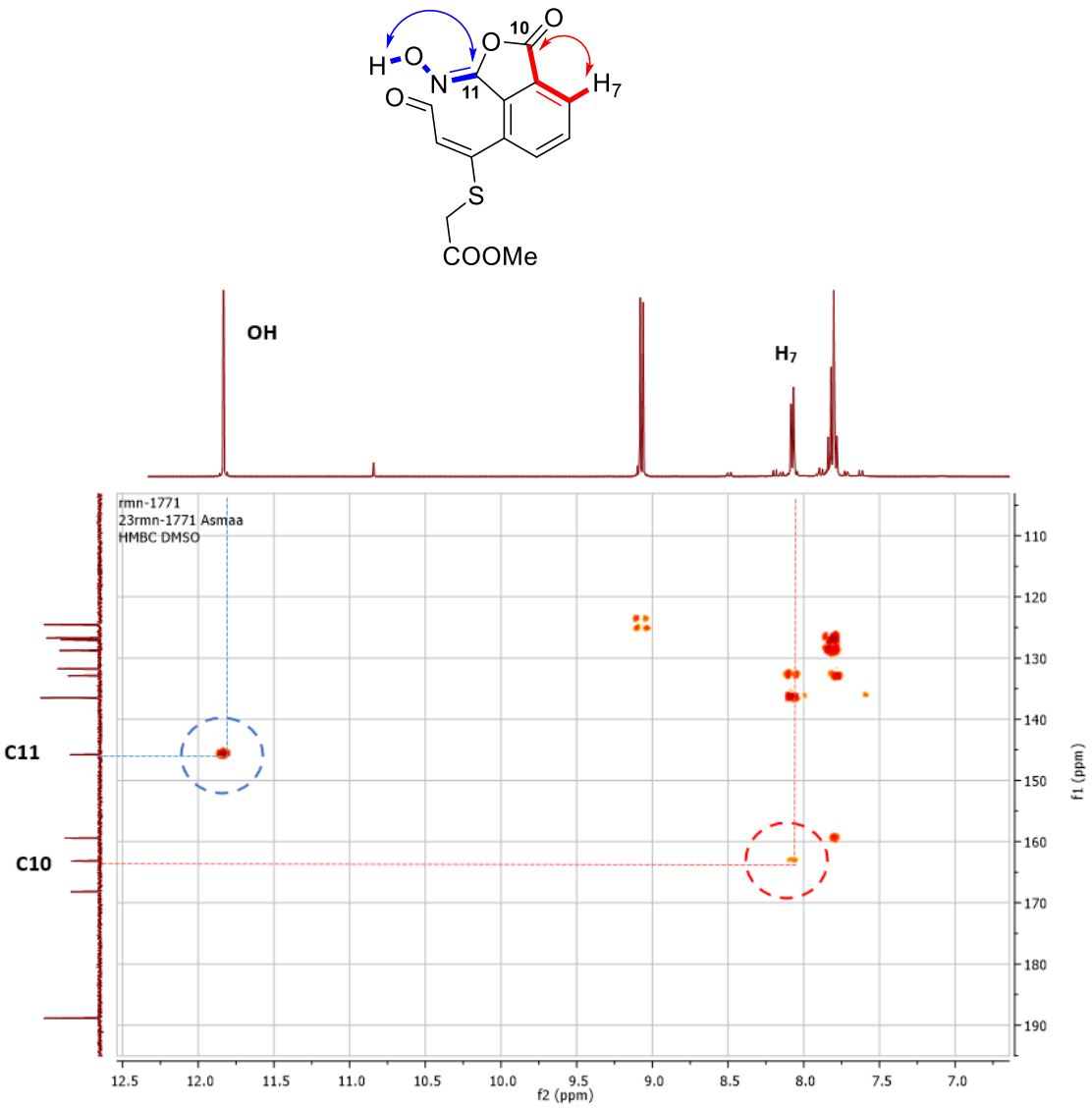


Figure S8. *Expansion of HMBC CIGAR spectrum of compound **4** in DMSO-d_6.*

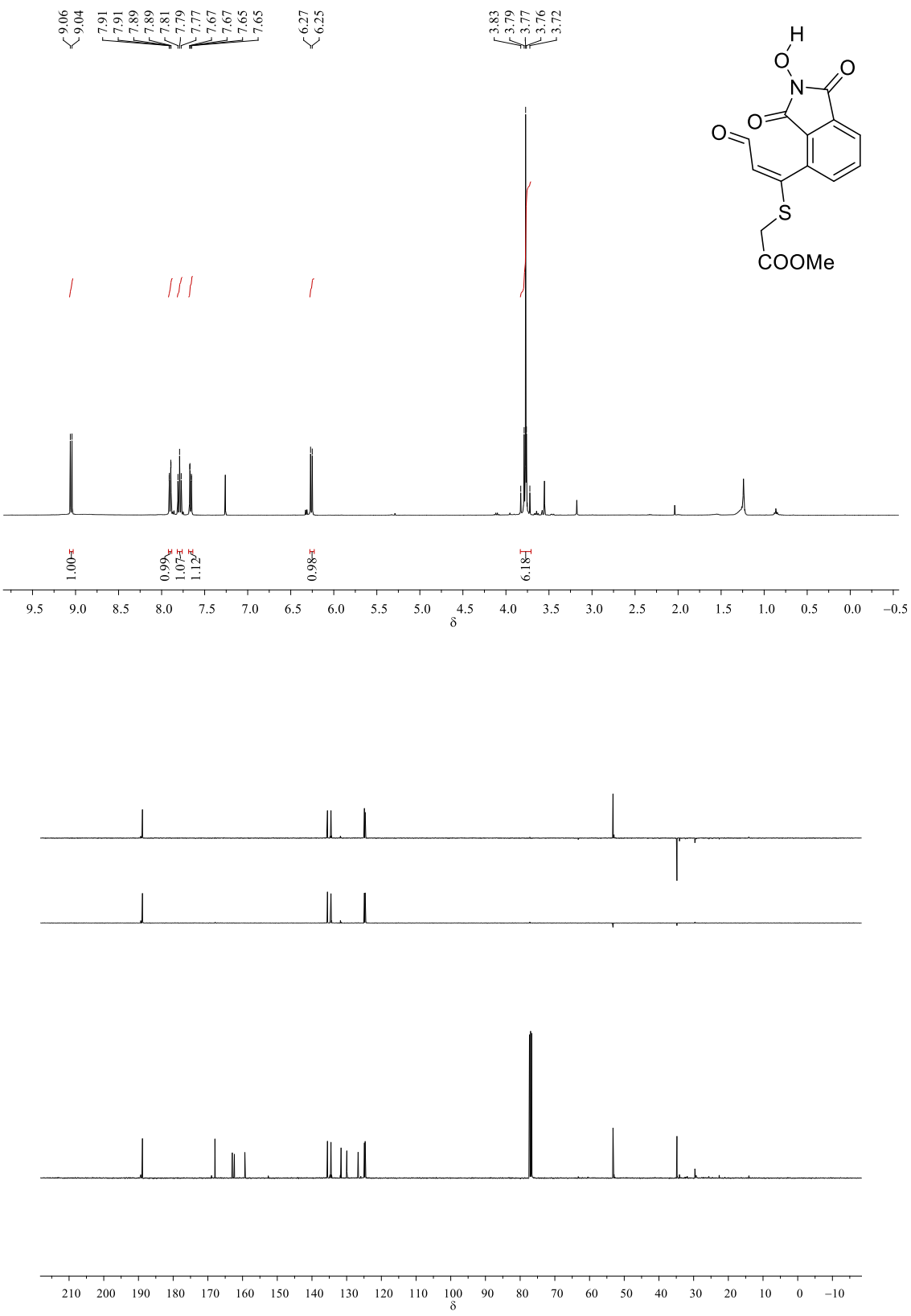


Figure S9. *^{1}H NMR ($CDCl_3$, 400 MHz) and ^{13}C ($CDCl_3$, 100 MHz) spectra of compound **5**.*

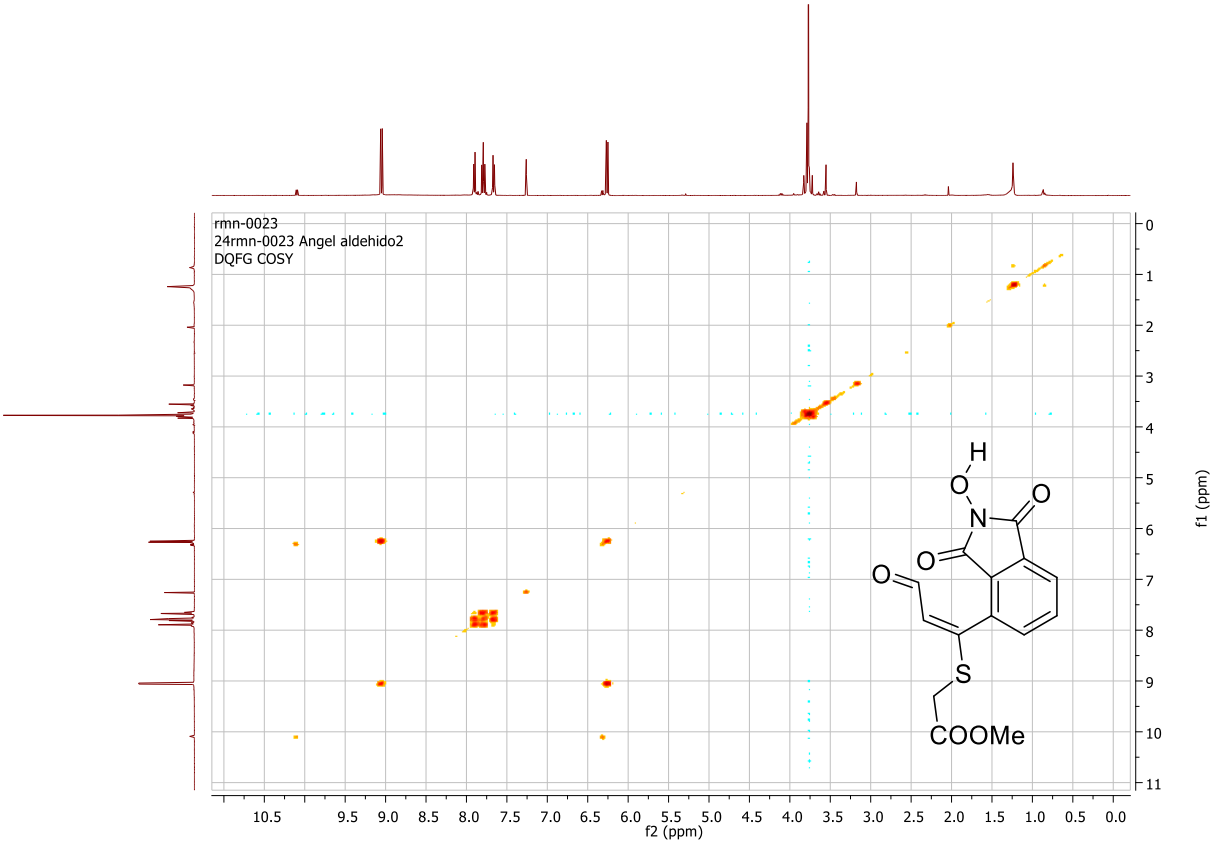


Figure S10. *COSY spectrum of compound* ***5*** *in* $CDCl_3$.

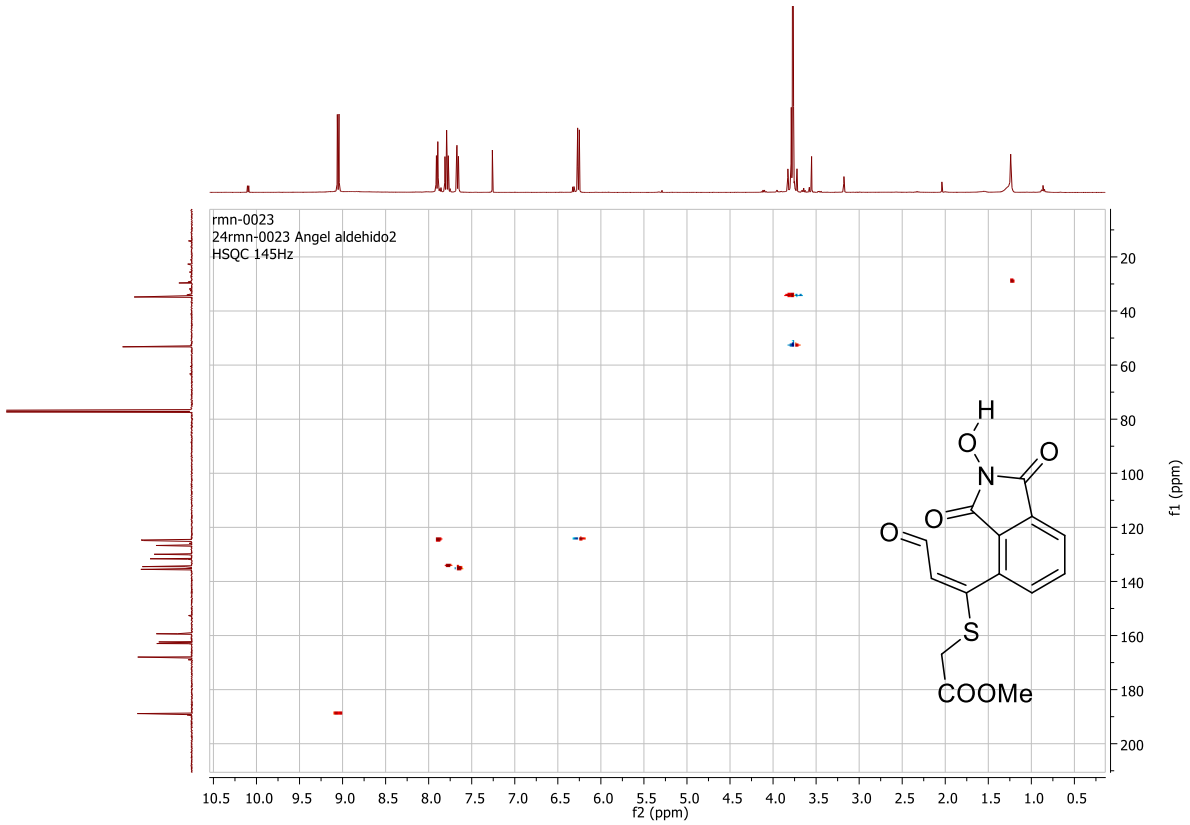


Figure S11. *HSQC 145 Hz spectrum of compound* ***5*** *in* $CDCl_3$.

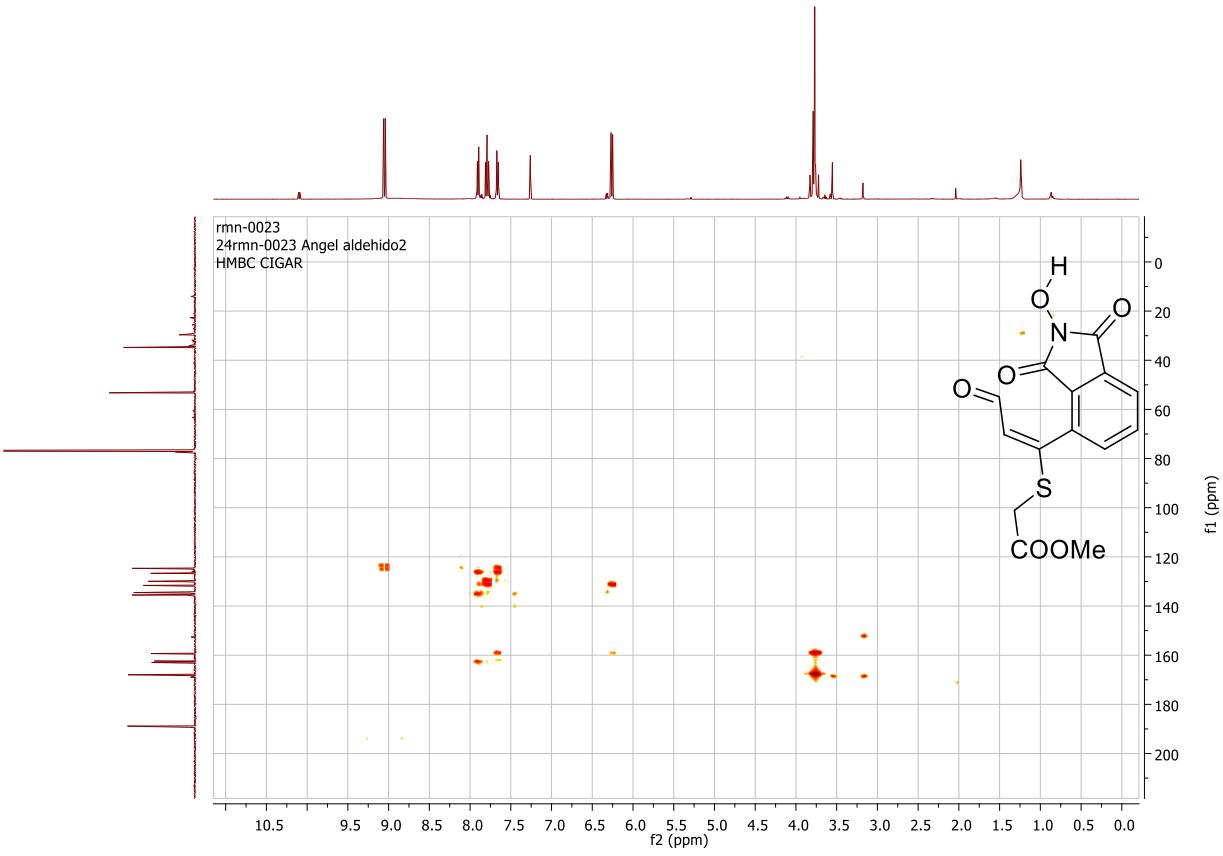


Figure S12. *HMBC CIGAR spectrum of compound* ***5*** *in* $CDCl_3$.

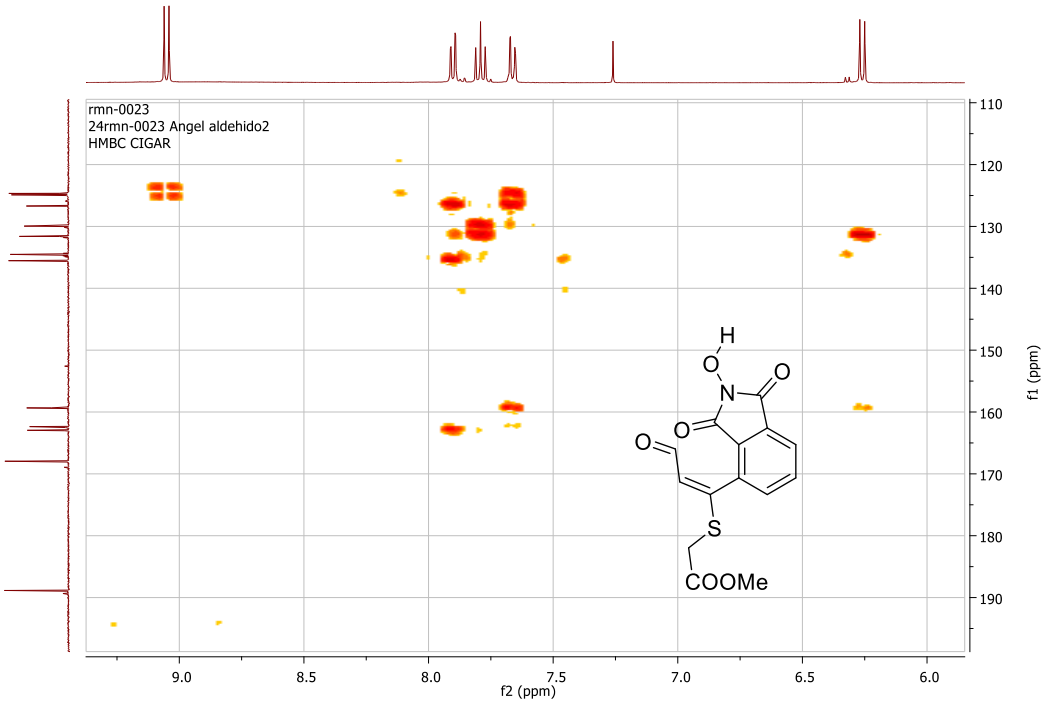


Figure S13. *Expansion of HMBC CIGAR spectrum of compound **5** in $CDCl_3$.*

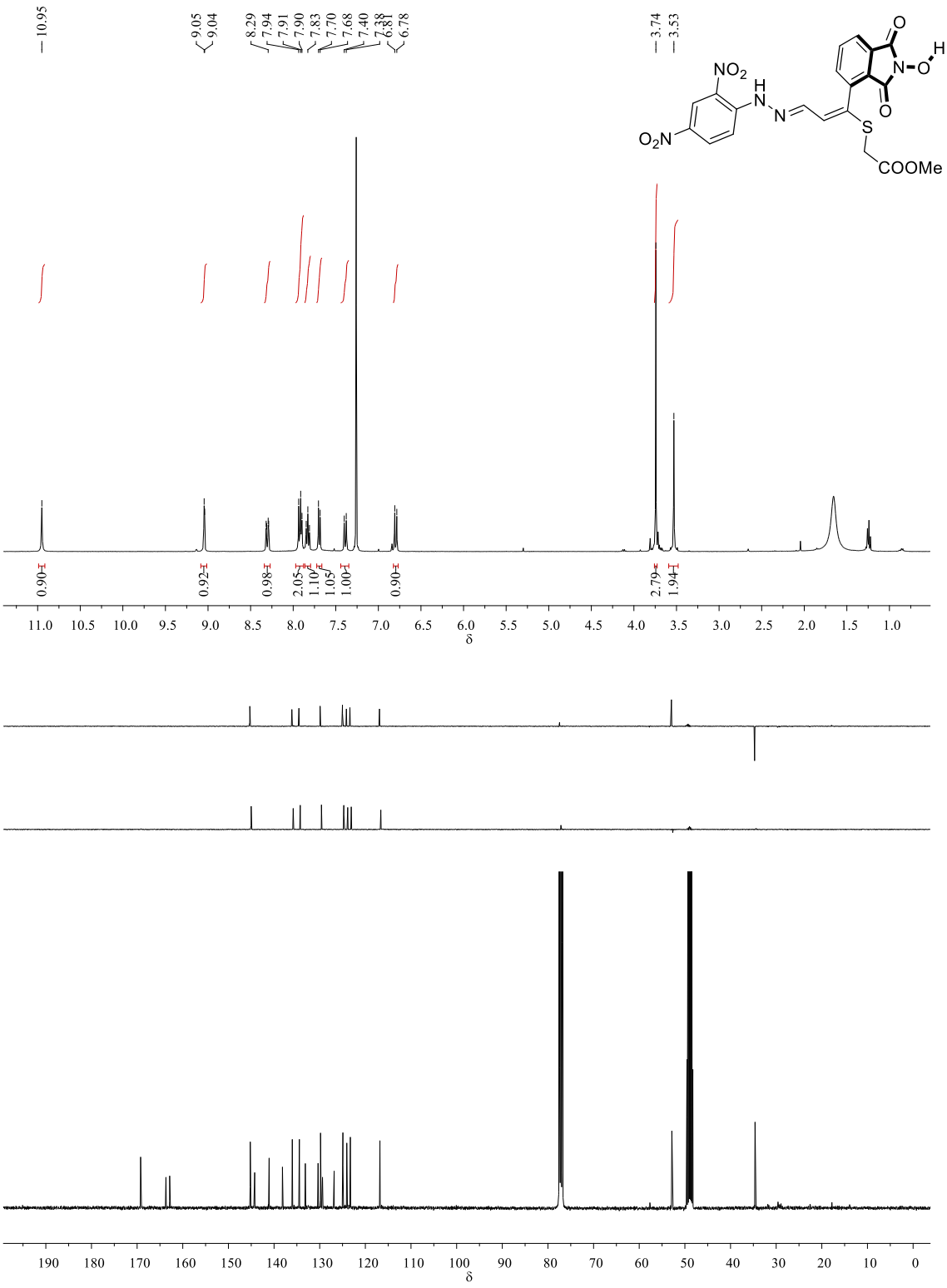


Figure S14. *^{1}H NMR ($CDCl_3$, 400 MHz) and ^{13}C ($CDCl_3$/* CD_3OD*, 100 MHz) spectra of compound* ***6***.

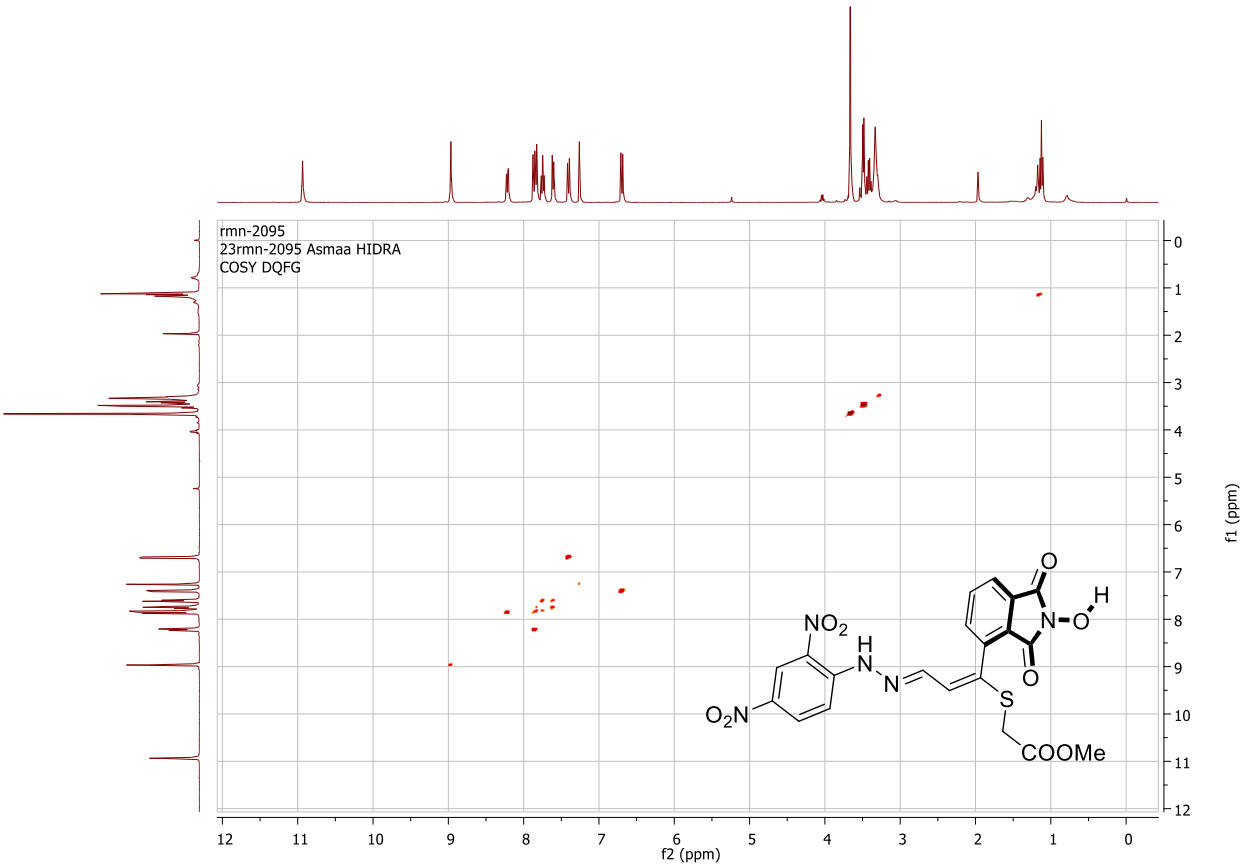


Figure S15. *COSY spectrum of compound* ***6*** *in $CDCl_3/CD_3OD$.*

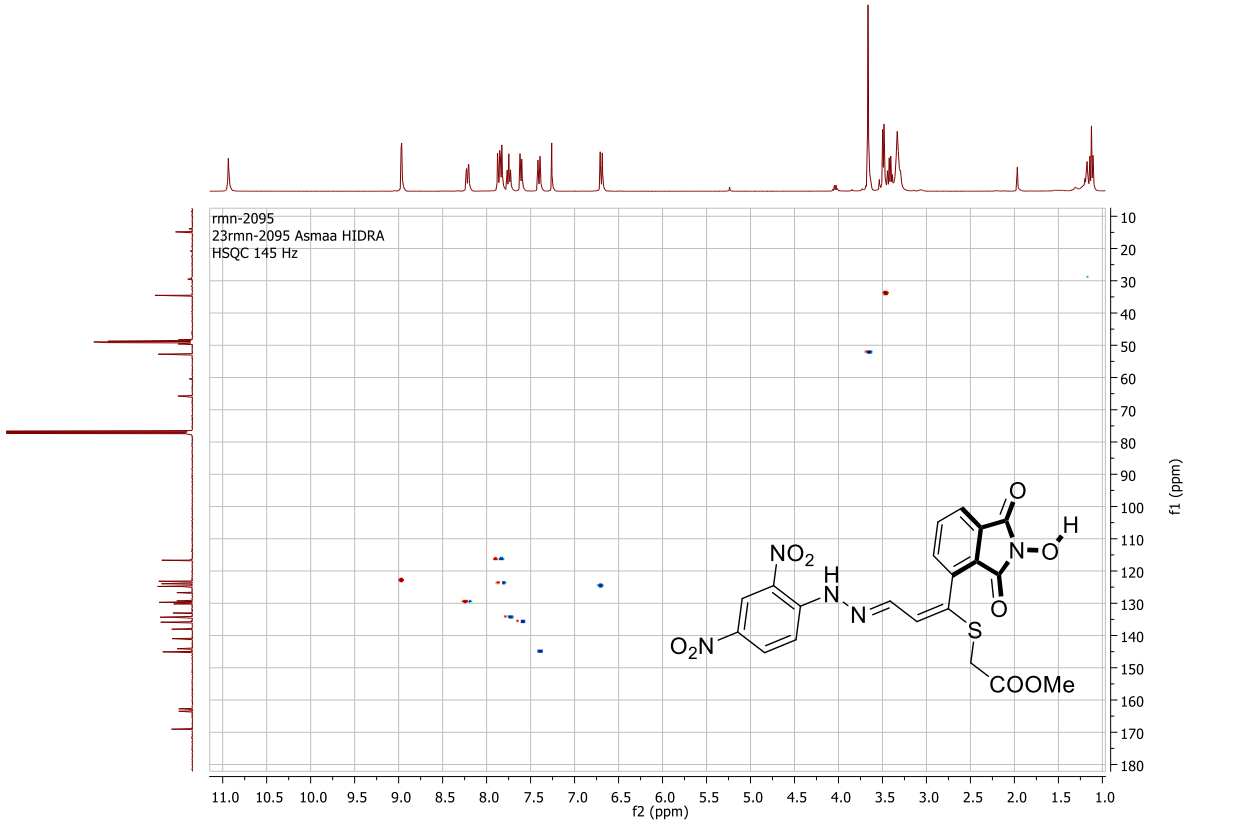


Figure S16. *HSQC 145 Hz spectrum of compound* ***6*** *in $CDCl_3/CD_3OD$.*

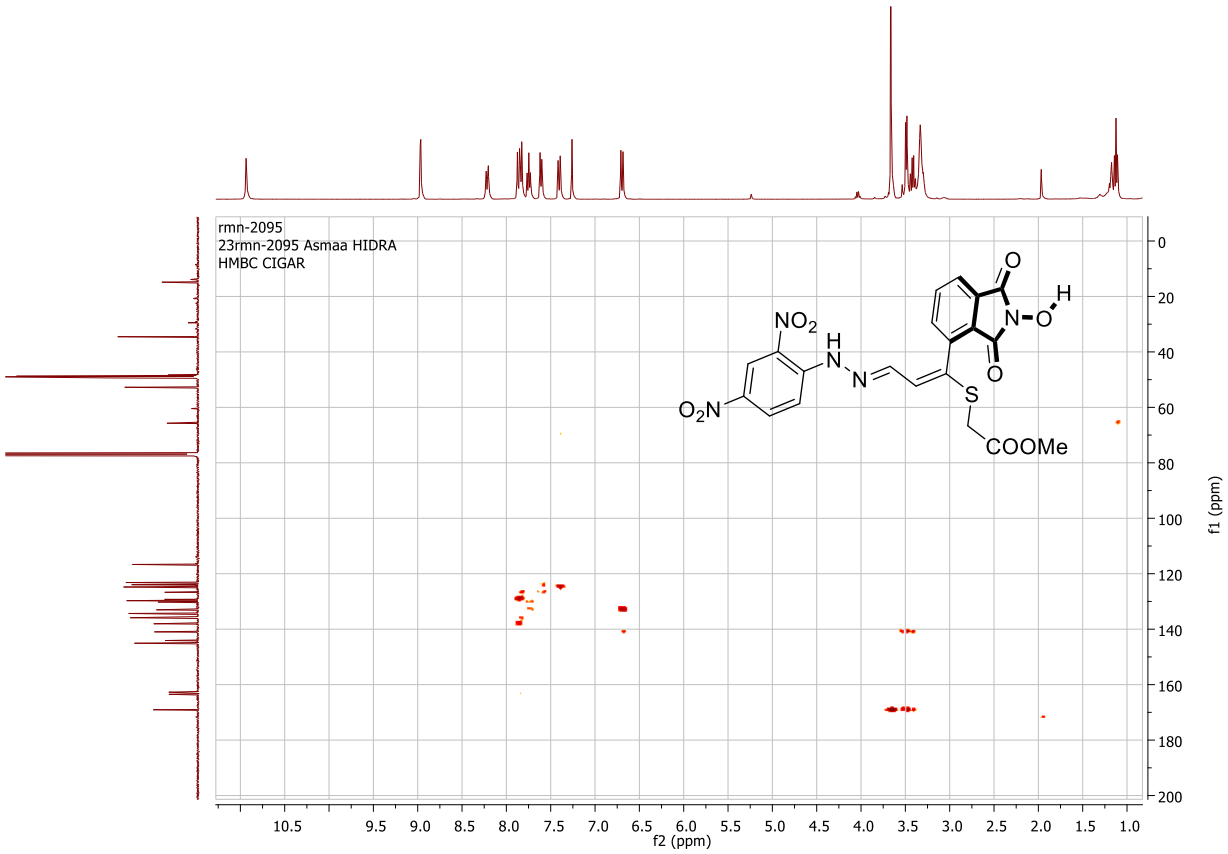


Figure S17. *HBMC CIGAR spectrum of compound* ***6*** *in* $CDCl_3/CD_3OD$.

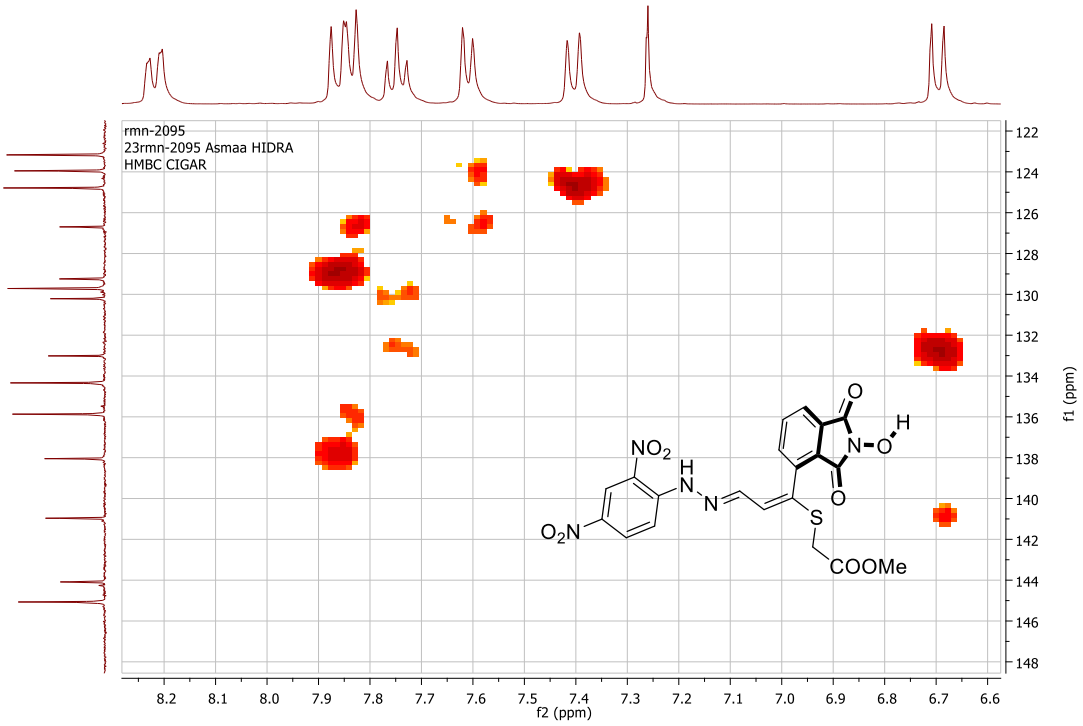


Figure S18. *Expansion of HMBC CIGAR spectrum of compound* ***6*** *in* $CDCl_3/CD_3OD$.

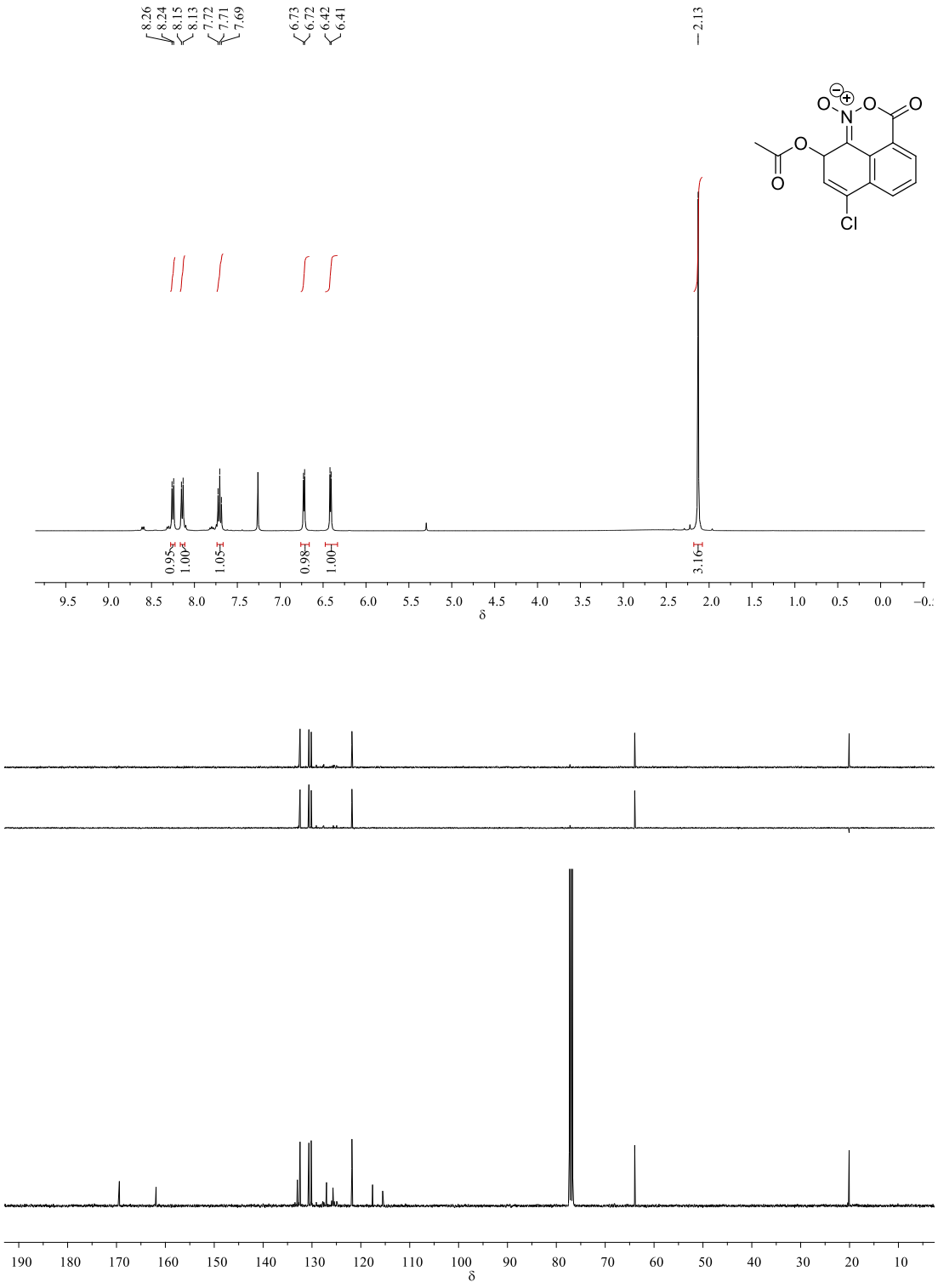


Figure S19. *^{1}H NMR ($CDCl_3$, 400 MHz) and ^{13}C ($CDCl_3$, 100 MHz) spectra of compound **12**.*

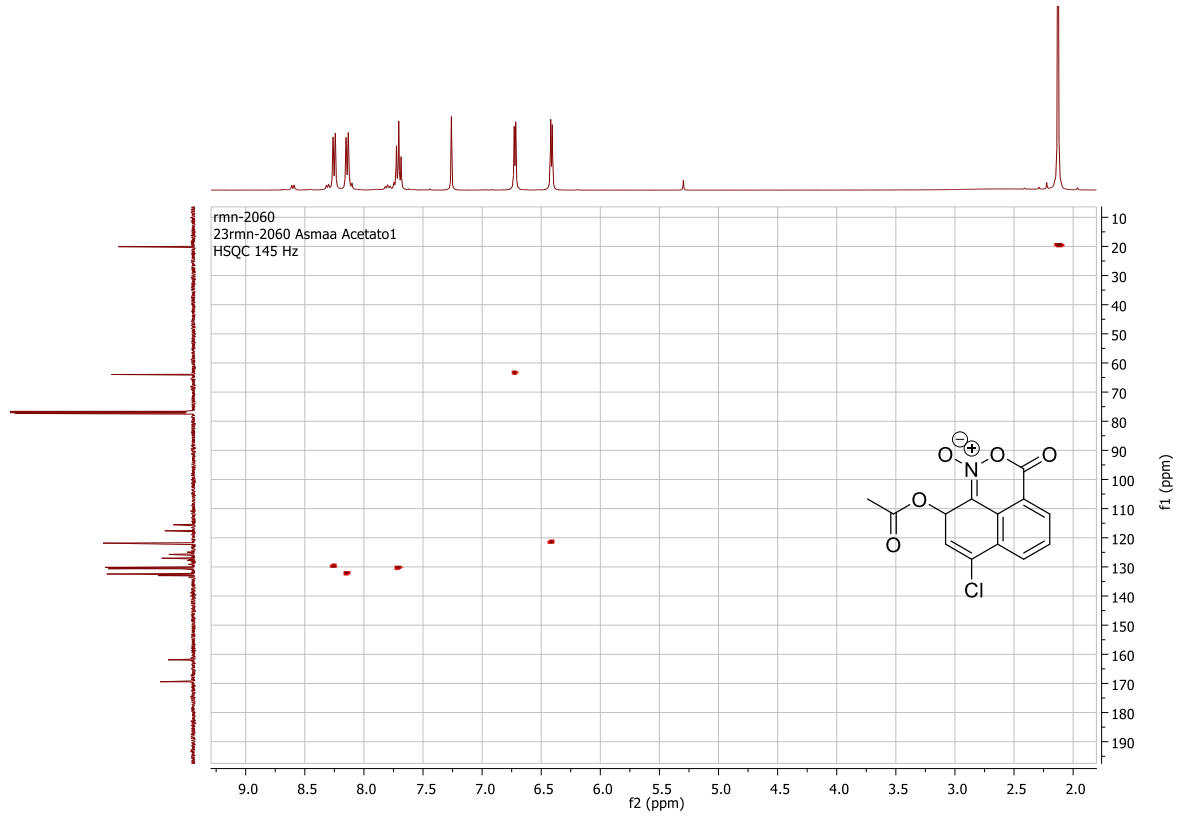


Figure S20. *HSQC 145 Hz spectrum of compound **12** in $CDCl_3$.*

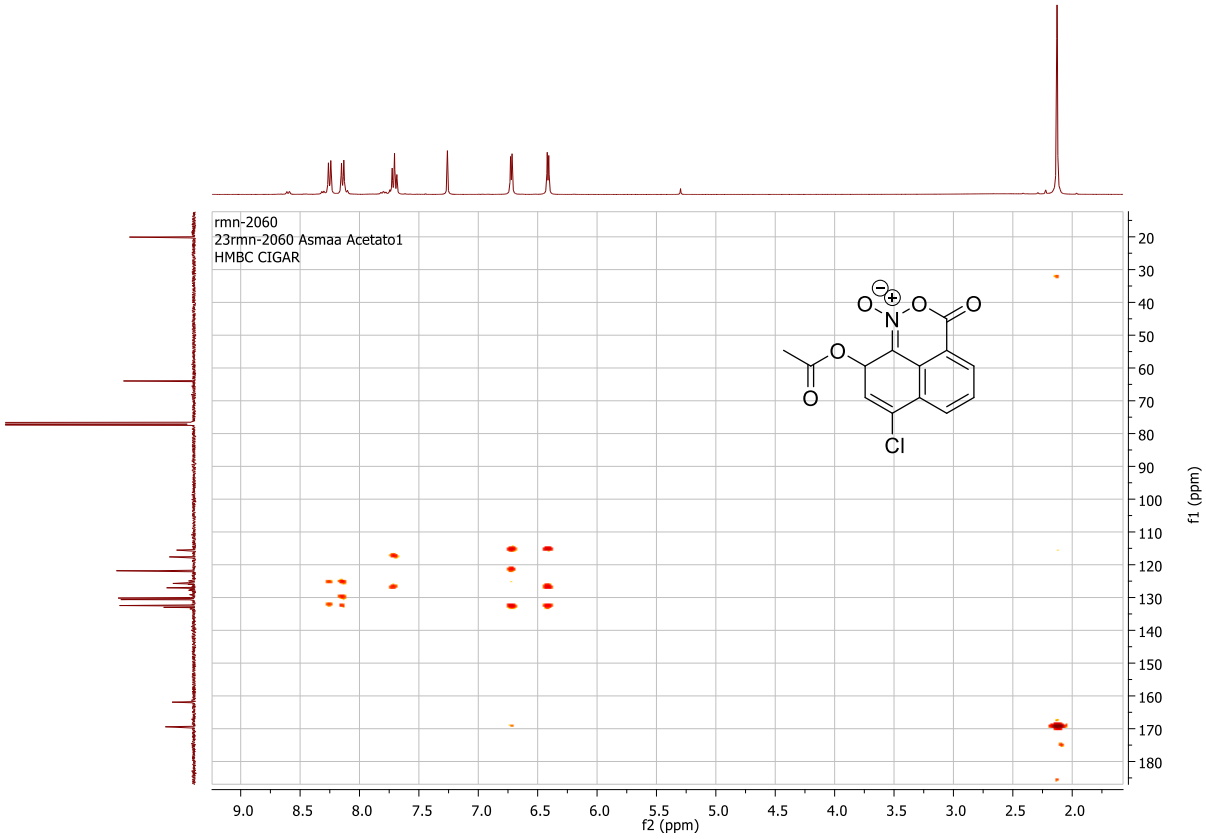


Figure S21. *HBMC CIGAR spectrum of compound **12** in $CDCl_3$.*

6. References

(1) Anderson, J. E.; Cooksey, C. J. Peri-Interactions in Naphthalene Derivatives. Rotation in 1,8-Disubstituted Naphthalenes. *J. Chem. Soc., Chem. Commun.* **1975**, No. 23, 942–943. https://doi.org/10.1039/C39750000942.

(2) Schweizer, W. B.; Procter, G.; Kaftory, M.; Dunitz, J. D. Structural Studies of 1,8-Disubstituted Naphthalenes as Probes for Nucleophile-Electrophile Interactions. *Helv. Chim. Acta* **1978**, *61* (8), 2783–2808. https://doi.org/10.1002/hlca.19780610806.

(3) Bristow, J. C.; Leslie, R.; Wallis, J. D. Incipient Nucleophilic Attack on a Carbonyl Group Adjacent to a Stereogenic Centre in Peri Naphthalene Derivatives. *Helv. Chim. Acta* **2023**, *106* (6), e202300021. https://doi.org/10.1002/hlca.202300021.

(4) Bristow, J. C.; Cliff, S. V. A.; Yang, S.; Wallis, J. D. Interaction, bond formation or reaction between a dimethylamino group and an adjacent alkene or aldehyde group in aromatic systems controlled by remote molecular constraints. *Cryst.Eng.Comm.* **2021**, *23*, 4500-4512; https://doi.org/10.1039/D1CE00377A

(5) Bristow, J. C.; Naftalin, I.; Cliff, S. V. A.; Yang, S.; Carravetta, M.; Heinmaa, I.; Stern, R.; Wallis, J. D. Modelling of an aza-Michael reaction from crystalline naphthalene derivatives containing peri–peri interactions: very long N–C bonds? *Cryst.Eng.Comm.* **2020**, *22*, 6783-6795; https://doi.org/10.1039/D0CE01137A.

(6) Saritemur, G.; Miralles, L. N.; Husson, D.; Pitak, M. B.; Coles, S. J.; Wallis, J. D. Two modes of peri-interaction between an aldehyde group and a carboxylate anion in naphthalaldehydate salts. *Cryst.Eng.Comm.* **2016**, *18*, 948-961; https://doi.org/10.1039/C5CE02282G.

(7) Mercadal, N.; Day, S. P. Day, S. P.; Jarmyn, A.; Pitak, M. B.; Coles, S. J.; Wilson, C.; Rees, G. J.; Hanna, J. V.; Wallis, J. D. O- vs. N-protonation of 1-dimethylaminonaphthalene-8-ketones: for-mation of a peri N–C bond or a hydrogen bond to the pi-electron density of a carbonyl group. *CrystEngComm.,* **2014**, *16*, 8363-8374. https://doi.org/10.1039/C4CE00981A.

(8) Lari, A.; Pitak, M. B.; Coles, S. J.; Rees, G. J.; Day, S. P.; Smith, M. E.; Hanna, V. J.; Wallis, J. D. Models for incomplete nucleophilic attack on a protonated carbonyl group and electron-deficient alkenes: salts and zwitterions from 1-dimethylamino-naphthalene-8-carbaldehyde. *Org. Biomol. Chem.* **2012**, *10*, 7763-7779. https://doi.org/10.1039/C2OB25929J.

(9) Wannebroucq, A.; Jarmyn, A. P.; Pitak, M. B.; Coles, S. J.; Wallis, J. D. Reactions and Interactions Between Peri Groups in 1- Dimethylamino-Naphthalene Salts: An Example of a "Through Space" Amide. *Pure Appl. Chem.* **2016**, *88*, 317−331. https://doi.org/10.1515/pac-2015-1103.

(10) Priestap, H. A.; Barbieri, M. A.; Johnson, F. Aristoxazole Analogues. Conversion of 8-Nitro-1-naphthoic Acid to 2-Methylnaphtho[1,2-d]oxazole-9-carboxylic Acid: Comments on the Chemical Mechanism of Formation of DNA Adducts by the Aristolochic Acids. *J. Nat. Prod.* **2012**, *75*, 1414–1418. https://doi.org/10.1021/np300137f.

(11) Ozeryanskii, V. A.; Pozharskii, A. F.; Antonov, A. S.; Filarowski, A. Out-Basicity of 1,8-Bis(Dimethylamino)Naphthalene: The Experimental and Theoretical Challenge. *Org. Biomol. Chem.* **2014**, *12* (15), 2360–2369. https://doi.org/10.1039/C3OB41986J.

(12) Kazim, M.; Siegler, M. A.; Lectka, T. Close Amide NH···F Hydrogen Bonding Interactions in 1,8-Disubstituted Naphthalenes. *J. Org. Chem.* **2020**, *85*, 6195-6200. https://doi.org/10.1021/acs.joc.0c00553.

(13) Reza, A. I.; Iwai, K.; Nishiwaki, N. A Study of the Correlation between the Bulkiness of peri-Substituents and the Distortion of a Naphthalene Ring. *Molecules* **2023**, 28, 5343. https://doi.org/10.3390/molecules28145343.

(14) Iwai, K.; Nishiwaki, N. Unsymmetrization of 1,8-Dibromonaphthalenes by Acid-Induced Halogen Dance Reaction. *J. Org. Chem.* **2024**, *89*, 7843–7847 https://doi.org/10.1021/acs.joc.4c00507.

(15) Repine, J. T.; Johnson, D. S.; White, A. D.; Favor, D. A.; Stier, M. A.; Yip, J.; Rankin, T.; Ding, Q.; Maiti, S. N. Synthesis of Monofluorinated 1-(Naphthalen-1-Yl)Piperazines. *Tetrahedron Lett.* **2007**, *48* (31), 5539–5541. https://doi.org/10.1016/j.tetlet.2007.05.156.

(16) Bauer, L.; Miarka, S. V. The Chemistry of N-Hydroxyphthalimide. *J. Am. Chem. Soc.* **1957**, *79* (8), 1983–1985. https://doi.org/10.1021/ja01565a061.

(17) Ames, D. E.; Grey, T. F. The Synthesis of Some N-Hydroxyimides. *J. Chem. Soc.* **1955**, 631-636. https://doi.org/10.1039/JR9550000631.

(18) Ames, D. E.; Grey, T. F. N-Hydroxy-imides. Part II. Derivatives of Homophthalic and Phthalic Acids. *J. Chem. Soc.* **1955**, 3518-3521. https://doi.org/10.1039/JR9550003518.

(19) Roderick, W. R.; Brown, W. G. Colorless and Yellow Forms of N-Hydroxyphthalimide. *J. Am. Chem. Soc.* **1957**, *79* (19), 5196–5198. https://doi.org/10.1021/ja01576a033.

(20) Mukaiyama, T.; Hoshino, T. The Reactions of Primary Nitroparaffins with Isocyanates. *J. Am. Chem. Soc.* **1960**, *82*, 5339–5342. https://doi.org/10.1021/ja01505a017.

(21) Kobayashi, S.; Jørgensen, K. A. Cycloaddition Reactions in Organic Synthesis, Wiley-VCH: Weinheim, **2002**. https://doi.org/10.1021/ja01505a017*10.1002/3527600256.*

(22) These numbers should be considered simply as a coincidence: a different choice of an acid-base pair to balance the number of atoms would show different results (for example, the energy would be -35.1 kcal/mol smaller if $H_2PO_4^-/HPO_4^{2-}$ were used to balance the number of atoms); the choice of the $H_3PO_4/H_2PO_4^-$ is more reasonable considering the conditions on which the reactions were carried out -and the amount of HPO_4^{2-} is probably very small in chloroform- but a more realistic model should imply explicitly solvated $H_3PO_4/H_2PO_4^-$ molecules. However, the use of explicit water molecules would make the calculations intractable since the number of conformations to consider would increase exponentially, and the simple model employed in the calculations is able to justify the experiments at least qualitatively.

(23) Armarego, W. L. F.; Perrin, D. D. Purification of Laboratory Chemicals; 3th ed.; Pergamon Press: Oxford, **1988**.

(24) Gottlieb, H. E.; Kotlyar, V.; Nudelman, A. NMR Chemical Shifts of Common Laboratory Solvents as Trace Impurities. *J. Org. Chem.* **1997**, *62*, 7512-7515. https://doi.org/10.1021/jo971176v.

(25) Habib, A.; Garrido-González, J. J.; Sánchez-Santos, E.; del Teso, I. B.; Sanz, F.; Alcázar, V.; Fuentes de Arriba, Á. L.; Morán, J. R. 5-Chloro-8-Nitro-1-Naphthoyl (NNap): A Selective Protective Group for Amines and Amino Acids. *Org. Lett.* **2023**, *25* (22), 4103–4107. https://doi.org/10.1021/acs.orglett.3c01334.

(26) SAINT-NT Version 6.0, Madison, Wisconsin, USA: Bruker–AXS, **2001**.

(27) SADABS 2008/1, Krause, L.; Herbst-Irmer, R.; Sheldrick, G. M.; Stalke. D. Comparison of Silver and Molybdenum Microfocus X-Ray Sources for Single-Crystal Structure Determination. *J. Appl. Crystallogr.* **2015**, *48*, (1), 3-10. https://doi.org/10.1107/S1600576714022985.

(28) (a) SHELXL 2014/4, Sheldrick, G. M. Crystal Structure Refinement with SHELXL. *Acta Cryst. A* **2015**, *71*, 3-8. https://doi.org/10.1107/S2053229614024218; (b) SHELXL 2014/7, Sheldrick, G. M. Integrated Space-Group and Crystal-Structure Determination. *Acta Cryst. A* **2015**, *71*, 3-8. https://doi.org/10.1107/S2053273314026370.

(29) Frisch, M. J.; Trucks, G. W.; Schlegel, H. B.; Scuseria, G. E.; Robb, M. A.; Cheeseman, J. R.; Scalmani, G.; Barone, V.; Petersson, G. A.; Nakatsuji, H.; Li, X.; Caricato, M.; Marenich, A. V.; Bloino, J.; Janesko, B. G.; Gomperts, R.; Mennucci, B.; Hratchian, H. P.; Ortiz, J. V.; Izmaylov, A. F.; Sonnenberg, J. L.; Williams; Ding, F.; Lipparini, F.; Egidi, F.; Goings, J.; Peng, B.; Petrone, A.; Henderson, T.; Ranasinghe, D.; Zakrzewski, V. G.; Gao, J.; Rega, N.; Zheng, G.; Liang, W.; Hada, M.; Ehara, M.; Toyota, K.; Fukuda, R.; Hasegawa, J.; Ishida, M.; Nakajima, T.; Honda, Y.; Kitao, O.; Nakai, H.; Vreven, T.; Throssell, K.; Montgomery Jr, J. A.; Peralta, J. E.; Ogliaro, F.; Bearpark, M. J.; Heyd, J. J.; Brothers, E. N.; Kudin, K. N.; Staroverov, V. N.; Keith, T. A.; Kobayashi, R.; Normand, J.; Raghavachari, K.; Rendell, A. P.; Burant, J. C.; Iyengar, S. S.; Tomasi, J.; Cossi, M.; Millam, J. M.; Klene, M.; Adamo, C.; Cammi, R.; Ochterski, J. W.; Martin, R. L.; Morokuma, K.; Farkas, O.; Foresman, J. B.; Fox, D. J. Gaussian 16 Rev. B.01, Wallingford, CT, **2016**.

(30) Chai, J.-D.; Head-Gordon, M. Long-range corrected hybrid density functionals with damped atom–atom dispersion corrections. *Phys. Chem. Chem. Phys.*, **2008**, *10*, 6615-6620. https://doi.org/10.1039/B810189B.

(31) (a) Hariharan, P. C.; Pople, J. A. Accuracy of AH_n equilibrium geometries by single determinant molecular orbital theory. *Mol. Phys.* **1974**, *27*, 209-214. https://doi.org/10.1080/00268977400100171; (b) Francl, M. M.; Pietro, W. J.; Hehre, W. J.; Binkley, J. S.; DeFrees, D. J.; Pople, J. A.; Gordon, M. S. Self-consistent molecular orbital methods. XXIII. A polarization-type basis set for second-row elements. *J. Chem. Phys.* **1982**, *77*, 3654-3665. https://doi.org/10.1063/1.444267; (c) Binning Jr., R. C.; Curtiss, L. A. Compact contracted basis sets for third-row atoms: Ga–Kr. *J. Comp. Chem.* **1990**, *11* 1206-1216. https://doi.org/10.1002/jcc.540111013; (d) Clark, T.; Chandrasekhar, J.; Spitznagel, G. W.; Schleyer, P. v. R. Efficient diffuse function-augmented basis sets for anion calculations. III. The 3-21+G basis set for first-row elements, Li–F. *J. Comp. Chem.* **1983**, *4*, 294-301. https://doi.org/10.1002/jcc.540040303.

(32) Marenich, A. V.; Cramer, C. J.; Truhlar, D. G. Universal Solvation Model Based on Solute Electron Density and on a Continuum Model of the Solvent Defined by the Bulk Dielectric Constant and Atomic Surface Tensions. *J. Phys. Chem. B* **2009**, *113*, 6378-6396. https://doi.org/10.1021/jp810292n.

(33) Grimme, S. Supramolecular Binding Thermodynamics by Dispersion-Corrected Density Functional Theory. *Chem. Eur. J.* **2012**, *18*, 9955–9964. https://doi.org/10.1002/chem.201200497.

(34) https://github.com/patonlab/GoodVibes

OL Organic Letters

pubs.acs.org/OrgLett

Letter

5-Chloro-8-nitro-1-naphthoyl (NNap): A Selective Protective Group for Amines and Amino Acids

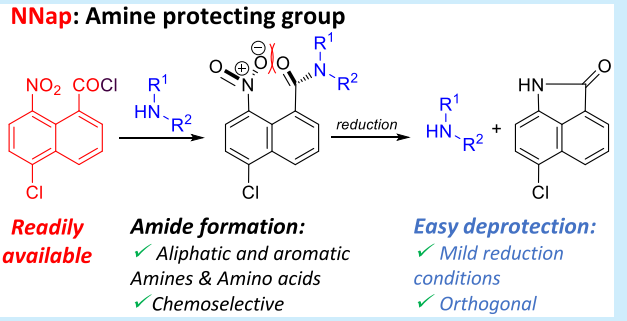
Asmaa Habib, José J. Garrido-González, Estela Sánchez-Santos, Irene Boya del Teso, Francisca Sanz, Victoria Alcázar,* Ángel L. Fuentes de Arriba, and Joaquín R. Morán*

Cite This: *Org. Lett.* 2023, 25, 4103–4107

Read Online

ACCESS | Metrics & More | Article Recommendations | Supporting Information

ABSTRACT: The synthesis of 5-chloro-8-nitro-1-naphthoyl chloride and its use as a protective group for amines is described. Protection is carried out with an auxiliary amine or under mild Schotten-Baumann conditions in high yield (>86%), while deprotection can be achieved easily under gentle reducing conditions due to the large steric tension between C-1 and C-8 naphthalene substituents. The reaction has been successfully tested in dipeptide synthesis and amino alcohols protection, and it has proved selective for the ε-amine group of lysine.



Downloaded via UNIV DE SALAMANCA on March 26, 2024 at 12:30:08 (UTC).
See https://pubs.acs.org/sharingguidelines for options on how to legitimately share published articles.

The protection of amino groups is a highly studied synthetic strategy.[1] Nevertheless the complexity of organic synthesis usually requires several different protecting groups with orthogonal properties, and therefore, new amine protective groups are welcome.

Amides are very stable functional groups, and thus, cleavage of the amide bonds usually requires strong acid or base-catalyzed hydrolysis to release the amines. To overcome this problem a popular solution is to use carbamates as the amine protecting groups.[2] Release of CO_2 is the main driving force of the deprotection reaction, which favors liberation of the amine. However, carbamates also present some drawbacks, such as their high toxicity or the presence of two different conformations, which, in many cases, might complicate the NMR spectra. Besides, chlorocarbonates are also unstable compounds which can decompose with generation of CO_2, creating high pressure inside the vessel that can lead to explosions.

In this paper we explore an alternative solution which implies the formation of a sterically stressed amide that can be later deprotected under unusual mild reductive conditions based on a strong release of steric strain. The protective group is the 5-chloro-8-nitro-1-naphthoyl (NNap) that can be introduced as an acid chloride under standard or Schotten-Baumann conditions[3] affording the corresponding amides in high yield (Table 1).

The large steric strain in 1,8-disubstituted naphthalenes is well-known,[4] and this steric strain is usually relieved by bond bending with the substituents twisted out of the plane of the aromatic rings. Thus, 1,8-bis(dimethylamino)naphthalene (pK_a = 12.1)[5] is a stronger base than dimethylaniline (pK_a = 5.15), because protonation reduces the electrostatic and steric strain

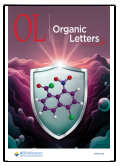
Table 1. Acylation of Amines with 5-Chloro-8-nitro-1-naphthoyl chloride 4 (NNapCl)[a]

entry	amine	amide (%)[b]
1	*n*-octylamine (**5**)	**12** (86%)
2	*n*-decylamine (**6**)	**13** (95%)
3	benzylamine (**7**)	**14** (87%)
4	*tert*-octylamine (**8**)	**15** (90%)
5	di-*n*-butylamine (**9**)	**16** (87%)
6	4-*tert*-butylaniline (**10**)	**17** (91%)
7	(1*S*,2*S*)-(+)-*trans*-1-amino-2-indanol (**11**)	**18** (86%)

[a]Reaction conditions: amine (1 equiv) in CH_2Cl_2 was added dropwise to a solution of the acid chloride NNapCl, **4** (1.0 equiv) in CH_2Cl_2 at 0 °C. After stirring 5 min, an aqueous Na_2CO_3 (5.0 equiv) solution was added and the mixture was allowed to warm to rt, stirring for an additional 25 min. [b]Isolated yields.

(Figure 1A). The X-ray crystal structure of 8-(dimethylamino)-1-naphthyl methyl ketone[6] illustrates the Burgi-Dünitz trajectory in which the combination of the steric compression and the bonding interaction between the lone pair of the amine and the carbonyl group deforms the molecule (Figure 1B).[7] Another example is the high reactivity of 8-dimethylamino-1-naphthaldehyde, in which treatment with benzoyl chloride[8] leads to benzoylation of the aldehyde oxygen and addition of

Received: April 23, 2023
Published: May 26, 2023



ACS Publications

© 2023 The Authors. Published by American Chemical Society

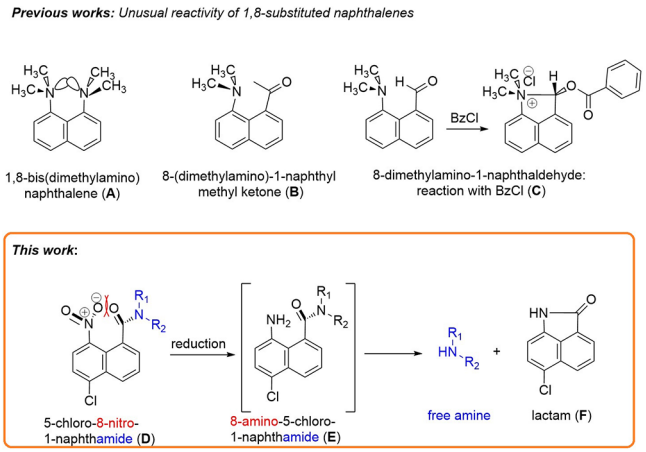


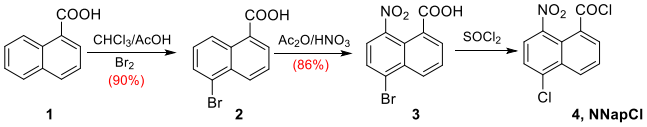
Figure 1. Unusual reactivity of some 1,8-substituted naphthalenes and sterically hindered amides synthesized in this work.

the *peri*-dimethylamino group to the former carbonyl group, setting a new N−C bond (Figure 1C).

In our case and in a similar way, reduction of the 8-nitro group to amine (**E**) leads to a decrease in the steric strain, due to the formation of a N−C bond between the *peri* substituents, the amine nitrogen at C-8, and the amide carbonyl group at C-1. Thus, formation of the five-membered lactam (**F**) is accompanied by release of the protected amine (Figure 1).

The preparation of the protecting group started from the commercially available 1-naphthoic acid **1** (Scheme 1). Direct

Scheme 1. Synthesis of the Protective Group (NNapCl)



nitration of this compound takes place in the C-5 position; therefore, previous bromination was carried out to block this position. Nitration in acetic anhydride using *p*-TsOH as catalyst yielded a clean reaction in the expected C-8 position. Treatment of the acid **3** with thionyl chloride afforded the acid chloride **4** with concomitant halogen exchange. The replacement of bromine by chlorine was experimentally confirmed: hydrolysis of the acid chloride **4** with water produced a carboxylic acid (**3a**), whose spectral properties (NMR and MS) showed that chlorine had replaced the C-5 bromine.

Both the carboxylic acid **3** and its potassium salt are highly crystalline compounds. Slow evaporation of an aqueous equimolar solution of potassium hydroxide and the acid **3** allowed us to obtain high-quality crystals suitable for X-ray diffraction analysis. The structure shows a strong steric interaction between substituents at C-1 and C-8 positions that are placed outside the plane of the naphthalene ring with torsion angles of 40°−48° (Figure 2).

Amine protection was carried out under Schotten-Baumann conditions in a two-phase reaction using methylene chloride and aqueous sodium carbonate solution; easy workup using liquid−liquid extraction was enough to obtain the amides (**D**) with high purity, and usually no chromatography was needed. Thus, reaction of the amine with 1.0 equiv of the acyl chloride **4** and in the presence of Na_2CO_3 (5.0 equiv) afforded the corresponding amide in good to excellent yields (Table 1,

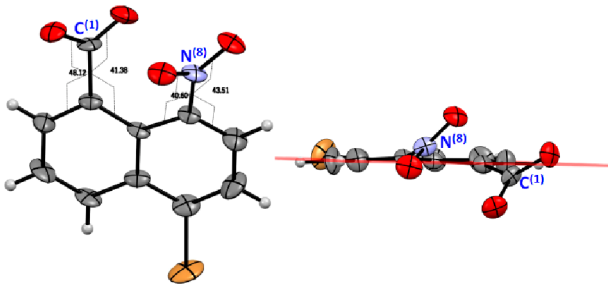


Figure 2. ORTEP diagram of the potassium salt of the carboxylic acid **3**. K^+ counterion and a crystallization water molecule have been omitted for clarity.

entries 1−6). Primary and secondary amines were tested: *n*-octylamine (**5**), *n*-decylamine (**6**), and benzylamine (**7**) afforded, in 30 min, a quantitative NMR yield of the desired amides (86−95% isolated yields). The more hindered primary amine *tert*-octylamine (**8**) and the secondary amine di-*n*-butylamine (**9**) also gave the corresponding amides in high yields (87−90% isolated yields). To further explore the substrate scope, an aromatic amine, 4-*tert*-butylaniline (**10**), was tested; as shown in Table 1 (entry 6), the aniline **10** was easily transformed to the target amide in 91% isolated yield under the same reaction conditions.

Pleasingly, single crystals of the amide **17** were obtained by slow evaporation of a methanol solution. The X-ray structure showed the same features as those of the potassium salt of acid **3**; the nitro and amide groups are twisted from the plane of the naphthalene ring, lying on opposite sides of the plane. Additionally, the replacement of bromine by chlorine at the C-5 position was corroborated (Figure 3).

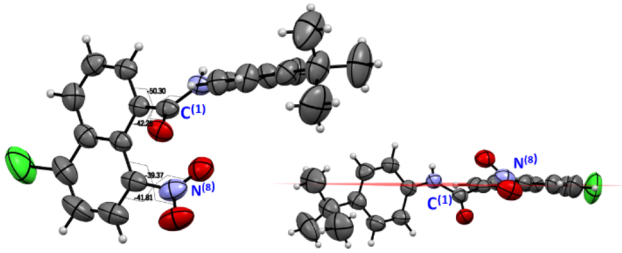


Figure 3. ORTEP diagram of amide **17**. The crystallization methanol molecule has been omitted for clarity.

Removal of the protecting group was studied using a variety of reducing conditions with amide **16** as model substrate (Table 2). The reduction of the nitro group is a widely used transformation, and many methods are available.[9] In our case, due to the unique reactivity of the *peri*-disubstituted naphthalenes, the reduction of the nitro group occurs under mild conditions producing cleanly the desired amine in high yields, along with the expected lactam **F**. Although our attempts to grow single crystals of the lactam **F** were not

Table 2. Removal of the Protecting Group

entry	conditions	yield of 9 (%)[a]
1	Zn/AcOH; 60 °C, 10 min	95%
2	$SnCl_2$/MeOH; 60 °C, 10 min	80%
3	H_2/Pd (C)/AcOEt; 20 °C, 12 h	90%

[a]Isolated yields.

https://doi.org/10.1021/acs.orglett.3c01334
Org. Lett. 2023, 25, 4103−4107

successful, the crystal structure of the closely related 1,8-naphtholactam is known.[10] The steric hindrance between *peri* positions in compounds **3** and **16**, twisted on either side of the naphthalene plane, is no longer present in the 1,8-naphtholactam, which possesses a nearly absolute planar configuration.

The best results in the reduction reaction were obtained using Zn/AcOH (Table 2, entry 1): a solution of the amide **16** in acetic acid was added to a preheated suspension of Zn in acetic acid affording di-*n*-butylamine **9** in 95% yield and lactam **F**.

The progress of the reduction could be monitored in an NMR tube (Figure 4). Starting from the 5-chloro-8-nitro-1-

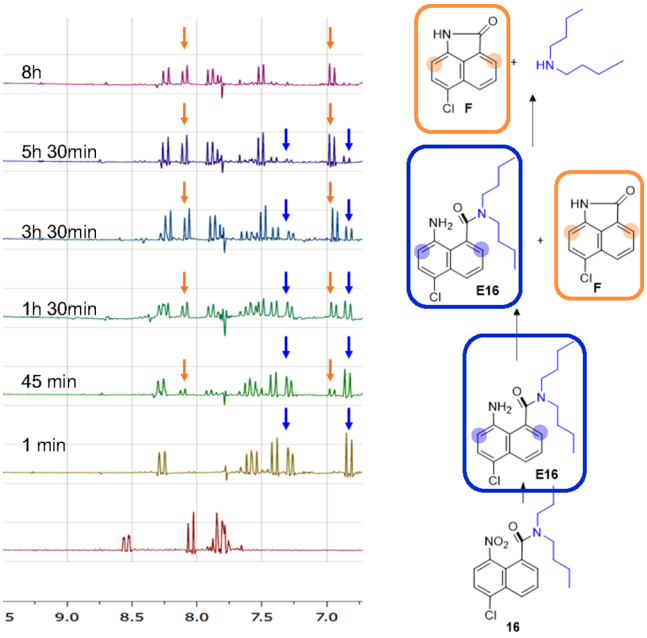


Figure 4. ^{1}H NMR spectra (aromatic region) of the progress of the reduction of amide **16** with Zn/AcOH: from the intermediate amine **E16** to the lactam **F**. Reaction conditions: amide **16** (10.0 mg), Zn (80.0 mg), and acetic acid (20 mg) were dissolved in 1.0 mL of CD_3OD at 20 °C.

naphthamide **16** (spectrum at the bottom), nitro group reduction to amine (**E16**) took place immediately following mixing (second spectrum from the bottom); however, in these dilute conditions (CD_3OD as solvent), intramolecular cyclization to lactam **F** required heating in a water bath at 60 °C for several hours. Thus, ^{1}H NMR signals corresponding to both the amine (**E16**) and lactam (**F**) could be easily identified in the different spectra until total conversion was achieved (lactam **F** spectrum at the top).

Attempts to isolate the intermediate aromatic amine (**E16**) were unsuccessful, but when the reaction mixture was treated with acetic anhydride, the amine (**E16**) was trapped as the acetamide (**Ac16**). Interestingly, one of the butyl chains of the acetamide **Ac16** is highly shielded: methyl triplet (4-Bu) at 0.53 ppm, probably because it is over the naphthalene ring (Figure 5). Rotating-frame nuclear Overhauser effect spectroscopy (ROESY) also shows a correlation of the methylene protons (1-Bu and 2-Bu) with the aromatic C-2 proton (7.28 ppm) of the naphthalene ring (Figure 5, inset). The absorption of the C-2 proton at 7.28 ppm is also very unusual, since it is *ortho* to a carboxylic group: the twist of the amide carbonyl

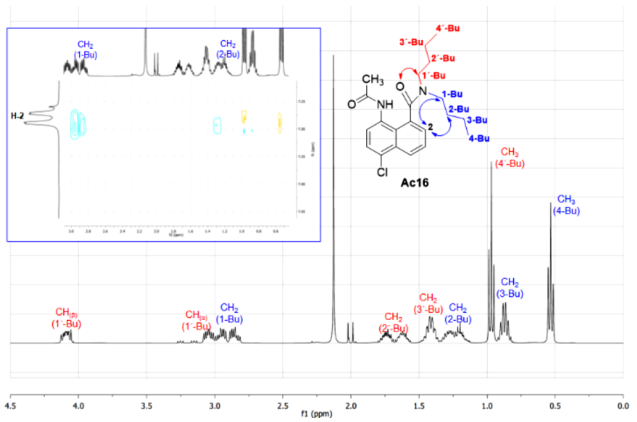


Figure 5. ^{1}H NMR spectra (aliphatic region) of acetamide **Ac16** in $CDCl_3$ at 20 °C and ROESY spectrum (inset) showing correlations between naphthalene C-2 proton and methylenes (1-Bu and 2-Bu).

group from the plane of the aromatic ring explains this unusual shift. On the other hand, one of the methylene protons of the other butyl chain (1′-Bu) is strongly deshielded (4.10 ppm) due to the proximity with the amide carbonyl group. These effects show a rigid conformation in this part of the molecule, probably due to an angular H-bond between the acetamide and the amide carbonyl group (Figure 5). Two-dimensional (2D) NMR spectra and molecular modeling studies allowed us to propose a possible geometry for the molecule with one butyl chain pointing toward the shielding zone of the naphthalene ring. A similar effect was observed for the nonacetylated compound, the amine **E16**.

Having optimized the reaction conditions, we explored the scope of the deprotection step with amides **12** (*n*-octylamide), **15** (*tert*-octylamide), and **17** (4-*tert*-butylanilide); in all cases, deprotection proceeded in excellent yields (>90%).

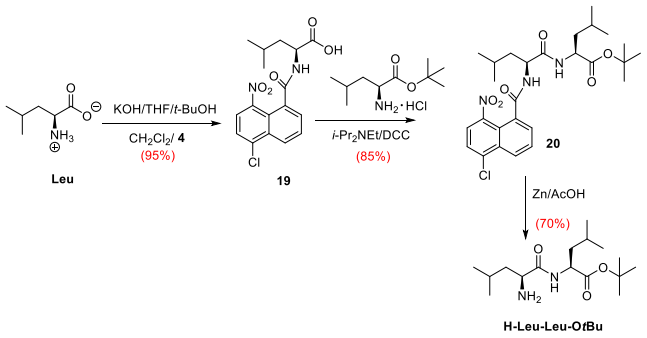
Finally, deprotection was tested using a reducing agent which mimics the physiological NADPH. Hantzsch ester reduced successfully the nitro group of amide **12** in the presence of eosin Y under 40 W white light irradiation. While the amine **5** (70% yield) is nicely liberated from the protecting group, surprisingly the lactam **F** was not obtained. Analysis of the reaction products showed 8-amino-5-chloro-1-naphthoic acid as the main product. Since this is not the expected compound the structure was confirmed through comparison with a synthesized compound obtained from the reduction of the nitroderivative **3a** under basic conditions.

As the protection of the amino functionality plays an essential role in peptide synthesis, we explored the utility of the NNap protective group in the synthesis of L-leucyl-L-leucine. Hence, L-leucine was first reacted with NNapCl **4** affording amide **19** in high yield (Scheme 2). The synthesis of the dipeptide **20** was completed by *i*-Pr_2NEt/DCC mediated coupling between H-Leu-O*t*Bu·HCl and **19** (Scheme 2). No racemization was observed.

One of the main challenges in peptide synthesis is related to selective protection of the ε- and α-amino groups of L-lysine.[11] Common protective groups such as benzyloxycarbonyl (Cbz) or fluorenylmethoxycarbonyl (Fmoc) are not selective, and protection of the ε-amino lysine usually requires blocking the α-amino group using copper salts.[12] Likewise, benzyloxycarbonylation of the α-amino group involves temporary blocking of the ε-amino by condensation with benzaldehyde.[13] These procedures are time-consuming and imply the use of additional

https://doi.org/10.1021/acs.orglett.3c01334
Org. Lett. 2023, 25, 4103−4107

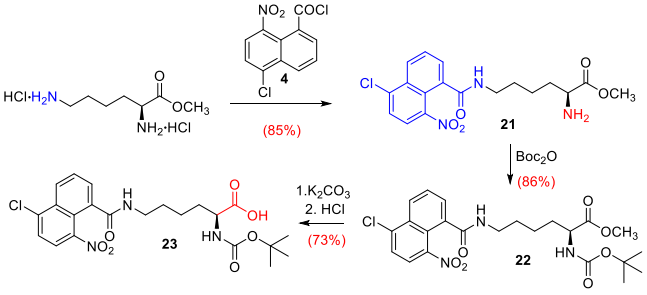
Scheme 2. Application to H-Leu-Leu-O*t*Bu Synthesis



reagents, so the development of new methods for orthogonal selective protection of the amino groups of lysine is highly desirable. A supramolecular approach using cyclodextrins (β-CDs) has shown strong regioselectivity and good yields in the Cbz protection of the ε- and α-amino groups.[14] The reaction has been performed on 1 mmol scale (1 mmol Lys; 0.1 mmol β-CD), and its selectivity appears to be limited to the Cbz group and the β-CD.

Prompted by our previous results, we explored the reaction with lysine; and after finding the optimal conditions, to our delight, treatment of the L-lysine methyl ester dihydrochloride (H-Lys-OMe 2HCl) with NNapCl **4** resulted in selective and high yield protection of the ε-amino group (Scheme 3).

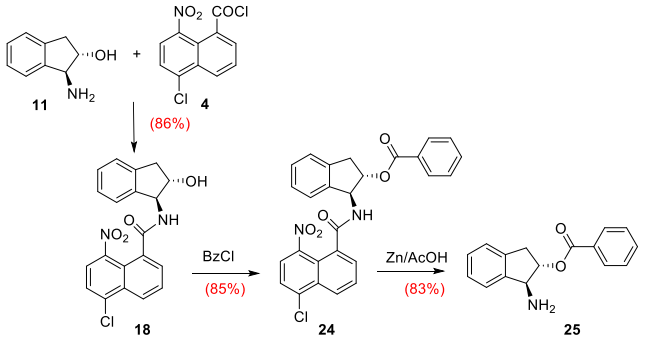
Scheme 3. Application to Orthogonal Protection of L-Lysine



The observed regioselectivity in favor of the ε-amino group yielding compound **21** might be justified by the highly sterically hindered naphthoyl chloride **4**. The amino ester **21** was amenable to further synthetic elaborations, such as protection of the α-amino group (**22**) or hydrolysis to carboxylic acid (**23**). Applying the strategy of orthogonal functional group protection, the free α-amino group was acylated with Boc_2O to afford **22** in good yield. Finally, the deprotected acid **23** was obtained by hydrolysis of the methyl ester under extremely mild conditions: aqueous potassium carbonate in methanol at room temperature. No sign of racemization was observed.

A further example showing the potential of this protecting group is demonstrated using indanolamines. First, indanolamine **11** was chemoselectively protected by treatment with NNapCl **4** (Table 1, entry 7), and next, the less nucleophilic hydroxyl group was esterified with benzoyl chloride. Finally, compound **24** was reacted with Zn/AcOH, and the amine functionality was deprotected without affecting the more sensitive ester group. No transposition to the amino group, neither racemization, was observed in compound **25** (Scheme 4).

Scheme 4. Application to Indanolamines



In conclusion, we have developed a readily available and efficient protective group for amines, the 5-chloro-8-nitro-1-naphthoyl (NNap). The steric hindrance between *peri* positions in the naphthalene ring allows deprotection under mild reduction conditions and selectivity in the case of lysine. This protective group is also suitable for aminoalcohols. The yields of the protection and deprotection steps are excellent, and both reactions proceed under mild reaction conditions. These promising results suggest that this new protective group has great potential to be further developed and included as an alternative for amine protection.

■ ASSOCIATED CONTENT

Data Availability Statement

The data underlying this study are available in the published article and its Supporting Information.

Supporting Information

The Supporting Information is available free of charge at https://pubs.acs.org/doi/10.1021/acs.orglett.3c01334.

Complete experimental procedures and characterization data for compounds, including ^1H, ^{13}C, 2D NMR, X-ray crystal analysis, and modeling studies (PDF)

Accession Codes

CCDC 2252216 and 2252212 contains the supplementary crystallographic data for this paper. These data can be obtained free of charge via www.ccdc.cam.ac.uk/data_request/cif, or by emailing data_request@ccdc.cam.ac.uk, or by contacting The Cambridge Crystallographic Data Centre, 12 Union Road, Cambridge CB2 1EZ, UK; fax: + 44 1223 336033.

■ AUTHOR INFORMATION

Corresponding Authors

Victoria Alcázar − *Environmental and Industrial Chemical Engineering Department, Polytechnic University of Madrid, Madrid 28006, Spain*; Email: mariavictoria.alcazar@upm.es

Joaquín R. Morán − *Organic Chemistry Department, University of Salamanca, Salamanca 37008, Spain*; Email: romoran@usal.es

Authors

Asmaa Habib − *Organic Chemistry Department, University of Salamanca, Salamanca 37008, Spain*

José J. Garrido-González − *Organic Chemistry Department, University of Salamanca, Salamanca 37008, Spain*

Estela Sánchez-Santos − *Organic Chemistry Department, University of Salamanca, Salamanca 37008, Spain*

https://doi.org/10.1021/acs.orglett.3c01334
Org. Lett. 2023, 25, 4103−4107

Irene Boya del Teso − *Organic Chemistry Department, University of Salamanca, Salamanca 37008, Spain*
Francisca Sanz − *X-Ray Diffraction Service, University of Salamanca, Salamanca 37008, Spain*
Ángel L. Fuentes de Arriba − *Organic Chemistry Department, University of Salamanca, Salamanca 37008, Spain*

Complete contact information is available at: https://pubs.acs.org/10.1021/acs.orglett.3c01334

Author Contributions

All authors have given approval to the final version of the manuscript.

Notes

The authors declare no competing financial interest.

■ ACKNOWLEDGMENTS

This work was supported by MICINN PID2020-118732RA-I00. J.J.G.-G. acknowledges support from the Margarita Salas postdoctoral grant. E.S.S. gratefully acknowledges University of Salamanca and Santander Bank for a predoctoral fellowship. A.H. is grateful to the Algerian Government for predoctoral fellowship for "Formation Doctorale résidentielle l'etranger". We also thank NUCLEUS platform at University of Salamanca, especially Anna Lithgow (NMR Service), César Raposo, Juan F. Boyero-Benito (MS Service), and José M. Compaña (X-ray Service).

■ REFERENCES

(1) (a) Wuts, P. G. M. *Greene's Protective Groups in Organic Synthesis,* 5th ed.; Wiley: NJ, 2014; p 895. (b) Kocieński, P. J. *Protecting Groups,* 3rd ed.; Georg Thieme Verlag: Stuttgart, NY, **2005**; p 488. (c) Omprakash Rathi, J.; Subray Shankarling, G. Recent Advances in the Protection of Amine Functionality: A Review. *ChemistrySelect* **2020**, *5*, 6861−6893. (d) Isidro-Llobet, A.; Álvarez, M.; Albericio, F. Amino Acid-Protecting Groups. *Chem. Rev.* **2009**, *109*, 2455−2504.
(2) (a) Ragnarsson, U.; Grehn, L. Dual Protection of Amino Functions Involving Boc. *RSC Adv.* **2013**, *3*, 18691−18697. (b) Shahsavari, S.; McNamara, C.; Sylvester, M.; Bromley, E.; Joslin, S.; Lu, B. Y.; Fang, S. An Amine Protecting Group Deprotectable Under Nearly Neutral Oxidative Conditions. *Beilstein J. Org. Chem.* **2018**, *14*, 1750−1757.
(3) Sonntag, N. O. V. The Reactions of Aliphatic Acid Chlorides. *Chem. Rev.* **1953**, *52*, 237−401. and references cited herein.
(4) (a) Antonov, A. S.; Tupikina, E. Y.; Karpov, V. V.; Mulloyarova, V. V.; Bardakov, V. G. Sterically Facilitated Intramolecular Nucleophilic NMe_2 Group Substitution in the Synthesis of Fused Isoxazoles: Theoretical Study. *Molecules* **2020**, *25*, 5977. (b) Saritemur, G.; Nomen Miralles, L.; Husson, D.; Pitak, M. B.; Coles, S. J.; Wallis, J. D. Two Modes of Peri-Interaction Between an Aldehyde Group and a Carboxylate Anion in Naphthalaldehydate Salts. *CrystEngComm* **2016**, *18*, 948−961. (c) Kirby, A. J.; Percy, J. M. Synthesis of 8-Substituted 1 -Naphthylamine Derivatives. Exceptional Reactivity of the Substituents. *Tetrahedron* **1988**, *44*, 6903−6910. (d) Robert, J.-B.; Sherfinski, J. S.; Marsh, R. E.; Roberts, J. D. 1,8 Interactions in Naphthalene Derivatives. An X-Ray Structure Determination and Nuclear Magnetic Resonance Studies of 1,8-Di(Bromomethy1)Naphthalene. *J. Org. Chem.* **1974**, *39*, 1152−1156.
(5) Ozeryanskii, V. A.; Pozharskii, A. F.; Antonov, A. S.; Filarowski, A. Out-Basicity of 1,8-Bis(Dimethylamino)- Naphthalene: The Experimental and Theoretical Challenge. *Org. Biomol. Chem.* **2014**, *12*, 2360−2369.
(6) Schweizer, W. B.; Procter, G.; Kaftory, M.; Dunitz, J. D. Structural Studies of 1,8-Disubstituted Naphthalenes as Probes for Nucleophile-Electrophile Interactions. *Helv. Chim. Acta* **1978**, *61*, 2783−2808.
(7) (a) Bürgi, H.B.; Dunitz, J.D.; Lehn, J.M.; Wipff, G. Stereochemistry of Reaction Paths at Carbonyl Centres. *Tetrahedron* **1974**, *30*, 1563−1572. (b) Burgi, H. B.; Dunitz, J. D.; Shefter, E. Geometrical Reaction Coordinates II. Nucleophilic Addition to a Carbonyl Group. *J. Am. Chem. Soc.* **1973**, *95*, 5065−5067.
(8) Wannebroucq, A.; Jarmyn, A. P.; Pitak, M. B.; Coles, S. J.; Wallis, J. D. Reactions and Interactions Between *Peri* Groups in 1-Dimethylamino-Naphthalene Salts: An Example of a "Through Space" Amide. *Pure Appl. Chem.* **2016**, *88*, 317−331.
(9) Orlandi, M.; Brenna, D.; Harms, R.; Jost, S.; Benaglia, M. Recent Developments in the Reduction of Aromatic and Aliphatic Nitro Compounds to Amines. *Org. Process Res. Dev.* **2018**, *22*, 430−445.
(10) Zhou, C.; Wang, M.; Guo, W.; Ye, G.; Wang, Y.; Yang, Y.; Xia, G.; Wang, H. Lactam node as a two-fold functional unit for achieving highly efficient and tunable dual-state emitters. *Dyes Pigment* **2023**, *213*, 111198 CCDC number 2046895..
(11) Su, J.; Sheng, X.; Li, S.; Sun, T.; Liu, G.; Hao, A. Effective regioselective protection of amino groups of lysine achieved by a supramolecular enzyme-mimic approach. *Org. Biomol. Chem.* **2012**, *10*, 9319−9324. and references cited herein.
(12) (a) Pícha, J.; Buděšínský, M.; Macháčková, K.; Collinsová, M.; Jiráček, J. Optimized syntheses of Fmoc azido amino acids for the preparation of azidopeptides. *J. Pept. Sci.* **2017**, *23*, 202−214. (b) Wiejak, S.; Masiukiewicz, E.; Rzeszotarska, B. Large Scale Synthesis of Mono- and Di-urethane Derivatives of Lysine. *Chem. Pharm. Bull.* **1999**, *47*, 1489−1490. (c) Albericio, F.; Nicolás, E.; Rizo, J.; Ruiz-Gayo, M.; Pedroso, E.; Giralt, E. Convenient syntheses of fluorenylmethyl-based side chain derivatives of glutamic and aspartic acids, lysine, and cysteine. *Synthesis* **1990**, *1990*, 119−122.
(13) Scott, J. W.; Parker, D.; Parrish, D. R. Syntheses of N^{ε} -Tert-butyloxycarbonyl-L-lysine and N^{α}-Benzyloxycarbonyl-N^{ε} -tertbutyloxycarbonyl-L-lysine. *Synth. Commun.* **1981**, *11*, 303−314.
(14) Su, J.; Sheng, X.; Li, S.; Sun, T.; Liu, G.; Hao, A. Effective regioselective protection of amino groups of lysine achieved by a supramolecular enzyme-mimic approach. *Org. Biomol. Chem.* **2012**, *10*, 9319−9324.

An unusual rearrangement of a 1,8-naphthalene derivative.

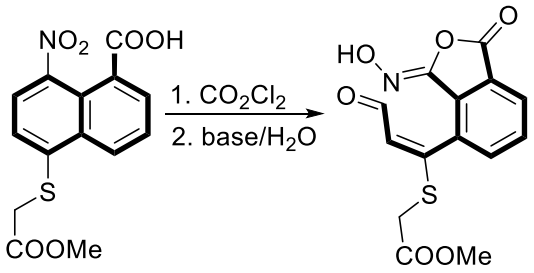
Asmaa Habib,[†] Estela Sánchez-Santos,[†] Irene Boya del Teso,[†] Francisca Sanz,[‡] Luis Simón,*[,‖] Joaquín R. Morán[†], Ángel L. Fuentes de Arriba *[,†]

[†] Organic Chemistry Department, University of Salamanca, Plaza de los Caídos s/n, Salamanca 37008, Spain. E-mail: angelfuentes@usal.es

[‡] X-Ray Diffraction Service, University of Salamanca, Plaza de los Caídos s/n, Salamanca 37008, Spain

[‖] Chemical Engineering Department, University of Salamanca, Plaza de los Caídos s/n, Salamanca 37008. E-mail: lsimon@usal.es

ABSTRACT: The steric strain between nitro- and carboxylic acid groups in a 8-nitro-1-naphthoic acid derivative is able to unexpectedly disrupt the aromaticity of the naphthalene core under mild reaction conditions. The addition of H_2O to the aromatic ring of a highly strained naphtho oxazinium intermediate induces a fragmentation of a Csp^2-Csp^2 bond, with a concomitant rearrangement to yield a conjugated aldehyde. Key intermediates have been characterized and the X-ray structure of a derivative has been obtained. DFT studies have been performed to confirm the proposed mechanism.



Introduction

1,8-napthalene derivatives are strained compounds due to the steric hindrance between substituents in 1,8- positions which produce unusual physical properties. Anderson studied in 1975 that the rotation-barrier energy of some naphthalene derivatives with *peri* interactions strongly depends on the planarity or tetrahedral character of the substituents.[1] In some cases, the short distance between *peri*-substituents facilitates a chemical reaction between them. Dünitz observed that 8-(dimethylamino)-1-naphthylmethyl ketone has the dimethylamino group tilted towards the ketone group to exploit the binding interactions provided by the Burgi-Dünitz trajectory. In this way, a dihedral angle of 116.65° instead of 120° was observed (Figure 1A).[2] This explains the reactivity observed by Wallis in many 1,8-substituted naphthalenes,[3] being one of the most remarkable the reaction between dimethylamino-1-naphthaldehyde with benzoyl chloride which produces the dihydro benzolinium compound shown in Figure 1B.[3e] Recently, Lectka has studied how the NH stretching frequency and the ^1H-^{19}F coupling constants of NH···F interactions are affected in 1,8-disubstituted naphthalenes (Figure 1C).[4] In addition, the strain experienced by the groups in *peri* position produces that some reactions proceed easily due to the activation caused by the steric repulsion. A highlighting example is the reaction reported by Priestap of 8-nitro-1-naphthoic acid which yields a naphthoxazole when treated with Zn and acetic acid (Figure 1D),[5] releasing the steric strain between the groups in 1- and 8- positions. The chemical properties are also strongly influenced, 1,8-bis(dimethylamino) naphthalene (Proton-sponge®) is a stronger base (pK_a=12.1) than the corresponding dimethylaniline (pK_a= 5.1) since amine protonation releases part of the steric strain between the two amino groups (Figure 1E).[6] Recently, Nishiwaki has studied how bulky substituents in *peri* position are able to distort the coplanarity of the naphthalene ring,[7] and affect the isomerization of bromine substituents (Figure 1F).[8]

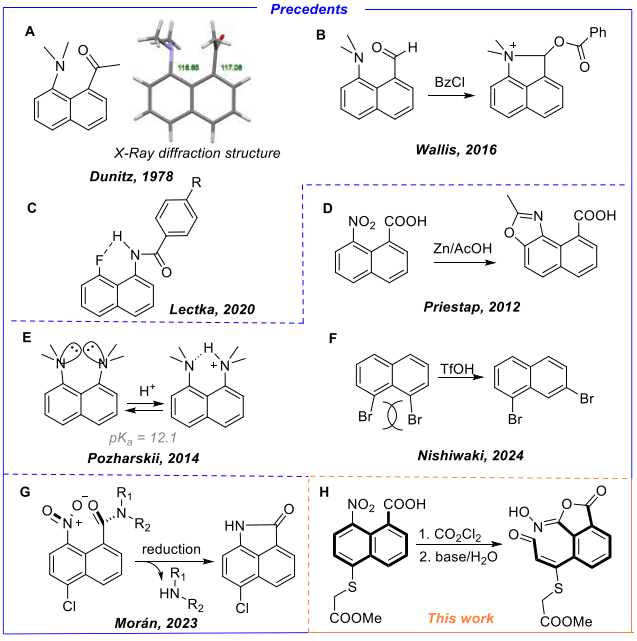


Figure 1. (A-G) Unusual chemical reactivity and physical properties of 1,8-disubstituted naphthalenes. (H) Unexpected rearrangement obtained in this work.

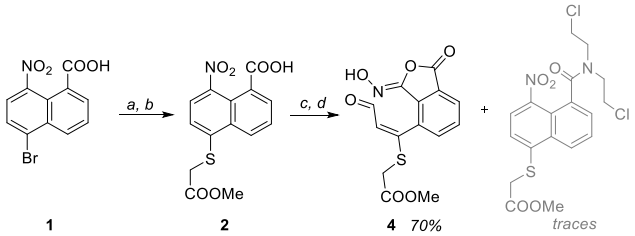
Recently, 5-chloro-8-nitro-1-naphthoyl (NNap) has been proposed by our group as an amine protecting group which easily liberates the amine and generates a lactam (Figure 1G).[9] The nitro- and amide groups suffer steric hindrance, and they are twisted from the naphthalene plane as has been already revealed from X-ray diffraction studies. After the reduction of the nitro- to amino- group, the proximity with the amide facilitates the formation of the lactam with the concomitant release of the amine and the disappearance of the steric tension.

We envisioned that NNap could be used as a drug carrier by anchoring a drug to the carboxylic acid group which could be released under reducing conditions. To overcome solubility issues the chlorine atom in C-5 was substituted by a water soluble moiety. Therefore, a thioglycolic fragment was included in the molecule as shown in Figure 1H. Nevertheless, an attempt to couple the naphthalene fragment with a nitrogenated mustard (a well-known intercrossing DNA molecule) under Schotten-Baumann conditions, led in good yield to an unexpected aldehyde (Figure 1H) with the concomitant fragmentation of the naphthalene ring. Intriguingly, this reaction was not observed when Cl atom was placed in the C-5 position of the naphthalene ring. Herein, we explain how this reaction takes place and propose a mechanism to explain this unusual rearrangement.

Results and Discussion

Compound **1** (Scheme 1) was synthesized following the literature procedure.[9] Then, thioglycolic acid fragment was introduced by nucleophilic aromatic substitution and the carboxylic acid attached to the thioglycolic moiety was selectively esterified with MeOH and $SOCl_2$. The putative acid chloride of compound **2** was prepared dissolving it in oxalyl chloride (see ESI). Then, Schotten-Baumann conditions with Na_2CO_3 and EtOAc were used to anchor nitrogen mustard **HCl·3**. However, the expected amide was only found at traces amounts, and an unexpected compound was obtained instead in high yield. The same outcome was obtained when the reaction was performed in wet DCM with excess of neutral bis(2-chloroethyl)amine or a biphasic reaction mixture with CH_2Cl_2 and aqueous phosphate buffer (Scheme 1).

Scheme 1. Synthesis of aldehyde 4 from reported compound 1.



Reaction conditions: a) 5 eq. thioglycolic acid sodium salt, 5 eq. KOH, DMSO/DMF/H_2O (25/5/2), 2M, 5°C, 89%; b) 0.3 eq. $SOCl_2$, MeOH/THF (3/1) 0.1M, 88%; c) 10 eq. CO_2Cl_2, 0.02 eq. NBu_4Cl, 40 °C, 99%; d) 4.5 eq. bis(2-chloroethyl)amine, wet DCM, 0.026 M, -30 °C, 70%.

Positive electrospray high resolution mass spectrometry showed a peak at 344.0193 corresponding with the molecular formula $C_{14}H_{11}NNaO_6S^+$ ($[M+Na]^+$). This formula is consistent with the protonated aldehyde **4** and also with a structural isomer of the starting naphthoic acid **2**. The presence of the aldehyde functional group in the rearranged compound **4** was supported by the IR spectrum with characteristic absorptions for aldehydes at 2850 and 2754 cm^{-1}. The stretching carbonyl band is hidden under two other carboxyl bands at 1730 cm^{-1}. ^1H NMR spectrum also supports the aldehyde functional group due to the presence of a 7.9 Hz doublet at 9.08 ppm coupled with an olefinic proton and the ^{13}C NMR spectrum presents a carbonyl carbon CH at 188.9 ppm. The presence of the aldehyde is also supported by the formation of a hemiacetal in CD_3OD after adding a trace of *p*TsOH to a compound **4** CD_3OD solution, showing two doublets at 6.00 and 4.50 ppm with *J*=6.7 Hz. The unusual (*Z*)-3-(hydroxyimino)isobenzofuran-1(3*H*)-one (phthaloxime) structure is consistent with the carboxyl carbon at 163.2 ppm and the imino carbon at 145.7 ppm. HMBC CIGAR long range proton-carbon correlations are also consistent with these assignations, since the hydroxyimino proton singlet at 11.83 ppm showed in the DMSO-d_6 spectrum a three-bond correlation with the hydroxymino carbon at 145.8 ppm, while the aromatic *ortho* proton at 8.07 ppm showed the corresponding correlation with the carboxyl carbon (Figure S8). All the other correlations are in agreement with the proposed structure (see ESI). An interesting fact is the splitting of the methylene protons in the ^1H NMR spectrum as an AB system at 3.95 and 3.89 ppm. This fact seems not to agree with a planar structure but can be explained due to the presence of atropoisomers. Modelling studies predict a rotational barrier for this structure around 20 kcal/mol (Figure 2), high enough to prevent rotation in the NMR scale.

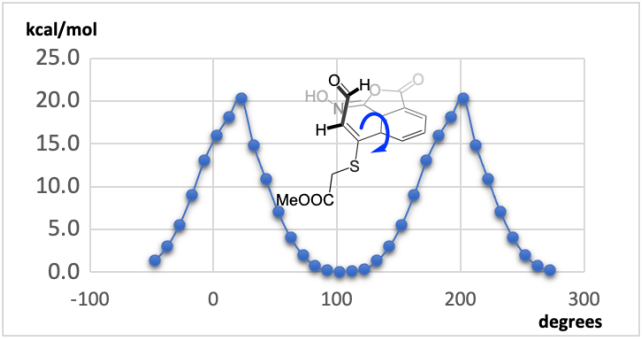
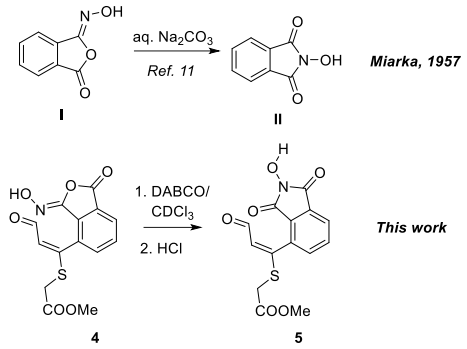


Figure 2. Modelling studies of the phthaloxime aldehyde showing the twisting between the aromatic ring and the substituent supporting the aldehyde.

The phthaloxime **I**[10] (Scheme 2) has been known for a long time, as the result of the reaction of phthalic anhydride and *O*-benzyl hydroxylamine, followed by hydrogenolysis. It has been reported that this structure is in equilibrium with the hydroxyphthalimide structure **II** thorough a deep red anion intermediate formed under basic conditions (Scheme 2, top) and assignation of the right structure has been a matter of considerable debate.[11]

Scheme 2. (Top) Rearrangement of (*Z*)-3-(hydroxyimino)isobenzofuran-1(3*H*)-one into *N*-hydroxyphthalimide under basic conditions reported in literature. (Bottom) Rearrangement found with aldehyde 4.



In our case, treatment of a $CDCl_3$ solution of the phthaloxime **4** with DABCO yielded indeed a deep red solution, from which, after acidulation with aqueous 2M HCl, the hydroxyphthalimide compound **5** was obtained (Scheme 2, bottom). The IR spectrum agreed with the hydroxyphthalimide structure with a characteristic band at 1787 cm^{-1}.[12] The most convincing fact is the appearance of the two carboxyl carbons in the ^{13}C NMR spectrum at 162.4 and 163.0 ppm while the imino carbon at 145.8 ppm has disappeared. All the other spectroscopic properties agree with the structure (ESI), therefore in this case there is no structure ambiguity between both compounds.

We have been unable to obtain suitable crystals from the previous aldehydes **4** or **5** for X-ray analysis, therefore the 2,4-dinitrophenyl hydrazones of both compounds were prepared with 2,4-dinitrophenyl hydrazine in THF. Both aldehydes rendered the same dinitrophenyl hydrazone which is a deep red crystalline compound from which the X-ray analysis was possible. The structure shown in Figure 3 corresponds to the hydroxyphthalimide compound **6**, since the phthaloxime rearranges under these conditions to the hydroxyphthalimide.

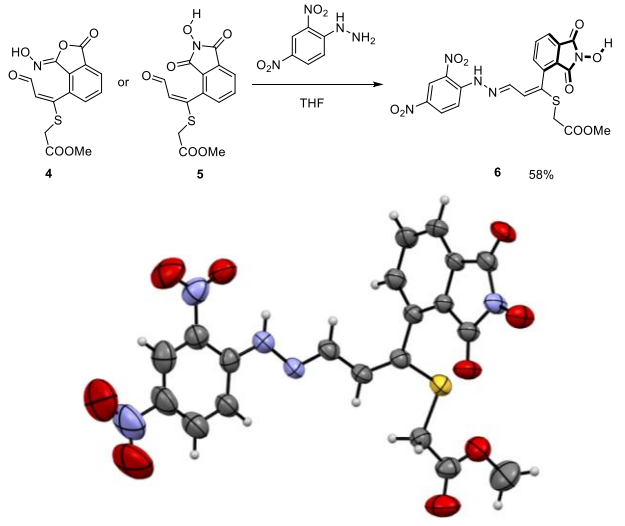


Figure 3. (Top) Synthesis of compound **6** from either **4** or **5**. (Bottom) ORTEP diagram of compound **6**. Displacement ellipsoids are drawn at 50 % probability level. Hydrogen atoms are shown as spheres of arbitrary radius.

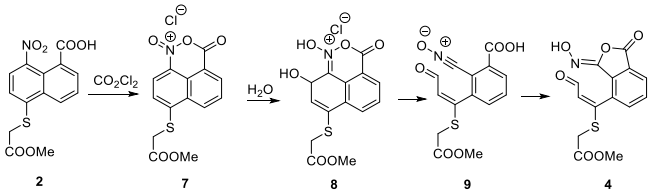
This structure is in good agreement with the previous modelling of the phthaloxime aldehyde **4** showing an almost 90° torsion angle between the hydroxyphthalimide aromatic ring and the substituent. This fact supports the presence of atropoisomers in these compounds.

A comparison of the ^{13}C-NMR spectra of the hydrazone with both previous aldehydes confirms the structure of the phthaloxime for the reaction of the acylnitronium chloride, since the hydrazone lacks the 145.8 ppm carbon from the imine while it shows the two carboxyl carbons at 162.9 and 163.7 ppm. This result shows that the phthaloxime rearranges to the hydroxyphthalimide in the presence of dinitrophenylhydrazine.

After elucidating the structure of the aldehyde **4** we aimed at investigating the mechanism to explain the unexpected formation of this compound from 1,8-disubstituted naphthalene **2**. We were suspicious of the reaction between compound **2** and oxalyl chloride to generate the acid chloride, since the reaction of an acid chloride with a secondary amine should obviously yield an amide. In order to explain the low yield of amide we discarded the acid chloride as intermediate, and we propose a naphtho oxazinium chloride **7** instead (Scheme 3) as the reaction product of the acid **2** with oxalyl chloride. This intermediate offers a plausible explanation to justify the preference for the nucleophilic attack on the C-7 position of the naphthalene ring instead of the carbonyl group of an acid chloride.

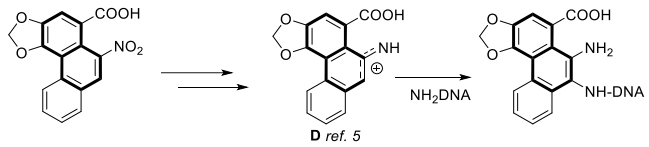
Although the naphtho oxazine chloride **7** is a highly unstable compound it has been possible to carry out a reasonable characterization. High resolution mass spectrometry shows a peak at 304.0273 corresponding to a molecular formula $C_{14}H_{10}NO_5S^+$. The lack of the chloride atom in the molecular formula ruled out the acid chloride structure. IR spectrum showed a broad band at 1728 cm^{-1} inconsistent with an acid chloride which is expected to absorb around 1800 cm^{-1}. ^{13}C NMR showed two carboxyl signals at 168.8 ppm and 167.7 ppm consistent with the expected chemical shifts for the naphtho oxazinium carbon and the ester group.

Scheme 3. Key intermediates proposed for the rearrangement of 1,8-disubstituted naphthalene 2.



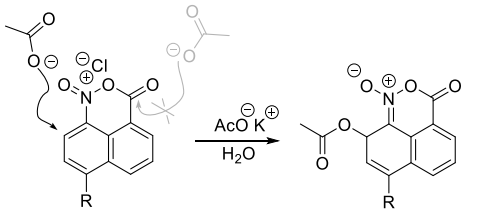
Although the addition of water to the naphthalene skeleton seems a counterintuitive reaction, as it should yield a big loss of aromatic energy, a good precedent can be found in the formation of the naphtho oxazole compound reported by Priestap (Figure 1D). In fact, these compounds also show interesting pharmaceutical and biological properties, since they have similar properties than aristolochic acids which have been proposed to act through a nitrenion ion to couple with DNA through the addition of the amino group of a DNA nucleobase (Scheme 4). However, no fragmentation was reported in this case.

Scheme 4. Naphtho oxazole derivatives with cytotoxic activity and the proposed nitrenium intermediate which reacts with the amino group of DNA nucleobases.



Trying to show that indeed the naphtho oxazinium chloride **7** undergoes nucleophilic attack in C-7, this compound was treated at 0 °C with potassium acetate. Two doublets with *J* = 5.2 Hz grow up during the reaction in the ^{1}H NMR spectrum in $CDCl_3$ at 6.67 and 6.15 ppm consistent with the addition of the acetate to C-7 naphthalene ring. However, the compound is unstable, and a further characterization has not been possible. We have been able to perform this study easier with the chloride derivative in position 5 instead of the thioglycolic fragment since a simple washing of the potassium acetate salt with cold water and evaporation of the solvent yielded a crystalline compound easier to handle. The structure of the acetate is shown in Scheme 5. The physical properties are in good agreement with the addition compound. The HRMS spectrum shows a peak at 315.9976 corresponding to the formula $C_{13}H_8O_5N^{35}Cl^{23}Na$ which matches the proposed acetate. This substitution is known to take place in the presence of oxalyl chloride, as already reported in the literature.[9] The ^{1}H NMR spectrum showed two doublets at 6.72 and 6.41 ppm corresponding to the proton geminal to the acetate group and the vinyl proton, respectively, confirming again the addition of the acetate (ESI). This easy nucleophilic addition to the naphthalene C-7 of the dioxo naptho oxazine may be an interesting clue for the addition of nucleic bases to aristolochic acids as an alternative to the reported nitrenium cation intermediates.

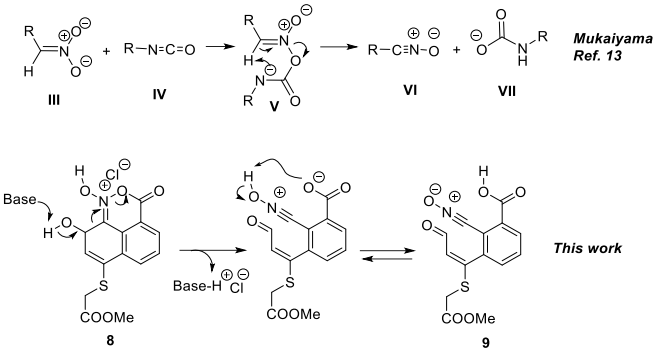
Scheme 5. Addition of potassium acetate to the naphthalene compounds 7 and 10 in position C-7.



As acetate **12** cannot undergo further reaction to the aldehyde, its hydrolysis to the alcohol was undertaken, however, hydrolysis of the naphtho oxazinium was obtained instead.

Therefore, in order for compound **7** to generate the observed product **4**, addition of water to C-7 should yield an alcohol (**8**) which can evolve to an aldehyde with concomitant ring opening and formation of the nitrile oxide **9** (Scheme 3, **7**→**8**→**9**). A precedent to this reaction can be found in the Mukaiyama nitrile oxide synthesis from nitroderivatives and isocyanates (Scheme 6).[13]

Scheme 6. (Top) Mukaiyama nitrile oxide synthesis. (Bottom) Rearrangement observed in this work.



The formation of the acyl nitronate is similar in both cases. While in the Mukaiyama reaction a proton is abstracted to yield the nitrile oxide and a carbamate, in our case is the C-C fragmentation which provides the pair of electrons to promote the carboxylate elimination, yielding in this process an aldehyde and a nitrile oxide.

Nitrile oxides are highly reactive species which readily undergo 1,3 dipolar additions.[14] All attempts to trap this intermediate, even with tetracyanoethylene were unsuccessful, probably because the intramolecular reaction with the carboxylic group in C-1 is faster (Scheme 3, **9**→**4**), and the phthalooxime **4** is formed.

To shed light into this unusual rearrangement, DFT calculations (see details in the SI section) were performed to understand the reaction mechanism and, specially the preference for the addition of H_2O to the C-7 position of the naphtho oxazinium cation instead of the carboxylic C carbon. To simplify the calculations, the 2-thioacetate group was replaced by a methylsulphane. Dihydrogenphosphate ($H_2PO_4^-$) and dimethylamine were studied as possible basic catalysts. Solvent effects (chloroform) were included by an implicit solvation model and in the reaction catalyzed by dimethylamine the chlorine counter anion was not included (the net charge of the molecule was +1 in the calculations), while in the case of the $H_2PO_4^-$ catalyzed reaction this group was used as counter anion (the net charge was 0). An exhaustive search of TSs structures with different orientations of the reacting groups was performed, although some of these orientations collapsed during the optimization to the same structure.

For the reaction catalyzed by dimethylamine, addition to the carboxylic C atom was favoured (≈2.0 kcal/mol energy difference between the most stable TSs, 95:5 ratio considering all TSs, see ESI). In the case of the reaction catalyzed by $H_2PO_4^-$, the major product corresponds to the addition to C-7 (energy difference of ≈2.5 kcal/mol between most stable TSs, 97:3 ratio, Scheme 7). These results agree with experimental observations. Not surprisingly, analogue calculations for the addition of one H_2O molecule to the acyl-chloride show a much larger preference for the addition on the carboxylic C atom (≈8.0 kcal/mol), confirming that the formation of the naphtho oxazinium chloride **A** is necessary to justify the reactivity observed (Scheme 7).

The reaction continues with the opening of two of the six-membered rings of intermediate **C**: the C7-C8 bond and the N-O bonds are broken to generate the aldehyde and the hydroxynitrile groups **C**. TS structures corresponding to this step (**TS-BC**), catalyzed by an additional dihydrogenphosphate group, were also found. The hydroxy group can adopt a *pseudo-axial* or a *pseudo-equatorial* position, but in the last case it is oriented in an almost planar *s-trans* conformation with respect to the conjugated double bond, an effect that probably contributes to stabilize the equatorial TS structure. The reaction is concerted but shows some degree of asynchronicity: N-O distance is 2.5 Å while the C-C distance is elongated to 1.9 Å (Figure 4). Finally, the reaction proceeds through **TS-CD** and product **D** (corresponding to compound **4**) is formed.

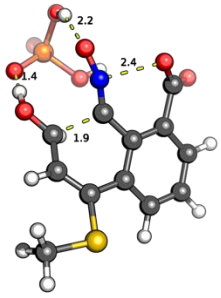
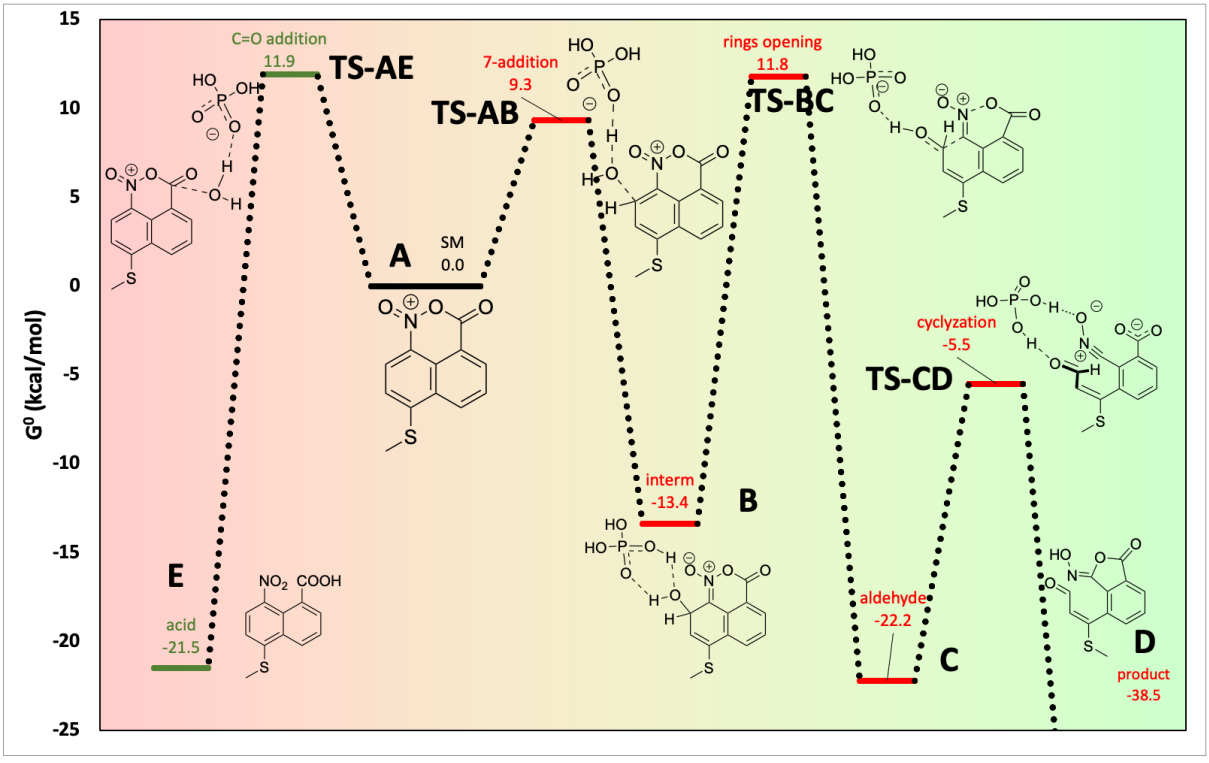


Figure 4. Miniminum energy transition state for the $H_2PO_4^-$ catalyzed fragmentation of C7-C8 and N-O bonds.

Since the addition of a water molecule to C-7 (the preceding step) is reversible, the accumulation of the aldehyde product also requires that the TSs corresponding to this second step are also more stable than the TSs (**TS-AE**) of the H_2O addition to the carbonyl C atom. Otherwise, the irreversible formation of the aldehyde from the intermediate would be slower than the protonation and elimination of the C-7 OH group and the addition of the resulting water molecule to the carbonyl C atom to yield the competing reaction towards the carboxylate **E**. However, direct comparison of the energies of these TSs is not possible since they have different number of atoms: the second step TSs are deprotonated with respect to the TSs for the addition of H_2O to the starting materials.

In order to correct for this effect, the energies of a neutral phosphoric acid structure and of a $H_2PO_4^-$ anion were added and subtracted from the energy of the second step TS structure. Formally, this balances the number of atoms under a condition in which the concentrations of phosphoric and dihydrogenphosphate are identical. Curiously, under these assumptions, the energy of the second step most stable TSs is 2.5 kcal/mol[15] higher than the energy of the most stable TSs corresponding to the H_2O addition to the C-7 atom, and very similar to the energy of the TSs for the addition on the carbonyl C atom, corresponding to the competing path. Under conditions in which the concentration of $H_2PO_4^-$ is higher (basic pK_a), the formation of the aldehyde should be favoured, while, in agreement with experimental results, acid pK_a should increase the effective barrier of the second step and the hydrolysis should follow the competing path.

Scheme 7. Computer reaction energy profile for the pathway through the lowest energy transition state structure leading to the rearranged aldehyde (green background) and competing hydrolysis reaction (red background).



Conclusions

In summary, an unprecedent rearrangement of a 1,8-nitronaphthalene carboxylic acid derivative towards an aromatic ring bearing aldehyde and a phthaloxime functional groups has been reported. The steric hindrance between the nitro and carboxylate groups in 1,8 positions promotes the formation of a strained naphtho oxazinium intermediate with an unusual reactivity. Addition of water under very mild reaction conditions under slightly basic conditions at 0-20 °C initiates a fragmentation reaction able to break the aromaticity of the naphthalene core. MS and NMR experiments support the intermediates proposed, and the final structure has been confirmed by X-ray diffraction analysis of a 2,4-dinitrophenylhydrazone derivative. DFT studies have been carried out and support the mechanism proposed. The naphtho oxazinium intermediate could find application as cytotoxic reagent by its similar properties to aristolochic acids which are able to react with DNA nucleobases.

ASSOCIATED CONTENT

Supporting Information. The Supporting Information is available free of charge at https://pubs.acs.org/doi/XXXXX. Complete experimental procedures and characterization data for compounds, including ^{1}H, ^{13}C, 2D NMR, X-ray crystal analysis, crystallographic data for **6** (CCDC 2351359) and modeling studies (PDF).

AUTHOR INFORMATION

Corresponding Author

Ángel L. Fuentes de Arriba – Organic Chemistry Department, University of Salamanca, Salamanca 37008, Spain; Email: angelfuentes@usal.es

Luis Simón – Chemical Engineering Department, University of Salamanca, Salamanca 37008; Email: lsimon@usal.es

Author Contributions

All authors have given approval to the final version of the manuscript.

Notes

The authors declare no competing financial interest.

ACKNOWLEDGMENT

This work was supported by MICINN PID2020-118732RAI00 and CNS2022-135656. A.H. is grateful to the Algerian Government for a predoctoral fellowship for "Formation Doctorale résidentielle l'etranger". E.S.S. and I.B.T. gratefully acknowledge Ministerio de Educación for a FPU predoctoral fellowship. We thank Dr. Anna M. Lithgow (NMR Service, NUCLEUS, University of Salamanca) for the NMR spectra done in the Bruker Avance NEO 400 MHz. Dr. César Raposo and Dr. Juan F. Boyero-Benito (Mass Spectrometry Service, NUCLEUS, University of Salamanca), and Dr. José M. Compaña (X-Ray Diffraction Service, NUCLEUS, University of Salamanca).

REFERENCES

(1) Anderson, J. E.; Cooksey, C. J. *peri*-Interactions in Naphthalene Derivatives. Rotation in 1,8-Disubstituted Naphthalenes. *J. Chem. Soc., Chem. Commun.* **1975**, 942-943.

(2) Schweizer, W. B.; Procter, G.; Kaftory, M.; Dünitz, J. D. Structural Studies of 1,8-Disubstituted Naphthalenes as Probes for Nucleophile-Electrophile Interactions. *Helv. Chim. Acta* **1978**, *61*, 2783–2808.

(3) (a) Bristow, J. C.; Leslie, R.; Wallis, J. D. Incipient Nucleophilic Attack on a Carbonyl Group Adjacent to a Stereogenic Centre in *Peri* Naphthalene Derivatives. *Helv. Chim. Acta* **2023**, *106*, e202300021; (b) Bristow, J. C.; Cliff, S. V. A.; Yang, S.; Wallis, J. D. Interaction, bond formation or reaction between a dimethylamino group and an adjacent alkene or aldehyde group in aromatic systems controlled by remote molecular constraints. *CrystEngComm.* **2021**, *23*, 4500-4512; (c) Bristow, J. C.; Naftalin, I.; Cliff, S. V. A.; Yang, S.; Carravetta, M.; Heinmaa, I.; Stern, R.; Wallis, J. D. Modelling of an aza-Michael reaction from crystalline naphthalene derivatives containing *peri*–*peri* interactions: very long N–C bonds? *CrystEngComm*. **2020**, *22*, 6783-6795; (d) Saritemur, G.; Miralles, L. N.; Husson, D.; Pitak, M. B.; Coles, S. J.; Wallis, J. D. Two modes of *peri*-interaction between an aldehyde group and a carboxylate anion in naphthalaldehydate salts. *CrystEngComm.* **2016**, *18*, 948-961; (e) Wannebroucq, A.; Jarmyn, A. P.; Pitak, M. B.; Coles, S. J.; Wallis, J. D. Reactions and Interactions Between Peri Groups in 1- Dimethylamino-Naphthalene Salts: An Example of a "Through Space" Amide. *Pure Appl. Chem.* **2016**, *88*, 317–331; (f) Mercadal, N.; Day, S. P. Day, S. P.; Jarmyn, A.; Pitak, M. B.; Coles, S. J.; Wilson, C.; Rees, G. J.; Hanna, J. V.; Wallis, J. D. *O- vs. N*-protonation of 1-dimethylaminonaphthalene-8-ketones: formation of a *peri* N–C bond or a hydrogen bond to the pi-electron density of a carbonyl group. *CrystEngComm.* **2014**, *16*, 8363-837; (g) Lari, A.; Pitak, M. B.; Coles, S. J.; Rees, G. J.; Day, S. P.; Smith, M. E.; Hanna, V. J.; Wallis, J. D. Models for incomplete nucleophilic attack on a protonated carbonyl group and electron-deficient alkenes: salts and zwitterions from 1-dimethylamino-naphthalene-8-carbaldehyde. *Org. Biomol. Chem.* **2012**, *10*, 7763-7779.

(4) Kazim, M.; Siegler, M. A.; Lectka, T. Close Amide NH···F Hydrogen Bonding Interactions in 1,8-Disubstituted Naphthalenes. *J. Org. Chem.* **2020**, *85*, 6195-6200.

(5) Priestap, H. A.; Barbieri, M. A.; Johnson, F. Aristoxazole Analogues. Conversion of 8-Nitro-1-naphthoic Acid to 2-Methylnaphtho[1,2-*d*]oxazole-9-carboxylic Acid: Comments on the Chemical Mechanism of Formation of DNA Adducts by the Aristolochic Acids. *J. Nat. Prod.* **2012**, *75*, 1414–1418.

(6) Ozeryanskii, V. A.; Pozharskii, A. F.; Antonov, A. S.; Filarowski, A. Out-Basicity of 1,8-Bis(Dimethylamino)- Naphthalene: The Experimental and Theoretical Challenge. *Org. Biomol. Chem.* **2014**, *12*, 2360–2369.

(7) Reza, A. I.; Iwai, K.; Nishiwaki, N. A Study of the Correlation between the Bulkiness of *peri*-Substituents and the Distortion of a Naphthalene Ring. *Molecules* **2023**, *28*, 5343.

(8) Iwai, K.; Nishiwaki, N. Unsymmetrization of 1,8-Dibromonaphthalenes by Acid-Induced Halogen Dance Reaction. *J. Org. Chem.* **2024**, *89*, 7843–7847.

(9) Habib, A.; Garrido-González, J. J.; Sánchez-Santos, E.; Boya del Teso, I.; Sanz, F.; Alcázar, V.; Fuentes de Arriba, Á. L.; Morán, J.

R. 5-Chloro-8-nitro-1-naphthoyl (NNap): A Selective Protective Group for Amines and Amino Acids. *Org. Lett.* **2023**, *25*, 4103-4107.

(10) Bauer, L.; Miarka, S. V. The Chemistry of N-Hydroxyphthalimide. *J. Am. Chem. Soc.* **1957**, *79*, 1983–1985.

(11) (a) Ames, D. E.; Grey, T. F. The Synthesis of Some N-Hydroxyimides. *J. Chem. Soc.* **1955**, 631-636; (b) Ames, D. E.; Grey, T. F. N-Hydroxy-imides. Part II. Derivatives of Homophthalic and Phthalic Acids. *J. Chem. Soc.* **1955**, 3518-3521.

(12) Roderick, W. R.; Brown, W. G. Colorless and Yellow Forms of N-Hydroxyphthalimide. *J. Am. Chem. Soc.* **1957**, *79*, 5196-5198.

(13) Mukaiyama, T.; Hoshino, T. The Reactions of Primary Nitroparaffins with Isocyanates. *J. Am. Chem. Soc.* **1960**, *82*, 5339–5342.

(14) Kobayashi, S.; Jørgensen, K. A. *Cycloaddition Reactions in Organic Synthesis*, Wiley-VCH: Weinheim, 2002.

(15) These numbers should be considered simply as a coincidence: a different choice of an acid-base pair to balance the number of atoms would show different results (for example, the energy would be -35.1 kcal/mol smaller if $H_2PO_4^-/HPO_4^{2-}$ were used to balance the number of atoms); the choice of the $H_3PO_4/H_2PO_4^-$ is more reasonable considering the conditions on which the reactions were carried out -and the amount of HPO_4^{2-} is probably very small in chloroform- but a more realistic model should imply explicitly solvated $H_3PO_4/H_2PO_4^-$ molecules. However, the use of explicit water molecules would make the calculations intractable since the number of conformations to consider would increase exponentially, and the simple model employed in the calculations is able to justify the experiments at least qualitatively.